ISSN 0990-7440
ALREEA

Aquatic Living Resources

Ressources vivantes aquatiques

Vol. 16 – No. 3
July 2003

ELSEVIER

Acoustics in Fisheries and Aquatic Ecology. Part 2

Jacques Massé & François Gerlotto - Co-Conveners

Aquatic Living Resources

Ressources vivantes aquatiques

Aquat. Living Resour. 16 (3) 2003, 105 – 338

Contents

ACOUSTICS IN FISHERIES AND AQUATIC ECOLOGY. PART 2

Contents (contd.)

NOTA

Acoustics in Fisheries and Aquatic Ecology:

Part 1. *ICES Journal of Marine Sciences*, vol. 60, n°3, 2003

Part 2. *Aquatic Living Resources*, vol. 16, n°3, 2003 (this volume).

Available online at www.sciencedirect.com
SCIENCE DIRECT®
Aquatic Living Resources 16 (2003) 105–106
Aquatic Living Resources
www.elsevier.com/locate/aquliv

Editorial

There is an increasing concern in the world about the potential effect that human pressure and climate change may introduce into the environment, and especially in marine ecosystems. Due to the fact that this ecosystem approach is recent, although many scientific observations and results show that climatic changes are already appearing, very little is known about the way marine communities are adapting to or affected by these changes. This ecological and ecosystem approach brings two constraints:

- there is a need to strengthen the capacity to detect, understand and predict the effects of the global change;
- this requires developing or adapting cost effective, reliable and efficient technologies, in order to be able to collect rigorous scientific data to develop indicators on the status of the ecosystem.

In the particular case of large pelagic ecosystems, the fish populations as well as the other animal groups remain difficult to study, as their dimension and variability do not allow performance of accurate, economic or synoptic observation of the different system parameters with the current state of technology. Thus, there is a strong need for adapted methods of direct observation.

These remarks have already lead ecologists towards the use of acoustic methods and techniques to sample and survey the ecosystem. For this reason, the sixth ICES Symposium on Acoustics in Fisheries and Aquatic Ecology (SAFAE) (France, June 2002) was the first to explicitly call for papers on the "Aquatic Ecosystem". In its three sessions (including behavioural ecology) 74 papers were devoted to this particular case.

This is certainly due to the fact that underwater acoustics represents an ideal tool for ecological analysis because it:

- allows a huge quantity of data to be collected in a rather short time;
- enables data collection at extreme scales: a single tool can obtain simultaneous information on zooplankton and large fish, with high definition (centimetres) at large range (hundreds of metres);
- is not intrusive (null or weak effect of the observer on the ecological medium);
- can be collected in conjunction with other data (on fisheries and biology, chemistry and physical oceanography, etc).
- Finally, the format of data acquired permits comprehensive use of the latest analysis methods: geostatistics, GAM, GLM, SIG, etc.

This ecological surveying and monitoring has to be done at several scales, and in some of them acoustic data can provide important information.

- At a large scale, it is important to be able to map the distribution of "global marine production", in terms of general biomass, regardless of the kind of organisms that form this biomass. Such data can help, for instance, to identify "hot spots" in the oceans, and through links with remote sensing data, to bring valuable information on the general distribution and abundance of marine life.
- At a fine scale, a more detailed series of observations can be made on the spatial distribution of biomass patches identified at the larger scale. These results are more dynamic, and relate to shape, size and density of the patches, persistence of the spatial structures, temporal patterns, etc., which underlie the process and function in ecological interaction. Here too, this kind of data are easily linked to remote sensing information, such as temperature and pressure which may structure biomass distribution and persistence.
- A singular advantage of acoustics over traditional methods (e.g. optical observation, net sampling) is the range of space—in 3D—which can be continuously sampled. When combined with net sampling (groundtruthing acoustical information) it is possible to identify and extrapolate the distribution of the major trophic groups, from micronekton to zooplankton to fish and other upper trophic species.
- Finally, fishing pressure in the last several decades has caused a significant change in the distribution and abundance of marine biodiversity in the world's oceans. Although we know the effects on major stocks, little work has been done on the other pelagic species indirectly affected by this loss of upper trophic biomass. However, significant amounts of information on these species are already contained within existing acoustic data, albeit unprocessed.

The ICES SAFAE was held in Montpellier, France, from 10 to 14 June 2002. There were 303 participants from 37 countries, emphasising the strongly international character of the meeting. This Symposium was the sixth organised on fisheries acoustics, and the fifth sponsored by ICES in a series concerned with acoustics in fisheries and related fields. The first of these was in Horten (1954), then there were two in Bergen (1973 and 1982), one in Seattle (1987) and the most recent was in Aberdeen (1995; *ICES Journal of Marine*

doi:10.1016/S0990-7440(03)00059-7

Science, Vol. 53, no. 2). To complete the historical picture, two Symposia on the special problems of shallow-water acoustics should be mentioned, held in London (1997) and in Seattle (1999; *Aquatic Living Resources*, Vol. 13, no. 5). By 2002, however, it was seen that shallow-water, marine and freshwater acoustics required a joint approach to problem solving and sharing of experience. It was therefore decided that the SAFAE would encompass all these applications within the general theme of acoustical methods for the study of aquatic biota and their exploitation.

The primary sponsors of the SAFAE were the ICES, the Institut de Recherche pour le Développement (IRD), and the Institut Français de Recherche pour l'Exploitation de la Mer (IFREMER); co-sponsors were the Acoustical Society of America, the UK Institute of Acoustics, the US National Marine Fisheries Service, and the Société Française d'Acoustique. The Symposium was convened by François Gerlotto (IRD) and Jacques Massé (IFREMER). They were assisted by a Scientific Steering Committee comprising Pablo Carrera (Spain), David Farmer (Canada), Masahiko Furusawa (Japan), D. Van Holliday (USA), Bill Karp (USA), Ole-Arve Misund (Norway), John Simmonds (UK), and Will Tesler (Russia). The conference Secretariat was efficiently organised by Laurence Vicens from the Centre Halieutique of the IRD which provided much logistical support, as did IFREMER, especially through the editorial work of Brigitte Milcendeau.

The main objectives of the SAFAE were to bring together scientists with diverse interests in fisheries and aquatic acoustics, covering a broad range of environments; to present their research in this rapidly evolving field; to review what can be achieved with new technology and theoretical approaches; and to consider future directions of study. There was a large response to the call for papers. The 256 submitted abstracts were allocated between the following 10 theme sessions:

1. Acoustic survey design, including data analysis.
2. Combination of methods, to compare acoustic and other methods of assessment.
3. Technology, innovations in equipment and data processing.
4. Identification and classification of echo-traces.
5. Ecology, freshwater.
6. Ecology, marine water.
7. Avoidance—the response of fish to vessel noise, and biological acoustics.
8. Fish and plankton behaviour, and physiological studies.
9. Target strength, methods and results.
10. Target strength, modelling and theory.

There were 106 verbal presentations, and 140 posters, which together gave participants a unique overview of a huge amount of multi-disciplinary research. Symposia like the SAFAE are essential if scientists are to have any chance of keeping up with the rapid pace of developments in this field.

The publication of proceedings is an important part of any symposium. The number of proposed manuscripts resulting from the SAFAE was substantial. It was therefore arranged that symposium papers would be published in special issues of two journals[1]—*Aquatic Living Resources* (this volume) and the *ICES Journal of Marine Science*. Papers were selected for each journal according to the relevant theme session. This volume contains 30 papers which are mainly on ecological or biological topics (themes 2, 5, 6, 7 and 8 above), A further 36 papers will be found in Vol. 60 of the *ICES Journal of Marine Science*, those mainly on technological or physical topics (themes 1, 3, 4, 9 and 10 above).

Readers are encouraged to consult both special issues, which together comprise the full SAFAE proceedings. Indeed, it is important to consider the full range of the activities explored at the SAFAE. This shows how cooperation between specialists from many disciplines can achieve much more than narrowly focussed research. Whatever the background, there is a common purpose in this work, namely the study and protection of sustainable aquatic resources.

The timely publication of these proceedings owes much to the referees (listed on last page), who prepared prompt and comprehensive reviews, and to the authors who made the required revisions to their manuscripts within tight deadlines.

Jacques Massé, François Gerlotto and David MacLennan.

Jacques Massé
Ifremer, Laboratoire d'écologie halieutique,
rue de l'Ile d'Yeu, BP 21105,
44311 Nantes cedex 3, France
E-mail address : jacques.masse@ifremer.fr

François Gerlotto
IRD, Roman Diaz 264
Santiago, Chile

David N. MacLennan
Perth, Scotland, UK

[1] Nota: **Acoustics in Fisheries and Aquatic Ecology.**
Part 1. *ICES Journal of Marine Sciences*, vol. 60, n° 3, 2003.
Part 2. *Aquatic Living Resources*, vol. 16, n° 3, 2003 (this issue).

Available online at www.sciencedirect.com
SCIENCE DIRECT®
Aquatic Living Resources 16 (2003) 107–112
Aquatic Living Resources
www.elsevier.com/locate/aquliv

Foreword

Introducing nature in fisheries research: the use of underwater acoustics for an ecosystem approach of fish population

The changes in environmental conditions require an "ecosystem approach" be adopted when considering fish populations. This new approach implies the design of new concepts and hypotheses including knowledge on ecology, behaviour and fisheries. Being able to observe in real time and in three dimensions the living organisms and their environment becomes essential. These are precisely the capabilities of underwater acoustics, which is going to play a major role in aquatic ecology research.

1. Introduction

Based on pioneer works in the 1950s by Schaefer (1954), Beverton and Holt (1957), Gulland (1969), Fox (1970), among others, fisheries biology and its associated models of the dynamics of populations represented a huge step forward in the analysis and monitoring of exploited fish populations. These models helped to manage a number of important fisheries in the world, initially with great success. A major advantage was the ability to manage a stock on the basis of limited data; mostly derived from the fishery itself. Implicit in these models was the concept of "stability" of the stock and its insensitivity to any other parameter than the fishery. Any change in the characteristics of the population was expected to be due to changes in the pattern of the fishery. The history of most studied fisheries has shown that these assumptions are not completely valid. The adaptation of fish populations to changes in environmental conditions has the potential to change the fundamental characteristics of the main parameters considered in conventional stock models. A good, well-described example is the pattern of area occupation by a stock with changes in abundance (Swain and Sinclair, 1994; Gauthiez, 1997; Fréon and Misund, 1998).

On the other hand, since its beginning in the 1970s, fisheries acoustics has been developed in order to correct the main biases present in indirect data such as fishing statistics. A well known bias is detailed by Fréon and Misund (1998) who show that, depending on the spatial strategy of a species, a decrease in the global biomass can result in a decrease or an increase of the catch per unit of effort (cpue). Contrarily to fisheries data, acoustic methods provide direct abundance estimates (MacLennan and Simmonds, 1992). The echo-integration results were generally used for two purposes: tuning virtual population analysis (VPA) models using actual biomass, or more directly establishing total allocated catches (TACs) based on the stock biomass. However, in many cases the contribution of fisheries acoustics remained limited.

Eventually we are entering a new era, which is based upon two observations.

- It is now recognised that fisheries activity in the world has reached and most probably exceeded its maximum sustainable yield (Pauly et al., 2002; Myers and Worm, 2003).
- The failures of stock management in many cases have demonstrated that the study of a fish stock independently from its biology and behaviour, and more generally from the ecosystem where this stock is living, usually lead to erroneous conclusions on its status.

These two observations have oriented towards new thoughts in fisheries biology, and to the conclusion that the understanding of stock dynamics would require an ecosystem approach.

2. Behavioural ecology in fisheries research

Such new approach implies new hypotheses, which should explicitly include behavioural and other biological or ecological parameters. Some of these hypotheses, in the design of which teams of our institutes were involved, are described below.

2.1. The "meeting point" hypothesis

Dagorn and Fréon (1999) have produced a simulation showing that tuna fish will form a school from an originally dispersed population faster when the fish are attracted by a floating object, than without one. This would be the basis of the use of fish aggregating devices (FADs). Essentially, the object serves as a "meeting point" for the fish, in an ocean environment that otherwise lacks obvious spatial references. This hypothesis has an impact on the way we understand (and use) the aggregative behaviour of such large pelagic fish.

2.2. The biological trap

The biological trap (Fréon and Dagorn, 2000) is basically a development of the FAD argument, and is also derived from

doi:10.1016/S0990-7440(03)00058-5

observations on the aggregative behaviour of tuna. Fishermen exploit the aggregation under FADs and introduce large numbers of rafts into the fishing area to concentrate the fish for more efficient capture. One possible secondary effect of this technique is that the fish may stay with the rafts as they drift. This drift may follow a different route from the normal migration pattern of the fish. In some situations and if the effect is strong enough, the tuna may be "trapped" by the FADs and end up in the "wrong" place, i.e. not where their migration would have placed them. If this area is unfavourable (poorer food resources, etc.) there would be a risk of additional mortality or reduction in recruitment. In this context the large number of human introduced floating objects in the ocean would be of concern.

2.3. Fish learning and catchability

It has been demonstrated that fishes are able to "learn" the effect of a fishing gear and increase their capability to avoid it (e.g. Soria et al., 1993; Pyanov, 1993). In an evolutionary perspective, the fish behaviour will adapt to high levels of fishing activity through selection for those fish, which are better at avoiding, capture. This would result in a decrease in catchability, proportional to the fishing effort (Fréon and Misund, 1998). This response has been documented in some fisheries (e.g. Brehmer and Gerlotto, 2001).

2.4. The "school trap" hypothesis (Bakun, 2001)

Alternate dominance of one species has been observed in many mixed pelagic fisheries. This has been well documented, for instance, for Peruvian anchovy (*Engraulis rigens*) versus sardine (*Sardinops sagax*). A fast change in dominance might be facilitated by the probability of individuals or groups of the declining species being included in a school of the dominant species. The fish may then be considered as "trapped" in this school with the possibility of them being in, for that species, sub-optimal biological conditions. Such behaviour would accelerate the declining of the dominated stock and be responsible for the fast changes in species dominance.

2.5. Other hypotheses

Other hypotheses along the same or similar lines, incorporating behaviour or other biological aspects, have also been postulated. These may also have important impacts on how we view and assess fish populations. Examples include concepts such as meta-populations (McQuinn, 1997), and more generally the evolutionary concepts synthesised by Cury (1994) and entitled "obstinate nature".

Such new sets of hypotheses are likely to improve dramatically the potential results of fisheries biology research. These present a strong requirement: to be able to observe the nature and the fish living in their environment.

This is the main reason of the parallel evolution of fisheries acoustics, described in details by Fernandes et al. (2002). This evolution can be seen simply through the changes in the titles of the ICES symposia related to underwater acoustics, from "*Fisheries Acoustics*" for the first ones (Bergen, 1973, 1982; Seattle, 1987) to "*Fisheries and Plankton Acoustics*" (Aberdeen, 1995), and finally "*Symposium on Acoustics in Fisheries and Aquatic Ecosystems*" (SAFAE) in Montpellier (2002).

3. Improving fisheries biology using acoustic data

In order to adapt underwater acoustics to "fisheries ecology", it is necessary to evaluate precisely the advantages that it can bring to ecological research, to gather the elements of techniques and methods that are directly applicable to this discipline, and to define the points that need specific research for an eventual adequacy of acoustics methods and techniques to ecology.

In this regard, three main objectives may be defined:

- Taking advantage of existing past research. To evaluate the quantity and quality of information already present in acoustic surveys. Since the 1970s, many countries have developed acoustic survey programs on the main pelagic stocks in their respective EEZs (Fernandes et al., 2002). At this time the ecological information (micronekton, bottom shape and type, school type and behav-

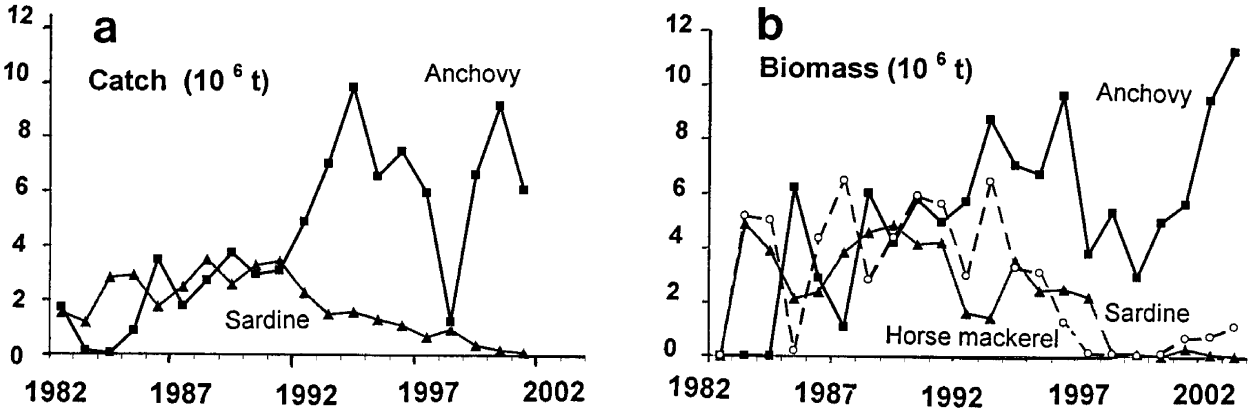

Fig. 1. Some acoustic results on behavioural ecology of pelagic fish. (a) Peruvian landings of anchovy and sardine since 1983; (b) biomass of anchovy, sardine and horse mackerel in Peruvian waters estimated by acoustics since 1983.

iour, hydrological information, etc.) was considered as background noise and not exploited. Under a new perspective, these data could be used to develop, define and extract ecological indicators, allowing observation of decades of change in pelagic ecosystems. It is likely that some methods will be needed for transforming acoustic data into ecological data.

- Preparing the future. The set of new hypotheses will require new series of data to be collected, in a more ecological and behavioural way. Being able to observe in real time and in three dimensions the living organisms and their environment will be essential. This will require new tools, such as multifrequency echo sounders (species and group identification), multibeam systems (3D observation) and omnidirectional sonars (kinematics of schools), which are already conceived and will need a wider use in the close future.
- Improving the present research. Two different kinds of improvements can be considered: technical and methodological. We will not discuss the first one, which was developed in the SAFAE and published in the Part 1, technological proceedings of this symposium (ICES J. Mar. Sci. 60, n° 3). The most promising method for ecological research and monitoring is the use of acoustic data collected and recorded aboard fishing vessels. Such method has been designed and applied for decades by Chile and Peru in the South-East Pacific Ocean (Gutierrez et al., 2000). Although it will require some technical improvement (principally the design of autonomous scientific echo sounders), it may already overcome a series of drawbacks that appear in a single vessel survey; it provides detailed information in the area of high production and abundance where fishing vessel are spending most of their time; and it makes possible real time survey of ecological changes at all scales in a given ecosystem.Anyway, there is a huge amount of acoustic data in the world, still unprocessed from an ecological point of view, which could already give some answers to the questions asked by the new hypotheses. We will give some preliminary examples on the use, for an ecosystem approach, of standard echo sounding survey data initially collected for fish stock study. They show how a stock can be observed and studied from an ecosystem perspective inside its environment. For such demonstration, we used long and detailed data series. One of them was provided by the Instituto del Mar del Peru (IMARPE), which is acknowledged here, on anchovy and sardine stocks off the Peruvian coast; the second one comes from the Bay of Biscay (IFREMER data base), on similar multispecific assemblage.

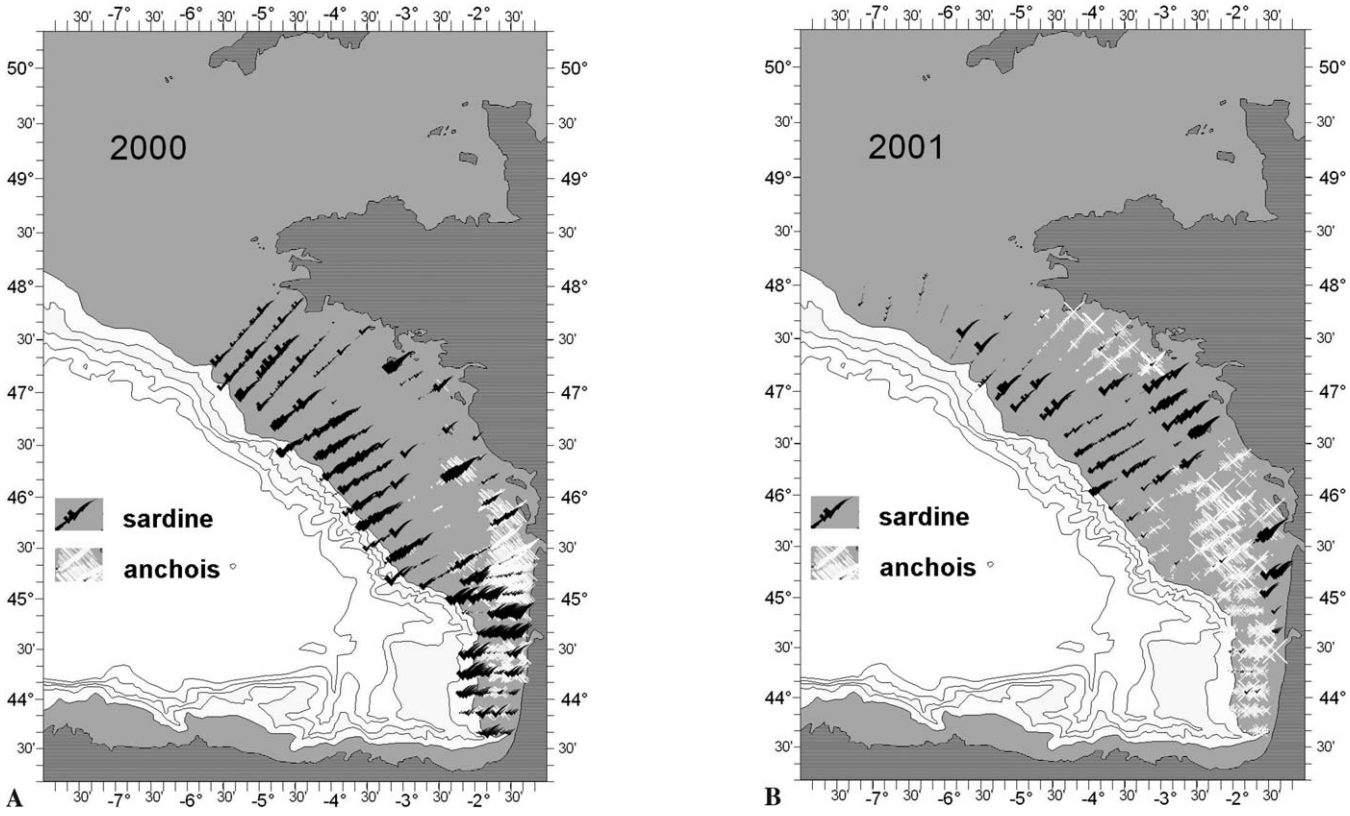

Fig. 2. Abundance of anchovy and sardine in the Bay of Biscay as observed during acoustic surveys in 2000 and 2001 from IFREMER acoustic surveys. Symbol size is proportional to scrutinised S_a values for each species.

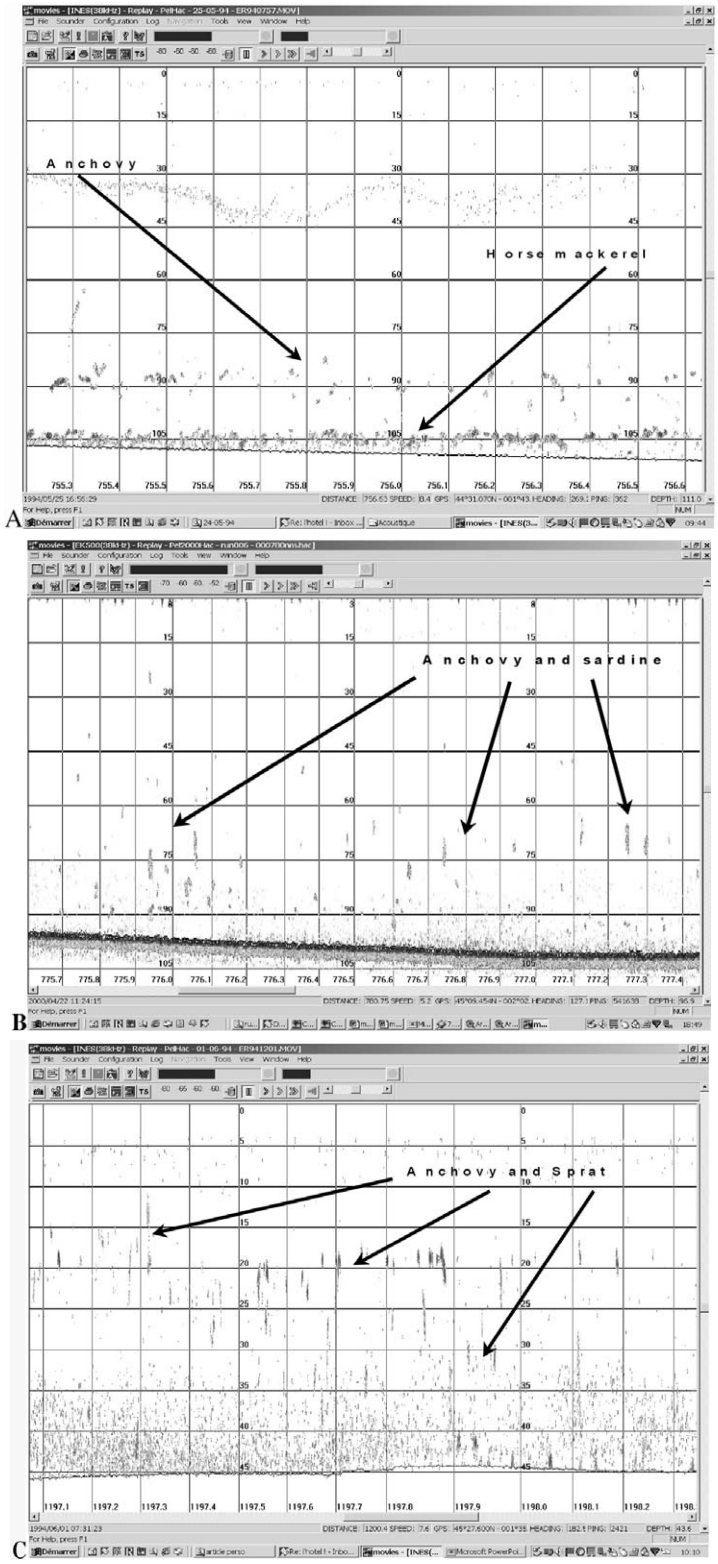

Fig. 3. Echograms in the Bay of Biscay showing the assemblage of anchovy with another pelagic species (anchovy with horse mackerel, sardine, sprat).

Three cases are given:

- Temporal change of stock biomass. Some of the hypotheses presented above have been drawn from long term catch data series, where some simultaneity of the population changes has been seen. This is the case in Peru, where a kind of "synchrony" of abundance of sardine and anchovy appears in the fishing data (Fig. 1a). Sardine and anchovy seem "incompatible", and collapse alternately according to climatic conditions. When observing the actual biomass values (Fig. 1b), the syn-

chrony does not present the same "absolute" character as seen with fishing data. It is confirmed that there are "Sardine–no anchovy" and "Anchovy–no sardine" periods, but the synchrony is only observed on rather long time scale and does not obviously need any behavioural hypothesis to exist: changes in the climatic condition (Chavez et al., 2003) are sufficient. Moreover, sardine and anchovy are able to coexist during rather long periods of "intermediate conditions" (e.g. Fig. 1b).

- Spatial distribution, competition and coexistence. The hypothesis of exclusion of a population from an area occupied by another one is not always demonstrated when the actual ecosystem is studied. For instance we observed in the Bay of Biscay that sardine and anchovy were present in two well differentiated areas in 2000, while they overlapped in 2001 (Fig. 2). The objective of this paper is not to study the determinism of such phenomena, but we may note that the water masses were quite differently distributed in these 2 years. The same observation was done in Peru. Although they usually do not share the same area, when anchovy and sardine in Peru are coexisting in a single place, their abundances are positively correlated (Gutierrez, personal communication). As in the case of time series, there is a "Sardine-no anchovy" and "Anchovy-no sardine" area pattern, but this remains a general drawing, which is likely more complex and more related to combinations and compromises of tropisms and taxis than to a simple competition/exclusion between two species.
- Occupation of space in three dimensions. Fish is occupying a space in three dimensions, and in most of the fisheries data, the vertical one is practically ignored, although it may be the most important for the species. This vertical dimension can allow the life of exclusive species in a single (horizontal) area but still remaining completely separated. Very often such evidence is not visible from fishery data, which cannot clearly describe this vertical dimension. In most of the cases, a vertical stratification of the species occurs. Moreover, the spatial organisation of pelagic fish may be affected by the presence of other species (Fig. 3): in the case of the Bay of Biscay, for instance, the shape and dimension of schools are strongly dependent on the other species sharing the space: the anchovy schools formed when a predator such as horse mackerel is present, are different from those organised when the species share the same trophic level (sardine, sprat) (Massé, 1996).

4. Conclusion

As these few examples show, a large part of the hypotheses that we listed, and more generally the ecosystem approach of fish stocks, can be explored using acoustic data. One interesting point is that standard fisheries acoustics is already able to answer many questions: it is clear that acoustic data have been dramatically underexploited so far.

Another point is that it seems extremely important and urgent to develop research to confirm or discard the behavioural hypotheses. In many cases, they were drawn without support of real in situ observations: the limited value of fisheries data for behavioural observation may bias strongly the conclusion that one can draw from them. For instance, we showed that in Peru the "school trap", which seemed agreeable when observing the catch statistics of anchovy and sardine, is unlikely to have any effect on these stocks.

But the ecosystem approach, including behavioural ecology, is indispensable. As acoustics is one of the very few methods able to provide real time in situ 3D observation data on living organisms and their ecosystem, it will be the responsibility of fisheries acousticians to develop tools to provide information on the fish living in their environment. The "Ecology Acoustics" is born.

References

Bakun, A., 2001. 'School-mix feedback': a different way to think about low frequency variability in large mobile fish populations. Progr. Oceanogr. 49, 485–511.

Beverton, R.J.H., Holt, S.J., 1957. On the Dynamic of Exploited Fish Populations. Chapman & Hall.

Brehmer, P., Gerlotto, F., 2001. Comparative analysis of swimming behaviour in different populations of *Sardinella aurita*: influence of environment and exploitation; effect on catchability. ICES CM 2001/Q:04.

Chavez, F.P., Ryan, J., Lluch-Cota, S.E., Niquen, M., 2003. From anchovies to sardines and back: multidecadal change in the Pacific Ocean. Science 299, 217–221.

Cury, P., 1994. Obstinate nature: an ecology of individuals. Thoughts on reproductive behaviour and biodiversity. Can. J. Fish. Aquat. Sci. 51, 1664–1673.

Dagorn, L., Fréon, P., 1999. Tropical tuna associated with floating objects: a simulation study of the meeting point hypothesis. Can. J. Fish. Aquat. Sci. 56, 984–993.

Fernandes, P.G., Gerlotto, F., Holliday, D.V., Nakken, O., Simmonds, E.J., 2002. Acoustic application in fisheries science: the ICES contribution. ICES Mar. Sci. Symp. 215, 473–492.

Fox, W.W., 1970. An exponential surplus yield model for optimizing exploited fish populations. Trans. Am. Fish. Soc. 99, 80–88.

Fréon, P., Misund, O.A., 1998. Dynamics of Pelagic Fish Distribution and Behaviour—Effects on Fisheries and Stock Assessment. Blackwell Science, Oxford, UK.

Fréon, P., Dagorn, L., 2000. Review of fish associative behaviour: toward a generalisation of the meeting point hypothesis. Rev. Fish Biol. Fish. 10, 183–207.

Gauthiez, F., 1997. Spatial structures of demersal fish populations. Characterization, biometric developments and fisheries science. Thèse Dr Université Claude Bernard, Lyon, France.

Gulland, J.A., 1969. Manual of methods for fish stock assessment Pt. 1. Fish Population Analysis. FAO Manuals Fish. Sci. 4, FRS/M4.

Gutierrez, M., Ñiquen,, M., Teraldilla, S., Herrera, N., 2000. Las operaciones EUREKA: una aproximación de la abundancia de anchoveta en el periodo 1982–1999. Bol. IMARPE 19, 83–102.

MacLennan, D., Simmonds, J., 1992. Fisheries Acoustics. Chapman & Hall, London.

Massé, J., 1996. Acoustics observation in the Bay of Biscay: schooling, vertical distribution, species assemblages and behaviour. Scient. Mar. 60 (Suppl. 2), 227–234.

McQuinn, I.H., 1997. Metapopulations and the Atlantic herring. Rev. Fish Biol. Fish. 7, 297–329.

Myers, R.A., Worm, B., 2003. Rapid worldwide depletion of predatory fish communities. Nature 423, 280–283.

Pauly, D., Christensen, V., Guenette, S., Pitcher, T.J., Sumaila, U.R., Walters, C.J., Watson, R., Zeller, D., 2002. Towards sustainability in world fisheries. Nature 418, 689–695.

Pyanov, A.I., 1993. Fish learning in response to trawl fishing. In: Olsen, S., Wardle, C.S., Hollingworth, C.E. (Eds.), Fish Behaviour in Relation to Fishing Operations. ICES Mar. Sci. Symp., 196, pp. 12–16.

Schaefer, M.B., 1954. Some aspects of the dynamics of populations important to the management of the commercial marine fisheries. IATTC Bull 1, 26–56.

Soria, M., Gerlotto, F., Fréon, P., 1993. Study of learning capabilities of tropical clupeoids using an artificial stimulus. In: Olsen, S., Wardle, C.S., Hollingworth, C.E. (Eds.), Fish Behaviour in Relation to Fishing Operations. ICES Mar. Sci. Symp., 196, pp. 17–20.

Swain, D.P., Sinclair, A.F., 1994. Fish distribution and catchability: what is the appropriate measure of distribution? Can. J. Fish. Aquat. Sci. 51, 1046–1054.

Jacques Massé *
Ifremer, Laboratoire d'Écologie halieutique,
rue de l'Ile d'Yeu, BP 21105,
44311 Nantes cedex 3, France
E-mail address: Jacques.Masse@ifremer.fr

François Gerlotto
IRD, Roman Diaz 264, Santiago, Chile

* Corresponding author.

Available online at www.sciencedirect.com
SCIENCE DIRECT®
Aquat. Living Resour. 16 (2003) 549
Aquatic Living Resources
www.elsevier.com/locate/aquliv

Erratum☆

Acoustics in Fisheries and Aquatic Ecology. Part 2

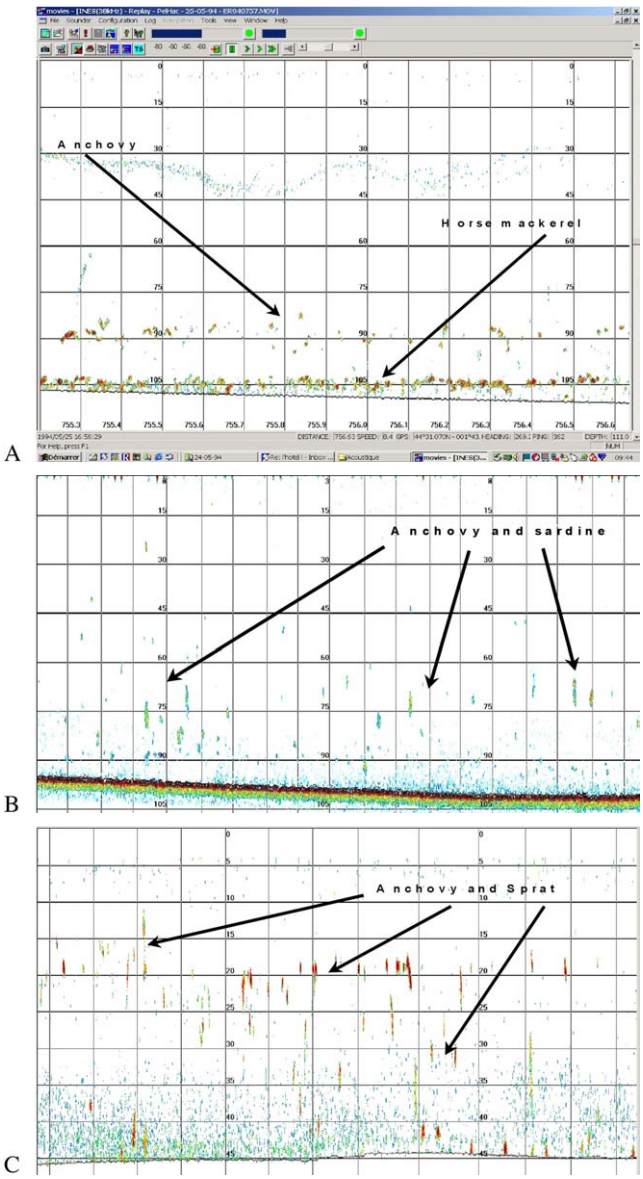

The Foreword to a special issue of Aquatic Living Resources, vol. 16, issue 3, "Acoustics in Fisheries and Aquatic Ecology. Part 2" on pages 107–112, was printed with its last set of figures in black and white due to a printing error. Theses figures should have been in color.

The correct figures to this article, "Foreword. Introducing nature in fisheries research: the use of underwater acoustics for an ecosystem approach of fish population" by J. Massé and F. Gerlotto, are printed below (Fig. 3).

Fig. 3. Echograms in the Bay of Biscay showing the assemblage of anchovy with another pelagic species (anchovy with horse mackerel, sardine, sprat).

☆ doi of original article 10.1016/S0990-7440(03)00058-5.

doi:10.1016/j.aquliv.2003.10.001

Available online at www.sciencedirect.com
SCIENCE DIRECT®
Aquatic Living Resources 16 (2003) 113–122
Aquatic Living Resources
www.elsevier.com/locate/aquliv

The three-dimensional morphology and internal structure of clupeid schools as observed using vertical scanning multibeam sonar

François Gerlotto [a,*], Jorge Paramo [b]

[a] *Institut de Recherches pour le Développement (IRD), Casilla 53390 Correo Central, Santiago-1, Chile*
[b] *Universidad de Concepcion, Casilla 160-C Concepcion, Chile*

Accepted 3 February 2003

Abstract

Fish schools are known to take a large number of different shapes and dimensions, in such a way that defining a school from its morphology is still an unanswered question. Nevertheless, some school typology and classification has been done successfully in different areas of the world using vertical echo sounding data. This implies that some morphological patterns may correspond to or reflect behavioural specificities. The objective of this paper is to take advantage of the 3D exhaustive observation capabilities of multibeam sonar to extract the morphological and internal characteristics of tropical clupeid schools. The main parameters measured are geometrical properties (overall dimensions, volume, surface, etc.) and relative distribution of densities inside the school (heterogeneity, existence of nuclei, etc.). The main results show that a school is usually formed of one or several nuclei of high density connected by less dense parts, including empty areas (vacuoles). The dimension of these sub-units is highly variable, but remains inside a diameter of 5-20 m. The reliability of these dimensions is evaluated, and some thoughts on the behavioural mechanisms constituting schools are presented.

Keywords: Fisheries acoustics; Fish school; Fish behaviour; 3D image; structure

1. Introduction

Pelagic fishes tend to gather into schools. These are innate structures for most of the Clupeidae, Engraulidae, Carangidae, and represent a major biological characteristic in the life of these species. Fishers take advantage of these aggregations of individuals to adapt their fishing effort, and several fishing gears have been designed specifically for exploiting fish schools. Nevertheless, even though the idea of a "school" is rather clearly understood, the knowledge of the structure of these features is weak, and attempts to provide a universal definition of a school, based on its morphology, have failed so far.

Fish schools are heterogeneous and variable structures. The heterogeneity was observed soon after the implementation of acoustic devices in fisheries research. One of the first images of the horizontal heterogeneity of a fish shoal has been drawn by Cushing (1977), using a scanning sonar with a 30° overall scanning angle. His results are descriptive and given in a single scale of presence/absence of fish, but the envelope of the fish distribution shows that the school morphology is complex and mostly amoeboid. Visual observations were more numerous, and gave some indications on the way individuals were behaving in a school. The inter-fish distance was often measured and the individual distribution within a school was modelled (Radakov, 1973). An "extreme" example was given by Breder (1976), who described a quasi-crystalline structure of the school, with each fish taking the position of an atom in a rhomboidal crystal. Such a regular distribution, noted through visual observation and at very short range (maximum 5 m) implies high densities within the school (Aoki and Inagaki, 1988) and is contradictory with the acoustic measures of fish school densities: Simmonds et al. (1992) have summarised the literature on the mean number of fish per cubic meter in schools for different species using different methods. The densities vary from 0.05 (20 cm herring) to 300 fish per m^3 (12 cm anchovy) for in situ studies, and up to 3000 fish per m^3 from modelling exercises. Although fish density has been found to depend on the species, the fish length, and the biological characteristics of the animals, a reasonable estimate would be in the 0.5-30 fish

* Corresponding author.
E-mail address: gerlotto@ird.fr (F. Gerlotto).

doi:10.1016/S0990-7440(03)00027-5

per m^3 range. A synthesis of these contradictory observations was given by Fréon et al. (1992), who described for the first time the global internal structure of a whole fish school in situ, observed by vertical echo sounding, visual observation (video camera) and aerial pictures. Their conclusions that at short distance fish remain almost always equidistant to one another were consistent with small scale visual and aquarium observations. However, on a global scale they observed that a fish school was a very heterogeneous 3D structure, with numerous empty sub-volumes that they named as vacuoles. Consequently, it was normal to obtain high fish densities per cubic meters when observing part of the school, or very weak densities when considering the whole structure.

Another characteristic was described by Misund (1993), as patchiness inside schools. The author observed "packing density structures" inside a school recorded by echo sounders, which were followed during several minutes. Inside these structures, the density was found similar to the densities measured with visual recording. He proposed the "moving mass hypothesis" for explaining the large variations in the packing density. This hypothesis is based on the individual fish dynamics and differences in speed and directions among individuals. It is worth noting that dense areas were recorded in the vertical (Fréon et al., 1992; Misund, 1993) as well as in the horizontal plan (Soria, 1994; Fréon et al., 1992; Axelsen et al., 2001), although only relative densities were given for the horizontal plan.

Another feature that has been studied is the external shape of the school. Since the beginning of fisheries acoustics, fishers were able to recognise species, with a rather acceptable precision, according to the shape of the school image on the echogram. Using this characteristic, two kinds of research were developed: one attempting to identify fish species (Rose and Leggett, 1988; Scalabrin, 1997); the other one focused on the variability of the school shapes (Petitgas and Lévenez, 1996; Gonzalez et al., 1998). Both approaches were successful, indicating that although the variability of the school shape is important, it is not completely random and depends on several characteristics, such as the species, the biology and behaviour conditions, and the global oceanographic conditions. A good synthesis on this "echo trace classification" is given by Reid (2000). All these studies were done using two kinds of acoustic devices: vertical echo sounder and horizontal omnidirectional multibeam sonar (MBS).

The vertical echo sounder presents a set of limitations for species classification/identification research, among which the most important are:

- Limited precision in image definition. A standard transducer typically has a 10° beam angle. This reduces dramatically the precision of the image with distance from the vessel. All the details of the internal structure and the external envelope are smoothed, and the external envelope is highly skewed by the location of the target inside the beam angle. Moreover, the horizontal dimensions of the school are biased and corrected (e.g. Johannesson and Losse, 1977; Diner, 2001).
- Limited biological value. The vertical echo sounder observes the most perturbed and noisy sector of the sea around the vessel. It only provides information on what has not avoided the vessel horizontally, and cannot discern whether the recorded structure corresponds to a natural behaviour of the fish or is strictly induced by its reactions to the vessel.

The horizontal MBS is much more accurate in observing and recording fish schools, as it is capable of observations at large horizontal distances from the vessel, and in two actual dimensions (independent of the vessel motion). This tool is particularly useful for observing the movements and dynamics of the schools (e.g. Diner and Massé, 1987). Nevertheless, the horizontal sonar is usually not applied for school shape analysis, because its definition is too low (i.e. beam angles are around 5-10°) and, as sound is emitted horizontally, school images at long distances can be biased or even hidden by the changes in sound direction due to the presence of a thermocline, for instance (e.g. Medwin and Clay, 1998). Some particularly narrow beam MBS was designed (Misund et al., 1995), which allowed for a very precise image of the fish distribution inside a school. Nevertheless, the third dimension was still lacking for an exhaustive view of a school structure.

This third (horizontal) dimension is obtained through the use of vertical MBS (Gerlotto et al., 1999; Mayer et al., 2002), which records a wide swath through successive pings along a vessel route. For the first time, questions regarding the dynamics of the school vs. the vessel were answered using this tool. Soria et al. (1996) showed that fish schools were avoiding horizontally, following a "double wave of avoidance". Bahri (2000) showed that the schools were presenting different lengths and widths depending on their location relative to the vessel, which she linked to the avoidance dynamics.

This paper explores the 3D structure and shape of fish schools using vertical MBS developed for fisheries acoustics.

2. Materials and methods

The acoustic device used in this study was developed in an European Project (AVITIS, FAIR CT96 1717) and presented by Gerlotto et al. (1999) and Fernandes et al. (1998). The system was a 455 kHz RESON model Seabat 6012 MBS with 60 beams of 1.5 × 15°, forming a 2D image on a 90° field, at a range setting up to a maximum of 100 m. The observation plan was vertical, normal to the vessel route, and observing from the surface to the vertical below the vessel (Fig. 1).

The digital data are recorded for each ping and stored. Once the complete school has been recorded, the data can be reconstructed into a 3D image of the structure using the software SBI Viewer (Lecornu et al., 1998). It calculates the morphological characteristics of the school, such as its over-

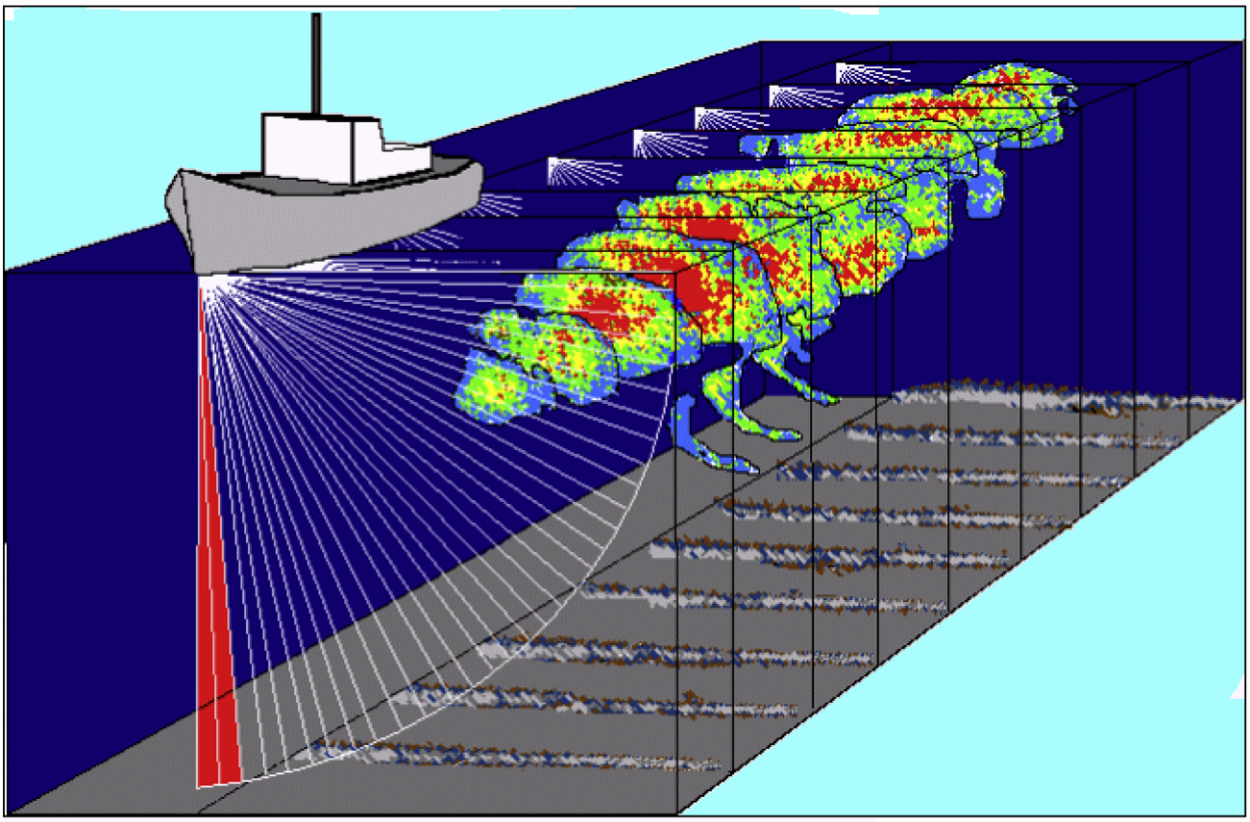

Fig. 1. Display of the MBS data in a vertical plan on the side of the vessel (from Fréon and Misund, 1999).

all dimension (length, width and height, which are the dimension of the rectangular box surrounding completely the school), its actual volume and surface, the number, surface and volume of holes inside the school, the school position in the water column with reference to the vessel and the relative density inside the school. The software also extracts all the voxels (defined as 3D volumetric pixels) inside the school and constructs a 4 column file, with the three spatial coordinates and the density value of each voxel. This allows for the calculation of 2D or 3D characteristics inside the school.

Some correction must be applied to the data, especially the length, using the classical correction related to the distance of the target (Johannesson and Losse, 1977). Simmonds et al. (1999) developed a calibration procedure for this MBS, which gives a beam angle of 22 × 1.5° for our sonar (instead of the nominal 15 × 1.5°), that we applied for correcting the length.

We must point out some potential sources of bias related to the data collection and processing methods. Data are collected during a survey, but the collection is not systematic, due to storage limitations. Therefore, the operator decides when a school has to be recorded. This may induce two biases: one on the location of schools, as it is easier to see and record a school in the centre of the screen than on the edges, and a bias in the actual dimensions of these schools, as small schools may be undersampled. When processing the data, some limitations due to the software may also affect the sampling, as the operator must have an implicit definition of a school, and applies particular thresholds. Finally, another point has to be taken into account when studying the linear dimensions: they represent the dimensions of a rectangular box surrounding the school. Therefore, when the school has a complex shape, these dimensions may not be completely realistic. For instance, in the case of a school with a shape in C: the length will be underestimated and the width largely overestimated.

The data were recorded during two acoustic surveys; Venezuela (survey VARGET 99/2) in March 1999, and Senegal (VARGET 99/1) in May 1999. These surveys were performed in order to measure the school behaviour. Data were collected during the day along transects aboard the R/V Antea, at a fixed speed of 8 knots. In tropical regions, the species assemblage is complex. For instance, in Venezuela we may observe up to 10 Clupeids, 15 Engraulids and 10 Carangids forming schools (less in Senegal: four Clupeids, one Engraulid, six Carangids), with no possibility to allocate with absolute precision each recorded school to a given species. Nevertheless, in the two areas the most abundant schooling fish is the Clupeid *Sardinella aurita*, which represents 60-80% of the total biomass in both countries (Gerlotto, 1993; Levenez, pers. comm.). Moreover, the recordings come from the part of the shelf where *S. aurita* is the most abundant, as proved by our own trawlings and the fisheries data. Hence, it is reasonable to assume that the majority of schools belong to *S. aurita*, and that the potential error in the species identification is probably less than 5% (which is the

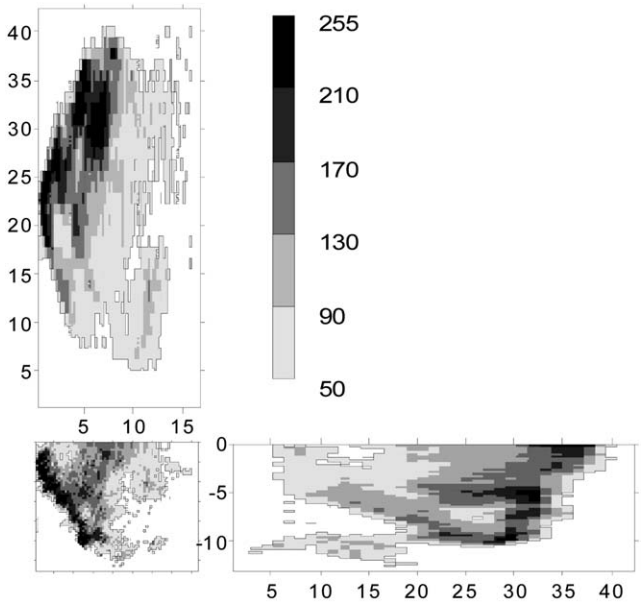

Fig. 2. The three images of the fish school structure in the three plans: above, horizontal plan; below left, vertical plan perpendicular to the vessel route; below right, vertical plan parallel to the vessel route. Densities represent a relative scale from 0 to 255, averaged on the dimension perpendicular to the plan. Same scale in m for the three dimensions (school # 770. Senegal).

proportion of the schooling biomass allocated to other pelagics).

Not all the schools can be processed by SBI Viewer. In some cases, the edges of the school were cut by the borders of the observed volume (e.g. for schools being observed vertically below the vessel), in other cases they are included in noisy volumes, and the discrimination between the school echoes and background noise is impossible. In a few cases, the structure of the school was extremely complex, the school belonging to a layer of schools with no clear borders, and no extraction of a single structure was possible. This reduced the field of our observations to well identified single schools.

The heterogeneity of fish distribution inside the schools was explored using geostatistics. For such measurements, we calculated a global horizontal section, by projecting each voxel on the horizontal plan to calculate the mean density for all the pixels of this horizontal image. The horizontal dimension was preferred to the vertical ones, as schools are usually more extended horizontally. An isotropic horizontal variogram was calculated for each school. In all the schools, dense patches are observed that allowed for extraction of information on the frequency and characteristics of these patches (that we called "nuclei"). The extraction of information was not always possible due to limitations of the software. We processed the information in two ways.

In the global analysis, the nucleus was defined as a single dense volume, with density superior to twice the "background density" of the school and linear dimensions greater than 1 m vertical and 3 m horizontal (these dimensions being decided after the results of geostatistical analysis). All the schools were mapped in 2D in the three plans (Fig. 2). Using these maps, we explored whether there were zero, one or several nuclei. No measurement of the nucleus dimension was performed.

In the second analysis, where additional processing was possible, we extracted the nucleus using the normal procedure for school extraction, but setting a higher threshold for the densities to be selected. For the extracted nucleus, we obtained the same morphological and density values as on the whole school.

3. Results

We extracted 427 schools, of which 359 were from Venezuela and 68 from Senegal. Among these 427 schools, 126 nuclei were extracted; a few of them belonging to the same school (Table 1).

Schools from Senegal and Venezuela are slightly different in shape. Curiously, even though the dimensions were different (i.e. the two groups differed in length, width, and surface, S_{sen} = 5326 m^2; S_{ven} = 3581 m^2; t = -2.07, $P < 0.007$), no significant difference was observed for height or volume (V_{sen} = 1576 m^3; V_{ven} = 1399 m^3; t = -0.62, $P < 0.53$).

It is also interesting to analyse the schools related to the distance from the vessel. Table 2 gives the mean values of the most important variables at intervals of 10 m from the vessel

Table 1
Mean values of the main morphological and density parameters of the schools and nuclei. Linear dimensions are given in m, surfaces in m^2, volumes in m^3. The density is the mean value of echo energy in a relative scale of 0-255. As the settings remained fixed, these relative values are comparable for all the schools. The fractal dimension is the ratio surface/volume. (*) The software SBI Viewer cannot count more than 1024 holes inside a single school (a hole is defined by an empty voxel). Only seven schools in our database have equal or more than 1024 holes

Parameter	School (n = 427)				Nucleus (n = 126)			
	All	Venezuela	Senegal	P-value	All	Venezuela	Senegal	P-value
Length	28.9	33.1	39.9	0.111	15.2	15.1	15.3	0.891
Width	17.4	16.9	20.1	0.026	8.4	8.3	8.6	0.661
Height	11.3	11.2	11.7	0.834	5.6	5.6	5.7	0.928
Volume	1427.0	1398.8	1576.0	0.239	203.8	203.4	205.8	0.911
Surface	3859.5	3581.8	5325.6	0.027	844.3	802.8	1029.1	0.720
Nb of holes (*)	125.4	120.1	153.4	0.051	23.0	20.9	32.4	0.821
Surface of holes	121.3	115.2	153.7	0.716	19.3	17.7	26.4	0.810
Volume of holes	13.8	13.0	17.6	0.035	2.1	1.9	2.8	0.947
Density	92.2	94.8	78.5	0.008	131.3	132.5	126.0	0.498

Table 2
Mean values of the morphological parameters of the schools depending on their distance to the vessel. Nb of schools = 427. All dimensions in m, surfaces in m^2, volumes in m^3. Holes in number of voxels. Density in relative units. Nuclei: number of nuclei per school

Parameter	Distance classes (m)								
	0/10	10/20	20/30	30/40	40/50	50/60	>60	*F*-value	*P*-value
Number of observations	92	101	60	48	58	43	25	–	–
Length	32.7	40.1	28.5	20.4	21.5	21.3	21	18.394	0.000
With	14.3	21.3	18.8	15.9	16.3	16.5	16.7	0.277	0.599
Height	9.8	13.1	11.3	10.1	11	12.1	11.8	1.119	0.291
Volume	690	1648.9	1610.2	1145.8	1501.5	2203.3	1980.6	30.314	0.000
Surface	2329.2	4750.1	4743.3	2863.5	4047.1	4648.3	4250.9	13.831	0.000
Holes	91.1	172.4	161.6	75.2	121.2	118.2	104.2	0.697	0.404
Density	107.61	98.73	87.95	73.93	77.03	88.47	91.91	29.719	0.000
Nuclei	0.96	1.16	0.77	0.67	0.66	0.53	0.41	12.650	0.000

(0-10, 10-20, etc.). We can see that the distance to the vessel may have an impact on the school shape.

3.1. General school morphology

We studied two points in this field: the main characteristics of the overall structure of the school and its anisotropy in length and width. *t*-Tests between length vs. width, length vs. height and width vs. height were calculated (Table 3).

As far as the overall structure is concerned, the question is whether a school can present a permanent regular shape. The first method was to compare the values of length, width, volume and surface. The linear dimensions cannot be compared easily with the volume and surface, as they are not calculated in the same way. Table 4 shows that most of the morphological parameters are correlated. The only parameter with no or weak correlation with the others is the density.

One important result is that there is a significant relationship between length and width (Tables 1 and 2). The width on an average represents 60.5% of the length (test $t = 12.3$, $P < 0.01$). If we consider the schools according to their distance from the vessel separately, we can calculate that the width varies from 47.3% (0-10 m) to 79.5% (>60 m) of the length. Although this is not the objective of the paper, we may note that this result is consistent with the avoidance scheme described by Soria et al. (this volume).

The second way to study the school shape is to consider the fractal dimension, which represents a "roughness factor". It is calculated by the ratio surface/volume (S/V). The mean roughness factor on the school studies has no real meaning, as the ratio S/V is inversely proportional to the radius R of the school. One other way to evaluate the roughness characteristics of the school is to compare the actual S/V values to a theoretical fractal dimension that would be obtained for regular shapes. We calculated two theoretical S/V ratios for two types of shapes: spherical and cylindrical. In the first case, we assumed that the volume of the school was the volume of a sphere and calculated the surface of this sphere, then we calculated the S/V on these values. We did the same with the cylinder, using the actual volume and height of the school to calculate the surface. Then we compared the three fractal

Table 3
Test *t* on relationships between length and width, length and height, width and height of the schools (d.f. = degrees of freedom). All the results below show a significant difference with $P < 0.005$

Variables	Mean	Standard error	*t*	d.f.
Length	28.97	24.12	12.3	426
Width	17.34	9.91		
Length	28.97	24.12	17.5	426
Height	11.30	6.67		
Width	17.34	9.91	20.5	426
Height	11.30	6.67		

Table 4
Correlation matrix of the morphological parameters of the 427 schools. Significant correlation at $P < 0.05$ are in italics

	Width	Height	Volume	Surface	Fractal	Hole	Density
Length	*0.633*	*0.596*	*0.669*	*0.706*	–0.0630	*0.594*	*0.135*
Width	1.000	*0.793*	*0.650*	*0.751*	*–0.1153*	*0.678*	0.016
Height		1.000	*0.628*	*0.664*	*–0.1209*	*0.616*	0.059
Volume			1.000	*0.878*	*–0.2779*	*0.740*	0.091
Surface				1.000	–0.0872	*0.861*	0.018
Fractal					1.0000	–0.010	*–0.219*
Hole						1.000	*0.128*

Table 5
Test *t* on roughness and fractal dimensions. *R*: roughness *S*/*V*; Fs = fractal dimension for a sphere; Fc = fractal dimension for a cylinder

	Mean	Standard deviation	*N*	Diff.	Diff. standard deviation	*t*	d.f.	P
R	3.15	1.057						
Fs	0.58	0.257	427	2.564	0.984	53.9	426	0.000000
R	3.15	1.057						
Fc	2.45	0.209	427	0.699	0.966	15.0	426	0.000000

dimensions, the actual roughness (*R*), and the ratios *S*/*V* for the cylinder (Fc) and the sphere (Fs). A *t*-test comparing the roughness and the fractal dimension of the sphere and cylinder, shows that they are significantly different at $P < 0.01$ (Table 5).

From these results, we can extract the following observation: a fish school has an irregular morphology, mostly amoeboid, which cannot be assimilated to any regular volume such as a cylinder or a sphere. Nevertheless, its morphology obeys some rules, and some constants in the shape can be recognised. The most important is the strong anisotropy between length, width, and height as already observed by several authors (Soria et al., 1996; Bahri, 2000).

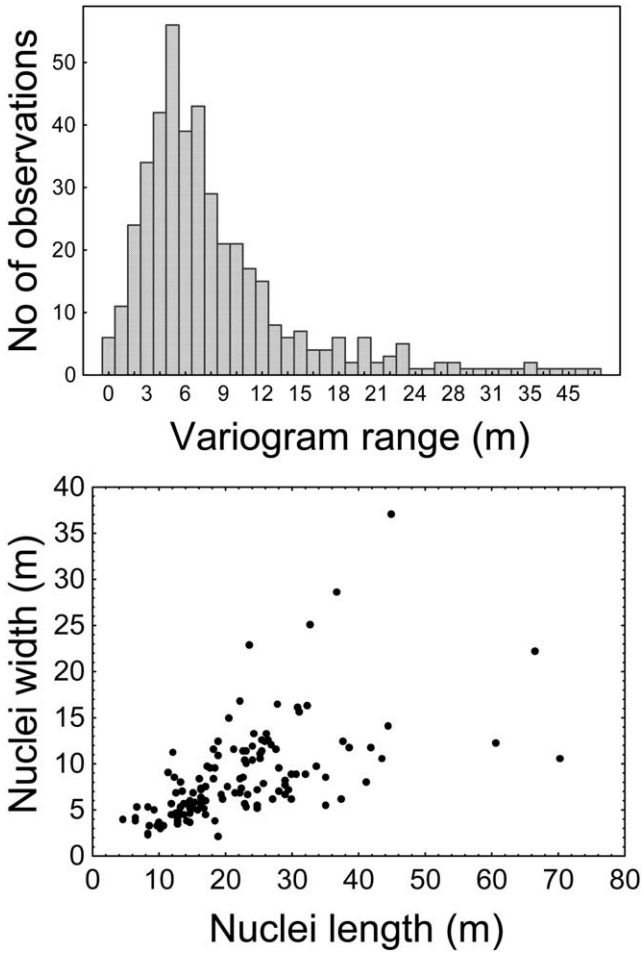

Fig. 3. Left: histogram of variogram ranges for the 427 schools; right: relations between length and width for the 126 extracted school nuclei.

3.2. Vacuole and nucleus morphology (Table 6)

3.2.1. Vacuoles

The vacuole information provided by SBI Viewer is limited to the number, global volume and global surface of empty voxels inside the extracted school. SBI Viewer cannot count more than 1024 "holes", which was the case for seven schools in our data base. It was also difficult to assimilate these holes to actual vacuoles as they did not have the same meaning. The holes were small empty spaces with no clear biological meaning, and more related to threshold and heterogeneity features. A single hole measures 0.1 m^3, which is much smaller than that observed by visual recordings (Fréon et al., 1992).

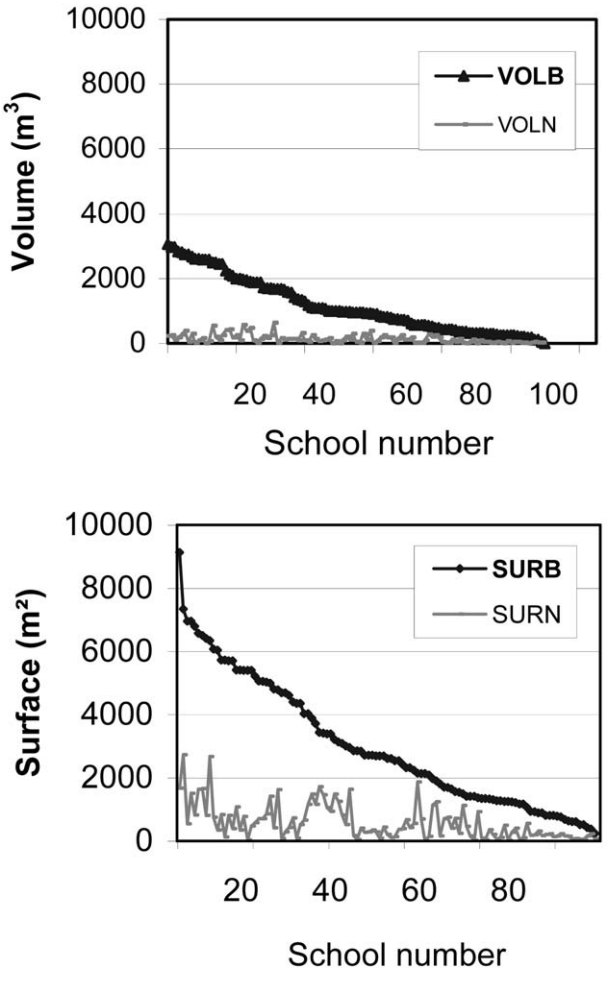

Fig. 4. Volume (above) and surface (below) of nuclei (N) for different values of surface and volume of schools (B). The 15 biggest schools have been removed to make the figure clearer.

Table 6
t-Test matrix on the main characteristics of schools, holes and nuclei. All the *t* tests show significant differences between the variables at $P < 0.001$ (except two pairs, Hon-Ln and Hos-Dn, in italics which are likely artificial similarities). The measurements on holes are done on the whole set of schools (427 individuals); the measurements on nuclei are done on the nuclei extracted in 126 schools

	Ws	Hs	Vs	Ss	Rs	Hos	Ds	Ln	Wn	Hn	Vn	Sn	Rn	Hon	Dn
Ls	14.4	17.4	–8.9	–8.8	19.9	–4.6	–12	14.2	18.4	19.9	–7	–7.4	19.1	3.9	–23.5
Ws	0	14.1	–9	–8.8	22	–5.7	–25.3	–3.2	17.2	21.8	–7.8	–7.6	19.4	–1.3	–35.1
Hs		0	–9	–8.8	16.3	–6	–29.9	–10.8	6.7	13.7	–8.1	–7.6	13.3	–2.7	–39.7
Vs			0	–7.9	9	9.2	8.6	9	9	9	8.6	6.1	9	9.1	8.4
Ss				0	8.8	8.9	8.7	8.8	8.8	8.8	8.7	8.5	8.8	8.9	8.6
Rs					0	–6.3	–34.7	–18.9	–12.8	–9.7	–8.4	–7.7	–17	–4.4	–42.8
Hos						0	2.3	5.5	6.1	6.2	–3.7	–7.4	6.3	6.2	0
Ds							0	24.1	32.2	33.3	–5.1	–7	34	10.6	–19.8
Ln								0	16.2	19.1	–7.8	–7.6	17	–0.8	–35.7
Wn									0	10	–8.2	–7.7	8.8	–3.5	–40.9
Hn										0	–8.3	–7.7	3.9	–4	–42.4
Vn											0	–7.3	8.3	8.9	3.2
Sn												0	7.7	7.8	6.6
Rn													0	–4.1	–42.5
Hon														0	–18

W, weight; H, height; V, volume; S, surface; R, roughness; Ho, hole number; D, density; L, length; s, school, n, nuclei.

3.2.2. Nuclei

The first analysis was to measure the existence of a non-random patchiness inside the schools. For this purpose, we measured an omnidirectional (horizontal) variogram on all of the 427 schools. On all of them, a bounded variogram was calculated, with a nugget presenting in average 66% of the sill and a mean range of 9.3 m (Fig. 3) indicating a patchy school distribution. Based on our definition of a nucleus, as a structure of more than 1 m vertical × 3 m horizontal dimensions, 126 structures were extracted and the global characteristics of the nuclei are presented in Table 6. The overall dimensions of a nucleus are on an average, 12.6 m long, 8.7 m wide, 5.7 m height. The mean elongation (ratio width/length) is 0.7. We compared the main parameters of the nuclei, which showed a series of significant correlations, indicating that these structures were not random.

The relationships between the nuclei and the schools have been considered by comparing the main morphological characteristics, specially the surface and volume (Fig. 4). When plotting a nucleus dimension with the similar dimension of its school, several significant relationships appear (e.g. surface of the nucleus vs. surface of the school: $r = 0.78$, $N = 126$, $P < 0.05$). Nevertheless, these relationships are mostly artificial and likely due to two facts: (1) a nucleus cannot be bigger than a school, (2) the variability of nucleus dimension increases when the dimensions of the schools increase. This is clear when we sorted the school dimension (surface or volume) from the smallest to the biggest, and plotted the corresponding values of the nuclei (Fig. 4). The relationship was tested using two methods. After sorting the data according to the school surface, we cut the data base into five classes (1-5, from very small to very large schools) of 25 data (26 for class 5), then compared the surface means between the schools and the nuclei for these five classes. The result is given on the Fig. 5. We did the same with the volume and obtained a similar result.

This figure shows several phenomena.

- By construction there are significant differences in the mean surface of schools in the five classes.
- The classes 1 and 5 of nuclei are significantly different from the three others and between them. This is due to the two following facts that we described above: (1) the

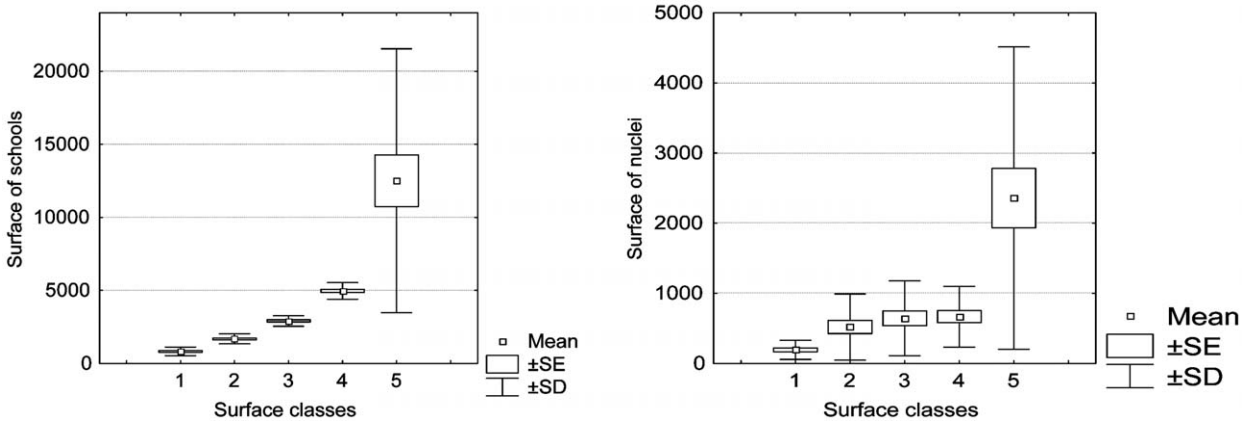

Fig. 5. Box-plot of the mean surface of schools and nuclei for five surface classes.

dimension of the nucleus is limited by the dimension of the school; (2) the class 5 is made of very large schools, most of them with several nuclei, and may represent a particular case that will be discussed below.

- The three other classes present no significant difference in the mean ($P < 0.35$).

A second test was to calculate the Pearson's correlation coefficient between the surfaces of schools and nuclei, and between the volumes of schools and nuclei for the 75 schools included in these three central classes, where the effect of the two above-mentioned artificial relationships are unlikely to bias the results. In this data set, the schools varied between 1300 and 5700 m^2, 260 and 3000 m^3. The correlations were, respectively, $r = 0.19$ for the surfaces and $r = 0.22$ for the volumes, showing no significant relationships ($P < 0.05$) between the corresponding dimensions in schools and nuclei for this set of data.

Therefore, we can conclude that there is no actual correlation between the surface and volume of the school and the surface and volume of its nuclei. Once the school is large enough, the nuclei maintain a relatively constant shape and dimension, with some increasing variability when the school is very large.

4. Discussion

Since the early 1990s, the importance of fish school behaviour and structure has been recognised as critical by fisheries acousticians (Anonymous, 1993), for several reasons, such as predation avoidance, physiologic facilitation, feeding, mating, etc. (Parrish and Turchin, 1997; Pitcher and Parrish, 1993), and effects of human pressure, which takes advantage of the schooling behaviour of the fish to increase the catch (Fréon and Misund, 1999). Until now, most of the works on fish structure and organisation inside a school have been performed at two scales:

- An individual scale (Radakov, 1973; Breder, 1976; Partridge et al., 1983; Pitcher and Parrish, 1993, etc.), with good results on the understanding of the collective behaviour inside a school, and the mechanisms that permit to maintain cohesion within the group. Successful individual-based models on fish schooling have been published at this scale (Huth and Wissel, 1993; Vabø and Nøttestad, 1997; Couzin et al., 2002).
- A global scale (Reid, 2000), where the whole structure of the school is studied and considered as an individual. At this level, successful results have been obtained on the possibility to identify a species using the school shape (Rose and Leggett, 1988; Scalabrin, 1997).

Although some attempts were made to model the school structure at an intermediate "collective" scale (Mackinson, 2000), the results that we present here are likely the first exhaustive observation on large schools in situ allowing for the analysis of their collective mechanisms. From these results, we may draw two main hypotheses.

The first one is that our observations are consistent with those at individual and global scales. We confirmed the existence of strong anisotropies between the three dimensions of the schools that was pointed out by numerous authors (e.g. Fréon and Misund, 1999). For instance, schools are much more extended in the horizontal dimension (L) than in the vertical one (h), and the overall height represents 39% of the length and 65% of the width in our data base. Nevertheless variations in these relationships may occur. We found a rather different ratio L/h than Oshihimo (1996) on anchovy, for instance, as the Sardinella schools have an $L/h = 2.6$, compared with the $L/h = 5$ calculated by this author. This indicates that although the horizontal dimensions are always larger than the height, they vary according to the species. But more likely, this anisotropy is linked with the horizontal dimensions of the schools: the Sardinella schools are rather small schools (mean diameter 23 m in our data set), while some schools studied in the literature are much wider (between 100 and 1000 m). The height cannot increase proportionally to the diameter, for biological, hydrological and geographical reasons. This shows that the differences are quantitative and adaptive to the local condition of the ecosystem. For instance, there is a neat effect of the distance to the vessel, which indicates that the schools we observed were under a dynamic process (avoidance). Concerning the effect of the distance, our results must be considered as preliminary, as the data base is small, but they are not contradictory with those of Soria et al. (1996): schools change their dimensions according to the distance from the vessel. Fig. 6 shows the values of length and width in relation to the distance for the whole data set.

These results are not in opposition with the conclusion that, although they have no regular morphology, schools are consistent structures that maintain some permanent feature and shape. From this observation, we may draw a first hypothesis: most of the small pelagic species develop similar mechanisms to maintain their cohesion inside a social structure and these mechanisms are the base of the school. Therefore, the results that we present on *S. aurita* are applicable to most of the Clupeids and other pelagic families.

The second kind of result is that schools are heterogeneous in their internal structure and that this heterogeneity is the consequence of an organisation. This observation leads to different conclusions than Parrish et al. (1997) who consider that schools are defined, among five criteria, by the fact that

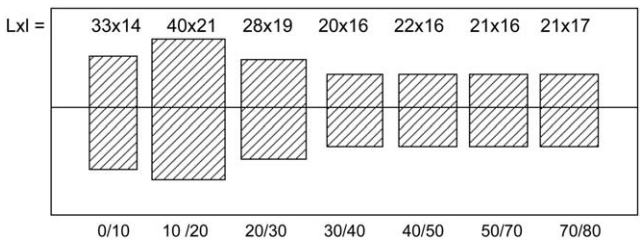

Fig. 6. Diagram of the relations length/width (Lxl. in m) for different classes of distance to the vessel (in m). This diagram is calculated on the whole data base (427 schools).

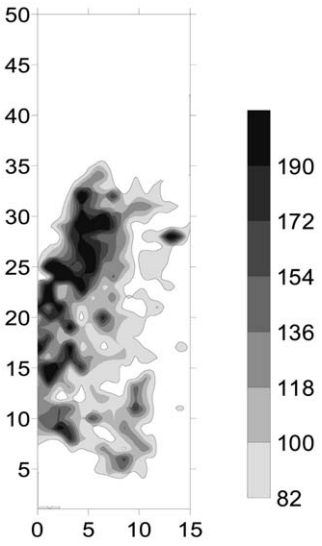

Fig. 7. Horizontal view of the distribution of mean density of fish in school # 770 (see Fig. 2). A nucleus is identified on the upper left part of the diagram. Small dense aggregates can be observed in the low density area (down right). Holes or vacuoles (mean density lower than 50) can be observed as well. Density in relative units on a scale 0-255. Dimensions in m. The density is calculated as the mean of the density on the vertical column below the point drawn on the figure. The threshold and the upper limit of the school densities are not those used for the extraction of the school and nucleus and are defined for the better visibility of the school heterogeneity.

"Many types of animal congregations have fairly uniform densities". Actually, this criterion is relevant for small groups of fish (even inside a larger school) and for small schools, especially when they are moving fast (Soria et al., 1996), but is no more valid for large concentrations of fish. The hypothesis that we propose to explain this apparent contradiction between permanent cohesion and global heterogeneity is the following. Fish tend to maintain a cohesive structure, which is ruled by the inter-individual distance, as observed by numerous authors. When the inter-individual distance is maintained, the school presents a high density. Inside these high density volumes, the fish must present a cohesive and polarised behaviour, otherwise the structure itself collapses. The mechanism that allows for maintaining this structure although the volume of the school is permanently changing, is the construction of vacuoles, which allow for the increase of the global volume of the school, with a local high permanent density of fish (Fréon et al., 1992; Soria, 1994). But such cohesive behaviour implies that the communications of information and decision on changes in the direction of the movement are quasi-instantaneous. Some of these mechanisms, such as the "wave of agitation" (Radakov, 1973), are well known. When the dimensions of the school increase, the quasi-instantaneity in the reactions is not possible anymore. Therefore, the dense structure is not cohesive above certain dimensions, and it must split. We believe that the nucleus represents the compromise between the need to maintain cohesive inter-fish distance and the delays in the transmission of dynamic instructions: for dimensions above 15-20 m, the nucleus cannot maintain its cohesion. This leads a part of the fish to stay in the "low density" volume, where either they tend to gather a nucleus or to build one. In fact, we may find numerous "pre-nucleus' structures, i.e. dense small patches of fish, inside the "low density" volume (e.g.Fig. 7).

In the case of very large schools (or when two schools are merging), two or several large nuclei can merge for a short period, due to the natural attraction of fish to any dense structure. But these "macro-structures" are not able to maintain their cohesion along a large period. This explains why the 10% larger ranges are above 18 m in our data set.

One interesting conclusion that can be drawn from these results is that the idea of a self-organisation of fish inside schools is confirmed: nuclei and vacuoles are emerging structures arising from elementary reaction of individuals (Soria, 1997). The combination of individual attraction, polarisation, synchronous reactions and delay of information transmission between the individuals implies the existence of dense nuclei and correlated empty vacuoles in a large aggregation of fish. This is what we observed in our 3D exhaustive observation of the internal structure of *S. aurita*.

Acknowledgements

This work is part of the Magister thesis of J. Paramo, University of Concepcion, Chile. The authors are grateful to an anonymous referee for the important remarks, which allowed for improving the statistical calculations, and for the edition of the text.

References

Anonymous, 1993. Foreword: the spatial organization of aquatic populations as observed using hydroacoustic methods. Aquat. Living Resour 6, 171–174.

Aoki, I., Inagaki, T., 1988. Photographic observations on the behaviour of Japanese anchovy *Engraulis japonica* at night in the sea. Mar. Ecol. Prog. Ser. 43, 213–221.

Axelsen, B.E., Anker-Nilssen, T., Fossum, P., Kvamme, C., Nøttestad, L., 2001. Pretty patterns but a simple strategy: predator-prey interactions between juvenile herring and Atlantic puffins observed with multibeam sonar. Can. J. Zool., 1586–1596.

Bahri, T., 2000. Relation entre des variables environnementales et la distribution et structure de la biomasse de poissons pélagiques côtiers en Méditerranée. Thèse Doct. Univ., Paris.

Breder Jr., C.M., 1976. Fish schools as operational structures. Fish. Bull. 74, 471–502.

Couzin, I.D., Krause, J., James, R., Ruxton, G.D., Franks, N.R., 2002. Collective memory and spatial sorting in animal groups. J. Theor. Biol. 218, 1–11.

Cushing, D.H., 1977. Observations on fish shoals with the ARL scanner. Rapp. P.-v. Réun. Cons. Int. Explor. Mer 170, 15–20.

Diner, N., 2001. Correction on school geometry and density: approach based on acoustic image simulation. Aquat. Living Resour. 14, 211–222.

Diner, N., Massé, J., 1987. Fish School Behaviour during Echo Survey Observed by Acoustic Devices International Symposium on Fisheries Acoustics, 1987 Seattle.

Fernandes, P.G., Gerlotto, F., Soria, M., Simmonds, E.J., 1998. Into the next dimension: three-dimensional acoustic observations of fish school aggregations ICES C.M 1998/J:33.

Fréon, P., Gerlotto, F., Soria, M., 1992. Changes in school structure according to external stimuli: description and influence on acoustic assessment. Fish. Res. 15, 45–66.

Fréon, P., Misund, O.A., 1999. Fishing News Books. Blackwell Science Dynamics of Pelagic Fish Distribution and Behaviour: Effects on Fisheries and Stock Assessment.

Gerlotto, F., 1993. Méthodologie d'observation et d'évaluation par hydroacoustique des stocks tropicaux de poissons pélagiques côtiers: impact du comportement et de la distribution spatiale. Thèse Doctorat Univ. Bretagne Occidentale, Brest.

Gerlotto, F., Soria, M., Fréon, P., 1999. From two dimensions to three: the use of multibeam sonar for a new approach in fisheries acoustics. Can. J. Fish. Aquat. Sci. 56, 6–12.

Gonzalez, L., Gerlotto, F., Cardenas, J.J., 1998. Pelagic fish populations in Eastern Venezuela: impact of the environmental characteristics on the morphology, aggregation and spatio-temporal distribution of *Sardinella aurita* schools ICES ASC.

Huth, A., Wissel, C., 1993. Analysis of the behavior and the structure of fish schools by means of computer simulation. J. Comments Theor. Biol. 3, 169–201.

Johannesson, K.A., Losse, G.F., 1977. Methodology of acoustic estimations of fish abundance in some UNDP/FAO resource survey projects. Rapp. P.-v. Réun Cons. Int. Explor. Mer 170, 296–318.

Lecornu, L., Burdin, V., Scalabrin, C., Hamitouche-Djabou, C., 1998. Fish school analysis from multibeam sonar image processing. Oceans 98, Engineering for sustainable use of the oceans: Conference Proceedings September 1998, Nice, vol. 1. IEEE Service Center, Piscataway, NJ, USA. vol: 1, pp. 587–591.

Mackinson, S., 2000. A adaptive fussy expert system for predicting structure, dynamics and distribution of herring shoals. Ecol. Model. 126, 155–178.

Mayer, L., Li, Y., Melvin, G., 2002. 3D visualisation for pelagic fisheries research and assessment. ICES J. Mar. Sci. 59, 216–225.

Medwin, H., Clay, C.S., 1998. Fundamentals of Acoustical Oceanography. Academic Press, San Diego, USA.

Misund, O.A., 1993. Dynamics of moving masses: variability in packing density, shape, and size among herring, sprat, and saithe schools. ICES J. Mar. Sci. 50, 145–160.

Misund, O.A., Aglen, A., Froenaes, E., 1995. Mapping the shape, size and density of fish schools by echo integration and a high-resolution sonar. ICES J. Mar. Sci. 52, 11–20.

Oshihimo, S., 1996. Acoustic estimation of biomass and school character of anchovy *Engraulis japonicus* in the East China Sea and the Yellow Sea. Fish. Sci. 62, 344–349.

Parrish, J.K., Hamner, W.M., Prewitt, C.T., 1997. Introduction—from individuals to aggregation: unifying properties, global framework, and the holy grails of congregation. In: Parrish, J.K., Hamner, W.M (Eds.), Animal Groups in Three Dimensions. Cambridge University Press, pp. 1–13.

Parrish, J.K., Turchin, P., 1997. Individual decisions, traffic rules, and emergent patterns in schooling fish. In: Parrish, J.K., Hamner, W.M (Eds.), Animal Groups in Three Dimensions. Cambridge University Press, pp. 126–142.

Partridge, B.L., Pitcher, T.J., Cullen, J.M., Wilson, J., 1983. The three-dimensional structure of fish schools. Behav. Ecol. Sociobiol. 6, 277–288.

Petitgas, P., Lévenez, J.J., 1996. Spatial organization of pelagic fish: echogram structure, spatio-temporal condition, and biomass in Senegalese waters. ICES J. Mar. Sci. 53, 147–153.

Pitcher, T.J., Parrish, J.K., 1993. Functions of schooling behaviour in treleosts. In: Pitcher, T.J (Ed.), Behavior of Teleosts Fish. Chapman & Hall, London, pp. 363–439.

Radakov, D.V., 1973. Schooling in the Ecology of Fish. Wiley, New York (USA), Jerusalem (ISR) (Israel Program for Scientific Translations).

Reid, D.G., 2000. Cooperative Report on Echo trace classification. ICES Coop. Res. Rep., 238.

Rose, G.A., Leggett, W.C., 1988. Hydroacoustic signal classification of fish schools by species. Can. J. Fish. Aquat. Sci. 45, 597–604.

Scalabrin, C., 1997. Identification acoustique des espèces pélagiques à partir d' attributs discriminants des bancs de poissons monospécifiques. Thèse dr. Univ. Bretagne Occidentale, Brest.

Simmonds, E.J., Gerlotto, F., Fernandes, P., MacLennan, D., 1999. Observation and extraction of three-dimensional information on fish schools. J. Acoust. Soc. Am. 105, 996.

Simmonds, E., Williamson, N.J, Gerlotto, F., Aglen, A., 1992. Acoustic survey design and analysis procedures: a comprehensive review of current practice. ICES Coop. Res. Rep., 187.

Soria, M., 1994. Structure et stabilité des bancs et agrégations de poissons pélagiques côtiers tropicaux: application halieutique. Thèse Doct., Univ., Rennes I.

Soria, M., 1997. Le banc de poissons: expression d'une motivation sociale ou comportement collectif d'un groupe auto-organisé? In: Theraulaz, G., Spitz, F (Eds.), Auto-organisation et comportement. Hermes, Paris, pp. 141–155.

Soria, M., Freon, P., Gerlotto, F., 1996. Analysis of vessel influence on spatial behaviour of fish schools using a multi-beam sonar and consequences for biomass estimates by echo-sounder. ICES J. Mar. Sci. 53, 453–458.

Vabø, R., Nøttestad, L., 1997. An individual based model of fish school reactions: prediction of antipredator behaviour as observed in nature. Fish. Oceanogr. 6, 155–171.

Available online at www.sciencedirect.com
SCIENCE DIRECT®
Aquatic Living Resources 16 (2003) 123–129
Aquatic Living Resources
www.elsevier.com/locate/aquliv

A conditional simulation of acoustic survey data: advantages and potential pitfalls

Alessandro Gimona [a,b,*], Paul G. Fernandes [b]

[a] *Macaulay Institute, Craigiebuckler, Aberdeen AB15 8QH, UK*
[b] *Marine Laboratory Aberdeen, P.O. Box 101, Victoria Road, Aberdeen AB11 9DB, UK*

Accepted 12 February 2003

Abstract

Standard geostatistical techniques provide effective methods for estimating the global abundance and precision of a variable of interest, for mapping its spatial distribution and for describing its spatial structure. In the case of acoustic survey data, however, obtaining a measure of precision of the global abundance estimate is confounded by the combination of variances from the interpolation of both the acoustic data and the concomitant fish length data. Even if the global estimation variance could be calculated, the distribution of the estimation error is not known and so confidence intervals cannot be determined. Furthermore, kriged distribution maps, in minimising the estimation variance, tend to smooth out local details of the attribute's spatial variation: small values can be overestimated and larger ones underestimated, such that the kriged map is smoother than reality. This can lead to serious shortcomings when trying to detect patterns of extreme attribute values, such as the high densities encountered in some fish schools. Stochastic geostatistical simulations, conditional on sampled locations, provide a solution to many of these problems. They can deliver a measure of uncertainty for local (density) estimates, a confidence interval estimation for the global mean density, and finally, reproduce global statistics, such as the sample histogram and variogram. In so doing, they also provide maps of the attribute, which are spatially realistic because the variogram is reproduced; these are generated as a number of equiprobable realisations. In the present paper, we apply these techniques to acoustic data from an acoustic survey of North Sea herring. Sequential gaussian simulations are used to generate realisations for fish length and values of the nautical area scattering coefficient. These are then combined to produce realisations of herring density. The combined set of multiple realisations is then used to provide confidence intervals for the global abundance estimate: 95% of the herring abundance estimates are between 5677 and 6271 millions of individuals. Although the method presented in this paper contributes to the assessment of total uncertainty for acoustic surveys, the approach may have suffered from bias due to the use of off-the-shelf data transformation algorithms on fisheries acoustic data, which are often very positively skewed. We discuss this limitation and propose corrections for future work.

Keywords: Geostatistics; Simulation; Fish density; Acoustic survey

1. Introduction

Fishery independent methods, such as research vessel surveys, are becoming increasingly important to determine the abundance and distribution of fish for effective stock assessment (NRC, 1998). Although these methods are not prone to the bias caused by illicit fishing activities that plague traditional fishery dependent methods, they are nonetheless subject to other uncertainties (such as sampling error). The widespread application of the precautionary approach (FAO, 1995) requires uncertainties relating to the size of stocks to be taken into account in its implementation. As a result, a variety of uncertainty estimates are now included in various assessment models (Patterson et al., 2001), but rarely are the variance estimates of the indices of abundance from research vessel surveys included.

There are various possible reasons for this omission. Overall, it is perhaps because uncertainty assessment is still a young science, and the techniques are yet to be established. There are very few examples where overall survey variability has been taken into account (Rose et al., 2000 give an example based on acoustic surveys). In most cases, measures of uncertainty have been based purely on sampling error, and even then, a wide variety of techniques have been proposed:

* Corresponding author.
E-mail addresses: a.gimona@macaulay.ac.uk (A. Gimona), fernandespg@marlab.ac.uk (A. Gimona).

doi:10.1016/S0990-7440(03)00028-7

Simmonds et al. (1992) have described a number for acoustic surveys; estimates of trawl survey variance have been calculated by Smith (1990), Pennington (1996), Stefansson (1996) and Smith (1997). Borchers et al. (1997) have described methods for egg surveys.

All survey data are similar in that they consist of estimates (samples) of a quantity (indicative of, or proportional to fish density) at a location (point). What usually differs is the placement of the sampling points in space (survey design) and this has implications for the analysis procedure. There are still disputes in fisheries science between advocates of systematic and random survey designs. In the presence of spatial gradients, it is widely acknowledged that a systematic design delivers a more precise estimate of (mean) abundance than a random design (Simmonds and Fryer, 1996). For this and other reasons, Hilborn and Walters (1992) have concluded that systematic grid sampling was better, despite their concession that the variance (precision) of the sample mean could not be assessed correctly using traditional formulas. This has long been the contention among advocates of random sampling design that has led various compromised schemes to be adopted to determine the variance (e.g. Jolly and Hampton, 1990). Geostatistics, however, has techniques that allow for the determination of sampling variance in a systematic design (Matheron, 1989).

In the case of acoustic survey data, the variances obtained from geostatistics refer to the sampling error of the acoustic data alone. To convert this to fish density, it is necessary to know the size of the fish (MacLennan and Simmonds, 1992), and so samples of fish length are required: these have their own inherent variability. Although Rivoirard et al. (2000) have described an analysis, which takes into account both of these quantities to produce an estimate of abundance, they could not estimate the combined variance. They have suggested that a method based on simulations would be needed to take into account both the uncertainties of the acoustic density and the biological parameters (length).

Geostatistical simulation is an approach to modelling that attempts to reproduce the range of values (fish densities) present in the data, as well as the spatial variability described by the variograms (Chiles and Delfiner, 1999). Instead of producing a single, average case estimate, a geostatistical simulation produces several alternative and equiprobable joint realisations of the local values of a variable of interest (e.g. Goovaerts, 1997). This contrasts with the more common geostatistical estimation procedure, kriging, which does not reproduce local spatial detail (it is unrealistically smooth, despite honouring the sample values) and provides estimates whose variance is usually smaller than the sample variance. Furthermore, and more importantly, a simulation is able to produce many realisations, which form a statistical distribution of abundance estimates from which, for example, confidence intervals can be determined.

The objective of this paper is to produce a conditional simulation of herring density, based on data from an acoustic survey. By individually applying geostatistical simulation to the acoustic data and length data, a set of realisations of these data are obtained. These realisations are then combined to produce a set of herring density realisations, from which global estimates of abundance are derived with an associated statistical distribution, confidence intervals and realistic distribution maps. The method, as applied to these data delivers useable confidence intervals and, therefore, assesses much of the uncertainty in the fishery independent estimate of herring abundance. Despite the fact that the paper achieves the objective of producing confidence intervals, the results are likely to suffer from bias due to the use of off-the-shelf data transformation algorithms on fisheries acoustic data, which are often very positively skewed. We discuss this limitation and propose corrections for future work.

2. Materials and methods

Data were taken from the Orkney Shetland herring acoustic survey carried out in July 1999 by the fisheries research vessel *Scotia*. The survey is the major component of the ICES international North Sea herring acoustic survey and accounts for 80% of the adult abundance estimate (ICES, 2000). A 38 kHz Simrad EK500 scientific echosounder was used to gather acoustic data. Echo traces were verified by regular "ground-truth" trawling with a pelagic trawl, and then allocated to the appropriate fish species by visual scrutiny of the echogram. The scrutinised acoustic data, along with position, were output as values of the nautical area scattering coefficient (NASC, in $m^2\ nm^{-2}$) ascribed to herring, for an equivalent distance sample unit (EDSU) of 1 km. This resulted in 5308 acoustic data points (see Fig. 1 for the data histogram and a further statistical description). The length of herring was measured from samples of each trawl haul and summarised as the root mean square length (RMSL, in cm).

Conversion of the scrutinised acoustic data into estimates of fish numbers was carried out according to the procedures in ICES (2000) based on the principles laid out in Simmonds et al. (1992) using the Marine Laboratory echo Integrator survey Logging and Analysis Programme (MILAP). Further details of the methods employed and results obtained are available in the survey report (ICES, 2000).

A detailed illustration and discussion of the gaussian sequential approach to simulation used in this study is provided by Goovaerts (1997). The simulation procedure used, assumes that the data are multivariate gaussian. In the first instance, this requires the univariate (one-point) cumulative distribution function (CDF) to be normal. Both variables were, therefore, subject to a normal-score transformation, that entails setting up a correspondence table between equal *p*-quantiles of the gaussian CDF and the original distribution (see Goovaerts, 1997).

The multigaussian assumption also requires the multivariate (two-point) CDF to be normal. To examine this two-point normality *h*-scatterplots for the two variables were inspected: these should appear elliptical with the long axis of the ellipse orientated along the one-to-one line (Tabachnick and Fidell,

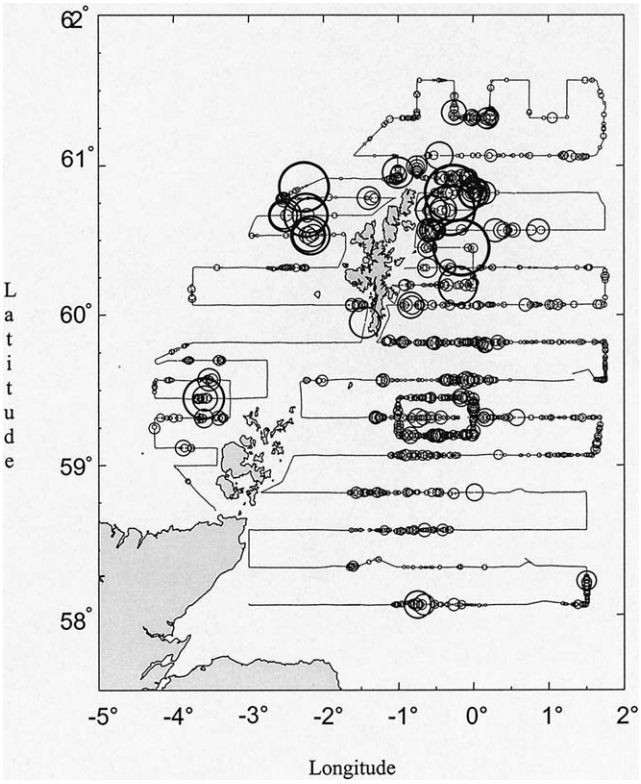

Fig. 1. Post plot with circle size proportional to NASC (m^2 nm^{-2}) attributed to herring, from the Orkney Shetland herring acoustic survey in July 1999.

1989). In the case of the NASC, the *h*-scatterplots were elliptical and there was reasonable agreement with this assumption. In the case of the RMSL, there was an insufficient number of samples (31) to determine the shape of the *h*-scatterplots, and so it was not possible to ascertain whether these data conformed to the assumption. Nonetheless, as discussed below, simulations of RMSL reproduced satisfactory global statistics, such as the variogram, mean, coefficient of variation and quantiles.

Variography and simulation were then carried out in "gaussian space". Omnidirectional experimental variograms were calculated at a lag of 1 km for the NASC (Fig. 2a) and 30 km for the RMSL (Fig. 2b). In this case, no evidence of anisotropy was found from calculation of directional variograms (this might not be the case for other acoustic surveys). Gaussian, exponential, spherical and linear models were fitted according to a weighted least squares procedure (Fernandes and Rivoirard, 1999). This resulted in the adoption of a linear isotropic model for RMSL and an exponential isotropic model for NASC (Fig. 2). A domain encompassing the data was chosen and discretised at 1 km grid nodes (162 470 nodes).

The independence of NASC and RMSL was verified using scatterplots, which indicated that no dependence was apparent. The algorithms for the simulations were implemented in GSLIB Fortran routines (Deutsch and Journel, 1992). In the gaussian conditional simulation procedure, a random walk was performed on grid nodes superimposed on the study area. At each node, a gaussian conditional cumulative distribution function (CCDF) was built, with mean and variance obtained by simple kriging the data values and any existing simulated values. A simulated value was then drawn from this CCDF and, finally, the results were backtransformed in the original "data space".

Two sets of realisations were produced using simple kriging as the interpolation algorithm of the simulation: a set of 100 for RMSL and a set of 100 for NASC. Each realisation of one set was then combined with each realisation of the other set using Eq. (1), to create a total of 10 000 fish density realisations.

The NASC values were extrapolated to a max of 40 000 rather than being cut off at observed maximum (35 000). This was a plausible value for the study area and reflected the possibility that the real maximum was not recorded. It should be stressed, however, that, because a hyperbolic model was

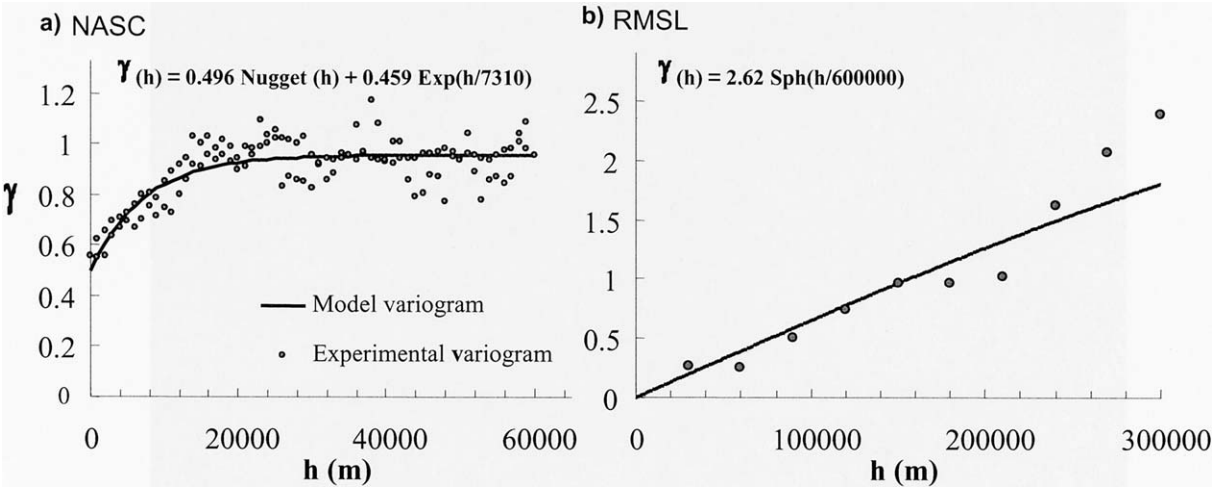

Fig. 2. Experimental variograms and fitted models for: (a) the NASC derived from the echosounder and attributed to herring; and (b) the RMSL of herring taken from pelagic trawls. Note, that the form of the variogram model in the case of RMSL (b) is linear, although the actual model fitted was a long range spherical model. This was a software requirement: the two models are equivalent inside the search radius used.

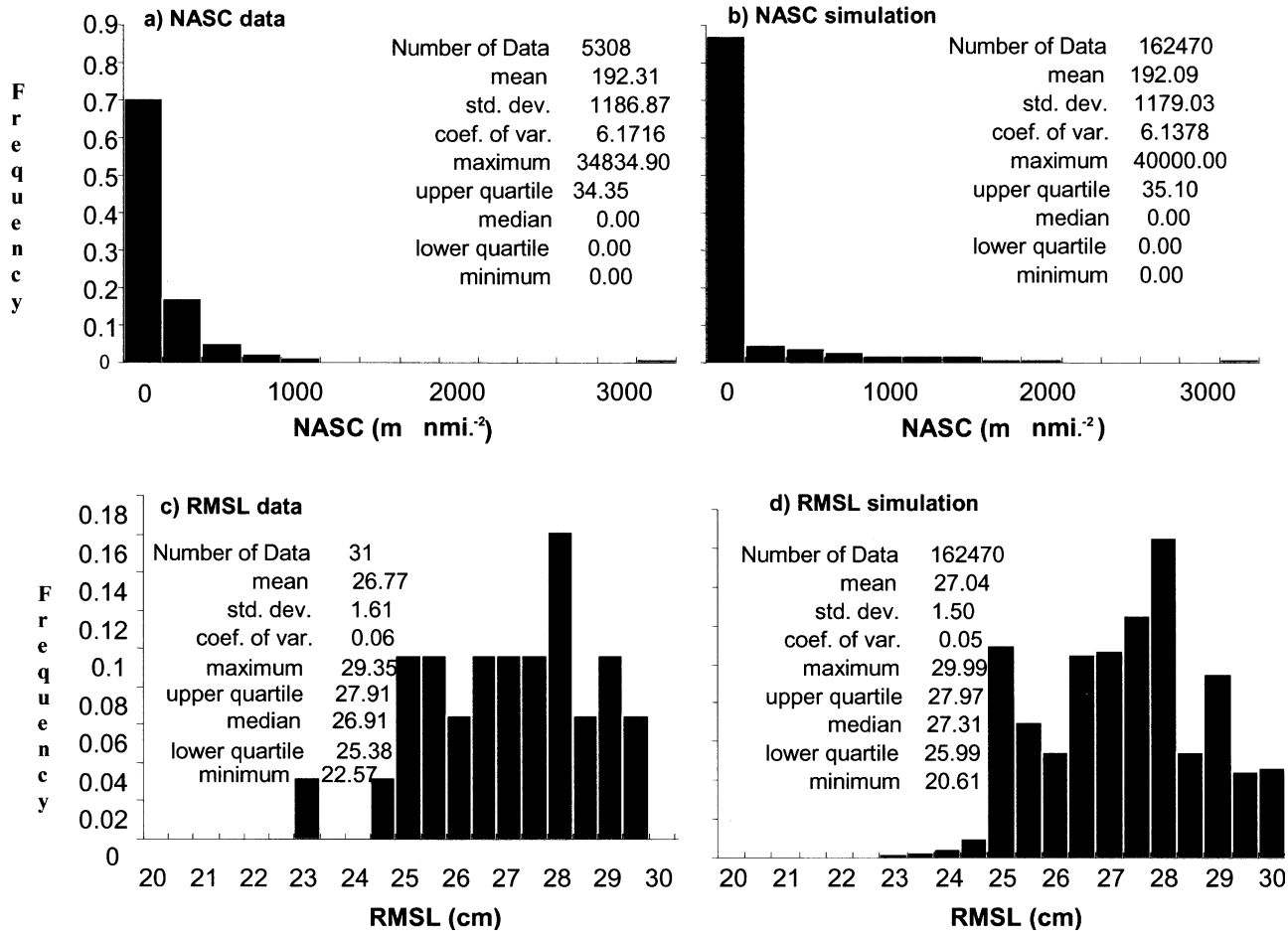

Fig. 3. Frequency distributions and summary statistics of: (a) the raw NASC data; (b) one realisation of the simulation of NASC; (c) the raw RMSL data; and (d) one realisation of the simulation of RMSL.

used for extrapolation with an *omega* parameter = 1.5, there were relatively few simulated values close to 40 000.

Eq. (1) used a target strength to length relationship for herring approved by ICES (2000). The calculation of fish density was performed at each grid node. Realisations of global abundance were then calculated by summing the individual grid nodes values for each abundance realisation.

$$\rho_a = \frac{S_A}{4\pi\,\mathrm{RMSL}^2 \times 10^{-7.12}\ 1.852} \quad (1)$$

To compare the estimates of the present study with those obtained by (ICES, 2000) for the same area and period, we applied a similar mask to the estimated values (see Fig. 5). The mask excluded pixels, where depth was greater than 200 m, as well as areas of land and areas not covered by the survey to which the simulation extrapolates, as it assumes a rectangular and continuous grid when performing the random walk. This stage might have introduced some bias in the reproduction of the statistics, and a more sound procedure would have been to avoid simulating the nodes to be masked out.

3. Results

One of the principal benefits of a conditional simulation is that each realisation broadly reproduces the statistics of the original data. This was shown here: the frequency distributions, means, minima, maxima and percentiles in the simulated realisations were close to the statistics of the sample data (e.g. Fig. 3). The reproduction of statistics in the NASC realisations (Fig. 3a) was better than those of RMSL (Fig. 3b): this is undoubtedly due to the former's much larger sample size and, therefore, the larger amount of conditioning data. The variograms were also reproduced. The realisations of RMSL reflect the high continuity expressed by the linear variogram. Each realisation (a single example is given in Fig. 4) represents an equiprobable distribution of RMSL, which is a more realistic distribution than a kriged map. The realisations of NASC were very similar in appearance to those of herring density (Fig. 5), as these are just conversions based on Eq. (1). The density realisation is difficult to visualise, because of the very high resolution coupled with the extremely skewed nature of the data (Fig. 3b). It should be borne in mind that the statistics of each realisation fluctuate

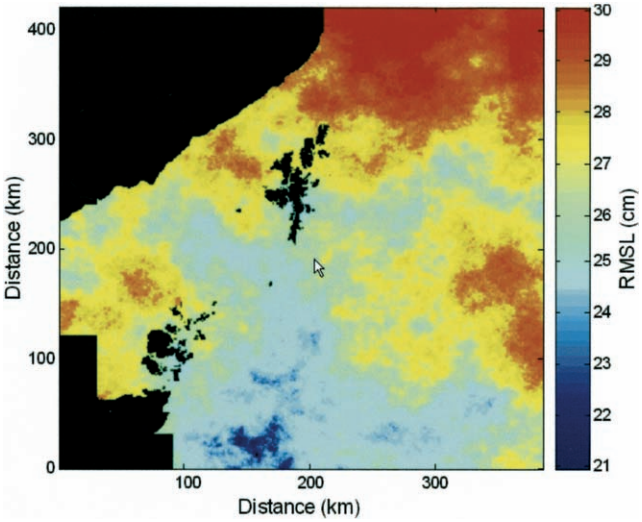

Fig. 4. A realisation of RMSL based on trawl data taken during the Orkney Shetland herring acoustic survey in July 1999. Blacked out regions indicate areas masked out due to land (Orkney Shetland Islands, Scottish mainland), sampled areas, and depths beyond the continental shelf (>200 m, top left).

around the real ones, as perfect reproduction with this approach could only be guaranteed on an infinite grid.

The frequency distribution of the 10 000 realisations of global fish abundance is presented in Fig. 6, and the summary statistics are given in Table 1. The mean abundance was 5942 million fish; 95% of the estimates were between 5677 and 6271 millions. This median-centred 95% probability interval was based on the whole set of 10 000 realisations.

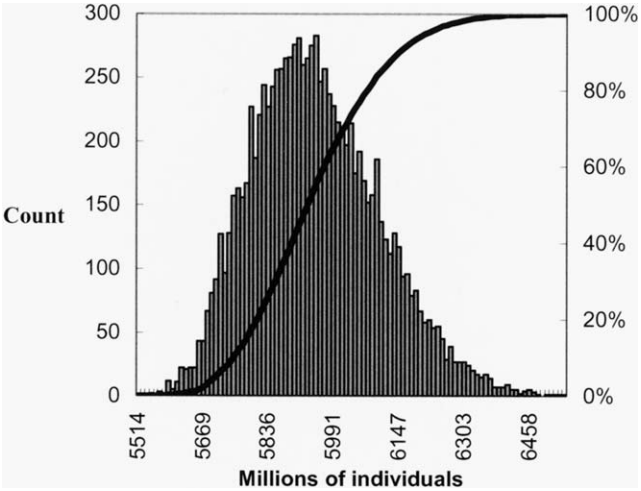

Fig. 6. Frequency distribution of 10 000 abundance estimates based on 100 × 100 realisations of NASC and RMSL combined according to Eq. (1).

4. Discussion

A number of attempts have been made to estimate the sampling error of a survey using a variety of techniques (Simmonds et al., 1992), including geostatistics (Petitgas, 1993; Porteiro et al., 1995; Williamson and Traynor, 1996; Rivoirard et al., 2000). However, in no case have the three factors of length variability, acoustic data variability, and the spatial autocorrelation (of each) been taken into account so far. The conditional simulation presented provides an example on how to both incorporate all of these factors and deliver a full statistical distribution of possible abundance estimates. The simulation provides an estimate of uncertainty

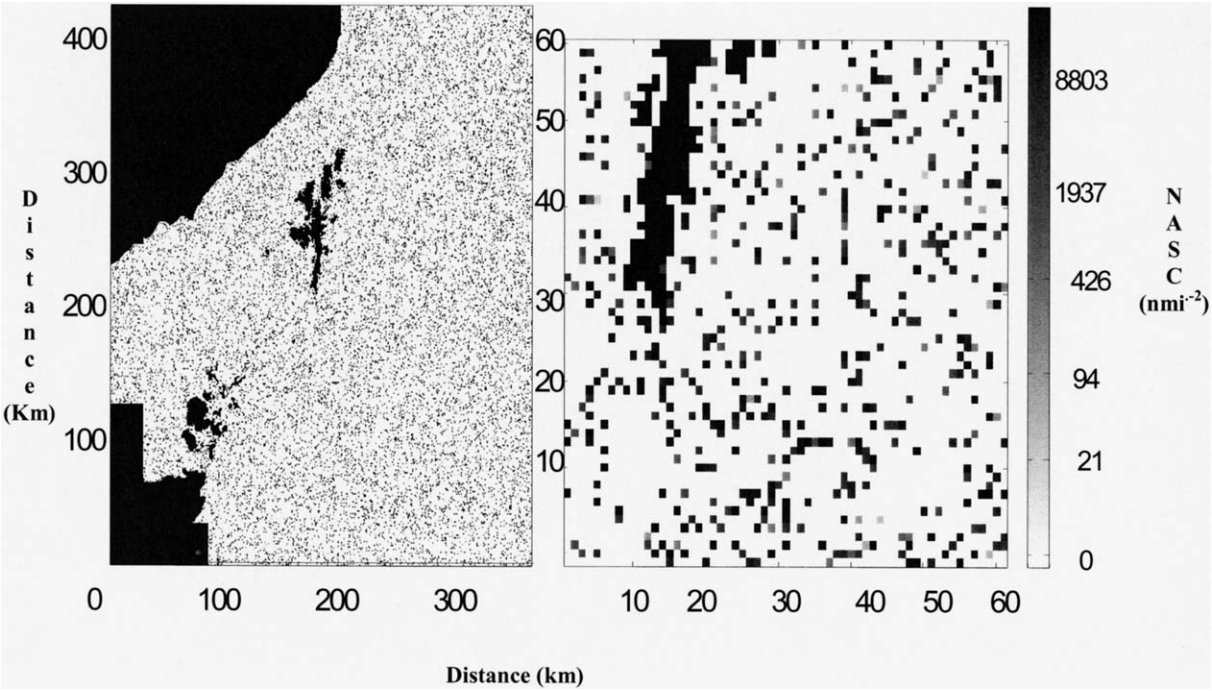

Fig. 5. A realisation of the NASC based on acoustic data taken during the Orkney Shetland herring acoustic survey in July 1999. The right panel is an expanded (zoomed) section of the left panel as illustrated. Blacked out regions indicate areas masked as per Fig. 3.

Table 1
Summary statistics of the 10 000 abundance estimates of herring based on 100 × 100 realisations of the NASC and the RMSL combined according to Eq. (1)

Mean	5 942
Median	5 930
Mode	5 961
Standard deviation	154
Sample variance	23 677
Kurtosis	–0.004
Skewness	0.398
Range	1 038
Minimum	5 514
Maximum	6 552
Count	10 000
2.5 percentile	5 677
97.5 percentile	6 271

that is easy to interpret—i.e. a 95% median based probability interval. This statistic may be used in current assessment models as a measure of uncertainty in the acoustic abundance index. An elaboration would be required to break the estimate down on the basis of fish ages, but this could be achieved by simulating proportions at age as an additional set of realisations (Rivoirard et al., 2000).

The success and wide adoption of geostatistics in fisheries science has, to date, also been compromised by the highly skewed nature of the density distributions, which renders poor structure when using the classical variogram estimator and low confidence in subsequent modelling (Murray, 1996; Maravelias et al., 1996). As structure is often evident in the log domain (Porteiro et al., 1995), a solution to this problem based on a log backtransformed variogram has been proposed (Guiblin et al., 1995). In the present paper, we used a normal score-transformation to estimate the variogram, because this is required by our simulation procedure. This proved to be less noisy (Fig. 2) than the log transform. The effective range of the modelled variogram (21 km) is in agreement with previous estimates of the autocorrelation range of this fish stock (Rivoirard et al., 2000).

Despite the success of this study in pooling length and acoustic data, to provide valid confidence intervals for the estimate of total abundance of fish, a potentially serious problem must be highlighted. The normal-score transformation and backtransformation procedure used (required by gaussian conditional simulations) is likely to have introduced some bias. Prior to transformation, the data must be ranked, and, because the transformation is monotonic, when data of the same value are encountered, ties are broken randomly in the GSLIB implementation. Given that there are many zeroes in our data sets, this is likely to have biased the nugget effect upwards, ultimately leading to a biased estimation of the data values. This is likely to contribute to explain the discrepancy between our results and those in ICES (2000). Therefore, our results caution against the use of "off-the-shelf" solutions for data sets with a high number of zeros. A possible alternative would be the implementation of a modified backtransformation, as described in Saito and Goovaerts (2000).

Providing a correction for backtransformation bias can be implemented, the method has distinct advantages in the estimation of local uncertainty when compared to the more popular kriging method. Kriging is locally optimal in the sense that the local error variance is minimised at each grid node. However, kriging does not reproduce local spatial detail (it is unrealistically smooth). Although it can honour the data, the degree of smoothing depends on their spatial configuration, increasing with distance from the data. This smoothing effect often results in a failure to reproduce the data variogram. Unlike kriging, in a simulation, the modelled values depend on the joint estimates of the variable of interest in the kriging neighbourhood. Uncertainty of local values also depends on data rather than just on their spatial configuration, as in the case of the kriging variance.

The maps produced by simulation are single realisations, which are a much better reflection of reality than smooth kriged maps. However, in the case of herring density, they are difficult to visualise (Fig. 5a,b), because the fish are distributed patchily and the patches are of high density and occur quite rarely in space. Nonetheless, this represents reality, in that most of the area does not actually contain herring. Expansion of scale improves the visual effect (Fig. 5b). The mean abundance obtained (5942 million fish) is somewhat lower than that reported (7635 million fish) using the same data in ICES (2000). The latter approach used the rectangular grid method of interpolation (MacLennan and Simmonds, 1992). The different methods should not in theory provide vastly different estimates of mean abundance, as the data were on a regular grid. One reason for the difference is likely to be due to a combination of factors: differences in the extent of the masks used in the two analyses, the masking procedure followed in this paper, and the bias introduced by the gaussian transformation. A further improvement in the estimates would be achieved by having additional length samples, although Rivoirard et al. (2000) suggest that the variability of density is mainly driven by the acoustic data. Further improvement of the length data could be obtained by considering the entire length distribution rather than using the summary RMSL value. As discussed above, the incorporation of age would also be very useful, particularly for this herring stock, because an index of abundance at age is used for stock assessment of North Sea herring (ICES, 2001).

This analysis provides steps towards an estimate of uncertainty specific to the sampling of length and acoustic data. Problems were encountered with some bias, due to the use of off-the-shelf transformation techniques, but solutions to these may be available as discussed above. Further uncertainties associated with the individual acoustic measurements could be incorporated by, for example, providing estimates of uncertainty associated with the coefficients of Eq. (1) and in the measurement of NASC and RMSL. The method could then approach a determination of total uncertainty, which would be invaluable to the rational management of fisheries resources.

Acknowledgements

We would like to thank E.J. Simmonds (FRS, Marine Laboratory Aberdeen, UK) for providing the data sets from the 1999 North Sea herring acoustic survey and J. Rivoirard (Centre de Géostatistique, France) for advice on geostatistics.

References

Borchers, D.L., Buckland, S.T., Priede, I.G., Ahmadi, S., 1997. Improving the precision of the daily egg production method using generalised additive models. Can. J. Fish. Aquat. Sci. 54, 2727–2742.

Chiles, J.-P., Delfiner, P., 1999. Geostatistics: Modeling Spatial Uncertainty. Wiley, New York.

Deutsch, C.V., Journel, A.G., 1992. GSLIB. Geostatistical Software Library and User's Guide. Oxford University Press, New York.

FAO, 1995. Precautionary approach to fisheries. Part 1: Guidelines on the precautionary approach to capture fisheries and species introductions. FAO Fish Tech. Pap. 350, 52 p.

Fernandes, P.G., Rivoirard, J., 1999. A geostatistical analysis of the spatial distribution and abundance of cod, haddock and whiting in North Scotland. Quant. Geol. Geostat. 10, 201–212.

Goovaerts, P., 1997. Geostatistics for natural resources evaluation. Oxford University Press, Oxford.

Guiblin, P., Rivoirard, J., Simmonds, E.J., 1995. Analyse structurale de données à distribution dissymétrique, exemple du hareng écossais. Cah. Géostat. 5, 137–159.

Hilborn, R., Walters, C.J., 1992. Quantitative Fisheries Stock Assessment: Choice, Dynamics and Uncertainty. Chapman and Hall, New York.

ICES, 2000. Report of the planning group for herring surveys ICES CM 2000/G:02, 106 p.

ICES, 2001. Report of the herring assessment working group for the area south of 62° N ICES CM 2001/ACFM:12, 126 p.

Jolly, G.M., Hampton, I., 1990. Some problems in the statistical design and analysis of acoustic surveys to assess fish biomass. Rapp. P.-v. Réun. Cons. Int. Explor. Mer 189, 415–420.

MacLennan, D.N., Simmonds, E.J., 1992. Fisheries Acoustics. Chapman and Hall, London.

Maravelias, C., Reid, D.G., Simmonds, E.J., Haralabous, J., 1996. Spatial analysis and mapping of acoustic survey data in the presence of high local variability: geostatistical application to North Sea herring (*Clupea harengus*). Can. J. Fish. Aquat. Sci. 53, 1497–1505.

Matheron, G., 1989. Estimating and Choosing. Springer-Verlag, Berlin.

Murray, A.W.A., 1996. Comparison of geostatistical and random sample survey analyses of Antarctic krill acoustic data. ICES J. Mar. Sci. 53, 415–421.

NRC, 1998. Improving Fish Stock Assessments. National Academic Press, Washington, DC.

Patterson, K., Cook, R., Darby, C., Gavaris, S., Kell, L., Lewy, P., Mesnil, B., Punt, A., Restrepo, V., Skagen, D.W., Stefansson, G., 2001. Estimating uncertainty in fish stock assessment and forecasting. Fish Fish. 2, 125–157.

Pennington, M., 1996. Estimating the mean and variance from highly skewed marine survey data. Fish. Bull. 94, 498–505.

Petitgas, P., 1993. Geostatistics for fish stock assessments: a review and an acoustic application. ICES J. Mar. Sci. 50, 285–298.

Porteiro, C., Carrera, P., Miquel, J., 1995. Analysis of Spanish acoustic surveys for sardine, 1991–1993: abundance estimates and inter-annual variability. ICES J. Mar. Sci. 53, 429–433.

Rivoirard, J., Simmonds, J., Foote, K.F., Fernandes, P., Bez, N., 2000. Geostatistics for Estimating Fish Abundance. Blackwell Science Ltd., Oxford.

Rose, G., Gauthier, S., Lawson, G., 2000. Acoustic surveys in the full monte: simulating uncertainty. Aquat. Living Resour. 13, 367–372.

Saito, H., Goovaerts, P., 2000. Geostatistical interpolation of positively skewed and censored data in a dioxin-contaminated site. Environ. Sci. Technol. 34, 4228–4235.

Simmonds, E.J., Fryer, R.J., 1996. Which are better, random or systematic acoustic surveys ? A simulation using North Sea herring as an example. ICES J. Mar. Sci. 53, 39–50.

Simmonds, E.J., Williamson, N.J., Gerlotto, F., Aglen, A., 1992. Acoustic survey design and analysis procedures: a comprehensive review of current practice. ICES Coop. Res. Rep. 187, 127 p.

Smith, S.J., 1990. Use of statistical models for the estimation of abundance from groundfish trawl survey data. Can. J. Fish. Aquat. Sci. 47, 894–903.

Smith, S.J., 1997. Bootstrap confidence limits for groundfish trawl survey estimates of mean abundance. Can. J. Fish. Aquat. Sci. 54, 616–630.

Stefansson, G., 1996. Analysis of groundfish survey abundance data: combining the GLM and delta approaches. ICES J. Mar. Sci. 53, 577–588.

Tabachnick, B.G., Fidell, L.S., 1989. Using Multivariate Statistics. second ed. Harper Collins, New York.

Williamson, N.J., Traynor, J.J., 1996. Application of a one-dimensional geostatistical procedure to fisheries acoustic surveys of Alaskan pollack. ICES J. Mar. Sci. 53, 423–428.

Available online at www.sciencedirect.com
SCIENCE DIRECT®
Aquatic Living Resources 16 (2003) 131–136
Aquatic Living Resources
www.elsevier.com/locate/aquliv

Advances in defining fine- and micro-scale pattern in marine plankton

Dale V. Holliday [a,*], Percy L. Donaghay [b], Charles F. Greenlaw [a], Duncan E. McGehee [a], Margaret M. McManus [c], Jim M. Sullivan [b], Jennifer L. Miksis [b]

[a] *BAE SYSTEMS, 4669 Murphy Canyon Road, San Diego, CA 92123, USA*
[b] *University of Rhode Island, Graduate School of Oceanography, Narragansett, RI 02882, USA*
[c] *University of California at Santa Cruz, Santa Cruz, CA 95064, USA*

Accepted 8 January 2003

Abstract

Since the June 1995 ICES Symposium on Fisheries and Plankton Acoustics in Aberdeen (MacLennan and Holliday, 1996), the use of acoustics for studying zooplankton has seen important advances. Acoustical monitoring of small-scale zooplankton distributions can now be done at intervals of a fraction of a minute. Resolution at vertical spatial scales of tens of centimeters is now easily achieved with commercially available sensors. Multiple-frequency echo-ranging sensors (TAPS™) have been deployed in an up-looking mode on the bottom, and on moorings looking up, down and horizontally. Real-time telemetry provides data on plankton distributions at ranges up to tens of meters from the sensors for periods of weeks to months. These sensors allow one to estimate total zooplankton biomass and the size-abundance spectrum of the animals in the water column at different depths and times. When a profiling CTD and multi-spectral optical sensors were used to define the physical environment and phytoplankton distributions near an acoustical zooplankton profiler, strong relationships were observed between measured spatial and temporal patterns. New methods in zooplankton acoustics are illustrated with data collected from these sensors while monitoring thin, sub-meter thick layers of plankton and diel migrations of benthopelagic crustaceans.

Keywords: Bioacoustics; Plankton acoustics; Thin layers; Benthopelagic migrators

1. Introduction

Since the mid-1990s, major improvements have been achieved in measuring fine- and micro-scale distributions of both phytoplankton and zooplankton. Advances have been made in using optical sensors to determine the distribution and characteristics of phytoplankton (primary producers). Advances continue to be made using optical techniques in studying phytoplankton, e.g., measurement of inherent and apparent optical water column properties using both multi- and hyper-spectral sensors (Twardowski et al., 1999) and flow cytometry for characterizing individual cells (Jochem, 2000). Striking advances have also been made in estimating the biomass, spatial distribution and temporal dynamics of assemblages of secondary producers, i.e., the zooplankton and micronekton. These advances stem largely from the evolution of multi-frequency acoustical sensors and from improvements in theory for describing scattering from small particles. Both marine optics and acoustics have also benefited from innovative changes in the way we deploy such instruments and from advances in theoretical descriptions of scattering and propagation.

2. Background and motivation

Even with the best technology of the late 20th century, it was a challenge to detect fine- and micro-scale spatial structure in the sea, much less to quantify it by describing the relationships between phytoplankton, zooplankton, and relevant small-scale physical features in the ocean. The vertical resolution of our best cast-deployed physical, chemical, acoustical, and optical sensors was limited by coupling of the wave and swell induced meter-scale vertical motions of a ship to an instrument or direct sampling device over periods of a few seconds. As sensor technologies and deployment modes evolved, we have finally begun to detect and describe some of the micro- and fine-scale structures that fisheries and plankton ecologists (Cassie, 1963; Lasker, 1975; Mullin and

* Corresponding author.
E-mail address: van.holliday@baesystems.com (D.V. Holliday).

doi:10.1016/S0990-7440(03)00023-8

Brooks, 1976) inferred from trophic arguments. We now describe and even monitor ecologically critical small-scale features in phytoplankton and zooplankton distributions which have been at best seriously under-sampled and often completely missed. We can now reveal patterns in primary and secondary producers at scales sampled adequately in both time and space, i.e., we can measure at scales that are not necessarily aliased by the sampling process (Platt and Denman, 1975). Sensors with high accuracy, resolution and precision can reveal zooplankton biomass and size spectra at tens of centimeters in the vertical, with horizontal resolutions of about a meter, and with temporal resolutions of better than a minute, for months. Modern acoustical zooplankton sensors have revealed that over 75% of the zooplankton biomass can be concentrated in a few sub-meter thick "thin layers" in a 50 m water column (Holliday, 1998). Similar "thin layer" vertical structures in physical, chemical and phytoplankton distributions have also been described (Donaghay et al., 1992; Cowles and Desiderio, 1993; Hanson and Donaghay, 1998). If, as Lasker and Mullin pointed out in the late 1960s, you are a fish larva, you may indeed be fortunate to find such a food resource.

We offer examples of data from studies where we have deployed instrumentation to allow high-resolution studies of fine- and micro-scale structures. These are scales, in both time and space, but especially in depth, which are relevant to the experiences of an individual organism. These tools are not only useful for small-scale work but have also been applied to problems that span hundreds of kilometers (McGehee et al., 2000; Pieper et al., 2001). Here, however, we focus on applications at small scales.

3. Evolutions in the modeling of acoustical scattering

In addition to advances in acoustical sensor technology, there have been important developments in mathematical modeling of acoustical scattering and in the software used to convert volume scattering data into measures that reflect the biophysical character of the scatterers and their distribution in relation to their environment.

During the late 1990s, the most widely used models of scattering from zooplankton and micronekton were analytical, the most useful being those of Anderson (1950), Faran (1951), Stanton (1988, 1989, 1990) and Stanton and Chu (1992). Simple adaptations of these models, such as the high-pass fluid sphere model (Johnson, 1977, 1978), the truncated versions of the fluid and elastic spheres (Holliday, 1992, 1987) were also available. While the stimulus for the newest models for scattering from zooplankton can often ultimately be traced to Stanton, through his students and research collaborators, the newest generation of models is largely numerical.

One such model involves the use of the Distorted Wave Born Approximation (DWBA). It was first implemented for micronekton in the late 1990s (McGehee et al., 1998; Martin-Traykovski et al., 1998) in 2-D, and in 3-D by Lavery and her collaborators (Lavery et al., 2002). In these models, the silhouettes (2-D) and volumes (3-D) of zooplankters are obtained photographically or via computerized tomography (CT-scans). Numerical integration yields estimates of scattering for realistic animal shapes at different sizes and selected orientations with respect to the incident sound waves.

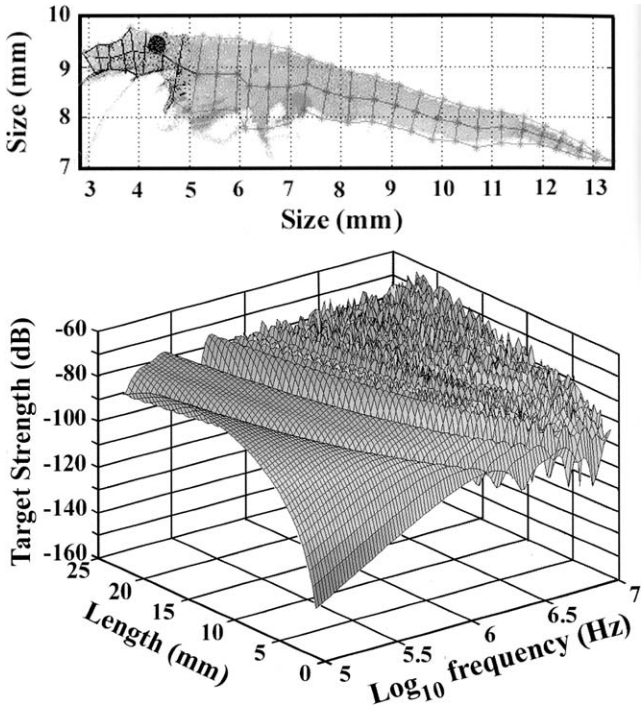

Fig. 1. Predicted ventral aspect scattering from a mysid. See McGehee et al., 1998 for details of modeling method.

To illustrate one of the new modeling techniques, the perimeter of a mysid was approximated by a series of cylinders whose radii were positioned orthogonally with respect to the central axis of the animal (Fig. 1, top panel). The dependence of the ventral target strength on animal length and the acoustic frequency, as computed with a 2-D DWBA model revealed a complex dependence of target strength on the acoustic frequency and the length of the mysid including both Rayleigh and geometric scattering domains (Fig. 1, bottom panel).

The shape of this mysid is similar to that of several common species of euphausiids. The ventral aspect angle was used to support an analysis of data where the acoustical system "looked" upward. Mysids have been observed swimming naturally in the approximate aspect illustrated (P. Jumars, pers. comm.).

4. Advances in inversion processing

Given accurate models of the scatterers in the water column and good multi-frequency estimates of acoustical volume scattering strength, one can estimate zooplankton abundance vs. size for each time-depth resolution cell (pixel) in a

sequence of echo-ranging profiles. Although the principles for multi-model inversion were outlined by Holliday (1977), implementation of the multi-frequency, multi-model process was not attempted in earnest until the late 1990s when modeling of scattering from animals of different morphologies had substantially advanced. Current versions of inverse codes optimally and simultaneously apportion the energy in the acoustic volume scattering strength spectra for each time and depth interval (pixel) into an estimated size-biomass spectrum for each scattering model supplied by the user.

5. Improvements in resolution of small-scale structure

Vertical spatial resolutions achievable in the mid-1990s were nominally >2 m, but are now ~0.125 m. From ships making stations along a transect, we were limited to making vertical casts about once an hour. With moored sensors in the coastal zone, we now routinely sample a 20–30 m water column at 0.5 min intervals, or better. Previously, casts along a transect from a ship were spaced at horizontal intervals not less than ~500 m. The surface footprint of an up-looking moored sounder at 20 m depth today resolves horizontal structure at ~1 m scales as the water is advected over the sensor. Similar horizontal resolutions could be achieved from moving platforms in an "echo sounder" mode. Data acquired with traditional research cruises on ships often span only a few days or weeks, often missing important variations in the distribution of biomass on both shorter and longer intervals of time, e.g., details of diel migrations, the responses of biota to storms, seasonal, and even annual changes. Data collected with today's multi-frequency moored acoustical zooplankton sensors may span several months at sampling intervals of less than a minute. With fairly minimal maintenance, e.g., removal of biological fouling on the sensors, even longer periods are entirely practical in some situations. This presents both an opportunity and a challenge. The opportunity involves being able to watch a distribution evolve and change on scales similar to the ambit and life-span of an individual zooplankter. The challenge involves the fact that the amount of data one must archive, process, visualize, correlate with environmental and trophic data at similar scales, and then interpret, is sometimes overwhelming.

Depending on the science objective of the deployment, we have arranged the sensors to look either up into the water column above them, or down to study the benthopelagic fluxes in the water column just above the seabed (Richardson et al., 2001). Volume scattering strength profiles can be reported at multiple acoustical frequencies, averaged over multiple echo-ranging cycles, at intervals of as often as every 30 s for months. As we have currently configured our acoustical sensor packages, a limited amount of internal sensor storage is available, but normally data are telemetered to a shore station via a spread spectrum radio with line-of-sight distances of about 30 km. This data link may also be used to remotely control a variety of sensor operating parameters. When it is desirable to use the system for more than about 3 weeks without changing the batteries, the system can be deployed at the end of an ~1 km cable, supplying power from shore and enabling two way communications.

To illustrate the difference these technological improvements have made, we use data from a TAPS deployment in a shallow fjord in northern Puget Sound, located between Seattle, WA, USA and Victoria, BC, Canada (Fig. 2). During the summer of 1998, the authors deployed several multi-frequency acoustical zooplankton sensors (TAPS™) on anchored sub-surface buoys. This sensor measured volume scattering strengths at 265, 420, 700, 1100, 1850 and 3000 kHz with a 12.5 cm range resolution with a set of approximately six° beams that insonify a common volume between the depth of a moored mid-water float and the surface. The maximum effective range for any active acoustical sensor depends on the abundance and kinds of scatterers in the water column and the acoustic frequency. In typical applications in the coastal ocean we have obtained useful results with the TAPS at ranges up to 20 or 30 m.

The differences between the spatial and temporal resolutions available from zooplankton acoustical sensors in the mid-1990s and today are graphically illustrated (Fig. 2, bottom panel) with data from an up-looking TAPS at the resolution available in 1998 (1 min, 0.125 m vertical). The high resolution (1998) data were re-sampled at the temporal and vertical spatial resolutions available in 1994 (1 h, 2 m vertical) to duplicate the aliasing that would have resulted from the lower sampling densities and a comparison illustrates the improvements achieved. Clearly, the higher resolution representation of the data conveys far more detail than was available less than a decade ago.

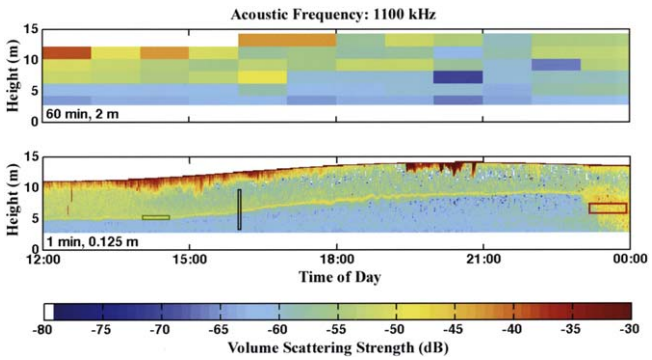

Fig. 2. An up-looking sounder record at 1.1 MHz was collected on June 25, 1998 in East Sound, Orcas Is., WA, USA. This record (lower panel) has been re-sampled once an hour and at 2 m intervals in depth (upper panel). The lower sampling density would have been comparable to the state-of-the-art in 1994 and illustrates the benefits of increases in resolution of acoustical volume scattering strengths measured from a mid-water mooring. The highest resolution data (bottom panel) reveal extensive detail of fine- and micro-scale structures in the water column during a 12-h period. The data in the upper panel is clearly under-sampled, and is aliased, causing major features to be missed or underestimated. It reveals little about the plankton fine structure. The "boxes" define specific times and depth ranges that are further discussed in the text.

6. Relating structure in biomass and environment

One obvious feature of this data set was the very thin layer of high acoustical scattering observed 5 m above the TAPS at noon (Fig. 2, bottom panel). This scattering layer shoaled slowly during the following 11 h. An autonomous winch which carried a CTD and sensors for O_2 and optical absorption was moored ~5 m from the TAPS and collected profiles once an hour. At 16:00 Pacific Daylight Time (PDT), the acoustical scattering layer was located 6.2 m above the TAPS, midway between the oxycline and the pycnocline (Fig. 3, arrow b). An O_2 minimum (3.8 ml l^{-1}) coincided with the scattering layer. Above the oxycline, O_2 levels were supersaturated by ~20%, while O_2 values below the pycnocline were well below saturation. Near the surface, bubbles, possibly generated by high phytoplankton production and brought out of the supersaturated solution by solar heating were episodically advected downward into the water column by Langmuir circulation during this period by light, variable (<4 m/s) winds. The acoustic spectra and scattering levels in the plumes near the surface (Fig. 2) are consistent with the presence of very small bubbles. At the same time, a thin (0.14 m) optical absorption layer was detected 7.1 m above the TAPS, or 0.9 m above the pycnocline and its associated zooplankton scattering layer. This thin optical layer, characterized by a peak total optical absorption value (a_{pg}) of 3.7 m^{-1} at 440 nm, was co-located with an O_2 maximum (7.2 ml l^{-1}). Sampling with a siphon revealed that it was due to phytoplankton. The acoustical scattering layers were only 22.5–45.0 cm thick for most of this particular 12-h period. A small packet of internal waves, with peak-to-peak amplitudes of less than a meter appeared at about 17:30 PDT, modulating the depth of the pycnocline and the acoustical scattering layer for about 2 h.

We illustrate the multi-model inverse method with three selections from the high resolution data of Fig. 2 (bottom panel). We employed two scattering models. The first was the truncated fluid sphere model often used as a generic description of scattering for small crustaceans such as copepods and amphipods (Costello et al., 1989). The second model was the DWBA elongate model of Fig. 1, chosen because *Neomysis* was collected during our occupation of this site and this organism often dominates nighttime emergence trap collections in this environment. Our inverse code optimally and simultaneously apportions the energy in the acoustic volume scattering strength spectra for each selected time and depth interval (pixel) into sizes supplied by the user with methods originally described by Holliday (1977).

An inverse calculation for pixels at the times and depths in the "box" on the thin scattering layer (Fig. 2, bottom panel, ~14:00 h) revealed that the layer was dominated by small copepod-size crustaceans averaging 1.2 mm total length. Several additional sizes were characterized by each of the modeled shapes (Fig. 4), but each with lesser biovolumes relative to the copepod-size animals.

The leftmost "box" in Fig. 2 included 220 independent estimates of volume scattering at each of five frequencies, spanned a 40-min time interval and 0.625 m in depth. Similar calculations revealed that the assemblage of small copepod-like scatterers just above and just below the layer at the same time were similar in size and relative abundance to those in the layer. This suggests that the layer was formed by aggregation of nearby small crustaceans—on the pycnocline in this instance. Average biovolumes of copepod-like organisms in the layer were ~300 mm^3 m^{-3}, while the biovolumes in the upper mixed layer averaged ~100 mm^3 m^{-3}. Immediately below the pycnocline, and to depths extending to ~2 m above the bottom, the copepod-size biovolumes averaged only ~15–20 mm^3 m^{-3}.

Acoustical data collected during the hourly CTD/optics profile (center "box", Fig. 2) were also examined with the two-model inverse code, revealing details of the fine-scale depth distribution of the different shapes and sizes of zooplankters in relation to their environment (Fig. 5). A layer of small "fluid-sphere-like" scatterers were bounded by the steepest point on the pycnocline (a) from below and by the oxycline (b) from above. Lesser concentrations of copepod-size scatterers were found above, but few were observed below the layer on the thermocline. The depth of the maxi-

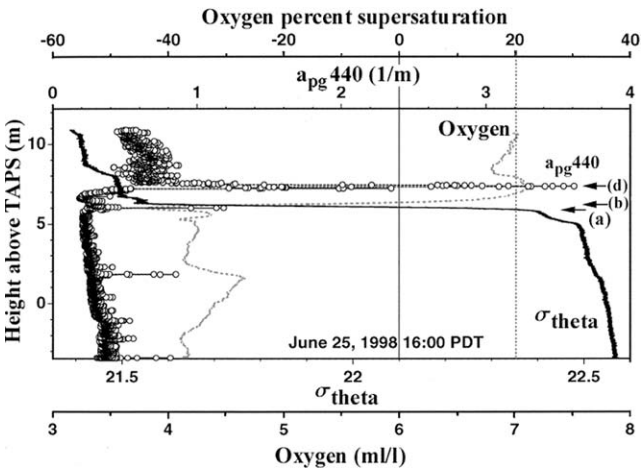

Fig. 3. σ_{theta}, O_2, percent supersaturation of O_2, and a_{pg} at 440 nm vs. depth at 16:00 PDT. Measurements are relative to the TAPS (0 m) which was moored at 20.6 m depth (MLLW). The locations marked (a), (b) and (d) are discussed in the legend for Fig. 5.

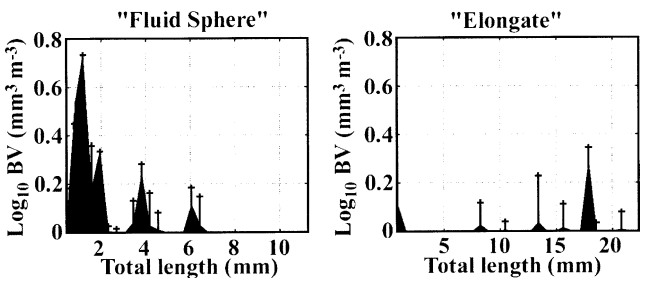

Fig. 4. Logarithmic biovolume spectra for thin layer averaged over all the time and depth pixels included in the green "box" in Fig. 2. Average biovolumes are defined by the top edge of the shaded areas while the mean plus one standard deviation of the biovolume is indicated by the vertical lines with the "+" at the top.

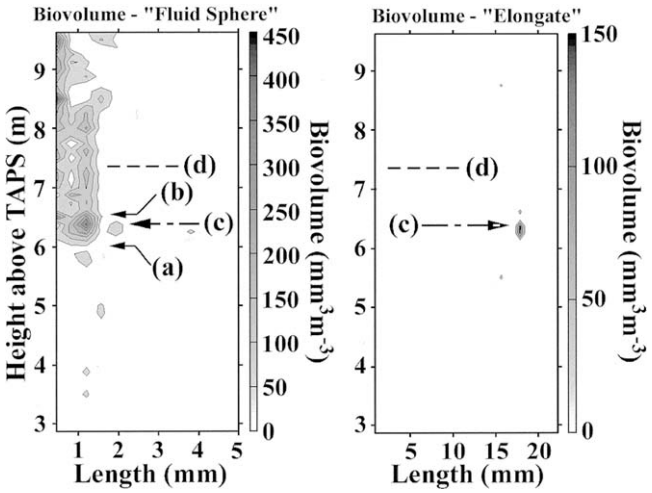

Fig. 5. Biovolume distributions for two distinct shapes of organisms at 16:00 PDT, June 25, 1998. The mid-point of the seasonal pycnocline (a); the mid-point of the oxycline (b); the mid-depth for 1.2 mm long copepods (c); and the depth of a thin layer of optically detected phytoplankton (d) are indicated. Contours are at intervals of 20 $mm^3\ m^{-3}$.

mum of this small crustacean distribution (c) was consistently just above that of the larger mysid-shaped (elongate) animals concentrated in a separate, but adjoining thin layer (<1 m thick) immediately below the seasonal thermocline. During the time designated by the center "box" (Fig. 2), peaks at several different sizes from ~7–22 mm total length were present, with biovolume peaks at different sizes reaching to as high as 180–200 $mm^3\ m^{-3}$.

The acoustically determined size distributions for organisms located just below the pycnocline were consistent with the presence of several distinct cohorts (stages) of mysids, similar in size structure and abundance to an assemblage independently observed earlier in a nearby fjord (West Sound) on the same island. At 16:00 PDT, however, only one size of the elongate scatterers was present at significant levels above 20 $mm^3\ m^{-3}$ (the contour interval). The thin layer of small crustaceans was at the shallow O_2 minimum (3.8 ml l^{-1}) and a second O_2 minimum (~4.1 ml l^{-1}) was observed at the depth of the larger mysid-shaped elongate animals. There was little evidence of small or large crustaceans scattering sound at the depth of the thin optical layer of phytoplankton (Fig. 5) during the daylight hours.

At the latitude of East Sound, the sun sets late during June. Sunset was at 21:17 PDT and nautical twilight ended at 23:00 PDT on the 25th. An increase in scattering at nautical twilight (Fig. 2) was consistent with the migration of several sizes of elongate scatterers to mid-water depths. Results of multi-model inverse calculations averaged over 504 pixels from below the layer after sunset (right 'box", Fig. 2) allows attribution of the increased nighttime scattering to larger organisms with both sphere-like and elongate shapes (Fig. 6).

7. Conclusions

Our ability to examine zooplankton in the coastal ocean has changed dramatically for the better during the last decade. Likewise, there have been major advances in sampling the physics, chemistry and the phytoplankton. Advanced telemetry and new modeling and computing assets suggest a need to consider how we will display so much data and how we can "see" it in ways that will lead to identification of causes and effects, e.g., behavior.

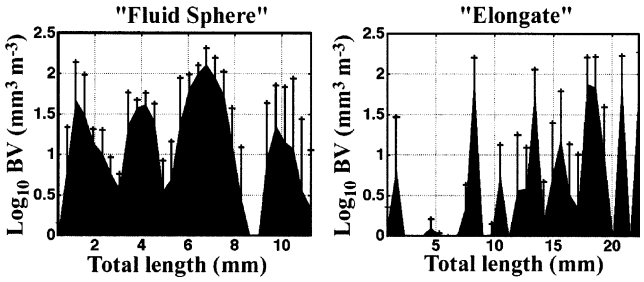

Fig. 6. Logarithmic biovolume spectra for thin layer averaged over all the time and depth pixels included in the red "box" on the right in Fig. 2.

Acoustical and optical methods can now be used to describe how some plankton distributions are related to fine-scale ocean physics and chemistry. Indeed, acoustics and optics are increasingly being used by investigators internationally to address their own science interests. The ability to observe plants and animals nearly continuously and with ever increasing spatial resolution, combined with future deployments on new, novel platforms, should accelerate the rate at which we learn how life survives, and even thrives, in the sea. It is also clear that making observations for sufficiently long periods to allow observation of the marine equivalent of the rare, but critical, terrestrial forest fire is needed. Technology, driven by external forces such as consumer electronics, is moving to lower power requirements, increased storage and improved data telemetry. These developments allow us to observe, at least at points in the ocean, for months now and likely for much longer—e.g., years or decades—in the future.

Finally, we are at the beginning of our exploration of acoustics and optics for studying zooplankton and phytoplankton. Improvements in modeling of scattering in both fields, doing inverse computations, and development of novel, enabling modes of deployment for a multitude of sensors are on the "drawing boards". Completely new approaches, such as multi-static, multi-frequency acoustics have not yet been developed for field use, but are being addressed. This is an iterative process, requiring both experiment and theoretical developments. It sometimes requires starting in the lab, going to sea, learning, going back to the lab. This approach rewards cooperating scientists with diverse heritages (e.g., physicists and biological oceanographers) who are interested in learning the language of other disciplines.

Acknowledgements

We appreciate the support of the Office of Naval Research's Oceanic Biology and Chemistry Program via Con-

tracts N00014–00-D-0122 and N00014–98-C-0025 to BAE SYSTEMS (Holliday, Greenlaw and McGehee) and Grant N00014–95–10225 to the Graduate School of Oceanography at the University of Rhode Island (Donaghay). Specific thanks go to the entire team of co-PIs who worked on thin layers in East Sound. Mr. and Mrs. Rick Bielfuss, Jim Youngren, and Leith Templeton each aided with logistics. Capt. Eric Boget from the R/V Joe Henderson (University of Washington) deserves recognition for an extraordinary effort in the field. Finally, we gratefully acknowledge the influence of Mike Mullin and Reuben Lasker, extraordinary teachers and researchers, whose legacy of curiosity and insight about the way the ocean works has outlived them.

References

Anderson, V.C., 1950. Sound scattering from a fluid sphere. J. Acoust. Soc. Am. 22, 426–431.

Cassie, R.M., 1963. Microdistribution of plankton. Oceanogr. Mar. Biol. Ann. Rev. 1, 223–252.

Costello, J.H., Pieper, R.E., Holliday, D.V., 1989. Comparison of acoustic and pump sampling techniques for the analysis of zooplankton distributions. J. Plankton Res. 11, 703–709.

Cowles, T.J., Desiderio, R.A., 1993. Resolution of biological microstructure through in situ fluorescence emission spectra. Oceanography 6, 105–111.

Donaghay, P.L., Rines, H.M., Sieburth, J.M., 1992. Simultaneous sampling of fine scale biological, chemical and physical structure in stratified waters. Arch. Hydrobiol. 36, 1–14.

Faran, J.J., 1951. Sound scattering by solid cylinders and spheres. J. Acoust. Soc. Am. 23, 405–418.

Hanson Jr., A.K., Donaghay, P.L., 1998. Micro to fine scale chemical gradients and layers in vertically stratified coastal waters. Oceanography 11, 10–17.

Holliday, D.V., 1977. Extracting bio-physical information from the acoustic signatures of marine organisms. In: Anderson, N.R., Zahuranec, B.J (Eds.), Ocean Sound Scattering Prediction, vol. 5. Plenum Press, Marine Science Series, New York, pp. 619–624.

Holliday, D.V., 1987. Acoustic determination of suspended particle size spectra. In: Kraus, N.C (Ed.), Proceedings of a Specialty Conference on Advances in Understanding of Coastal Sediment Process, Coastal Sediments - 1987, vol. 1. American Society of Civil Engineers, New York, pp. 260–272.

Holliday, D.V., 1992. Zooplankton acoustics. In: Desai, B.N (Ed.), Oceanography of the Indian Ocean. Oxford and IBH Publishing Co. Pvt. Ltd., New Delhi, pp. 733–740.

Holliday, D.V., 1998. Acoustical sensing of small-scale vertical structures in zooplankton assemblages. Oceanography 11, 18–23.

Jochem, F.J., 2000. Probing the physiological state of phytoplankton at the single-cell level. Sci. Mar. 64, 183–195.

Johnson, R.K., 1977. Sound scattering from a fluid sphere revisited. J. Acoust. Soc. Am. 61, 375–377.

Johnson, R.K., 1978. Erratum: sound scattering from a fluid sphere revisited. J. Acoust. Soc. Am. 63, 626.

Lasker, R., 1975. Field criteria for survival of anchovy larvae: the relation between inshore chlorophyll maximum layers and successful first feeding. Fish Bull. 73, 453–462.

Lavery, A., Stanton, T.K., McGehee, D.E., Chu, D., 2002. Three-dimensional modeling of acoustic backscattering from fluid-like zooplankton. J. Acoust. Soc. Am. 111, 1197–1210.

MacLennan, D.N., Holliday, D.V., 1996. Fisheries and plankton acoustics: past, present, and future. ICES J. Mar. Sci. 53, 513–516.

Martin-Traykovski, L.V., O'Driscoll, R.L., McGehee, D.E., 1998. Effect of orientation on broadband acoustic scattering of Antarctic krill *Euphausia superba*: implications for inverting zooplankton spectral acoustic signatures for angle of orientation. J. Acoust. Soc. Am. 104, 2121–2135.

McGehee, D.E., O'Driscoll, R.L., Martin-Traykovski, L.V., 1998. Effect of orientation on acoustic scattering from Antarctic krill at 120 kHz. Deep-Sea Res. 45, 1273–1294 (Part II).

McGehee, D.E., Greenlaw, C.F., Holliday, D.V., Pieper, R.E., 2000. Multi-frequency acoustical volume backscattering patterns in the Arabian Sea - 265 kHz to 3 MHz. J. Acoust. Soc. Am. 107, 193–200.

Mullin, M.M., Brooks, E.R., 1976. Some consequences of distributional heterogeneity of phytoplankton and zooplankton. Limnol. Oceanogr. 21, 784–796.

Pieper, R.E., McGehee, D.E., Greenlaw, C.F., Holliday, D.V., 2001. Acoustically measured seasonal patterns of zooplankton in the Arabian Sea. Deep-Sea Res. 48, 1325–1343 (Part II).

Platt, T., Denman, K., 1975. Spectral analysis in ecology. Ann. Rev. Ecol. Systemat. 6, 189–210.

Richardson, M.D., Briggs, K.B., Bibee, L.D., Jumars, P.A., Sawyer, W.B., Albert, D.G., Bennett, R.H., Berger, T.K., Buckingam, M.J., Chotiros, N.P., Dahl, P.H., Dewitt, N.P., Fleischer, P., Food, R., Greenlaw, C.F., Holliday, D.V., Hulbert, M.G., Hutnak, M.P., Jackson, P.D., Jaffe, J.S., Johnson, H.P., Lavoie, D.L., Lyons, A.P., Martens, C.S., McGehee, D.E., Moore, K.D., Orsi, T.H., Piper, J.N., Ray, R.I., Reed, A.H., Self, R.F.L., Schmidt, J.L, Schock, S.G., Simonet, F., Stoll, R.D., Tang, D., Thistle, D.E., Thorsos, E.I., Walter, D.J., Wheatcroft, R.A., 2001. An overview of SAX99: environmental considerations. IEEE J. Ocean. Eng. 26, 26–53.

Stanton, T.K., 1988. Sound scattering by cylinders of finite length: I. Fluid cylinders. J. Acoust. Soc. Am. 83, 55–63.

Stanton, T.K., 1989. Sound scattering by cylinders of finite length: III. Deformed cylinders. J. Acoust. Soc. Am. 86, 691–705.

Stanton, T.K., 1990. Sound scattering by spherical and elongated shelled bodies. J. Acoust. Soc. Am. 88, 1619–1633.

Stanton, T.K., Chu, D., 1992. Sound scattering by rough elongated elastic objects: II. Fluctuations of scattered field. J. Acoust. Soc. Am. 92, 1665–1678.

Twardowski, M.S., Sullivan, J.M., Donaghay, P.L., Zaneveld, J.R.V., 1999. Microscale quantification of the absorption by dissolved and particulate material in coastal waters with an ac-9. J. Atmos. Ocean. Tech. 16, 691–701.

Available online at www.sciencedirect.com
SCIENCE DIRECT®
Aquatic Living Resources 16 (2003) 137–144
Aquatic Living Resources
www.elsevier.com/locate/aquliv

Three-dimensional acoustic mapping and simulation of krill distribution in the Saguenay—St. Lawrence Marine Park whale feeding ground

Yvan Simard [a,*], Denis Marcotte [b], Keyvan Naraghi [b]

[a] *Institut des Sciences de la Mer de Rimouski, Université du Québec à Rimouski, 310 Allée des Ursulines, Rimouski, Québec, Canada G5L 3A1, and Institut Maurice-Lamontagne, Pêches et Océans Canada, C.P. 1000, Mont-Joli, Québec, Canada G5H 3Z4*
[b] *Département des Génies Civil, Géologique et des Mines, École Polytechnique, C.P. Centre-ville, Montréal, Québec, Canada H3C 3A7*

Accepted 10 January 2003

Abstract

Geostatistical conditional simulations are used to get a family of non-smoothed three-dimensional (3D) images of the St. Lawrence krill aggregation from echointegration data at 38 and 120 kHz on a systematic grid of transects. These maps respect the inherent patchiness of krill. Their ensemble gives an histogram of the krill density estimates at any point of the 3D grid, not only the mean density as in kriging. The spatially consistent simulations are conditional to match the observations and their histogram and variogram. The 3D problem is by-passed by transposing to a short series of 2D ones, which simplifies the modelling of the autocorrelation function and has the additional advantage of reducing by a factor of 5 the number of points to simulate. The spatially structured krill density profile is summarised by the first few factors of a principal component analysis, where the variables are the volume backscattering strength at 120 kHz for the integrated vertical bins along the profiles and the observations are the different profiles. The principal component scores are simulated over a 2D-grid and then used to reconstruct the full 3D-image. The method adequately reproduces the histogram, variogram and mean profile of krill density, and cross-validations replicate the observations. It is as precise as an alternative kriging approach to estimate the mean density, but has the additional advantages of requiring less computing time for our particular application. These conditional simulations enable estimating the probability density function of the krill density at any point, an essential information for predator-prey interactions and other ecosystem studies.

Keywords: Acoustics; Conditional simulation; Geostatistics; St. Lawrence estuary; Whale feeding ground

1. Introduction

Oceans are three-dimensional (3D) spaces. Many properties measured in these ecosystems exhibit a structure over a range of scales in space and time (Haury et al., 1978; Mackas et al., 1985). Such structuring plays a fundamental role in ecosystem function from plankton (Steele, 1978) to whales (e.g. Simard et al., 2002). Vertical gradients tend to be several times larger than the horizontal ones. Oceans are also in motion and sampling effectively in time and space can be difficult. Acoustics tools can sample these huge 3D-environments remotely, rapidly and continuously. Acoustics has been used for seafloor mapping and, given sufficient time, a complete high-resolution image of the seabed on continental shelves can be obtained from multibeam sonar imaging. The equivalent for the moving pelagic environment and its drifting or actively mobile content is not possible, nor relevant. At best, acoustic imaging can produce a time-distorted tomography of the pelagic systems, via the assembly of a series of slices through the body of water (e.g. Greene et al., 1998; Stanley et al., 2000). Multibeam sonars can be used to get high-resolution series of slices in close range of a sampling vessel (e.g. Gerlotto et al., 1999). Though this is useful for increasing the information available at small scales, it only slightly enlarges the slice width when we consider the scale of the transects covered by the sampling vessel over what are often very large study areas. Furthermore, because the observation angle varies for each beam of the multibeam sonar, these observations must be interpreted with caution because of the strong directivity patterns of the backscattering from fish or zooplankton targets (Medwin and Clay, 1998). Low frequency sonars could help to enlarge the observation slice width up to kilometres for highly reflective large targets, but

* Corresponding author.
E-mail address: simardy@dfo-mpo.gc.ca (Y. Simard).

doi:10.1016/S0990-7440(03)00026-3

the sampled field then is still only a fraction of the water column, that depends on the propagation characteristics in the medium (Farmer et al., 1999).

To get a best estimate of the 3D-distribution of a resource in large pelagic ecosystems from limited survey transects, the 3D-image must be reconstructed from the series of comparable observation slices, ideally from the same vertical viewing angle because of the sound scattering directivity of the targets. This can be done by 3D-kriging (Chilès and Delfiner, 1999), taking advantage of the strong autocorrelation in acoustic data (e.g. Simard et al., 1993) to estimate the values at unvisited locations between the observed slices[1]. The required anisotropic 3D-variogram is, however, difficult to define with accuracy because it must take into account a gradient along the vertical axis that is very different from those along the horizontal axes in combination with krill patchiness. For example, krill scattering layers (SLs) can extend several tenths of kilometre horizontally, but start and stop abruptly at a scale of metre in the vertical (e.g. Lavoie et al., 2000). An alternative solution is to convert the 3D-problem to a 2D one, by summarising the vertical profiles of observations by a fitted function (e.g. Goulard and Voltz, 1993), and kriging its parameters. The function is then used with the estimated parameter to produce a mean estimate of the studied variable at each node of the series of nodes making the 3D-estimation grid. Since kriging is a smoother, this value does not represent the full range of values that could be observed at a node. This variability (i.e. patchiness) is, however, an important characteristic of the ecosystem, that must be taken into account to understand the interactions between predators and preys in 3D pelagic ecosystems (e.g. Zamon et al., 1996). Any feeding functional response is dependent on prey density. In optimising this function through their feeding strategies, predators must preferably look for the richest densities, not for the mean density. This is particularly true for whales, for which efficient feeding in the ocean is critical (e.g. Acevedo-Gutierrez et al., 2002). Conditional geostatistical simulations (Chilès and Delfiner, 1999) is a spatial approach that can take this relevant local prey density distribution into account, by producing a series of realisations of the grid estimates, from which a probability density function (pdf) of prey density can be computed for each node of the grid. Chilès and Delfiner (1999) define these methods as "spatially consistent Monte Carlo simulations". They produce realistic pictures of spatial variability by introducing an autocorrelated random component in the geostatistical estimation process, which is not done in kriging. Therefore, conditional simulations produce non-smoothed pictures of the reality contrary to kriging estimates. On an average, the same patchiness as that of the unknown reality is expected on the simulation.

In this paper, we apply a 2D-approach and conditional simulations to estimate multiple realisations of the 3D krill aggregation of the Saguenay—St. Lawrence Marine Park, from a series of acoustic echointegration slices. Several species of toothed and baleen whales frequent this traditional feeding ground in summer (Michaud et al., 1997). Understanding the local trophic interaction dynamics that is acting during research surveys requires realistic estimations of the prey fields available to these predators, whose success relies on large amounts of densely concentrated food. The method we adopted here is general and can be easily applied to several other studies, where a multivariate signal has to be generated over a continuous field from spatially structured sparse observations.

2. Material and methods

2.1. Sampling

Sampling was carried out aboard the Canadian Coast Guard Ship "*F.G. Creed*" in the St. Lawrence estuary on 31 July and 1 August 1994, along a regular grid of 10 transects crossing the head of the Laurentian channel (Fig. 1). Sampling procedures are briefly outlined here; details can be found in Simard and Lavoie (1999). The grid was surveyed during daytime only, when the krill SLs were at their daytime depth (Simard et al., 1986) and well separated from fish echoes in the upper water column. CTD profiles and zooplankton samples from 0.28-m^2 Bongo nets were taken at stations along the transects (Fig. 1). Acoustic backscattering coefficient (s_v) data at 120 kHz (3.3° beam) and 38 kHz (10° beam) were acquired from a Biosonics 102 echosounder linked to a computer via a Biosonics ESP A/D interface and the ESP_EI echointegration software, which simultaneously recorded positions from a GPS receiver. At the beginning of the survey, the ambient noise level at the survey speed was recorded for each frequency, with the transducers in listening mode (i.e. not transmitting). ESP_EI software was then set up to only accept echoes, whose voltage exceeded the measured noise level for each vertical stratum. Echointegration (MacLennan and Simmonds, 1992) was done along transects on 5-m vertical strata, from ranges of 2 to 207 m, which included all the krill SLs. Horizontally, echointegration was done every 20 pings (20 s), which corresponded to steps of ~80 m at the survey speed of 8 knots. The acoustic data used hereafter were, therefore, s_v profiles with a vertical resolution of 5 m and spaced every 80 m along transects. The system was calibrated using the standard sphere method for each frequency (Foote et al., 1987).

2.2. Data analysis

The acoustic backscattering coefficient data were cleaned of acoustic interference and the first meter off the bottom was ignored. They were corrected for the absorption (François and Garrison, 1982) and sound speed profile associated to the vertical structure of the water column. The resulting s_v at 120 kHz was used for the present krill biomass simulations,

[1] Introductions to geostatistical methods in fisheries applications can be found in Petitgas (1996) or Rivoirard et al. (2000).

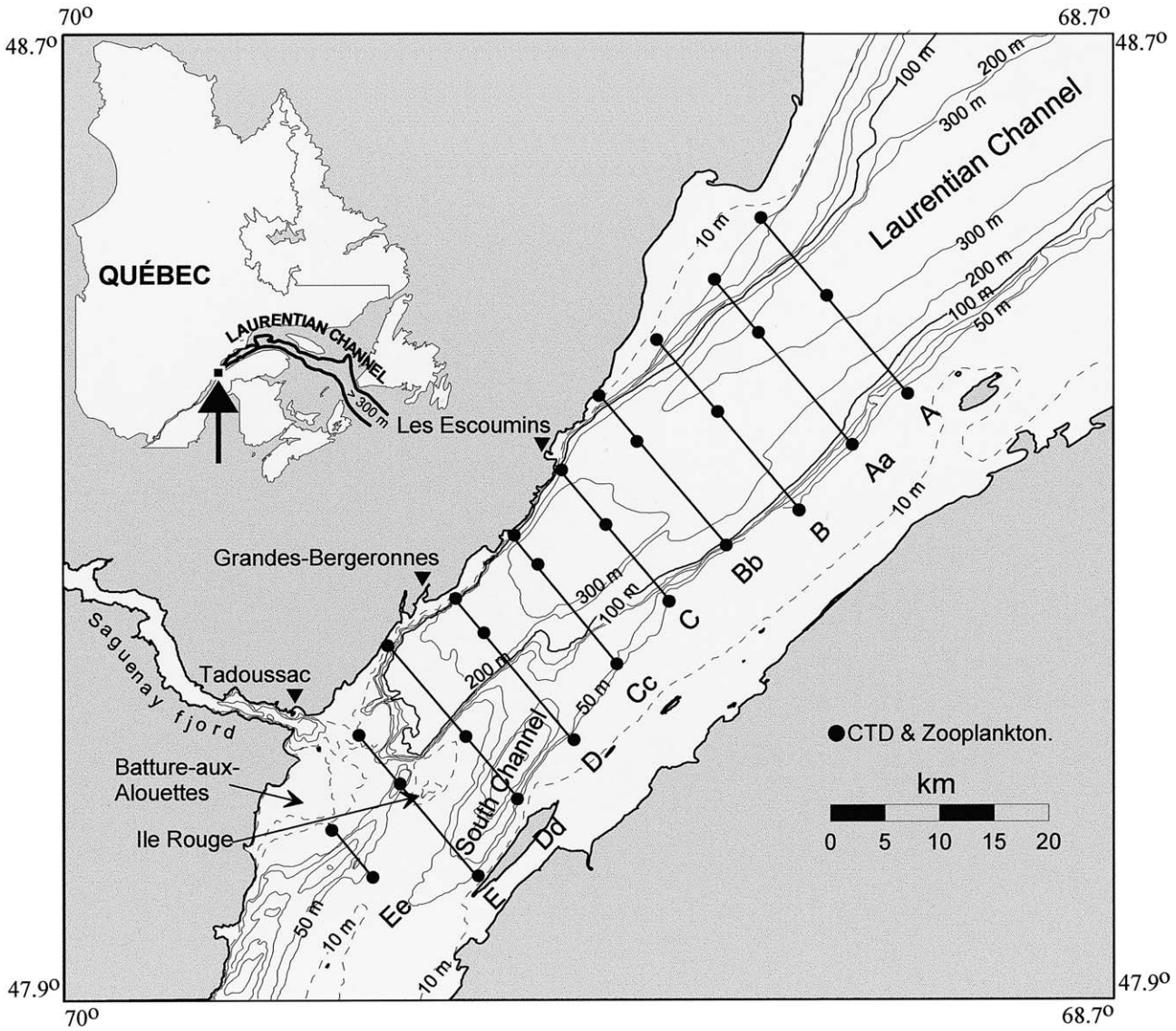

Fig. 1. Map of the study area showing the acoustic transects, and the hydrographic and plankton stations.

after the fish echoes were sorted out using the s_v ratio at the two frequencies (Simard and Lavoie, 1999). The acoustic densities were converted to biomass using a mean target strength of –69 dB g^{-1} (see Simard and Lavoie, 1999). The s_v profiles containing krill in more than 2 strata between the depth limits of the krill SL (ranges of 27–207 m) were used as the basis for the simulation (Fig. 2a, red). The simulation domain was limited to areas, where the bottom depths exceeded 50 m, the observed krill SLs being confined to deeper waters (Fig. 2a–c).

The simulation proceeded in four steps. First, the data were prepared for a principal component analysis (PCA, Lebart et al., 1984), whose output will be used for summarising the s_v profile shapes by a few orthogonal (i.e. uncorrelated) principal components (PCs). Each profile was represented by the 37 s_v values corresponding to the 5–m bin strata, where the krill SL was present. The zeros present on some profiles and the strata below the bottom depth were assigned an artificial small s_v value of 3.16×10^{-9} m^{-1} (or an equivalent volume backscattering strength, $S_v = 10 \log_{10}(s_v) = -85$ dB) to provide complete profiles of 37 values everywhere and to allow for a log transformation prior to the PCA analysis. This artificial s_v value was derived from a simulation study, where different candidate values were tested. The value was selected to ensure a non-biased mean s_v value computed from 100 realisations obtained following the same method as described below. The data were log-transformed to S_v to stabilise the variances, thus, giving a more stable PCA analysis than with the raw data.

Second, a PCA was performed on the centred S_v profiles to reduce the representation of their shapes from initially 37 variables (strata) to 7 orthogonal PCs. The number of significant PCs retained was determined by requiring a minimum of 85% of the total variance be accounted for, by

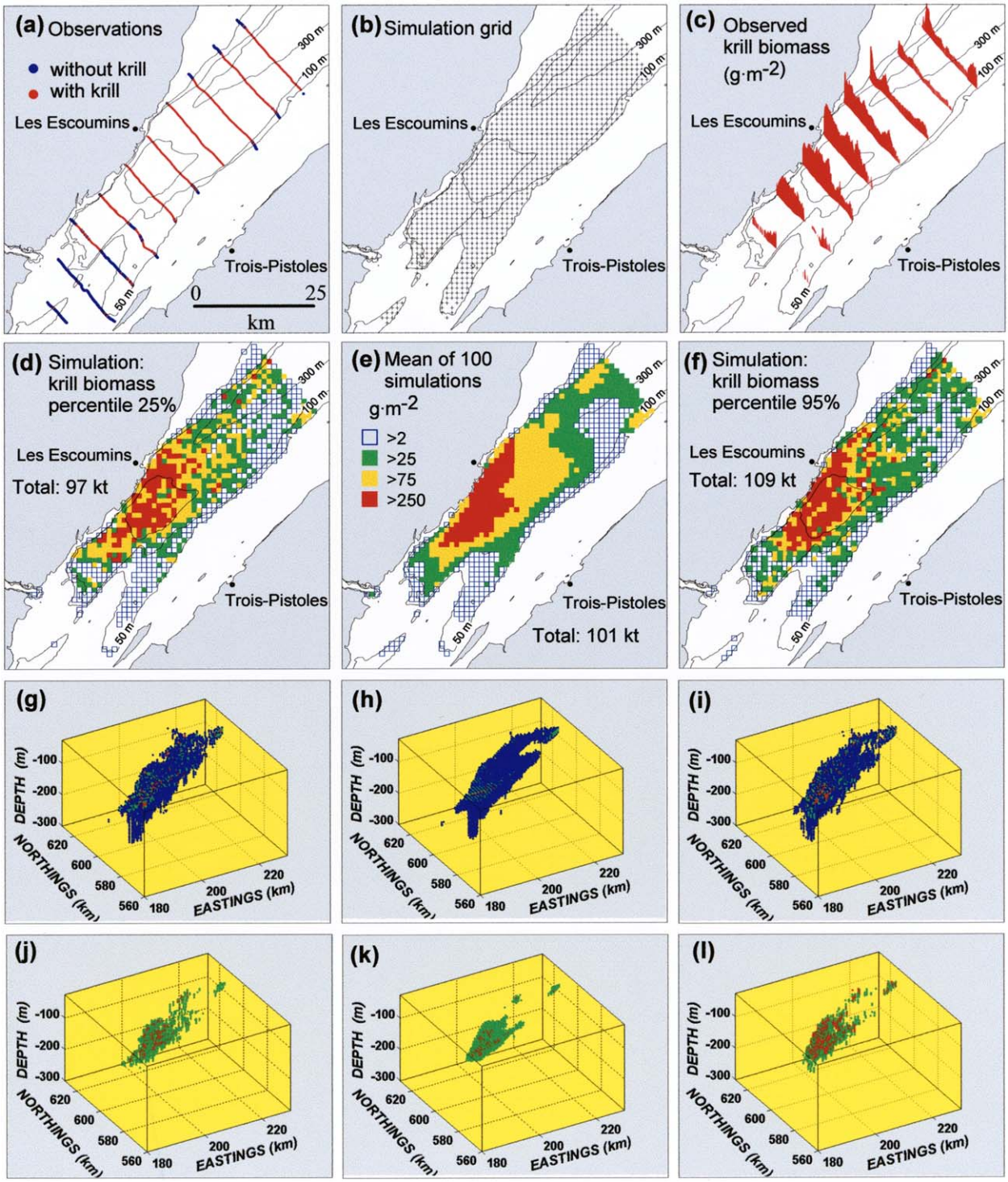

Fig. 2. Simulation of the krill aggregation. Location of the observed acoustic profiles with (red) and without (blue) krill (a), grid nodes used for simulating the S_v profiles (b), observed vertically integrated krill biomass with a square-root symbol height scale (c). Vertically integrated krill biomass maps for a simulation where the total biomass corresponded to the first quartile of cumulated density function of the total biomass of the 100 simulations (d), to the mean of the 100 simulations (e), and to the 95th percentile of the same cumulated density function of the total biomass (f). 3D view of the simulated biomass corresponding to d–f for the richest quartile (g–i) or the richest 5% (j–l) based on the krill concentration cut-offs from the mean of the 100 simulations; the three-colour palette cut-offs being blue, >0.6 gm^{-3}; green, >3.7 gm^{-3}; red, >8.1 gm^{-3}.

examination of the eigenvalues plot searching for a clear break in the slope, and by retaining only the PC scores with the nugget component on the experimental variograms smaller than half the sill.

Third, the scores on the retained PCs were graphically gaussian-transformed (required for the simulation method below) and subjected to geostatistical conditional simulations (Chilès and Delfiner, 1999). Each gaussian-transformed

Table 1
Percentage of variance explained by the first seven PCs and parameters of the anisotropic spherical model [a] fitted to the variograms of the observed PC scores. Directions are geometric degrees, 45° being the channel axis. C_0 is the nugget parameter

PC	% Variance	Direction 1	Dir. 2	a_1	a_2	C_0	C	C/C_0
1	52.5	45°	135°	38.00	14.80	0.154	0.898	5.83
2	11.7	45°	135°	38.00	13.70	0.167	1.288	7.71
3	10.0	45°	135°	12.36	19.96	0.364	0.727	2.00
4	5.7	45°	135°	8.77	7.40	0.320	0.710	2.22
5	3.5	45°	135°	14.80	5.96	0.407	0.639	1.57
6	2.3	45°	135°	7.34	4.40	0.474	0.522	1.10
7	1.7	45°	135°	11.10	5.10	0.451	0.597	1.32

[a] Model: $\gamma(h) = C_0 + \begin{cases} C\left(\frac{3h}{2a} - \frac{1}{2}\left(\frac{h}{a}\right)^3\right), & \text{if } h \leqslant a \\ C, & \text{if } h \geqslant a \end{cases}$

where h is the distance between the observations.

PC score was simulated separately using the covariance matrix decomposition (i.e. LU) method (Cholesky decomposition; Chilès and Delfiner, 1999). The covariance matrix, C, containing the covariances from the vector of the M conditional observation points plus the N points to simulate, is decomposed in a lower triangular matrix L so that $LL' = C$. The matrix L can be partitioned into four different blocks:

$$L = \begin{bmatrix} L_{MM} & 0 \\ L_{NM} & L_{NN} \end{bmatrix} \quad (1)$$

where L_{MM} corresponds to the set of conditioning points, L_{NN} to the set of points to simulate, and L_{NM} to the interaction between the two sets. A vector U, composed of $M + N$ independent $N(0,1)$ variables, completes the linear equation system:

$$\begin{bmatrix} Z_M \\ Z_n \end{bmatrix} = \begin{bmatrix} L_{MM} & 0 \\ L_{NM} & L_{NN} \end{bmatrix} \begin{bmatrix} U_M \\ U_N \end{bmatrix}$$

where Z_M is the conditional data and Z_N is the simulated data. The solution is:

$$\begin{aligned} Z_M &= L_{MM}\, U_M \\ U_M &= L_{MM}^{-1}\, Z_M \\ Z_N &= L_{NM}\, U_M + L_{NN}\, U_N \end{aligned} \quad (2)$$

One advantage of this LU decomposition method is that for computing another realisation of the simulation set Z_N, only the vector U_N of Eq. (2) has to be updated, which allows to realise several simulations without much additional computing cost. The simulation 1-km mesh grid (Fig. 2b) contained 1015 nodes where the bottom depth exceeded 50 m.

Fourth, the simulated gaussian-transformed PCA scores were back-transformed and then used, with the eigenvectors, to reconstruct the centred S_v profiles (Lebart et al., 1984). To insure that the histograms of the simulated and observed S_v are the same, a graphical transform (Chilès and Delfiner, 1999) mapping the simulated cumulative density function (cdf) to the observed cdf was applied.

An alternative to the above procedure, consisting of feeding the PCA with profiles that are limited to the water column and summarised by an equal number of points corresponding to relative (and not absolute) depths, was also tested. Local centring and standardisation of each profile combined with kriging of the mean and the variance in the final step was also explored, but did not performed better than the above global approach.

The accuracy of the method was tested through the following validation tests. First, we checked if the simulation reproduced the main descriptive statistics, the variogram, and the pdf of the observed data. Second, a cross validation at small distances was performed by removing one S_v profile every two profiles and simulating the removed profiles using the remaining profiles as conditional data. Third, the performance at larger distances was checked by randomly picking up 100 conditional observations from a selection of one transect every two transects in the study area and simulating the profiles at 400 randomly chosen observations on the unselected alternating transects. Actual simulation conditions were less severe than those used for this test, the interpolation distances being at most half those of this test. Fourth, the means of the simulated data at the nodes of the 3D grid were also compared to those of a kriging using the same conditional data and the variogram computed for the first PC.

3. Results

The first seven PCs explained 87% of the variance of the S_v profiles (Table 1) and were retained for the simulation. The structural component (C,Table 1) of the corresponding PC scores was always larger than the unresolved variability (C_0,Table 1), up to more than five times for the first two PCs. The simulations closely reproduced the mean and the other distribution statistics of the observations (Table 2). The variograms of the simulated S_v were generally similar to the corresponding S_v, notably for the main krill concentration depth of about 80 m (Fig. 3). The small-distance cross validation showed that the simulations performed almost as well

Table 2
Descriptive statistics of the observed and simulated mean volume backscattering strength (S_v) of the profiles. Computed as acoustic backscattering coefficients (S_v), for each simulation, then averaged and transformed to s_v

Data	*n*	Mean	First quartile	Median	Third quartile	Max
Observed	1368	–70.2	–77.4	–72.8	–68.5	–59.4
Simulated	1015	–71.0	–78.6	–74.8	–69.6	–61.8

as kriging to replicate the observations (Fig. 4a,b). Results of the two approaches of cross validation at large distances were nearly identical (Fig. 4c,d). The 2D-map of the krill biomass obtained from the mean of all simulations (Fig. 2e) was almost identical to that computed by Lavoie et al. (2000, Fig. 9d) from a 2D-kriging. Its total integrated biomass of 101 kt fell within the 95% confidence interval of Simard and Lavoie's (1999) kriging estimate for this survey. The individual simulation having a total biomass equal to that of the first quartile of the total biomass cdf of all simulations (Fig. 2d) presented much more "grain" or patchiness than that of the mean, as expected. The same was true for the simulation corresponding to the 95th percentile of the same cdf (Fig. 2f). This enhanced patchiness of the individual simulations compared to the mean of all simulations (or kriging results not shown) was also evident in 3D (Fig. 2g–l).

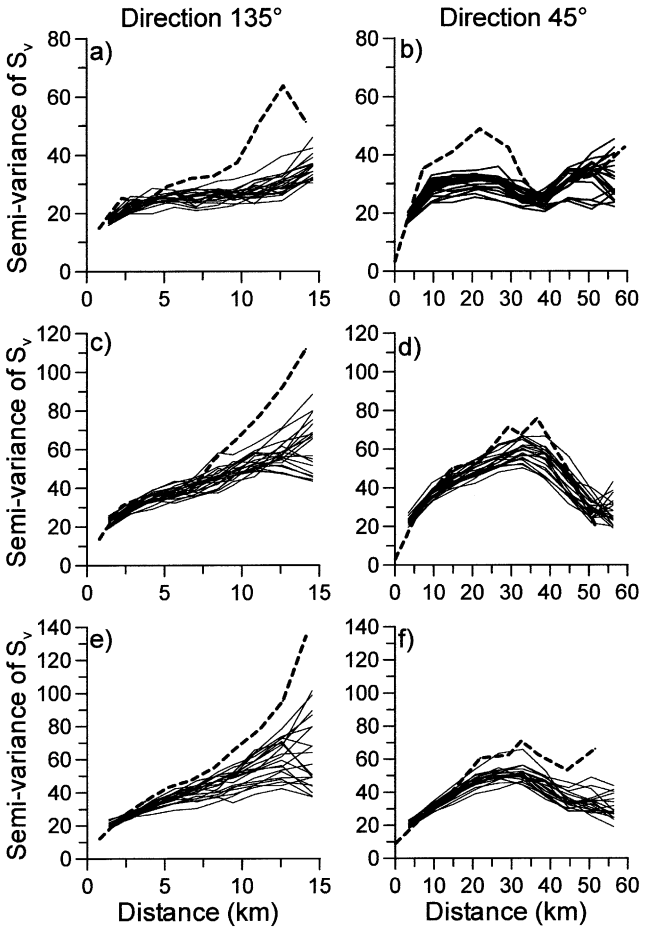

Fig. 3. Comparisons of variograms of simulated S_v for 20 randomly selected simulations (thin lines) with the variograms of observed S_v (bold line) in the transect direction (135°) and along channel (45°) for three depths: 59.5 m (a, b), 79.5 m (c, d), and 99.5 m (e, f).

The mean simulated biomass profile had the same amplitude, envelope and modal depth than the observed one (Fig. 5).

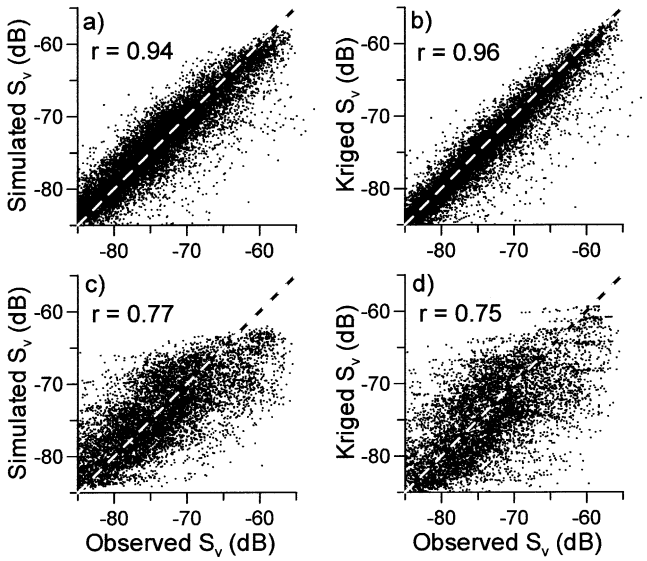

Fig. 4. Comparison between kriged estimates and the mean of 100 simulations with the observations for short distances (along transects) (a, b) and longer distances (to the next transect) (c, d). Lines are $y = x$.

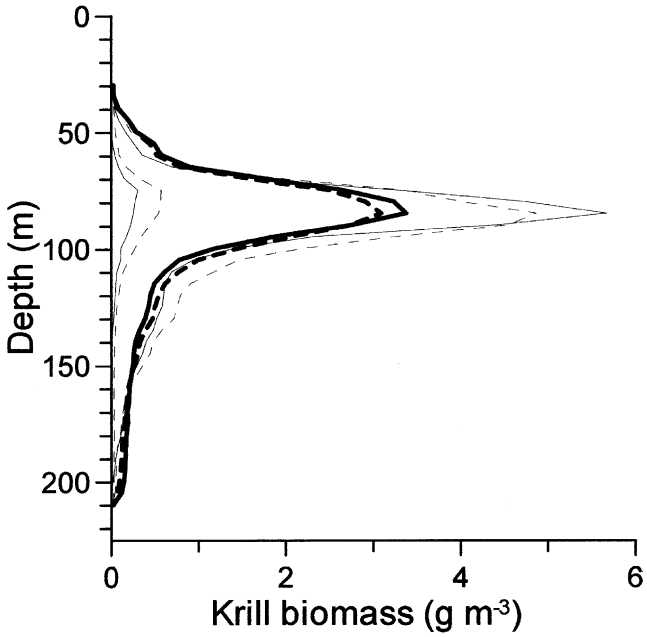

Fig. 5. Comparison of observed (continuous lines) and simulated (dashed lines) krill biomass profiles. Means (bold lines), first and third quartiles (thin lines).

4. Discussion

The proposed 2D approach to solve the difficulty of geostatistically mapping a structured variable in 3D appears to perform relatively well with krill acoustic densities collected along line transects. Coupled with conditional simulations, this approach becomes an efficient way of exploring the space of variability of 3D-structured data, such as the S_v at several acoustic frequencies, or exploitations of such information to generate secondary variables, including taxonomic composition or acoustical description of the bottom. The interest of having a series of realistic simulations instead of only a mean estimate allows for much more possibilities of using the information for better interpretation of the results. For example, 3D-maps of the probability to exceed the given krill density thresholds, an important variable for predator/prey interactions, can be obtained directly from the simulated data. The fraction of the total biomass above this threshold (e.g. exploitable biomass) is another information directly available. Simulations also allow to see realistic pictures of krill patchiness, the distribution of the rich nuggets that predators could detect and exploit, which are totally invisible to alternative smoothing methods. The exploitation of such methods appears, therefore, very useful for helping to understand the actual functioning of our 3D-structured ocean ecosystems.

Though the numerical methods are relatively simple, their applications to actual observed data ask for particular attributes of the data set and require some data conditioning to satisfy the numerical conditions. First, the zero profiles pose problems in defining the simulation field. In our case, the krill aggregation was a continuous cloud and the zero profiles were located at its periphery. It was then simple to limit the simulation grid to the contour of the aggregation. If this had not been the case, the simulation grid nodes would have been to be determined first, from 2D indicator conditional simulations (Chilès and Delfiner, 1999) of the null node locations. Second, the zero part of the profiles and the empty cells below the seafloor need to be filled for performing the PCA. A possible practical solution is to use a relative vertical scale, such as the proportion of the water column, instead of the absolute depth. Though this solution was initially tried, we preferred to work in absolute units because krill are vertically distributed along the depth. This structure is distorted by relative units. Instead, we chose to fill the empty cells of the profiles by a non-biasing low s_v value. This step is the most demanding in terms of computing time. An alternative approach would be to use a transformation that could handle zeros more easily than the log one (e.g. square root, cubic root, Box-transform). Third, the PCs must be spatially uncorrelated among them for all lag distances, not only for zero lag as PCA provides by construction. This is especially important for small distances, such as half the transect spacing. Cross-correlations at larger distance have less impact because the conditioning observations are imposing the larger scale spatial structure, a characteristic of conditional simulations. We checked if the main PCs were cross-correlated over small lag distances and found only low correlations ($r < |0.25|$), often linearly sloping around zero. Our implicit assumption of negligible cross-correlation of PCs was therefore reasonable. Fourth, LU decomposition method of the covariance matrix is limited to small matrices. The size of our data set was at about the limit for this method. For larger data sets (or lower level computers) a solution to this problem, is to partition the study area into adjacent small neighbourhoods and perform the simulation in a sliding window. To prevent the creation of artificial discontinuities between the neighbourhoods, the conditional data for the neighbourhoods can include the simulated data of the preceding neighbourhood (Alabert, 1987). Also, several simulation methods are able to handle large grids (e.g. turning bands, SGS, FFT-MA, etc.; see Chilès and Delfiner, 1999).

References

Acevedo-Gutierrez, A., Croll, D., Thershy, B., 2002. Feeding costs limit dive time in large whales. J. Exp. Mar. Biol. 205, 1747–1753.

Alabert, F., 1987. The practice of fast conditional simulations through the LU decomposition of the covariance matrix. Math. Geol. 19, 369–386.

Chilès, J.-P., Delfiner, P., 1999. Geostatistics: Modeling Spatial Uncertainty. John Wiley and Sons, Inc., New York.

Farmer, D.M., Trevorrow, M.V., Pedersen, B., 1999. Intermediate range fish detection with a 12–kHz sidescan sonar. J. Acoust. Soc. Am. 106, 2481–2490.

Foote, K.G., Knudsen, H.P., Vestnes, G., MacLennan, D.N., Simmonds, E.J., 1987. Calibration of acoustic instruments for fish density estimation: a practical guide. ICES Coop. Res. Rep. No. 144 .

François, R.E., Garrison, G.R., 1982. Sound absorption based on ocean measurements: Part II: Boric acid contribution and equation for total absorption. J. Acoust. Soc. Am. 72, 1879–1890.

Gerlotto, F., Soria, M., Fréon, P., 1999. From two dimensions to three: the use of multibeam sonar for a new approach in fisheries acoustics. Can. J. Fish. Aquat. Sci. 56, 6–12.

Goulard, M., Voltz, M., 1993. Geostatistical interpolation of curves: a case study in soil science. In: Soares, A (Ed.), Geostatistics Troia '92, vol. 2. Kluwer Academic Publisher, Dordrecht, pp. 805–816.

Greene, C.H., Wiebe, P.H., Pelkie, C., Benfield, M.C., Popp, J.M., 1998. Three-dimensional acoustic visualization of zooplankton patchiness. Deep-Sea Res. II. 45, 1201–1217.

Haury, L.R., McGowan, J.A., Wiebe, P.H., 1978. Patterns and processes in the time-space scales of plankton distributions. In: Steele, J.H (Ed.), Spatial Pattern in Plankton Communities. Plenum Press, New York, pp. 277–327.

Lavoie, D., Simard, Y., Saucier, F.J., 2000. Aggregation and dispersion of krill at channel heads and shelf edges: the dynamics in the Saguenay—St. Lawrence Marine Park. Can. J. Fish. Aquat. Sci. 57, 1853–1869.

Lebart, L., Morineau, A., Warwick, K.M., 1984. Multivariate Descriptive Statistical Analysis: Correspondence Analysis and Related Techniques for Large Matrices. John Wiley and Sons, New York.

Mackas, D.L., Denman, K.L., Abbott, M.R., 1985. Plankton patchiness: biology in the physical vernacular. Bull. Mar. Sci. 37, 652–674.

MacLennan, D.N., Simmonds, E.J., 1992. Fisheries Acoustics. Chapman and Hall, London.

Medwin, H., Clay, C.S., 1998. Fundamentals of Acoustical Oceanography. Academic Press, New York.

Michaud, R., Bédard, C., Mingelbier, M., Gilbert, M.C., 1997. Les activités d'observation en mer des cétacés dans l'estuaire maritime du Saint-Laurent 1985–1996 : une étude de la répartition spatiale des activités et des facteurs favorisant la concentration des bateaux sur les sites d'observation. GREMM, 108 de la Cale Sèche, Tadoussac, Québec G0T 2A0. Final report to Parks Canada, Canadian Heritage Department, Ottawa 17 p.

Petitgas, P., 1996. Geostatistics and their applications to fisheries survey data. In: Megrey, B.A., Mokness, E (Eds.), Computers in Fisheries Research. Chapman and Hall, UK, London, pp. 113–142.

Rivoirard, J., Simmonds, J., Foote, K.G., Fernandes, P., Bez, N., 2000. Geostatistics for Estimating Fish Abundance. Blackwell Science, Oxford.

Simard, Y., Lacroix, G., Legendre, L., 1986. Diel vertical migrations and nocturnal feeding of a dense coastal krill scattering layer (*Thysanoessa raschi* and *Meganyctiphanes norvegica*) in stratified surface waters. Mar. Biol. 91, 93–105.

Simard, Y., Lavoie, D., 1999. The rich krill aggregation of the Saguenay—St. Lawrence Marine Park: hydroacoustic and geostatistical biomass estimates, structure, variability and significance for whales. Can. J. Fish. Aquat. Sci. 56, 1182–1197.

Simard, Y., Lavoie, D., Saucier, F.J., 2002. Channel head dynamics: Capelin (*Mallotus villosus*) aggregation in the tidally-driven upwelling system of the Saguenay—St. Lawrence Marine Park's whale feeding ground. Can. J. Fish. Aquat. Sci. 59, 197–210.

Simard, Y., Marcotte, D., Bourgault, G., 1993. Exploration of geostatistical methods for mapping and estimating acoustic biomass of pelagic fish in the Gulf of St. Lawrence: size of echointegration unit and auxiliary environmental variables. Aquat. Living Resour. 6, 185–199.

Stanley, R.D., Kieser, R., Cooke, K., Surry, A.M., Mose, B., 2000. Estimation of a widow rockfish (*Sebastes entomelas*) shoal off British Columbia, Canada as a joint exercise between stock assessment staff and the fishing industry. ICES J. Mar. Sci. 57, 1035–1049.

Steele, J.H., 1978. Spatial Pattern in Plankton Communities. Plenum Press, New York.

Zamon, J.E., Greene, C.H., Meir, E., Demer, D.A., Hewitt, R.P., Sexton, S., 1996. Acoustic characterization of the three-dimensional prey field of foraging chinstrap penguins. Mar. Ecol. Prog. Ser. 131, 1–10.

Available online at www.sciencedirect.com
SCIENCE DIRECT®
Aquatic Living Resources 16 (2003) 145–157
Aquatic Living Resources
www.elsevier.com/locate/aquliv

Effect of external factors (environment and survey vessel) on fish school characteristics observed by echosounder and multibeam sonar in the Mediterranean Sea

Marc Soria [a,*], Tarub Bahri [b], François Gerlotto [c]

[a] *IRD, BP 172, 97492 Sainte-Clotilde cedex, France*
[b] *FAO-MedSudMed, via Luigi Vaccara, 61, 91026 Mazara del Vallo (TP), Italy*
[c] *IRD, Instituto de Fomento Pesquero (IFOP), Huito 374, Casilla 8-V, Valparaiso, 5a Region, Chile*

Accepted 5 February 2003

Abstract

The size of pelagic fish schools depends on several parameters related to internal factors such as species, number of fish, fish swimming speed and physiological status and to external factors, such as hydrological factors and presence of predators. In order to better understand these relations, results coming from echosounder and multibeam sonar databases are analysed. Field data are collected during four acoustic surveys in the Mediterranean Sea in two different areas (Catalan and Adriatic Seas). The analysis shows differences between the two areas regarding size and position in the water column: schools are deeper and their mean size is lower in the Catalan Sea in comparison with Adriatic Sea. The differences in size of schools are mainly related to differences in school length. Moreover, the elongation of schools seen with the sonar is greater than one and half higher in the Adriatic Sea than in the Catalan Sea, whereas one would expect similar values for the two areas. The results are discussed in terms of environmental influence, avoidance reaction and acoustic capabilities of both tools. A hypothesis is proposed: the variation of school length and consecutively the variation of the correlated dimensions is first related to the strength of the avoidance reaction in front of the vessel and this effect can be reinforced depending on the environmental conditions. The model takes into account the effect of the boat, the vertical constraints undergone by the schools, and the internal requirements of the schools, such as the necessity for fish to keep visual contacts and the cohesion of the group.

Keywords: Acoustic; Multibeam sonar; Echosounder; Fish school behaviour; Avoidance; Environment

1. Introduction

Spatial dynamics are of paramount importance to the understanding of the forces governing population dynamics. In the particular case of fish stocks, studying the factors inducing and maintaining the aggregation of fish within schools could be helpful to better understand the spatial heterogeneity of small pelagic fish populations and the mechanisms that lead to the particular mode of distribution of schools (Pitcher et al., 1996; Mackinson, 1999; Fréon and Misund, 1999; Booth, 2000). Moreover, schooling behaviour is a powerful mechanism to sort fish by length (Fréon, 1984, 1985), an improved understanding of the mechanisms driving space-time variations in school size should greatly improve the estimation of demographic parameters. According to previous investigations, the size and the shape of pelagic fish schools depend on several parameters related to internal and external factors. Among the internal factors, the most commonly quoted are the species (Partridge et al., 1980; Misund, 1993a; Maes and Ollevier, 2002), the swimming speed or the body length of fish (Hara, 1987; Peukhuri et al., 1997; Dagorn et al., 1997; Hoare et al., 2000), the foraging behaviour (Pitcher and Partridge, 1979; Pitcher and Parrish, 1993; Mackinson et al., 1999) or the physiological status (Morgan, 1988; Robinson and Pitcher, 1989; Robinson, 1995). With regard to the external factors, related literature reports the influence of the stock abundance (Misund, 1993b; Petitgas and Lévénez, 1996; Petitgas et al., 2001), the interactions between species like the presence of predators (Fréon et al., 1992; Parrish, 1992; Krause and Godin, 1995; Pitcher et al., 1996) or the trophic competitors (Massé et al., 1996),

* Corresponding author.
E-mail address: soria@univ-reunion.fr (M. Soria).

doi:10.1016/S0990-7440(03)00025-1

the environmental conditions such as thermocline depth (Swartzman et al., 1994), the food availability and the food density (Nøttestad et al., 1996) or the specific disruptive events like strong gales (Scalabrin and Massé, 1993) or the arrival of a boat (Olsen et al., 1983; Gerlotto and Fréon, 1992). Finally, an important phenomenon must be pointed out: the avoidance behaviour of the schools, which has an impact on factors such as catchability and abundance estimates. The recent development of 3D acoustic technology might lead to a better accuracy of school size estimations and to a better understanding of adaptation mechanisms of schools to local variations (Gerlotto et al., 1999; Misund and Coetzee, 2000; Mackinson et al., 1999). In order to study this issue, we analysed the morphological and spatial characteristics of schools measured by echosounder and multibeam sonar during acoustic surveys in relation to the external conditions measured in the near field of these schools. We focus on both environmental changes occurring during the day in the vertical plane (thermocline, halocline and chlorophyll concentration) and local perturbations induced by the vessel. Data composed of two species (sardine and anchovy). Two surveys were conducted during successive years (1994, 1995), using the same research vessel in two different areas of the Mediterranean Sea showing different environmental conditions. Based on our database and on previous studies (Bahri and Fréon, 2000), the object of this paper is to compare the school characteristics in these two areas, measured with two acoustic devices, so as to test the hypothesis that the differences are related to environmental conditions and to the impact of the vessel.

2. Materials and methods

2.1. Survey designs

The surveys were carried out during 1994 and 1995 in Catalan Sea (39–41°N/0–2°E) during spring, and in Northern Adriatic Sea (43°30'–45°30'N/12°15'–13°30'E) at the end of summer (Fig. 1). In Catalan Sea, the studied area is characterized by a wide continental shelf (30–40 nmi wide by 90 nmi long) and receives in its northern part freshwater from Ebra River. Two back-to-back coverages of the zone were performed during each of the two cruises. In the North Adriatic, the area includes the plume of the Pô River characterized by turbid freshwater. A single coverage was performed during each of the two cruises. The surveys were all performed aboard the R/V *García del Cid*, in the framework of the European programme T-ECHO (AIR1 CT92 0314). For both zones, the vessel's track was designed as parallel transects separated by 7 nmi, roughly perpendicular to the coastline (from 15 to 100 m isobath). Vessel speed was about 5–7 knots. A CTD cast every 7 nmi was performed.

2.2. Acoustic instruments

The echo-integration was performed utilizing a 38 kHz dual beam echosounder BioSonics operating at 2 s ping rate

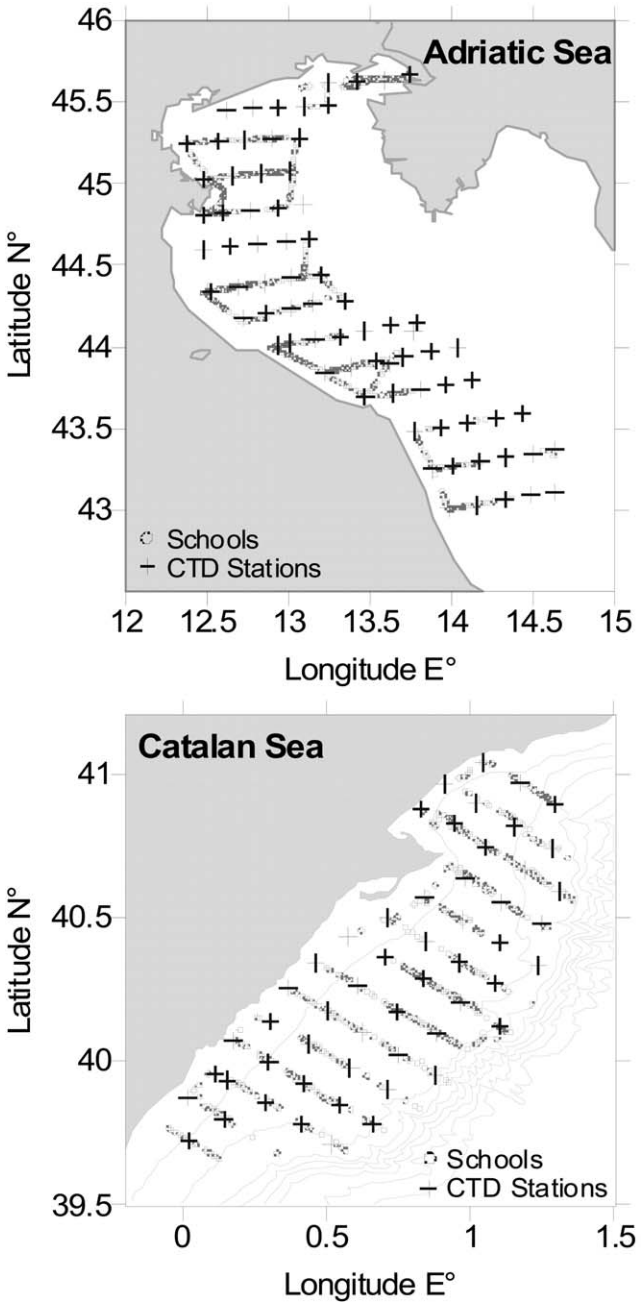

Fig. 1. Sampling design in the areas surveyed during the T-ECHO Project (50 m isobaths are shown in Catalan Sea).

and 0.4 ms pulse rate. The beam width was 10° between the –3 dB points on the narrow beam. The transducer was mounted on a V-fin body, towed at 4–6 m depth. The sonar recordings were made by a 455 kHz multibeam sonar Reson SEABAT 6012 with a pulse length of 0.06 ms and with a total receiving beam angle of 90° (60 beams of 1.5° each) in the vertical plane and 21° in the perpendicular direction. The 60 beams were simultaneously updated seven times per second using the 100 m range. The efficient range was 80 m due to the background noise. The sonar was mounted on a vertical pipe along the vessel. The transducer was at 4 m depth and oriented transversally to the boat in order to scan the side

of the vessel route and exhaustively explore the water volume (Bahri et al., 1997; Soria et al., 1997; Gerlotto et al., 1999).

2.3. Databases

2.3.1. Schools

An acoustic data processing system, INES-Movies-B (Weill et al., 1993; Diner et al., 1994), was connected to the echosounder and allowed for the extraction of acoustical and morphological characteristics of schools. Thresholds, corrections and filtering used in this analysis were chosen empirically in order to take into account the specific acoustical conditions met during the surveys.

According to several authors (Kieser et al., 1993; Fréon et al., 1996; Patty, 1996; Scalabrin et al., 1996; Bahri, 2000; Bahri and Fréon, 2000), we defined an acoustic pelagic school using the following four settings.

(1) For echosounder, a school was defined as a set of pings having amplitude values above the processing threshold. The value of this threshold was chosen in order to avoid possible detections through the side lobes of the acoustic beam. Depending on the background noise, the value was ranged between 50 and 100 mV. The samples must also satisfy a contiguity law, both for vertical and horizontal axes.

(2) INES-Movies-B was set with the following thresholds: successive pings > 3, signal digital sampling units (height 10 cm) > 30, backscattering energy > 100 (in mV^2). These thresholds were empirically chosen in order to discriminate individual echoes from patches on the echogram.

(3) As during night time, fish tend to disperse in layers and few schools were observed, only daytime data were taken into account. Dawn and dusk have not been included in the database. According to Fréon et al. (1996) and Beare et al. (2002), school formation and school dispersion dynamics during these periods are very specific. Diffuse layers observed during daytime, very likely containing a mixture of plankton and fish, have been discarded from the school dataset on the basis of length and density criteria.

(4) The minimum area and volume of a school were set, respectively, to 5 m^2 and 5 m^3. Echoes smaller than 2 m long, 2 m wide and 2 m high were eliminated from the datasets. Since we considered that pelagic fish schools in contact with the bottom had a greater vertical dimension than demersal species schools, a school was considered as being pelagic when the distance between the seabed and the top of the school was greater than or equal to 6 m.

Due to the lack of calibration procedure of the sonar, neither precise absolute values of the echo-signal nor comparable inter-survey relative measurements could be provided. Therefore, the morphological parameters were the only usable data, they were measured manually on the video screen in our laboratory, after the survey (Soria et al., 1996). The school descriptors are listed (Appendices 1 and 2). School size corrections were based only on nominal beam opening, despite the low accuracy of this type of correction (Diner, 2001). This correction still provided negative length values for few schools that were removed from the database.

2.3.2. CTD data

In addition to the collection of acoustic data, vertical profiles of hydrological data were also collected during CTD stations. In order to analyze relationships between school characteristics and environmental parameters, and because of the inertia of environmental characteristics of the water column, each school was associated to the closest CTD cast. The measured values were: thermocline depth, halocline depth, first fluorescence peak depth and second fluorescence peak depth, we considered both absolute and relative depths (in percentage relative to the bottom depth). We calculated the vertical distance between the fish schools and the thermocline, the halocline and the fluorescence peaks, and we assigned either positive or negative sign, depending on whether the school is above (positive distance) or below (negative distance). Spatio-temporal descriptors were also attributed to each school (longitude, latitude, date and time, vessel speed, bottom depth).

2.3.3. Biological sampling

Biological sampling was also performed, using pelagic trawls, in order to identify fish species and size composition. The main species were sardine (*Sardina pilchardus*) and anchovy (*Engraulis encrasicolus*). The two occasional species were the gilt sardine *Sardinella aurita* in the Catalan Sea and the sprat *Sprattus sprattus* in the Adriatic Sea (Bahri and Fréon, 2000).

2.4. Statistical analysis

The comparison between areas and between acoustic tools of the main school descriptors was done using a *t*-test for independent samples by groups.

A principal component analysis (PCA) was performed in order to reduce the number of variables and to identify components, which best explain the observed variability, thereby making it possible to describe differences between the geographical areas. The analysis was performed for each acoustic device. A varimax-normalized rotation was applied in order to maximize the variance. Eigenvalues were calculated and factor coordinates of variables were plotted.

In order to evaluate the contribution of environmental variables to the variability of the school size (see results), a multiple ANOVA was performed on sonar and echosounder data. Since the effect of the predictors on the dependent variable may not be linear in nature, relationships cannot adequately be summarized by a simple linear equation, and categorical predictor variables were then computed. Effects for these variables are represented using the sigma-restricted parameterization. The backward stepwise method was used to select the best model. Intercept is included in the model. In addition to environmental variables, the vessel speed and the lateral distance of the school to the boat were taken into account at the initial step of the process.

Table 1
Summary statistics of survey characteristics

Survey	Covered distance (nmi)	Sonar		Echosounder	
		Number of schools	School density (Nb nmi^{-1})	Number of schools	School density (Nb nmi^{-1})
Catalan94	534	380	0.71	307	0.58
Catalan95	595	158	0.27	310	0.52
Total Catalan	1129	538	0.48	617	0.55
Adriatic94	303	333	1.10	87	0.29
Adriatic95	298	599	2.01	156	0.52
Total Adriatic	601	932	1.55	243	0.40
Total	1730	1470	0.85	860	0.50

3. Results

3.1. Survey characteristics

General survey characteristics are indicated (Table 1). First, we noted a difference between the density of schools recorded by the sonar in Adriatic Sea in 1994 and 1995 (respectively, 1.1 and 2 school nmi^{-1}). This difference can be partly due to the change in the image smoothing rate (from 4 to 2). Nevertheless, this interpretation is minimized by the fact that similar results are obtained with the echosounder (0.3 and 0.5 school nmi^{-1}, respectively). Since the sonar has a greater sampling area, the number of schools was expected to be higher than echosounder schools. This is not the case in Catalan Sea: differences are surprisingly weak in 1994 (Nb_{sonar} = 380, $Nb_{echosounder}$ = 307) and in inverse order in 1995 (Nb_{sonar} = 158, $Nb_{echosounder}$ = 310). On the one hand, this could be due to a lower reception gain of the sonar in 1995 in comparison with 1994 (4 vs. 5); this, implies that the size of schools in 1995 should be smaller than in 1994 and that a lower number of small schools should be detected in 1995 in comparison with 1994. On the other hand, the differences in detection thresholds and acoustic properties of the echosounder and the sonar, imply that the sonar does not detect small schools and therefore underestimates the number of schools (MacLennan and Simmonds, 1992; Misund and Coetzee, 2000). This last hypothesis is confirmed by the analysis of morphological characteristics of schools detected in Catalan Sea. The mean size of schools, recorded in Catalan Sea by the sonar in 1994, is similar to those recorded in 1995 (e.g. on an average: area in 1995 = 63 m^2 and area in 1994 = 64.6 m^2; t-value = 0.98, P = 0.32), whereas the mean size of schools, recorded by the echosounder in 1995, is smaller than those recorded in 1994 (mean area = 195 m^2 in 1995, and mean area = 355 m^2 in 1994; t-value = 9.4, $P < 0.0001$). Moreover, mean school sizes of schools recorded by the echosounder in Catalan Sea are higher than mean school sizes of schools recorded with the sonar (e.g. mean $length_{echosounder}$ = 24.5 m and mean $length_{sonar}$ = 9.7 m; t-value = –18.5, $P < 0.001$). Therefore, the data cannot be compared between years and acoustic device. The analysis was performed separately on the two database, and the years were not take into account.

3.2. Morphological and spatial characteristics of schools and environmental parameters

Table 2 shows, for each acoustic device, the results of the comparison between the two areas for selected variables describing morphological and spatial characteristics of schools and environmental parameters. Student t-tests reveal significant differences between the areas for all the descriptors. Regarding morphological parameters, the difference of school size recorded by the sonar is mainly dependent on the variation of the school length. Moreover, the mean school length is significantly higher in Adriatic Sea than in Catalan Sea. This difference is also observed with the echosounder. The other parameters are significantly different, even though they show less striking results. The most important result concerns the elongation (ratio length/width) of schools recorded with the sonar. The mean value is twice higher in Adriatic Sea than in Catalan Sea, whereas similar values were expected. The value of this ratio was expected to be 1. This is not observed in Adriatic Sea, where the average value is 1.5, which means that in this area, schools are in average more or less half longer than wide. Regarding external factors, mean bottom depth of Adriatic Sea is lower than in Catalan Sea. This induces differences between the means of related factors, such as the school depth and vertical distance between the schools and the thermocline, the halocline or the depth of the fluorescence peaks. The comparison of the mean relative depth of the schools indicates that schools in Adriatic Sea tend to occupy the upper part of the water column compared to those of Catalan Sea. The mean lateral distance to the boat might reflect the horizontal avoidance reaction of the fish to the vessel. This distance is significantly greater in Adriatic Sea than in Catalan Sea. Moreover, the vessel sailed faster in Adriatic Sea than in Catalan Sea.

3.3. Principal component analysis

The PCA of the correlation matrix allows for the description of the linear interactions between descriptors of schools and environmental parameters. Analysis of echosounder data (Table 3) showed that the variables, describing school characteristics, are grouped into three sets (morphological, acoustical and environment-related descriptors). Respec-

Table 2
Means of selected variables describing morphological and spatial characteristics of schools and environmental parameters for each area and each acoustic tool, *P* value is the level of significance of student *t*-test

Variables	Sonar			Echosounder		
	Catalan Sea	Adriatic Sea	$P < 0.05$	Catalan Sea	Adriatic Sea	$P < 0.05$
Nb School	538	932		617	243	
Boat speed (knot)	6.6 ± 0.1	6.7 ± 0.1	*	6.3 ± 0.1	6.5 ± 0.2	*
Bottom depth (m)	60 ± 4	27 ± 2	*	78 ± 4	36 ± 4	*
School depth (m)	29 ± 3	11 ± 1	*	53 ± 4	18 ± 4	*
Relative depth of the school (%)	50 ± 4	36 ± 3	*	67 ± 3	46 ± 5	*
Length (m)	10 ± 2	18 ± 2	*	25 ± 3	29 ± 6	*
Height (m)	8 ± 1	6.2 ± 0.5	*	12 ± 1	9 ± 1	*
Ratio length/height	1.6 ± 0.3	3.3 ± 0.5	*	2.4 ± 0.2	3.5 ± 0.6	*
Area (length × height) m^2	64 ± 16	95 ± 17	*	274 ± 69	252 ± 87	*
Thermocline depth (m)	12 ± 1	12 ± 1	*	13 ± 1	16 ± 2	*
Halocline depth (m)	19 ± 3	9 ± 1	*	20 ± 3	12 ± 2	*
First fluorescence peak depth (m)	6 ± 1	8 ± 1	*	6 ± 1	8 ± 1	*
Second fluorescence peak depth (m)	38 ± 2	24 ± 2	*	44 ± 2	27 ± 4	*
Relative depth of the thermocline (%)	22.3 ± 2.3	42.8 ± 2.8	*	19.2 ± 2.4	44.3 ± 4.8	*
Relative depth of the halocline (%)	31.8 ± 3.9	28.9 ± 2.8	*	27.8 ± 3.3	30.8 ± 4.3	*
Relative depth of the first fluorescence peak (%)	11.7 ± 2.4	20.7 ± 2.6	*	8.3 ± 1.5	21.3 ± 4.0	*
Relative depth of the second fluorescence peak (%)	62.5 ± 2.6	75.0 ± 2.3	*	58.9 ± 2.7	71.7 ± 4.9	*
Distance to the thermocline (m)	–17 ± 3	2 ± 1	*	–40 ± 4	–2 ± 3	*
Distance to the Halocline (m)	–10 ± 4	–1 ± 1	*	–33 ± 5	–6 ± 3	*
Distance to the first fluorescence peak depth (m)	–23 ± 3	–3 ± 1	*	–47 ± 4	–9 ± 4	*
Distance to the second fluorescence peak depth (m)	9 ± 3	11 ± 2	*	–9 ± 4	9 ± 3	*
Integrated back-scattered energy (relative value)				131 ± 67	684 ± 317	*
Volume reverberation index (dB m^{-3})				–54 ± 1	–40 ± 2	*
Roughness				1.4 ± 0.03	1.4 ± 0.04	*
Perimeter (m)				196 ± 57	147 ± 49	*
Width (m)	14 ± 1	14 ± 1	NS			
Volume (m^3)	729 ± 267	1 291 ± 394	*			
Ratio length/width	0.8 ± 0.1	1.4 ± 0.2	*			
Ratio width/height	2.1 ± 0.3	2.7 ± 0.3	*			
Lateral distance to the boat (m)	34 ± 3	42 ± 2	*			

tively to Adriatic and Catalan Seas, the first component explained 42% and 49% of the total variance, the second component 19% and 18% and the third component 14.5% and 16%. In both areas, the first component is highly correlated with the environmental-related descriptors, the second component to morphological descriptors, and the third to acoustical characteristics of schools associated with the roughness. This result indicates that the morphological and acoustical characteristics (related to internal density and biomass) of schools are independent from the variations of environment-related parameters. Nevertheless, the PCA allows for a classification according to the environmental conditions measured near the schools. Moreover, the factor coordinates of the schools were plotted for each geographical area, according to the two components representing environmental conditions and school morphology. Variations along

Table 3
Factor loadings of the principal components extracted from the echosounder data set and percents of variance explained

Class of descriptors	Variable	Factor loadings (varimax-normalized)					
		Adriatic Sea; Nb = 243			Catalan Sea; Nb = 617		
		Factor 1	Factor 2	Factor 3	Factor 1	Factor 2	Factor 3
Environmental-related descriptors	Relative depth of the school	**0.82**	–0.29	0.05	**0.81**	–0.42	0.13
	Distance to the thermocline	**0.96**	–0.03	0.07	**0.94**	0.05	0.15
	Distance to the halocline	**0.95**	–0.04	0.09	**0.88**	0.15	0.23
	Distance to the first fluorescence peak	**0.94**	0.04	0.20	**0.94**	0.04	0.20
	Distance to the second fluorescence peak	**0.61**	–0.39	–0.13	**0.92**	0.06	0.23
Acoustic descriptors	Integrated back-scattered energy	–0.11	0.57	**–0.68**	–0.16	0.31	**–0.92**
	Volume reverberation index	–0.18	–0.07	**–0.75**	–0.19	–0.09	**–0.94**
Morphological descriptors	Roughness	–0.05	0.29	**0.81**	0.22	0.25	**0.58**
	Height	–0.02	**0.81**	0.12	–0.21	**0.85**	0.03
	Length	–0.19	**0.79**	0.09	0.30	**0.82**	0.03
	Percentage of inertia	41.7	19.3	14.6	49.4	17.7	16.2

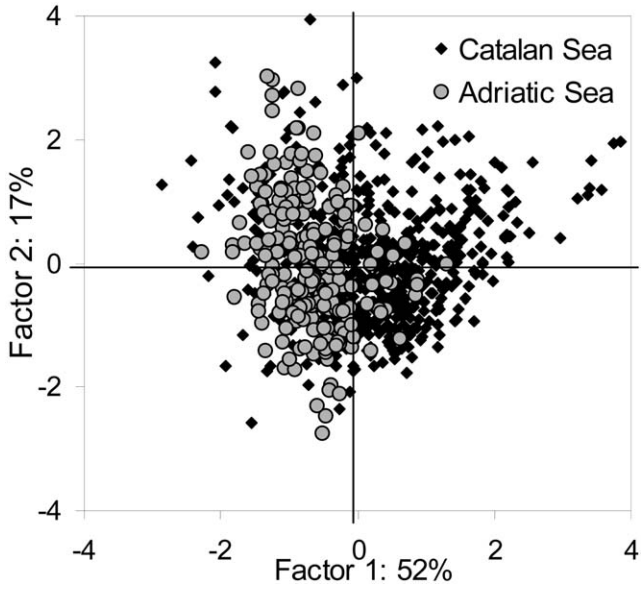

Fig. 2. Scatter plots of the schools detected in both geographical area and for echosounder, according to the two components representing environmental conditions (factor 1) and school morphology (factor 2).

the horizontal axe induced two separated clouds of points (Fig. 2), which means that the first component discriminates the two geographical areas. Concerning sonar school data, the main result is similar to the one obtained with echosounder data: morphological characteristics of schools are independent of environmental parameters. Nevertheless, the factor coordinates of the schools of each geographical area, plotted on the first plane, induced two superposed clouds of points.

3.4. Multiple analysis of variance

Results of analysis on sonar and echosounder are shown (Tables 4 and 5). The variables explaining the variance of the school length are similar in Adriatic and Catalan Seas. They regard parameters related both to the influence of the vessel (vessel speed and lateral distance to the boat) and to the vertical stratification of the water column (principally parameters related to the thermocline and the halocline). Nevertheless some differences appear. First, in Catalan Sea the most important variables of the model are: the vessel speed, the distance of schools to the thermocline or the relative depth of the thermocline and the relative depths of the first and second fluorescence peaks. In Adriatic Sea, the most important variables of the model are: the lateral distance to the boat, the distances of the schools to the halocline and to the second fluorescence peak and the relative depths of the first and second fluorescence peaks. These variables enter both in the sonar and echosounder models. Secondly, the most important difference between sonar and echosounder models is that variables related to the seabed (bottom depth, relative depth of schools and altitude) have significant influence on the length of schools recorded with the echosounder, whereas this influence is not marked on the length of schools recorded with the sonar. A consequence of this influence is a higher multiple correlation coefficient for echosounder model than for sonar model (Tables 4 and 5). However, despite the low values shown by the sonar model, statistical analysis suggests relations between the size of fish schools and vertical distribution of schools, strength of the vertical stratification of the water column and intensity of the vessel perturbation.

In order to visualize the results of the MANOVA, we drew the 2D-categorized box plots of the school mean length vs. the relative school depth, the lateral distance to the boat, and the vessel speed (Fig. 3), the distances of the schools to the thermocline, the halocline and the second fluorescence peak (Fig. 4). Three conclusions can be drawn: (i) in both areas, the higher is the vessel speed, the greater is the school length (Fig. 3c); (ii) the schools close to the surface or above the thermocline, the halocline and the depth of the second fluorescence peak are longer than those far from the surface or below the thermocline, the halocline and the depth of the second fluorescence peak (Figs. 3a and 4); (iii) in Adriatic

Table 4
Results of the MANOVA performed on sonar data. Contributions of variables to the variability of the school length in Adriatic and Catalan Seas

	Sonar				
	Sum of squares	d.f.	Mean square	F	*P*
Catalan Sea (r^2 = 0.17)					
Intercept	402.6	1	402.6	4993	* * *
Vessel speed	1.70	3	0.57	7.02	* * *
Distance to the thermocline	2.87	9	0.32	3.95	* * *
Relative depth of the first fluorescence peak	1.93	9	0.21	2.67	* *
Relative depth of the second fluorescence peak	2.15	9	0.24	2.97	* *
Error	40.64	504	0.08		
Adriatic Sea (r^2 = 0.20)					
Intercept	74.4	1	74.4	682	* * *
Lateral distance to the boat	5.39	9	0.60	5.49	* * *
Distance to the Halocline	3.60	9	0.40	3.66	* * *
Distance to the second fluorescence peak	3.09	9	0.34	3.15	* *
Relative depth of the first fluorescence peak	1.86	8	0.23	2.13	*
Relative depth of the second fluorescence peak	1.98	7	0.28	2.59	*
Error	67.06	614	0.11		

Table 5
Results of the MANOVA performed on echosounder data. Contributions of variables to the variability of the school length in Adriatic and Catalan Seas

	Echosounder				
	Sum of squares	d.f.	Mean square	F	*P*
Catalan Sea (r^2 = 0.48)					
Intercept	873.2	1	873.2	31904	* * *
Vessel speed	0.48	3	0.16	5.87	* * *
Relative depth of the school	1.40	9	0.16	5.67	* * *
Relative depth of the thermocline	1.05	9	0.12	4.27	* * *
Relative depth of the halocline	0.49	9	0.05	2.00	*
Relative depth of the first fluorescence peak	0.52	9	0.06	2.09	*
Relative depth of the second fluorescence peak	1.37	9	0.15	5.56	* * *
Altitude	0.96	9	0.11	3.89	* * *
Error	14.67	536	0.03		
Adriatic Sea (r^2 = 0.37)					
Intercept	380.8	1	380.8	7178	* * *
Bottom depth	1.01	9	0.11	2.11	*
Distance to the thermocline	1.97	9	0.22	4.13	* * *
Relative depth of the first fluorescence peak	1.59	8	0.20	3.75	* * *
Altitude	2.54	9	0.28	5.33	* * *
Error	10.93	206	0.05		

Sea, there is a negative correlation between school length and lateral distance to the boat, and this is not observed in Catalan Sea (Fig. 3b).

4. Discussion and conclusion

Few restrictions must be done regarding our database. We did not use the algorithm proposed by Diner (2001) in order to "correct" school length, because as stressed by this author, schools resulting from complex shapes and varying internal densities do not fill the conditions for the use of the algorithm, and this was the case for most of the schools of our database. Besides, as usual in fisheries acoustics, the change of settings may have a dramatic effect on the results, mostly by changing the actual sampled volume and the echo threshold. This was the case in our surveys, where some important changes in the settings were decided. Therefore, a careful check must be done prior to any analysis, to see whether the possible differences in the results (from one year to the other and/or from one acoustic device to the other) are due to the settings. The preliminary analysis of our data regarded the number and size of schools detected by each acoustic device and in each zone. We checked that the differences observed were not due to changes in the settings from one year to the other. Moreover, it appeared that the properties of each acoustic device did not allow for a global analysis of the whole dataset, and we therefore decided to perform separate analysis.

The comparison of the characteristics of schools in the two areas evidenced important differences: it appears that, observed with the sonar, schools in the Adriatic Sea are longer, tend to occupy the upper part of the water column and are detected further from the boat. In this area, the vessel showed higher sailing speed compared to the Catalan Sea.

The PCA indicated a clear independence between environmental, morphological and acoustic descriptors in each zone. The main difference between sonar and echosounder data is that environmental factors of the two zones can be discriminated only in echosounder dataset (Fig. 2).

The variability of the length of schools appears to be mostly explained by the vessel speed, the lateral distance to the boat and the thermocline and halocline depth. In addition, echosounder schools' length is sensitive to parameters related to the bottom depth and to variables related to the bottom, which is not the case for sonar schools. This is very likely due to the range of the device which enables the detection of deeper schools in comparison with the sonar. In this respect, the echosounder allows the analysis of the depth effect on school characteristics, which is not the case of the sonar, as this device has a much more limited vertical range. On the other hand, the lateral range of the sonar allows for the analysis of the boat effect on schools size (as evidenced by the multiple analysis of variance). Therefore, our results show in which way these two devices can be complementary.

The PCA indicated that the components were explained by distinct sets of descriptors. Nevertheless, this classification does not allow for the discrimination of sonar schools between the Adriatic and Catalan Seas, despite their morphological differences and does not allow the relation of morphological differences of echo-sounder schools between the Adriatic and Catalan Seas with the differences of their environmental-related factors. These results are similar to those obtained by Coetzee (2000) on the sardine schools along the South-African coasts. This suggests that variability of school size is governed by specific factors not taken into account in our analysis. These factors could be related to the physiological status and motivation of individuals, such as feeding motivation (Mackinson et al., 1999) or to the species composition of schools and size of fish. These behavioural and biological characteristics imply different capabilities of reaction and different types of internal organization in terms of structural homogeneity, minimum approach distance or

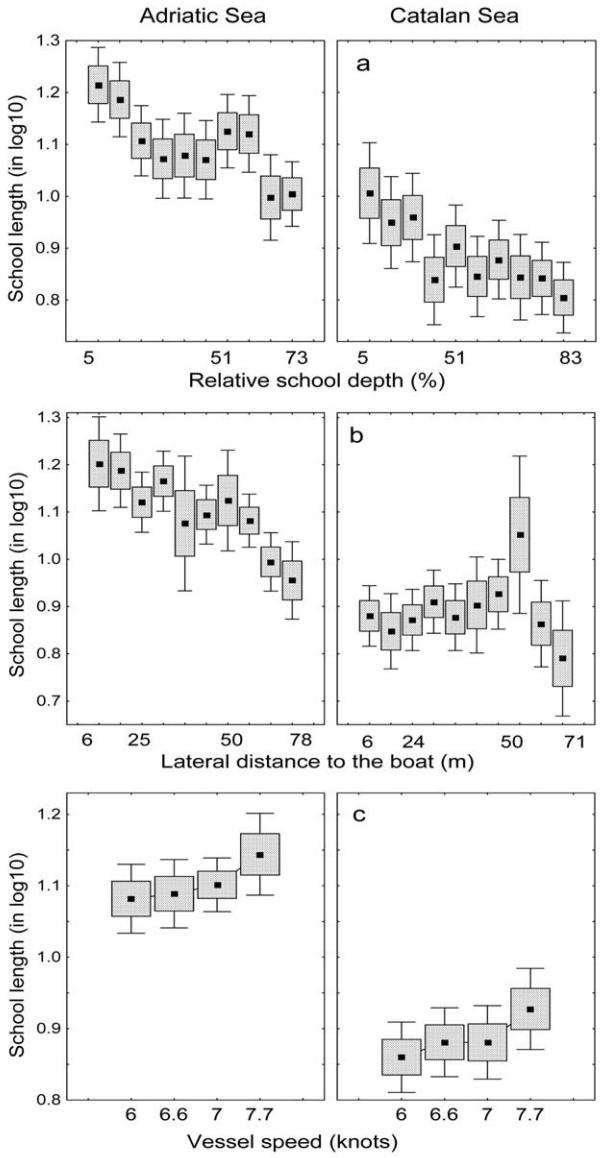

Fig. 3. Categorized box plots of the school mean length vs. the relative school depth (a), the lateral distance to the boat (b) and the vessel speed (c).

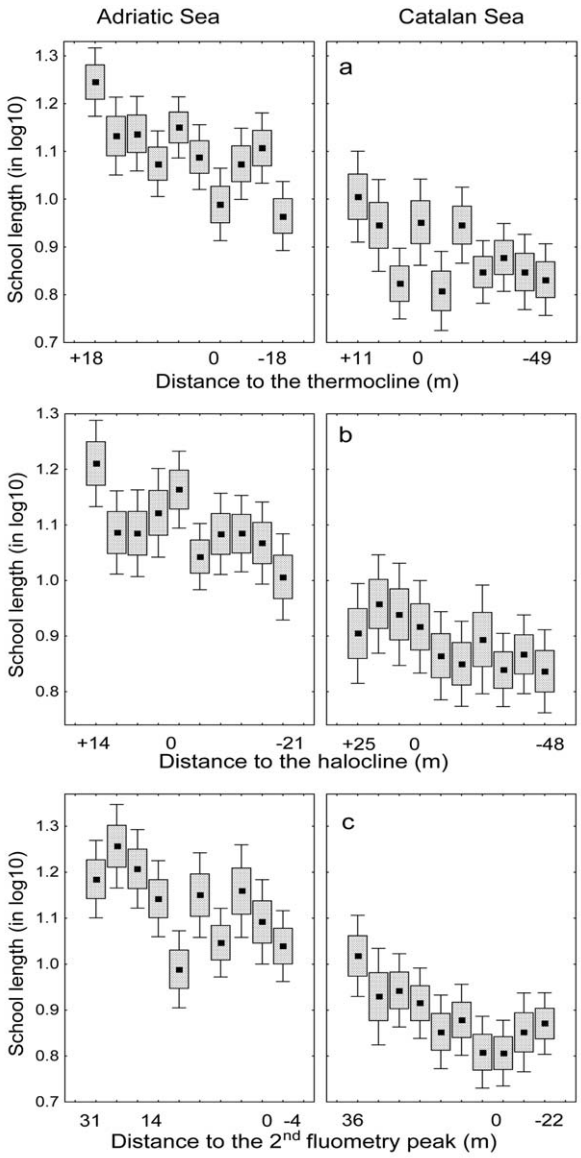

Fig. 4. Categorized box plots of the school mean length vs. the distance of the schools to the thermocline (a), the distance of the schools to the halocline (b), the distance of the schools to the second fluorescence peak (c).

swimming speed and polarization, which have positive relationships with school size (review in Hoare et al., 2000). Near environmental field conditions such as the presence of predators can also influence the behavioural dynamics of pelagic schools and contribute to the variation of their size (Swartzman et al., 1994; Massé et al., 1996; Pitcher et al., 1996; Misund et al., 1998). This analysis is in agreement with those done by other authors (review in Fréon and Misund, 1999), and confirms the necessity to go deeper in to the behavioural observations at micro-scale.

The difference in the length of schools between Adriatic Sea and Catalan Sea, is the most surprising result, since this dimension represents the horizontal dimension of the schools along the vessel track. No bias was found regarding the beam correction, vessel speed estimation and sonar settings for image acquisition. According to several authors, environmental factors such as temperature, bottom depth (Swartzman, 1997), or biological factors such as species and interactions between species (Massé et al., 1996) may explain variations observed in morphological parameters of schools. Neural networks developed by Haralabous and Georgakarakos (1996), or the linear discriminant model approach proposed by Scalabrin et al. (1996) take into account school descriptors extracted from echo-integration data. Our analysis validates these works, however, we suggest an alternative to the hypothesis of a direct influence of these factors on school morphology: the variation of school length and consecutively the variations of the correlated dimensions in 2D and 3D are first related to the intensity of the avoidance reaction in front of the vessel and this effect can be reinforced depending on the environmental conditions.

Our investigation focuses on the differences, between two areas, of the mean school length measured by the sonar and

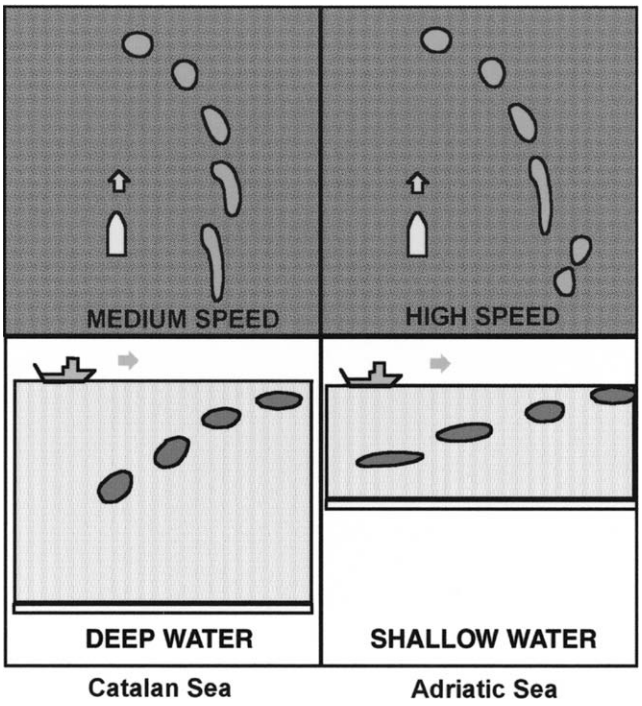

Fig. 5. Schematic diagram of the behavioural mechanism, that may explain differences of school length and elongation between the Catalan and Adriatic Seas (see text).

the echosounder. The MANOVA shows that, depending on the geographical zone, the school length may be explained alternatively by the schools' position in the water column, their lateral distance to the boat, the vessel speed and the vertical stratification of the water column. Due to the high variability of the measured values, the sonar model applied on Adriatic and Catalan database did not explain more than 20% and 17% of the variation observed. However, the echosounder model and the analysis of the box plots (Figs. 3 and 4) confirm the results of the sonar model and allow for proposing a behavioural model of avoidance (Fig. 5). School avoidance occurs both in the horizontal and vertical plans (Olsen et al., 1983; Soria et al., 1996; Misund et al., 1998; Misund and Coetzee, 2000). In the absence of vertical constraints, fish far away from the boat are disturbed by the noise of the vessel and react by polarizing their swimming. This polarization induces a fast compression and enables the fish to avoid the vessel laterally and vertically by a fast and coordinated movement of the school (Pitcher and Parrish, 1993; Fréon et al., 1993; Soria et al., 1996). We assume that under shallow water conditions and environmental constraints related to the vertical distribution of temperature and/or salinity, vertical movement of fish is restricted. Since the mean bottom depth, the halocline depth and the depth of the second fluorescence peak are lower in Adriatic Sea than in Catalan Sea (Table 2), pelagic fish schools in Adriatic Sea tend to stay in subsurface area and disturbed schools escape rather in the horizontal direction than in vertical one. Fish are forced both by the vertical constraint and by the necessity of keeping visual contacts and minimum

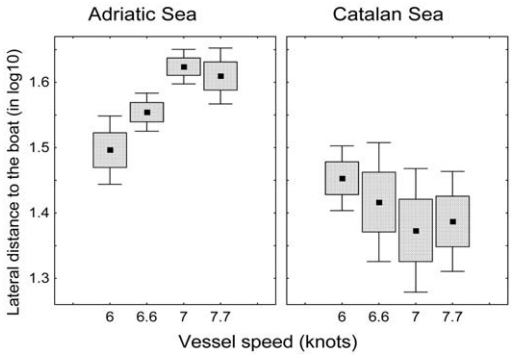

Fig. 6. 2D categorized box plots of the mean lateral distance to the boat vs. the vessel speed.

inter-distances in order to maintain the cohesion of the group. After the works of Radakov (1973), Breder (1959), Shaw (1978), Fréon et al. (1992) and Soria (1994), we assume that these constraints induce a stretching of the schools in the field of the lowest gradient of disturbances. Since this field is parallel to the vessel path, the school elongation is expected to be greater than in non-disturbed conditions. This effect can be amplified by vertical restrictions, such as the depth of the halocline and/or the depth of the thermocline, which could play the role of horizontal fences. This hypothesis is supported by the environmental characteristics of the two prospected zones during our sampling periods: in September, Northern Adriatic Sea shows a strong thermal stratification (Russo and Artegiani, 1996), whereas the stratification is still weak in the Catalan Sea at the beginning of spring, both for temperature and salinity (Castellón et al., 1985). Following the schematic pattern of gradual reaction of fish, the more they detect external stimuli, the stronger is their reaction. Then there is evidence that this reaction is proportional to the vessel speed (Fig. 3c). This hypothesis is validated by the analysis of the relationship between the mean lateral distance to the boat and the vessel speed (Fig. 6). The vessel speed has no effect on the lateral position of schools in Catalan Sea, while in Adriatic Sea the highest lateral distances to the boat were recorded for schools, detected at the highest vessel speeds. Nevertheless, above a threshold of disturbance, the cohesion of a school cannot be kept and the schools might split. This last hypothesis could explain the highest number of small schools observed far from the boat in Adriatic Sea. An alternative explanation is that schools furthest from the vessel are relatively undisturbed and then fish gather again and form small schools in length with a more regular shape (Fig. 7).

The above results allow to improve our knowledge on the vertical and lateral avoidance patterns of schools in relation to their position in the water column, and allow for describing the influence of external factors on school characteristics. After our results, it seems very hazardous to estimate fish biomass from size of schools. Nevertheless, we need more information to be able to quantify the impacts of avoidance reaction on size of schools and biomass estimates. In order to establish the relations between the intensity of factors, like

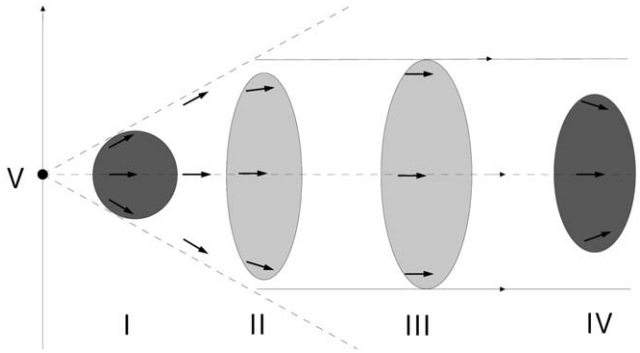

Fig. 7. Diagram presenting the dynamics of a school avoiding a source of noise. In this scheme, we have identified three fish represented by darts, at two sides and in the centre of the school. Dotted lines represent the noise vectors; solid lines the maximum length of the school. (a) At the beginning of the noise emission, the school is circular, each fish tends to escape, following the line of maximum noise avoidance (i.e. in direct opposition to the source). (b) The inter-individual distance increases; if the stress is not too strong, the gregarious tropism will allow the fish to maintain contact. The volume of the school has increased, i.e. fish are on an average at larger inter-individual distances from each other. (c) The inter-individual distance reaches the maximum and the school is not stretching anymore; if the dispersal effect of the noise is stronger than the gregarious behaviour of the fish, the school will split. Otherwise, it will maintain this anisotropic shape until the noise becomes lower and fish may closely aggregate again. (d) The school is at enough distance from the source of noise and goes back to its original shape, i.e. roughly circular. (e) Vessel route (source of noise). This example is presented as if the vessel was static and began to transmit noise close to the school. The reality is slightly different, due to the slow approach of the vessel, all schools already present an elliptical shape when the vessel approaches.

the bottom depth or the vessel speed and the intensity of the stretching behaviour of schools, more investigations are required. Moreover, environmental factors like the thermocline depth or the halocline depth and the chlorophyll concentration seem to have an effect on this behaviour and should systematically be taken into account when observing schools. Several scientists have noted that the aggregation of schools in clusters is a key factor, affecting both precision of acoustic surveys and catchability in the fishery (Fréon and Misund, 1999; Booth, 2000; Petitgas et al., 2001). From our point of view, the spatial dynamics of fish at a micro-scale (e.g. at the level of the school), could be a key factor affecting both precision of acoustic surveys and catchability in the fishery, at the same level of importance than the dynamics of clusters.

Acknowledgements

This work was funded by a grant from the European Union (T-ECHO, project AIR1-CT9200314). We are grateful to our colleagues for their help in data collecting and processing and to J. Rucabado, A. Castillón and P. Schneider, deck officers, and crew from the Instituto de Ciencas del Mar of Barcelona for the excellent cooperation on board RV “Garcia del Cid”. Comments and constructive criticism from two anonymous referees are acknowledged.

Annex 1. List of school descriptors of the echosounder database (see Weill et al., 1993)

Descriptor (abbreviated)	Signification and unit	Calculation method
H	Maximum height (m)	
L	Maximum length (m)	The beam pattern effect on length estimation was taken into account by removing $2R\tan(\alpha/2)$ of the maximal horizontal length, where R is the depth of the gravity centre of the school; and α the beam angle (Johannesson and Losse, 1973).
Elong	Elongation	Ratio maximal length (L) to the maximal height (H).
Ar	Area (m^2)	$Ar = \pi/2(HL)$ assuming that the schools have an ellipsoid shape.
RO	Roughness	$RO = 2\ln(Per/4)/(\ln(Ar)$. RO is close to 1 for schools having a very smooth outline shape and close to 2 for the very irregularly shaped schools.
Per	Perimeter (m)	Corrected from the beam angle error.
MinDep	Minimum depth (m)	Distance between the sea surface and the upper limit of the school.
RelDep	Relative depth (m)	RelDep = 100(MinDep/depth), where: MinDep is the minimum depth of the school (distance between the water surface and the upper limit of the school). Depth is the bottom depth.
σ_s	Integrated back-scattered energy (relative value)	It is the sum of squared echo amplitude computed with the samples used to define the school detection. This value is proportional to the total biomass of the school. $\sigma_s = 1/\varepsilon\sum_{j=1}^{N} S_j \quad T_j \sum_{i=1}^{n} V_{ij}^2$ where ϵ = number of samples per meter, N is the number of pings over the integrated school length, n is school sample number integrated for each ping, S is vessel speed (ms^{-1}), T is ping period in seconds, V is the integrated sampling amplitude, measured in volts.
	Volume reverberation index ($dB\ m^{-3}$)	$Sv = 10\log(\sigma_s/A)$, where A is the school area (m^2). This value is proportional to the mean density of the school.

Annex 2. List of school descriptors of the sonar database

Descriptor	Signification and unit	Calculation method
H	Maximum height (m)	
L	Maximum length (m)	The maximum horizontal length of each school is the maximum dimension of the school along the vessel path. It is estimated using parameters of image acquisition (Gerlotto et al., 1994). The same beam correction applied on the echosounder school lengths was used
W	Maximum width (m)	Perpendicular to the vessel path
Elong1	Elongation 1	Ratio maximum length (L) to the maximal height (H)
Elong2	Elongation 2	Ratio maximum length (L) to the maximal width (W)
Elong3	Elongation 3	Ratio maximum width (W) to the maximal height (H)
Ar1	Area 1 (m^2)	$\pi/2(LH)$, calculated assuming and ellipsoid form of the school
Ar2	Area 2 (m^2)	$\pi/2(LW)$, calculated assuming and ellipsoid form of the school
Ar3	Area 2 (m^2)	$\pi/2(WH)$, calculated assuming and ellipsoid form of the school
V	Volume (m^3)	$V = 4/3\pi(HWL/2)$, calculated assuming and ellipsoid form of the school
MinDep	School depth	Distance between the sea surface and the upper limit of the school
RelDep	Relative depth	RelDep = 100(MinDep/depth)
LatDiB	Lateral distance to the boat (m)	Horizontal distance from the school centre to the vertical line under the boat

References

Bahri, T., 2000. Relations entre des variables environnementales et la distribution et structure de la biomasse de poisons pélagiques côtiers en Méditerranée. Thèse dr. Univ. Pierre et Marie Curie, Paris VI.

Bahri, T., Fréon, P., 2000. Spatial structure of coastal pelagic schools descriptors in the Mediterranean Sea. Fish. Res. 48, 157–166.

Bahri, T., Soria, M., Fréon, P., Gerlotto, F., 1997. Preliminary description of the pelagic fish school database obtained during the T-ECHO project using multibeam sonar (Reson Seabat 6012). Scientific and Technical Annexes T-ECHO (AIR1 CT92 0314) Project Final Report.

Beare, D.J., Reid, D.G., Petitgas, P., 2002. Spatio-temporal patterns in herring (*Clupea harengus* L.) school abundance and size in the northwest North Sea: modelling space-time dependencies to allow examination of the impact of local school abundance on school size. ICES J. Mar. Sci. 59, 469–479.

Booth, A.J., 2000. Incorporating the spatial component of fisheries data into stock assessment models. ICES J. Mar. Sci. 57, 858–865.

Breder Jr., C.M., 1959. Studies on social groupings in fishes. Bull. Am. Museum Nat. Hist. 117, 393–482.

Castellón, A., Salat, J., Masó, M., 1985. Some observations of Rhone fresh water plume in the Catalan coast. Rapp. Comm. Int. Mer. Médit. 29, 119–120.

Coetzee, J., 2000. Use of shoal analysis and patch estimation system (SHAPES) to characterise sardine schools. Aquat. Living Resour. 13, 1–10.

Dagorn, L., Petit, M., Hallier, J.P., Cayré, P., Simier, M., 1997. Does yellowfin tuna *Thunnus albacares*, school size in the western Indian ocean depend on individual size? Coll. Vol. Sci. Pap.— ICCAT 46, 122–128.

Diner, N., 2001. Correction on school geometry and density: approach based on acoustic image simulation. Aquat. Living Resour. 14, 211–222.

Diner, N., Scalabrin, C., Weill, A., 1994. Automatic shoal recognition and classification bases on MOVIES-B software. Institute of Electrical and Electronic Engineers Proceedings of Oceans 94 with OSATES 94.

Fréon, P., 1984. La variabilité des tailles individuelles à l'intérieur des cohortes et des bancs de poissons : observations et interprétations. Oceanol. Acta 7, 457–468.

Fréon, P., 1985. La variabilité des tailles à l'intérieur des cohortes et des bancs de poissons. Application à la biologie des pêches. Oceanol. Acta 8, 87–99.

Fréon, P., Misund, O.A., 1999. Dynamics of pelagic fish distribution and behaviour: effects on fisheries and stock assessment. Blackwell Science Ltd Fishing News Books.

Fréon, P., Gerlotto, F., Soria, M., 1992. Changes in school structure according to external stimuli: description and influence on acoustic assessment. Fish. Res. 15, 45–66.

Fréon, P., Gerlotto, F., Soria, M., 1993. Variability of *Harengula* spp. School reactions to boats or predators in shallow water. ICES Mar. Sci. Symp. 196, 30–35.

Fréon, P., Gerlotto, F., Soria, M., 1996. Diel variability of school structure with special reference to transition periods. ICES J. Mar. Sci. 53, 459–464.

Gerlotto, F., Fréon, P., 1992. Some element of vertical avoidance of fish schools to a vessel during acoustic surveys. Fish. Res. 14, 251–259.

Gerlotto, F., Fréon, P., Soria, M., Cottais, P.-H., Ronzier, L., 1994. Exhaustive observation of 3D school structure using multibeam side scan sonar: potential use for school classification, biomass estimation and behaviour studies. ICES C.M. 1994, B:26.

Gerlotto, F., Soria, M., Fréon, P., 1999. From two dimensions to three: the use of multibeam sonar for a new approach in fisheries acoustics. Can. J. Fish. Aquat. Sci. 56, 6–12.

Hara, I., 1987. Swimming speed of sardine school on the basis of aerial survey. Nippon Suisan Gakkaishi 53, 223–227.

Haralabous, J., Georgakarakos, S., 1996. Artificial neural networks as a tool for species identification of fish schools. ICES J. Mar. Sci. 53, 173–180.

Hoare, D.J., Krause, J., Peukhuri, N., Godin, J.-G.J., 2000. Body size and shoaling in fish. J. Fish Biol. 57, 1351–1366.

Kieser, R., Mulligan, T.J., Richards, L.J., Leaman, B.M., 1993. Bias correction of rockfish school cross section widths from digitized echosounder data. Can. J. Fish. Aquat. Sci. 50, 1801–1811.

Krause, J., Godin, J.-G.J., 1995. Predator preferences for attacking particular group sizes: consequences for predator hunting success and prey predation risk. Anim. Behav. 50, 465–473.

Johannesson, K., Losse, G., 1973. Methodology of acoustic estimations of fish abundance in some schools. UNDP/FAO Resource Survey Projects. Rapp. Proc. Réun. Cons. Int. Explor. Mer 170, 296–318.

Mackinson, S., 1999. Variation in structure and distribution of pre-spawning Pacific herring shoals in two regions of British Columbia. J. Fish Biol. 55, 972–989.

Mackinson, S., Nottestad, L., Guénette, S., Pitcher, T., Misund, O.A., Fernö, A., 1999. Cross-scale observations on distribution and behavioural dynamics of ocean feeding Norwegian spring-spawning herring (*Clupea harengus* L.). ICES J. Mar. Sci. 56, 613–626.

MacLennan, D.N., Simmonds, E.J., 1992. Fisheries Acoustics. Chapman and Hall, London.

Maes, J., Ollevier, F., 2002. Size structure and feeding dynamics in estuarine clupeoid fish schools: field evidence for the school trap hypothesis. Aquat. Living Resour. 15, 211–216.

Massé, J., Koutsikopoulos, C., Patty, W., 1996. The structure and spatial distribution of pelagic fish schools in multispecies clusters: an acoustic study. ICES J. Mar. Sci. 53, 155–160.

Misund, O.A., 1993. Dynamics of moving masses: variability in packing density, shape and size among herring, sprat and saithe schools. ICES J. Mar. Sci. 50, 145–160.

Misund, O.A., 1993. Abundance estimation of fish schools based on the relationship between school area and school biomass. Aquat. Living Resour. 6, 179–194.

Misund, O.A., Coetzee, J., 2000. Recording fish schools by multibeam sonar: potential for validating and supplementing echo integration recordings of schooling fish. Fish. Res. 47, 149–159.

Misund, O.A., Fernö, A., Pitcher, T., Totland, B., 1998. Tracking herring schools with a high resolution sonar. Variation in horizontal area and relative echo intensity. ICES J. Mar. Sci. 55, 58–66.

Morgan, M.L., 1988. The effect of hunger, shoal size and the presence of a predator on shoal cohesiveness in bluntnose minnows, Pimephales notatus Rafinesque. J. Fish Biol. 32, 963–971.

Nøttestad, L., Aksland, M., Beltestad, A., Fernö, A., Johannessen, A., Misund, O.A., 1996. Schooling dynamics of Norwegian spring spawning herring (*Clupea harengus* L.) in a coastal spawning area. Sarsia 80, 277–284.

Olsen, K., Angell, J., Peterson, F., 1983. Observed fish reactions to a surveying vessel with special reference to herring, cod, capelin, and polar cod. FAO Fish Rep. 300, 131–138.

Parrish, J.K., 1992. Do predators "shape" fish schools: interactions between predators and their schooling prey. Neth. J. Zool. 42, 358–370.

Partridge, B.L., Pitcher, T.J., Cullen, J.M., Wilson, J., 1980. The three-dimensional structure of fish schools. Behav. Ecol. Sociobiol. 6, 277–288.

Patty, W., 1996. Déterminisme de la répartition spatio-temporelle des populations de poissons pélagiques à partir d'observations acoustiques et environnementales. Thèse dr. Univ. UBO, Sciences et Techniques, Brest.

Petitgas, P., Lévénez, J.J., 1996. Spatial organisation of pelagic fish: echogram structure, spatio-temporal condition and biomass in Senagalese waters. ICES J. Mar. Sci. 53, 147–154.

Petitgas, P., Reid, D., Carrera, P., Iglesias, M., Georgakarakos, S., Liorzou, B., Massé, J., 2001. On the relation between schools, clusters of schools, and abundance in pelagic fish stocks. ICES J. Mar. Sci. 58, 1150–1160.

Peukhuri, N., Ranta, E., Seppä, P., 1997. Size-assortative schooling in free-ranging sticklebacks. Ethology 103, 318–324.

Pitcher, T.J., Partridge, B., 1979. Fish school density and volume. Mar. Biol. 54, 383–384.

Pitcher, T., Parrish, J., 1993. Functions of shoaling behaviour in teleosts. second ed. In: Pitcher, T (Ed.), The Behaviour of Teleost Fishes. Chapman and Hall, London, pp. 363–427.

Pitcher, T., Misund, O.A., Fernö, A., Totland, B., Melle, V., 1996. Adaptative behaviour of herring schools in the Norwegian seas as revealed by high resolution sonar. ICES J. Mar. Sci. 53, 449–452.

Radakov, D.V., 1973. Schooling in the Ecology of Fish. J. Wiley and Sons, New York.

Robinson, C.J., 1995. Food competition in a shoal of herring: the role of hunger. Mar. Behav. Physiol. 24, 237–242.

Robinson, C.J., Pitcher, T.J., 1989. Hunger motivation as a promoter of different behaviour within a shoal of herring: selection for homogeneity in a fish shoal? J. Fish Biol. 35, 459–460.

Russo, A., Artegiani, A., 1996. Adriatic Sea hydrography. Scientia Marina 60, 33–43.

Scalabrin, C., Massé, J., 1993. Acoustic detection of the spatial and temporal distribution of fish shoals in the Bay of Biscay. Aquat. Living Resour. 6, 269–283.

Scalabrin, C., Diner, N., Weill, A., Hillion, A., Mouchot, M.C., 1996. Narrowband acoustic identification of monospecific fish shoals. ICES J. Mar. Sci. 53, 181–188.

Shaw, E., 1978. Schooling fishes. The school, a truly egalitarian form of organization in which all members of the group are alike in influence, offers substantial benefits to its participants. Am. Scient. 66, 166–175.

Soria, M., 1994. Structure et stabilité des bancs et agrégations de poissons pélagiques côtiers tropicaux : application halieutique. Thèse Doct. Univ. Rennes I.

Soria, M., Fréon, P., Gerlotto, F., 1996. Analysis of vessel influence on spatial behaviour of fish schools using a multibeam sonar and consequences for biomass estimates by echosounder. ICES J. Mar. Sci. 53, 453–458.

Soria, M., Bahri, T., Gerlotto, F., Fréon, P., 1997. Preliminary description of the pelagic fish school database obtained during the T-ECHO project using INES-MOVIESB school classification system. T-ECHO (AIR1 CT92 0314) Project Final Report. Scientific and Technical Annexes.

Swartzman, G., 1997. Analysis of the summer distribution of fish schools in the Pacific Eastern Boundary Current. ICES J. Mar. Sci. 54, 105–116.

Swartzman, G., Stuetzle, W., Kulman, K., Powojowski, M., 1994. Relating the spatial distribution of pollack schools in the Bering Sea to environmental factors. ICES J. Mar. Sci. 51, 481–492.

Weill, A.C., Scalabrin, C., Diner, N., 1993. MOVIES-B: an acoustic detection description software. Application to shoal species classification. Aquat. Living Resour. 6, 255–267.

Available online at www.sciencedirect.com
SCIENCE DIRECT®
Aquatic Living Resources 16 (2003) 159–165
Aquatic Living Resources
www.elsevier.com/locate/aquliv

Spatial distribution and temporal changes in the fish populations of Lake Victoria

Albert Getabu [a], Rhoda Tumwebaze [b], David N. MacLennan [c,*]

[a] *Kenya Marine and Fisheries Research Institute, P.O. Box 1881, Kisumu, Kenya*
[b] *Department of Fisheries Resources, P.O. Box 4, Entebbe, Uganda*
[c] *The Orchard, Muirhall Road, Perth PH2 7BQ, Scotland, UK*

Accepted 17 December 2002

Abstract

The fisheries of Lake Victoria in East Africa must be managed effectively to ensure sustainable food supplies. This has been impossible in the past due to inadequate knowledge of commercially important fish stocks. Here we present the first acoustic abundance estimates of fish in Lake Victoria. Five lakewide acoustic surveys were conducted between 1999 and 2001, using the Simrad EY500 echo-integrator with a 120 kHz split-beam transducer. There are many species of fish in Lake Victoria, however, only limited identification of targets can be achieved by present methods. Broad categories were distinguished by visual examination of echo-traces. The echo-integrals were partitioned between four target groups: (1) the Nile perch (*Lates niloticus*), a top predator, (2) small pelagics comprising mainly the dagaa *Rastrineobola argentea* together with mixed species of haplochromines, (3) the crustacean *Caridina nilotica* and (4) other species. Spatial and temporal differences in the Standing Crop were observed between north and south, and between shallow and deep water. Most fish were found inshore but the spatial distribution varied between seasons. Mid-lake fish densities were higher in August compared to February. In August, the water column is well mixed while in February it is stratified with a low-oxygen layer inhospitable to fish near the bottom. There are consequent changes in the characteristics of observed echo-traces. Over the survey series, Nile perch biomass showed a consistent decline, while the stocks of small pelagic species increased. We emphasize the need for simple rules to identify species, and hydrographic monitoring to assist echo-trace classification. In the absence of any other source of comprehensive biomass estimates, the value of acoustic surveying in Lake Victoria is demonstrated.

Keywords: Acoustic survey; Fish stock estimation; Species identification; Lake Victoria

1. Introduction

Lake Victoria is the second largest lake in the world by surface area, covering 68 000 km^2 in East Africa. It has a mean depth of 40 m and a shoreline of 3450 km, which is shared by the bordering states of Kenya, Tanzania and Uganda. The lake is an important source of food, employment and earnings for the riparian communities through the exploitation of fish resources.

The fisheries of Lake Victoria have undergone drastic changes in its recent history. The introduction of the Nile perch *Lates niloticus* has had major ecological consequences (Goudswaard et al., 2002). It is thought that some 200 endemic species of haplochromines (which previously comprised about 90% of the fish biomass) have become extinct from the lake due to predation by the Nile perch (Witte et al., 2000). In the 1960s, the fisheries sustained a production of around 100 000 ton per year, although even then there were signs of overexploitation (Reynolds and Greboval, 1988). The fisheries now produce over 500 000 ton of fish annually. The considerable increase after 1979 came from the developing Nile perch population. The present fisheries are much simpler than before, being dominated by only three species: the Nile perch, the Nile tilapia (*Oreochromis niloticus*) and the dagaa (*Rastrineobola argentea*). In recent years, however, as fishing pressure on the Nile perch intensified, there have been signs of recovery in at least some of the prey species (Witte et al., 2000).

Research on the lake fisheries is essential to support management initiatives intended to ensure sustainable food sup-

* Corresponding author.
E-mail address: maclennan22@aol.com (D.N. MacLennan).

doi:10.1016/S0990-7440(03)00008-1

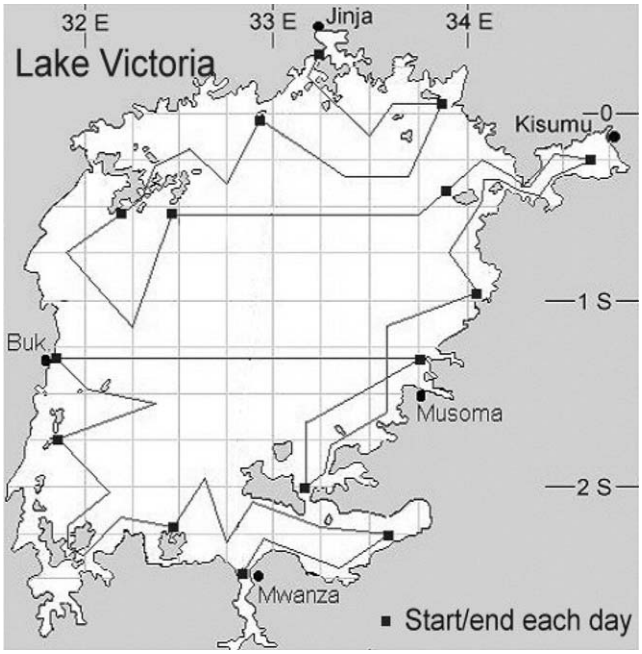

Fig. 1. Stratified track design with most effort applied inshore, as used in August 1999. Fourteen-day survey from Mwanza to Jinja.

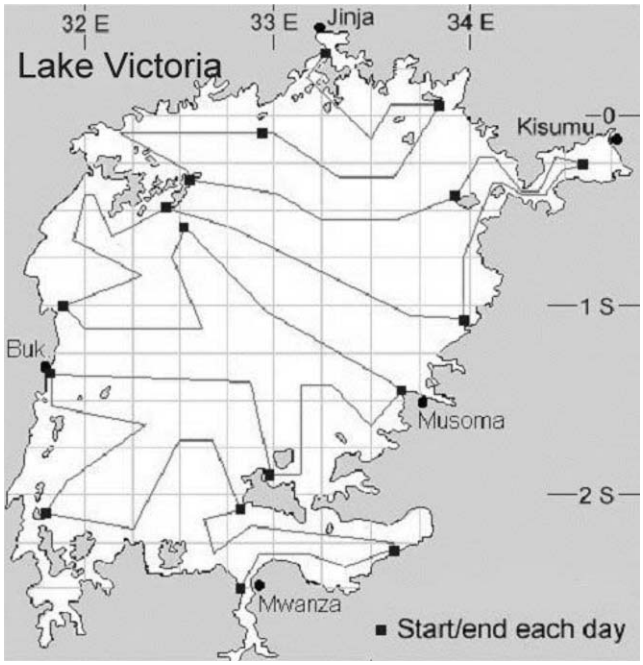

Fig. 2. Uniform design giving a more even coverage of the whole lake, as used in February 2000 onwards. Sixteen-day survey from Mwanza to Jinja.

plies in the region. In recognition of this need, Phase II of the Lake Victoria Fisheries Research Project (LVFRP) was implemented from 1997 until the end of 2001. Acoustic surveying was a central component of the LVFRP programme. Five surveys were conducted at 6-month intervals starting in August 1999. Each survey covered the whole of Lake Victoria. In this paper, we describe the methods used and some of the results obtained from these surveys.

2. Materials and methods

The surveys were done using the research vessel "Victoria Explorer" which is a 16.5 m long stern trawler. A 120 kHz split-beam transducer with 9° beam width between 3 dB down points was mounted on the vessel's hull. The transducer was connected to a Simrad EY500 echo-integrator controlled by a Toshiba Satellite laptop computer. The echo-integrator was calibrated twice during each survey using the standard target method (MacLennan and Simmonds, 1992). The reference target was initially a 23 mm copper sphere (TS = –40.4 dB) and, for the fifth survey only, a 33.2 mm tungsten carbide sphere (TS = –40.6 dB).

2.1. Survey design

The surveys were designed as a series of transects crossing the lake, normally starting from Mwanza, Tanzania and ending in Jinja, Uganda (Figs. 1, 2). Practical constraints limited the extent to which a completely even transect design could be achieved. There are many islands scattered throughout Lake Victoria. The surveys were conducted primarily during the daylight hours, with the vessel going to anchor or lying at a jetty overnight. The transect design had to allow the vessel to reach a suitably sheltered location at the end of each day. The surveying speed of "Victoria Explorer" is about 10 knots. The cross-lake transects are up to 140 miles long, thus some 30% of the longest transect had to be covered in darkness. The behaviour of fish is well known to depend on the light level, and after dark there were concentrations of plankton in the water not seen in the daytime. We were unable to fully allow for these day-night differences. It was, therefore, important to minimise the amount of survey track covered at night. The logistical constraints, however, did not allow a daytime-only survey. The first survey, in August 1999, was designed as a stratified sampling scheme, which provided more intensive surveying of the shallow inshore areas (Fig. 1). The results showed that more sampling was needed in the offshore mid-lake areas. Extra survey time was, therefore, allocated to allow additional cross-lake transects. Fig. 2 shows the resulting design, which was more uniform than before. The new transect scheme was followed with minimal modification on the second and later surveys.

2.2. Echo-trace sampling

During the first four surveys, a 3.5 × 3.5 m frame trawl with 26 mm mesh and a 5 mm liner in the codend was used to sample the echo-traces in midwater. The frame trawl was effective in sampling small haplochromines and the dagaa, *R. argentea*. It caught very few of the larger Nile perch which can easily escape from such a small net. A bottom trawl with 22.6 m headrope, codend mesh 25 mm and a vertical opening of 3.5 m was used alternately with the frame trawl to sample the largest fish, which were mostly found close to the lakebed. A pelagic trawl (codend mesh size 26 mm and 5 mm

liner) was obtained for "Victoria Explorer" in May 2001. During the last survey, this gear was used instead of the frame and bottom trawls. The mouth opening of the pelagic trawl is about 10 × 10 m. The pelagic trawl proved to be much more effective at catching the larger Nile perch. Fish up to 96 cm in length were caught. After each trawl haul, the catch was sampled to determine the species and size composition.

2.3. Data recording

The echo-integration was performed in a series of consecutive layers covering the whole water column from 5 m below the transducer (changed to 3 m in the 2001 surveys) to 0.5 m above the bottom. The layers were 5 m thick down to 20 m depth and 10 m thick in deeper water. Echograms and tables showing the nautical area scattering coefficient (NASC) for each layer were printed at 6 min intervals. This corresponds to about 1 nautical mile (1852 km) of cruise track. Position data (from a Garmin GPS Navigator) and the NASC values for each 6 min interval were entered on an Excel spreadsheet for subsequent analysis of biomass and distribution. Additionally, the echo data (ping interval 0.5 s) were stored on the Toshiba hard disk in real time, and later downloaded to recordable compact disks for permanent archiving.

2.4. Partitioning the echo-integrals

The NASC is a single measure of all the detected targets. This needs to be partitioned among such target categories as can be separately identified, i.e. individual species or species groups. There was a limit to what could be achieved in this respect. A complete breakdown to species level was not practicable. Some knowledge of aquatic ecology and the behaviour of fish as regards aggregation and vertical movement was necessary to decide what level of partitioning was reasonable.

In our surveys, the partitioning was done in two stages. Firstly, the total NASC was divided among "selections". This was based on general knowledge revealed by the trawl catches, the appearance of characteristic echo-traces and their depth. We adopted five selections, called Sel 1 through 5, which are defined as follows.

- Sel 1: Near-surface dagaa schools; strong, individual marks down to 15 m depth.
- Sel 2: Mixed pelagic layer; mostly dagaa and haplochromines, some Nile perch.
- Sel 3: Mixed bottom layer; mostly haplochromines and Nile perch, some dagaa.
- Sel 4: Diffuse deep layer; mostly composed of *Caridina nilotica* with some *Barbus profundus*.
- Sel 5: Mixture of fish and plankton; diffuse traces everywhere, only seen at night.

Fig. 3 shows an example where Sel 1, Sel 2 and Sel 3 appear in the same echogram. The selections are distinguished by the appearance and/or the depth of the echo-traces.

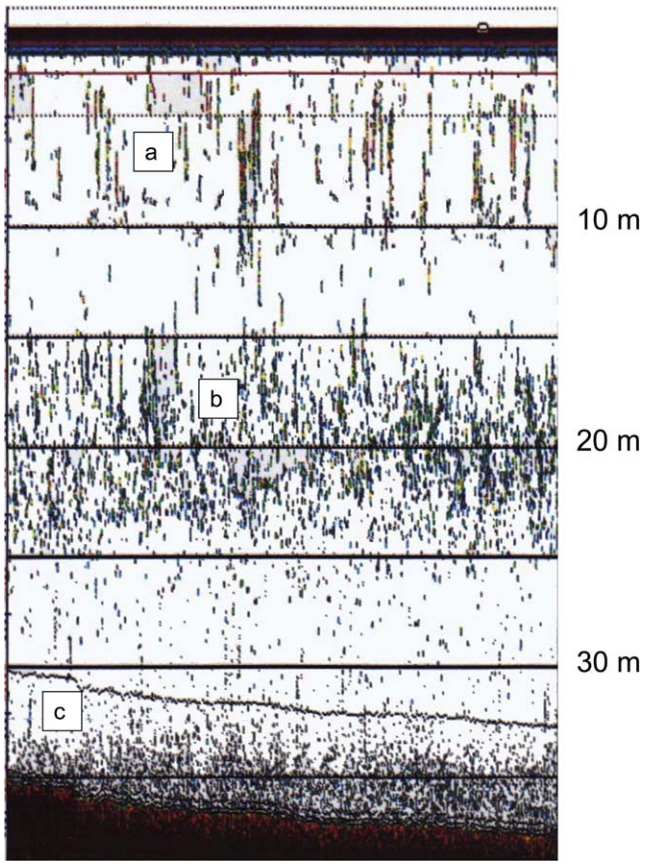

Fig. 3. Example of three of the selections used for echo-trace partitioning. (a) The strong narrow marks above 15 m are dagaa schools; (b) the patchy marks 15–20 m are the pelagic mixture—Nile perch, dagaa and Haplochromines; (c) the diffuse weak echoes near the bottom are mainly Caridina shrimp.

The first stage of partitioning was done for each integration interval, by allocating the NASC for each 5 or 10 m depth interval to one selection. Only measurements above 15 m were relevant to the single-species Sel 1. The other selections required further subdivision to determine useful groupings of the target ensemble. This second stage of partitioning was based on the species composition of the trawl catches. For each integration interval, the species proportion by weight in the nearest trawl catch, taken at an appropriate depth, was assumed to be representative of the echo-traces. Where trawl catches were small, two or more hauls in the vicinity were combined to give more precise species proportions. If the catches were large enough to provide well-defined size histograms, the catch proportions of each species or species group were averaged. If the catches were very small, the fish quantities were summed and the total was treated as though it was one haul.

During the first four surveys, Sel 2 and Sel 3 were partitioned using the catch compositions of the frame trawl and the bottom trawl, respectively. During the fifth survey, only the pelagic trawl was used for echo-trace sampling. No allocations to Sel 3 were made in the absence of bottom trawl data. In the fifth survey, the echo-traces previously allocated to Sel 3 were now included in Sel 2, which was then parti-

tioned according to the pelagic trawl catches. The change of sampling gear has introduced some uncertainty in the partitioning in the fifth survey compared to the earlier results. However, the pelagic trawl is clearly superior to the methods previously used for echo-trace sampling. This one gear is capable of sampling all the stock components, which previously required two gears. The main question to be considered for all the gears is the relative catching efficiency between large and small fish, in particular, between the Nile perch and the small pelagics i.e. dagaa and haplochromines. Conversion factors were determined from catch comparison experiments to ensure that the catch proportions registered by all the gears are comparable between the five surveys. The two-stage partitioning ended with the NASC being divided between the following five categories: (1) dagaa; (2) haplochromines; (3) Nile perch; (4) Caridina (*C. nilotica*) and (5) others.

The "others" category included all the additional species, which could not be individually determined, notably *B. profundus*, *Synodontis* spp. and the tilapia, *O. niloticus*. The acoustic and fishing data collected on our surveys did not allow any finer discrimination of the species composition than that indicated above.

2.5. Data analysis

To obtain total abundance estimates, we assumed the NASC of the unobserved near-surface water would be the same as that of the top layer. The observed NASC was increased accordingly.

The acoustic abundances were determined from the mean NASC multiplied by the water area of each square in a 15 × 15 nmi grid. To compare changes with latitude and water depth, the abundances were aggregated in the four zones illustrated in Fig. 4. The zonal boundaries were chosen on convenient political and bathymetry lines. The northern/southern divide was at the Tanzanian border (latitude 01°S). The offshore/inshore zones corresponded to water depths more or less than 40 m, respectively.

Target strength functions are required to convert the acoustic measurements to biomass. These have the form $TS = 20 \log_{10}(L) - b_{20}$ where the factor b_{20} depends on the species but not on the fish length L (Foote, 1987). The TS functions relevant to Lake Victoria are not well known. We conducted limited experimental investigations on Nile perch, *L. niloticus* and dagaa, *R. argentea* in cages. The results suggest the following values for b_{20}, although their accuracy is uncertain: *L. niloticus* 66 dB; *R. argentea* 72 dB.

In the absence of any other information, we have assumed the same TS function for all the small pelagics in the lake. In the case of *C. nilotica*, we have assumed a bulk TS of -49 dB kg^{-1}, taken from the results on similar crustaceans reported by Pieper (1979). In view of the uncertainty in these assumptions, it is emphasised that our biomass estimates must be considered as indices rather than absolute abundances.

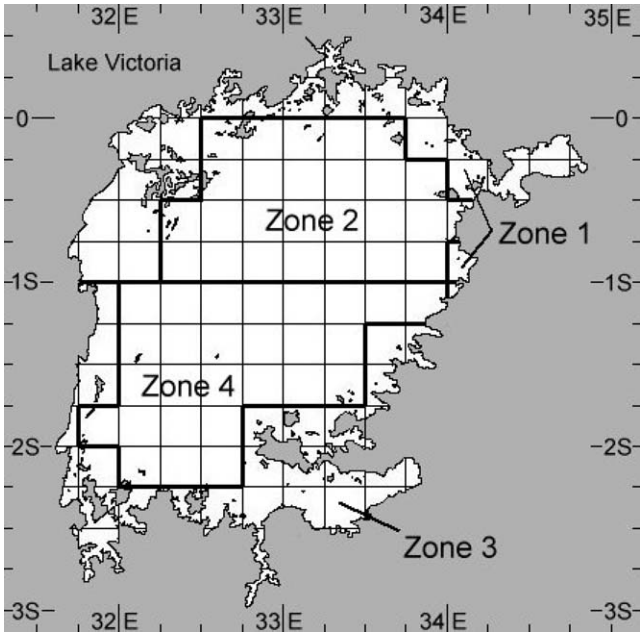

Fig. 4. Chart of the squares grid and the zones used in the analysis. The zones are (1) north inshore, (2) north offshore, (3) south inshore and (4) south offshore. The offshore/inshore divide is based on the mean water depth in the square being more or less than 40 m.

3. Results

3.1. Biomass trends

Fig. 5 shows the total biomass and the partitioned indices for four of the species groups described above. The "small pelagic" group comprises all of the dagaa and *Haplochromis* species combined. The small pelagics were further divided in the analysis, however, the results were highly variable. A much clearer picture of the ecological trends emerges when the small pelagics are considered as one species group.

The mean total biomass index from all the surveys was 2.17×10^6 ton, corresponding to a Standing Crop (SC) of 31.0 ton km^{-2}, of which *L. niloticus* constituted 59.3%, *R. argentea* 22.4%, haplochromines 15.0%, *C. nilotica* 1.1% and other species 2.2%. For comparison, Moreau (1995) found SC values around 27 ton km^{-2} in the early 1970s, before the Nile perch upsurge, rising to 43 ton km^{-2} in the mid 1980s.

The trends were investigated by linear regression of the aggregated biomass indices against time ($n = 5$, Fig. 5). Each index had a coefficient of variation (CV) around 25% due to sampling error. A strong seasonal dependence is evident. The average biomass index in August is 18.6 ± 0.5% higher than that in February. The regression slope should, nevertheless, give a good indication of the trends over the 2 years. Any consistent seasonal effect could influence the regression intercept, but not the slope.

The total biomass index did not change much over the 2 years of the acoustic survey programme. At the species level, however, considerable changes were observed. Comparing the same seasons between years, our results show a

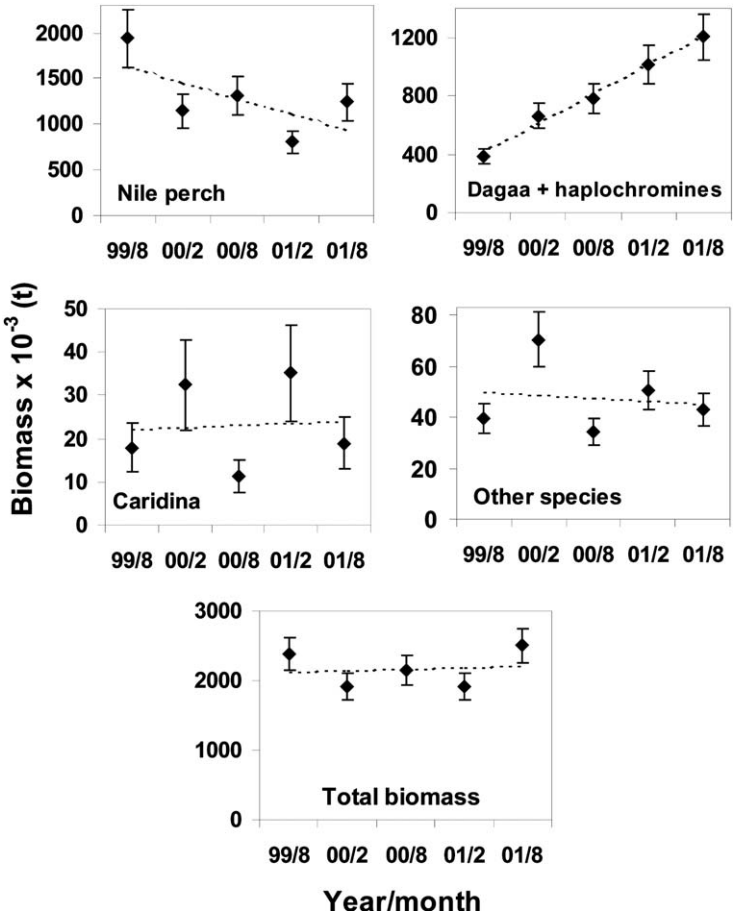

Fig. 5. Biomass indices from acoustic surveys of Lake Victoria 1999–2001. Points are the individual survey results. Bars show standard errors. Dashed lines: trends from linear regression of the five indices against time.

declining Nile perch stock (significance level 95%), while the small pelagics increased substantially over the same 2-year period. This is consistent with the observation of Witte et al. (2000) that the haplochromine population was increasing in the late 1990s.

3.2. Bathyspatial distribution

The acoustic surveys showed how fish were distributed through the water column and across the lake. Fig. 6 shows how the mean SC changed between the four zones.

In the shallow zones the all-species SC was around twice that in the offshore zones. Most of the variation comes from the Nile perch, which are primarily near the bottom. When the lake was stratified, there were few echoes below the oxycline.

In the case of the small pelagics, substantial quantities were observed in the upper waters throughout the lake. The dominant species in the pelagic zone were dagaa, *R. argentea* in surface layers and haplochromines, which were generally in deeper layers. The dagaa were less abundant inshore in August compared to February. The SC was much the same in

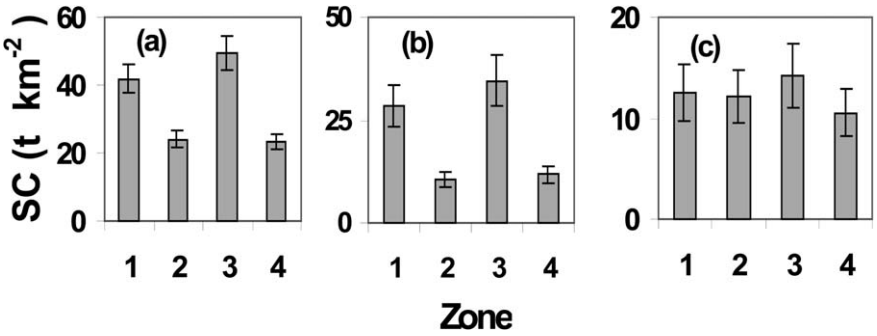

Fig. 6. Distribution of the Standing Crop (means for all five surveys) between the zones of Lake Victoria—1, 2 north; 3, 4 south; 1, 3 shallow; 2, 4 deep. Bars show standard errors. (a) Total biomass, (b) Nile perch, (c) small pelagics.

Table 1
Dissolved oxygen concentrations ± 1 standard error (mg l^{-1}) near the lakebed by water depth and season. Mean results from measurements during surveys in 2000

	Season	
	February	August
Inshore (<40 m depth)	4.3 ± 0.8	6.2 ± 0.6
Offshore (>40 m depth)	1.2 ± 0.7	6.3 ± 0.3

all zones. The small pelagics were patchily distributed in open water, but more uniformly than the less abundant *C. nilotica*, *B. profundus* and *Synodontis* species.

The consistency of the spatial distribution was investigated through paired comparisons between surveys of the SC in each 15 × 15 nmi square. Backward stepwise regression was used to determine the Pearson moment correlation coefficient. The August distributions were positively and significantly correlated with one another, as were those of the February surveys ($P < 0.01$). The cross-correlations between the February and August surveys were much less consistent.

3.3. Environmental factors

During February, most of the deeper lake is stratified with richly oxygenated water lying above a nearly anoxic layer. In August the water is well mixed with a much higher concentration of dissolved oxygen. Table 1 shows the concentrations recorded during the two surveys in 2000. Note that 3 mg l^{-1} is the critical level of dissolved oxygen below which most fish species are not able to survive (Chapman et al., 1995; Wanink et al., 2001).

The inshore oxygen concentration remained high throughout the year. The seasonal changes were much stronger in the deeper water.

4. Discussion

This paper describes the first comprehensive acoustic assessment of fish stocks in Lake Victoria. Due to the pioneering nature of the work, some changes in methodology were adopted as techniques developed. The initial survey design was more stratified than that adopted later, the survey duration was extended to allow more fishing and a higher degree of area coverage, and a new gear was introduced to improve echo-trace sampling. These changes could bias the observed trends and the species proportions from echo-trace partitioning. The results are, nevertheless, our best estimates of the biomass indices and the distribution of fish stocks. The experience gained should allow future surveys to be conducted with a more consistent methodology. Consistency in acoustic surveying is important for reliable indication of trends in the biomass and its principal components.

The vertical echo-sounder cannot integrate fish in the near-surface layer. Corrections can be made if the near-surface aggregations are similar to those observed further down, however, substantial coastal areas of Lake Victoria are less than 10 m deep. Estimates made by present techniques are unsatisfactory in these circumstances. Horizontal sonar might be used in future surveys as a novel way to improve the coverage of the lake.

Better knowledge of the fish TS is needed to determine the biomass as an absolute measure rather than an index. Our experiments showed that the caged-fish technique works well for the robust Nile perch, however, they were restricted to juvenile specimens. Further work on larger fish is required. In the case of *R. argentea*, the mortality rate in the experimental cage was too high to give good results. Improved techniques are needed to maintain the captive fish in good condition. Future TS experiments should include other species, notably the pelagic haplochromines and the tilapia *O. niloticus*. It would also be useful to determine the TS of the lake fly larvae, *Chaoborus* spp., since they can produce strong planktonic echoes at night.

In addition to oxygen, the chlorophyll-*a* concentration, water temperature and salinity were measured during the surveys. Seasonal differences in all these parameters were observed which could further influence the fish distribution. For example, higher fish densities were observed in warmer water i.e. in the coastal shallows compared to the central areas of the lake. This suggests that the water temperature is also an important determinant of the spatial distribution and variability of the fish stocks.

Understanding the behavioural ecology of fish is essential to the interpretation of acoustic surveys. Fish aggregation behaviour can change with the time of day and environmental conditions. This affects the characteristics of the echo-traces (Aglen, 1994; Misund, 1997). In Lake Victoria, the scattering layers containing fish have different features from time to time. Inshore, the main layer was usually near the bottom during morning hours and in midwater during the afternoon. In the evening, fish were scattered all over the water column. In the open deeper part of the lake, the layer was always in midwater.

When periods with different fish aggregation behaviour are being compared, different criteria are needed for partitioning the echo-integrals. We used simple rules to make the partitioning as objective as possible, however, the possible bias in the partitioned results is unknown. The reliance on trawl catches for the species and size proportions could introduce substantial error. The relative catch selectivity on species as different as Nile perch and dagaa is a particularly difficult question.

There was a significant ($P > 0.95$) decline of the *L. niloticus* stock over the 2 years of our investigations. Fishing pressure is a primary reason for the decline, however, environmental changes could also be important. Oxygen depletion can deny large areas of the bottom to fish. This is thought to have contributed the past decline of the haplochromine stocks (Hecky et al., 1994). Anoxia forces the demersal population to concentrate inshore where they are more vulnerable to predation by *L. niloticus* (Witte et al., 1992, Kudhongania and Cordone, 1974).

Some spatial separation of the species may be maintained, depending on the precise environmental conditions, since the small haplochromines can tolerate low-oxygen water unsuitable for the large perch (Fish, 1956; van Oijen et al., 1981; Chapman et al., 1995).

The important point here is that environmental and biological studies need to be included in the stock assessment process. All the factors motivating change must be considered together, to determine the true risk to the long-term future of sustainable fisheries.

Acknowledgements

Phase II of the LVFRP was supported by the European Development Fund and the Governments of Kenya, Tanzania and Uganda. We acknowledge the advice and support provided by many colleagues from the regional fishery research institutes (FIRRI, KMFRI and TAFIRI), the FRS Marine Laboratory in Scotland and the Hull International Fisheries Institute in England.

References

Aglen, A., 1994. Sources of error in acoustic estimation of fish abundance. In: Ferno, A., Olsen, S. (Eds.), Marine Fish Behaviour in Capture and Abundance Estimation. Fishing News Books, Oxford, UK, pp. 107–133.

Chapman, L.J., Kaufman, L.S., Chapman, C.A., Mckenzie, F.E., 1995. Hypoxia tolerance in 12 species of East African cichlids—potential for low-oxygen refugia in Lake Victoria. Conserv. Biol., 1274–1288.

Fish, G.R., 1956. Some aspects of respiration of six species of fish from Uganda. J. Exp. Biol. 33, 186–195.

Foote, K.G., 1987. Fish target strengths for use in echo-integrator surveys. J. Acoust. Soc. Am. 82, 981–987.

Goudswaard, P.C., Witte, F., Katunzi, E.F.B., 2002. The tilapiine fish stocks of Lake Victoria before and after the Nile perch upsurge. J. Fish Biol. 60, 838–856.

Hecky, R.E., Bugenyi, F.W.B., Ochumba, P., Talling, J.F., Mugidde, R., Gophen, M., Kaufman, L., 1994. Deoxygenation of Lake Victoria, East Africa. Limnol. Oceanogr. 39, 1476–1481.

Kudhongania, A.W., Cordone, A.J., 1974. Bathospatial distribution patterns and biomass estimates of the major demersal fishes in Lake Victoria. Afr. J. Trop. Hydrobiol. Fish. 3, 15–31.

MacLennan, D.N., Simmonds, E.J., 1992. Fisheries Acoustics. Chapman and Hall, London p. 325.

Misund, O.A., 1997. Underwater acoustics in marine fisheries and fisheries research. Rev. Fish Biol. Fish. 7, 1–34.

Moreau, J., 1995. Analysis of species changes in Lake Victoria using ECOPATH, a multispecies trophic model. In: Pitcher, T.J., Hart, P.J. (Eds.), The Impact of Species Changes in African Lakes. Chapman and Hall, London, pp. 137–161.

van Oijen, M.J.P., Witte, F., Witte-Maas, E.L.M., 1981. An introduction to ecological and taxonomic investigations on the cichlids from the Mwanza Gulf of Lake Victoria. Neth. J. Zool. 31, 149–174.

Pieper, R.E., 1979. Euphausid distribution and biomass determined acoustically at 102 kHz. Deep Sea Res. 26, 687–702.

Reynolds, J.E., Greboval, D.F., 1988. Socio-economic effects of the evolution of Nile perch fisheries in Lake Victoria: a review. Com. Inland Fish. Afr. Tech. Pap., 17. Food and Agriculture Organisation of the United Nations, Rome, Italy.

Wanink, J.H., Kashindye, J.J., Goudswaard, P.C., Witte, F., 2001. Dwelling at the oxycline: does increased stratification provide a predation refugium for the Lake Victoria sardine *Rastrineobola argentea*? Freshwater Biol. 46, 75–85.

Witte, F., Goldschimidt, T., Wanink, J., van Oijen, M., Goudswaard, K., Witte-Maas, E., Bouton, N., 1992. The destruction of an endemic species flock: quantitative data on the decline of the haplochromine cichlids of Lake Victoria. Environ. Biol. Fishes 34, 1–28.

Witte, F., Msuku, B.S., Warink, J.H., Seehausen, O., Katunzi, E.F.B., Goudswaard, P.C., Goldschmit, T., 2000. Recovery of cichlid species in Lake Victoria: an examination of factors leading to differential extinction. Rev. Fish Biol. Fish. 10, 233–241.

Available online at www.sciencedirect.com
SCIENCE DIRECT®
Aquatic Living Resources 16 (2003) 167–173
Aquatic Living Resources
www.elsevier.com/locate/aquliv

Hydroacoustical parameters of fish in reservoirs with contrasting levels of eutrophication

Małgorzata Godlewska [a,*], Andrzej Świerzowski [b]

[a] *International Centre for Ecology, Polish Academy of Sciences, ul. Konopnickiej 1, 05-092 Łomianki, Poland*
[b] *Institute of Inland Fisheries, ul. Oczapowskiego 10, 10-719 Olsztyn, Poland*

Accepted 15 January 2003

Abstract

Hydroacoustical estimation of fish abundance and distribution is performed in three reservoirs that are characterised by different levels of eutrophication. The Biosonics 101 dual beam echosounder with a frequency of 420 kHz and the ESP software for acoustical data analyses are used. A clear dependence between fish density and the level of eutrophication is observed. In the mesotrophic Solina reservoir, fish abundance is over an order of magnitude lower than that in the eutrophic Dobczyce and Sulejów reservoirs. Fish length distributions have different shapes in the three reservoirs, which indicates the changes in fish size structure due to eutrophication; however, the mean target strength of fish does not differ significantly. These results suggest that hydroacoustically collected data may help to assess the ecological state of inland waters and may be used together with other methods in monitoring the water quality.

Keywords: Hydroacoustics; Eutrophication; Fish stocks; Reservoirs; Water quality

1. Introduction

Eutrophication of inland waters, which leads to fast deterioration of water quality and to the commonly observed phytoplankton blooms (Tarczyńska et al., 2001), is a worldwide problem for the managers of water resources. If sustainable management and restoration of aquatic ecosystems is to be successful, it is important to have cost-effective methods for reliable, large scale monitoring of water quality. New technology has an increasing role to play in the classification and management, and methodologies for classification and evaluation of lake state should be developed (see requirements of the new Water Framework Directive).

Classification schemes for standing waters have been a subject of research for over a century. The major focus of most research has been the trophic status, which is principally determined by phosphorus and nitrogen. However, it is well known that the concentrations of nutrients in reservoirs undergo natural fluctuations dependent on the physical, chemical and biological characters of their watersheds. This leads to significant difficulties in sampling, measurement, evaluation and classification of lakes. One of the major problems is that the trophic parameters are determined from point measurements, while in fact they are changing within the water body both horizontally and vertically. Thus, point measurements are not always representative of the trophic state of the whole ecosystem of reservoir or lake. Carlson (1977) has attempted to develop a universal trophic state index for lakes that could be calculated on the basis of any of several parameters, such as Secchi disk transparency, chlorophyll *a* or total phosphorus, thus, that would retain the expression of the diverse aspects of the trophic state, yet still could have the simplicity of a single parameter index. However, comparatively high fluctuations of the index, which are dependent on the parameter used for calculations, and high seasonal sensitivity have limited its routine application.

Changes in nutrient loading result in changes in community structure at each trophic level including fish. To quantify such changes, numerous indices have been developed, see review by Washington (1984), but their validity has been questioned, as contrasting results have been obtained for relationships between species richness and trophic state. Classification using various taxonomic groups, or assemblages from specific habitats have encountered difficulties, because such indices often reflect local conditions rather than

* Corresponding author.
E-mail address: mce-pan@mail.unicom.pl (M. Godlewska).

doi:10.1016/S0990-7440(03)00014-7

Table 1
Characteristics of the reservoirs under study

Reservoir	State of eutrophication	Total phosphorus (μmg dm^{-3})	Retention time (month)	Area (ha)	Volume (10^6 m^3)	Mean depth (m)	Maximum depth (m)
Solina	Mesotrophic	6	6	2105	472	22	65
Dobczyce	Eutrophic	93	4	1120	127	11	35
Sulejów	Highly eutrophic	366	1	2200	75	3	10

the quality of the water as a whole. Classification schemes based upon phytoplankton and zooplankton, or zoobenthos, while offering probably the most directly relevant information to water managers as related to the whole water column, have limited usefulness due to the complexity of interpretation and difficulties in separating natural variation from those caused by the impact of man. The classification of standing water state using macrophytes (Melzer, 1999; Ozimek and Kowalczewski, 1984) is also limited by the fact that macrophytes may obtain their phosphorus from long accumulation in sediments and therefore may be largely independent of the current water column concentrations.

The existing different measures of the ecological state of the ecosystem, based on chemical, physical and biological parameters (Carlson, 1977; Washington 1984) are as yet not sufficient for the effective monitoring and management of a lake, and leave a considerable room for improvement. New methods for evaluation and assessment of a lake state should be developed. In this respect, hydroacoustical methods deserve more attention than that they have been given so far. In contrast to conventional point measurements, the hydroacoustical methods provide high resolution area-based synoptic data that are collected on a regular basis adequate for GIS presentation. Thus, they enable to visualise, evaluate and compare the outcome resulting from different reservoirs, or different moments in time (daily, seasonally, annually). The digital format of remotely sensed data makes it easy to retrieve and analyse large amounts of information at low cost and in a short period of time.

Eutrophication leads to undesirable changes in fish species composition, size distribution and abundance (Colby et al., 1972; Kubecka, 1993). Salmonids characteristic of oligotrophic conditions are replaced by cyprinids with rapidly decreasing share of predatory fish. The density of fish at the beginning increases, then falls dramatically with the number of species and their body lengths continuously decreasing (Bachmann et al., 1996; Jeppesen et al., 2000a, b). Fishery methods can give us detailed information about the population structure of fish, which is an important indicator of the water quality, but to assess fish biomass these methods are very tedious, time and labour consuming and not always applicable. By contrast, fish abundance can be easily estimated using acoustics. The length distributions of fish populations, measured acoustically, have lower precision than traditional fishery methods, but for comparison purposes, it is probably sufficient. In spite of the advantages of acoustical methods, they are as yet seldom used to study freshwater ecosystems.

Application of hydroacoustics for ecological studies is very promising and rapidly developing nowadays. Echo sounding techniques can provide the basic information not only on fish stocks, sizes and spatio-temporal distribution patterns (Świerzowski et al., 2000), but also on zooplankton (Stanton and Chu, 1998; Stanton et al., 2001), bottom characteristics (LeBlanc et al., 1992; Anderson et al., 2002) and macrophytes coverage (Sabol and Burczyński, 1998). Thus, acoustical methods can integrate several of the quality indices that have been used so far, in addition offering the scale and accuracy not available with other methods. Knowledge of the relationships between fish, macrophytes and zooplankton that can be assessed using acoustics is of great importance for the conservation of high water quality.

The paper presents the preliminary results, whose aim was to check which of the fish parameters derived from hydroacoustical monitoring of the reservoir can be used as indices of its trophic state. For this purpose, the hydroacoustical data concerning fish abundance and size distribution are compared with the environmental parameters for three reservoirs, which differed substantially as regarding their condition and water quality.

2. Materials and methods

2.1. Study sites

Three reservoirs with contrasting levels of eutrophication (total phosphorus loadings in each of them differed roughly by one order of magnitude) were studied: the montane mesotrophic Solina reservoir, the submontane eutrophic Dobczyce reservoir and the lowland highly eutrophic Sulejów reservoir. Their principal morphometric and trophic characteristics are summarised in Table 1.

The largest reservoir, Solina, situated in the Carpathian Mountains, comprises about 15% of the total water storage in Poland. Due to the power station activity, the fluctuation of the water level is up to 10 m, which leads to the absence of littoral area. Concentrations of phosphorus and nitrogen compounds in the reservoir correspond to mesotrophy. The most frequent fish species are: bream (*Abramis brama*) 57.8%, crucian carp (*Carassius carassius*) 16.1%, roach (*Rutilus rutilus*) 9.2%, pike-perch (*Stizostedion lucioperca*) 4.5% and perch (*Perca fluviatilis*) 4.8% (Bieniarz and Epler, 1993). Information on the physical, chemical and biological characteristics of the reservoir is available (Godlewska et al., 2000).

The Dobczyce reservoir supplies the drinking water for Kraków, one of the largest cities in Poland. Hence, the qual-

ity of water is the main concern for both the authorities and the inhabitants. The fish management applied in the reservoir is based on a biomanipulation, which is directed to an increase in the number of predatory fish by stocking and by prohibition of angling, and the limitation of planktivorous fish by regular catches. These practices ensure a good quality of water, in spite of a fairly high loading of nutrients. The most frequent species are the same as in the Solina reservoir, i.e. bream, roach, pikeperch and perch, but they are present in different proportions (Jelonek and Godlewska, 2000).

The Sulejów is a shallow lowland reservoir situated in central Poland. The reservoir is eutrophic due to high nutrient loads. Total phosphorus concentrations (TP) of about 150-500 µg dm^{-3}, and total nitrogen (TN) of 1500-2500 µg dm^{-3} are maintained throughout the year (Tarczyńska, 2001). This leads to the occurrence of toxic algal blooms during periods of mean water temperatures exceeding 18 °C. Since the Sulejów reservoir is one of the important freshwater resources for the city of Łódź (over one million people) the utilisation of water may be highly dangerous.

2.2. Field measurements

Hydroacoustical records of fish distribution were obtained along closely separated zigzag transects covering the whole area of the reservoirs with depths exceeding 3 m. Surveys were performed during summer seasons of 1999-2002 on day and night bases: three surveys in the Solina reservoir, three in the Dobczyce reservoir and one survey in the Sulejów reservoir. The echosounder used was a Biosonic 101 dual beam, 420 kHz, with a narrow beam width of 6° and a wide beam width of 15°. To estimate fish abundance and size distribution, the echo counting method was applied with the TVG set to 40 log *R*. Due to time limitations and the fact that the echosounder used did not allow for the simultaneous recording of 20 log *R* and 40 log *R*, the echo integration was not performed. The echo sounding results were analysed using the ESP software system supplied by the manufacturer. The instrument settings for data acquisition were the following: pulse length $\tau = 0.4$ ms, single target criteria $0.8 < \tau < 1.2$, repetition rate 0.1 or 0.5 s, threshold -65 dB (200 mV), The parameters settings in the post-processing software were the same for all three reservoirs The maximum half-angle for processing targets was set to three and the beam pattern factor > zero had threshold 3 dB. The acoustic system was routinely calibrated with a -43.2 dB tungsten carbide sphere before each measurement series (Foote et al., 1987).

In the Solina reservoir, water samples for the analysis of chlorophyll *a*, nutrients, and zooplankton were taken at nine stations at which temperature, oxygen concentration and Secchi disk visibility were also measured. The stations were situated in the main basin near the dam, as well as in the two branches of the reservoir; the Solinka and San supply rivers, which were characterised by different trophic levels. For the Dobczyce and Sulejów reservoirs, environmental data were taken from one monitoring station during the year when acoustical data were collected (M. Tarczyńska and E. Wilk-Woźniak, personal communications).

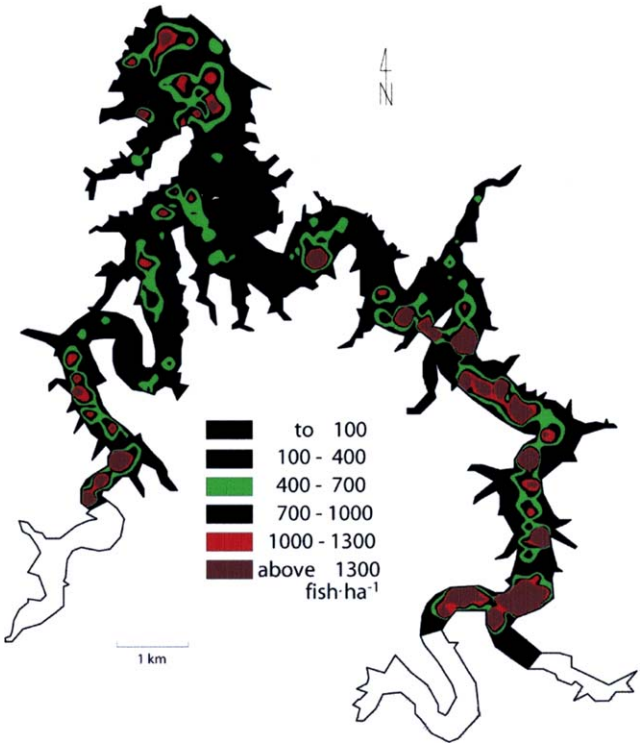

Fig. 1. Fish spatial distribution in the Solina reservoir (Poland).

3. Results

3.1. The Solina reservoir

Fish spatial distribution in the Solina reservoir (Fig. 1) exhibits a typical longitudinal pattern with higher concentrations in shallow areas close to the river discharge, and lower concentrations in a deep part near the dam. The fish density gradient corresponds to the enhancement in the productivity of the reservoir. Patchiness in fish distribution also clearly reveals the locations of agricultural and tourist pollution (source of nutrients).

Acoustical fish characteristics, such as mean density and mean target strength (TS) along the longitudinal axis (Fig. 2) are correlated with the nutrient gradient represented by such

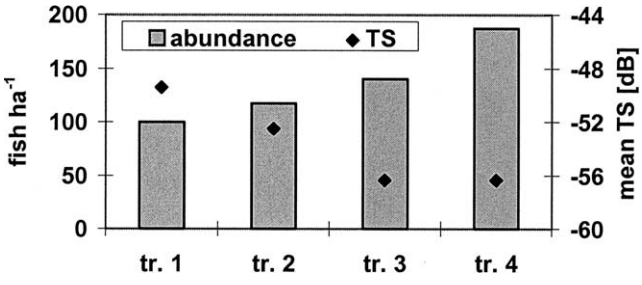

Fig. 2. Fish densities and their mean TSs in four transects in the Solinka branch of the Solina reservoir along the increasing trophic level (from the dam towards the river discharge).

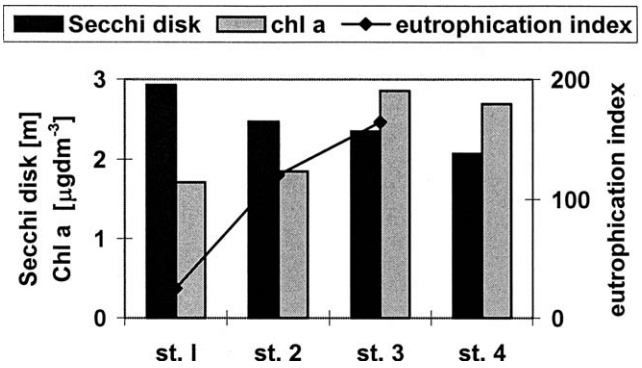

Fig. 3. Environmental parameters at four stations along the Solinka branch of the Solina reservoir. Secchi disk visibility and chlorophyll *a* concentration are taken as mean for the season, from May to October (T. Półtorak, personal communications) and eutrophication index based on the *Oligochaeta* to Chironomidae ratio in benthos was determined by T. Prus et al. (personal communications).

environmental characteristics as Secchi disc visibility, chlorophyll *a* concentration and eutrophication index based on the *Oligochaeta* to Chironomidae ratio in benthos (Fig. 3). Comparison of the Figs. 2 and 3 shows that fish abundance increases with increased eutrophication level, while the mean size of fish represented by its TS decreases.

3.2. Comparison of dam reservoirs

As expected, the three reservoirs with the contrasting levels of eutrophication also differed strongly in the levels of fish densities and fish length distributions. Similar to the Solina reservoir alone, fish abundance first increased with an increased concentration of chlorophyll *a* in the Dobczyce reservoir, then dropped in the Sulejów reservoir, although the chlorophyll *a* was further increasing (Fig. 4). Using the echo counting method, instead of echo integration, could lead to some underestimation of fish abundance, especially in the shallowest Sulejów reservoir. This makes it impossible to decide whether the observed drop in fish density was caused by the bias in the acoustical fish density estimate or was the real one and caused by eutrophication. In the Solina and Dobczyce reservoirs, fish were fairly well dispersed at night and the bias due to multiple targets was negligible. The

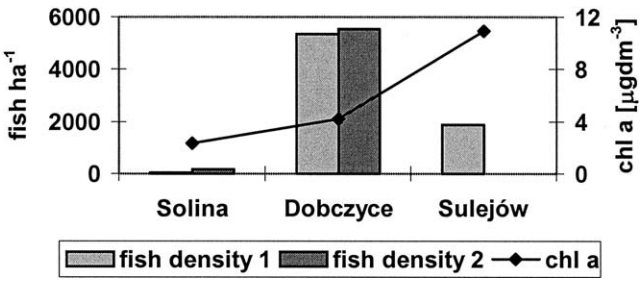

Fig. 4. Fish density estimates (night only, threshold -65 dB) in three reservoirs with different levels of eutrophication. Fish density 1: the Solina reservoir surveyed on 14 July 2000, the Dobczyce reservoir surveyed on 19 June 2000, the Sulejów reservoir surveyed on 16 July 2002. Fish density 2: the Solina reservoir surveyed on 23 August 2001, the Dobczyce reservoir surveyed on 1 August 2002 (see Table 2).

seasonal and year-to-year fluctuations of fish densities within a given reservoir were much smaller than the variations between the reservoirs (Table 2).

In the mesotrophic Solina reservoir, fish concentrations were over one order of magnitude lower than that in the other two eutrophic reservoirs, independently of the threshold applied for the analysis (Table 2). This was true for both day and night estimates. In the Solina reservoir, the day estimates were regularly slightly higher than those of the night ones, probably due to diurnal vertical migrations of fish (Godlewska et al., 2000). On the other hand, in the Dobczyce and Sulejów reservoirs, which are shallower, night estimates were usually higher than the estimates during the day, probably due to predominance of the horizontal over the vertical migrations, from the littoral during the day to open water at night (Godlewska, 2002).

The fish length distributions represented by their TS differed markedly in all three reservoirs. The distributions presented were based on all echoes considered as independent samples (Fig. 5). Since the different number of fish was registered in each of the reservoirs, the frequency of every TS class was shown as the percentage of total number of fish. In the Solina reservoir, all but very large sizes (in dB) were present in similar proportions. In the Dobczyce reservoir, pressure of the predatory fish was demonstrated by a little contribution of small specimens into the population structure (due to biomanipulation the predatory pike-perch and perch made over 30% of fish population and efficiently eliminated small specimens). In the Sulejów reservoir, the situation was opposite, the smallest sizes dominated and larger fish were entirely absent.

In spite of clear differences in the shape of fish length distributions in the three reservoirs, the mean values of fish acoustical lengths did not differ significantly (Table 2). It was to be expected, as the TS values varied greatly, and in this case the mean value was almost meaningless. To characterise the fish size distributions, instead of the mean value, one should rather use the percentage of fish belonging to a certain size classes.

4. Discussion

By studying systems at the extremes of the trophic gradient (low trophy Solina reservoir and highly eutrophic Sulejów reservoir), we hoped to obtain a more clear picture of the relationship between lake productivity and fish parameters in a broad spectrum of the reservoir ecosystems. The reservoirs, as expected, differed strongly in the levels of fish density. Fish concentrations in the two eutrophic reservoirs were more than an order of magnitude higher than that in the mesotrophic reservoir. It is obvious, that for the purpose of comparison, measurements should be taken at the same time of the season—preferably at the end of summer, and the same time of day—preferably at night, when a majority of fish are dispersed in the pelagial. The TS threshold is very important, although its proper choice may be difficult at the present,

Table 2
Fish densities and the TS for the studied reservoirs

Reservoir name	Date	Fish (ha^{-1})	Mean TS [a]	S.D.	TS max	Mean *s* (in dB) [b]	Number of fish [c]	Day or night
Threshold 200 mV (TS = –65 dB)								
Solina reservoir	14 July 2000	48	–52.39	6.7	–35.8	–47.52	229	D
	14 July 2000	43	–53.76	6.1	–37.0	–46.64	107	N
	23 August 2001	178	–55.63	5.2	–34.3	–51.32	2287	N
Dobczyce reservoir	19 June 2000	3030	–54.34	4.8	–32.9	–51.33	5944	D
	19 June 2000	5340	–55.04	4.3	–29.0	–52.44	9200	N
	13 August 2001	2610	–53.23	5.6	–30.3	–49.75	13 074	D
	13 August 2001	3390	–53.74	5.2	–34.4	–50.97	16 355	N
	01 August 2002	5625	–55.48	5.2	–31.0	–52.10	7889	N
Sulejów reservoir	16 July 2002	1743	–56.47	4.8	–35.5	–53.13	1662	N
	16 July 2002	574	–56.58	5.9	–36.3	–50.38	80	D
Threshold 500 mV (TS = –57 dB)								
Solina reservoir	14 July 2000	35	–49.29	4.2	–35.8	–46.78	164	D
	14 July 2000	23	–49.03	4.4	–37.0	–46.27	58	N
	23 August 2001	43	–50.47	4.0	–34.3	–47.99	1176	N
	24 September 2002	58	–47.90	4.9	–30.6	–44.17	733	D
	24 September 2002	43	–48.84	4.4	–30.5	–45.91	535	N
Dobczyce reservoir	19 June 2000	1875	–50.87	3.3	–32.9	–49.06	3672	D
	19 June 2000	2865	–51.69	2.6	–29.0	–50.12	4939	N
	13 August 2001	1605	–49.34	3.4	–30.3	–47.70	8057	D
	13 August 2001	2055	–49.98	2.9	–34.4	–48.97	9930	N
	01 August 2002	2805	–50.67	2.9	–31.0	–49.24	3882	N
Sulejów reservoir	16 July 2002	151	–48.55	5.1	–35.5	–45.08	21	D
	16 July 2002	618	–51.00	3.3	–36.3	–49.00	431	N
Threshold 1000 mV (TS = –50 dB)								
Solina reservoir	14 July 2000	13	–45.18	3.0	–35.8	–43.99	58	D
	14 July 2000	8	–44.51	3.6	–37.0	–42.97	22	N
	23 August 2001	10	–46.10	3.3	–34.3	–44.57	314	N
	24 September 2002	28	–44.98	3.7	–30.6	–43.11	361	D
	24 September 2002	20	–45.33	3.3	–30.5	–43.87	239	N
Dobczyce reservoir	19 June 2000	345	–46.26	2.9	–32.9	–44.95	685	D
	19 June 2000	180	–46.33	3.9	–29.0	–43.24	321	N
	13 August 2001	690	–46.58	2.3	–30.3	–45.54	3485	D
	13 August 2001	735	–47.36	1.8	–34.4	–46.86	3549	N
	01 August 2002	690	–47.73	2.4	–31.0	–46.42	1164	N
Sulejów reservoir	16 July 2002	63	–44.02	4.4	–36.3	–42.01	9	D
	16 July 2002	98	–45.46	3.2	–35.5	–43.96	70	N

[a] Mean TS averaged in logarithmic domain.
[b] Mean TS averaged in linear domain and then recalculated to dB.
[c] Number of fish taken for statistics.

with a limited knowledge of the TS of inland fishes at different frequencies. The threshold used in this study (-65 dB) may seem to be low as compared with other investigations done at frequencies 120 and 200 kHz. The reason for this low threshold was that at frequency 420 kHz, the TS of fish is considerably smaller than at lower frequencies. According to Mason and Schaner (2001), who measured the TS of fish simultaneously by a few different echosounders, the 420 kHz system consistently had the lowest estimates of TS, with a 13 dB average deviation from other systems at -70 dB threshold, and 17 dB at -80 dB. In our observations (not published), the TSs of roach and perch were considerably lower than it would be expected from the commonly used Love's formula (1977). The TS distributions can be directly compared only if they were received with the same frequencies. Observed differences in fish density and fish length distributions, along the nutrient gradient, suggest that both parameters can be used as indices of the quality of the ecosystem.

We are aware of the fact that fish populations are subject to large fluctuations seasonally, and from year to year. These changes may arise through fish management (fishing pressure or stocking) or from natural causes, mainly affecting the survival of juveniles. This considerably weakens the strength of the fish abundance as an indicator of the quality of the ecosystem. Nevertheless, a relationship between fish densities and the eutrophication level has been demonstrated in the literature. Jeppesen et al. (1997) observed that the total catch of fish per net (CPUE) in multimesh gillnets placed in the

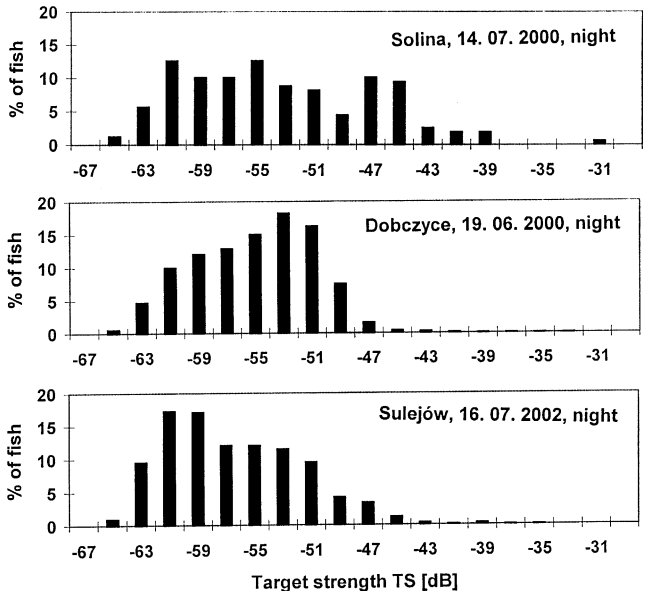

Fig. 5. Fish length distributions in three reservoirs with different trophic levels.

open water and the littoral zone of 42 north temperate Danish lakes was positively related to nutrient level. The relationships between fish abundance and nutrients and fish abundance and zooplankton/phytoplankton ratio and between chlorophyll *a* and total phosphorus measured in 25 New Zealand lakes (Jeppesen et al., 2000a) have largely followed the pattern obtained for Danish lakes. A similar pattern was observed in 65 Florida (USA) lakes, which were selected to range from oligotrophic to hypereutrophic. The total fish biomass per unit area was positively correlated with total phosphorus, total nitrogen, chlorophyll *a*, and inversely correlated with Secchi disc transparency. On an average, the standing crops increased about one order of magnitude from the oligotrophic to the hypereutrophic (Bachmann et al., 1996). According to these authors, there was a considerable unexplained variance (about 75%) in these relationships, due in part to other factors influencing fish stocks and the practical sampling problems of estimating the biomass of wild fish populations. It is apparent, that a large number of interlinking ecological factors operate, especially in shallow lakes, to make at present only a general guidance possible in which fish populations can be associated with lakes of different environmental conditions. The application of acoustics may lead to a better understanding of these linkages and a more precise estimation of fish stocks.

The changes in fish abundance and size distribution received in this study, using hydroacoustical methods, correspond well to the results received by traditional fishery methods for other lakes, both in temperate and tropical regions. Many factors may introduce biases in the fish density measured by acoustics (MacLennan and Simmonds, 1992), but other methods are not free of them either. Diurnal variation in fish behaviour affects the results of surveys, especially the ratio of apparent biomass measured by day and night (Godlewska, 2002). Among the different biases, the majority leads to underestimation rather than overestimation. During the day, factors leading to underestimation include: vessel avoidance (Olsen, 1990), the acoustic shadow in dense aggregations (Appenzeller and Leggett, 1992), daily horizontal migrations causing that fish are located in inaccessible area, littoral zone for instance (Godlewska, 2002), the decrease in TS associated with an increase in the tilt angle, when fish dive below the boat (Fréon et al., 1993), and the bottom blind area when during the day important part of the biomass is located very close to the bottom. During the night, the major underestimation, in measured acoustic density, is due to a subsurface blind area dependent on the depth of the transducer and its dead zone. This problem may be solved using additional horizontally looking transducer (Kubecka, 1996). In spite of all these difficulties, the use of hydroacoustics to estimate fish abundance, instead of traditional fishery methods, has many advantages, e.g. such as time and cost effectiveness, coverage of large areas, high spatial resolution. If additionally accompanied by control catches for species composition, acoustics can provide the basis for an integrated fish-oriented indicator of the ecosystem quality. The efforts of incorporating fish into lake quality measures should be supported because fish have both economic and aesthetic values, and thus help to raise awareness for the necessity of conserving aquatic habitats. Among the biological indices, fish should be considered as key organisms because they are present in nearly all water bodies, are indicative of habitat quality at various spatial scales, occupy variety of trophic levels, and play a central role in lake restoration and management (Lammens, 1999).

Acoustical methods need many more investigations before they can be used as a standard monitoring tool and a source of ecosystem quality indices, but the results so far justify efforts applied. A standard protocol, for the collection and processing of acoustic data, should be done before implementation of the new Water Framework Directive. Currently, there are at least 13 different scientific echosounders encompassing seven models and four frequencies (70, 120, 200 and 420 kHz), which make it very difficult to compare data between different hydroacoustic systems, lakes and individual users. The intercalibration of different acoustical systems should be encouraged.

Acknowledgements

We are very grateful to Bill Acker for lending to us the Biosonics echosounder. We are also grateful to anonymous referees who greatly contributed to improving the manuscript. The work has been supported by the Committee of Scientific Research in Warsaw, Grant no. 6 P04F 00720.

References

Anderson, J.T., Gregory, R.S., Collins, W.T., 2002. Acoustic classification of marine habitats in coastal Newfoundland. ICES J. Mar. Sci. 59, 156–167.

Appenzeller, A.R., Leggett, W.C., 1992. Bias in hydroacoustic estimates of fish abundance due to acoustic shadowing: evidence from day-night surveys of vertically migrating fish. Can. J. Fish. Aquat. Sci 49, 2179–2189.

Bachmann, R.W., Jones, B.L., Fox, D.D., Hoyer, M., Bull, L.A., Canfield Jr., D.E., 1996. Relations between trophic state indicators and fish in Florida (USA) lakes. Can. J. Fish. Aquat. Sci. 53, 842–855.

Bieniarz, K., Epler, P., 1993. Fish catching by anglers in the Solina dam reservoir. Rocz. Nauk. PZW 6, 5–18.

Carlson, R.E., 1977. A trophic state index for lakes. Limnol. Oceanogr. 22, 361–369.

Colby, P.J., Spangler, G.R., Hurley, D.A., McCombie, A.M., 1972. Effects of eutrophication on salmonid communities in oligotrophic lakes. J. Fish. Res. Board Can. 29, 975–983.

Foote, K.G., Knudsen, H.P., Vestnes, G., MacLennan, D.N., Simmonds, E.J., 1987. Calibration of acoustic instruments for fish density estimation: a practical guide. Coop. Rep. Cons. Int. Explor. Mer 144, 69 p.

Fréon, P., Soria, M., Mullon, C., Gerlotto, F., 1993. Diurnal variation in fish density estimate during acoustic survey in relation to spatial distribution and avoidance reaction. Aquat. Living Resour. 6, 221–234.

Godlewska, M., 2002. The effect of fish migration pattern on the acoustical estimates of fish stocks. Acta Acust. Acust. 88, 748–751.

Godlewska, M., Półtorak, T., Świerzowski,, A., 2000. Hydroacoustical Estimation of fish abundance and distribution in the Solina reservoir. In: Kozaczka, E., Grelowska, G (Eds.), Naval Academy, Gdynia. Hydroacoustic, 3. Naval Academy, Gdynia. Hydroacoustic, pp. 173–177.

Jelonek, M., Godlewska, M., 2000. Ichtiofauna. In: Starmach, W., Mazurkiewicz-Boroń, J.I., Zbiornik Dobczycki, G. (Eds.), Ekologia-eutrofizacja-ochrona, pp. 137–148 ZBW PAN, Kraków.

Jeppesen, E., Jensen, J.P., Sondergaard, M., Lauridsen, T.L., Pedersen, L.J., Jensen, L., 1997. Top-down control in freshwater lakes: the role of nutrient state, submerged macrophytes and water depth. Hydrobiologia 342/343, 151–164.

Jeppesen, E., Jensen, J.P., Sondergaard, M., Lauridsen, T.L., Landkildehus, F., 2000. Trophic structures, species richness and biodiversity in Danish lakes: changes along a phosphorous gradient. Freshwat. Biol. 45, 201–218.

Jeppesen, E., Lauridsen, T.L., Mitchell, S.F., Christoffersen, K., Burns, C.W., 2000. Trophic structure in the pelagial of 25 shallow New Zealand lakes: changes along nutrient and fish gradients. J. Plankton Res. 22, 951–968.

Kubecka, J., 1993. Succession of fish communities in reservoirs of Central and Eastern Europe. In: Straskraba, M., Tundisi, J.G., Duncan, A (Eds.), Comparative Reservoir Limnology and Water Quality Management. Kluwer Academic Publishers, Netherlands, pp. 153–168.

Kubecka, J., 1996. Use of horizontal dual-beam sonar for fish surveys in shallow waters. In: Cowx, I.G (Ed.), Stock Assessment in Inland Fisheries. Blackwell Science, Oxford, pp. 165–178.

Lammens, E.H.R.R., 1999. The central role of fish in lake restoration and management. Hydrobiologia 395/396, 181–190.

LeBlanc, L.R., Mayer, L.A., Rufino, M., Schock, S.G., King, J., 1992. Marine sediment classification using the chirp sonar. J. Acoust. Soc. Am. 91, 107–115.

Love, R.H., 1977. Target strength of an individual fish at any aspect. J. Acoust. Soc. Am. 62, 1397–1403.

Mason, D.M., Schaner, T., 2001. Great Lakes Acoustics Workshop IV. Inter-Calibration of Scientific Echosounders in the Great Lakes.

MacLennan, D.N., Simmonds, E.J., 1992. Fisheries Acoustics. Fish and Fisheries Ser5. Chapman & Hall, London.

Melzer, A., 1999. Aquatic macrophyts as tools for lake management. Hydrobiologia 395/396, 181–190.

Olsen, K., 1990. Fish behaviour and acoustic sampling. Rapp. P.-v. Reun. Cons. Int. Explor. Mer 189, 147–158.

Ozimek, T., Kowalczewski, A., 1984. Long-term changes of the submerged macrophytes in eutrophic Lake Mikolajskie (North Poland). Aquat. Bot. 19, 1–11.

Sabol, B.M., Burczyński, J., 1998. Digital echo sounder system for characterising vegetation in shallow-water environments. In: Allipi, A., Cannelli, G.B (Eds.), Proceedings of the Fourth European Conference on Underwater Acoustics, pp. 165–171 Rome.

Stanton, T.K., Chu, D., 1998. Sound scattering by several zooplankton groups. I. Scattering models. J. Acoust. Soc. Am. 103, 236–253.

Stanton, T.K., Chu, D., Traykowski, L.V.M., Reeder, D.B., Warren, J.D., Wiebe, P.H., 2001. Broadband acoustic classification of individual zooplankton and fish: a review of recent work. In: Leighton, T.G., Herald, G.J., Griffiths, G (Eds.), Acoustic Oceanography, vol. 23, pp. 181–188 Proceedings of the Institute of Acoustics Part 2.

Świerzowski,, A., Godlewska, M., Półtorak, T., 2000. The relationship between the spatial distribution of fish, zooplankton and other environmental parameters in the Solina reservoir. Poland. Aquat. Living Resour. 13, 373–377.

Tarczyńska, M., Romanowska-Duda, Z., Jurczak, T., Zalewski, M., 2001. Toxic cyanobacterial blooms in a drinking water reservoir—causes, consequences and management strategy. Water Sci. Technol. Water Supply 1, 237–246.

Washington, H.G., 1984. Diversity, biotic and similarity indices. A review with special relevance to aquatic ecosystems. Water Res. 18, 653–694.

Available online at www.sciencedirect.com
SCIENCE DIRECT®
Aquatic Living Resources 16 (2003) 175–184
Aquatic Living Resources
www.elsevier.com/locate/aquliv

Observations of fish migration in a macrotidal mangrove channel in Northern Brazil using a 200-kHz split-beam sonar

Uwe Krumme *, Ulrich Saint-Paul

Zentrum für Marine Tropenökologie (ZMT), Fahrenheitstr. 6, 28359 Bremen, Germany

Accepted 11 April 2003

Abstract

A 200-kHz split-beam echosounder (BioSonics, DT6000) with a 6° circular-beam transducer was applied in a mangrove channel in Northern Brazil to study the migratory patterns of intertidal fish. Acoustic sampling was conducted horizontally across the channel perpendicular to the tidal current during two lunar cycles in the dry season 2000 and the wet season 2001. The complex acoustic environment of the mangrove channel was characterized by small target sizes (juvenile fish), multiple targets (aggregated fish), high reverberation and background noise levels due to sediment loads, plankton and mangrove litter transport. Dry seasons provided less noisy acoustic conditions resulting in clearer echo data than wet seasons. Neap tide data were less complex than spring tide data. During a tidal cycle, low water provided the clearest acoustic conditions. Mangrove leaves generated fish-like echoes. Analysis of two dry season wax moon cycles revealed fish flux maxima at low water, flood start and high water in the daytime and the night cycle. Night fish fluxes were significantly higher than at daylight. Throughout the tidal cycles, 60% of the fish traveled with the tide and 40% against, suggesting active foraging against the tide to be a major component of fish movements. Resident mangrove fish entered the intertidal creeks at early flood tide, leaving at late ebb tide at fairly shallow-water depths. Estuarine fish required a minimum water depth (about 2 m) for tidal migration. Since time delays during spring tides between immigration of resident and estuarine fish were reduced, foraging time and habitat accessibility would be enhanced and fish catches and fishes' feeding success would be greater.

Keywords: Shallow-water echosounder; Mangrove; Fish migration; Tide; Tidal cycle

1. Introduction

Mangroves—the highly productive evergreen tidal forests—are considered important nursery areas for young fish throughout the tropical and subtropical coasts of the world (Bell et al., 1984; Robertson and Duke, 1987; Louis et al., 1995; Laroche et al., 1997; Barletta-Bergan et al., 2002). Interannual, seasonal, lunar and diel changes have been observed in mangrove ichtyofauna (Davis, 1988; Laegdsgaard and Johnson, 1995; Laroche et al., 1997; Barletta, 1999). These changes are caused by active movements of the fish in response to variations in food availability, presence of competitors, predation risk and environmental suitability (Gibson et al., 1998) on short-, medium- and long-term scales.

Since tidal-related short-time movements may play a large part in the everyday survival strategies of juvenile fish, comprehensive information about such movements is essential for understanding the life of the young fish in their nursery habitats. Optimized small-scale movements within a nursery probably enhance growth, survival and thus recruitment success.

Although short-time changes in intertidal fish communities have been the focus of several studies (Davis, 1988; Laroche et al., 1997; Gibson et al., 1998; Krumme, own obs.), there is a considerable lack of detailed investigations on this particular time scale.

However, sampling in tidal habitats is often difficult to carry out (Horn et al., 1999). Generally, high tidal dynamics require high sample resolution and thus, sampling soon becomes labor-intensive. Additionally, strong tides and floating mangrove litter can considerably impede sampling with conventional fishing gear. Finally, low water clarity prevailing in many mangroves hampers visual observations of fish movements.

* Corresponding author.
E-mail address: uwe.krumme@zmt.uni-bremen.de (U. Krumme).

doi:10.1016/S0990-7440(03)00046-9

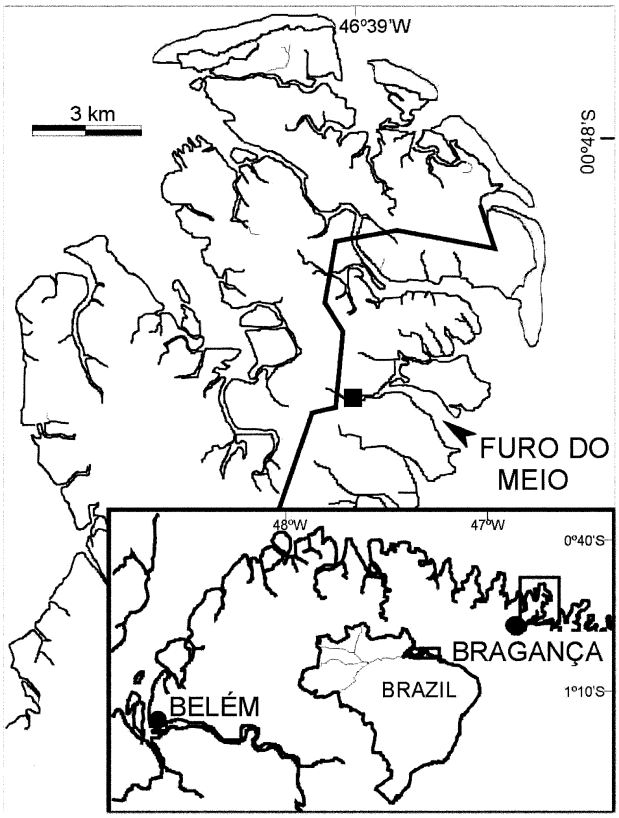

Fig. 1. Mangrove peninsula southeast of the Amazon estuary, 200 km east of Belém, North Brazil; location of the study site (Furo do Meio) in the center of the mangrove peninsula (black square) near the city of Bragança. Black line indicates road from Bragança to the beach.

Modern hydroacoustic equipment allows for non-intrusive, high-resolution sampling even in shallow-water environments. The tidally influenced fish behavior has been commonly observed in many estuaries and tidally influenced rivers (e.g. Levy and Cadenhead, 1995), albeit we found only one study which was conducted in a tropical mangrove environment (Guillard, 1998).

Within the scope of the MADAM project (Mangrove Dynamics and Management; Berger et al., 1999) we could apply a 200-kHz split-beam sonar (BioSonics) in a macrotidal mangrove channel in Northern Brazil. Here, we present results about the tidal-related migratory dynamics of mangrove fish; critical phases for data acquisition in a mangrove environment are discussed.

2. Materials and methods

2.1. Study area and site

The study area, a 180 km^2 peninsula located in the second largest mangrove area in the world (Spalding et al., 1997), is situated about 200 km east of Belém in the estuary of the Caeté river (Fig. 1). More than 4/5 of the mangrove peninsula is covered by mangroves, predominantly *Rhizophora mangle*, *Avicennia germinans* on the more elevated sites, and rarely *Laguncularia racemosa*. A detailed description of the study area can be found in Krause et al. (2001).

The tidal regime is semidiurnal, ranging between 2.5 and 5 m at neap tides and spring tides, respectively. The region receives about 2500 mm of rainfall per year (INMET, 1992), mainly from January to June. Salinities (psu) can be below 5 in April and exceed 35 in November. Air and water temperatures are high year-round, ranging from 25 to 33 °C and 27–30 °C, respectively. Water clarity is low (5–30 cm, max. 100 cm Secchi depth). Dittmar and Lara (2001a, b) provide further details about the dynamics of abiotic parameters.

The study site was located in the Furo do Meio, a large creek in the central part of the peninsula (Fig. 1) that has already been the sample site for several fisheries studies (Barletta, 1999; Barletta-Bergan, 1999; Krumme, own obs.; Leal-Flórez, pers. comm.; Brenner, pers. comm.). The Furo do Meio is a cul-de-sac channel with a length of about 4.5 km. An extensive sand bank characterizes the lower reaches until 2.5 km upstream of the mouth. The upper reaches are composed entirely of mud providing an acoustically absorptive bottom boundary. Both the extreme upper and the entire lower reaches of the Furo do Meio are almost completely exposed to the air during low water (LW) (the deepest channel holds less than 5 m of water at LW). The sonar site was situated in the upper sector of the extensive subtidal section (1 km length) that extended to where the sand-dominated lower reaches started. Water depth at the sample site was 4 m at LW and could exceed 8 m at high water (HW). The channel width at the sonar site was 30 m at LW and about 50 m at HW (Fig. 2).

2.2. Tidal-related acoustic sampling

The 200-kHz split-beam sonar (Biosonics, DT6000) with a 6° circular-beam transducer was employed horizontally across the channel perpendicular to the tidal flux (Fig. 2) with acoustic ranges at neap tide between 14 m at LW and 23 m at HW. The transducer was fixed to an aluminum frame (35 cm below the water surface), which was attached on two plastic floating bodies (130 × 25 × 25 cm each). The horizontal position of the floating device was adapted to the changing water levels using four different positions (P1: HW, P2 and P3: intermediate, P4: LW). At each position, the four corners of the floating device were moored on four wooden sticks that determined the position. Thus, the transducer could float within each position while the transducer's orientation remained steady (no pitch and roll).

2.3. Data acquisition

Acoustic data were collected during two successive lunar cycles: a dry season from September to November 2000, and a wet season from March to May 2001. For each lunar phase, data were continuously acquired for 50 h, thus covering four consecutive tidal cycles. The transmission rate of the sound pulses was four pings per second. A narrow pulse-width of 0.2 ms was chosen to maximize the range-resolution of

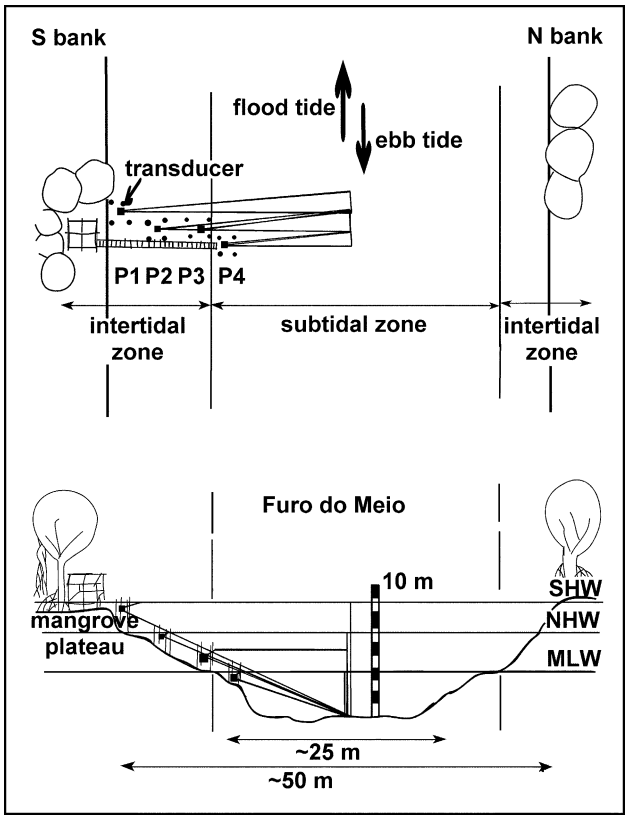

Fig. 2. Tidal-related acoustic sampling in the Furo do Meio. Aerial (above) and cross-sectional view (below) of sonar site. Insonified portions of the channel at different tidal stages (schematic drawing). P1: transducer high water position, P2 and P3: intermediate positions, P4: LW position. SHW = spring tide high water; NHW = neap tide high water; MLW = mean low water.

individual fish and to minimize reverberation levels. Low ambient noise (beyond –80 dB) allowed for a threshold of –70 dB. The acquisition software (Visacq 4.0.2, BioSonics) was run 5 min on and 5 min off continuously throughout 50 h.

Abiotic cycles were measured constantly during each sonar sampling (water level, salinity, Secchi depth, water temperature, wind). We inferred current velocities from a relationship established between current velocity (m s^{-1}) and water level change (height change min^{-1}) during 16 neap tide tidal cycles in the Furo do Meio in October and November 2002. The neap tide tidal curve was subdivided into five different parts and five linear or polynomial regressions were calculated fitting best the relationship between water level change and current velocity: (1) LW until about 1.1 m after start of flood tide, (2) >1.1 m until HW, (3) HW until maximum ebb tide, (4) maximum ebb until about 1.1 m, (5) <1.1 m until LW. Approximately 1.1 m above LW corresponds to the topographical height where the lateral mangrove creeks enter the main channel.

2.4. Calibration

The DT6000 was professionally calibrated by BioSonics (Seattle, USA). Since in situ calibration was uncorroborated by the tidal current and in the occasionally strong wind, calibration (tungsten carbide sphere) was performed in a black water pool (0 psu, 28 °C) in Bragança (Pará, Brazil) and in a brackish water mangrove lagoon (10 psu, 29 °C) near the sample site. The mean target strength (TS) value for the sphere of –39.8 dB (±2.59 S.E., n = 229 echoes; pool) and –40.5 dB (±1.00 S.E., n = 1727 echoes, lagoon) corresponded closely with the theoretical value of –40.0 dB (both calibration files analyzed with VisAnal4.0.2).

2.5. Data processing

Two dry season wax moon tidal cycles (October 6–7 and November 5–6) were analyzed for fish tracks using Vtrack1.0.1 (BioSonics software). Since different acoustic conditions occurred at different tidal stages, we adopted an analysis strategy in which each 5-min-file was run several times with varying parameter sets. Thus, we tried to minimize the noise and maximize fish echo recognition performance. The Vtrack software showed the track formation results visually, and track formation parameters were selected to optimize the formation of fish tracks. Thus, different minimum TS limits were used for different files acquired during a tidal cycle. One single TS limit would have provided a better interfile-comparability in terms of target size. The median Vtrack TS limits applied during tracking analysis for the neap tide cycles in October and November were –52 dB (S.D. = 4, S.E. = 0.3, min –60 dB, max –43 dB) and –55 dB (S.D. = 4, S.E. = 0.3, min –63 dB, max –43 dB), respectively. We found a range-dependent bias in the TS measurements between Vtrack and VisAnal (both programs BioSonics) that followed a power function ($y = 7.8906 \times x^{-0.7481}$) with highest bias in less than 5 m range (e.g. Vtrack TS was 6 dB higher at 3.5 m range) and decreasing bias with increasing range (>1 dB beyond 15 m; J. Dawson, pers. comm.). All other parameters like range, angles or beam pattern correction values were calculated the same by the two programs (J. Dawson, pers. comm.). Given the TS difference, we decided to leave out a detailed analysis of the TS values.

To determine the fish flux in front of the transducer, we calculated the cross-section intercepting the movements of the fish; dividing the number of up- and downstream fish tracks by the cross-section area per unit time provided a straightforward algorithm in the form number of fish m^{-2} min^{-1}.

3. Results

3.1. Acoustic characterization

3.1.1. Season

The dry season provided better acoustic conditions than the wet season, when terrestrial run-off in the catchment area increased sediment loads in the entire Caeté estuary and in the mangrove channels. In the mangrove proper, rains eroded fine sediments from the forest floor into the channels, with poorest acoustic conditions in the channels' upper reaches

(increased background reverberation, decreased signal-to-noise ratio). During wet season neap tide-LW, when the tide was almost stagnant, the water had quasi-viscose properties due to the high concentrations of fine sediment particles. Sound was completely absorbed for hours (white sonar files) until the next flood tide. This phenomenon disappeared when the rains retreated. During rain showers, ambient noise levels in the water increased and occasionally completely concealed targets, thus generating phases of the missing data.

3.1.2. Tide

Acoustic conditions at spring tide were by far more complex and hence poorer than at neap tide. At spring flood tides, the water level rose more than 2 m in less than 1 h (Fig. 6). Extreme tidal rise or fall at spring tide always correlated with minimum Secchi readings and maximum seston transport, thus deteriorating acoustic conditions (see above). At spring tide HW, the mangrove floor was usually inundated. About ¾ h after HW, the export of huge amounts of mangrove litter (particularly buoyant leaves) started and lasted for about 1½ h. During each spring ebb tide, this phenomenon was observed on the channel surface as concrete convergence-like surface bands at the zone where the ebb current was supposed to be strongest, and on the echogram as undulating bands with high TS values. Common software cannot analyze the increased structural complexity in the channel.

3.1.3. Tidal phase

The tide was asymmetric, flood and ebb tide lasting between 4 and 8 h, respectively. In the last 4 h, ebb tide was extremely weak with an almost negligible fall in the water level. Consequently, different acoustic conditions occurred at different tidal stages. The best acoustic conditions prevailed during weak ebb tide when the tidal impact was insignificant (signal-to-noise ratio (SNR) at LW: ca. 15 dB).

Acoustic conditions at strong flood tide and strong ebb tide were poorest due to increased background reverberation. Weak flood tide, HW and weak ebb tide provided intermediate acoustic conditions (SNR at HW: ca. 7 dB).

3.2. Abiotic parameters

Secchi disc readings at dry season-neap tide were positively correlated with water level (LW 20–30 cm; HW 70–90 cm). Extreme tidal rise or fall coincided with minimum Secchi readings, maximum seston transport and current velocity maxima. Neap tide current velocitieswere asymmetric. Flood and ebb tide speeds reached maxima of almost 25 and 15 cm s^{-1}, respectively (Fig. 3, upper figures). Current velocities were highly dynamic, with irregular and strong changes in speed within a few minutes. During weak flood tide intervals, even complete changes to ebb direction occurred. Salinity (psu) increased from 29 in October to 33 in November. Salinity was negatively correlated with water level (cycle maxima at LW, minima at HW). Oxygen and water temperature followed a 24 h cycle, reaching highest values in the late afternoon at ebb tide (9.5 mg l^{-1} and 30 °C,

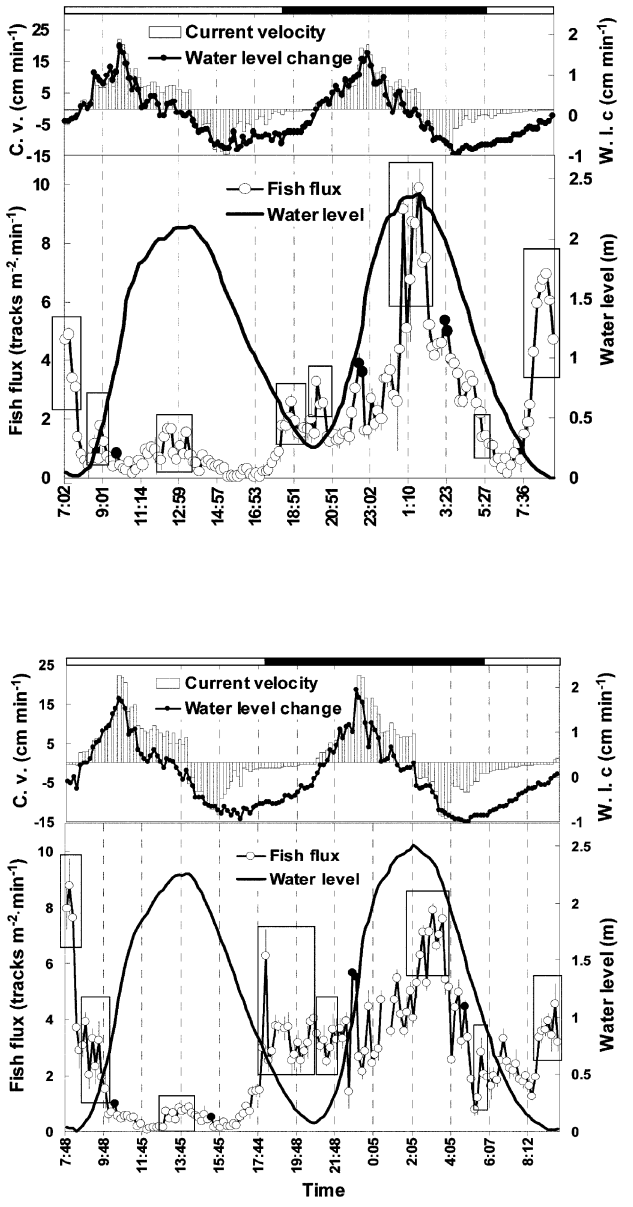

Fig. 3. Mean fish flux (fish m^{-2} min^{-1}) ± 1 S.E. and tidal curve (lower figure) and current velocities (bars) derived from the water level change (upper figure) at two wax moon cycles (neap tide), October 6–7 (above) and November 5–6 (below), during dry season 2000, in the Furo do Meio. Horizontal bars on top indicate night (18 h 00–5 h 45). Lower figure: rectangles indicate fish flux peaks at daytime-LW, daytime-flood start, daytime-HW, night-LW, night-flood start, night-HW, dawn and again daytime-LW (from left to right). Closed circles indicate distinct fish flux peaks at increased current velocities.

respectively). Lowest water temperatures were recorded during the night-HW (28 °C). Lowest oxygen values were recorded at 7:30 (6 mg l^{-1}). Wind consistently blew in from the northeast with stronger periods both in the afternoon and in the night.

3.3. Fish tracking

About 30 000 fishes were detected during each neap tide cycle. Assuming that half of the channel cross-section was

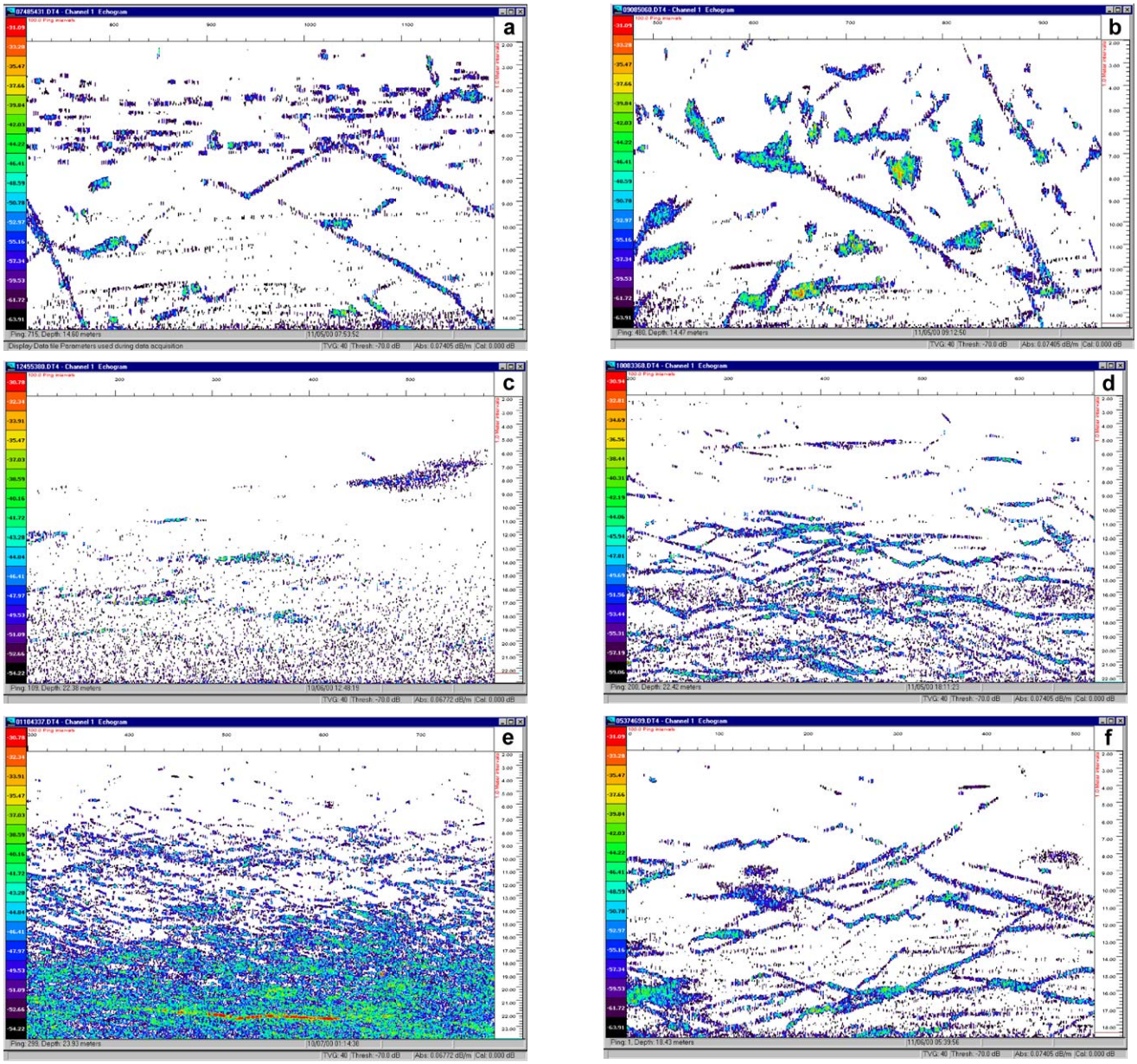

Fig. 4. Examples of echograms from fish flux peaks in the mangrove channel Furo do Meio near Bragança, PA, North Brazil, neap tides, during dry season 2000, at (a) daytime-LW, 7 h 54, November 5, 2000; (b) flood tide start at daytime, 9 h 13, November 5, 2000; (c) daytime-high water, 12 h 48, October 6, 2000; (d) night-LW at sunset, 18 h 11, November 5, 2000; (e) night-high water, 1 h 14, October 7, 2000 and (f) sunrise, 5 h 40, November 6, 2000. Echogram axis, left: echo intensity (dB; red strongest); right: range in front of transducer (m); top: time (2 min period or about 480 pings at a ping rate of 4 pings s^{-1}); bottom: first bottom echo. Note different scales for range and echo intensity between echograms.

insonified and considering only fish moving upstream, we calculated a mean of 6000 and 28 000 fish immigrating into the mangrove during the daytime and the night flood tide, respectively.

The fish flux curves of both dry season neap tide cycles had seven peaks: at daytime-LW, the start of daytime flood, daytime-HW, night-LW (starting at dusk), the start of night flood, night-HW and at dawn (Fig. 3). The daytime-LW peak occurred in the morning (5–9 fish m^{-2} min^{-1}) with highest values at slack low tide just before the water level started to rise again. A unique migratory pattern was observed during the daytime-LW peak when many targets occurred in a near-range corridor along the southern side of the channel and several tracks were visible in the far range (Fig. 4a). At the start of the daytime flood tide when current velocity increased sharply, fish fluxes peaked to about 2 fish m^{-2} min^{-1} showing an upsurge in activity with many multiple targets occurring and crisscrossing throughout the range (Figs. 3 and 4b). At the end of the daytime flood tide, fish flux increased slightly to form the daytime-HW peak, albeit reaching only about 1 fish m^{-2} min^{-1} (Figs. 3 and 4c). The night-LW peak started at dusk. The fish flux remained high throughout the night LW phase and ended when the night-flood tide started (about 2–3 fish m^{-2} min^{-1}; Figs. 3 and 4d). The night flood

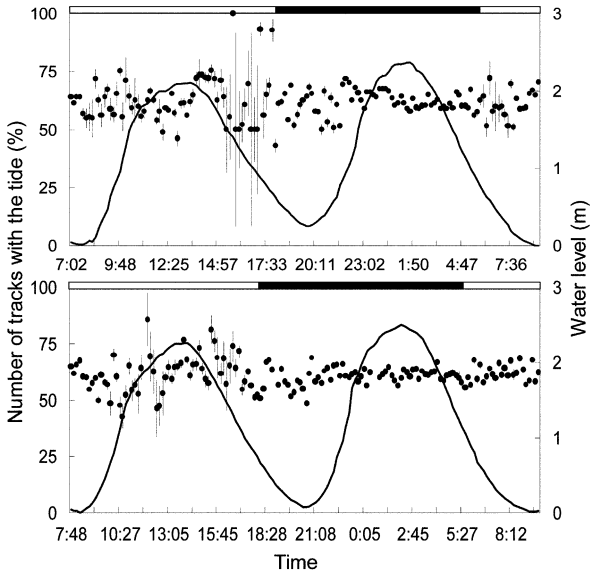

Fig. 5. Proportion of fish tracks going with the tide (solid circle ± 15 S.E.) and tidal cycle (solid line) for two neap tide cycles, October 6–7 (above) and November 5–6 (below). Black bars on top indicate night (18 h 00 until 5 h 45). High S.E. is related to low sample size (number of fish tracks) since variance was $p \times [(1–p) \times n^{-1}]$ with p = proportion of fish tracks going with the tide.

start peak occurred at a fish flux level similar to the previous night-LW peak (about 2–3 fish m^{-2} min^{-1}). The distribution pattern of target tracks resembled the night-LW situation; unlike the start of daytime flood tide, night flood start lacked multiple targets. The night-HW peak also started at the end of flood tide (5–10 fish m^{-2} min^{-1}); many target tracks occurred throughout the range (Figs. 3 and 4e). At dawn, fish fluxes increased briefly (Fig. 4f). After sunrise, fish flux was low until the daytime-LW was formed again towards the end of weak ebb tide. In contrast to the clear fish flux increase at dusk, fish flux increase at dawn was weak (Figs. 3 and 4d,f). Individual fish flux maxima coincided with strong flood and ebb tide intervals (Fig. 3). Mean fish flux was 2.4 fish m^{-2} min^{-1} ± 2.1 S.D. The night fish fluxes, especially at HW were several times higher than those at daytime. Due to the particular flux patterns at daytime-LW, however, the LW fish flux peak was usually higher at daytime than at night.

Target sizes were generally small (–43 ± 4 dB, n = 55 727; results from Vtrack), indicating the presence of mainly juvenile or small-sized fish. Larger echoes (>–30 dB) were usually only caused by multiple targets.

Throughout the tidal cycles, about 60% of the fish tracks were directed with and about 40% against the tide (Fig. 5), with higher variability in the proportions occurring during the daytime cycle. A tidal periodicity was not apparent.

4. Discussion

4.1. Acoustic characterization

It was a clear advantage that the sampling period started in the dry season. Thus, we became acquainted with the yet unknown acoustic conditions in the mangrove environment under a minimum of external influences. The poor acoustic conditions encountered in the wet season might hold true for turbid shallow-water environments on tropical coasts in general. Experiments using vertical transducer orientation or the use of a lower frequency echosounder (120 kHz instead of 200 kHz) could be worthwhile alternatives.

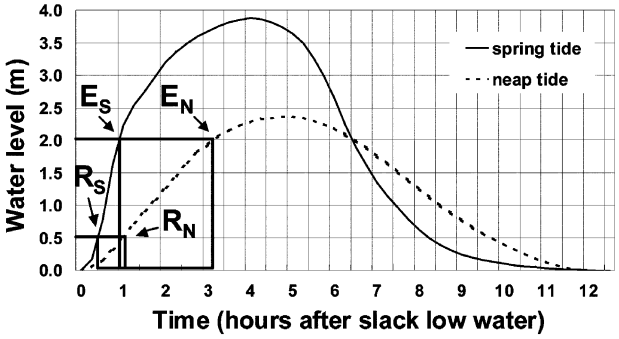

Fig. 6. Time delay threshold between spring tide and neap tide in mangrove accessibility at two water levels; E_S: Estuarine fish at spring tide, E_N: Estuarine fish at neap tide, R_S: Resident fish at spring tide, R_N: Resident fish at neap tide.

When studying intertidal migration patterns of fish acoustically, it is very problematic when the clearest conditions for sonar application occur at weak ebb tide when tidal impact is negligible. Fortunately, weak neap tide currents allowed for sonar file analysis throughout the tidal cycles.

4.2. Fish tracking

Considerable numbers of fish entered the upper reaches of the mangrove during flood tides. The high numbers can be attributed to the high abundances of juvenile fish commonly found in mangroves (Sasekumar et al., 1992; Laedgsgaards and Johnson, 1995; Barletta, 1999).

The high number of target tracks, their relatively low TS values and a mean fish size of 14 cm in the mangrove channels (Krumme, own obs.) clearly emphasized the importance of this habitat as a fish nursery.

The hypothesis that intertidal fish behave like passive particles can be readily rejected since a considerable proportion of the tracks (about 40%) was directed against the tidal current irrespective of flood or ebb tide. However, the high background noise levels observed in the channel may have added higher variability to the positional data of the split-beam system (Kieser et al., 2000; Fleischman and Burwen, 2000) and could have led to incorrect results when assigning the track directions. It is nevertheless clear that the fish are not passively transported by the tides but may in fact actively move to, and concentrate in resource-rich intertidal habitats when accessible. Obviously, swimming against the direction of the tide was a major component of fish movements in the mangrove channel at neap tide. Thus, surface and midwater fish may take advantage of the fact that food is passively transported towards their mouth. *Colomesus psittacus* (Tetraodontidae) was observed maintaining its relative position

in the channel while actively swimming against the current near the water surface. Thus, they patrolled a certain corridor for several minutes searching for prey. This particular swimming behavior of *C. psittacus* was reflected on the echogram as extraordinarily long tracks. Position shifts to the left or to the right may have caused the zick-zack tracks visible on the echograms (Figs. 4a,f).

We assume that the fish swam and crisscrossed in the flooding and ebbing water body to inter- and intraspecifically increase their particular foraging areas while taking advantage of the tidal transport into and out of the intertidal area. Weak neap tide current speeds did not constrain fish to show strong directional movements. Nevertheless did fish fluxes noticeably increase during short intervals of increased current speed suggesting a positive response of the fish to increased tidal current speeds (Fig. 3).

4.3. Tidal stage

LW and HW phases represented stable stages with established fish assemblages at increased fish fluxes; unlike flood and ebb tides that can be considered as transitional stages during the tidal migration of fishes. Detailed stomach analysis of the catfish *Cathorops* sp., predominant in the upper reaches of the channels (Barletta, 1999), revealed that flood tide stomachs were generally empty, whereas ebb tide stomachs were already well filled briefly after HW (Leal-Flórez, pers. comm.). Apparently, the tidal stages before and around HW were the principal phases for catfish feeding. This pattern corresponded well with the fish flux peaks around HW in the channel. Although benthic catfish may not have been well represented by horizontal beaming, their foraging pattern can serve as a general rule for more pelagic fish species as well since the water level likewise determines the degree of habitat accessibility for other intertidal fish.

It seems contradictory that fish fluxes increased at HW when the water volume was greatest. However, we assume that the immigration and import of organisms from downstream was maximum at HW. Both nekton abundance and species richness were significantly greater at slack high tide than either flood or ebb tide on a temperate marsh surface (Kneib and Wagner, 1994). HW is the short period where insignificant current speed and maximum intertidal accessibility coincide. Water transparency was highest at and after HW. Fish that actively immigrated into the mangrove during flood tide probably milled around at HW in the main channel, especially during the night-HW (Fig. 4e). The increased fish flux at HW clearly indicates that active movements in the water column increased. We assume that negligible current speed and high water transparency around HW favored visual focusing of pelagic prey by the fish in the mangrove water, both at day and at night. Insignificant current speeds at slack HW probably favored localization and oral fixing of benthic prey in the mud.

The high fish fluxes at LW resulted from the resident fishes' active swimming in the subtidal parts of the channel. The population of resident mangrove fish probably achieved successful maintenance in the channels' upper reaches by late emigration out of the intertidal mangrove creeks. Thus, they would both achieve avoidance of undesirable downstream transport and optimize the time for feeding in the intertidal creeks. Staying horizontally in distance to the main channel is probably linked to rather bottom-oriented movements at ebb tide. Interconnected to the fish community, similar temporal patterns with stable assemblage structures during HW and LW can be proposed for other tidally influenced nekton communities, e.g. zooplankton (Krumme and Tsui-Hua, submitted) and phytoplankton organisms (Schories et al., unpubl.).

4.4. Migratory cycle

The course of the flux curve and the series of sonar files suggest a schematic migratory cycle for intertidal mangrove fish. The migratory pattern found for the two wax moon cycles to all appearances also applies to wane moon cycles, thus reflecting a typical dry season neap tide pattern in 2000.

1. Resident mangrove fish were clearly concentrated in the subtidal parts of the channel forming both the LW peak at daytime and at night (Fig. 3).
2. As soon as the water level started to rise at the start of flood tide, fish flux first peaked and then decreased. Resident fish either left the channel horizontally entering the shallow (less than 50 cm) intertidal creeks, or went down towards the channel bottom. We assume early horizontal immigration into the mangrove creeks since a clear upsurge in fish activity during the first 30 min after slack low tide was observed on the echograms (Fig. 4b). Cattrijsse et al. (1994), using a fyke net in a Dutch marsh, found that most species migrate during the first and the last hours of the tidal cycle when the current velocities were low; gill net catches of summer flounder in New Jersey were greatest in early flood tides and in mid and late ebb (Rountree and Able, 1992).
3. During flood tide, distinct fish flux maxima coincided with current speed maxima. The mangrove fish community apparently directly responded to the tidal current regime on a very short time scale.
4. During flood tide, the fish fluxes increased towards HW. Many resident mangrove fish were probably foraging in the intertidal mangrove creeks at this time and hence absent from the main channel. Fish fluxes in the mangrove channel did not increase until the flood tide water level had risen about 2 m above the previous LW level and flood current speeds had fallen below 10 cm s^{-1} (upper figures in Fig. 3). Estuarine fish that immigrated with the flood tide from the Caeté estuary to the upper reaches (a distance of at least 4 km) probably contributed to the HW fish flux peak. Several other authors have assumed that some estuarine fish require a minimum water level to enter an intertidal area (Davis, 1988; Blaber et al., 1994). Interestingly, Gibson (1973) counted most fish in an intertidal Scottish sandy beach when the water was 1–2 m deep. Prey search of pelagic

Table 1
Lift net catches in main channel of the mangrove creek Furo do Meio, dry season 2000; sunrise was at 5 h 45, sunset at 18 h 00; data from Leal-Flórez (pers. comm.)

Species	Total	%	Day	Night
Cathorops sp.	735	39	316	419
Sciaenidae	468	25	158	310
C. psittacus	229	12	192	37
Engraulidae	137	7	81	56
Others	312	17	169	143
Sum	1881	100	916	965

and benthic fish in the channel was probably facilitated (see above) and hence resulted in increased milling in front of the transducer around HW.

5. When the water levels in the mangrove channel started to fall with the receding tide, fish flux decreased again. The decrease in fish flux during ebb tide occurred at water depths apparently symmetrical to those at flood tide (Fig. 3). When we assume that estuarine fish returned to the start points of their tidal migration, they covered distances of at least 8 km for each tidal cycle between the estuary and the upper mangrove reaches. The emigration of estuarine fish out of the mangrove channels during ebb tide is exploited by local fishermen with large fish traps (*corrals*) on the sand banks of the lower reaches of the channels and in the estuary (Barletta et al., 1998; Schaub, pers. comm.). Resident mangrove fish may have returned from the intertidal creeks to the channel at mid or late ebb tide as observed by Rountree and Able (1992) for summer flounder where they stay until the next flood tide enters again. A signal from this emigration was not apparent in the sonar files, possibly due to more bottom-oriented movements. The fish flux rather showed a continuous decrease. However, like at flood tide did distinct ebb fish flux maxima coincide with ebb current speed maxima.
6. At neap tides, twilight coincided with the semistagnant LW phase. Especially at dusk fish flux increased significantly whereas sunrise only produced a weak signal in the fish flux curves. Most mangrove fish are rather nocturnal or show at least negative phototaxis (own obs.); only *C. psittacus* is a clear diurnal species (Table 1).

4.5. Delay in accessibility

The accessibility of the intertidal area is determined by the water level, i.e. the height of the tide. Since resident and estuarine fish apparently accessed the intertidal mangrove area at different water levels, the time delay between the two access levels determines the time available for mangrove foraging. Fig. 6 shows the extremely short-time delay between habitat accessibility for resident and estuarine fish at spring tide and the rather marked time delay for neap tides. Resident mangrove fish may spend more time feeding in the mangrove than estuarine fish whose foraging activity is more restricted in time, especially at neap tide (Fig. 6). The high standing stocks of resident *Cathorops* sp. and *Anableps anableps* (Barletta, 1999; Krumme, own obs.) compared to other fish species captured in the upper reaches of the mangrove channel at HW support this argument. For estuarine fish, the time delay between the start of flood tide until a minimum water depth provides access to the intertidal area, may be a crucial parameter for intertidal migration of estuarine fish. Hence, the hydrodynamics at spring tide provide excellent conditions for immigration of estuarine fish since the mangrove becomes accessible in less than an hour after slack LW, unlike more than 3 h during neap tides (Fig. 6). The numbers of 11 fish species were greater at spring tides (Krumme, own obs.) when both the periods available for foraging and the habitat accessibility in the mangrove are increased (Fig. 6). Foraging success of *A. anableps*, *Arius herzbergii* and *Anchovia clupeoides* was clearly greater at spring than at neap tide (Brenner, pers. comm.).

4.6. Four assemblages

We assume that different fish assemblages caused each of the fish flux peaks at LW and HW during a neap tide cycle. Krumme (own obs.) already found that HW assemblages of mangrove fish at neap tide differ significantly between day and night with the neap tide-daytime assemblage being poorest in both biomass and diversity. This might explain the marked increase of fish tracks throughout the night cycle compared to the desolated track situation during the daytime cycle. Morrison et al. (2002) found clear differences in the fish fauna composition between both low and high tides and day and night samples in a temperate New Zealand tidal mudflat. Simultaneously to the sonar application during the dry season 2000, Leal-Flórez (pers. comm.) caught migrating fish 500 m upstream of the sonar site in the open channel from a bridge using lift nets. Day and night catches were similar in terms of abundance but differed clearly in their species composition (Table 1). *Cathorops* sp. was constantly present in the catches. Sciaenidae, a mainly nocturnal family (Helfman, 1993) was more abundant at night and may have caused the high numbers of targets at night-HW. The diurnal pufferfish *C. psittacus* was mainly caught during daylight. Engraulidae tended to be more abundant at daytime as well. These species may have contributed to the daytime-HW fish flux peak. Unfortunately, there was no relationship between the number of fish caught (lift nets) and the number of fish

tracked (counting of acoustic traces). The lift net did not produce representative catches. It suffered from several shortcomings: during strong spring flood and ebb tide the lift nets flouted. They became frequently entangled in the channel bottom near the bridge, and clearing of the net might have expelled fish from the area. LW depth at the Furo do Meio bridge was less than 1 m, hence complicating lift net use.

Our findings suggest that different assemblages also existed for LW day and LW night during neap tide. Increasing fish fluxes at the night-LW coincided with sunset and remained high throughout the LW phase (Figs. 3 and 4d). During the daytime LW phase, fish fluxes peaked weakly at sunrise. This was probably caused by an activity upsurge of *C. psittacus*. At dawn, lift nets again caught *C. psittacus* (Leal-Flórez, pers. comm.). Fish fluxes then only increased after 7:00, peaking towards 9:00 at slack low tide. Maybe the formation of the near-range corridor at LW, i.e. increasing fish fluxes, was related to the increased oxygen concentrations after the oxygen minimum at around 7:00 (start of phytoplankton activity during the stable weak ebb tide). Barletta-Bergan (1999) found at neap tide in the same mangrove area, high densities of five fish species: early larval stages of <10 mm of *A. clupeoides* (Engraulidae), *Stellifer* sp. (Sciaenidae), *Rhinosardinia amazonica* (Clupeidae), *Archirus* sp. and *Guavina guavina* (Eleotridae) in the morning (9:00), predominantly occurring at the surface, probably feeding on plankton. Densities of larval and juvenile fish were significantly lower during the night-LW (21:00) for most taxa except for *Stellifer rastrifer*, which showed significantly higher values at night (Barletta-Bergan, 1999). Furthermore, Fig. 4d shows clearly that the horizontal distribution and movement pattern of targets was different between the daytime and the night LW situation. During the night-LW, multiple targets did not occur and the near-range corridor was absent, suggesting different assemblages to be active at these periods. However, it remains unclear whether the near-range band of targets at daytime-LW represented a typical feature of the system or whether it was merely caused by an extraordinary abundant cohort in its nursery ground. Spring tide LW lacked any similar horizontal pattern in the target distribution.

5. Conclusions

The observation of fish movements using shallow-water acoustics was feasible in a mangrove environment. Shallow-water acoustics provided a reasonable approach to obtain high-resolution samples in a dynamic environment where conventional fishing methods have become limited. For acoustic studies in tropical estuarine environments, we recommend sampling during the dry season and at weaker tides, that is, at neap tide and/or during LW.

Fisheries studies conducted under meso- or macrotidal regimes should consider the importance of temporal changes on the short-term scale determined by the factors “tide”, “photoperiod” and “tidal stage” in both the survey design and choosing a sampling method.

The tidal-induced fish flux changes together with the considerable proportion of fish tracks directed against the tide indicate clearly that the tidal migration of fish was an active movement to and from intertidal areas promoted by the tide.

Our data suggest that resident mangrove fish enter the intertidal mangrove creeks at early flood tide and leave them at late ebb tide at fairly shallow water depths. The estuarine fish enter and leave the upper reaches of the mangrove channel when water level was about 2 m above the previous LW level, thus requiring a minimum water depth for tidal migration. At HW, maximum habitat accessibility, reduced current speeds and maximum visibility probably helped in the foraging of pelagic and benthic fish in the channel and hence resulted in high fish fluxes due to increased milling in front of the transducer. The time delay between immigration of resident and estuarine fish is shorter at spring than at neap tide (Fig. 6). Hence, the period available for foraging and the habitat accessibility are enhanced at spring tide; both catches of fish (Davis, 1988; Laroche et al., 1997; Krumme, own obs.) and the fishes’ feeding success are greater at spring tide (Colombini et al., 1996; Brenner, pers. comm.).

Acknowledgements

We would like to thank all our Brazilian and German colleagues for their cooperation. We are very grateful to Jenny Leal-Flórez, Matthias Brenner and Christoph Schaub who provided insight into their thesis’ results. Special thanks go to Chico Amanço, Falko Berger, Jim Dawson (BioSonics), Andreas Hanning, Ilson, Gesche Krause, Anne Lebourges (IRD), Darlan Smith and Ulf Stühmer for help, practical support and discussions. This work resulted from the cooperation between the Center for Tropical Marine Ecology (ZMT), Bremen, Germany and the Universidade Federal do Pará (UFPa), Belém, Brazil, under the Governmental Agreement on Cooperation in the Field of Scientific Research and Technological Development between Germany and Brazil financed by the German Ministry for Education, Science, Research and Technology (BMBF) [Project number: 03F0253A5, Mangrove Dynamics-Management and MADAM], and the Conselho Nacional de Pesquisa e Tecnologia (CNPq) [MADAM contribution 47].

References

Barletta, M., 1999. Seasonal changes of density, biomass and species composition of fishes in different habitats of the Caeté estuary (North Brazilian coast-east Amazon). Bremen Univ., (FRG) Fachbereich 2 (Biologie/Chemie) ZMT Contrib. No. 7, Zentrum fuer Marine Tropenoekologie, Bremen (FRG).

Barletta, M., Barletta-Bergan, A., Saint-Paul, U., 1998. Description of the fisheries structure in the mangrove-dominated region of Bragança (state of Pará, North Brazil). Ecotropica 4, 41–53.

Barletta-Bergan, A., 1999. Structure and seasonal dynamics of larval and juvenile fish in the mangrove-fringed estuary of the Rio Caeté in North Brazil. Bremen Univ., (FRG) Fachbereich 2 (Biologie/Chemie), ZMT Contrib. No. 8, Zentrum fuer Marine Tropenoekologie, Bremen (FRG).

Barletta-Bergan, A., Barletta, M., Saint-Paul, U., 2002. Structure and seasonal dynamics of larval fish in the Caeté River estuary in North Brazil. Estuar. Coast. Shelf Sci. 54, 193–206.

Bell, J.D., Pollard, D.A., Burchmore, J.J., Pease, B.C., Middleton, M.J., 1984. Structure of a fish community in a temperate tidal mangrove creek in Botany Bay, New South Wales. Aust. J. Mar. Freshw. Res. 35, 33–46.

Berger, U., Glaser, M., Koch, B., Krause, G., Lara, R., Saint-Paul, U., Schories, D., Wolff, M., 1999. An integrated approach to mangrove dynamics and management. J. Coast. Cons. 5, 125–134.

Blaber, S.J.M., Brewer, D.T., Harris, A.N., 1994. Distribution, biomass and community structure of demersal fishes of the Gulf of Carpentaria, Australia. Aust. J. Mar. Freshw. Res. 45, 375–396.

Cattrijsse, A., Makwaia, E.S., Dankwa, H.R., Hamerlynck, O., Hemminga, M.A., 1994. Nekton communities of an intertidal creek of a European estuarine brackish marsh. Mar. Ecol. Prog. Ser. 109, 195–208.

Colombini, I., Berti, R., Nocita, A., Chelazzi, L., 1996. Foraging strategy of the mudskipper *Periophthalmus sobrinus* Eggert in a Kenyan mangrove. J. Exp. Mar. Biol. Ecol. 197, 219–235.

Davis, T.L.O., 1988. Temporal patterns in the fish fauna entering a tidal swamp system in tropical Australia. Env. Biol. Fish. 21, 161–172.

Dittmar, T., Lara, R.J., 2001. Do mangroves rather than rivers provide nutrients to coastal environments south of the Amazon River? Evidence from long-term flux measurements. Mar. Ecol. Prog. Ser. 213, 67–77.

Dittmar, T., Lara, R.J., 2001. Driving forces behind nutrient and organic matter dynamics in a mangrove tidal creek in North Brazil. Estuar. Coast. Shelf Sci. 52, 249–259.

Fleischman, S.J., Burwen, D.L., 2000. Correcting for positional-related bias in estimates of the acoustic backscattering cross-section. Aquat. Living Resour. 13, 283–290.

Gibson, R.N., 1973. The intertidal movements and distribution of young fish on a sandy beach with special reference to the plaice (*Pleuronectes platessa* L.). J. Exp. Mar. Biol. Ecol. 12, 79–102.

Gibson, R.N., Pihl, L., Burrows, M.T., Modin, J., Wennhage, H., Nickell, L.A., 1998. Diel movements of juvenile plaice *Pleuronectes platessa* in relation to predators, competitors, food availability and abiotic factors on a microtidal nursery ground. Mar. Ecol. Prog. Ser. 165, 145–159.

Guillard, J., 1998. Daily migration cycles of fish populations in a tropical estuary (Sine-Saloum, Senegal) using a horizontal-directed split-beam transducer and multibeam sonar. Fish. Res. 35, 23–31.

Helfman, G.S., 1993. Fish behaviour by day, night and twilight. Second ed. In: Pitcher, T.J. (Ed.), Behavior of Teleost Fishes. Chapman & Hall, London, Fish & Fisheries Ser. 7, pp. 479–512.

Horn, M.H., Martin, K.L.M., Chotkowski, M.A., 1999. Intertidal Fishes: Life in Two Worlds. Academic Press, San Diego, CA.

INMET (Instituto Nacional de Metereologia), 1992. Normais climatológicas (1961–1991). Tech. Rep. Instituto Nacional de Metereologia, Brasilia DF, Brasil.

Kieser, R., Mulligan, T., Ehrenberg, J., 2000. Observation and explanation of systematic split-beam angle measurement errors. Aquat. Living Resour. 13, 275–281.

Kneib, R.T., Wagner, S.L., 1994. Nekton use of vegetated marsh habitats at different tidal stages of tidal inundation. Mar. Ecol. Prog. Ser. 106, 227–238.

Krause, G., Schories, D., Glaser, M., Diele, K., 2001. Spatial patterns of mangrove ecosystems: the bragantinian mangroves of northern Brazil (Bragança, Pará). Ecotropica 7, 93–107.

Laegdsgaard, P., Johnson, C.R., 1995. Mangrove habitats as nurseries: unique assemblages of juvenile fish in subtropical mangroves in eastern Australia. Mar. Ecol. Prog. Ser. 126, 67–81.

Laroche, J., Baran, E., Rasoanandrasana, N.B., 1997. Temporal patterns in a fish assemblage of a semiarid mangrove zone in Madagascar. J. Fish Biol. 51, 3–20.

Levy, D.A., Cadenhead, A.D., 1995. Selective tidal stream transport of adult sockeye salmon (*Oncorhynchus nerka*) in the Fraser River estuary. Can. J. Fish. Aquat. Sci. 52, 1–12.

Louis, M., Bouchon, C., Bouchon-Navaro, Y., 1995. Spatial and temporal variations of mangrove fish assemblages in Martinique (French West Indies). In: Wong, Y.S., Tam, F.Y. (Eds.), Asia-Pacific Symposium on Mangrove Management, pp. 275–284.

Morrison, M.A., Francis, M.P., Hartill, B.W., Parkison, D.M., 2002. Diurnal and tidal variation in the abundance of the fish fauna of a temperate tidal mudflat. Estuar. Coast. Shelf Sci. 54, 793–807.

Robertson, A.I., Duke, N.C., 1987. Mangroves as nursery sites: comparisons of the abundance and species composition of fish and crustaceans in mangroves and other nearshore habitats in tropical Australia. Mar. Biol. 96, 193–205.

Rountree, R.A., Able, K.W., 1992. Foraging habits, growth, and temporal patterns of salt-marsh creek habitat use by young-of-year summer flounder in New Jersey. Trans. Am. Fish. Soc. 121, 765–776.

Sasekumar, A., Chong, V.C., Leh, M.U., D'Cruz, R., 1992. Mangroves as a habitat for fish and prawns. Hydrobiologia 247, 195–207.

Spalding, M., Blasco, F., Field, C.D. (Eds.), 1997. World Mangrove Atlas. International Society for Mangrove Ecosystems, Okinawa.

Available online at www.sciencedirect.com
SCIENCE DIRECT®
Aquatic Living Resources 16 (2003) 185–190
Aquatic Living Resources
www.elsevier.com/locate/aquliv

Upstream migration activity of cyprinids and percids in a channel, monitored by a horizontal split-beam echosounder

Juha Lilja [a,*], Tapio Keskinen [a], Timo J. Marjomäki [a], Pentti Valkeajärvi [b], Juha Karjalainen [a]

[a] *University of Jyväskylä, Department of Biological and Environmental Science, P.O. Box 35, 40351, Jyväskylä, Finland*
[b] *Finnish Game and Fisheries Research Institute, Laukaa Fisheries Research and Aquaculture, Vilppulantie 415, 41360 Valkola, Finland*

Accepted 17 December 2002

Abstract

A 200 kHz digital echosounder (HTI) with two split-beam transducers was aimed horizontally to monitor the upstream migration activity of fish, from 24 April to 28 June, in Äijälänsalmi channel (mean width 35 m, length 700 m, and maximum depth 5 m) from large mesotrophic Lake Päijänne to small eutrophic Lake Jyväsjärvi. This study was part of a larger project which aims to analyse the movement of commercially unimportant fish species and reduce the abundance of these fish in L. Jyväsjärvi. Catch samples were collected with a trap net located immediately upstream from the acoustic beams. The most common species in the catch were roach (*Rutilus rutilus*), perch (*Perca fluviatilis*), bream (*Abramis brama*), ruffe (*Gymnocephalus cernuus*), and white bream (*Abramis bjoerkna*). The upstream migration of fish was correlated with water temperature ($r = 0.40$) with time lag of 1 d. In spring, L. Jyväsjärvi warmed faster than L. Päijänne, causing spawning migration from L. Päijänne to L. Jyväsjärvi. Clear diurnal rhythm in activity was observed. The migration rate through the channel peaked around dawn and dusk. Catch per unit effort of the trap net suggested that the peak of the spawning migration of different species was separate. Upstream migration was induced by the temperature difference between two lakes, and the activity of the migration was regulated by temperature changes and light rhythm.

Keywords: Horizontal acoustics; Migration; Temperature; Diel rhythm; Cyprinids; Percids

1. Introduction

The split-beam three-dimensional target tracking technique enables detection of the swimming direction and speed of individual fish in real time. This system also permits the study of migration changes in the short term. These systems are usually used to non-intrusively count upstream migration of anadromous salmonids returning up their parent river (Ransom et al., 1998). Fixed location hydroacoustic methods can also be used to study the diel behaviour and movements of fish on lakes and other shallow waters (Cuillard, 1998; Gonzalez and Gerlotto, 1998; Kubecka and Duncan, 1998a).

Fish migrations can be classified as reproductive, feeding and refuge migrations (Lucas and Baras, 2001). The timing of spawning migrations in freshwater is generally determined by light rhythm and temperature changes. The scale of migrations in freshwater habitats is usuallysmall compared to anadromous species, but it can be ecologically important. This study was the first attempt to assess the upstream migration of cyprinids and percids in a Finnish channel by using hydroacoustics.

A few decades ago, L. Jyväsjärvi was the dumping place of the city of Jyväskylä, and its water quality was extremely low. A water purification plant was completed in the end of 1970s and water quality began to improve. Currently, L. Jyväsjärvi is an important location for development, growth and reproduction of many commercially unimportant fish species. The aim of this study was to monitor the upstream migration of the commercially unimportant fish species through the Äijälänsalmi channel, and to identify the role of water temperature and air pressure affecting it.

2. Materials and methods

2.1. Study site

Äijälänsalmi channel is located in central Finland and connects L. Jyväsjärvi to L. Päijänne (Fig. 1). The channel is

* Corresponding author.
E-mail address: julilja@cc.jyu.fi (J. Lilja).

doi:10.1016/S0990-7440(03)00016-0

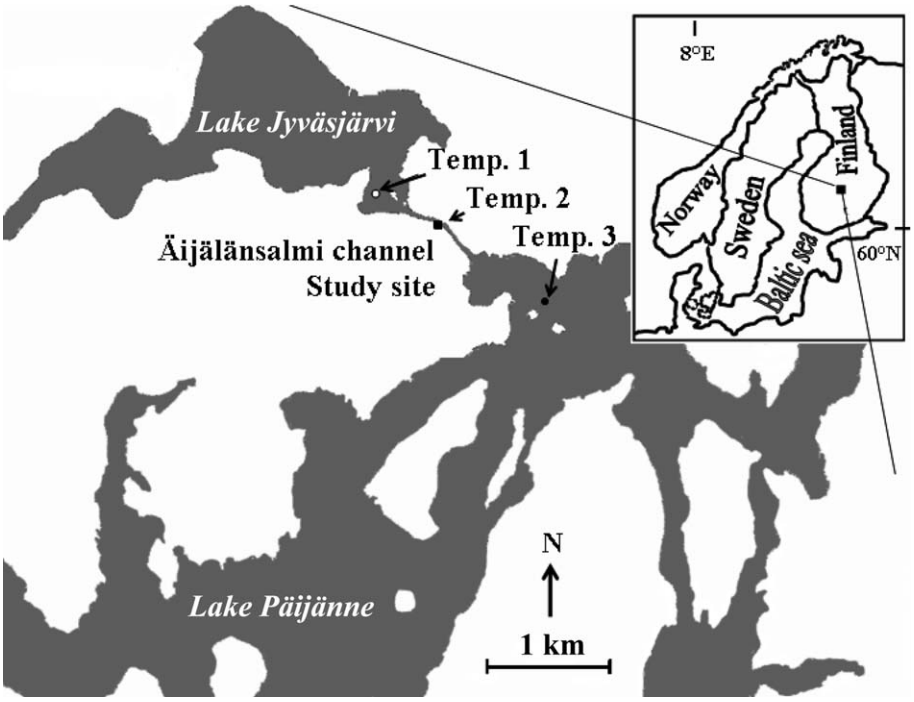

Fig. 1. Map of Äijälänsalmi channel, Lake Jyväsjärvi, and the northern part of Lake Päijänne. The arrows show the location of the hydroacoustic study site and the location of the temperature measurements (Temp. 1, 2, and 3).

700 m long and 4 m deep, with a width of about 30 m. The channel has been dredged, hence the bottom profile is quite similar throughout its length. The bottom substrate in the echosounding site consists generally of mud or clay. L. Jyväsjärvi discharges via the channel to L. Päijänne. During spring and earlysummer (April-June), the current is towards L. Päijänne, and is laminar. However, the direction of current in Äijälänsalmi channel can sometimes change, especially, in late summer. In winter, both the lakes and the channel are covered by ice.

L. Jyväsjärvi is eutrophic and northern L. Päijänne is mesotrophic (Table 1). The fish population in L. Jyväsjärvi and northern part of L. Päijänne consists mainly of roach (*Rutilus rutilus*), bream (*Abramis brama*), white bream (*Abramis bjoerkna*), perch (*Perca fluviatilis*) and ruffe (*Gymnocephalus cernuus*). The main predator species are pikeperch (*Sander lucioperca*) and pike (*Esox lucius*).

2.2. Hydroacoustic counting

A 200 kHz digital split-beam echosounder HTI (Hydroacoustic Technology, Inc.) Model 243 was used at a fixed location in this study. Two elliptical (4 × 10°) transducers were mounted across the channel, one for each bank, and once properly mounted, were kept stationary. The system also included dual-axis transducer rotators, an oscilloscope, a printer, and a computer. The transmitter pulse length was 1.25 ms and a 10 kHz frequency-modulated (FM) slide/chirped signal was used to maximize the signal-to-noise ratio (Ehrenberg and Torkelson, 2000). The sampling rate was 8 pings s^{-1} and a 40 log *R* TVG (Time Varied Gain) function was used. The sensitivity threshold value of the detected echoes was –58 dB (–52 dB at full beam) due to the low level of the background noise. Before and after the study, the echosounder system was in situ calibrated using a tungsten-carbide standard sphere (∅ = 38.1 mm). The echosounder was in operation 24 h a day and each hour was split into four sequences. Both transducers collected data in turn for 30 min every hour. On both banks, the position scanning was set at two vertical aiming angles, each scanning for 15 min. The rotator controllers communicated with the echosounder, processor, and dual-axis rotators to automatically scan pre-set of aiming angles. Aiming angles near the surface could not be used, due to boat traffic in the channel. The angles of the beams were defined by in situ beam mapping. They were on the north bank –21.7° (seq. 1) and –12.2° (seq. 2) and on the south bank –22.7° (seq. 3) and –13.2° (seq. 4) (Fig. 2). Guiding nets were used to exclude fish from swimming behind the transducers. Acoustic data were analysed by means of the analysis software HTI EchoScape. The auto-tracking mode was used, and auto-tracking parameters were tested with manual tracking. In all, 1567 hourly files were analysed between 24 April and 28 June.

Table 1
Hydrological characteristics of Lake Jyväsjärvi and Lake Päijänne

	Lake Jyväsjärvi	Lake Päijänne (northern part)
Area (km^2)	3.37	54
Maximum depth (m)	26	48
Total phosphorus (μg l^{-1})	35–40	15
Total nitrogen (μg l^{-1})	850	650
Colour (Pt mg l^{-1})	80–100	30–50
pH	6.9	6.9

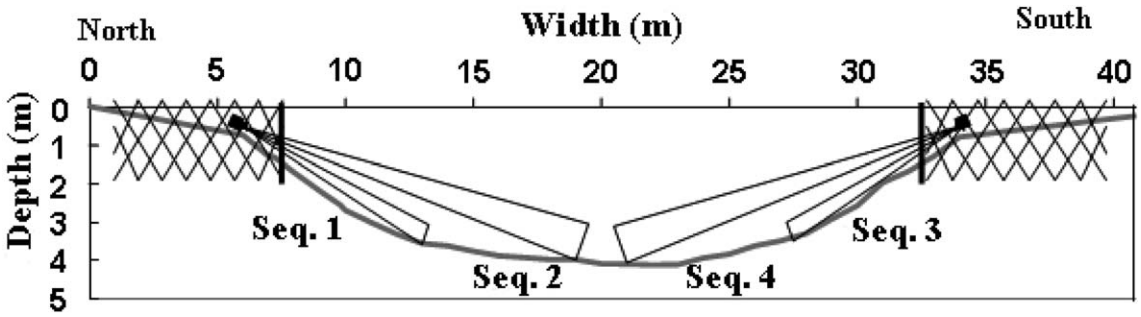

Fig. 2. The cross-sectional view of Äijälänsalmi channel. Two transducers with elliptical beams were aimed sloping downward. Guide nets kept the fish from swimming behind the transducers. Acoustic data were collected at four sampling periods per hour (seq. 1–4).

2.3. Trap net catch and environmental variables

The species and length distribution of migrating fish populations were estimated from trap net catches. The trap net was placed 50 m towards L. Jyväsjärvi from the echosounding site, and was set to catch fish migrating upstream to L. Jyväsjärvi. The trap net was sampled from 26 April to 28 June. It was examined at 1–7 d intervals. The length and species distribution of each catch were measured. The total length of each fish was measured to the nearest mm. If the total catch exceeded 10 kg, a sample was taken. The catch per unit effort (ind h^{-1}) (CPUE) was also calculated for total catch and each species separately.

The water temperature in the epilimnion was measured from 25 May to 28 June from L. Jyväsjärvi (Temp. 1) and L. Päijänne (Temp. 3) in 1–5 d intervals (Fig. 1). The temperature at the echosounding site (Temp. 2) was measured by data logger in 3-h intervals from 26 April to the end of the study. The air pressure at Tikkakoski (20 km from study site) was measured four times per day by the Finnish Meteorological Institute.

2.4. Statistical analysis

The daily numbers of upstream migrating fish detected by the echosounder, were used for the cross-correlation analysis. All the time series were first differenced ($Y = X_t - X_{(t-1)}$, where X is the measured value at point of time t) to render them stationary and prevent autocorrelations. Cross-correlation functions between the fish count series and the series of the environmental variables were estimated with a time lags of ±5 d. The numbers of upstream migrating fish for the same period as the interval between the trap net examinations were also calculated. Then, a Spearman rank order correlation between the trap net CPUE and the quantity of upstream migrating fish was calculated.

3. Results

Altogether, about 124 000 fish were detected moving upstream past the sample site between 24 April and 28 June in 2001. Some upstream migrating fish were observed instantly after the onset of monitoring, and clear peaks in upstream migration activity were detected as the monitoring progressed (Fig. 3). The first peak was detected on 10 May, followed by a sharp decrease in water temperature which seemed to delay the migration. The highest daily migration of fish was observed on 17 May, when about 11 000 fish passed the sample site.

Temperature in L. Jyväsjärvi and in the channel was generally higher than in L. Päijänne (Fig. 3). A significant cross-correlation ($r = 0.40$, $P < 0.01$) was found between the change in the number of upstream migrating fish and the change in temperature the day earlier (time lag 1 d) (Fig. 4). Air pressure changes had no effect on migration activity. Diurnally, migration activity was typically highest at dawn and dusk (Fig. 5).

In all, 13 fish species were caught from Äijälänsalmi channel by the trap net during the study period. The peak of the CPUE of the trap net occurred in the first part of May, the catch consisting mainly of perch and roach (Fig. 6). The upstream migration of ruffe started a few days later. The maximum CPUE of bream and white bream occurred in June. Perch and ruffe observed in the latter part of the study period (after Julian day 151) were small immature specimens, which were probably local fish. The temporal pattern of CPUE resembled the pattern of migration activity (Figs. 3 and 6). The CPUE and the number of fish observed by echosounder, however, did not correlate.

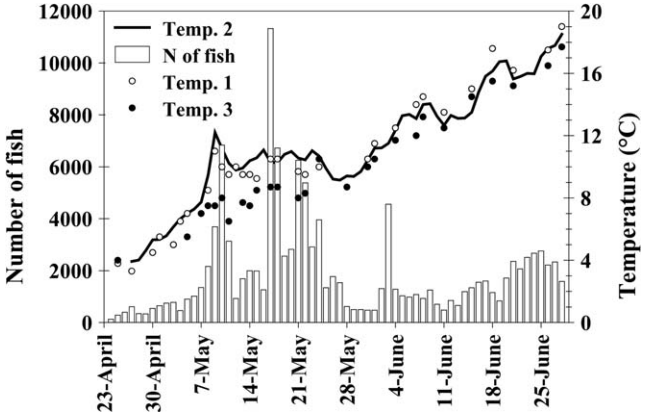

Fig. 3. Daily summary of fish migrating upstream in Äijälänsalmi channel and temperature observations (Temp 1, 2, and 3, refer to Fig. 1).

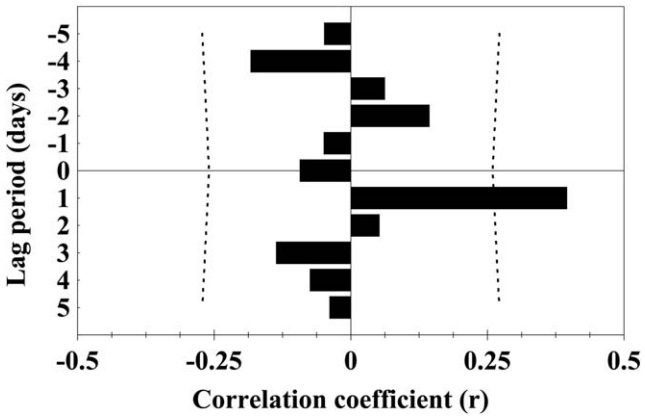

Fig. 4. Cross-correlation analysis between upstream migrating fish and water temperature. Broken lines refer to statistical significance at level of $P = 0.05$.

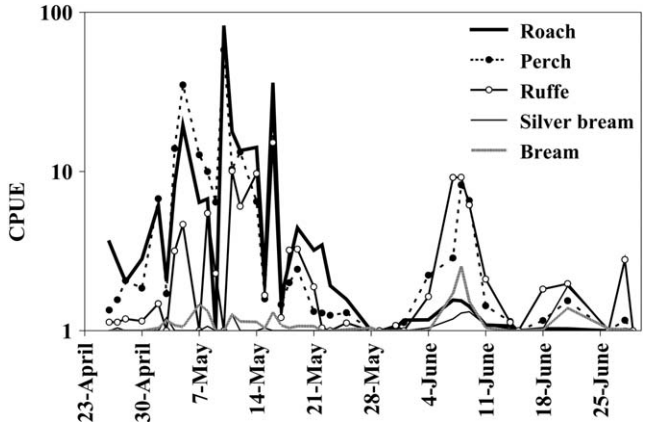

Fig. 6. Catch per unit effort ($(n+1)$ h^{-1}) of trap net for different species in Äijälänsalmi channel. Julian day 113 was 23 April and 176 was 25 June.

The distributions of target strength (TS) and $\log_{10}$(fish length, mm) of the trap net catch had similar patterns in days when the catch was high (Fig. 7). On 10 May, the comparison between the peak of the TS distribution and the peak of the fish length distribution gave the values of –43.5 dB and 135 mm, respectively. On 8 June, the TS distribution was somewhat flatter than on 10 May, and some larger fish were caught by trap net on this day.

4. Discussion

Spawning migrations of bream (Prignon et al., 1998; Molls, 1999; Grift et al., 2001), perch (Craig, 1987), roach (Vøllestad and L'Abee-Lund, 1987; Molls, 1999), ruffe (Lucas and Baras, 2001) and white bream (Prignon et al., 1998; Molls, 1999) were documented. However, an interest in migration of these species is low, because they are usually not economically important. For lake ecosystems, these migrations can be significant. When one considers how to improve L. Jyväsjärvi by intensive fishing for commercially unimportant species, one should consider how removed coarse fish might be replaced by recolonisation from L. Päijänne. All the species observed, migrating from L. Päijänne, are also found in L. Jyväsjärvi. The migrating fish are probably a subpopulation which overwinters in larger L. Päijänne, but migrate to warmer L. Jyväsjärvi to spawn.

Migrations of cyprinids and percids from L. Päijänne to L. Jyväsjärvi are triggered by the temperature difference between these lakes. L. Jyväsjärvi is typically a few degrees

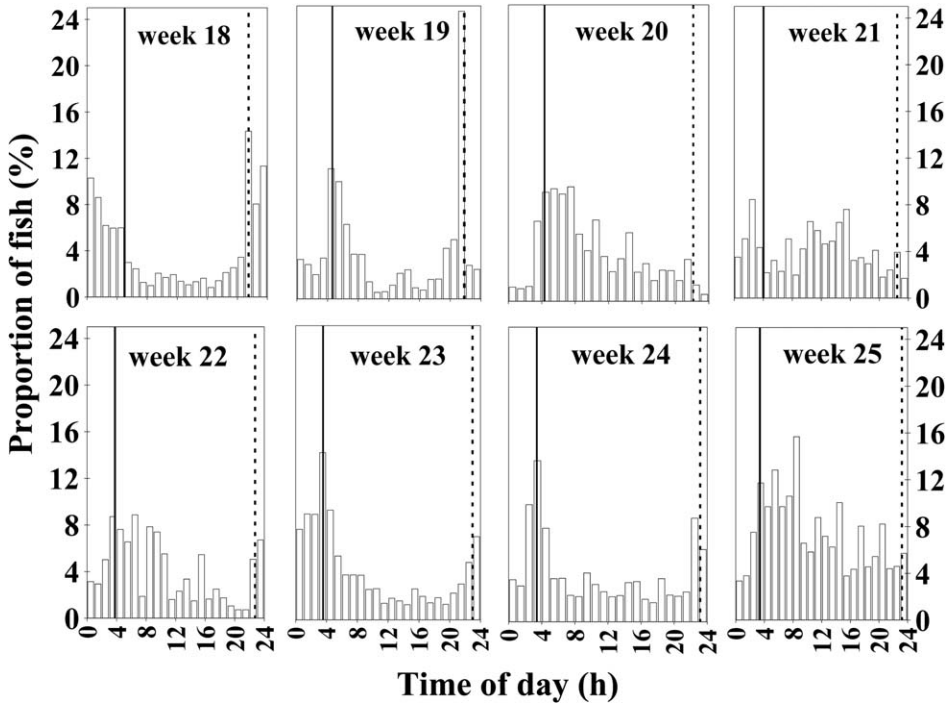

Fig. 5. Daily distribution of the upstream migrating fish in Äijälänsalmi channel. Weekly data pooled, solid line is sunrise and broken line is sunset.

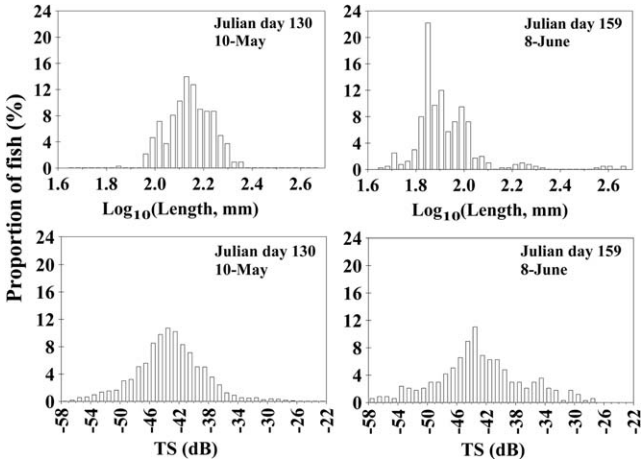

Fig. 7. Target strength (TS) distribution and fish length distribution of trap net catch for 10 May (Julian day 130) and 8 June (Julian day 159).

warmer than L. Päijänne. Temporal changes in temperature seem to regulate the migration activity, as has also been found by Vøllestad and L'Abee-Lund (1987) for roach and Craig (1987) for perch. Between Julian days 127–129, the temperature increased to 4.5 °C, and the largest CPUE was observed on day 130.

In our data, the maximum CPUE of roach, perch, and ruffe in the trap net occurred when water temperature had risen up to about 12 °C. This is higher than the 4–6 °C observed by Vøllestad and L'Abee-Lund (1987). According to the review by Lucas and Baras (2001), the migration temperature trigger for roach varied between 6 and 15 °C in different studies. In the River Ängerån, the spawning migration of perch started when the water temperature was about 10 °C (Berglund, 1978). Hokanson (1977) reported the spawning temperature to be 5–18 °C for perch and 12–18 °C for ruffe. According to Prignon et al. (1998), the spawning migration of white bream and bream was triggered at 10–15 °C. Our data showed that the maximum CPUE of these species occurred at 14–16 °C, generally in agreement with previous studies.

Light rhythm seems to drive the diurnal activity of fish. Lucas et al. (1999) observed a clear diurnal rhythm for adult male chub (*Leuciscus cephalus*) during their spawning migration. Many other species have a diel component to their migration (Lucas and Baras, 2001). We observed the maximum activity near dawn and dusk. In weeks 21 and 22 (Fig. 5), the pattern is not so obvious probably due to low number of migrating fish. In these weeks, much of the catch consisted of non-migrating fish. According to Lucas and Baras (2001), one reason for diurnal migration activity is predation avoidance. Our trap net catch showed that many fish species migrated through the Äijälänsalmi channel. During the first third of the monitoring period, the trap net CPUE and fish counts from echosounder were in good agreement. The poor correlation after 17 May was due to poor and variable catchability of the trap net. This was primarily due to fouling of the trap net. The day after cleaning the trap net, the CPUE was usually higher than before. In addition, during the catch peaks, gear saturation may have decreased catchability. Moreover, different fish species swim in different parts of the channel, avoiding the trap net. Also, decreases in water level and velocity may change the migration route of fish.

According to Kubecka and Duncan (1998b), the relationships between full-side aspect TS (dB) and standard length (SL, mm) of roach and perch were $TS = 26.7 \log_{10}(SL) - 91.0$ and $TS = 23 \log_{10}(SL) - 83$ dB, respectively. In our data, the comparison between the peak of the TS distribution and the peak of the length distribution gives a lower relationship between TS and fish length than the models of Kubecka and Duncan (1998b). There are at least two potential explanations for this difference. First, our beams were directed sloping downward which decreased the TS of our fish. Second, the fish in Äijälänsalmi channel did not necessarily swim perpendicular to the acoustic axis of the beam, in which case, the observed TS would be lower than for full-side aspect (e.g. Love, 1977; Lilja et al., 2000).

Our results confirm that horizontal split-beam echosounding is a suitable method for monitoring upstream migration and activity of fish in a small and slowly flowing channel. In general, the species discrimination is impossible with echosounders in waters, where multiple species are present. Where the fish community is dominated by one species, or an important fish species dominates, species discrimination is less problematic (e.g. Horne, 2000; Romakkaniemi et al., 2000). This study demonstrated that split-beam hydroacoustics gives fish migration information in real time, and allows us to study migration changes in the short term.

Acknowledgements

We are very grateful to R. Riikonen who helped with system setup and logistics.

References

Berglund, I., 1978. Spawning migration of the perch, *Perca fluviatilis* L. in a subarctic Swedish coastal stream. Aquilo Ser. Zool 18, 43–48.

Craig, J.F., 1987. The Biology of Perch and Related Fish. Croom Helm, London 333 p.

Cuillard, J., 1998. Daily migration cycles of fish populations in a tropical estuary (Sine-Saloum, Senegal) using a horizontal-directed split-beam transducer and multibeam sonar. Fish. Res. 35, 23–31.

Ehrenberg, J.E., Torkelson, T.C., 2000. FM slide (chirp) signals: technique for significantly improving the signal-to-noise performance in hydroacoustic assessment systems. Fish. Res 47, 193–199.

Gonzalez, L., Gerlotto, F., 1998. Observation of fish migration between the sea and a mediterranean lagoon (Etang de l'Or, France) using multibeam sonar and split beam echo sounder. Fish. Res 35, 15–22.

Grift, R.E., Buijse, A.D., Klein Breteler, J.G.P., van Densen, W.L.T., Machiels, M.A.M., Backx, J.J.G.M., 2001. Migration of bream between the main channel and floodplain lakes along the lower River Rhine during the connection phase. J. Fish Biol 59, 1033–1055.

Hokanson, K.E.F., 1977. Temperature requirements of some Percids and adaptations to the seasonal temperature cycle. J. Fish. Res. Board Can 34, 1524–1550.

Horne, J.K., 2000. Acoustic approaches to remote species identification: a review. Fish. Oceanogr 9, 356–371.

Kubecka, J., Duncan, A., 1998. a. Diurnal changes of fish behavior in a lowland river monitored by a dual-beam echosounder. Fish. Res 35, 55–63.

Kubecka, J., Duncan, A., 1998. b. Acoustic size vs. real size relationships for common species of riverine fish. Fish. Res 35, 115–125.

Lilja, J., Marjomäki, T.J., Riikonen, R., Jurvelius, J., 2000. Side-aspect target strength of Atlantic salmon (*Salmo salar*), brown trout (*Salmo trutta*), whitefish (*Coregonus lavaretus*), and pike (*Esox lucius*). Aquat. Living Resour 13, 355–360.

Love, R.H., 1977. Target strength of an individual fish at any aspect. J. Acoust. Soc. Am 62, 1397–1403.

Lucas, M.C., Baras, E., 2001. Migration of Freshwater Fishes. Blackwell Science, London 420 p.

Lucas, M.C., Mercer, T., McGinty, S., Armstrong, J.D., 1999. Use of a flat-bed passive integrated transponder antenna array to study the migration and behavior of lowland river fishes at a fish pass. Fish. Res. 44, 183–191.

Molls, F., 1999. New insights into the migration and habitat use by bream and white bream in the floodplain of the River Rhine. J. Fish Biol 55, 1187–1200.

Prignon, J.D., Micha, J.C., Gillet, A., 1998. Biological and environmental characteristics of fish passage at the Tailfer dam on the Meuse River, Belgium. In: Jungwirth, M., Schmutz, S., Weiss, S. (Eds.), Fish migration and bypasses, Fishing News Books. Blackwell Science Ltd, Oxford, pp. 69–84.

Ransom, B.H., Johnston, S.V., Steig, T.W., 1998. Review on monitoring adult salmonid (*Oncorhynchus* and *Salmo salar*) escapement using fixed-location split-beam hydroacoustics. Fish. Res 35, 33–42.

Romakkaniemi, A., Lilja, J., Nykänen, M., Marjomäki, T.J., Jurvelius, J., 2000. Spawning run of Atlantic salmon (*Salmo salar*) in the river Tornionjoki monitored by horizontal split beam echosounding. Aquat. Living Resour 13, 349–354.

Vøllestad, L.A., L'Abee-Lund, J.H., 1987. Reproductive biology of stream-spawning roach. *Rutilus rutilus*. Environ. Biol. Fish 18, 219–227.

Available online at www.sciencedirect.com
SCIENCE DIRECT®
Aquatic Living Resources 16 (2003) 191–196
Aquatic Living Resources
www.elsevier.com/locate/aquliv

Spatial overlap and distribution of anchovies (*Anchoa* spp.) and copepods in a shallow stratified estuary

J. Christopher Taylor [a,*], Peter S. Rand [b]

[a] *Department of Zoology, Center for Marine Sciences and Technology, North Carolina State University, 303 College Circle, Morehead City, NC 28557, USA*
[b] *Department of Zoology, North Carolina State University, Campus Box 7617, Raleigh, NC 27695, USA*

Accepted 16 January 2003

Abstract

Juvenile pelagic fishes are integral members of many coastal river communities. Many of these systems are strongly influenced by variable wind stress and freshwater inputs that can increase heterogeneity in estuarine habitat for fishes. We use mobile sonar surveys within the Neuse River Estuary System, NC, USA to assess the distribution and behavioral patterns of juvenile anchovies, *Anchoa* spp. 25-65 mm TL, over a broad range of spatial scales in relation to diel and seasonal changes in water quality including stratification, hypoxic events and copepod distribution. Results from our study indicate that episodic stratification-induced hypoxic events can reduce suitable habitat volume for anchovies by more than 50%. Furthermore, our sampling suggests that hypoxia causes spatial separation between plankton and the grazing fishes. Under stratified oxygen conditions, we observe higher densities of copepods in hypoxic bottom water. Finally, we report that reductions in available habitat caused an increase in local densities of fishes and may result in increased competition for resources. These spatially explicit data are critical for developing trophic dynamic models that predict the response of fish communities to natural and anthropogenic impacts on the system.

Keywords: Hydroacoustics; Estuary-dependent; Spatial structure; Hypoxia; Zooplankton; *Anchoa*

1. Introduction

Estuary-dependent fishes occupy spatially complex and temporally dynamic habitats during portions of their life-history. Juvenile stages of numerous commercially and ecologically important fish species rely on the estuarine habitats as a nursery for rapid growth and as a refuge from predation (Minello, 1999). Several factors influence the spatial distribution of juvenile fishes in estuaries. These factors can be broadly categorized as abiotic factors, such as salinity, temperature, pH, dissolved oxygen (DO), and benthic structure, and biotic factors, such as prey availability and predator abundance.

Numerous studies have documented relationships between the abundance of juvenile estuarine fishes and the presence and complexity of physical structure such as oyster reefs, sea grasses, and salt marshes (Minello, 1999). DO is an additional abiotic factor that can structure estuarine fish populations in estuaries (Breitburg, 1992; Howell and Simpson, 1994). Several studies have focused on the effects of low DO (hypoxia) on the distribution of demersal fishes (Pihl et al., 1991; Howell and Simpson, 1994), but only a few studies have been devoted to an understanding of the interactions between hypoxia and predator-prey relationships (Pihl et al., 1992; Keister et al., 2000). We are not aware of any studies that have focused on the interactions of DO and prey dynamics on the distribution of juvenile pelagic fishes in shallow estuaries; however, recent work has documented relationships between larval anchovies and zooplankton and bottom-layer DO (Keister et al., 2000). Dominant pelagic fishes such as anchovies, *Anchoa* spp., and menhaden, *Brevoortia* spp., comprise the majority of the fish biomass in many estuaries of eastern North America. These species serve important commercial (in the case of menhaden) and ecological roles as prey resources for commercially important piscivores. It may be counter-intuitive to suppose that pelagic fish populations would be impacted by hypoxic events that occur in the

* Corresponding author.
E-mail address: Chris_Taylor@ncsu.edu (J.C. Taylor).

doi:10.1016/S0990-7440(03)00012-3

hypolimnion. As a result, previous studies examining the distribution of pelagic fishes in US estuaries have focused primarily on their distribution in relation to biotic factors, and more specifically prey fields such as zooplankton patchiness and phytoplankton dynamics (Peebles et al., 1996; Friedland et al., 1989).

The pelagic environment of shallow aquatic systems presents a challenge for sampling fish communities. Previous assessments of the distribution of estuarine fishes in relation to habitat quality have primarily used trawls, which are restricted to coarse spatial scales and do not adequately sample the near surface. Fisheries hydroacoustics provides an improved, non-invasive method of collecting information on the distribution of fishes within aquatic habitats, over a continuum of spatial scales throughout the water column (MacLennan and Simmonds, 1992). Furthermore, in shallow aquatic habitats (<10 m), depth-discrete active or passive sampling gear has proved ineffective at determining the distribution of small fishes in the vertical dimension (Taylor and Rand, unpublished data). Split-beam hydroacoustic technology now gives us the ability to describe 3D distribution patterns of estuarine fishes and to better assess the relationship between fish populations and the spatially complex, physicochemical environment.

The aim of this paper is to characterize the spatial structure of fish distribution as a function of water column stratification and hypoxia in the lower water column. Understanding the spatial structuring of the grazing fishes will lead us to better estimates of grazing impact and trophic efficiencies in estuarine food webs impacted by adverse water quality.

2. Methods

Surveys were conducted in the lower Neuse River Estuary (NRE), NC, USA (Fig. 1). The Neuse River is one of two major rivers that provide freshwater input into the Pamlico Sound, the largest lagoon-type estuary in the eastern US. A single transect was sampled at night on two dates. The first date, 26 June 2001, was during a period of severe density stratification and the hypolimnion was hypoxic (DO < 2 mg O_2 l^{-1}). The second date, 2 August 2001, was during a period when the water column was mixed and oxygen was nearly homogeneous throughout.

The survey was conducted between 23:30 and 00:30 on both occasions. We used a 200-kHz HTI Model 241 split-beam echosounder coupled with an elliptical (4° × 10° nominal beam dimension) transducer and a circular (15° nominal beam dimension) transducer to assess abundance of fish in the vertical and horizontal dimensions from the surface to within 0.25-m from the bottom. The elliptical transducer was oriented perpendicular and lateral to the vessel path and sampled the top 1.5-m of the water column from 10 to 30-m athwart ship. The circular transducer was oriented vertically and sampled from 1-m below the surface to within 0.25 m from the bottom. Vessel speed was constant at about

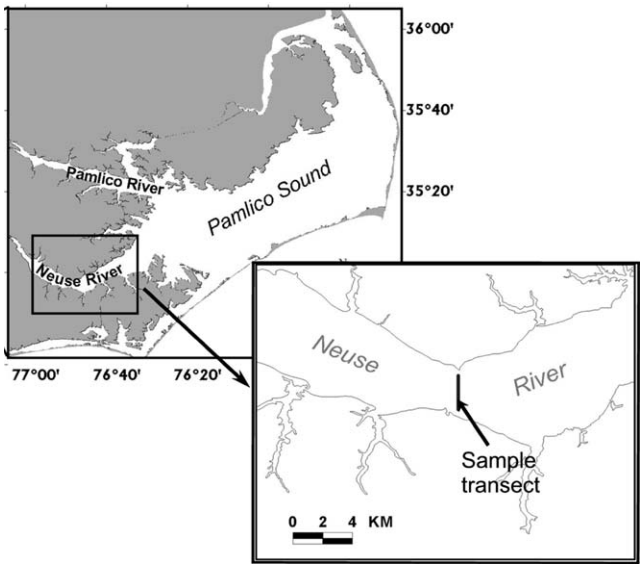

Fig. 1. Sample transect in the lower Neuse River Estuary, NC, USA.

1.8 m s^{-1}. A ping rate of 10 pulses s^{-1} was multiplexed between the two transducers, resulting in 5 pulses s^{-1} to each transducer. Each sampling occasion was preceded by an in situ system calibration using a tungsten-carbide reference sphere of known target strength placed greater than 5-m from the transducers. Gain parameters were adjusted accordingly based on calibration results. Returned acoustic signals were simultaneously adjusted for spreading loss by applying 40-log R and 20-log R time-varied gain for split-beam and echo-integration processing, respectively. The data were processed in real-time for split-beam and echo-integration (HTI DEP v. 3.53, HTI Seattle, WA, USA) and stored on a laptop computer for later data analyses.

The acoustic survey coincided with a sampling of water quality using a data logger (YSI Model 6600) at 4-5 stations along the transect. The data logger recorded temperature, salinity, and DO at 0.1-m increments through the water column. All parameters were interpolated along the cross-section of the river to provide a visualization of the water quality observed during the hydroacoustic sampling. Discrete zooplankton samples were taken at 2 or 3 depths at each station using a 30-l Schindler-Patalis plankton trap fitted with a 63 μm mesh net. Samples were preserved in 2-5% buffered formalin, and subsamples were counted for juvenile and adult (copepodite) stages in the laboratory. Densities of copepods were calculated and reported in ind. m^{-3}. To verify fish size and species composition in the surveyed area, we sampled 18 stations using a surface trawl (1.2 m width, 0.7 m height, 3.5 m length, 3.2 mm knotted mesh) that was towed between two small boats and targeted the top 1 m of the water column. Results from this survey indicated that anchovies, *Anchoa* spp., comprised over 98% by number of the fishes encountered.

Acoustic data were processed using split-beam and echo-integration analyses. Split-beam analysis was used to determine the acoustic size (target strength) of individual fish

targets in decibels. Using equations for clupeiform species, target strengths were converted to approximate fish size and to wet weight (Foote, 1986; Taylor, unpublished data). Echo-integration provided a measure of relative density that can be converted to absolute density by scaling the integrated acoustic signal within a cell by the average target size within the cell. For this study, down-looking echo-integration data were divided into cells approximately 25-m long by 0.5-m deep from 2.0-m below the surface to the bottom. The side-looking integration data were divided into cells 25-m long and 1.5-m deep and was calculated as the average voltage return from 10 to 30-m athwart ship. Average target strength was calculated for each cell and during each sampling occasion. Only fish targets between -57 and -43 dB (ca. 20-100 mm TL) were used for the split-beam and echo-integration analyses, representing the range of fish sizes sampled in the surface trawl samples. All targets were assumed to be *Anchoa* spp. based on the surface trawl samples. Densities, measured in no. m^{-3} and g m^{-3}, were calculated for each cell by scaling the mean voltage returned from the ensonified volume by the average fish size calculated from split-beam analysis and verified using the surface trawl survey.

2.1. Data visualization and statistical analyses

Summary statistics for fish size and densities were computed for each of the surveys. Echo-integration data were analyzed for large- (trend) and small-scale (autocorrelation) spatial structures. We used a generalized additive model (GAM) to characterize the spatial trend in the data for the transect on each sampling occasion. Distance-along-transect (in meters) and depth in the water column (in meters) were used as covariates to explain the variability in root-transformed echo-integrated density. The root-transformation of the echo-integration data appeared to best normalize the data, since the data were highly skewed and there were many zero-densities in the dataset. A stepwise regression technique was used to optimize the degrees of freedom used for each covariate in the smoothing functions of the GAM. Predictions from the GAM and its residuals were plotted to examine them for normality. Approximate *r*-squares were calculated to determine the amount of variability explained by the spatial covariates. Residuals from the GAMs were then analyzed for the remaining spatial structure by calculating the semivariance as a function of the distance between measures (Cressie, 1993). The behavior of the empirical variogram suggested that a Gaussian model would best fit the data. The range, sill and nugget parameters were estimated using non-linear least squares procedures to estimate the spatial extent of correlation, the range parameter of the theoretical variogram. Significant model variogram parameters were compared between the two surveys to assess differences in the spatial patterns of densities that may be explained by the differences in habitat quality between the two sampling occasions. All statistical analyses were performed using S-plus (v. 6.0, Insightful Corporation, 2001).

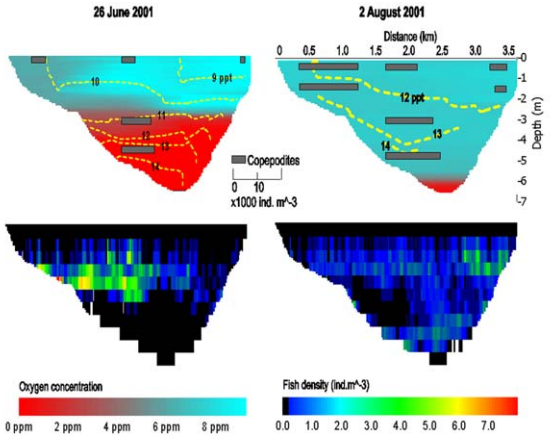

Fig. 2. Cross section of the transect sampled in June and August 2001. Viewing direction is toward the west with the south on the left and north on the right of each plot. Vertical and horizontal dimensions of each plot are according to axes in top right panel. Interpolations of water quality (top panels) are represented by salinity (broken yellow lines) and DO (color bar at lower left). Copepod densities are represented by gray bars at sample locations and are proportional to the scale inset. Echo-integrated fish density is represented in the lower panels. Densities ranged from 0 to 8 fish m^{-3} represented by a color spectrum (lower right).

3. Results and discussion

Patterns in water quality were quite different between the two sampling occasions with respect to DO and salinity.

3.1. June sampling

During the night of 26 June 2001, the transect was stratified with the pycnocline (12-13 ppt) and thermocline (28.0-27.0 °C) at a depth of 3-m and >50% of the water column under hypoxic conditions (Fig. 2). Hypoxic events during the late-spring to early-fall in the Neuse River were strongly correlated with stratification caused by spring freshwater input, early-spring organic matter decomposition, and the magnitude and direction of wind stress (Borsuk et al., 2001; Paerl et al., 1998). Low wind stress before the June sampling contributed to density stratification, which was caused primarily by salinity differences between the intruding high salinity water from the Pamlico Sound and net downstream flow of the freshwater from the Neuse River. Copepodites that were sampled concurrently during the hydroacoustic survey indicated higher densities at and below the pycnocline in DO concentrations lethal to larval anchovies (Fig. 2; Breitburg, 1994). This pattern was in contrast to the observations in the Chesapeake Bay, where copepodites avoided bottom-layer DO < 3 mg O_2 l^{-1} (Keister et al., 2000). Large copepodites were the preferred prey of the anchovies (Peebles et al., 1996) and represented the majority of the stomach contents of anchovies captured during this study (Taylor and Rand, unpublished data).

Average estimated fish size for June was 32.8 ± 0.6 mm TL (mean ± SE, Table 1) and corresponded well with our surface trawl sampling in the region, which averaged 35 ± 1 mm TL. The distribution of June density values was highly

Table 1
Summary of fish size and distribution of echo-integrated densities

Date	Estimated TL (SE) (mm)	Mean density (SE) (no. m^{-3})	Median density (no. m^{-3})	Min/Max density (no. m^{-3})	Biomass (g)
26 June 2001	32.8 (0.6)	0.50 (0.04)	0.04	0/8.31	809
2 August 2001	30.3 (0.3)	0.66 (0.02)	0.50	0/3.42	1054

skewed and contained many zeros. Density values along the transect averaged 0.50 fish m^{-3} (median = 0.04 fish m^{-3}) and ranged from 0 to 8.31 fish m^{-3} (Table 1). High variability and frequent zeros were common in the surveys of pelagic species (Freon and Misund, 1999).

The GAM covariates of horizontal distance and depth explained 60.5% of the variability in the density distribution in June. There was a weak effect of horizontal distance, with higher densities toward the middle of the river (Fig. 3). This pattern may be better explained by the effect of depth on the vertical distribution, especially in the middle of the river. The results from the GAM indicated a significant positive relationship of fish density and depth from the surface to approximately 3-m depth (Fig. 3). Vertical density distributions generally matched the pattern of oxygen stratification with very few fish encountered below 3.5-m. Larval stages of anchovies in the Chesapeake Bay were also observed to avoid hypoxic waters (Breitburg, 1994). Our results also suggested that the fish were aggregating near the pycnocline. In larger ocean and coastal systems, the evidence of changes in vertical distribution was attributed to depleted oxygen in the lower water column. Mathisen (1989) reported changes in the maximum depth of anchoveta during extreme El Nino events that resulted in an oxygen depletion closer to shore. Further work is required to better characterize the movements of pelagic fishes that may help explain this pattern.

Presence of aggregations was further supported by the analysis of the spatial structure of the residuals of the GAM. Small-scale spatial correlation was present in the residuals to an estimated range of 400 m (Fig. 4). High degrees of correlation were especially evident from 20 to approximately 200-m lag distance. These small to medium sized patches can be seen in the data plotted in Fig. 1. We were surprised to see residual spatial structure in the data since other pelagic species that have been studied generally show disaggregate patterns during the night while shoaling or schooling during the day (reviewed in Freon and Misund, 1999). Dense aggregations may indicate that these fish were occupying microhabitats with high prey resources. Such high local densities of grazers, however, may lead to increased competition for resources, decreased feeding rates by individuals, and possible increases in activity costs. These mechanisms can lead to decreased individual growth rates and lower population production.

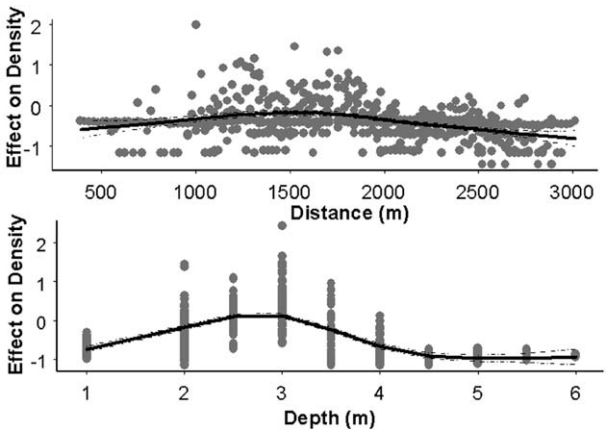

Fig. 3. GAM results for June 2001 fish density. Closed circles represent the residuals. Spline fit (solid line) is bound by 95% confidence intervals (dotted lines).

3.2. August sampling

Water quality sampling on 2 August 2001 showed a generally mixed water column with high DO down to approximately 5.5-m (Fig. 2). Just prior to this period, the NRE experienced moderate wind stress that served to mix the water column and bring oxygenated water to the hypolimnion. Zooplankton abundances were higher than those observed in June and were also generally homogeneous throughout the water column (Fig. 2).

Average estimated fish size for August was 30 ± 0.3 mm TL, and, as with sampling in June, corresponded well with our surface trawl samples, which averaged 31.8 ± 0.2 mm TL (Taylor and Rand, unpublished data). The distribution of August density values was not nearly as skewed as June

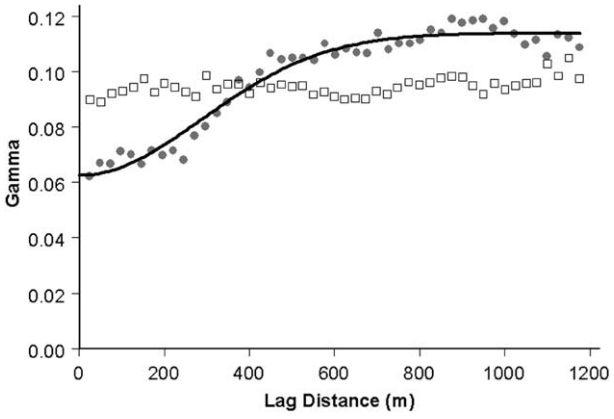

Fig. 4. Variogram plots from analysis of spatial structure of residuals from GAMs for June (closed circles) and August (open squares). Data points represent calculated semivariance (gamma) at lag distances along the *x*-axis. Dark line is a fitted theoretical variogram to the June data with parameters for the Gaussian model, range: 406.32, sill: 0.05, nugget: 0.06. No significant model was found for the August data.

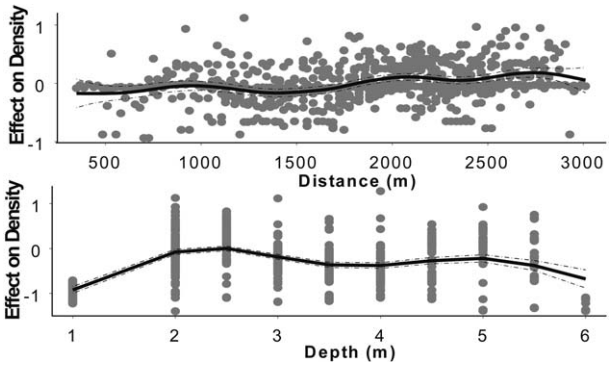

Fig. 5. GAM results for August 2001 fish density. Closed circles represent the residuals. Spline fit (solid line) is bound by 95% confidence intervals (dotted lines).

values and contained fewer zeros. Density values along the transect during August averaged 0.66 fish m^{-3} (median = 0.50 fish m^{-3}) and ranged from 0 to 3.42 fish m^{-3} (Table 1).

The GAM model for the August density distributions explained 48% of the variability in the data. In contrast to June, there was a weak positive effect of distance along the transect, with more fish present near the end of the transect (Fig. 5). This pattern was opposite to the trend in zooplankton abundances across the transect (Fig. 2), and may be a result of localized grazing effects on the plankton. Vertical distribution was also quite different from the pattern observed in June, with fish generally evenly distributed from 2-m to near bottom (6-m). The more uniform distribution of fish in the water column appeared to be a more typical pattern observed with nighttime acoustic data (reviewed in Freon and Misund, 1999), and served as a stark contrast to what we observed in June.

Unlike the results from the analysis of small-scale spatial structure in the June sampling, there was no spatial pattern in the GAM residuals for August (Fig. 4). The empirical variogram indicated a pure nugget effect, and neither the sill nor the range parameters of the model variogram were significant. With evidence of only a weak trend... “with the sentence” Given the prevalence of normoxia, and the overall higher densities and more uniform distribution of zooplankton prey during this sampling period (Fig. 2), we hypothesize fish exhibit a more uniform distribution throughout the system as a result of less restrictive limits on available oxygen and prey resources in the system. The apparent inverse relationship between grazing fish and zooplankton densities observed across the horizontal dimension may indicate how these grazing fishes may affect copepod dynamics through localized grazing pressure. This latter conclusion is speculative and requires further investigation.

4. Conclusion

Hydroacoustic data analyzed with modern statistical methods provides us with new insights into the environmental factors that structure the distribution of pelagic estuary-dependent fish populations in shallow systems. These results represent the first reported efforts to quantify the spatial structuring of pelagic fishes in response to oxygen stratification in a periodically stratified estuary. Under stratified conditions, we found that fish form dense aggregations at night, in conditions when overall prey concentrations in the epilimnion were low. This suggests that fish may be depleting prey concentrations in the epilimnion or concentrating in prey patches that we cannot resolve with our current plankton sampling methods and argues for an approach where we can more closely match the scale and resolution of sampling of both fish and plankton communities. Future hydroacoustic sampling coupled with intense sampling of the zooplankton community will allow us to extend the analysis to important biotic processes, particularly with regard to better assessing the interactions of abiotic and biotic factors in determining the spatial distribution of pelagic fishes in estuaries. These data are important to develop trophic models that will predict population dynamics as a function of habitat quality. Physical models suggest that anthropogenic sources of nutrients increase the propensity of hypoxic events during periods of low wind stress (Paerl et al., 1998; Borsuk et al., 2001). Varying durations and severity of stratification and hypoxia will likely result in complex interactions between the zooplankton populations and the grazing fish community, the transfer of energy between the two trophic levels, and system-wide fish production.

Acknowledgements

This project was made possible by funding through an US EPA STAR Fellowship to J.C.T. and a NOAA Sea Grant College Program grant to North Carolina Sea Grant at North Carolina State University (grant no. R/MRD-44) to P.S.R. We greatly appreciate the assistance of J. Jenkins, B. Belazsi, C. Bergeron, N. Hall, S. Searcy, and J. Arnott during field collections. L. Avens, B. Burke, K. Craig, M. Fuentes and S. Searcy provided valuable comments on this manuscript.

References

Borsuk, M.E., Stow, C.A., Leuttich, R.A., Paerl, H.W., Pinckney, J.L., 2001. Modelling oxygen dynamics in an intermittently stratified estuary: estimation of process rates using field data. Estuar. Coast. Shelf Sci. 52, 33–49.

Breitburg, D.L., 1992. Episodic hypoxia in the Chesapeake Bay: interacting effects of recruitment, behavior and physical disturbance. Ecol. Monogr. 62, 525–546.

Breitburg, D.L., 1994. Behavioral response of fish larvae to low dissolved oxygen concentrations in a stratified water column. Mar. Biol. 120, 615–625.

Cressie, N.A.C., 1993. Statistics for Spatial Data. Wiley,, New York.

Foote, K.G., 1986. Fish target strengths for use in echointegrator surveys. J. Acoust. Soc. Am. 82, 981–987.

Freon, P., Misund, O.A., 1999. Dynamics of Pelagic Fish Distribution and Behaviour: Effects of Fisheries and Stock Assessment. Blackwell, MA.

Friedland, K.D., Arenholz, D.W., Guthrie, J.F., 1989. Influence of plankton on distribution patterns of the filter-feeder *Brevoortia tyrannus* (Pisces: Clupeidae). Mar. Ecol. Prog. Ser. 54, 1–11.

Howell, P., Simpson, D., 1994. Abundance of marine resources in relation to dissolved oxygen in Long Island Sound. Estuaries 17, 394–402.

Insightful Corporation, 2001. S-PLUS 6 for Windows. Seattle, WA, USA.

Keister, J.E., Houde, E.D., Breitburg, D.L., 2000. Effects of bottom-layer hypoxia on abundances and depth distributions of organisms in Patuxent River. Chesapeake Bay. Mar. Ecol. Prog. Ser. 205, 43–59.

MacLennan, D.N., Simmonds, E.J., 1992. Fisheries Acoustics. Chapman and Hall,, New York.

Mathisen, O.A., 1989. Adaptation of the anchoveta to the Peruvian upwelling system. In: Pauly, D., Muck, P., Mendo, J., Tsukayama, I (Eds.), The Peruvian Upwelling Ecosystem: Dynamics and Interactions, ICCLARM Conference Proceedings, 18, pp. 220–234 Callao, Peru.

Minello, T.J., 1999. Nekton densities in shallow estuarine habitats of Texas and Louisiana and the identification of essential fish habitat. In: Benaka, L (Ed.), Fish Habitat AFS Symposium 22 Bethesda, MD.

Paerl, H.W., Pinckney, J., Fear, J., Peierls, B., 1998. Ecosystem responses to internal and watershed organic matter loading: consequences for hypoxia in the eutrophying Neuse River Estuary, NC, USA. Mar. Ecol. Prog. Ser. 166, 17–25.

Peebles, E.B., Hall, J.R., Tolley, S.G., 1996. Egg production by the bay anchovy *Anchoa mitchilli* in relation to adult and larval prey fields. Mar. Ecol. Prog. Ser. 131, 61–73.

Pihl, L., Baden, S.P., Diaz, R.J., 1991. Effects of periodic hypoxia on distribution of demersal fish and crustaceans. Mar. Biol. 108, 349–360.

Pihl, L., Baden, S.P., Diaz, R.J., Schaffner, L.C., 1992. Hypoxia-induced structural changes in the diet of bottom-feeding fish and Crustacea. Mar. Biol. 112, 349–361.

Available online at www.sciencedirect.com
SCIENCE DIRECT®
Aquatic Living Resources 16 (2003) 197–203
Aquatic Living Resources
www.elsevier.com/locate/aquliv

Acoustics for ecosystem research: lessons and perspectives from a scientific programme focusing on tuna-environment relationships

Arnaud Bertrand [a,*], Erwan Josse [b], Pascal Bach [c], Laurent Dagorn [d]

[a] IRD, c/o Escuela de Ciencias del Mar, ECM-UCV, Av. Altamirano 1480, Casilla 1020, Valparaiso, Chile
[b] Institut de recherche pour le développement, IRD, Centre de Bretagne, BP 70, 29280 Plouzané, France
[c] IRD, Pôle Halieutique Méditerranéen et Tropical, avenue Jean Monnet, BP 171, 34203 Sète cedex, France
[d] IRD, c/o Hawaii Institute of Marine Biology, P.O. Box 1346, Coconut Island, Kaneohe, HI 96744, USA

Accepted 10 December 2002

Abstract

Fisheries management now extends from the stock to the ecosystem. The foundation for fisheries management on an ecosystem basis must lie in appropriate modelling of the ecosystems. A prerequisite for such models requires data on the two interactive components of the ecosystem: the biotope (physical environment), and the community of living species. In this context, acoustics become essential, as this tool can provide qualitative and quantitative data on various communities of species, and furthermore allows the seldom-attainable study of their interactions. In fact, acoustics allow the monitoring of entire communities, from plankton to large predators, as well as certain aspects of the physical environment, such as substratum characteristics. Acoustics have been used during the last two decades mainly to provide fishery-independent estimates of stocks. The intention of this paper is to promote the use of acoustics for studying marine ecosystems and to encourage the emergence of new generations of ecosystem models. As an example of integrative research based on acoustic data, we will present the approach and the results of a scientific programme (ECOTAP) carried out to study the tuna pelagic ecosystem in French Polynesia. We then discuss the use of acoustics as a tool for ecosystem-based studies and management.

Keywords: Acoustics; Behaviour; Ecosystem approach; Pelagic ecosystem

1. Introduction

Ecosystem-based fisheries management has been widely promoted by fisheries management agencies and non-governmental organisations, and will soon be the preferred mode of management (e.g. FAO Reykjavik conference on responsible fisheries in the marine ecosystem: http://www.refisheries2001.org/). Interactions between organisms and their environment, and between organisms themselves, are complex and fishing is only one of the factors influencing aquatic communities. The foundation for fisheries management on an ecosystem-basis must lie in appropriate modelling of the ecosystems. Such modelling requires data on the two components of the studied ecosystem: the biotope (physical environment), and the community of living species, the biocoenosis. Some models often considered to be "ecosystem models" are already available (e.g. Ecopath, Ecosim, Ecospace; Pauly et al., 2000) but these are based mainly on trophic relationships between components of the studied communities. In addition, these models do not take explicitly into account the variability of the physical environment and the interactions between the physical environment and species communities. The search for a quantitative understanding of the dynamics of interactions between the biotic and abiotic components of marine ecosystems, and their effects on the dynamics of fish populations constitutes the foundation of modern fisheries oceanography (Dower et al., 2000). Furthermore, as stated by Denman (2000), "it is almost axiomatic to state that confidence in forecast will increase with the increased use of observations". In other words, we need to develop our understanding to model better ecosystems. At present, the main difficulty resides in our lack of knowledge about the true functioning of ecosystems, primarily due to a lack of available data. In most cases, the only available data concern the exploited species (plus some punc-

* Corresponding author.
E-mail address: arnaud.bertrand@ird.fr (A. Bertrand).

doi:10.1016/S0990-7440(03)00018-4

tual data on plankton or other parameters). As a consequence, most current models are based only on multi-species catch data, without any information on other key components of the system (micronekton for instance). These models might be using the term "ecosystem" in an incorrect way. From our point of view, it is of great importance to take care when using the term "ecosystem" else there is a strong risk of it losing its true meaning. An ecosystem approach seeks to study the main components of an ecosystem, knowing that a truly exhaustive study is impossible.

To comply with such an objective, acoustic techniques become essential. Acoustics represent the only tool allowing the simultaneous collection of qualitative and quantitative data on various communities of an ecosystem, from plankton to large predators, and also on abiotic parameters, such as substratum characteristics. Acoustic observations allow the user to investigate ecological relationships in a direct manner. Of course, other methods of observation should also be used in order to collect complementary data.

The purpose of this paper is to promote the use of acoustics for studying aquatic ecosystems and to encourage the emergence of new generations of ecosystem models. As an example of integrative research based on acoustic data, we will present a synthesis of the approach and results of a scientific programme (ECOTAP: Etude du comportement des thonidés par acoustique et par pêche/study of tuna behaviour using acoustics and fishing) carried out to study the tuna pelagic ecosystem in French Polynesia. We will then discuss the potential of acoustics as a tool for ecosystem-based studies and management. It is important to note that our intention is not to provide an exhaustive review of the studies that have used acoustics coupled with other observation tools to observe different communities of pelagic ecosystems (e.g. Axelsen et al., 2000; Croll et al., 1998; Fiedler et al., 1998; Lebourges-Dhaussy et al., 2000; Marchal et al., 1996; Young et al., 2001), but rather to illustrate our approach through the example of one integrative study.

2. Example of an ecosystem approach: the ECOTAP programme

The integrative objective of the ECOTAP programme was the direct and simultaneous observation of tuna (i.e. albacore, *Thunnus alalunga*; bigeye, *Thunnus obesus* and yellowfin tuna, *Thunnus albacares*), their prey and the hydrologic environment using acoustics, CTD probes, ultrasonic tracking, instrumented longline fishing, pelagic trawling and the analysis of stomach contents (Fig. 1).

3. Materials and methods

Data were collected on-board the IRD R/V "Alis" (28 m long) during ECOTAP experiments carried out in the French Polynesian exclusive economic zone. The study was conducted between 4 and 20°S and 134 and 154°W, in the

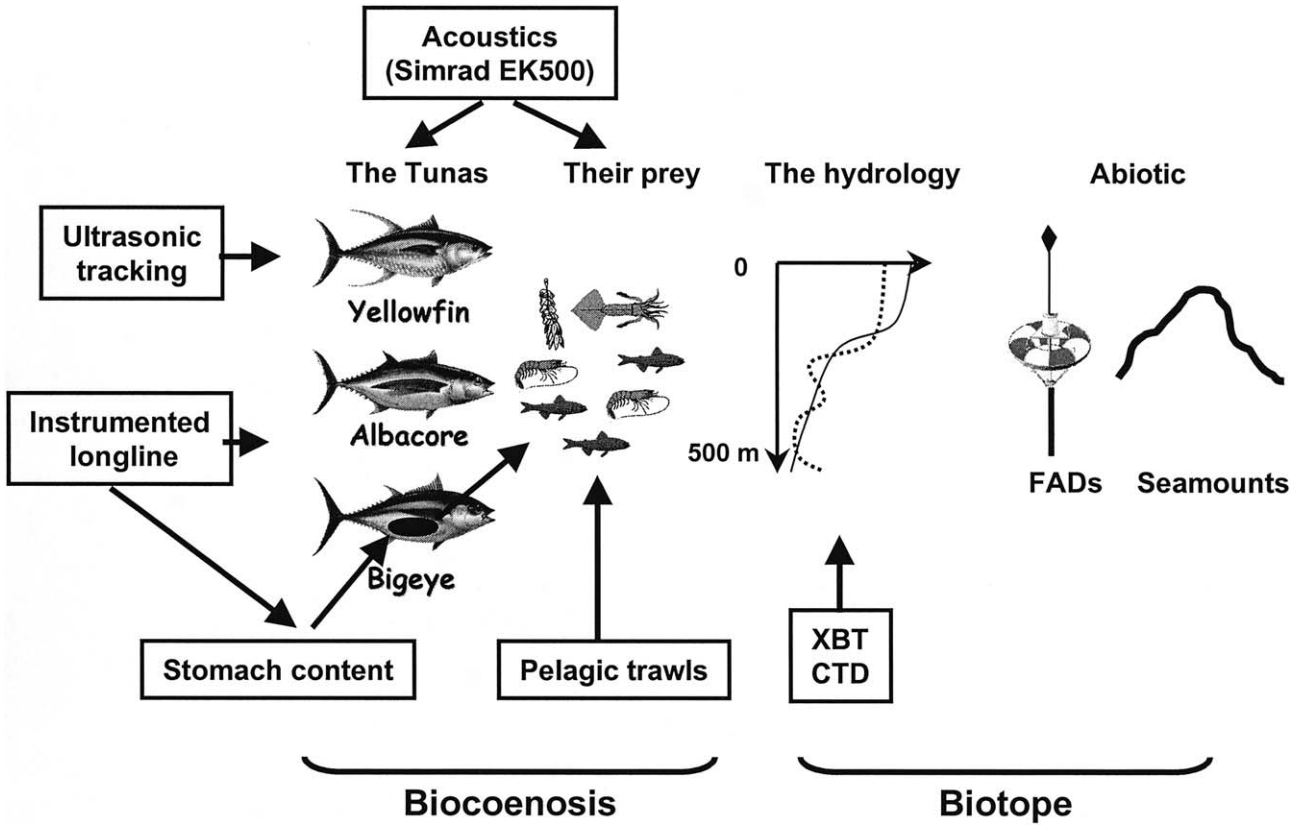

Fig. 1. Schematic outline of the ecosystem approach used during the ECOTAP programme.

vicinity of the Society, Tuamotu and Marquesas Archipelagos, from October 1995 to August 1997. Acoustic data collected with a SIMRAD EK500 connected to a 38 kHz split beam transducer, were recorded to observe both tuna (by echo counting or echo-integration) and their prey (by echo-integration) (Bertrand et al., 1999b; Bertrand and Josse, 2000a; Josse et al., 1999). Acoustic observations were also performed around fish aggregating devices (FADs) to study tuna aggregations (Josse et al., 1999). Temperature, salinity and dissolved oxygen profiles were collected using a probe Seacat SBE 19 (Seabird Electronics, Inc.) between the surface and more than 500 m in depth. A total of 80 000 hooks were deployed during 163 fishing operations conducted using an experimental longline instrumented with hook timers and time-depth recorders (Bach et al., 2003) in order to estimate both time and depth of capture using a model developed by Bach et al. (1996). Micronekton sampling was done using a fry pelagic trawl (5 mm mesh) coupled with echo sounding (Bertrand et al., 2002a). Stomach contents of fish caught by longline were fixed in 10% formalin, then organisms were sorted and weighed at the laboratory (Bertrand et al., 2002a). The tracking equipment we used was a VEMCO system (Shad Bay, Nova Scotia, Canada), 50 kHz, 500 and 1000 PSI equipped with pressure sensor (Josse et al., 1998; Dagorn et al., 2000a).

All of these observational techniques were used to study the relationships between tuna and their environment (biotic and abiotic) as shown in Fig. 1. The main results obtained using an echosounder as the central tool and some potential applications of these results in fisheries science are presented in Table 1.

3.1. Tuna observation

Tuna horizontal and vertical distribution was studied indirectly using an instrumented longline and directly using sonic tracking and acoustics (Fig. 2, Table 1). The simultaneous use of acoustic and ultrasonic tracking allowed studying the fine scale behaviour of tunas and to precise the role of the biotic and abiotic parameters on their horizontal and vertical movements (Josse et al., 1998; Dagorn et al., 2000a, b; Dagorn et al., 2001). Another application of such approach was the measurement of the target strength (TS) of fish individually identified, swimming free in their environment (Bertrand et al., 1999a). An example of spin off of such study was the demonstration that bigeye tuna was more able to adjust the volume of its swimbladder than other physoclists (Bertrand and Josse, 2000b). Furthermore, knowledge on tuna TS allowed the direct observation and assessment of adult tuna dispersed in their environment (Bertrand and Josse, 2000a). Performing tuna direct observation is essential as indirect methods are known to be biased particularly when fishing gears do not sample the whole vertical habitat of tunas. Catchability is a key parameter when using fishing data and a comparison of acoustic tuna observations and longline catch data thus allowed tackling the issue of longline tuna catchability.

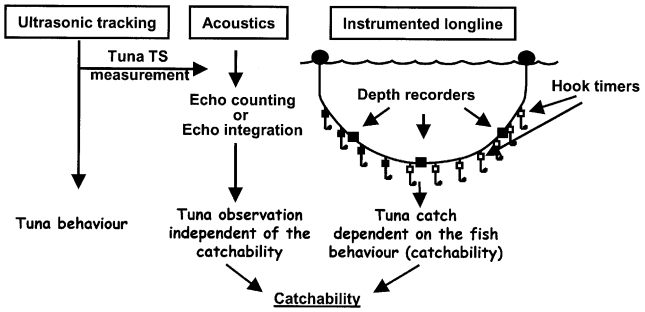

Fig. 2. Schematic outline of tuna observation.

3.2. Tuna preyobservation

Tuna prey (i.e. micronekton) distribution was studied through acoustics, pelagic trawls and stomach content analysis (Fig. 3, Table 1). Micronekton and particularly mesopelagic fish such as myctophids plays a major role in the pelagic ecosystems. The importance of this component was often underestimated in the past due to a lack of efficient observation methods. Actually mesopelagic fishes and squids are very poorly sampled by direct methods. However, acoustics allows the direct study of micronekton distribution and structuring at large and small scales. In the Central Pacific using acoustics and pelagic trawls data we showed that micronekton distribution was different from general ideas raised in bibliographical data but not supported bydirect observations. Direct data allowed us to propose a schematic model of ecosystem functioning (Bertrand et al., 1999b). Stomach contents were then considered in order to determine (1) how tuna forage according to a given environment, and (2) whether stomach contents are a good indicator of prey diversity and of actual diet. The comparison of pelagic trawl catches, stomach contents and echo-integration data highlights a number of contradictions but each method gives complementary data (Bertrand et al., 2002a, Table 1). We could put into perspective the concept of reduced food availability for tunas in the pelagic environment. Tuna have developed physiological capacities (e.g. thermal inertia and swimbladder efficiency) to dive enough during daytime to exploit the migrant micronektonic species. Each tuna species foraging in specific ecological niche defined in the vertical plan. Finally acoustic observation of tuna prey allowed showing that studies of tuna feeding behaviour may be biased when carried out on tuna caught by a passive gear such as longline.

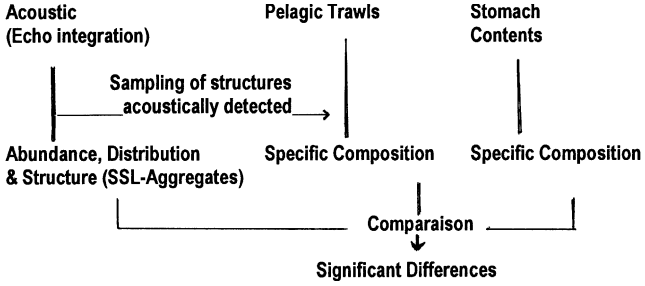

Fig. 3. Schematic outline of tuna prey observation.

Table 1
A synthesis of results obtained during the ECOTAP programme based on acoustic data. Some potential applications of these results in fisheries science are also listed. (1) Bertrand et al. (1999a); (2) Bertrand and Josse (2000a); (3) Josse and Bertrand (2000); (4) Bertrand and Josse (2000b); (5) Josse et al. (1998); (6) Dagorn et al. (2000a); (7) Dagorn et al. (2001); (8) Dagorn et al. (2000b); (9) Dagorn et al. (2000d); (10) Josse et al. (1999); (11) Josse et al. (2000); (12) Dagorn et al. (2000c); (13) Bertrand et al. (1999b); (14) Bertrand et al. (2002a); (15) Bertrand et al. (2002b)

Topics	Tools	Main results	Secondary results	Fisheries science application
Tuna acoustic observation	Echosounder, Ultrasonic tag, Trolling	First tuna TS measurements (1, 2, 3). Preliminary tuna TS relationships to fish length and swimbladder volume (3)	Bigeye ability to adjust the volume of their swimbladder better than might be supposed for other physoclists fish (1, 4)	Direct acoustic tuna observation.
Tuna distribution	Echosounder, Experimental longline	Tuna observation and abundance estimation independent of commercial fishing activities (i.e. independent of catchability) (4)	At a regional scale, tuna distribution related to prey distribution (4)	Direct tuna biomass estimators, particularly when the population is not fully exploited and/or the whole vertical range of vertical habitat is not sampled by longliners.
Tuna swimming behaviour	Echosounder, Ultrasonic tag, CTD, Agent based model	Role of the biotic and abiotic environment in the horizontal and vertical behaviour of tuna (5, 6, 7, 8). Modelling tuna vertical behaviour according to the biotic environment (9)	Respective role of biotic and abiotic conditions	Model tuna horizontal and vertical swimming behaviour, e.g. (9).
Tuna aggregation behaviour	Echosounder, Vertical longline, Fuzzy logic model	Typology and behaviour of tuna aggregated around floating objects (7, 10, 11). Modelling tuna aggregation behaviour according to the local environment (12)	Size dependant behaviour of fish around FADs (11)	Method for tuna aggregation studies. Aggregated tuna densities direct estimation. Data for tuna management. Model tuna aggregative behaviour, e.g. (12).
Micronekton distribution	Echosounder, pelagic trawl, stomach content data, CTD	Direct observation and typology of micronekton distribution. Schematic model of ecosystem functioning (13), Role of deoxygenated water and remineralisation process. No direct relation between plankton and micronekton distribution in the Central Equatorial Pacific (13). Fine characterisation of scattering structures (14)	Role of micronekton spatial structure in ecosystem functioning (13, 15)	Predictive models of tuna forage should incorporate environmental limiting factors. Necessity to take into account the structure of micronekton distribution (scattered vs. patchy).
Tuna feeding behaviour	Echosounder, pelagic trawl, Experimental longline, stomach content data	Determination of how tuna forage according to a given environment, and how tuna diet as ascertained from stomach content, can be a good indicator of prey diversity and of actual diet (14)	The classic concept of reduced tuna food availability in the tropical pelagic environment seems relative (14)	Studies of tuna feeding behaviour when carried out on tuna caught by longlining may be biased (should be taken into account in tropho-dynamic models).
Tuna spatial occupation	Echosounder, pelagic trawl, Experimental longline, CTD	Definition of an index for the vertical volume of tuna habitat according to abiotic conditions. Determination of the biotic and abiotic factors influencing bigeye, albacore and yellowfin tuna spatial occupation (15)	Revisiting of the role assigned to oxygen gradients on tuna distribution. New data on habitat limits of tropical tuna (tolerance vs. temperature and dissolved oxygen) (15)	Quantitative and qualitative data to fit models on tuna behaviour, distribution, etc.
Tuna catchability with a longline	Echosounder, pelagic trawl, Experimental longline, stomach content data, CTD	Determination of the biotic and abiotic factors influencing tuna catchability. Role of the scale of observation and of the prey spatial structure in the tuna catchability with a longline (15)	Observation of a “cryptic” biomass of bigeye tuna (15)	Elements allowing better interpretation of longline CPUE (e.g. prey patch characteristics should be taken into account for resource management or modelling).

3.3. Tuna-environment relationships

Knowledge on precise tuna distribution and habitat characteristics allows an examination of tuna-environment relationships (Fig. 4, Table 1). We defined an index of the vertical volume of tuna habitat according to abiotic conditions. Inside such “abiotic habitat”, we showed that tunas are likely to adopt depths where prey are presents rather than depth of preferred temperature or dissolved oxygen (DO). A spin off of such study was a new interpretation of the role assigned to oxygen gradient in tuna distribution (Bertrand et al., 2002b). The relation between tunas and their environment have strong impacts in their catchability. To interpret longline catch data, in addition to abiotic parameters, the scale of observation and the type of prey distribution are key factors. On a regional scale, tuna CPUE and prey abundance are positively correlated. On a finer scale, when prey are abundant and patchy distributed this correlation become negative

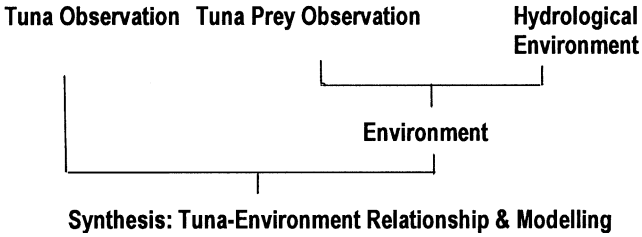

Fig. 4. Schematic outline of tuna-environment approach.

as if tunas preferred to feed on prey rather than on dispersed baits. Longline rates are thus higher in area with high prey-density, but at a small scale inside such areas, very dense patches reduced the catchability of albacore and bigeye tunas (Bertrand et al., 2002b).

3.4. Tuna behaviour modelling

Observations of the prey of tuna distribution and structuring allowed the construction of a simplified model of prey spatial distribution and temporal dynamics. Models of tuna behaviour based on ultrasonic and acoustic observations were then developed to reproduce tuna horizontal (near floating objects, Dagorn et al., 2000c) and vertical (Dagorn et al., 2000d) behaviour according to their environment (Table 1). Modelling applications can be much larger. Predictive models of tuna forage should incorporate environmental limiting factors as we showed that assuming a direct relationship between micronekton and lower trophic levels is not always appropriate (Bertrand et al., 1999b). Modelling tuna distribution and behaviour is a multi-parameter work. For instance, in the vertical plan, inside their range of abiotic habitat, tuna distribution is related to the distribution of prey. Prey vertical position is controlled by irradiance (e.g. Widder and Frank, 2001; Frank and Widder, 2002), but also by the presence of deoxygenated waters at depth or the structure of the food web (Bertrand et al., 1999b, 2002a, b). Finally acoustics, which was the central tool allowing the construction of such theoretical scheme is also needed to validate potential models on tuna distribution according to the ecosystem structure.

4. Acoustics for ecosystem research: lessons and perspectives

In the case of the present programme (Table 1), as in the case of other integrative studies based on acoustics (e.g. Croll et al., 1998; Lebourges-Dhaussy et al., 2000), such an approach led to significant scientific findings. However, as already stated by Brandt and Mason (1994), acoustics should be used much more often as a central tool for the study of ecosystems and ecological modelling. Although these techniques are certain to become increasingly popular, using acoustics and interpreting data with relevance are not always simple tasks, particularly for non-acousticians.

A research programme focusing on ecosystem functioning is based foremost on biology, ecology and ethology. For

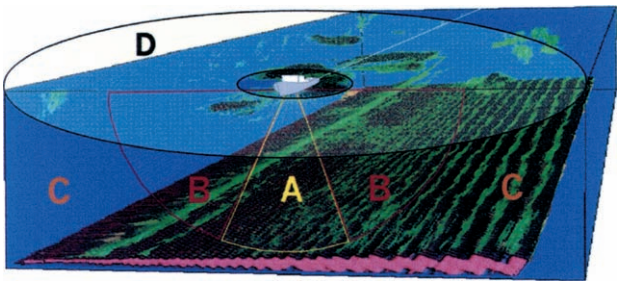

Fig. 5. Drawing of the future "ideal" multibeam system for fisheries acoustics and ecosystem research (Gerlotto, personal communication). (A) beams forming the "vertical multi-beam echosounder" area (in this area, TS values can be calculated using standard methods, assuming the organisms are normally insonified on their dorsal aspect); (B) beams forming the "school structure and biomass measurement" area (here, the background noise due to side lobe echoes on the bottom are not present, and the characteristics of the schools can be measured with precision); (C) area at distance longer than the depth, for shoal counting and cluster analysis; (D) combined with a 360° long range sonar to study school behaviour.

the scientists involved, acoustics represent a tool (i.e. not a research topic) allowing qualitative and/or quantitative, direct and simultaneous observations of the main biotic and some abiotic components of an ecosystem.

Studying ecosystems and understanding the functional relationships connecting the various compartments of the ecosystem at various space-time scales often requires observations on large vertical and/or horizontal ranges. The limitations of acoustics are dynamic and vary according to ambient noise levels and many other parameters (e.g. frequency, acoustic power). For example, at 38 kHz, with the vertical range we used during the ECOTAP programme (i.e. 500 m), we were continuously close to the echosounder's limits for echo-integration and echo-counting (Josse et al., 1999). This kind of limitation is often difficult to explain to non-acoustians. As more and more researchers are brought to use these techniques, it is essential that acousticians make an effort towards non-specialists in order to promote acoustics and to make these techniques accessible and comprehensible. The acoustician must adapt tools and methods to these new objectives. In addition, it is the role of the acoustician to validate and to interpret acoustic data in relation to data from other observation tools.

Carrying out ecosystem studies often implies the need for huge amounts of data. Acoustic data are known to be extremely voluminous, particularly if we want to be able to re-process them with different thresholds. Finally, studies on fish behaviour (mainly schooling and avoidance behaviour) and also on TS, etc. should remain important research focuses, as they still constitute major biases when observing aquatic ecosystems acoustically.

The number of acoustic tools available for ecosystem approaches is increasing from year to year. However, no universal tool exists. Choosing an echosounder, for example, is not solely limited to the choice of a manufacturer, but also implies compromises such as choosing one or several frequencies, a beam width, etc.; decisions which themselves depend on the desired range, the studied communities, and so

on. These choices, which can sometimes appear commonplace for an "expert" acoustician, are again often difficult to explain to non-acousticians. Furthermore, to perform an "ideal" ecosystem study you may actually need one or several research vessels, a multifrequency echosounder to maximise species recognition, a multibeam sonar to take full advantage of school behaviour observation, a TAPS™ acoustical zooplankton sensor vertically undulating to maximise plankton observation, high performance software for acoustic data processing (e.g. Movies + or Echoview), an autonomous underwater vehicle, as well as CTD probes, micronekton and plankton pelagic trawls (and/or purse seine, longline, etc.), remote sensing data on SST, chlorophyll, and more. In other words, you need something near to an armada. Of course, such a deployment of force is often out of reach and sometimes inoperative due to interference and other concerns.

In the near future we can reasonably hope that new integrative tools will be available to study ecosystems. New systems should be derived from recent developments in multibeam echosounders (Gerlotto et al., 1999, 2000; Mayer et al., 2002). An "ideal" system for fisheries acoustics (Fig. 5) could be composed of a "180° multi-beam echo sounder" where central beams calculate TS values using standard methods; lateral beams are used to determine 3D structures and perform biomass measurement; and long range lateral beams are employed in shoal counting and cluster analysis (Fig. 5). All of this could be combined with a 360° long-range sonar to study school behaviour. With such a tool we should obtain a real scan of the ecosystem's composition and be able to study fish behaviour. Acousticians and ecologists will need to collaborate in the development of such a tool. Number of "non-acousticians" still believe that acoustics are only used for biomass estimation, since many "acousticians" use acoustic data only in this way (see Fernandes et al., 2003 for a review of acoustic applications in fisheries science). When acoustically assessing a stock, much effort is devoted to removing echoes from plankton or micronekton. This information is considered to be pure noise and simply eliminated. However, such information is fundamental to the study of predator-prey relationships and more generally to understand and model resource distribution and ecosystem functioning. We can reasonably consider that micronekton is a key component when modelling pelagic ecosystem. In that way acoustics should play a major role when constructing theoretical models of ecosystem functioning but also to validate mathematical models. Many laboratories all over the world dispose of a huge amount of data stocked with information about the biomass and distribution of "non-targeted species" (predator, prey, competitor, etc.). Fisheries ecologists should capitalise on these data for the purpose of integrative studies. This implies that researchers who may not have any knowledge of acoustics should make the effort to exploit such data in a fruitful way. In the future, estimates could be made routinely for targeted species, and also for other organisms. Such efforts are unavoidable if we want to move towards truly ecosystem-based management. This implies for instance that all the frequencies available on a research vessel should be used on a routine basis. To move further in this direction, some projects are seeking to develop "plug on play" echosounders and other acoustic tools in order to make routine observations of ecosystems from moored buoys, merchant ships, fishing ships (e.g. Melvin et al., 2002), and others.

The joint application of acoustic techniques, which allow direct monitoring of the ecosystems at different spatiotemporal scales, and powerful new modelling methods, should lead to considerable progress in our knowledge and management of ecosystems, but will require that acousticians, ecologists, and modellers work hand in hand. If this challenge is undertaken, acoustics will certainly be the most important and commonly used observation tool of aquatic ecosystems in coming decades.

Acknowledgements

The Government of French Polynesia supported this research. The authors wish to thank the officers and crew of the R/V "ALIS" for their kind assistance during experiments. Sincere thanks are extended to all of our colleagues from SRM, IFREMER and IRD, who worked with us during the ECOTAP programme. We are also grateful to François Gerlotto for very helpful comments. Gareth Lawson is warmly thanked for revisiting the English of this paper.

References

Axelsen, B.E., Nøttestad, L., Fernö, A., Johannessen, A., Misund, O.A., 2000. "Await" in the pelagic: dynamic trade-off between reproduction and survival within a herring school splitting vertically during spawning. Mar. Ecol. Prog. Ser 205, 259–269.

Bach, P., Wendling, B., Abbes, R., Josse, E., 1996. Characteristics of albacore (*Thunnus alalunga*) catches achieved by experimental fishing with an instrumented longline in the French Polynesia EEZ. Sixth SPAR Workshop, Rarotonga, 5-7 March 1996. pp. 10.

Bach, P., Dagorn, L., Bertrand, A., Josse, E., Misselis, C., 2003. Acoustic telemetry versus instrumented longline fishing for studying the vertical distribution of pelagic fish: the example of the bigeye tuna (*Thunnus obesus*) in French Polynesia. Fish. Res 60, 281–292.

Bertrand, A., Josse, E., Massé, J., 1999. In situ acoustic target-strength measurement of bigeye (*Thunnus obesus*) and yellowfin tuna (*Thunnus albacares*) by coupling split-beam echosounder observations and sonic tracking. ICES J. Mar. Sci 56, 51–60.

Bertrand, A., Le Borgne, R., Josse, E., 1999. Acoustic characterisation of micronekton distribution in French Polynesia. Mar. Ecol. Prog. Ser 191, 127–140.

Bertrand, A., Josse, E., 2000. Acoustic estimation of longline tuna abundance. ICES J. Mar. Sci 57, 919–926.

Bertrand, A., Josse, E., 2000. Tuna target-strength related to fish length and swimbladder volume. ICES J. Mar. Sci 57, 1143–1146.

Bertrand, A., Bard, F.X., Josse, E., 2002. Tuna food habits related to the micronekton distribution in French Polynesia. Mar. Biol 149, 1023–1037.

Bertrand, A., Josse, E., Bach, P., Gros, P., Dagorn, L., 2002. Hydrological and trophic characteristics of tuna habitat: consequences on tuna distribution and longline catchability. Can. J. Fish. Aquat. Sci 59, 1002–1013.

Brandt, S.B., Mason, D.M., 1994. Landscape approaches for assessing spatial patterns in fish foraging and growth. In: Stouder, D.J., Fresh, K.L., Feller, R.J. (Eds.), Theory and Application in Fish Feeding Ecology, vol. 18. The Belle W. Baruch Library in Marine Science, pp. 211–238.

Croll, D.A., Tershy, B.R., Hewitt, R.P., Demer, D.A., Fiedler, P.C., Smith, S.E., Armstrong, W., et al., 1998. An integrated approach to the foraging ecology of marine birds and mammals. Deep Sea Res. II 45, 1353–1371.

Dagorn, L., Bach, P., Josse, E., 2000. Movement patterns of large bigeye tuna (*Thunnus obesus*) in the open ocean determined using ultrasonic telemetry. Mar. Biol 136, 361–371.

Dagorn, L., Josse, E., Bach, P., 2000. Individual differences in horizontal movements of yellowfin tuna (*Thunnus albacares*) in nearshore areas in French Polynesia, determined using ultrasonic telemetry. Aquat. Living Resour 13, 193–202.

Dagorn, L., Josse, E., Bach, P., Bertrand, A., 2000. Modeling tuna behaviour near floating objects: from individuals to aggregations. Aquat. Living Resour 13, 203–211.

Dagorn, L., Josse, E., Bach, P., 2001. Association of yellowfin tuna (*Thunnus albacares*) with tracking vessels during ultrasonic telemetry experiments. Fish. Bull 99, 40–48.

Dagorn, L., Menczer, F., Bach, P., Olson, R.J., 2000. Co-evolution of movement behaviours by tropical pelagic predatory fishes in response to prey environment: a simulation model. Ecol. Model 134, 325–341.

Denman, K.L., 2000. Can we see the future? In: Harrison, P.J., Parsons, T.R. (Eds.), Fisheries Oceanography: An Integrative Approach to Fisheries Ecology and Management. Blackwell Science Ltd., Oxford, UK, pp. 200–206.

Dower, J.F., Leggett, W.C., Frank, K.T., 2000. Commentary: improving fisheries oceanography in the future. In: Harrison, P.J., Parsons, T.R. (Eds.), Fisheries Oceanography: An Integrative Approach to Fisheries Ecologyand Management. Blackwell Science Ltd., Oxford, UK, pp. 263–281.

Fernandes, P.G., Gerlotto, F., Holliday, D.V., Nakken, O., Simmonds, E.J., 2003. Acoustic application in fisheries science: the ICES contribution. ICES J. Mar. Sci in press.

Fiedler, C.P., Barlow, J., Gerrodette, T., 1998. Dolphin prey abundance determined from acoustic backscatter data in eastern Pacific surveys. Fish. Bull 96, 237–247.

Frank, T.M., Widder, E.A., 2002. Effects of a decrease in downwelling irradiance on the daytime vertical distribution patterns of zooplankton and micronekton. Mar. Biol 140, 1181–1193.

Gerlotto, F., Georgakarakos, S., Eriksen, P.K., 2000. The application of multibeam sonar technology for quantitative estimates of fish density in shallow water acoustic surveys. Aquat. Living Resour 13, 385–393.

Gerlotto, F., Soria, M., Fréon, P., 1999. From two dimensions to three: the use of multibeam sonar for a new approach in fisheries acoustics. Can. J. Fish. Aquat. Sci 56, 6–12.

Josse, E., Bach, P., Dagorn, L., 1998. Simultaneous observations of tuna movements and their prey by sonic tracking and acoustic surveys. Hydrobiologia 371/372, 61–69.

Josse, E., Bertrand, A., Dagorn, L., 1999. An acoustic approach to study tuna aggregated around fish aggregating devices: methods and validation. Aquat. Living Resour 12, 303–313.

Josse, E., Bertrand, A., 2000. In situ acoustic target strength measurements of tuna associated with a fish aggregating device in French Polynesia. ICES J. Mar. Sci 57, 911–918.

Josse, E., Dagorn, L., Bertrand, A., 2000. Typology and behaviour of tuna aggregations around fish aggregating devices from acoustic surveys in French Polynesia. Aquat. Living Resour 13, 181–190.

Lebourges-Dhaussy, A., Marchal, E., Menkès, C., Champalbert, G., Biessy, B., 2000. *Vinciguerria nimbaria* (micronekton), environment and tuna: their relationships in the Eastern Tropical Atlantic. Oceanol. Acta 23, 515–528.

Marchal, E., Josse, E., Lebourges-Dhaussy, A., 1996. Prédateurs et proies: une approche acoustique. Océanis 22, 117–132.

Mayer, L., Li, Y., Melvin, G., 2002. 3D visualization for pelagic fisheries research and assessment. ICES J. Mar Sci 3 (59), 216–225.

Melvin, G., Li, Y., Mayer, L., Clay, A., 2002. Commercial fishing vessels, automatic acoustic logging systems and 3D data visualization. ICES J. Mar. Sci 59, 179–189.

Pauly, D., Christensen, V., Walters, C., 2000. Ecopath, Ecosim, and Ecospace as tools for evaluating ecosystem impact of fisheries. ICES J. Mar. Sci 57, 697–706.

Young, J.W., Bradford, R., Lamb, T.D., Clementson, L.A., Kloser, R., Galea, H., 2001. Yellowfin tuna (*Thunnus albacares*) aggregations along the shelf break off south-eastern Australia: links between inshore and offshore processes. Mar. Freshwater Res 52, 463–474.

Widder, E.A., Frank, T.M., 2001. The speed of an isolume: a shrimp's eye view. Mar. Biol 138, 669–677.

Available online at www.sciencedirect.com
SCIENCE DIRECT®
Aquatic Living Resources 16 (2003) 205–213
Aquatic Living Resources
www.elsevier.com/locate/aquliv

An 8-year cycle in krill biomass density inferred from acoustic surveys conducted in the vicinity of the South Shetland Islands during the austral summers of 1991–1992 through 2001–2002

Roger P. Hewitt *, David A. Demer, Jennifer H. Emery

Antarctic Ecosystem Research Division, Southwest Fisheries Science Center, 8604 La Jolla Shores Drive, La Jolla, CA 92037, USA

Accepted 7 January 2003

Abstract

Data from single and multi-frequency active acoustic surveys conducted annually in the vicinity of the South Shetland Islands, Antarctica were re-analyzed using updated procedures for delineating volume backscattering due to Antarctic krill, adjusting for signal contamination due to noise, and compensating for diel vertical migration of krill outside of the acoustic observation window. Intra-and inter-seasonal variations in krill biomass density and dispersion were derived from the re-processed data set for surveys conducted in the austral summers of 1991/1992 through 2001/2002. Estimated biomass density ranged from 1 to 60 g m^{-2}, decreasing from mid-range levels in 1991/1992 to a minimum in 1992/1993–1993/1994, increasing to a peak in 1996/1997–1997/1998, and decreasing again through 2000/2001–2001/2002. Although this variability may be attributed to changes in the spatial distribution of krill relative to the survey area, comparisons with the proportion of juvenile krill in simultaneous net samples suggest that the changes in biomass density are consistent with apparent changes in reproductive success. A truncated Fourier series fit to the biomass density time series is dominated by an 8-year cycle and predicts an increase in krill biomass density in 2002/2003 and 2003/2004. This prediction is supported by an apparent association between cycles in the extent of sea ice cover and per-capita krill recruitment over the last 23 years and indications that ice cover in the winter of 2002 is seasonally early and extensive.

Keywords: Krill; Antarctica; South Shetland Islands

1. Introduction

A series of active acoustic surveys were conducted in the vicinity of the South Shetland Islands as part of a larger effort to understand the relationships between krill and their predators, the influence of the environment and the potential effects of a fishery on krill. Aggregations of krill, moving past the islands with the Antarctic Circumpolar Current, are preyed on by land-breeding predators who consume approximately 800 000 ton annually (Croll and Tershey, 1998). The krill fishery operating in this area currently takes less than 10% of this estimate on an annual basis (Convention on the Conservation of Antarctic Marine Living Resources, CCAMLR, 2000); however, 90% of the catch is within 80 km of the breeding colonies (Agnew, 1992). Large variations in krill recruitment success and age structure have been described from net samples obtained in the vicinity of the islands (Siegel and Loeb, 1995; Loeb et al., 1997; Siegel et al., 1998). Strong year classes appear to be auto-correlated in time such that several years of poor recruitment are followed by 1 or 2 good years, describing a repeating cycle with a 4–5-year period. Loeb et al. (1997) suggested a link between krill reproductive success and the extent of sea ice. Brierley et al. (1999) suggested that the similarities in results from krill surveys conducted in the South Shetland Islands and near South Georgia (ca. 1000 km to the east) implied large-scale physical influences on krill reproduction.

Data describing long-term trends and cycles in Antarctic krill (*Euphausia superba*) biomass density can be useful when making inferences regarding factors that may regulate the growth of the krill population (Loeb et al., 1997) and the spatial and temporal scales over which these factors may operate (Brierley et al., 1999). While relative estimates of biomass derived from a series of surveys conducted and analyzed in a consistent manner have value, accurate esti-

* Corresponding author.
E-mail address: rhewitt@ucsd.edu (R.P. Hewitt).

doi:10.1016/S0990-7440(03)00019-6

mates are critical to comparisons between surveys conducted by different investigators in different locales (Brierley et al., 1999). Absolute estimates of biomass density are also important to the development of models underpinning an ecosystem approach to the management of the krill fishery (e.g. Constable et al., 2000; Constable, 2001).

The surveys reported here were originally conducted and analyzed following the methods described by Hewitt and Demer (1993) and reported in a series of annual reports available from the US Antarctic Marine Living Resources, AMLR Program[1]. For these analyses, contamination by noise was avoided by thresholding measurements of volume backscattering before integrating; bias due to diurnal vertical migration of krill (Demer and Hewitt, 1995) was ignored; and delineation of backscattering due to krill was accomplished by visual inspection of reconstructed echograms. The re-analyses of the surveys reported here improve accuracy by: (1) characterizing system noise for portions of survey transects and then subtracting it from reconstructed echograms; (2) deleting from consideration those portions of transects that were conducted after local sunset and before local sunrise when an unknown portion of krill were in the surface layers above the observation window; and (3) employing a multi-frequency technique for objectively delineating volume backscattering due to krill.

The time series of krill biomass densities generated from the re-analysis of the surveys in the South Shetland Islands are examined as they relate to variations in reproductive success. A truncated Fourier series is also fit to the data, following Brierley et al. (1999). The predictive value of such a model is dependent on the continuation of cycles apparent in the Antarctic Peninsula environment over the last 20 years.

2. Materials and methods

Two surveys were conducted each year during mid-January to early March. Although survey design varied between years, at least five transects were conducted in the vicinity of Elephant Island during each survey (Fig. 1, Table 1). During each survey, oceanographic profiles and net samples were obtained over a grid of regularly-spaced stations. Acoustic transects were conducted between stations. Transects were oriented across bathymetric gradients and for the purposes of estimating krill biomass density, transects between a line of stations were aggregated and treated as a single transect.

Measurements of volume backscattering strength were obtained using a Simrad EK500 echosounder and various frequencies and transducer configurations. From 1992 through 1995, surveys were conducted aboard the NOAA Ship *Surveyor* using a 120 kHz transducer deployed on a towed-body (1992 and 1993) or installed in a hull blister (1994 and 1995). From 1996 through 2002, surveys were conducted aboard the R/V *Yuhzmorgeologiya* using 38, 120, and 200 kHz transducers installed in a hull blister. System calibrations using standard spheres were conducted under ambient conditions before and after survey operations each year.

Echograms were reconstructed from samples of volume backscattering strength obtained at a vertical resolution of 0.5 m and a horizontal resolution of approximately 10 m, assuming 2 s ping repetition rate and nominal surveyspeed of 10 knots. Portions of the echograms corresponding to the surface layer (0–15 m depth), bottom (5 m above the bottom and deeper), and periods when the ship was on station were excluded from further consideration. Various methods to compensate for bias due to diel migration of krill into the surface layer (Demer and Hewitt, 1995) were explored. The additional uncertainty associated with applications of these methods was difficult to quantify, however, and it was decided to instead eliminate sampling periods between local apparent sunset and sunrise. The effects of this decision on sampling variance are discussed in Section 3. Post-survey adjustments for system calibration and water density effects on sound absorption, wavelength and two-way beam angle were made where appropriate.

Initial measurements of noise at each frequency under survey conditions were used to generate time-varied echograms of only noise. These were visually compared to echograms reconstructed from the original data using similar absorption coefficients and display thresholds. Noise levels were then adjusted until the effects of noise at long ranges appeared equal on each display; another 2 dB was then added in order to arrive at a conservative adjustment for noise. The time-varied noise echograms were subtracted from the original data in manner similar to that described by Watkins and Brierley (1995).

Regions of the noise-free echograms were attributed to backscattering from krill swarms and layers by making use of the expected frequency-specific target strength of krill over the size range of krill encountered during the survey. Volume backscattering strength from an aggregation of krill at 38, 120 and 200 kHz was modeled by Demer (2003) using a Distorted Wave Born Approximation model of krill target strength (McGehee et al., 1998) and assumed distributions for body orientation (Kils, 1981) and the density of animals within an aggregation. The distributions of expected differences of volume backscattering strength at 120 vs. 38 kHz ($S_{V,120} - S_{V,38}$), and 200 vs. 120 kHz ($S_{V,200} - S_{V,120}$) had modes of 11 dB (range ca. 4 dB) and –1 dB (range ca. 3 dB), respectively (Demer, 2003). In order to account for random variability in the sound scattering process, these ranges were expanded to 12 and 6 dB, respectively, and were used to construct filters. Regions of a noise-free echogram were

[1] US AMLR Program Field Season Reports, published on an annual basis from 1989 through 2002 as SWFSC Administrative Reports (1989–1999) and NOAA Technical Memoranda (2000–2002). See also a series of short papers under the general heading of US AMLR Program in the 1991–1997 review issues of the Antarctic Journal of the US published by the US National Science Foundation. Copies available from US AMLR Program, 8604 La Jolla Shores Drive, La Jolla, CA 92037, USA.

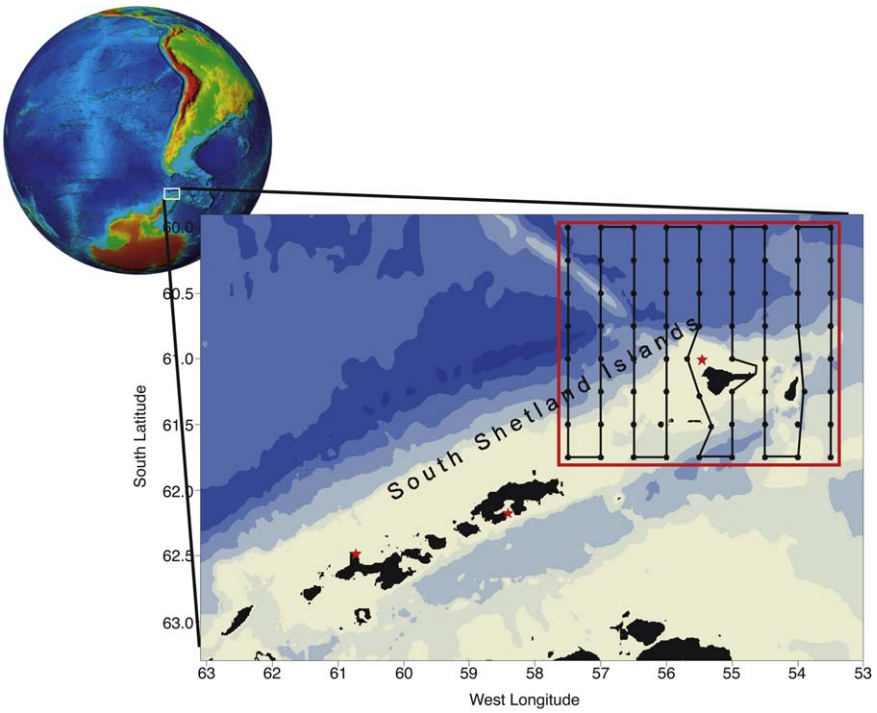

Fig. 1. Study area for the US Antarctic Marine Living Resources, AMLR Program. Solid circles indicate oceanographic and net sampling stations, solid lines indicate acoustic transects between stations, and stars indicate field camps where the reproductive success of land-breeding krill predators was monitored. Survey designs varied from year to year depending on the number of stations sampled in the grid. The most consistent sampling was conducted in the Elephant Island stratum delineated by the red rectangle.

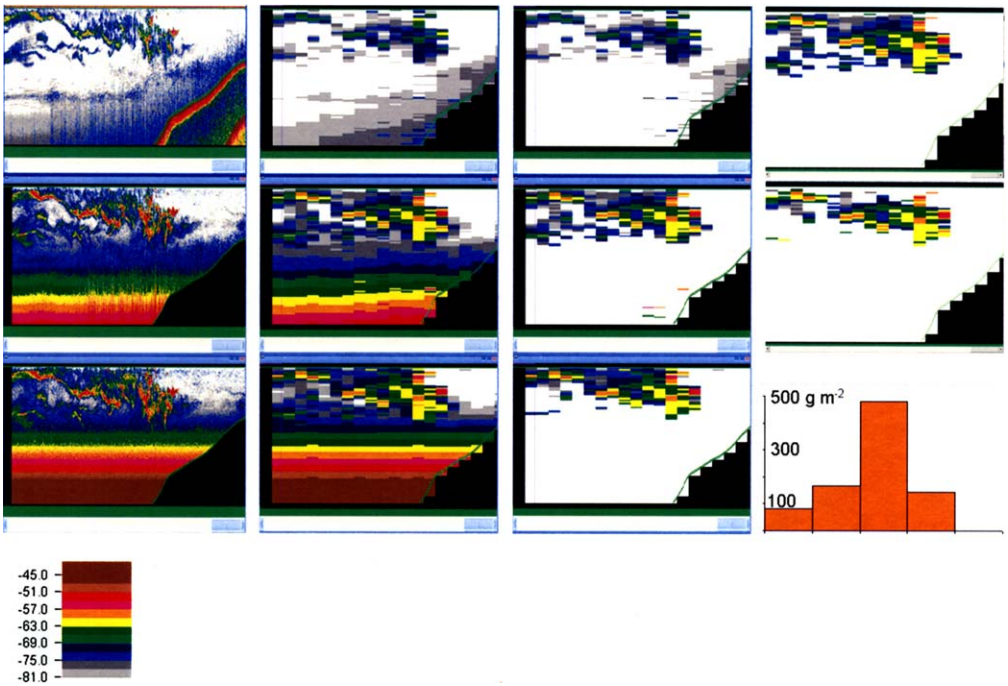

Fig. 2. The processing of samples of volume backscattering strength is illustrated byand example section of a transect. Echograms constructed from 38, 120 and 200 kHz data are shown in the first column. An irregular layer of krill is shown above the remnants of an extensive layer of myctophid fish and below more diffuse aggregations of zooplankton. Re-sampled versions of these echograms are shown in the second column where each block represents the average of 500 samples. Re-sampled noise-free echograms are shown in the third column. In the fourth column the re-sampled noise-free 120 kHz echogram is shown filtered for those regions where $4 \leq (S_{V,120} - S_{V,38}) \leq 16$ dB (top, where most of the backscatter attributed to myctophids is eliminated), and for those regions where $-4 \leq (S_{V,200} - S_{V,120})$ 2 dB (middle, where backscatter attributed to zooplankton and the remainder of backscatter due to myctophids is eliminated). In the final step, volume backscattering strength at 120 kHz is vertically integrated, averaged over 1 nautical mile intervals and converted to krill biomass density (bottom).

Table 1
US AMLR Program surveys in the vicinity of Elephant Island. CCAMLR: Convention on the Conservation of Antarctic Marine Living Resources

Austral summer	Survey	Dates	Number of transects	Frequencies (kHz)	Mean density ($g\ m^{-2}$)	Coefficient of variation (%)	Original estimate of mean density ($g\ m^{-2}$)
1991/1992	Survey A	19 January–31 January	6	120	38.0	20.1	61.2
	Survey D	29 February–10 March	9	120	7.9	14.3	29.6
1992/1993	Survey A	18 January–31 January	9	120	1.2	52.1	–
	No data	–	–	–	–	–	–
1993/1994	Survey A	19 January–28 January	8	120	3.1	34.7	9.6
	Survey D	26 February–5 March	9	120	2.1	33.7	7.7
1994/1995	Survey A	19 January–29 January	9	120	7.5	23.5	27.8
	Survey D	16 February–23 February	9	120	13.2	28.8	35.5
1995/1996	Survey A	25 January–4 February	9	38, 120, 200	26.8	29.0	80.8
	Survey D	25 February–5 March	9	38, 120, 200	17.0	36.0	70.1
1996/1997	Survey A	31 January–9 February	9	38, 120, 200	50.0	21.4	100.5
	No data	–	–	–	–	–	–
1997/1998	Survey A	16 January–25 January	9	38, 120, 200	60.2	19.3	82.3
	Survey D	16 February–25 February	9	38, 120, 200	20.8	16.3	47.1
1998/1999	Survey A	22 January–28 January	5	38, 120, 200	14.8	38.1	
	Survey D	16 February–23 February	5	38, 120, 200	13.4	39.8	
1999/2000	CCAMLR 2000	29 January–1 February	8	38, 120, 200	25.7	25.2	
	Survey D	26 February–5 March	9	38, 120, 200	34.6	28.6	
2000/2001	Survey A	17 January–24 January	9	38, 120, 200	6.6	19.1	
	Survey D	17 February–25 February	9	38, 120, 200	5.6	10.4	
2001/2002	Survey A	20 January–26 January	7	38, 120, 200	3.3	~60	
	Survey D	28 February–6 March	7	38, 120, 200	1.2	31.2	

attributed to krill when both of the following conditions were true: $4 \leq (S_{V,120} - S_{V,38}) \leq 16$ dB and $-4 \leq (S_{V,200} - S_{V,120}) \leq 2$ dB. The effects of these decisions are discussed in Section 3.

The multi-frequency filters were used to process survey data collected on surveys conducted in 1996 through 2002. The distribution of volume backscattering strength attributed to krill ranged between –50 and –90 dB, with approximately 80% of the integrated energy between –50 and –70 dB. For surveys conducted during 1992 through 1995, when data collection was limited to 120 kHz, volume backscattering strength was thresholded to include values >–70 and <–50 dB as a means of delineating regions of the echograms attributed to backscattering from krill. Visual inspection of the echograms indicated that this was an effective, but conservative, method of eliminating backscattering due to animals other than krill.

Comparisons of single samples of volume backscattering strength were too variable to allow contiguous regions of the echogram to be delineated as krill and it was judged necessary to average volume backscattering strength over bins of finite vertical and horizontal dimensions (resample). Bin size was set at 5 m vertical and 50 pings horizontal (ca. 500 m). The effects of this decision are discussed in Section 3.

Resampled, noise-free 120 kHz echograms were filtered to include only those regions where volume backscattering was attributed to krill. Volume backscattering coefficients ($m^2\ m^{-3}$) were vertically integrated and averaged over 1 nautical mile distance intervals. Integrated volume backscattering area ($m^2\ m^{-2}$) was converted to krill biomass density ($g\ m^{-2}$) by applying a factor equal to the ratio of the weight of an individual krill (g) and its backscattering cross sectional area (m^2) summed over the length frequency distribution of krill sampled in the survey area (Hewitt and Demer, 1993).

The procedures outlined above are illustrated in Fig. 2 for an example section of a survey transect. Mean biomass density and its sampling variance were estimated for each survey following Jolly and Hampton (1990) where the mean density along each transect is considered a representative sample of the survey mean (Shotton and Bazigos, 1984). It should be noted, however, that transect spacing was not random, and therefore, a violation of their requirement for a ratio estimate of sampling variance. Other investigators defend the validity of systematic transect spacing when using this method to estimate variance by noting that the surveyed population is most often randomly distributed relative to transect spacing (Williamson, 1982; Francis, 1984, 1985). In their manual for the conduct of acoustic surveys Simmonds et al. (1992) recommended a survey design of systematically spaced parallel transects for populations, exhibiting both high and low contagion in their spatial distribution, where the distribution can be assumed to be random with respect to transect location. No evidence to the contrary was discovered with respect to the surveys reported here.

3. Results

Estimates of mean krill biomass density and coefficient of variation are listed for each survey in Table 1. The second

surveys in 1992/1993 and 1996/1997 were compromised due to problems with the towed-body(1993) and the ship's propulsion system (1997); consequently, no results for these surveys are presented. The results presented for the first survey in 2000 were estimated from data collected in the South Shetland Island stratum of the CCAMLR 2000 Survey (Hewitt et al., 2002). The large error associated with the first survey of 2001/2002 is a combined error due to sampling error between transects plus measurement error due to equipment malfunction during a portion of the survey (estimated by processing the entire survey twice using gain settings before and after replacement of a faulty power supply). With the exception of 1991/1992 and 1997/1998 the first and second surveys of each year are not significantly different from each other. In both 1991/1992 and 1997/1998 krill biomass density decreased sharply from the first to second surveys and continued to decrease in subsequent years.

Survey estimates of krill biomass densities and coefficients of variation were re-calculated using all of the data and compared to results where nighttime sampling was excluded. As expected, mean density was consistently higher when sampling during the dark hours was not considered. It should be noted, however, that the Jolly and Hampton (1990) method used to estimate mean density assumes that the transect mean is a representative sample of the survey mean. Thus a reduction in the number of intervals in a single transect does not impose a penalty with regard to the estimate of sampling variance between transects. The increased density estimates when only daytime sampling is considered, however, confirms the expected negative bias when sampling krill at night and justifies their exclusion.

The ranges for the multi-frequency filters used to delineate regions of the echogram attributed to krill scattering were initially selected based on theoretical expectations of the frequency-specific differences in volume backscattering strength from aggregations of krill (Demer, 2003). Selected echograms were processed using these initial values and the resulting echograms were compared against the original echograms. The initial ranges were judged to be too conservative and were expanded so that more aggregations presumed to be composed of krill were included. Aggregations were presumed to be composed of krill based on their size, shape, intensity, edge gradient and depth as verified by directed net sampling. Application of the first filter ($4 \leq (S_{V,120} - S_{V,38}) \leq 16$ dB) captured most aggregations visually identified as krill, but also included aggregations identified as myctophid fish and smaller zooplankton. Narrowing the filter range excluded the non-krill scatterers at the expense of excluding more krill aggregations. Application of the second filter ($-4 \leq (S_{V,200} - S_{V,120}) \leq 2$ dB) eliminated the non-krill scatterers while retaining most of the krill aggregations. The multi-frequency filters used here should be considered conservative; that is, their application will result in an underestimate of the krill biomass density.

The effect of changing the dimensions of the re-sampling bins was investigated. It was expected that the selection of bin size would necessitate a tradeoff: if the bins were too small the variability between samples of volume backscattering strength would cause the continuous nature of krill swarms and layers apparent on the original echograms to be lost; if the bins were too large the power to distinguish krill would be diminished because backscattering from krill and non-krill scatterers would be averaged together. Experimentation with bin size on selected echograms indicated little change in integrated energyattributed to krill when the bin size was larger than some nominal dimensions and smaller than very large regions of the echograms. Bin size was selected at 5 m vertical and 50 pings in the horizontal direction, but comparable results could have been obtained if the bin size was half or double these dimensions.

4. Discussion

The revised estimates of krill biomass density in the Elephant Island area were consistently lower than the original estimates (Table 1). As noted above the filter ranges used in the current analysis were chosen such that aggregations that were presumed to be composed of krill were included and all else was excluded. In contrast, the visual classification procedure used in the original analyses lumped krill and non-krill zooplankton; although, the non-krill zooplankton component (including other euphausiids, copepods, amphipods, chaetognaths, pteropods, and ostracods) was estimated to contribute less than 10% of the total volume backscattering strength at 120 kHz (Hewitt and Demer, 1993). Not included in this estimate were contributions from salps and myctophid fish. The numerical abundance of the non-krill zooplankton component was an order of magnitude higher in 1994/1995 and 1995/1996 than it was in 1991/1992 and 1997/1998 (V. Loeb, personal communication). The largest discrepancies between the current estimates of krill biomass densities and the original estimates also occur during 1994/1995 and 1995/1996, suggesting that the proportion of volume backscattering attributed to non-krill zooplankton was underestimated and variable from survey to survey. Variations in the abundance of myctophid fish (primarily *Electrona antarctica* and *Gymnoscopelus nicholsi*) and salps (primarily *Salpa thompsoni*) may have also contributed to the variations in the difference between the original estimates (which included a portion of the backscatter from these taxa) and the current estimates (which did not). Perhaps the largest and least quantifiable source of variability was the subjective nature of the visual interpretation of the original echograms.

The procedures described here provide a more objective method for delineating backscatter from aggregations of Antarctic krill. Verification of the method, however, is dependent on an accurate and unique characterization of krill aggregations derived from a comparison of acoustic records and net sampling. Underestimates of krill biomass density will arise if unknown forms of krill aggregations (or mixed species aggregations) have not been characterized and hence not considered when comparing the performance of various filter

ranges in delineating krill aggregations. Dispersed krill were also not explicitly considered when selecting the filter ranges, although it was noted that low density regions of krill were often delineating in the vicinity of denser krill aggregations when the filters were applied. The advantages of the method are that it can be described in specific terms, and therefore, applied consistently to a series of surveys; the filters can be adjusted, new ones added and analyses redone as warranted; and it can be used in a complementary way to other techniques for delineating krill aggregations such as discriminate functions and neural networks (Woodd-Walker, 2003).

The coefficients of variation reported here represent sampling error as distinguished from measurement error (Hewitt and Demer, 2000). Demer (2003) analyzed the total uncertainty associated with a similar survey of Antarctic krill across the Scotia Sea. He considered errors associated with system calibration, characterization of krill target strength, probability of detection, and the efficiency of algorithms used to delineate backscatter attributed to krill. He concluded that measurement variance was negligible relative to sampling variance. Demer (2003) also noted a disparity in krill target strength predicted by an empirical model (Greene et al., 1991) vs. a theoretical model (McGehee et al., 1998), and concluded that uncertainty with regard to krill target strength remains the largest source of potential bias. The empirical model, where target strength is estimated as a function of body length, is used in the current analyses to convert integrated volume backscattering strength to krill biomass density. The theoretical model, where target strength is a function of body length, shape, curvature, orientation angle and material properties, is impractical to apply under survey conditions because so many parameters must be characterized. One approach is to randomize the sound scattering process by assigning appropriate probability density functions to various parameter values and estimating a range of target strength values for various body lengths (Demer and Conti, 2003). The results of this and similar work will be improved estimates of krill target strength under natural conditions and the possibility of systematic changes in estimates of krill biomass density.

Assuming that the character of krill aggregations and their target strength are not influenced by overall abundance, the trends apparent in the time series presented here may be helpful when making inferences regarding factors that control the growth of the krill population. One must also assume that a representative sample of the krill population (both biomass densityand demographic structure) can be obtained from sampling in the vicinityof Elephant Island.

Siegel (1988) proposed a model of spatial succession of age groups in the vicinity of the South Shetland Islands. He described an order of magnitude increase in krill abundance as the austral spring progressed into summer and fall, and then a sharp decline as krill apparently left the area before the expansion of sea ice into the region. The seasonal change in abundance has a spatial component with an increase in the numbers of juvenile krill near the islands and in the Bransfield Strait between the islands and the Antarctic Peninsula, and by an influx of sexually maturing adults farther offshore. Siegel further proposed that, as the summer progresses, postbreeding adults move shoreward and juveniles leave the area. Lascara et al. (1999) suggested that shoreward migration could explain large differences between summer and winter krill densities observed along the western Antarctic Peninsula south west of the South Shetland Islands. Results from net sampling in the Elephant Island area have confirmed that this movement is a consistent phenomenon from year to year (V. Loeb, personal communication). The juvenile and immature component of the population is reduced from the first survey to the second survey of each year. Over the course of four surveys conducted in the vicinity of the South Shetland Islands from mid-December 1999 through early March 2000, small and intermediate krill length modes were reduced, but differences in biomass density were not detectable (Gutierrez et al., 2003). Similarly, krill biomass density, as estimated from acoustic surveys reported here, does not describe a consistent pattern from the first to second surveys. Only in 1991/1992 and 1997/1998 were significant differences detectable between the first and second surveys.

Although krill are only seasonally abundant in the South Shetland Islands (Siegel, 1988; Siegel et al., 1997), results from net sampling during the early summer suggest that the relative contribution of year classes, and their effect on population size, can be tracked over several years (Fig. 3). The strong 1987/1988 year class (45 mm mode following Siegel, 1987) was still evident in the population when the first acoustic surveys reported here were conducted. Also evident was another strong year class (27 mm mode) produced by spawning in 1990/1991. Recruitment from spawning in 1991/1992 was negligible and biomass density sharply declined. Weak recruitment from spawning in 1992/1993 and 1993/1994 was associated with modest increase in biomass density. The 1994/1995 year class was very strong, followed by moderately successful recruitment from spawning in 1995/1996 and 1996/1997, and biomass density rapidly increased peaking in 1997/1998. Recruitment from spawning in 1997/1998 was negligible and biomass density sharply declined. The increase in biomass density in 1999/2000 was associated with moderate reproductive success from spawning in 1998/1999 but was not sustained in 2000/2001. The most recent surveys in 2001/2002 suggest a slight decrease in biomass density associated with relatively good reproductive success from spawning in 2000/2001. Reid et al. (1999a, b) also demonstrated a correlation between krill abundance and the length-frequency distribution of krill in the diets of krill predators breeding at South Georgia.

Brierley et al. (1999) concluded that variations in krill abundance were influenced by broad-scale variations in the physical environment. They documented 2-, 3-, 4-, 5- and 8-year cycles in the power spectra of a 15-year record of air temperature and a 17-year record of sea-ice extent in the Antarctic Peninsula region, and a 15-year record of sea-

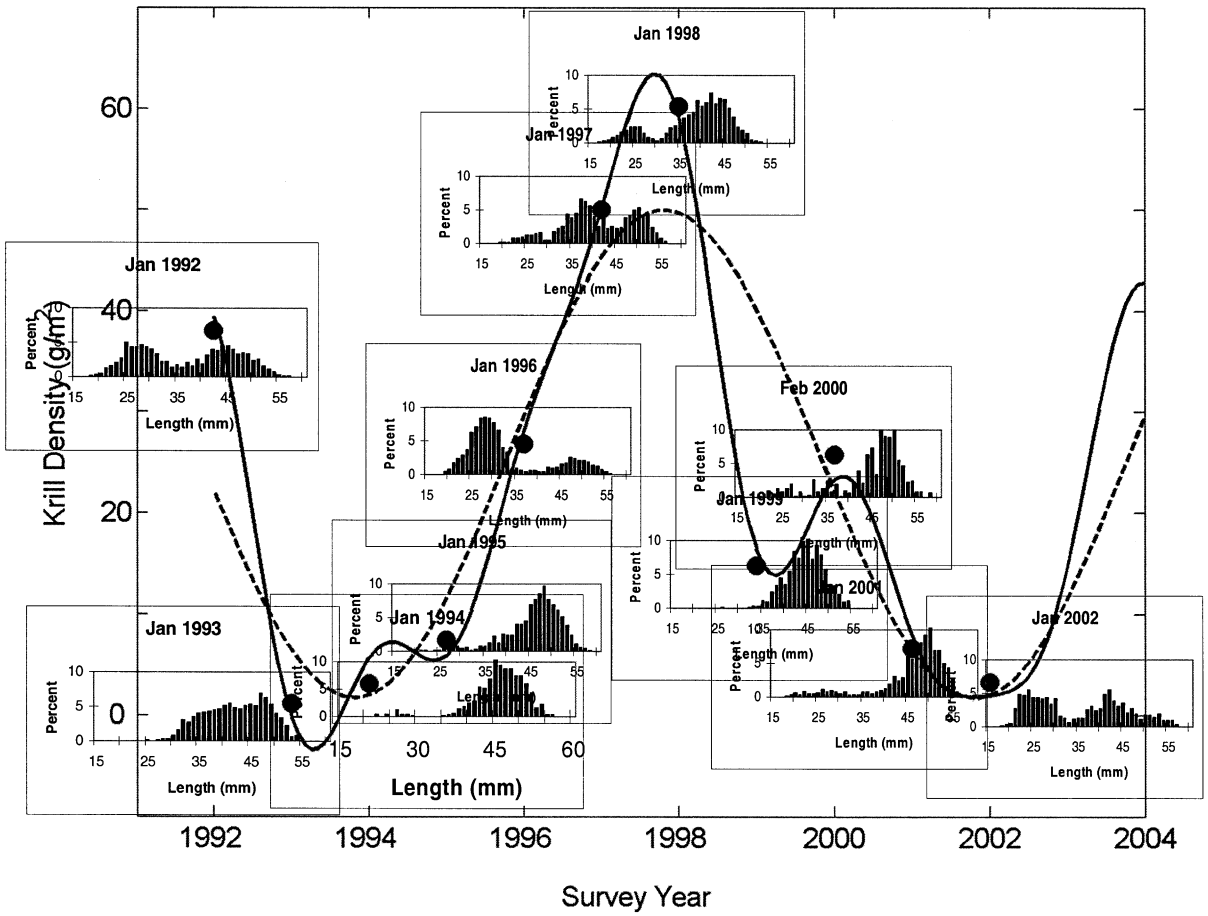

Fig. 3. Annual estimates of krill biomass density in the vicinityof Elephant Island from the first surveyof each year (filled circles). Also shown are krill length frequency distributions corresponding to the surveys (number of net tows per survey ranged from 75 to 105; 150 krill or less measured per tow). The solid line is a truncated Fourier series fit to the data, using cycles of 2, 3, 4, 5 and 8 years, which explains 98% of the variability in the time series. Of these, the 8-year cycle (dashed line) dominates explaining 75% of the variance; addition of a 3-year cycle explains another 9%.

surface temperatures near South Georgia. They then fit a truncated Fourier series to a time series of acoustic estimates of krill biomass density in the Elephant Island area drawn from a variety of sources. A majority of the variance between annual surveys was explained by 5- and 8-year cycles. Similar analyses were applied to the data in Table 1, considering all of the surveys, only the first surveys in each year, only the second surveys in each year and the mean of both surveys in each year. In all cases, 3- and 8-year cycles explained the majority of the variance in the time series (Fig. 3). The model also suggests an increase in krill biomass density over the next 2 years. This prediction is dependent on the continuation of cycles in the environment and associated changes in krill reproductive success.

An association between the extent of sea ice cover and per-capita krill recruitment is apparent in indices derived from satellite imagery of sea ice concentrations west of the Antarctic Peninsula and net sampling data in the vicinity of the South Shetland Islands over the last 23 years (Fig. 4). These records suggest cyclical variation, and mechanisms have been proposed to link sea ice extent and krill reproductive success (e.g. Loeb et al., 1997). However, the period is irregular and the association is not perfect. Interestingly, although the extent of ice cover in 2001 was low, the most current satellite images indicate seasonally early and extensive sea ice cover in the Antarctic Peninsula area through the winter and early spring of 2002 [2] . Recruitment from spawning in 2000/2001 and a second good or stronger year class from spawning in 2001/2002 could be expected to increase krill biomass density over the next 2 years as happened following the recruitment of the 1994/1995 year class.

Acknowledgements

We wish to express our gratitude to our long-term colleague Dr. Valerie Loeb for her generosity in sharing data and insights, to the small army of people who diligently helped us collect the data over the years, and the Captains and crews working aboard the NOAA Ship *Surveyor* and the R/V *Yuhzmorgeologiya* for their conscientious adherence to our sampling protocols. We also wish to acknowledge the advice and guidance that we have received over the years from col-

[2] Near Real-Time DMSP SSM/I Daily Polar Gridded Sea Ice Concentrations from National Snow and Ice Data Center (http://www.nsidc.org).

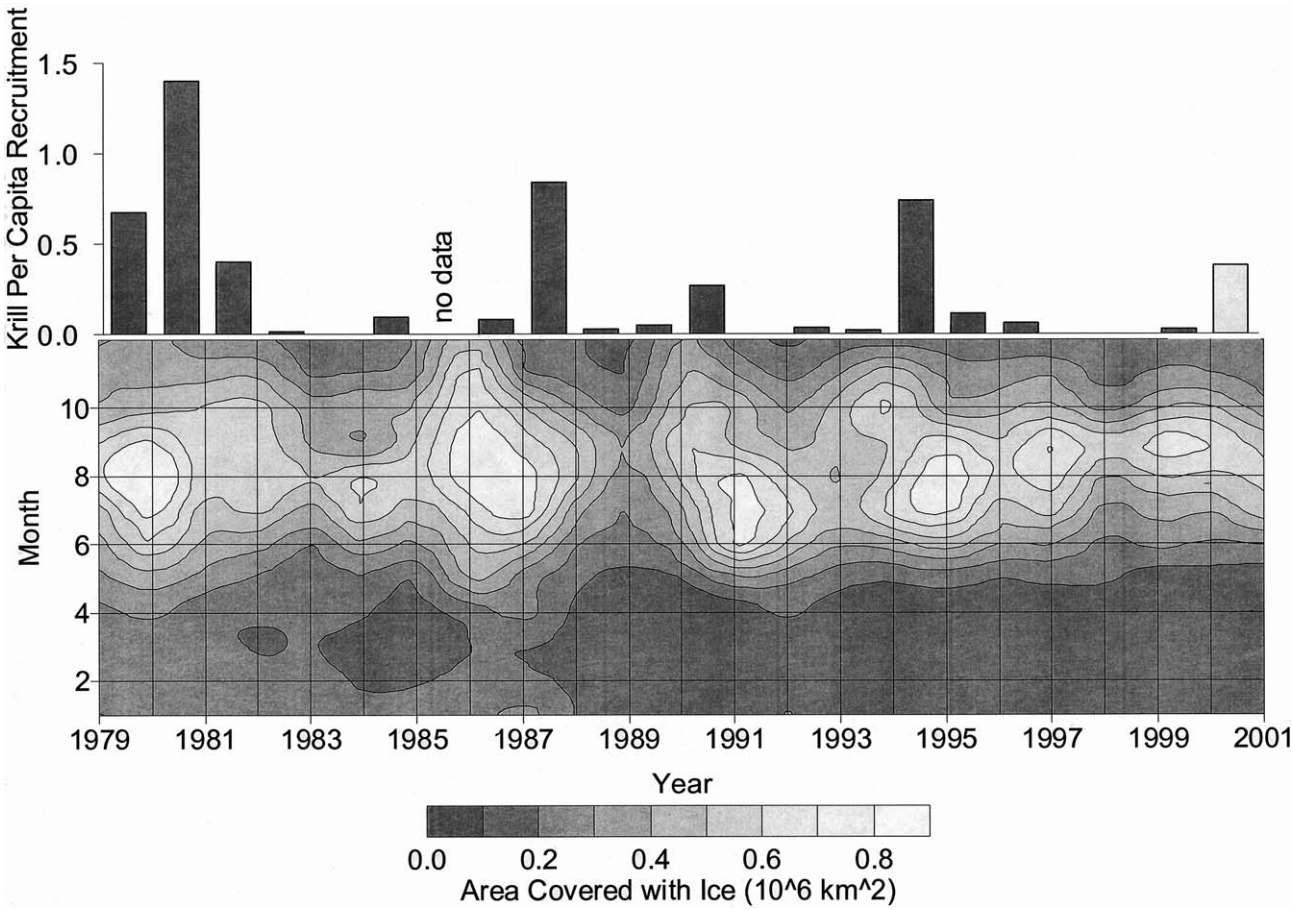

Fig. 4. Area covered by sea ice off the northwestern side of the Antarctic Peninsula (updated from Hewitt, 1997) and per capita krill recruitment as calculated from the proportion of age one krill (Siegel, personal communication) following Hewitt (2000). The estimate of per capita recruitment from spawning in 2001 (shaded in light gray) should be considered preliminary.

leagues who have used acoustic technology to assess marine resources in the Southern Ocean, including A. Brierley, I. Everson, K. Foote, C. Greene, C. Greenlaw, I. Hampton, I. Higgenbottom, V. Holliday, M. Macaulay, T. Pauly and J. Watkins.

References

Agnew, D.J., 1992. Distribution of krill (*Euphausia superba* Dana) catches in the South Shetlands and South Orkneys. Selected Scientific Papers (SC-CAMLR-SSP/9) CCAMLR, Hobart, Australia, pp. 287–303.

Brierley, A.S., Demer, D.A., Watkins, J.L., Hewitt, R.P., 1999. Concordance of interannual fluctuations in acoustically estimated densities of Antarctic krill around South Georgia and Elephant Island: biological evidence of same-year teleconnections across the Scotia Sea. Mar. Biol. 134, 675–681.

CCAMLR, 2000. Statistical Bulletin, 12. CCAMLR, Hobart, Australia (1989–1999).

Constable, A.J., de la Mare, W.K., Agnew, D.J., Everson, I., Miller, D., 2000. Managing fisheries to conserve the Antarctic marine ecosystem: practical implementation of the Convention for the Conservation of Antarctic Marine Living Resources (CCAMLR). ICES J. Mar. Sci. 57, 778–791.

Constable, A.J., 2001. The ecosystem approach to managing fisheries: achieving conservation objectives for predators of fished species. CCAMLR Sci. 8, 37–64.

Croll, D.A., Tershy, B.R., 1998. Penguins for seals, and fishing: prey requirements and potential competition in the South Shetland Islands, Antarctica. Polar Biol. 19, 365–374.

Demer, D.A., 2003. An estimate of error for the CCAMLR 2000 estimate of krill biomass. Deep Sea Res. II (Special issue), in press.

Demer, D.A., Conti, S.G., 2003. Reconciling theoretical versus empirical target strengths of krill; effects of phase variability on the distorted wave Born approximation. ICES J. Mar. Sci. (in press).

Demer, D.A., Hewitt, R.P., 1995. Bias in acoustic biomass estimates of *Euphausia superba* due to diel vertical migration. Deep-Sea Res. I 42, 455–475.

Francis, R.I.C.C., 1984. Variability in hydroacoustic estimates (comment). Can. J. Fish. Aquat. Sci. 41, 825–826.

Francis, R.I.C.C., 1985. Two acoustic surveys of pelagic fish in Hawk Bay, New Zealand, 1980. New Zealand J. Mar. Freshwater Res. 19, 375–389.

Greene, C.H., Stanton, T.K., Wiebe, P.H., McClatchie, S., 1991. Acoustic estimates of Antarctic krill. Nature 349, 110.

Gutierrez, M., Kang, D., Takao, Y., Quinones, J., Lee, Y.H., 2003. Variation in the biomass density and demography of Antarctic krill in the vicinity of the South Shetland Islands during the 1999/2000 austral summer. Deep Sea Res. II (Special issue), in press.

Hewitt, R.P., 1997. Areal and seasonal extent of sea ice cover off the northwestern side of the Antarctic Peninsula: 1979 through 1995. CCAMLR Sci. 4, 65–73.

Hewitt, R.P., 2000. An index of per-capita recruitment. CCAMLR Sci. 7, 179–196.

Hewitt, R.P., Demer, D.A., 1993. Dispersion and abundance of Antarctic krill in the vicinity of Elephant Island in the 1992 austral summer. Mar. Ecol. Prog. Ser. 99, 29–39.

Hewitt, R.P., Demer, D.A., 2000. The use of acoustic sampling to estimate the dispersion and abundance of euphausiids, with an emphasis on Antarctic krill. Fish. Res. 47, 215–229.

Hewitt, R.P., Watkins, J.L., Naganobu, M., Sushin, V., Brierley, A.S., Demer, D.A., Kasatkina, S., Takao, Y., Goss, C., Malyshko, A., Brandon, M., Kawaguchi, S., Siegel, V., Trathan, P., Emery, J.H., Everson, I., Miller, D., 2002. Setting a precautionary catch limit for Antarctic krill. Oceanography 15, 26–33.

Jolly, G.M., Hampton, I., 1990. A stratified random transect design for acoustic surveys of fish stocks. Can. J. Fish. Aquat. Sci. 47, 1282–1291.

Kils, U., 1981. The swimming behavior, swimming performance and energy balance of Antarctic krill, Euphausia superba, BIOMASS Scientific Series No. 3, 122 pp.

Lascara, C.M., Hofmann, E.E., Ross, R.M., Quetin, L.B., 1999. Seasonal variability in the distribution of Antarctic krill, *Euphausia superba*, west of the Antarctic Peninsula. Deep-Sea Res. I 46, 951–984.

Loeb, V., Siegel, V., Holm-Hansen, O., Hewitt, R., Fraser, W., Trivelpiece, W., Trivelpiece, S., 1997. Effects of sea-ice extent and krill or salp dominance on the Antarctic food web. Nature 387, 897–900.

McGehee, D.E., O'Driscoll, R.L., Martin Traykovski, L.V., 1998. Effects of orientation on acoustic scattering from Antarctic krill at 120 kHz. Deep-Sea Res. II 45, 1273–1294.

Reid, K., Watkins, J.L., Croxall, J.P., Murphy, E.J., 1999. Krill population dynamics at South Georgia 1991-1997, based on data from predators and nets. Mar. Ecol. Prog. Ser. 177, 103–114.

Reid, K., Barlow, K.E., Croxall, J.P., Taylor, R.I., 1999. Predicting changes in the Antarctic krill, *Euphausia superba*, population at South Georgia. Mar. Biol. 135, 647–652.

Shotton, R., Bazigos, G.P., 1984. Techniques and considerations in the design of acoustic surveys. Rapp. P.-v. Reun. Cons. int. Explor. Mar. 184, 34–57.

Siegel, V., 1987. Age and growth of Antarctic Euphausiacea (Crustacea) under natural conditions. Mar. Biol. 96, 483–495.

Siegel, V., 1988. A concept of seasonal variation of krill (*Euphausia superba*) distribution and abundance west of the Antarctic Peninsula. In: Sahrhage, D. (Ed.), Antarctic Ocean and Resources Variability. Springer-Verlag, Berlin, Heidelberg, pp. 219–230.

Siegel, V., Loeb, V., 1995. Recruitment of Antarctic krill, *Euphausia superba*, and possible cause for its variability. Mar. Ecol. Prog. Ser. 123, 45–56.

Siegel, V., de la Mare, W.K., Loeb, V., 1997. Long-term monitoring of krill recruitment and abundance indices in the Elephant Island area (Antarctic Peninsula). CCAMLR Sci. 4, 19–35.

Siegel, V., Loeb, V., Groger, J., 1998. Krill (*Euphausia superba*) density, proportional and absolute recruitment and biomass in the Elephant Island region (Antarctic Peninsula) during the period 1977–1997. Polar Biol. 19, 393–398.

Simmonds, J.E., Williamson, N.J., Gerlotto, F., Aglen, A., 1992. Acoustic survey design and analysis procedure: a comprehensive review of current practice. ICES Coop. Res. Rep. 187, 1–127.

Watkins, J.L., Brierley, A.S., 1995. A post-processing technique to remove background noise from echo integration data. ICES J. Mar. Sci. 53, 339–344.

Williamson, N.J., 1982. Cluster sampling estimation of the variance of abundance estimates derived from quantitative echo sounder surveys. Can. J. Fish. Aquat. Sci. 39, 229–231.

Woodd-Walker, R.S., Watkins, J.L., Brierley, A.S., 2003. Identification of Southern Ocean acoustic targets using aggregation backscatter and shape characteristics. ICES J. Mar. Sci. (in press).

Available online at www.sciencedirect.com
SCIENCE DIRECT®
Aquatic Living Resources 16 (2003) 215–221
Aquatic Living Resources
www.elsevier.com/locate/aquliv

Statistical analysis of acoustic echoes from underwater meadows in the eutrophic Puck Bay (southern Baltic Sea)

Jarosław Tęgowski, Natalia Gorska *, Zygmunt Klusek

Institute of Oceanology, Polish Academy of Sciences, ul. Powstańców Warszawy 55, 81-712 Sopot, Poland

Accepted 20 January 2003

Abstract

In order to monitor the recovery of vegetation from pollution and the success of re-seeding efforts, acoustic echoes from the sea floor, covered and uncovered by underwater vegetation, were collected in Puck Bay (southern Baltic sea) using a 208 kHz Biosonics DT 4200 scientific echo sounder. The echo envelopes were examined and several of their parameters were recommended for further analysis. The possibility of using these parameters to distinguish between a bare sea floor and underwater meadows was tested. The parameters may be helpful in the identification of the species composition of the meadows and in accurate biomass assessment.

Keywords: Echo signals; Underwater meadows; Parametric analysis

1. Introduction

In many environmental applications, it is important to assess the spatial distribution and biomass of underwater meadows and to identify their species composition. This requires monitoring techniques that are sufficiently cheap, neither time-consuming nor labour-intensive, and which permit the synoptic coverage of a large area. It has been shown that the hydroacoustic method satisfies these requirements and is useful for detecting and characterising submersed aquatic vegetation in fresh water (Maceina and Shireman, 1980; Maceina et al., 1984; Duarte, 1987; Thomas et al., 1990) and in sea water (Spratt, 1989; Miner, 1993; Bozzano et al., 1998; Carbó and Molero, 1997; Sabol et al., 1997, 2002a; Sabol and Burczinski, 1998).

The paper scrutinises the utility of the hydroacoustic technique for monitoring the buoyant, bottom-rooted, submersed aquatic vegetation covering the acoustically hard, sandy, nearly flat bottom of Puck Bay (southern Baltic Sea). Before the 1970s, this bay was one of the biologically richest areas in southern Baltic coastal waters—multispecific underwater meadows covered most of the bottom, providing a refuge and foraging conditions for various marine organisms, including economically valuable species of fish. During the 1970s, pollution caused the state of the meadows to deteriorate drastically—the species diversity and their spatial extent shrank dramatically. At present, signs of recovery have been observed, which has encouraged efforts to restore the marine plant population. It is important to determine the extent of this recovery by monitoring the submersed vegetation. The hydroacoustic method could be useful in this respect.

The properties of the echo envelope of signals collected with a 208 kHz Biosonics DT 4200 scientific echo sounder in Puck Bay were studied. The analysis included a comparison of the echoes from the bare and plant-covered parts of the sea floor. The parameters for which a difference between echoes was noted are presented, and the significance of the difference is analysed. The effectiveness of the cluster analysis approach, based on selected parameters, in distinguishing the bare and plant-covered seabed is also discussed.

Selected features of the echo envelopes may be helpful in detecting the presence of underwater vegetation, especially where the actual bottom is undetectable. The problem of poor detection is discussed in Sabol et al. (2002b). Indeed, there was a problem with bottom detection for the hydroacoustic data we collected in some particularly dense patches of vegetation.

The analysis may also be important as a preliminary step in the identification of plant species and the accurate assessment of biomass. Identification of the brown filamentous

* Corresponding author.
E-mail address: gorska@iopan.gda.pl (N. Gorska).

doi:10.1016/S0990-7440(03)00015-9

algae *Pilayella* sp., which flourishes in the polluted, eutrophic waters of Puck Bay, could be significant in the accurate assessment of biomass. Clouds of these algae, saturated with air bubbles trapped in the underwater meadows, can significantly distort the echoes from rooted underwater vegetation.

Biological observations show that the vertical structure of the vegetation canopy depends on the plant species involved, as this may influence the properties of the echo envelopes. Hence, it is important to define the echo envelope parameters sensitive to this effect. The parameters investigated in the paper could be interesting from this point of view. As a further step, the possibility of using these parameters to identify plant species (including *Pilayella* sp. algae) will be investigated.

2. Materials and methods

2.1. Site conditions

The data were collected in a 500 × 500 m area in the northern part of the outer Puck Bay in May and September 2001. The sediments were homogeneous (sandy bottom) throughout the area. The bathymetry exhibited relatively little variability; the mean depth was approximately 1.7 m.

The area was colonised by submersed, vascular plants. The buoyancy of the bladders is due to the inter-cellular space, which is involved in the exchange of gases between the plant and the surrounding water. The maximum height of the vegetation canopy was around 40 cm.

The spatial distribution of the vegetation was patchy. The species composition of most patches was complex, the dominant species being *Zostera marina*, *Zanichellia* sp. and *Potamogeton* sp. However, almost monospecific patches were also found. The brown filamentous algae *Pilayella* sp., typical of eutrophic waters, was present in many patches (up to 8% of total biomass).

2.2. System description and data collection

The study was conducted from a small survey boat with precise navigational instrumentation. The acoustic measurements were performed using a downward-looking Biosonics dual-beam echo-sounder with a working frequency of 208 kHz. The narrow, 6° width beams were used for emitting and receiving. The transducer pulsed at the rate of 8 pulses s^{-1} and the signal duration was 0.1 ms. The envelope of the received echoes was sampled at 41.7 kHz. Simultaneously with the acoustic measurements, positional data were recorded using a D-Global Positioning System (DGPS) TRIMBLE SE4000 sampled at 1 Hz. The positioning precision of this system is approximately 0.3–1 m. Both acoustic and position data were stored on a laptop PC.

Fifty transects parallel to the local shoreline with a fixed distance between them were sampled using the echosounder and DGPS.

Additional observations involved stationary ground truth sampling and detailed visual inspection of the underwater meadows, enabled by the optically transparent shallow water conditions of Puck Bay.

The stationary ground truth samples were collected at random locations (one in May and seven in September) within the study area. The applied methodology closely resembled that described in Sabol et al. (2002a). The data collected were used mainly to verify the algorithm for detecting the bottom and measuring the height of the vegetation canopy (the algorithm is discussed in detail in another paper currently in preparation). Nevertheless, the information on the spatial distribution of the vegetation and the species composition of the underwater meadows also contributed to the present analysis.

Detailed visual inspection of the spatial distribution of the meadows, together with DGPS localisations of the boundaries between vegetated and bare areas, was carried out over some of the hydroacoustic transects. The visual observations were helpful in evaluating the differences between the relevant parameters for the vegetated and bare sea floor.

2.3. Data processing

The position-referenced hydroacoustic data were processed in order: (1) to develop an algorithm for detecting the bottom and measuring the height of the vegetation canopy; and (2) to analyse the echo envelopes.

A signal-processing algorithm for bottom detection and tracking, and vegetation detection was developed. A separate paper, which discusses this algorithm and its precision in detail is in preparation. Here we will only describe it briefly. Analysis of the echo signal envelope has shown that, unlike the algorithm of Sabol et al. (2002a), the depth of the sharpest rise of the echo envelope cannot be used to localise a vegetation-covered sea floor. The algorithm we have developed is based on the observed difference of echo levels for the bottom and the plants. In the majority of echoes from a vegetated bottom the highest echo level corresponds to backscattering from the water-bottom boundary. The algorithm uses the locations of the maxima in the series of echo envelopes to determine the bottom position. For detecting the presence of vegetation, an acceptable level of accuracy of this algorithm was demonstrated for a flat bottom and a relatively sparse vegetation.

The present paper focuses on the analysis of the envelopes of the collected echoes. The signals reflected from a bare sea floor and underwater meadows were compared. Examples of echo envelopes for plant-covered and bare sea floors are presented in Fig. 1a, b, respectively. These show that the echo duration from a non-vegetated sandy bottom is approximately defined by the pulse width, whereas the echoes from vegetated areas are significantly longer. The figure also highlights the difference in shape of the echo envelopes. The envelopes are smoother for the echoes from the non-vegetated bottom. These distinctions should be reflected in

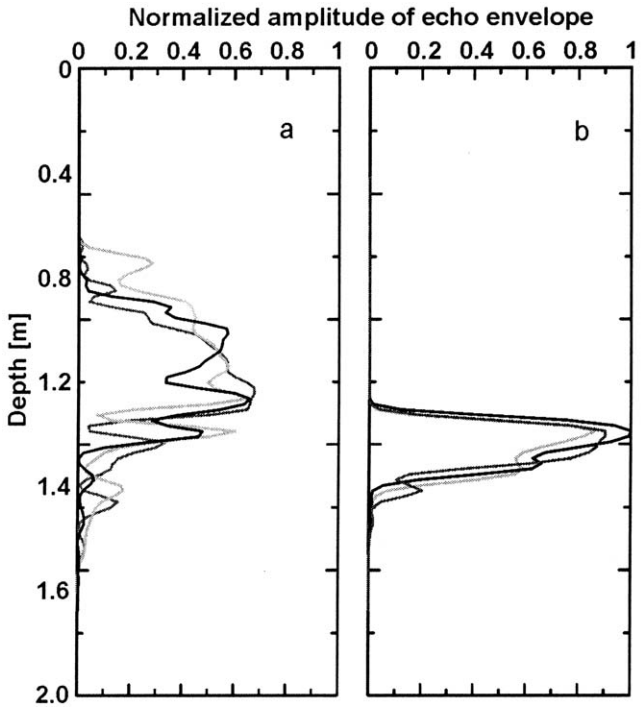

Fig. 1. (a, b) Normalised echo envelopes for the vegetated (a) and uncovered sea floor (b).

the values of the parameters controlled by the echo signal width and "smoothness".

A series of echo envelope parameters was studied. The analysis involved calculating the moments of different orders (up to the fourth order) for the echo envelopes in time- and frequency-domains and combinations of moments. The fractal dimension of an echo envelope, dependent on the variability of the echo envelope, was also computed. Two approaches were tested in parallel. One was based on the calculation of this parameter as the log–log slope of the power density spectrum (Hastings and Sugihara, 1994). It should be noted that a large set of echo envelope samples is required for this approach. However, this condition is not satisfied for short echoes from a sandy bottom, so this technique cannot be used for them. Therefore, an alternative approach, free from this limitation, was employed: this uses the wavelet transform (Simonsen and Hansen, 1998). The calculations were done for several classes of wavelets.

The analysis yielded three parameters whose values with respect to a bare sea floor and underwater meadows display the most conspicuous differences. These parameters are described in the next section.

3. Results and discussion

The echoes from covered and uncovered bottoms were compared with respect to the following parameters.

3.1. Description of the selected parameters

1. The normalised moment of inertia of the echo intensity, with respect to its centre of gravity, is defined as

$$M_i = \frac{\sum_{i=1}^{N} (i - i_c)^2 \cdot p_i^2}{\sum_{i=1}^{N} p_i^2} \quad (1)$$

where i is the number of the echo sample, p_i denotes the acoustic pressure for the ith sample, and N is the total number of echo samples. Here, i_c describes the sample number corresponding to the position of the centre of gravity for the echo signal intensity, which can be expressed as

$$i_c = \text{int}\left[\frac{\sum_{i=1}^{N} i \cdot p_i^2}{\sum_{i=1}^{N} p_i^2}\right] \quad (2)$$

where int stands for the integer inside the brackets.
The normalised moment of inertia indicates how the echo energy is concentrated around the centre of gravity. The smaller the value of M_i, the shorter the echo pulse duration; conversely, a larger value of M_i reflects a longer echo pulse duration, which may indicate the presence of vegetation.

2. The spectral width parameter v^2 is expressed as (Clough and Penzin, 1975)

$$v^2 = \frac{m_0 \; m_2}{m_1^2} - 1 \quad (3)$$

where m_r (r = 0, 1, 2) are spectral moments of the 0th, 1st and 2nd orders, respectively. The rth order moment is defined as

$$m_r = \int_0^{\infty} \omega^r \, S(\omega) \, \mathrm{d}\omega \quad (4)$$

where $S(\omega)$ is the power spectral density of the echo signal envelope and ω denotes the frequency. The mean frequency can be given by $w = m_1 / m_0$.
The spectral width parameter is defined by the mean frequency $\bar{\omega}$ and by the concentration of the spectral power density around it. The larger the mean frequency, the smaller the parameter. The spectral width parameter is larger in a spectrum where the spectral energy is more broadly distributed among the frequencies; it is smaller in the opposite case.

3. The fractal dimension was calculated using the wavelet transform approach (Simonsen and Hansen, 1998), as discussed in section 2.
The wavelet transform of a signal $y(x)$ in a domain x for a shifted and scaled version of a mother wavelet $\psi(x; a, b)$ can be expressed by

$$c(a,b) = \int_{-\infty}^{\infty} y(x) \, \frac{1}{\sqrt{a}} \psi\left(\frac{x-b}{a}\right) dx \quad (5)$$

where a and b are scale and translation parameters. The wavelets can be created by choosing $a = 2^j$ and $b = 2^j k$, where j and k are both integers. Wavelets are non-zero over only small intervals of x. They are formed by dilation and translation of the function $\psi(x)$ and the scaling function $\phi(x)$, using the relationships

$$\psi_k^j(x) = 2^{-j/2}\,\psi(2^{-j}x - k) \text{ and } \phi_k^j(x) = 2^{-j/2}\,\phi(2^{-j}x - k).$$

To estimate the fractal dimension, the use of several wavelets was checked. The best results were obtained for Daubechie's orthonormal wavelets of order M. Their first M moments are zero, and functions $\psi(x)$ and $\phi(x)$ are related to those on the finer length scales by

$$\phi(x) = \sqrt{2}\sum_{k=0}^{L-1} h_k\,\phi(2x - k),$$

$$\psi(x) = \sqrt{2}\sum_{k=0}^{L-1} g_k\,\psi(2x - k),$$

where $L = 2M$. The coefficients h_k and g_k are linked by the relationship: $g_k = (-1)^k h_{L-k-1}$, with $k = 0, 1, ..., L - 1$.

The wavelet transform of the self-affine function $y(x)$, defined as $y(x) \cong \lambda^{-H} y(\lambda x)$, where H is the Hurst exponent ($0 \le H \le 1$) and λ is a constant, is expressed using the result of Simonsen and Hansen's (1998) derivations

$$W_{y\lambda x a,b} = W_{\lambda - H\, y\lambda x a,b} = \lambda^{-(1/2)-H}\, W[y(x)](\lambda a, \lambda b) \quad (6)$$

as

$$W[y](\lambda a, \lambda b) \cong \lambda^{(1/2)+H}\, W[y](a, b). \quad (7)$$

Here $W[y(x)](a, b)$ is a wavelet transform of the self-affine function $y(x)$. On averaging both parts of this expression over the translation parameter b, the following expression can be derived:

$$W[y](\lambda a) \cong \lambda^{(1/2)+H}\, W[y](a)$$

where

$$W[y](a) = \langle |W[y](a, b)| \rangle_b. \quad (9)$$

Here, the brackets $\langle ... \rangle_b$ describe the averaging over the b translation parameter. The Hurst exponent H and the respective Hausdorff dimension (or fractal dimension) $D = 2 - H$ can be calculated from the slope of a log-log plot of $W[y](a)$ versus a using a linear regression algorithm.

The fractal dimension is defined by the variability of the echo envelope and is smaller for smoother envelopes.

3.2. The results of calculations

The parameters described in section 3.1. were calculated for the echo signals collected over the study area (Figs. 2a, e).

The echogram for the part of the acoustic transect crossing the central part of the study area is shown in Fig. 2a. The solid black line above the echogram indicates the presence of vegetation as confirmed by visual inspection. Two underwater meadows almost uniformly covered by plants were visually examined. Their boundaries were localised using the DGPS.

Fig. 2b presents the variation in plant height along the transect. The algorithm briefly described in section 2.3 was used to determine the height of the vegetation. The presence of visually confirmed vegetation is indicated in the same way as in Fig. 2a. There was good correlation between the underwater meadow boundaries as indicated by the echogram and the field observations.

The normalised moment of inertia M_i, the spectral width parameter v^2, and the fractal dimension D_{Db7} for the signals scattered from underwater meadows and the bare sea floor are shown (Fig. 2c–e). The figures demonstrate the growth of all the parameters in the vegetated areas.

Further interesting result (Fig. 3a–c) show the spatial distributions of the spectral width parameter v^2 (a), the normalised moment of inertia M_i (b) and the fractal dimension D_{Db7} (c) calculated for the study area. The logarithmic scale is used on the map for the normalised moment of inertia. The scale bars are given on the plots. It is important to note the apparent identity of the patchiness structure of the different parameters, which the maps show up (Fig. 3a–c). For example, the patch corresponding to the largest values of the parameters is clearly visible in the central part of the investigated area on all three maps. To understand the reasons for the correlation in the spatial distribution of the parameters, it should be remembered that they are defined by the various properties of the collected echoes: the moment of inertia is influenced by the echo thickness, the fractal dimension depends on the echo envelope variability, while the frequency width parameter can be defined by both the echo thickness and the echo envelope "smoothness". The parameters are not functionally dependent, and the correlation in their spatial distribution is explained by the fact that their values differ for a sandy bottom and underwater meadows. Indeed, the parameters can probably be regarded as indicators of underwater meadows.

Accuracy analysis was carried out in order to assess the significance of the differences between the parameters for a plant-covered and a bare sea floor, and the possibility of using them as indicators of underwater meadows. In an attempt to classify the collected echoes reflected from a bare and a plant-covered sea floor ("bare sea floor" and "plant" pings, respectively), suitable thresholds were considered for each of the parameters. The thresholds divide the parameter variability range into two parts corresponding to covered and uncovered bottom conditions. Then, for each of the parameters, the pings for which the parameter is larger than the threshold are classified as a "plant" ping. In the opposite case, they are defined as "bare sea floor" pings. The results of the classification are illustrated in Figs. 2c–e using the vegetation occurrence indicator—thick solid black (c) or grey and black (d, e) lines. The black and grey lines correspond to the various threshold values stated in the legends.

The accuracy of classification was assessed for the each parameter. This was done by comparing the results of the classification with the result obtained using our detection algorithm (Fig. 2b, see section 2.3). The results of the detection algorithm were selected for the comparison because it

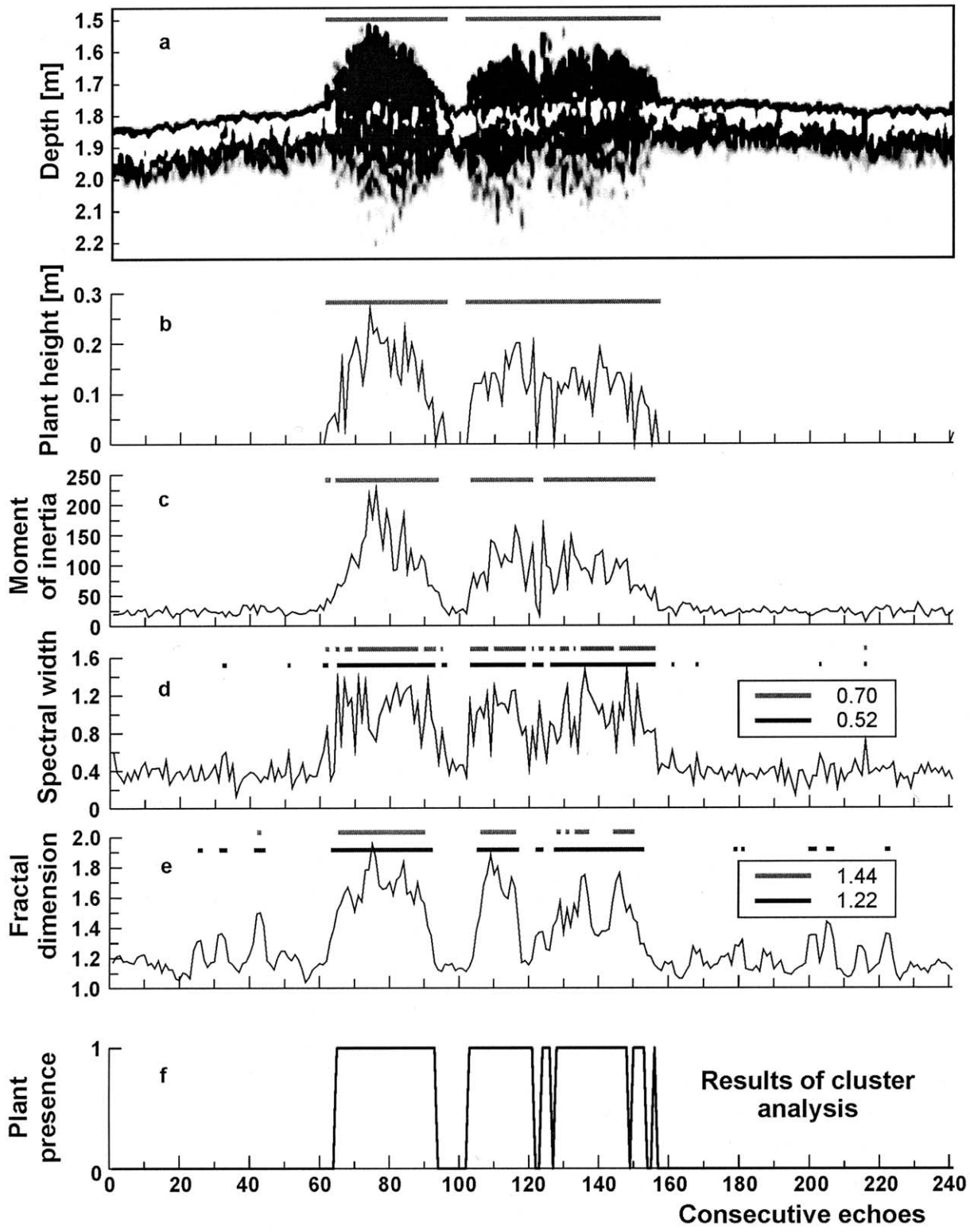

Fig. 2. (a-f) Echogram (a) and variability in echo parameters along a selected acoustic transect—variations in height of the vegetation canopy (b); variability of the normalised moment of inertia M_i (c), spectral width parameter v^2 (d) and fractal dimension D_{Db7} (e). The results of the cluster analysis classification procedure are presented in plot *f*. The thick, unbroken black lines in plots *a* and *b* indicate the presence of plants, verified bya non-acoustic method. The thick unbroken lines in plots c–e, indicating the occurrence of vegetation, were obtained from a comparison of the calculated parameters with the respective selected thresholds, given in the legends.

was sufficiently accurate to detect the presence of the vegetation on a flat bottom. This algorithm was verified using a combination of visual inspection (September 2001 measurements, results of which are presented in this paper) or video

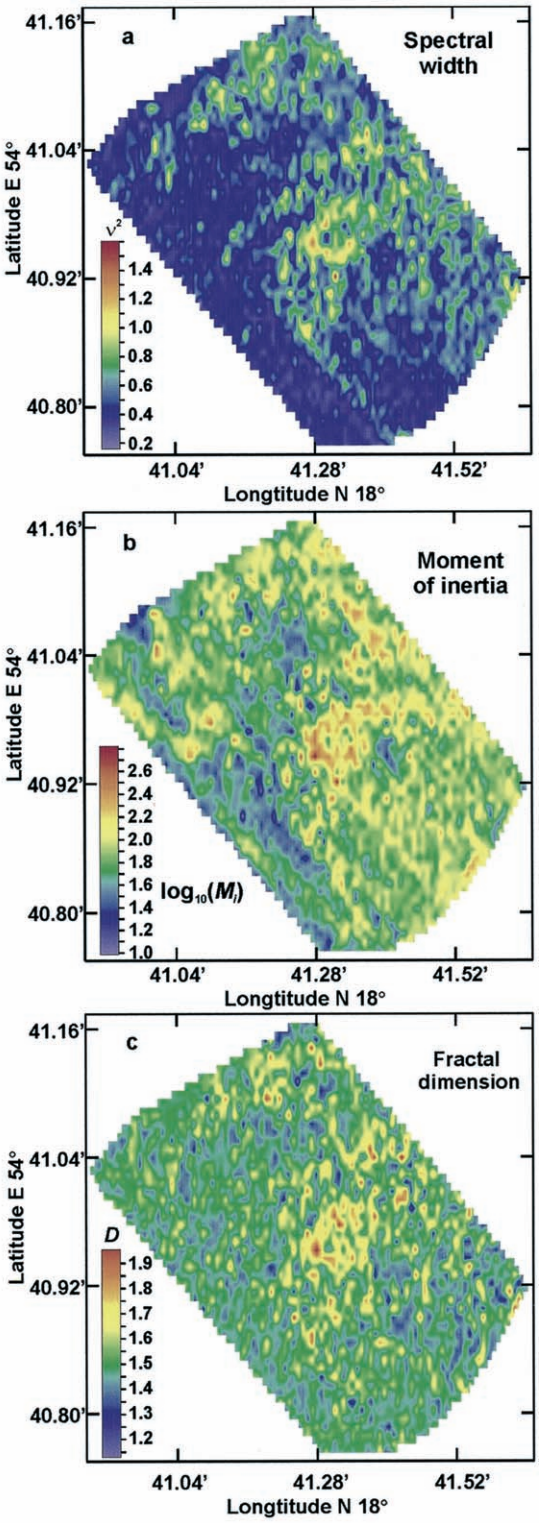

Fig. 3. The spatial distribution of the selected parameters in the study area.

filming data (later measurements made in 2002) and DGPS to localise the boundaries of the underwater meadows. The correlation with respect to the detection of the boundaries positions of underwater meadows was high.

Comparing the vegetation indicators (Fig. 2c–e) with the indicator (Fig. 2a, b), it can be concluded that using the moment of inertia gives the best agreement with the results of the detection algorithm. Agreement is poorest for the fractal dimension parameter. A more accurate comparison demonstrated that:

1. for the moment of inertia M_i (Fig. 2c), the false alarm and miss detection errors are, respectively, equal to 2.5 and 2.4% for the chosen threshold of 38.61.
2. for the spectral width parameter v^2 (Fig. 2d), the false alarm error decreases from 8.3 to 1.9% and the miss detection error increases from 4.8 to 14.3% for thresholds from 0.52 to 0.70.
3. for the fractal dimension D_{Db7} (Fig. 2e), the false alarm error decreases from 14 to 1.3% and the miss detection error grows from 16.7 to 38.1% for thresholds from 1.28 to 1.44.

For the data presented in the echogram (Fig. 2a), the selected parameters can be regarded as indicators of underwater vegetation. However, these data were collected under "ideal" conditions—a flat bottom of constant depth and vegetation patterns of comparable height. Sea floor conditions of greater complexity were also examined, including variability of bottom depth and meadows where the plant height is very variable. Our study demonstrated that the use of just one parameter is not sufficient to detect vegetation under such conditions. Therefore, the possibility of cluster analysis for detecting underwater meadows was also studied. A number of clustering algorithms were tested for the data presented in the echogram (Fig. 2a). They differed in the number of parameters used, the number of groups classified, and the classifying procedure. The K-MEAN algorithm of clustering (Späth, 1982), applied in the three-dimensional space of the selected parameters for three classes—"high plants", "low plants" and "bare sea floor" pings, displayed better accuracy. The classification results are comparable with those based on the one-parameter approach using the moment of inertia. The results of applying the clustering procedure are shown in (Fig. 2f) where the vegetated and non-vegetated bottom conditions are indicated by the unit-and zero-values, respectively.

Using this classifying procedure, a map of the vegetation distribution along the acoustic transects (Fig. 4) was constructed. The vegetation specified by cluster analysis (both groups—"high" and "low" plants) is indicated by dots, which correspond to the geographical co-ordinates of the respective echo signal measurements. The results of the clustering analysis were verified by detailed visual inspection of a given transect (4000 echoes were collected over this transect). The calculated false alarm and miss detection errors were found to be 3.2 and 37.7%, respectively. It was demonstrated that cluster analysis gives better results than just one of the selected parameters in distinguishing shorter vegetation in cases where the height of the vegetation varies.

4. Conclusion

The paper analyses the properties of the envelope of the echoes collected using a 208 kHz Biosonics DT 4200 scien-

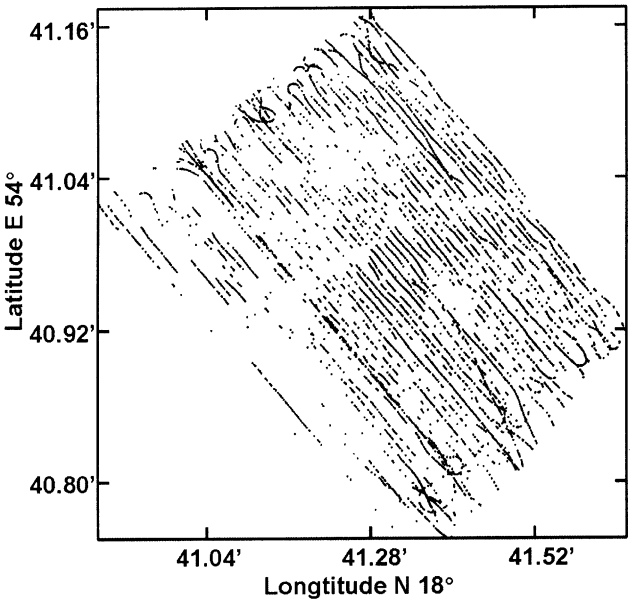

Fig. 4. Map showing the occurrence of vegetation in the study area; the map was constructed on the basis of cluster analysis classification.

tific echo sounder in Puck Bay. Comparison of the echoes from bare and vegetated sea floors shows that for the echo envelope parameters—the moment of inertia, the spectral width parameter and the fractal dimension—the difference is significant. This difference is evaluated. It is the most significant for the moment of inertia, and this parameter can be used to distinguish a bare sea floor from underwater meadows wherever the bottom is flat and the vegetation patches are of comparable height.

The effectiveness of cluster analysis (K-MEAN clustering algorithm, applied in the three-dimensional space of the selected parameters for three classes—"high plants", "low plants" and "bare sea floor" pings) in distinguishing a vegetated from a non-vegetated sea bed is demonstrated. This procedure is more effective for detecting shorter vegetation where there is significant variability in the height of the meadows than if onlyone of the selected parameters is used.

Acknowledgements

This study was supported financially by the State Committee for Scientific Research of Poland (Research Project No. 6 PO4 051 20). We greatly appreciate the efforts of the crew of the research vessel "Doktor Lubecki" and the survey boat "IMOROS" (Maritime Institute, Gdańsk) for their assistance in the field. We also extend our gratitude to biologists L. Kruk-Dowgiałło and R. Opioła (Maritime Institute, Gdańsk) for the sampling and processing of biological data. Finally, we would like to thank the two anonymous reviewers for their very valuable comments for improving the text.

References

Bozzano, R., Castellano, L., Siccardi, A., 1998. Characterization of submerged aquatic vegetation by a sector-scanning sonar. Fourth European Conference on Underwater Acoustics, Rome. pp. 159–164.

Carbó, R., Molero, A.C., 1997. Scattering strength of a *Gelidium* biomass bottom. Appl. Acoust 51, 343–351.

Clough, R.W., Penzien, J., 1975. Dynamics of structure. McGraw-Hill, New York.

Duarte, C.M., 1987. Use of echo sounder tracing to estimate the aboveground biomass of submersed plants in lakes. Can. J. Fish. Aquat. Sci. 44, 732–735.

Hastings, H.M., Sugihara, G., 1994. Fractals. A User's Guide for the Natural Sciences. Oxford University Press, Oxford, New York, Tokyo, pp. 7–77.

Maceina, M.J., Shireman, J.V., 1980. The use of a recording fathometer for determination of distribution and biomass of Hydrilla. J. Aquat. Plant Manage 18, 34–39.

Maceina, M.J., Shireman, J.V., Langland, K.A., Canfield, D.E., 1984. Prediction of submerged plant biomass by use of a recording fathometer. J. Aquat. Plant Manage. 22, 35–38.

Miner, S.P., 19–23 July 1993. Application of acoustic hydrosurvey technology to the mapping of eelgrass (Zostera marina) distribution in Humboldt Bay, California. Sixth Symposium on Coastal and Ocean Management, New Orleans, LA.

Sabol, B.M., Burczinski, J., 1998. Digital echo sounder system for characterizing vegetation in shallow-water environments. Fourth European Conference on Underwater Acoustics, Rome. pp. 165–171.

Sabol, B., McCarthy, E., Rocha, K., 1997. Hydroacoustical basis for detection and characterization of eelgrass. Fourth Conference on Remote Sensing for Marine and Coastal Environments, Orlando, FL. pp. I-679–693.

Sabol, B., Melton, R.E., Chamberlain, R., Doering, P., Haunert, K., 2002a. Evaluation of a digital echo sounder for detection of submersed aquatic vegetation. Estuaries 25, 133–141.

Sabol, B., Burczyński, J., Hoffman, J., 2002b. Advanced digital processing of echo sounder signals for characterization of submersed aquatic vegetation. 6 ICES Symposium on Acoustics in Fisheries and Ecology, Montpellier, France, 10–14 June 2002, 1732–1747.

Simonsen, I., Hansen, A., 1998. Determination of the Hurst exponent by use of wavelet transforms. Phys. Rev. 58, 2779–2787.

Spratt, J.D., 1989. The distribution and density of eelgrass, *Zostera marina*, in Tomales Bay, California. Calif. Fish Game 75, 204–212.

Späth, H., 1982. Cluster Analysis Algorithms for Data Reduction and Classification of Objects. Wiley, New York.

Thomas, G.L., Thiesfield, S.L., Bonar, S.A., Crittenden, R.N., Paulely, G.B., 1990. Estimation of submergent plant bed biovolume using acoustic range information. Can. J. Fish. Aquat. Sci. 47, 805–812.

Available online at www.sciencedirect.com
SCIENCE DIRECT®
Aquatic Living Resources 16 (2003) 223–230
Aquatic Living Resources
www.elsevier.com/locate/aquliv

Use of multi-beam sonar to map seagrass beds in Otsuchi Bay on the Sanriku Coast of Japan

Teruhisa Komatsu [a,*], Chiaki Igarashi [a], Kenichi Tatsukawa [a], Sayeeda Sultana [a], Yasuaki Matsuoka [b], Shuichi Harada [b]

[a] *Ocean Research Institute, The University of Tokyo, 1-15-1, Minamidai, Nakanoku, Tokyo 164-8639, Japan*
[b] *Toyo Corporation, 1-1-6, Yaesu, Chuoku, Tokyo 103-8234, Japan*

Accepted 7 April 2003

Abstract

Seagrass beds play an important role in coastal ecosystems as primary producers and providers of habitat and environmental structure. Therefore, mapping seagrass beds is indispensable in the management and conservation of sound littoral ecosystems, and in the development of sustainable fisheries in coastal waters. Multi-beam sonar is often used to map bottom topography. We developed a mapping method to quantify the volume of seagrass using a multi-beam sonar. Seagrass beds were scanned with the multi-beam sonar and quadrat sampled to verify the distribution of seagrasses. We used software to discriminate seagrass signals from echoes to obtain a topographic profile of the bottom without seagrass; this was then subtracted from the topography including the seagrass. We then mapped seagrass distribution, calculated seagrass volume, and estimated biomass using volume and quadrat samples. We applied these methods to map a seagrass bed of *Zostera caulescens* in Otsuchi Bay, on the Sanriku Coast of Japan, during the growing season of 2001. A transducer was attached to a boat (one gross ton) equipped with a differential-GPS, a motion sensor, and a gyrocompass. The vessel completed a grid survey scanning whole seagrass bed with an area of 115 m × 156 m at bottom depths between 2 and 8 m within about 40 min when traveling at a speed of 1.5 m s^{-1} (3 knots). The multi-beam sonar was able to visualize three-dimensional seagrass distribution without interpolation and easily to estimate area and volume occupied by the seagrass using hydrography software. The results indicated that *Z. caulescens* was distributed at bottom depths of 6–7 m with a surface area of 3 628 m^2 and a volume of 1 368 m^3. The mean biomass of above- and below-ground parts of seagrass were estimated to be 28.6 gDW m^{-2} (range 26.6–30.9) and 15.9 gDW m^{-2} (range 14.1–17.7). Our study demonstrated that multi-beam sonar is effective for mapping and quantifying the spatial distribution of seagrass beds, and for visualizing the landscape of the seagrass canopy.

Keywords: Seagrass; Seaweed; Mapping methods; Remote sensing; Multi-beam sonar

1. Introduction

Seagrass beds play an important role in marine coastal ecosystems. They support flora and fauna, including epiphytic organisms, as well as coastal fisheries (Coles et al., 1993), and contribute to the marine environment by stabilizing bottom sediments and maintaining coastal water quality and clarity (Ward et al., 1984; Jeudy de Grissac and Boudouresque, 1985; Komatsu and Nakaoka, 2000; Komatsu and Yamano, 2000). Additional effects of seagrass meadows include those of seaweed forests such as buffering of water flow (Komatsu and Murakami, 1994), pH distribution (Komatsu and Kawai, 1986), and dissolved oxygen distribution (Komatsu, 1989; Komatsu et al., 1990). Many commercially important species spawn in seagrass beds (e.g., sea urchins, balaos, cuttlefish); larvae and juveniles use the beds as nursery grounds (Arasaki and Arasaki, 1978). Thus, seagrass beds support biodiversity and are an important habitat for marine animals.

Increased seafloor reclamation and industrial and agricultural pollution as a result of economic development have decreased the size of large areas of seagrass beds in coastal zones (e.g., Hoshino, 1972; Komatsu 1997). Since seagrass beds are sensitive to pollution and water quality deterioration, they serve as "bio-indicators". Altered seagrass depth distribution in Chesapeake Bay was used as a bio-indicator when runoff impacted water quality, causing changes in light

* Corresponding author.
E-mail address: komatsu@ori.u-tokyo.ac.jp (T. Komatsu).

doi:10.1016/S0990-7440(03)00045-7

penetration and consequently affecting seagrass abundance and distribution patterns (Dennison et al., 1993; Short and Willie-Echeverria, 1996). Monitoring has also been carried out at 24–33 survey sites along the coast of Provence and the French Riviera since 1984, using the lower limit of *Posidonia oceanica* as a bio-indicator (Boudouresque et al., 2000). Mapping of seagrass beds is a very practical method to assess the condition of coastal environments. Recently, it has been stressed that preservation, restoration, and creation of seagrass beds are necessary to recover coastal environments, biodiversity, and bioresources for sound littoral ecosystems and for the sustainable development of fisheries. To preserve or conserve seagrass beds, it is very important to map and monitor them (Lee Long et al., 1996).

The methods of mapping seagrass and seaweed beds can be classified into two categories (Komatsu et al., 2002; 2003); one involves direct observation or measurement, whereas the other involves indirect methods using remote sensing equipment. The former category includes ground surveys (walking, diving, or sampling from the surface). In France, observations from a submarine were used to map the lower limits of seagrass, *P. oceanica*, along the French Riviera (Meinesz and Laurent, 1978). Because they require much time and labor, direct methods are not very efficient. Indirect methods are classified into two groups, based on the type of remote sensing equipment that is used: optical remote sensing or acoustic remote sensing. Aerial photographs and satellite imagery are efficient for mapping areas in which dense seagrass beds can be identified on very coarse scales (Belsher, 1989; Long et al., 1994). However, these methods cannot always be used successfully to map seagrass biomass or to find seagrasses at low densities, and they are not effective in waters that are too turbid or deep for optical remote sensing.

One acoustic method that has been developed since the 1970s to map seagrass beds in the Mediterranean Sea is the use of scanning sonar, which is more efficient than ground surveying. With this method, swaths of the sea bottom 50–500 m in width are scanned, and individual seagrass beds can be successfully distinguished (Meinesz et al., 1981; Pasqualini et al., 1998; Piazzi et al., 2000). However, the major disadvantages of this system are that it is difficult to apply on a small boat in shallow waters; it is impossible to measure vertical height distributions; and it is difficult to convert horizontal distribution data to mapping data from the position data for the boat. Other acoustic methods use echosounders to detect vertical seagrass distribution (e.g., Hatakeyama and Maniwa, 1978; Komatsu and Tatsukawa, 1998). The disadvantage of echosounders is that only a narrow area can be scanned; since seagrass is often patchily distributed, the narrow strips deform the distribution. Thus, a broader scan width is recommended.

Recently, narrow multi-beam sonar was developed and used to map bottom topography in shallow waters. This narrow multi-beam sonar can scan broad strips, as well as provide vertical topography, making it suitable for mapping seagrass beds. Therefore, we aimed to develop an efficient method of mapping seagrass beds by using multi-beam sonar to measure their horizontal and vertical distribution.

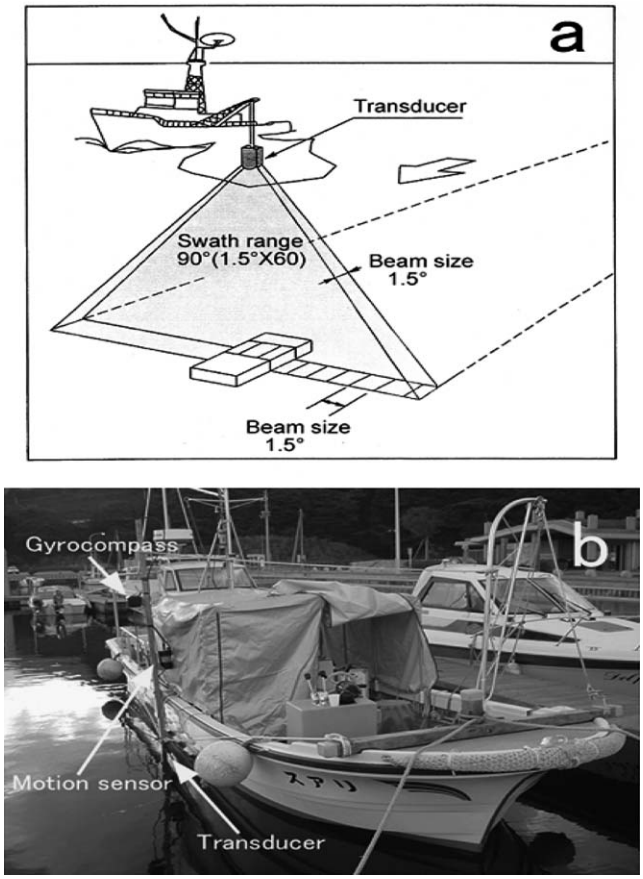

Fig. 1. Schematic view of multi-beam sonar (a) and photography of R/V *Rias* equipped with the multi-beam sonar, gyrocompass and motion sensor utilized for mapping seagrass beds (b). Map of Otsuchi Bay on the Sanriku Coast facing the Northwestern Pacific (left panel) and the study site off Nebama in Otsuchi bay (right panel).

2. Materials and methods

2.1. Multi-beam sonar

A multi-beam sonar, SeaBat 9001 (RESON Inc.) was used for mapping seagrass beds. The SeaBat 9001 multi-beam echosounder measures 60 soundings in a single pass from a lightweight and portable transducer head. The operating frequency of the ultrasound is 455 kHz. Sixty sonar beams within each swath (combined to form a 90°-wide by 1.5°-long geometrically correct cross-section) provide simultaneous sonar coverage equivalent to about two times the measured depth (Fig. 1a). Because of its small size, the SeaBat 9001 was installed on a small vessel (one gross ton), the R/V *Rias* of the Otsuchi Marine Research Center, Ocean Research Institute, The University of Tokyo (Fig. 1b).

A motion sensor (Model DMS2-10, TSS Ltd.) and a gyrocompass (Model ADGC, KVH Inc.) were combined with SeaBat 9001 to compensate for the motion and direction of

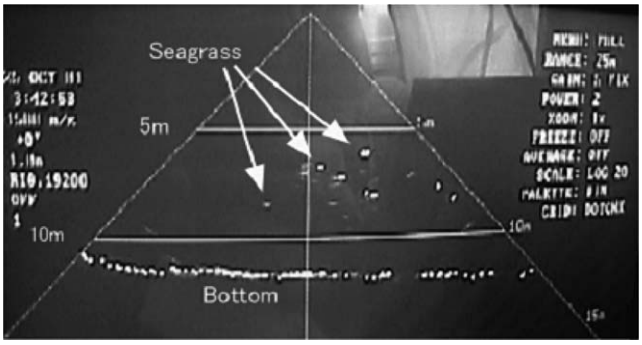

Fig. 2. Echoes of multi-beam sonar reflecting from seagrass and sand bottom.

the vessel (Fig. 1b). The position of the boat and the transducer were localized using differential-GPS (Model AgGPS 132, Trimble). The transducer was fixed vertically on the side of the boat to scan the bottom topography. The data were stored in a notebook computer and analyzed with hydrography software (Hypack Max, Coastal Oceanography Inc.).

2.2. Estimation of seagrass volume and biomass

Most seagrasses, including *Zostera caulescens* Miki, grow on sandy beds. If the seagrass canopy is much higher than the sand bed, we can distinguish the seagrass from the bottom (Fig. 2) by the multi-beam sonar.

We estimated the volume occupied by the seagrass using the difference in depth between the above-ground part of the seagrass and the sand bed. The procedure for this estimation was as follows: (1) a seagrass bed was mapped; (2) data of bottom depth distribution were stored in the computer; (3) using the hydrography software, the seagrass data were removed from the bottom depth data to obtain the bottom distribution of only the sand bed (Fig. 3); (4) the bottom depth distribution of the sand bed was subtracted from the data including the seagrass to obtain the volume occupied by the seagrass. In Fig. 3a, we can observe seagrass signals sticking out upward from the base lines on the hydrography software (Hypack Max). These signals were echo reflecting from the leaves or stems of seagrass on the bottom of which substratum was only sand in this area. Therefore we obtained a topographic profile of the bottom without seagrass (Fig. 3b) by processing seagrass signals as noise on the software. We estimated volume occupied by seagrass subtracting the topographic profile of the bottom without seagrass from that with seagrass (canopy depth) on the software for dredging canals and ports that can calculate the volume between two layers with different bottom depths in an identical area.

Seagrass biomass is estimated by the following steps. In July and October, *Z. caulescens* grew two kinds of shoots in Funakoshi Bay, which neighbors Otsuchi Bay (Sultana and Komatsu, 2002, 2003): flowering and vegetative shoots. The former were >80 cm and the latter were ≤80 cm. Since the vegetative shoots are positioned below the flowering shoots, their biomass depends on the aerial cover of seagrass on the bottom.

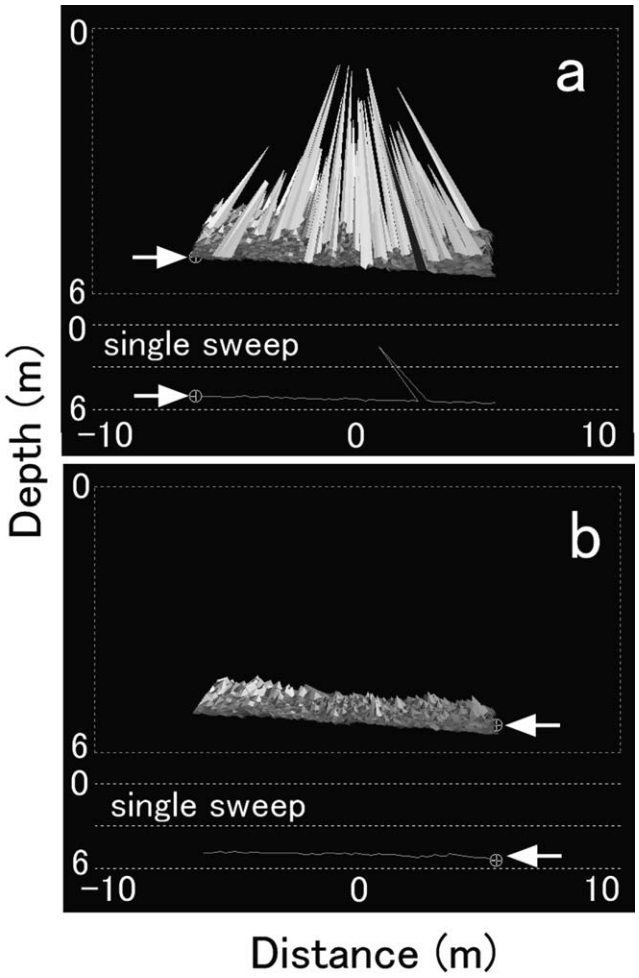

Fig. 3. Bottom depth distributions including sand bottom and seagrass sticking from the sand bed (a) and those of only the sand bed without the seagrass data removed from the bottom depth data by using the hydrography software. Bottom depth data were set along the vessel course. Single sweep shows the bottom depth distribution with a solid line connecting data obtained by one sweep of multi-beam sonar. The corresponding bottom distributions are represented by the white arrows in each panel.

We can estimate vegetative shoot biomass by multiplying the area covered by seagrass and the vegetative shoot biomass per unit area obtained by quadrat sampling. If we assume that the volume occupied by flowering shoots between the bottom and 80 cm above the bottom is vertically constant, the volume can be obtained by multiplying the height of 80 cm and the area occupied by the seagrass at the level of 80 cm above the bottom. Total volume occupied by the flowering shoots is calculated from the sum of that from the bottom to 80 cm above the bottom and that from 80 cm above the bottom to the canopy of seagrass above 80 cm. We can estimate flowering shoot biomass by multiplying the volume occupied by flowering shoots and the flowering shoot biomass per unit volume obtained by quadrat sampling.

The definition of the shoot length is from the base of stem to the tip of maximum leave attaching to the top of stem. However, leaves attaching to the top of flowering shoot stem trail downward in situ. Since the canopy heights of *Z. caulescens* greater than 80 cm are proportional to stem length,

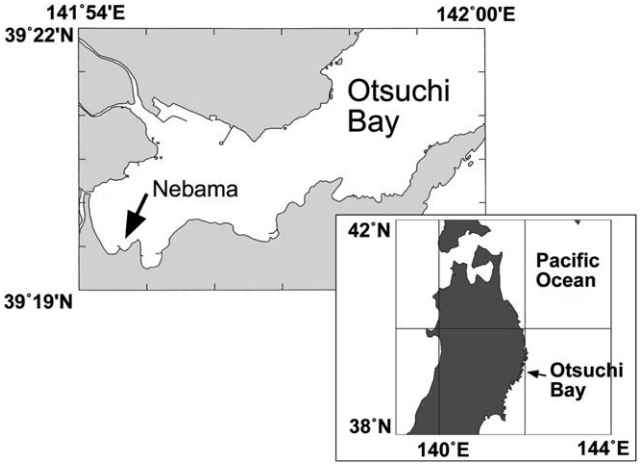

Fig. 4. Map of Otsuchi Bay on the Sanriku Coast facing the Northwestern Pacific (right panel) and the study site off Nebama in Otsuchi bay (left panel).

flowering shoot biomass per unit volume was calculated dividing above-ground biomass of flowering shoots by mean stem length based on the quadrat sampling of seagrass.

2.3. Study area and ground-truthing survey

We selected a seagrass bed off Nebama Otsuchi Bay on the Sanriku Coast of Japan, facing the Northwestern Pacific (Fig. 4). Otsuchi Bay is a *rias*-type bay neighboring Funakoshi Bay, where the longest seagrass on record, *Z. caulescens*, is distributed (Aioi et al., 1996, 1998). The boat, equipped with the multi-beam sonar, scanned the bottom at a speed of 3 knots (about 1.5 m s^{-1}) from 10:22 to 11:03 on 23 October 2001.

To verify the seagrass distribution, a diver made in situ observations and sampled two quadrats (0.5 m × 0.5 m) of seagrass in the area where the acoustic survey was performed at bottom depths of 5.1 and 6.1 m. Samples of seagrass were preserved in plastic bags with 10% formalin seawater. Since seagrass, *Z. caulescens*, is classified as a threatened species by Division of Wildlife, the Ministry of Environment of Japan (2000), it was necessary to limit number of quadrat sampling that destroyed the seagrass beds of *Z. caulescens* (Orth et al., 1984).

To estimate the error of depth detection by the multi-beam system, we compared differences of bottom depth at a quadrat of 20 cm × 20 cm on the sand bed, which is roughly equivalent to the foot print of each sound beam at the study area, sounded at three times. Since surveyed area was 2 m × 2 m, we obtained 100 samples of the difference in the bottom depth.

2.4. Seagrass biomass

Plant material was rinsed in freshwater and cleaned off sand and shells in the laboratory. Shoot density (i.e., density of only the above-ground foliar portions of a plant) and shoot length (i.e., length from the bottom end of a shoot to the top of the longest blade) were measured. Samples were also sorted into above- and below-ground parts. Epiphytic plants and animals were removed from leaves by dipping the plants into 5% acetic acid water. Wet weights were taken prior to drying the seagrass in a hot-air oven (DX300, Yamato Scientific Co. Ltd) at 60 °C for 48 h. Dry weights of the samples were then obtained and used to calculate above- and below-ground biomass. Biomass was expressed as dry weight (g) per unit area (i.e., gDW m^{-2}), which is the most widely used expression for biomass.

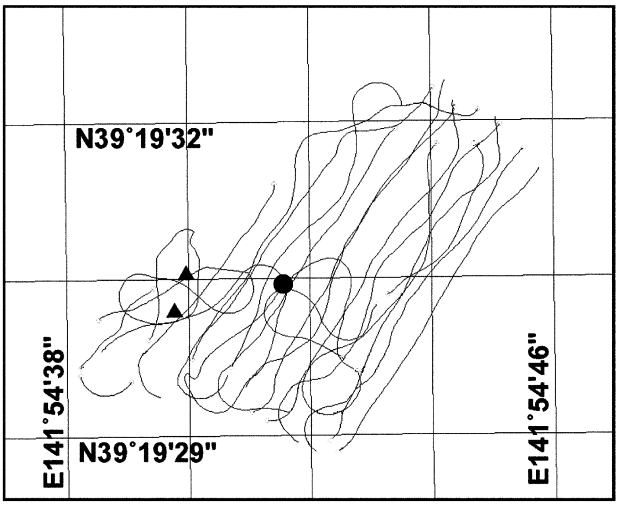

Fig. 5. Map of traces made by the R/V *Rias*, which was equipped with a multi-beam sonar for mapping a seagrass bed of *Z. caulescens* in Otsuchi Bay. Triangles show quadrat-sampling stations. Circle represents the area (2 m × 2 m) to estimate the error of depth detection by the multi-beam sonar system where three courses of bottom measurements were crossing..

3. Results

Boat traces with the multi-beam sonar are shown in Fig. 5. Bottom topographic profiles with and without seagrass were mapped with the triangulated irregular network (TIN) model using the hydrography software (Fig. 6), and we found that *Z. caulescens* formed a band-like distribution.

To estimate the error of depth detection, the differences of bottom depth at a quadrat of 20 cm × 20 cm on the sand bed sounded at three times in an area of 2 m × 2 m were classified into 5 cm intervals (Fig. 7). Mean of differences of the bottom depth was 11.4 cm (S.D. = 5.4 cm). Therefore, the bottom depth measured by the multi-beam system had an error of ±16.8 cm.

Longer, flowering shoots of *Z. caulescens* were distributed on the western part of the scanned area, where the bottom depth was greater (Fig. 8). The northwestern part of the scanned area was occupied by rafts used in aquaculture, whereas the southeastern part was occupied by buoys. The blank areas on the top and bottom of Fig. 9 correspond to these rafts and buoys. The horizontal distribution of *Z. caulescens* suggests that it was mainly limited to a maximum bottom depth of about 6.5 m (Fig. 9). Dense patches of

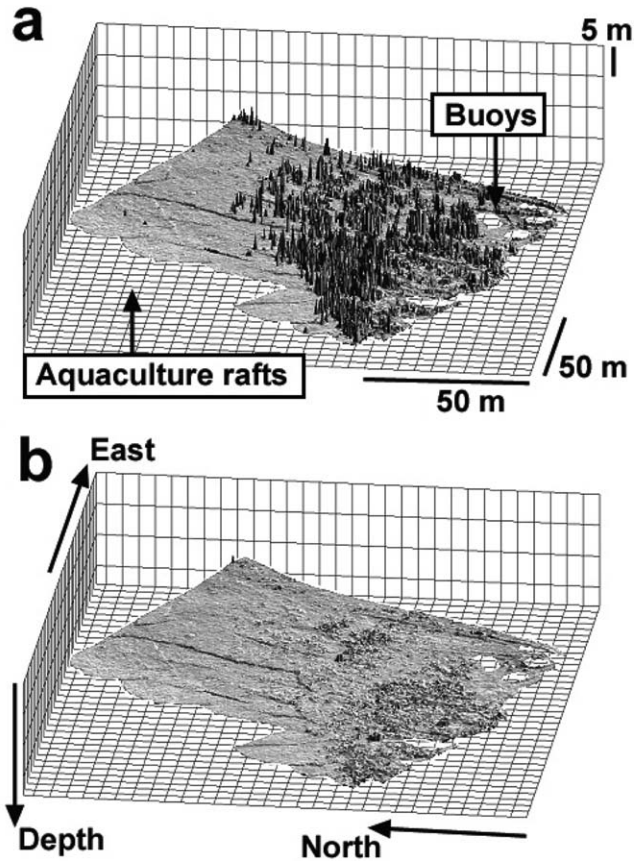

Fig. 6. Three-dimensional distributions of *Z. caulescens* on the bottom (a) and bottom profile without seagrass (b) in Otsuchi Bay using the TIN model. Intervals of grid lines on the East-West, North-South and depth axis are 5 m.

seagrass were observed at bottom depths between 6 and 4.5 m.

Using the software (Hypack Max), we calculated that the areas occupied by seagrass at 1 and 80 cm above the bottom were 3628 and 543 m^2, respectively. The reason for cutting

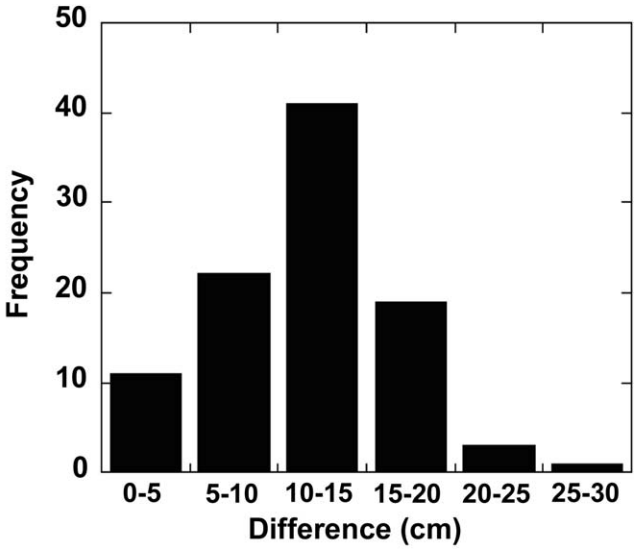

Fig. 7. Frequency distribution of differences between maximum and minimum bottom depths at a quadrat of 20 cm × 20 cm on the sand bed sounded at three times in an area of 2 m × 2 m.

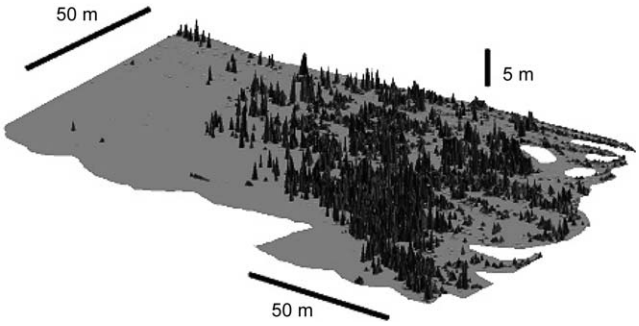

Fig. 8. Three-dimensional distribution of *Z. caulescens* in Otsuchi Bay using the TIN model after subtracting the bottom with the seagrass from the bottom topography including the seagrass.

seagrass at 1 cm above the bottom is to separate seagrass from the bottom. Since three-dimensional distribution of seagrass was extracted from the bare bottom, the aerial cover of the sand bed was 10,205 m^2. The volumes occupied by the seagrass greater than 1 and 80 cm above the bottom were 1354 m^3 (±610 m^3) and 342 m^3 (±91 m^3). Therefore, volume occupied by the seagrass was 1368 m^3. The mean height of seagrass greater than 1 cm was 19.7 cm when we excluded the area covered by shoots greater than 80 cm from the volume and area estimates. The mean height of shoots above 80 cm was 143.1 cm (±16.8 cm).

Shoot lengths determined by quadrat sampling were divided into two categories: groups of shoots below and above 80 cm (Fig. 10). We pooled samples at depths of 5 and 6 m to calculate the mean lengths and total weights of the two groups of shoots. The mean lengths of shoots below and above 80 cm were 21.7 cm (±50.3 cm) and 311.4 cm (±96.5 cm). The mean stem length of flowering shoots was 263.4 cm (±103.0 cm). The total dry weights of vegetative and flowering shoots per unit area were 24.3 gDW m^{-2} (range 23.4–25.3) and 52.7 gDW m^{-2} (range 33.6–71.7). The dry

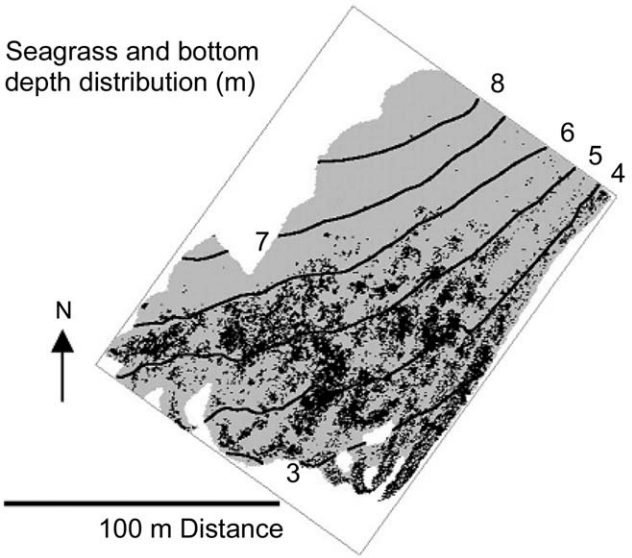

Fig. 9. Horizontal distribution of the area occupied by *Z. caulescens*, as well as bottom depth.

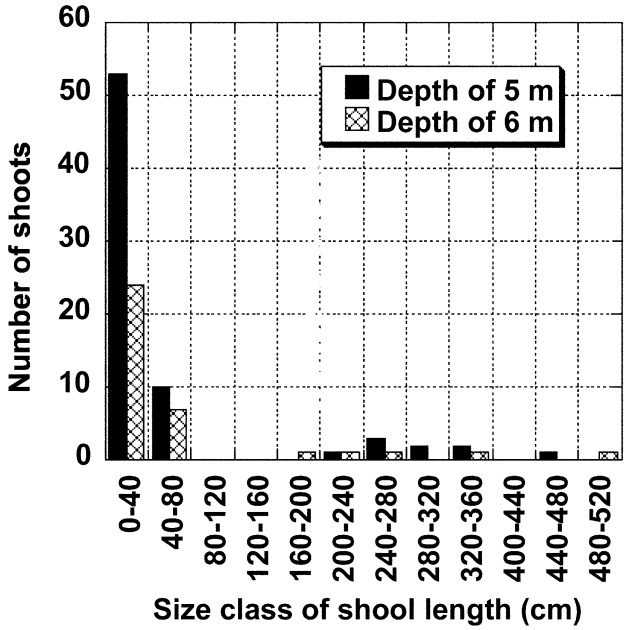

Fig. 10. Distribution of shoot lengths of *Z. caulescens* sampled at bottom depths of 5.1 and 6.1 m in Otsuchi Bay in October during the growing season.

weight of flowering shoot per unit volume was 20.8 gDW m^{-3} (range 15.1–26.4). Roots attaching to vegetative and flowering shoots were classified into two categories of roots: roots of vegetative shoots and flowering shoots. Biomass of the former and the latter were 15.3 gDW m^{-2} (range 13.8–16.8) and 3.5 gDW m^{-2} (range 1.4–5.5).

Biomass of vegetative and flowering shoots were estimated to be 88 kg (range 85–92) and 16 kg (range 12–20). Root biomass of vegetative and flowering shoots were 56 kg (range 50–61) and 2 kg (range 1–3). Biomass of above- and below-ground parts were 104 kg (range 97–112) and 58 kg (range 51–64). Biomass of above- and below-ground parts averaged in total seagrass area were 28.6 gDW m^{-2} (range 26.6–30.9) and 15.9 gDW m^{-2} (range 14.1–17.7), respectively. Consequently, mean seagrass biomass including above- and below-ground parts was 44.5 gDW m^{-2} (range 40.7–48.6).

4. Discussion

Many studies that have mapped seagrass beds using side-scan sonar were unable to show three-dimensional images of the seagrass beds, and provided only horizontal images. On the other hand, mapping studies that relied on echosounders produced only vertical images of seagrass beds. Our study demonstrated that multi-beam sonar could detect seagrass meadows precisely and visualize three-dimensional structure on a computer display. Three-dimensional images of seagrass beds can be used to analyze the formation of seagrass beds, including considerations of gap regeneration, horizontal and vertical development of seagrass patches, and landscape ecology. By quadrat-sampling of seagrass beds, Sultana and Komatsu (2002; 2003) reported that blade length was proportional to bottom depth. We observed a similar phenomenon when we mapped the landscape of the seagrass canopy (Fig. 8).

Colantoni et al. (1982) attempted to use a low-frequency echosounder (3.5 kHz), which proved to be rather ineffective in distinguishing the acoustic characters of *P. oceanica* beds from those of the bottom. Although high-resolution continuous seismic reflection (3.5 kHz) can distinguish *P. oceanica* beds from others (Rey and Diaz del Rio, 1989), the long wavelengths of ultrasound result in worse vertical precision of the echosounder. Echosounders with an ultrasonic wave of 200 kHz are more appropriate for detecting seagrass beds (Komatsu and Tatsukawa, 1998). The multi-beam sonar (SeaBat 9001) used 455 kHz and was reflected by the seagrass. Beam frequencies above 200 kHz are necessary to detect seagrass beds.

Hatakeyama and Maniwa (1978) used echosounding to map a *Zostera* bed, but they calculated only an index of biomass, i.e., the sum of canopy heights per unit sector along a transect scanned by the echosounder. Since it is necessary to estimate seagrass biomass for a quantitative understanding of the seagrass ecosystem, Komatsu and Tatsukawa (1998) proposed a simple method using echosounder and global positioning system to convert the shading grades of seagrass on echograms to above-ground biomass based on quadrat samplings. However, they did not estimate the volume occupied by the seagrass. Multi-beam sonar measurement of seagrass beds and subsequent software processing of data allowed us to estimate the area and volume occupied by seagrass. Incorporating these data with quadrat sampling, we could then estimate the biomass of the seagrass beds.

Sabol et al. (2002) presented a technique for rapid detection of submersed aquatic vegetation (SAV) using a high-frequency, high-resolution digital echosounder linked with global positioning system equipment. The acoustic reflectivity of SAV allows for detection and explicit measurement of canopy geometry using a digital signal processing algorithm. However, it is difficult for this system to map three-dimensional shape of seagrass patches because the echosounder detects only narrow area along survey course of the vessel equipped with the echosounder. The single beam needs interpolation and geostatistics of data between survey courses. Patch distribution of shoots prevents the reconstruction of seagrass canopy by using only one single beam. Thus the multi-beam sonar is more precise than the single beam for detection and explicit measurement of canopy geometry, and estimation of the volume occupied by the seagrass.

The lower depth limit of seagrass beds is related to the light extinction coefficient, which affects the minimum degree of light required for seagrass growth (Duarte, 1991). Thus, it can be used as an indicator of water quality. In France, the lower depth limit of *P. oceanica* was monitored by placing concrete markers (Meinesz, 1977). In this case, the results were very precise, but the area of observation was limited. In contrast, multi-beam sonar can be used to define

the vertical distribution and the lower depth limits of seagrass beds by correcting depths measured by the echosounder to mean sea level. Therefore, monitoring the lower depths with multi-beam sonar is useful for detecting the lower limits of seagrass beds precisely over a wide area.

Multi-beam sonar can scan a seagrass bed with an area of 115 m × 156 m at bottom depths between 2 and 8 m within about 40 min when traveling at about 1.5 m s^{-1} (3 knots). The survey produces bottom distributions in the entire scanned area, except in places that the boat cannot approach. It is therefore possible to investigate about 500 m × 800 m per day at bottom depths of 6 m with 60 s per turn of a boat at the end of survey line, and under a condition of 25% overlap of width scanned along two neighboring lines when a boat with an echosounder travels at 1.5 m s^{-1} for 10 h. In this way, multi-beam sonar is a very useful apparatus for mapping seagrass beds and visualizing the underwater landscape.

5. Conclusion

Mapping with multi-beam sonar is a simple, labor-saving, and efficient method to assess the three-dimensional distribution of seagrass canopies. It can be used to estimate the volume and area occupied by seagrass, and, in conjunction with quadrat sampling, the biomass of seagrass beds can also be estimated. The results of such a three-dimensional investigation can then be used to study seagrass ecology from a landscape approach.

Acknowledgements

We thank Mr. Koichi Morita and other staff of the Otsuchi Center for Marine Science, and Mrs. Hiroko Aoyama, University of Tokyo, for their help during our field survey and research. We are also grateful to Prof. Yoshinobu Miyazaki of the University of Tokyo and Mr. Toshio Oyagi and Kazuhiro Hantani of Toyo Corporation for their encouragement. This study was supported in part by a grant from the Ministry of Education, Culture, Sports, Science, and Technology and by a grant from the Ministry of Agriculture, Forestry, and Fisheries.

References

Aioi, K., Komatsu, T., Morita, K., 1996. Giant seagrass, *Zostera caulescens*, discovered in Funakoshi Bay, Iwate Prefecture. Bull. Japan. Soc. Fish. Oceanogr. 60, 7–10 (in Japanese with English Abstract).

Aioi, K., Komatsu, T., Morita, K., 1998. The world's longest seagrass, *Zostera caulescens* from northeastern Japan. Aquat. Bot. 61, 87–93.

Arasaki, M., Arasaki, T., 1978. Compilation of Stories on Algae. Tokai University Press, Tokyo (in Japanese).

Belsher, T., 1989. Apports du satellite SPOT à la cartographie des végétaux marins. La Mer 27, 144–145.

Boudouresque, C.-F., Charbonel, E., Meinesz, A., Pergent, G., Pergent-Martini, C., Cadiou, G., Bertrandy, M.C., Foret, P., Ragazzi, M., Rico-Raimondino, V.A., 2000. Monitoring network based on the seagrass *Posidonia oceanica* in the northwestern Mediterranean Sea. Biol. Mar. Medit. 7, 328–331.

Colantoni, P., Gallignani, P., Fresi, E., Cinelli, F., 1982. Patterns of *Posidonia oceanica* (L.) Delile beds around the Island of Ischia (Gulf of Naples) and in adjacent waters. P.S.Z.N. Mar. Ecol. 3, 53–74.

Coles, R.G., Lee Long, W.J., Watson, R.A., Derbyshire, K.J., 1993. Distribution of seagrasses, and their fish and penaeid prawn communities, in Cairns Harbour, a tropical estuary, northern Queensland, Australia. Aust. J. Mar. Freshw. Res. 44, 193–210.

Dennison, W.C., Orth, R.J., Moore, K.A., Stevenson, J.C., Carter, V., Kollar, S., Bergstrom, P.W., Batiuk, R.A., 1993. Assessing water quality with submerged aquatic vegetation: Habitat requirements as barometers of Chesapeake Bay health. Bioscience 43, 86–94.

Division of Wildlife, the Ministry of Environment of Japan, 2000. Threatened Wildlife of Japan: Vascular Plants: Red Data Book. second ed. Japan Wildlife Research Center, Tokyo (in Japanese).

Duarte, C.M., 1991. Seagrass depth limits. Aquat. Bot. 40, 363–377.

Hatakeyama, Y., Maniwa, Y., 1978. On the investigation of seaweed distribution by utilizing a fish finder. Tech. Rep. Fishing Boat 73, 155–168 (in Japanese).

Hoshino, Y., 1972. Pollution in the Seto Inland Sea. Iwanami, Tokyo (in Japanese).

Jeudy de Grissac, A., Boudouresque, C.-F., 1985. Rôle des herbiers de Phanérogames marines dans les mouvements des sédiments côtiers : les herbiers à *Posidonia oceanica*. In: Ceccaldi, H.J., Champalbert, G. (Eds.), Acte du Colloque Pluridisciplinaire Franco-Japonais d'Océanographie. Soc.Franco-Japonaise Océanogr. vol. 1, Marseille, pp. 143–151.

Komatsu, T., 1989. Day-night reversion in the horizontal distributions of dissolved oxygen content and pH in a *Sargassum* forest. J. Oceanogr. Soc. Japan 45, 106–115.

Komatsu, T., 1997. Long-term changes in *Zostera* bed area in the Seto Inland Sea (Japan), especially along the coast of Okayama Prefecture. Oceanol. Acta 20, 209–216.

Komatsu, T., Igarashi, C., Tatsukawa, K., Nakaoka, M., Hiraishi, T., Taira, A., 2002. Mapping of seagrass and seaweed beds using hydro-acoustic methods. Fish. Sci. 68 (Suppl. 1), 580–583.

Komatsu, T., Kawai, H., 1986. Diurnal changes of pH distributions and the cascading of shore water in a *Sargassum* forest. J. Oceanogr. Soc. Japan 42, 447–458.

Komatsu, T., Kawai, H., Sakamoto, W., 1990. Influences of *Sargassum* forest on marine environments. Bull. Coast. Oceanogr. 27, 115–126 (in Japanese with English abstract).

Komatsu, T., Mikami, A., Sultana, S., Ishida, K., Hiraishi, T., Tatsukawa, K., 2003. Hydro-acoustic methods as a practical tool for cartography of seagrass beds. Otsuchi Mar. Sci. 28, 72–79.

Komatsu, T., Murakami, S., 1994. Influence of a *Sargassum* forest on the spatial distribution of water flow. Fish. Oceanogr. 3, 256–266.

Komatsu, T., Nakaoka, M., 2000. Water flow and sedimentation rate in seagrass beds off Khao Bae Na in Trang Province, Thailand. Biol. Mar. Meditter. 7, 240–242.

Komatsu, T., Tatsukawa, K., 1998. Mapping of *Zostera marina* L. beds in Ajino Bay, Seto Inland Sea, Japan, by using echosounder and global positioning systems. J. Rech. Océanogr. 23, 39–46.

Komatsu, T., Yamano, H., 2000. Influence of seagrass vegetation on bottom topography and sediment distribution on a small spatial scale in the Dravuni Island Lagoon, Fiji. Biol. Mar. Meditter. 7, 243–246.

Lee Long, W.J., Mckenzie, L.J., Rasheed, M.A., Coles, R.G., 1996. Monitoring seagrasses in tropical ports and harbours. In: Kuo, J., Phillips, R.C., Walker, D.I., Kirkman, H. (Eds.), Seagrass Biology: Proceedings of an International Workshop, Rottnest Island, Western Australia, 25–29 January 1996. Faculty of Science, The University of Western Australia, Nedlands, pp. 345–350.

Long, B.G., Skews, I.D., Pointer, I.R., 1994. An efficient method for estimating seagrass biomass. Aquat. Bot. 47, 277–292.

Meinesz, A., 1977. Balisage de la limite inférieure de l'herbier de *Posidonia oceanica* en rade de Villefranche-sur-Mer (Alpes-Maritimes, France) Rapp. P.V. Réunion Comm. Int. Explor. Sci. Medit. 24, 143–144.

Meinesz, A., Laurent, R., 1978. Cartographie et état de la limite inférieure de l'herbier de *Posidonia oceanica* dans les Alpes-Maritimes (France) – Campagne Poseidon 1976. Bot. Mar. 21, 513–526.

Meinesz, A., Cuvelier, M., Laurent, R., 1981. Méthode récentes de cartographie et de surveillance des herbiers de Phanérogames marines. Vie Milieu 31, 27–34.

Orth, R.J., Heck, K.L.J., Van Monfrans, J., 1984. Faunal communities in seagrass beds. A review of the influence of plant structure and prey characteristics on predator-prey relationships. Estuaries 7, 339–350.

Pasqualini, V., Pergent-Martini, C., Clabaut, P., Pergent, G., 1998. Mapping of *Posidonia oceanica* using aerial photographs and side scan sonar: Application off the Island of Corsica. Estuar. Coast. Shelf Sci. 47, 359–367 (France).

Piazzi, L., Acunto, S., Cinelli, F., 2000. Mapping of *Posidonia oceanica* beds around Elba Island (western Mediterranean) with integration of direct and indirect methods. Oceanol. Acta 23, 339–346.

Rey, J., Diaz del Rio, V., 1989. Cartographia de los fondos marinos de la Bachia de Palma (Baleares, Espana): Distribution de las praderas vegetales y sedimentos superficiales. In: Boudouresque, C.-F., Meinesz, A., Fresi, E., Gravez, V. (Eds.), International Workshop on Posidonia Beds 2. GIS Posidonie Press, Marseille, pp. 29–41.

Sabol, B.M., Melton, R.E., Chamberlain, R., Doering, P., Haunert, K., 2002. Evaluation of a digital echo sounder for detection of submersed aquatic vegetation. Estuaries 25, 133–141.

Short, F., Willie-Echeverria, S., 1996. Natural and human-induced disturbance of seagrasses. Environ. Conserv. 23, 17–27.

Sultana, S., Komatsu, T., 2002. Preliminary study on shoot density and biomass of seagrass, *Zostera caulescens*, in Funakoshi Bay off the Sanriku Coast, Japan. Otsuchi Mar. Sci. 27, 23–27.

Tatsukawa, K., Komatsu, T., Aioi, K., Morita, K., 1996. Distribution of seagrasses off Kirikiri in Funakoshi Bay, Iwate Prefecture, Japan. Otsuchi Mar. Res. Cent. Rep. 21, 489–494 (in Japanese).

Ward, L.G., Kemp, W.M., Boyton, W.R., 1984. The influence of waves and seagrass communities on suspended particulates in an estuarine embayment. Mar. Geol. 59, 85–103.

Available online at www.sciencedirect.com
SCIENCE DIRECT®
Aquatic Living Resources 16 (2003) 231–238
Aquatic Living Resources
www.elsevier.com/locate/aquliv

Foraging behaviour of tuna feeding on small schooling *Vinciguerria nimbaria* in the surface layer of the equatorial Atlantic Ocean

Frédéric Ménard [a,*], Emile Marchal [b]

[a] *IRD, Centre de Recherche Halieutique Méditerranéenne et Tropicale, BP 171, 34203 Sète cedex, France*
[b] *IRD, Institut Océanographique, 195, rue St Jacques, 75005 Paris, France*

Accepted 25 March 2003

Abstract

The feeding behaviour of small tuna on the mesopelagic fish *Vinciguerria nimbaria* was studied in an equatorial area of the Atlantic Ocean (10–20° W, 0–5° N). Acoustic data (from a scientific cruise) and tuna stomach content data (from the tuna purse-seine fishery) were combined. *V. nimbaria* formed loose schools that occurred in clusters during daytime, and large aggregations during the night. The characteristics of the schools and clusters were analysed. The average length, size and packing density of the day-school were estimated at 48.5 m, 24 400 individuals, and 5.8 fish m^{-3}, respectively. The average length of clusters was close to 10 km. The packing density of night-school was estimated at 1.6 fish m^{-3}. The preying of tuna on *V. nimbaria* was modelled as a stochastic process based on two Poisson processes. Daily rations of tuna were estimated at 3.5% and 7% of the body weight. Taking into account the swimming performance of the prey and the predator, we showed that tuna were able to feed on day-schools in a very short time, whereas feeding during the night by filtering was not competitive. Furthermore, a cluster is able to feed a single tuna school during 2 months, proving the sustainability of the biomass of small tuna in the area by *V. nimbaria*.

Keywords: Acoustics; Feeding; Foraging behaviour; Predator-prey interactions; Schools; Tuna; *Vinciguerria nimbaria*

1. Introduction

Fish develop a broad variety of feeding strategies (Lazzaro, 1987; Gerking, 1994). Two main feeding behaviours are observed among pelagic species: particulate feeding (including fish that eat other fish) and filter feeding. The former is distinguished from the latter by the visual detection of prey. Both types of feeding may be sequenced in successive events. Faced with prey that form schools, the predation-act can be split into two phases: seeking out the school, and then catching prey inside the school. The first phase includes detection and pursuit, the second, capture by sight or filtration, according to the packing density of the school, the reaction of the prey, the illumination and the retention ability (mouth and branchial filters).

Tropical tuna grow rapidly and have high swimming performance. They live in the pelagic ocean environment which has been generally considered as poor in prey (Blackburn, 1968). They can shift from one food source to another, preying upon anything they encounter (if they can capture and ingest it). They thus feed on varied prey including numerous fish, crustaceans, squid and gelatinous organisms. They do not always chase individual prey but commonly seek out schools of favoured targets (Gerking, 1994). To feed on fast swimming epi-pelagic fish, like sardines or anchovies that form highly dense schools on the continental shelves, tuna have to track and eat them as quickly as possible. Faced with small prey that form loose schools and swim slowly, tuna have to adapt their capture strategy. Are tuna able to use some kind of filtration? Indeed, most species of tuna have well developed gill rakers (Magnuson and Heitz, 1971). If the tuna feed during the night, such an apparatus could prevent food loss through the operculum gap.

In an equatorial area of the Atlantic Ocean (10–20° W, 0–5° N), where large purse-seine fishery occurs, the presence of seasonal tuna concentrations was studied within the context of a research programme, PICOLO, conducted by Institut de Recherche pour le Développement (IRD) (Ménard et al., 2000a). In this area, skipjack (*Katsuwonus pelamis*) and

* Corresponding author.
E-mail address: menard@ird.fr (F. Ménard).

doi:10.1016/S0990-7440(03)00040-8

juveniles of yellowfin (*Thunnus albacares*) and bigeye tuna (*Thunnus obesus*) of the same size (average fork length 46 cm) feed mainly on small-size mesopelagic fish *Vinciguerria nimbaria* (Phosichthyidae) (Ménard et al., 2000b). This foraging fish aggregates day and night in the top 200 m of the sea (Marchal and Lebourges, 1996). In this context, the feeding behaviour of the tuna and the predator-prey relationships were studied based on acoustic data and tuna stomach content data. Concentrations of *V. nimbaria* were observed during the scientific sea cruise P1 that took place in January-February 1997. This survey was conducted onboard the IRD R/V "Antea" in the area extending from 5° N to 0°. North south transects along the longitude 15° W was replicated eight times. The aim was to estimate the size of the schools, the distances between the schools and the packing densities of the schools. We also looked at the number of *V. nimbaria* in a dataset of tuna stomach content. We estimated the average meal size and the daily consumption using a mixed Poisson-Poisson model for a predator preying on a homogeneous prey (Magnússon and Aspelund, 1997). Taking into account the swimming performance of the prey and the predator, we then investigated the feeding behaviour of tuna during the day vs. the night, and the sustainability of the biomass of small tuna in the area by *V. nimbaria*.

2. Materials and methods

2.1. Acoustics

The R/V "Antea" was equipped with a dual-frequency (120 and 38 kHz) hull-fixed transducer echo sounder (OSSIAN, trademark). Continuous records were made during the entirety cruise. For this study, only the 38 kHz frequency was used. The packing density inside the aggregations, the size and the dimension of the schools, as well as the distance between schools have been acoustically assessed in relation to the time of the day and the depth, using the software Movies+ (Diner et al., 1989; Weil et al., 1993). Acoustic settings are displayed in Appendix A. Data is processed by layer (average Sv) and by school in the depth range 10–200 m. Movies+ provides many characteristics of each school, as physical or acoustics properties (Scalabrin and Massé, 1993). The data was corrected for geometry and density descriptors (Diner, 1999). When the correction was seemed improbable after the algorithm was applied, the school was discarded. We also applied a statistical correction to convert the average observed length of the school into "true" diameter by a factor of $4/\pi$, assuming a circular horizontal section (MacLennan and Simmonds, 1992). Packing densities were computed from Sv values, using a target strength (TS) of –56.7 dB for a 43 mm standard length (SL) and 0.6 g wet weight *V. nimbaria* (Lebourges-Dhaussy et al., 2000). A backscatter threshold for schools was defined as a minimum packing density (Swartzman and Hunt, 2000). We used 1 fish m^{-3} for night time and 2 fish m^{-3} for daytime, i.e. –56.7 and –53.7 dB, respectively. An efficient recursive function of S+SpatialStats (Kaluzny et al., 1998) was used to find the nearest neighbour distances between the day-schools. Frequency distributions of the variables characterising the schools are highly asymmetrical, and maximum values are outliers. In our approach, the population mean is the characteristic of interest. We used a robust procedure from a library of S-PLUS 6 to fit lognormal distributions and to estimate the lognormal means and the standard errors. There is several ways to define a cluster of schools. Petitgas et al. (2001) used a distance threshold. Here, cluster size was investigated using two independent methods with two datasets: the number of recorded schools per kilometre and the integration by depth layer per kilometre (i.e. the area backscattering strength averaged per kilometre; MacLennan et al., 2002), assuming that all the detected biomass was in schools. The first dataset we collected was smoothed with a moving average of order 1: a cluster was encountered when the number of schools per kilometre was greater than the mean in the smoothed series. In the second approach, the cluster size was estimated by the range of the variogram of the integration by depth layer per kilometre. This second method seems confident because it takes into account the intensity of the detection, the depth range in which the day-schools occurred, and avoid the use of a threshold. A spherical function was chosen to model the empirical variogram.

2.2. Micronekton observation and sampling

Observations included trawl sampling with a young-fish mid-water trawl (mouth of 10 m high and 15 m wide, 10 mm mesh in the cod-end), equipped with a trawl echo sounder. Trawling was targeted on school groups or scattering layers detected by echo sounding. Hauls ranged from depths of 20–135 m, with an averaged duration of 30 min. SLs of *V. nimbaria* specimens were measured and some fish were weighed (wet) at the laboratory.

2.3. Stomach content analysis

Stomachs were collected on tuna caught during daylight hours by the purse-seine fishery operating in the area. The length of each sampled fish was measured and the stomach was preserved in formalin or was deep-frozen. Stomach contents were weighed (wet) and sorted according to the food item and the degree of digestion. Four degrees of digestion similar to those used by Magnuson (1969) were assigned to each item, according to the state of the ingested prey. The rate of empty stomachs was very high, but a substantial number of small size tuna had only *V. nimbaria* as prey (for more details, see Ménard et al., 2000b). For these stomachs, *V. nimbaria* were counted and measured (empty stomachs were not taken into account). When identification was not possible, an empirical method based on the degrees of digestion was used for reconstructing the initial prey-weight prior to the digestion (Bard, 2001). In this approach, a "test animal" is selected (*Brama orcini* for the ingested fish) in order to compute weight loss factors of prey for each digestion

index. These coefficients allowed us to estimate the initial weight of the stomach content before it was digested. The reconstructed weight was divided by the average weight of an adult of *V. nimbaria* (0.6 g) in order to estimate the number of *V. nimbaria* in the stomach.

Based on the stochastic model of Magnússon and Aspelund (1997), the feeding of tuna that prey on schooling *V. nimbaria* can be described by two random variables. Let X be the number of encounters with prey per unit time interval (i.e. meal frequency), and Y be the amount of food obtained in each encounter (i.e. meal size). The former variable gives the number of schools encountered per unit interval, and the latter the number of prey captured in each encounter with a school. Let T be the length of time a *V. nimbaria* is identifiable in the stomach of a tuna, the amount of food obtained in this interval is

$$Z = \sum_{i=1}^{X} Y_i$$

assuming that the number of prey consumed in a time interval of length T is the same as the number found in the stomach, and that Y_i is the number of *V. nimbaria* obtained in the ith encounter. A common assumption for foraging models is that both X and Y have Poisson distributions with parameter λ and μ, respectively. Observed frequency distribution of stomach content allows us to estimate both parameters using the method of moments: $\mu = s^2/\bar{z} - 1$, and $\lambda = \bar{z}/\mu$, where $\bar{z}$ and s^2 are the calculated mean and variance of the number of prey in the stomach, respectively. Several assumptions of independence have to be stated. This simple model gives estimates of the average number of meals per unit of time ($\hat{\lambda}$) and the average meal size ($\hat{\mu}$) for small size tuna. These estimates allow us to compute the mean ($\hat{C}_W$) and variance ($s^2_{C_W}$) of the total consumption (wet weight) in the time interval T:

$$\hat{C}_W = \hat{\lambda}\hat{\mu}\hat{\mu}_W, \quad \text{and} \quad s^2_{C_W} = \hat{\lambda}(\hat{\mu}\hat{\sigma}^2_W + \hat{\mu}\hat{\mu}^2_W) + \hat{\lambda}\hat{\mu}^2\hat{\mu}^2_W \quad \text{with}$$

$\hat{\mu}_W = 0.6$ and $\hat{\sigma}_W = 0.21$ g, the average and the standard deviation of the weight of *V. nimbaria* in the area, respectively. If an estimate of T is available, the mean daily consumption can also be estimated (for more details, see Magnússon and Aspelund, 1997). Olson and Boggs (1986) gave values of T from gastric evacuation experiments on yellowfin tuna. T was estimated at 10 h using a mixed group of prey. However, for the small prey *Stolephorus purpureus* (nehu) similar to *V. nimbaria*, T was estimated at 5 h. We thus took these two limits to compute estimates of the total daily consumption by weight and per unit of body weight of a tuna.

3. Results

3.1. Schools during daytime

During the daytime, *V. nimbaria* were schooling (Fig. 1a). The usual depth is around 100 m. We assumed that the schools are circular in horizontal cross-section. The results

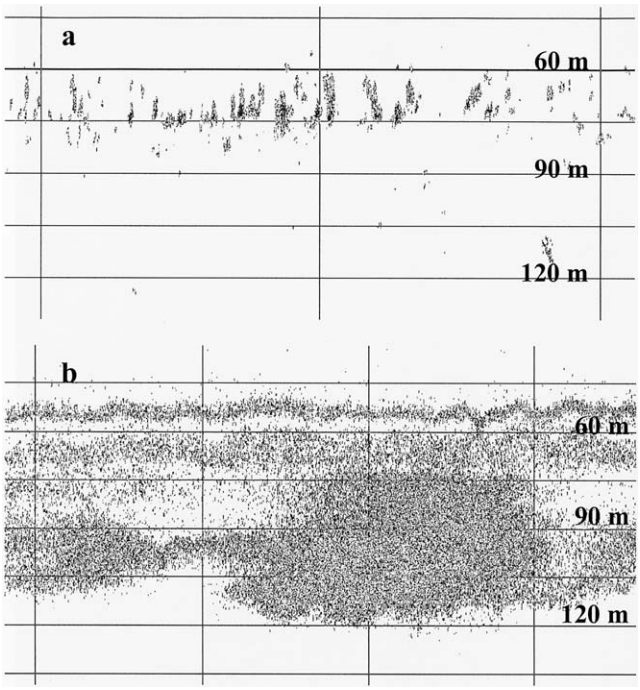

Fig. 1. Echogram showing (a) schools of *Vinciguerria nimbaria* adults during daytime, and (b) one "swarm" during the night. The distance between each vertical line is 1 nautical mile.

on the size of the schools are displayed in Fig. 2. The lognormal mean of the observed length was estimated at 38.1 m (standard error = 0.8). The mean diameter of the schools was 48.5 m after correction by a factor of (4/π). The lognormal mean of the height was estimated at 8.3 m (standard error = 0.2). The packing densities of the day-schools were highly variable but rather low given their small size and weak weight (0.6 g in average). The lognormal mean was estimated at 5.8 m^{-3} (standard error = 0.1). The number of fish in a school was then deducted, assuming a school in the shape of a cylinder. The observed cross-section was assumed to be equal to the section of an equivalent cylinder whose height was unknown. The volume of the school was computed from the estimate of the lognormal mean of the section (110.5 m^2), and from the mean diameter of the schools (48.5 m). In average, the number of fish in a school of *V. nimbaria* was thus estimated at 24 400 individuals.

The distances between the day-schools were computed from the relative coordinates in the horizontal cross-section and the depth of the centres of gravity of each of the schools. We selected the schools identified between 50 and 110 m only, because (i) schools were the most abundant in this range, (ii) we limited the bias linked to the acoustic records (variability of the scattering volumes), (iii) and small size tuna can dive to feed at this depth. The lognormal mean of the nearest distance between neighbouring schools was estimated at 124 m (standard error = 5). This is thus a robust estimate of the nearest distance between the gravity centres of the day-schools inside a cluster of schools.

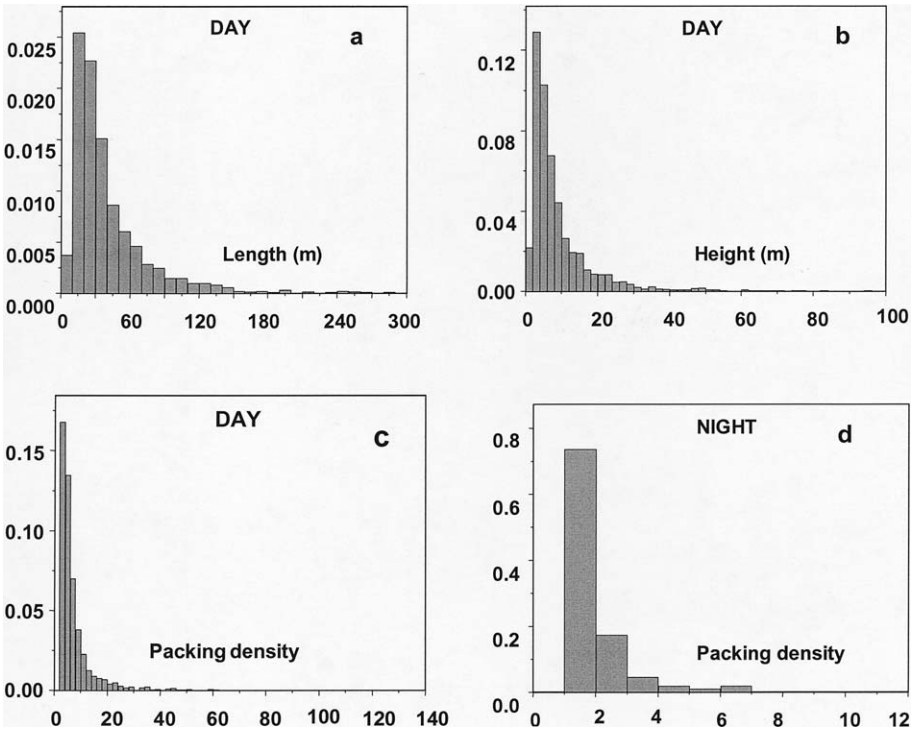

Fig. 2. Histograms scaled as probability densities for (a) the length and (b) the height of the day-schools of *Vinciguerria nimbaria*, and for the packing densities during (c) the day and (d) the night. Robust estimates of lognormal means (standard errors) were 38.08 m (0.77), 8.29 m (0.20), 5.78 fish m^{-3} (0.09), and 1.61 fish m^{-3} (0.06), respectively.

3.2. Clustering

Schools of *V. nimbaria* occurred in clusters during daytime. The total average number of schools per kilometre is 5.5. This threshold allowed us to estimate the average size of a cluster (12.6 km), the average distance between the clusters (11.3 km), and the average number of schools per kilometre inside a cluster (9.7 schools km^{-1}). The empirical variogram for the area backscattering strengths averaged per kilometre shows a plateau (Fig. 3). The range of the corresponding spherical model was estimated at 10.4 km that was very close to the preceding estimation of the size of a cluster. The distance between clusters was highly variable. The clusters probably occurred in groups of clusters. But the acoustical observations recorded during the cruise did not allow us to precisely estimate this spatial organisation. However, the frequency distribution of the distances between clusters showed two patterns (Fig. 4): the main one at short distance (2–19 km), and the other at large distance (41, 61 and 90 km).

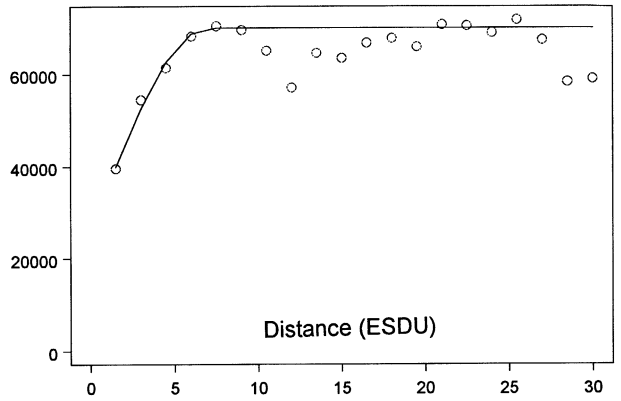

Fig. 3. Empirical variogram and fit of a spherical model for the integration by depth layer and per kilometre (range = 7, sill = 44 000, nugget = 26 000). *X*-axis is expressed in ESDU and can be converted into kilometre by a factor of 1.482.

3.3. Schools during the night

During the night, *V. nimbaria* were also schooling. Schools were localised at the bottom of the thermocline (80–100 m) or just below (110–130 m). The shape and the size of the schools were completely different from those observed during daytime (Fig. 1b). The sizes we observed were very large, around 3000 m, sometimes twice that. Since the software Movies+ is not adapted to such length of schools, these lengths were directly read on the echograms. The packing density was very low: the lognormal mean is

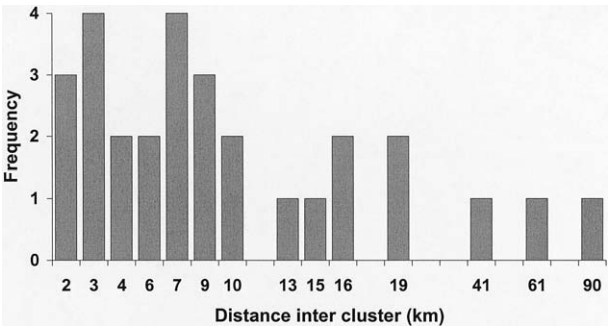

Fig. 4. Frequency distribution of the distances between clusters.

estimated at 1.6 fish m^{-3}, with a standard error of 0.1 (Fig. 2d). The average distance between these schools was about two times their length. They were also grouped in clusters, with very variable but sometimes long distances between them (20 km in average). In reference to krill, we named this type of school "swarm".

3.4. Vinciguerria sampling

The adults of *V. nimbaria* (SL ≥ 30 mm) sampled during the day and the night had the same length distribution (Fig. 5). The juveniles were caught in the surface layer during the night only. These juveniles were not mixed with the adults, instead they were dispersed in layers at the thermocline level.

3.5. Tuna stomach contents

Nearly all of the *V. nimbaria* found in the stomachs of the sampled tuna were adults: they fell into a narrow size range, 39–48 cm. Fig. 6 displays the observed frequency distribution of *V. nimbaria* numbers in the tuna stomachs. The sample mean was 45.4 (variance = 1149; maximum = 150). The average meal frequency based on the Poisson-Poisson

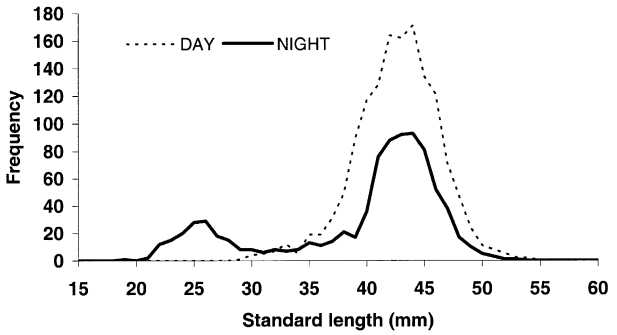

Fig. 5. Frequency distribution of *Vinciguerria nimbaria* standard length, caught night and day by trawling.

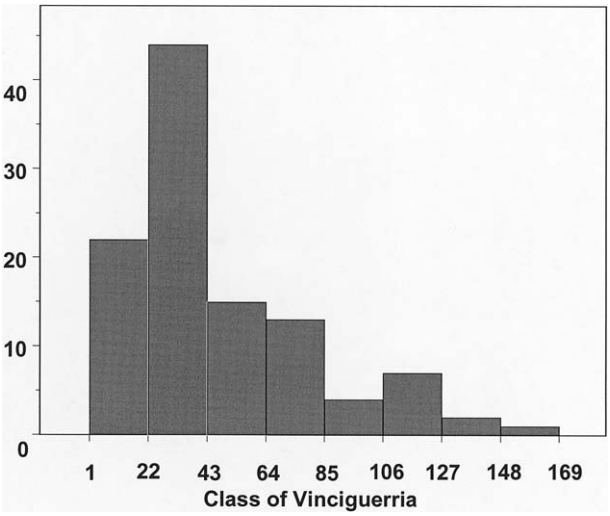

Fig. 6. Frequency distribution of *Vinciguerria nimbaria* number in stomachs of the sampled tuna.

Table 1
Estimates of average number of meals per unit time (λ), meal size (μ), and average time between meals (1/λ) using the method of moments

Parameter	λ	μ	$1/\lambda$
Estimates	1.9	24.3	0.53

Table 2
Average daily consumption and average daily consumption per unit of body weight as a function of *T*, the length of time a *V. nimbaria* is recognisable in the tuna stomach

T (h)	Time between meals (h)	Daily consumption (g d^{-1})	Daily ration (per body weight)
5	2 h 50 min	133	7%
10	5 h 40 min	66.5	3.5%

model was estimated at 1.9 meals per unit interval (*T*), i.e. the time a *V. nimbaria* is recognisable in the stomach, and the average meal size of almost 25 individuals (Table 1). The average and standard deviation of consumption in time *T* were estimated at 27.7 and 20.9 g, respectively. A tuna with a fork length of 46 cm has an average weight of 1.9 kg. Using the two limits of *T* (5 and 10 h) based on the gastric evacuation experiments on yellowfin tuna, estimates of the daily consumption and consumption as a percentage of body weight were computed (Table 2). For *T* equals to 5 h, the daily ration is estimated at 7% of the tuna body weight and at 3.5% for *T* equals to 10 h.

3.6. Feeding behaviours

The acoustical results and the stomach data are now combined to analyse the foraging behaviour of tuna feeding on *V. nimbaria* schools. Let us consider one single tuna which encounters a cluster of *V. nimbaria* schools during daytime. The feeding involves successive captures of prey with a feeding speed that we ranged from 0.5 to 6 tuna body lengths per second (BL s^{-1}). Equally, we considered that *V. nimbaria* cannot avoid an attack of a tuna predator, because of its small size (no predator avoidance reaction was assumed for the prey). We assumed that the tuna that has encountered a school in the cluster, simply swam at the same depth and at a regular speed, feeding on all the prey he met in front of him. The size of the meal for the tuna was established at 100 *V. nimbaria*. This is a very conservative hypothesis regarding our estimations ($\hat{\mu} = 25$), but it represents roughly 3.1% of the body weight of the predator. An average packing density of 6 fish m^{-3} leads to an average distance between fish inside the school of $1/\sqrt[3]{6} = 0.55$ m. According to its speed, the tuna filled its stomach in less than 15 min (Fig. 7a). At 6 BL s^{-1}, the computed time to catch 100 preys was only 2 min. Now, let us consider the same tuna encountering a swarm of *V. nimbaria* during the night. Since visual detection of prey is not possible, the tuna is assumed to feed by filtration. In this theoretical case, the time to prey on the same number of *V. nimbaria* depends on the packing density, the gap of the mouth and the speed of the fish. The mouth section was assumed to be circular and the radius was estimated at

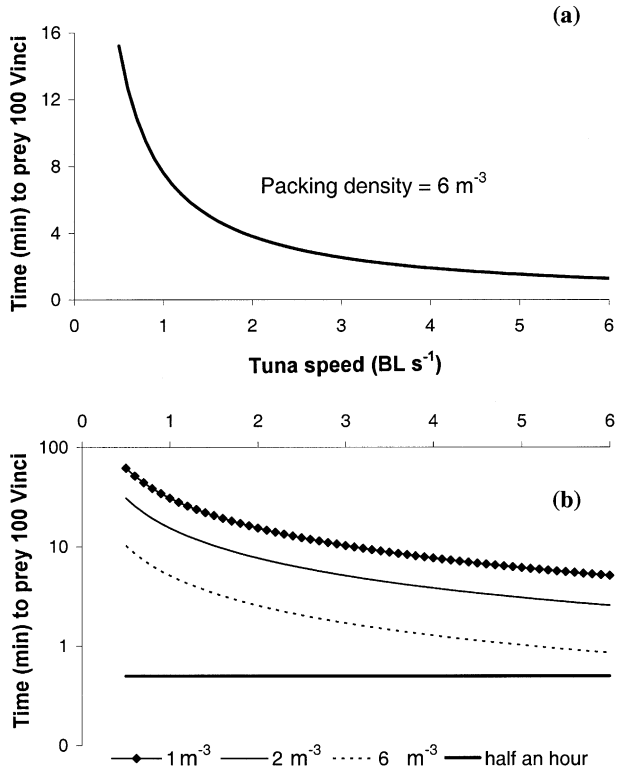

Fig. 7. Computed time for one tuna to fill its stomach with 100 *Vinciguerria nimbaria* as a function of tuna speed and packing density. (a) Model for the day; (b) model for the night.

0.025 m (unpublished data). We supposed that the tuna swam with its mouth open. The time necessary to fill its stomach was calculated as a function of the packing density (varying from 1, 2 and 6 fish m^{-3}) and of the tuna velocity (Fig. 7b). At 2 BL s^{-1}, the tuna needed between 3 and more than 15 h to fill its stomach, depending on the increasing values of the packing density.

Now let us consider a school of small tuna (mean individual weight = 1.9 kg). Such a school, which weighs 38 metric tons on average (purse seine catch statistics in the area), has 20 000 individuals. Based on the estimated daily rations (mean of 7% and 3.5%), 3 million *V. nimbaria* have to be fed on by tuna each day (prey biomass = 1.8 metric tons), corresponding to 126 day-schools. Assuming that a cluster of schools is isotropic, considering the number of schools per kilometre inside the cluster, and the average diameter of a cluster, the number of schools inside a cluster is estimated at 8000. Thus, a cluster is able to feed a single tuna school during 2 months, or 63 schools of tuna during 1 d.

4. Discussion

The estimate of the packing density is dependent on the TS of *V. nimbaria*. TS measurements of mesopelagic fish are scarce. Bagøien et al. (2001) measured the TS of adults of two mesopelagic fish, *Maurolicus muelleri* and *Benthosema glaciale* (–59.3 and –58.0 dB, respectively), using a split-beam 38 kHz. Both species are close in shape and size to *V. nimbaria*. According to their data, we computed the average SL of their samples: 42.9 and 55.5 mm, respectively. Thus, for the same size, the difference is 2.6 dB between *M. muelleri* and *V. nimbaria*. Measurements were made in the near-surface waters during the diel vertical migration, following the same procedure we followed for *V. nimbaria*. Bias could affect both measurements, especially if the fish was swimming up during the experiment (Torgersen and Kaartvedt, 2001). It is thus difficult to interpret this difference that could be related to the species. For example, the swimbladder of *V. nimbaria* is well developed, probably more than the other species (Marshall, 1960). Anyway, even a bias of ±3 dB (that doubles or divides by 2 our packing density estimates) could not modify the conclusions with respect to the tuna feeding pattern. The packing density we estimated looks very low in comparison with those of true pelagic fish. However, such low densities were also recorded with other mesopelagic fish in "dense" layers. In the Gulf of Oman, trawling by the R.V. *Dr. Fridtjof Nansen* equipped with a krill trawl led to a catch of 0.6–1.6 fish m^{-3} during the night, and 8 fish m^{-3} during the day, of *Benthosema pterotum*, a very common small Myctophid (Sætersdal et al., 1999).

The thresholds and the acoustical parameter setting are also key parameters. Moreover, the day-schools of *V. nimbaria* appear to be very loose, and the night-swarms very large. In order to compare day and night data, we set the same signal thresholds for both aggregations, but we made different choices for schools and layer. Indeed, the –59 dB acoustical value used for schools also catches other scatters during the night. The –50 dB threshold discards most of them and reduces slightly the integrated day-values in comparison with the –59 dB threshold (about 10% less). But in this study, the integration layer process was only used for characterisation of the clusters, and not strictly for biomass estimation. However, the relation between the night-swarms and the clusters should be more investigated.

The preying of tuna on *V. nimbaria* is modelled as a stochastic process based on two Poisson processes. No satiation effect are taken into account, and the underlying hypotheses of independence are sometimes hard to hold, i.e. the time between meals is independent of the size of the meal, schools are assumed to be randomly distributed. This simple approach can be extended using, for instance, a Poisson-negative binomial model, as proposed by Magnússon and Aspelund (1997). However, the aim here was to have simple estimates of meal size and of daily consumption of tuna feeding on schooling *V. nimbaria*, using stomach content data that were not sampled at the same time as the acoustic data. We thus did not take into account the empty stomachs and other prey than *V. nimbaria* was ignored. Especially, the time spent by one tuna to seek a cluster of prey schools has not been assessed. But the time for one tuna to join one school to another inside a cluster is negligible, because of the short average distance between them. Therefore, our daily consumption results concern tuna who found schools of

V. nimbaria. If empty stomachs would had been included in the analysis (but no representing sample was available), the overall encounter rate and the consumption estimates would have been lower. But our results in terms of daily rations (between 3.5% and 7%) were similar to those obtained elsewhere. Using a completely different approach based on stomach contents, Olson and Boggs (1986) estimated the ration of yellowfin tuna of the Eastern Tropical Pacific Ocean at 3.9% of the fish's body weight. Ménard et al. (2000b) followed the same procedure and found that the daily ration varies from 1% to 6%. Furthermore, Magnuson (1969) quoted that the maximum capacity of the stomach of a captive skipjack tuna was about 7% of its body weight.

Tuna clearly do not always hunt individual prey but seek out schools of favoured targets. Once a concentration is detected (the encounter with a group of prey), the feeding involves successive captures of individuals, given a handling time and a "feeding" swimming speed for tuna that in this case fed on a quasi-static prey. Actually, skipjack tuna is one of the scombrids species with the fastest recorded cruising speeds. But the sustained speed in scombrids is variable, ranging from 1 to 10 BL s^{-1}, whereas burst speeds can reach 12–15 BL s^{-1} (Altringham and Shadwick, 2001). On the other hand, the small size of *V. nimbaria* leads to a swimming speed of one order of magnitude less than the swimming speed of tuna. Measurements were made with a split-beam on a similar species (Torgersen and Kaartvedt, 2001). These authors found an average speed of about 30 cm s^{-1}. We thus considered that *V. nimbaria* cannot avoid an attack from a tuna predator. Furthermore, this mesopelagic species is probably not adapted to support a high level of light. The length of time tuna feed on *V. nimbaria* during daytime remains very short. We did not take into account the handling time, and we certainly slightly underestimated the total feeding time. But the computed time for feeding during the night is probably higher. Actually, the speed of a tracked skipjack tuna was recorded in the area. This tuna swam in a cluster of schools during daytime (Fig. 11 in Marchal et al, 1996). Its average speed was about 2 BL s^{-1} and its track was linear in direction and depth. During the night, the same fish was swimming more slowly. Thus, small surface tuna are able to feed during daytime on very loose schools of small fish in a very short time. On the opposite, feeding during the night by filtering is definitely not competitive in this context, and may explain why tuna do not use this type of feeding.

Schooling behaviour is common among fish, but the characteristic pattern of schooling behaviour is variable (see Fréon and Misund, 1999). For epi-pelagic fish (e.g. anchovy), the schools are generally large and their overall packing density is very high in comparison with *V. nimbaria*. However, *V. nimbaria* compensate by a high number of small day-schools grouped in clusters in the surface layer, whereas such a fish normally lives at depth during daytime. In that sense, *V. nimbaria* is a favourable target-prey for small size tuna in the equatorial Atlantic Ocean. The underlying simple assumptions we used to study the foraging behaviour of tuna feeding on schooling *V. nimbaria* allow us to make more qualitative, rather than quantitative, conclusions. Simple feeding models based on information on school density and distances, swimming speed and detection range of the predator, combined with independent assessment of encounter rate estimated from stomach analysis, seem a promising tool for investigating foraging behaviour.

Appendix A

A.1. *Acoustic settings*

Acquisition threshold = –65 dB.

A.2. *Processing settings*

Parameters	Day	Night
(1) Schools		
Minimum signal threshold (dB)	–59	–59
Maximum signal threshold (dB)	–10	–10
Minimum school Sv threshold (dB)	–53.7	–56.7
Minimum length (m)	10	500
Maximum length (m)	5000	5000
Minimum height (m)	2	20
Maximum height (m)	100	100
Minimum area (m^2)	20	500
Maximum area (m^2)	100 000	100 000
Authorized horizontal gap (ping)	2	0
Authorized vertical gap (m)	2	0
Minimum depth processed (m)	20	80
Maximum depth processed (m)	200	200
Processing distance (nautical mile)	2	10
(2) Layers		
Minimum depth processed (m)	10	10
Maximum depth processed (m)	200	200
Total number of layers	10	10
Processing distance (nautical mile)	1	1
Minimum signal threshold (dB)	–50	–50
Maximum signal threshold (dB)	–10	–10
(3) Target strength (dB)		
Vinciguerria nimbaria 43 mm SL	–56.7	–56.7

References

Altringham, J.D., Shadwick, R.E., 2001. Swimming and muscle function. In: Block, B.A., Stevens, E.D. (Eds.), Tuna. Physiology, Ecology, and Evolution. Academic Press, San Diego, pp. 313–344.

Bagøien, E., Kaartvedt, S., Aksnes, D.L., Eiane, K., 2001. Vertical distribution and mortality of overwintering *Calanus*. Limnol. Oceanogr. 46, 1494–1510.

Bard, F.X., 2001. Apparent effect of stomach repletion on catchability of large tunas to longline gear. Comparison with other fishing gears. Collect. Vol. Sci. Pap. ICCAT 52, 452–465.

Blackburn, M., 1968. Micronekton of the eastern tropical Pacific Ocean: family composition, distribution, abundance and relations to tuna. Fish. Bull. 67, 71–115.

Diner, N., 20–22 April 1999. Corrections on school geometry and density descriptors; use of the algorithm on school actual detection. FAST working group, St John, Newfoundland.

Diner, N., Weil, A., Coail, J.Y., Coudeville, J.M., 1989. INES-MOVIES: a new acoustic data acquisition and processing system. ICES C.M. 1989/B.45.

Fréon, P., Misund, O.A., 1999. Dynamics of pelagic fish distribution and behaviour: effects on fisheries and stock assessment. Fishing News Books.

Gerking, S.D., 1994. Feeding Ecology of Fish. Academic Press, San Diego.

Kaluzny, S.P., Vega, S.C., Cardoso, T.P., Shelly, A.A., 1998. S+SpatialStats: User's Manual for Windows and UNIX. Springer, New York.

Lazzaro, X., 1987. A review of planktivorous fishes: their evolution, feeding behaviours, selectivities, and impacts. Hydrobiologia 146, 97–167.

Lebourges-Dhaussy, A., Marchal, E., Menkès, C., Champalbert, G., Biessy, B., 2000. *Vinciguerria nimbaria* (Micronekton), environment and tuna: their relationships in the Eastern Tropical Atlantic (ETA area). Oceanol. Acta 23, 515–528.

MacLennan, D.N., Simmonds, E.J., 1992. Fisheries Acoustics. Chapman & Hall, London.

MacLennan, D.N., Fernandes, P.G., Dalen, J., 2002. A consistent approach to definitions and symbols in fisheries acoustics. ICES J. Mar. Sci. 59, 365–369.

Magnuson, J.J., 1969. Digestion and food consumption by skipjack tuna (*Katsuwonus pelamis*). Trans. Am. Fish. Soc. 98, 379–392.

Magnuson, J.J., Heitz, J.G., 1971. Gill raker apparatus and food selectivity among mackerels, tunas, and dolphins. Fish. Bull. 69, 361–370.

Magnússon, K.G., Aspelund, T., 1997. A model for estimating meal frequency and meal size from stomach data with an application to Atlantic cod (*Gadus morhua*) feeding on capelin (*Mallotus villosus*). Can. J. Fish. Aquat. Sci. 54, 876–889.

Marchal, E., Lebourges, A., 1996. Acoustic evidence for unusual diel behaviour of a mesopelagic fish (*Vinciguerria nimbaria*) exploited by tuna. ICES J. Mar. Sci. 53, 443–447.

Marchal, E., Josse, E., Lebourges, A., 1996. Prédateurs et proies: une approche acoustique. Oceanis 22, 117–132.

Marshall, N.B., 1960. Swimbladder structure of deep-sea fishes in relation to their systematics and biology. Discovery Rep. 31, 1–122.

Ménard, F., Fonteneau, A., Gaertner, D., Nordstrom, V., Stéquert, B., Marchal, E., 2000. Exploitation of small tunas by a purse seine fishery with fish aggregating devices and their feeding ecology in an eastern tropical Atlantic ecosystem. ICES J. Mar. Sci. 57, 525–530.

Ménard, F., Stéquert, B., Rubin, A., Herrera, M., Marchal, E., 2000. Food consumption of tuna in the Equatorial Atlantic ocean: FAD-associated versus unassociated schools. Aquat. Living Resour. 13, 233–240.

Olson, R.J., Boggs, C.H., 1986. Apex predation by yellowfin tuna (*Thunnus albacares*): independent estimates from gastric evacuation and stomach contents, bioenergetics, and Cesium concentrations. Can. J. Fish. Aquat. Sci. 43, 1760–1775.

Petitgas, P., Reid, D., Carrera, P., Iglesias, M., Georgakarakos, S., Liorzou, B., Massé, J., 2001. On the relation between schools, clusters of schools, and abundance in pelagic fish stocks. ICES J. Mar. Sci. 58, 1150–1160.

Sætersdal, G., Bianchi, G., Strømme, T., Venema, S.C., 1999. Dr. Fridtjof Nansen programme 1975– 1993. Investigations of fishery resources in development regions. History of the programme and review of results. F.A.O. Fish. Tech. Pap., 391.

Scalabrin, C., Massé, J., 1993. Acoustic detection and the spatial and temporal distribution of fish shoals in the Bay of Biscay. Aquat. Living Resour. 6, 269–283.

Swartzman, G., Hunt, G., 2000. Spatial association between murres (*Uria* spp.), puffins (*Fratercula* spp.) and fish shoals near Pribilof Islands, Alaska. Mar. Ecol. Prog. Ser. 206, 297–309.

Torgersen, T., Kaartvedt, S., 2001. In situ swimming behaviour of individual mesopelagic fish studied by split-beam echo target tracking. ICES J. Mar. Sci. 58, 346–354.

Weil, A., Scalabrin, C., Diner, N., 1993. MOVIESB: an acoustic detection description software. Application to shoal species classification. Aquat. Living Resour. 6, 255–267.

Available online at www.sciencedirect.com
SCIENCE DIRECT®
Aquatic Living Resources 16 (2003) 239–245
Aquatic Living Resources
www.elsevier.com/locate/aquliv

Relationship between abundance of small pelagic fishes and environmental factors in the Colombian Caribbean Sea: an analysis based on hydroacoustic information

Jorge Paramo [a,*], Renato A. Quiñones [b], Argiro Ramirez [b,c], Rodrigo Wiff [b]

[a] *Instituto de Investigación Pesquera (Inpesca), Av. Cristóbal Colón 2780, Casilla 350, Talcahuano, Chile*
[b] *Departamento de Oceanografía, Universidad de Concepción, Casilla 160-C, Concepción, Chile*
[c] *Instituto Nacional de Pesca y Acuicultura, Apartado Aéreo 10140, Buenaventura, Colombia*

Accepted 1 April 2003

Abstract

The most important pelagic artisanal fishery of the Colombian Caribbean Sea is the Atlantic thread herring (*Opisthonema oglinum*) and the associated species scaled herring (*Harengula jaguana*), round sardinella (*Sardinella aurita*), and scad (*Decapterus punctatus*). The largest aggregations of these small pelagics were found in the La Guajira area, where the local oceanography is modulated by seasonal upwelling intensity. We analysed the associations between the distribution of these small pelagic fishes and the environmental variables. A cumulative frequency method and a Monte Carlo randomization were used to detect associations between fish density and environmental variables. The adults of Atlantic thread herring were found in the upwelling area of La Guajira Peninsula and were associated to waters with temperature and salinity values higher than 25.5 and 36.7 °C, respectively. During December, a nursery area was found in the southern portion of the study area and the juveniles of Atlantic thread herring showed preference for temperatures higher than 27.4 °C. Scaled herring was found to be associated with temperatures (>25.7 °C) and salinities (>36.8). Scad and round sardinella were also associated to temperatures and salinities higher than 25 and 36.6 °C. Our results suggest that the dynamics of the upwelling area may influence the spatial distribution and abundance of small pelagics in the Colombian Caribbean Sea.

Keywords: Hydroacoustic; Small pelagic fish; Environmental factors; Colombian Caribbean

1. Introduction

The most important pelagic artisanal fishery of the Colombian Caribbean Sea is the Atlantic thread herring (*Opisthonema oglinum*) and the associated species scaled herring (*Harengula jaguana*), round sardinella (*Sardinella aurita*), and scad (*Decapterus punctatus*). These fisheries are mainly located off the La Guajira Peninsula, Ciénaga Grande de Santa Marta, and the Magdalena River Delta. Only few surveys have been carried out on these small pelagic fishes in order to assess the abundance and spatial distribution using hydroacoustic methods. The first one was conducted in 1985 (Blanco, 1986), and the other in 1988 was conducted by the Institute of Marine Research (Norway) using acoustic echo-integration (Anon., 1989). Major concentrations of pelagic fishes were found in the Riohacha area for the 1985 survey and in the northern La Guajira Peninsula for the 1988 survey (Fig. 1). Another two surveys were carried out by the Fishing Program of the Instituto Nacional de Pesca y Acuicultura (INPA-VECEP/UE) in 1997 using acoustic-geostatistical methods leading to a biomass estimation and spatial distribution updates for the small pelagic fishes (Paramo and Roa, 2003). These last few surveys found that the patches of small pelagic fishes were distributed mainly in southern La Guajira Peninsula (Paramo and Roa, 2003; Paramo and Viaña, 2003). All studies conducted coincide with the fact that the largest aggregations of small pelagics are found in the La Guajira area.

In the northern Colombian Caribbean, the continental shelf is very narrow, with the 200 m isobath at a distance of only 10 nautical miles (nmi) from the coast. To the west, the shelf widens to a maximum of 25 nmi off Riohacha and then

* Corresponding author.
E-mail address: jparamo@inpesca.cl (J. Paramo).

doi:10.1016/S0990-7440(03)00043-3

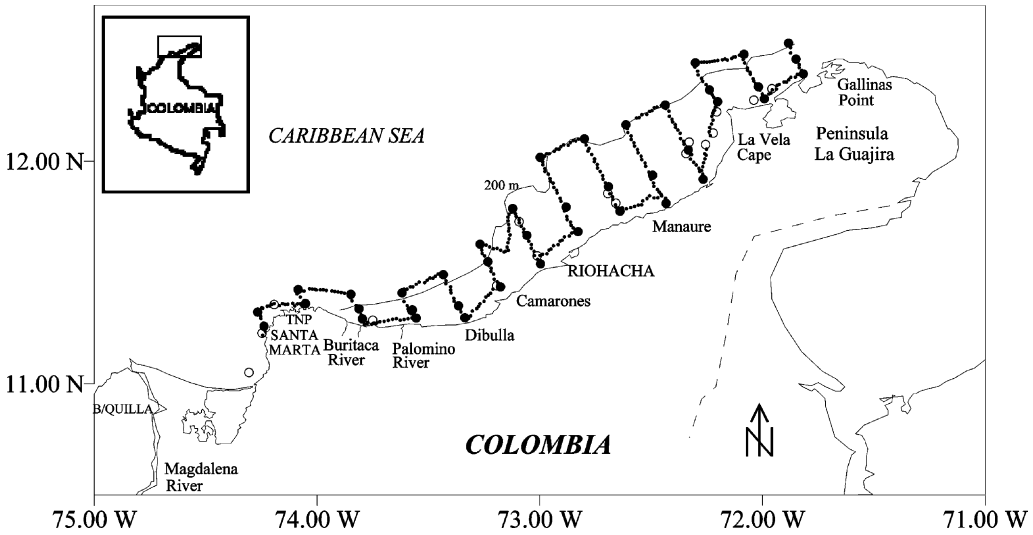

Fig. 1. Acoustic track performed on the Colombian Caribbean during the research surveys. Small circles: elementary distance sampling units; large empty circles: directed fishing trawls; large grey circles: oceanographic stations.

narrows again and almost disappears off the Tayrona National Park (TNP) (Fig. 1). The Colombian Caribbean is under the influence of the north–south displacement of the Inter Tropical Convergence Zone (ITCZ). When the ITCZ is towards the south (dry season), the high-pressure system forces strong and constant westward trade winds. During the same period, the Caribbean current is displaced towards the west. When this current is near the Panama coast, it is deflected southward and then eastward. In this way, the counter-current is formed. When the ITCZ is towards the north (rain season), the trade winds relax and their direction becomes variable due to the low-pressure system. This condition promotes the extension of the counter-current in the northwest axis. In this way, the counter-current forcing is seasonally dependent (Pujos et al., 1986); during the dry seasons (major summer: August–September; minor summer: December–January), the northern zone is affected by the Caribbean current and the upwelling of deep waters. The upwelling magnitude is stronger at La Guajira Peninsula, whose effects reach the waters near the TNP (Blanco, 1986). During the rainy seasons (major winter: September–November; minor winter: May–June), the counter-current reaches even La Vela Cape in La Guajira Peninsula (Bula-Meyer, 1990). However, Blanco (1986) considered that this counter-current would not cross Boca de Ceniza (Magdalena river's mouth). On the other hand, Pujos et al. (1986) mentioned that during dry seasons, this counter-current reaches the Magdalena River's mouth, until it reaches a maximum off the Guajira coast during the most rainy period of the year (October–November).

The major aggregations of these small pelagic fishes found in the La Guajira area, where the local oceanography is modulated by the seasonal upwelling intensity, suggest that environmental conditions were important determinants of their spatial distribution and abundance. Here, we analysed the associations between the distribution of the small pelagic Atlantic thread herring, scaled herring, round sardinella and scad with environmental variables (temperature, salinity, and oxygen) in the northern part of the Colombian Caribbean Sea. We used data from the two surveys carried out by the INPA-VECEP/UE Fishing Program during 1997.

2. Materials and methods

2.1. Survey designs and equipment

Two hydroacoustic surveys were carried out during July/August and December 1997 between Gallinas Point (12° 24' N–71° 48.69' W) and Santa Marta (11° 16' N–74° 14' W), of the northern area of the Colombian Caribbean Sea. Both surveys had a similar systematic sampling design with 14 parallel transects located perpendicular to the coast covering the entire continental shelf. The inter-transect distance was 12 nmi and elementary distance sampling unit (EDSU) was 1 nmi (Fig. 1).

Nine transects were carried out from 1 to 25 nmi offshore in the areas where the shelf was wider. Five transects were carried out from 1 to 15 nmi offshore in the zone between Dibulla and Santa Marta. On the 25 nmi transects the oceanographic sampling stations were positioned at 1, 15, and 25 nmi from the coast, while on the 15 nmi transects, the stations were located at 1, 5, and 15 nmi from the coast (Fig. 1). Temperature, salinity, and oxygen concentration were measured at a depth of 5 m with a CTDO (Sea Bird Electronics). During the July/August survey, no oxygen data were available because the CTDO sensor was not working appropriately.

The acoustic data were collected using a SIMRAD EK500 echo-sounder and echo-integrator at a frequency of 38 kHz. An equipment calibration was conducted according to SIMRAD specifications (SIMRAD, 1993) before the start of each

survey. Midwater trawls were used to identify echo-traces and to determine the species size-frequency distribution (MacLennan and Simmonds, 1992). The target strength (TS) was assumed from the equation suggested by Foote (1987) for physostome fishes:

$$\mathrm{TS} = 20 \log \bar{L} - 71.9 \ (\mathrm{dB}) \quad (1)$$

where $\bar{L}$ is the average length (cm) of the fish sample obtained by fishing trawls.

The nautical area scattering coefficient (S_A) measured in $m^2\ nmi^{-2}$ was converted to fish density ($t\ nmi^{-2}$) using this TS and values of echo-integration for each EDSU.

2.2. Habitat–fish density relationships

A cumulative frequency method and a Monte Carlo randomization (D'Amours, 1993; Perry and Smith, 1994) were used to detect associations between fish density and environmental variables (i.e. temperature, salinity, and oxygen). First, the relative cumulative frequency distribution (CFD) was calculated for each of the environmental variables. Subsequently, we weighted the CFD for each environmental variable by fish density. The comparison of the unweighted CFD of the environmental variable with the weighted CFD of the environmental variable provides evidence as to whether the population is associated with the environmental variable or not. If the population is randomly distributed in relation to the environmental variable, the two curves will accrue similarly and the two curves will not be significantly different. In contrast, if the population is associated with a particular environmental variable, the slope of the weighted CFD should be steeper than that of the unweighted environmental variable. The opposite is valid in the case of no association between a particular range of the environmental variable and fish density. The CFDs for the environmental variables (i.e. temperature, salinity, and oxygen) were calculated as follows:

$$f(t) = \frac{1}{n}\sum_{i=1}^{n} I(x_i) \quad (2)$$

with the indicator function

$$I(x_i) = \begin{cases} 1, \text{ if } x_i \leq t, \\ 0, \text{ otherwise} \end{cases}$$

where t represents an index ranging from the lowest to the highest value of the habitat variable at a step size appropriate for the desired resolution.

In order to relate the environmental variables with the fish density, only the EDSUs within a 2 nmi radius from each oceanographic station were used. Then, we used the CFD of the environmental variable multiplied by fish density:

$$g(t) = \frac{1}{n}\sum_{i=1}^{n} \frac{y_i}{\bar{y}} I(x_i) \quad (3)$$

where y_i is a specific fish density variable in the set i within the t range of the environmental variable and $\bar{y}$ is the mean fish density.

In order to determine the statistical significance (P) of the difference between the curves, the maximum absolute vertical distance between $g(t)$ and $f(t)$ was calculated as:

$$\max_{\forall t} |g(t) - f(t)| = \max_{\forall t} \left| \frac{1}{n}\sum_{i=1}^{n} \left(\frac{y_i - \bar{y}}{\bar{y}} \right) I(x_i) \right| \quad (4)$$

and its probability under the hypothesis of a random relation between both CFDs was evaluated by producing a Monte Carlo frequency distribution for the statistic in Eq. (4). Thus, after determining the maximum absolute difference between the two curves (s), we compare it with the distribution of the maximum absolute differences from 2000 randomizations of the Monte Carlo resampling for fish density and the environmental variable.

3. Results

During both the July/August (Fig. 2a) and December (Fig. 2b) surveys, sea surface temperature (SST) increased in a southwesterly direction from the area of the main source of upwelling (north of La Vela Cape). This tendency was more pronounced during the second survey. During the first survey, warm water was retained close inshore between Manaure and the Palomino River, and the thermal gradient diminished with increasing distance offshore. During the second survey, a similar pattern was seen in the area between Camarones and Dibulla.

Results of the statistical analysis show that during the July/August survey, all small pelagics, except the scaled herring, were primarily associated with the sea surface temperature (SST) ($P < 0.01$ and $P < 0.05$). The only species that showed a significant association ($P < 0.05$) with salinity were the adults of the Atlantic thread herring and the round sardinella (Table 1, Fig. 3). It should be noted that in this analysis the adults and the juveniles of the Atlantic thread herring were separated. This was possible since the identification fishing hauls and the echo-integration records showed a more coastal spatial distribution for the juveniles than the adults. Off Camarones, the adults were found approximately 17 nmi offshore and between Santa Marta and Dibulla they were closer inshore. The Atlantic thread herring adults were associated with temperature ($P < 0.01$) and salinity ($P < 0.05$), while the juveniles were only associated with temperature ($P < 0.01$). The scaled herring showed no significant association with either of the two oceanographic variables. The round sardinella showed consistent association with temperature ($P < 0.01$) and salinity ($P < 0.05$), while the scad was only associated with temperature ($P < 0.05$). Atlantic thread herring were associated with warmer temperatures while round sardinella and scad with cooler temperatures. The patterns of salinity associations

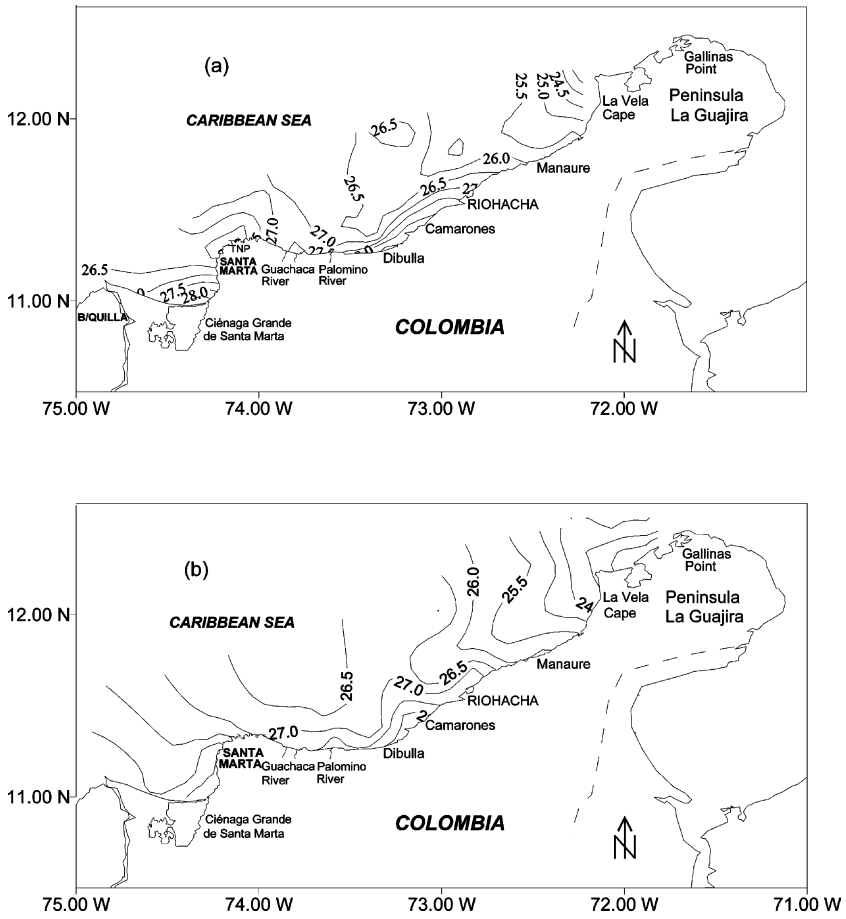

Fig. 2. SST: (a) during the July/August survey; (b) during the December survey.

showed that the Atlantic thread herring adults were associated with lower salinities and round sardinella with higher salinities (Fig. 3).

Results of the randomization test of association between fish density with environmental variables (temperature, salinity, and oxygen) during the December survey (Table 1), show significant associations mainly with temperature and salinity for most species. When the analysis was carried out using the data of the entire study area, a significant association was found for the Atlantic thread herring with salinity and oxygen, but not with temperature. However, Paramo and Roa (2003) found two spatially separated aggregations of the

Table 1
Results of the univariate randomization test of association between fish density and surface temperature, salinity and oxygen during the July/August and December 1997 surveys. The number below each *P*-value is the preference range for the environmental variable

Fish species	July/August, 1997		December, 1997		
	Temperature (°C)	Salinity (psu)	Temperature (°C)	Salinity (psu)	Oxygen (ml l^{-1})
Atlantic thread herring, all areas	0.00 *	0.04 * *	0.07	0.05 * *	0.00 *
	(26.68–27.48)	(36.50)		(36.71–36.76)	(3.09–3.14)
Atlantic thread herring adults	0.00 *	0.04 * *	0.00 *	0.001 *	0.17
	(26.76–27.46)	(36.50)	(24.44–24.54)	(36.81–36.84)	
Atlantic thread herring juveniles	0.002 *	0.78	0.01 * *	0.51	0.24
	(26.70–27.50)		(27.37–27.47)		
Scaled herring	0.11	0.23	0.00 *	0.00 *	0.01 *
			(25.78)	(36.81–36.82)	(3.20)
Round sardinella	0.001 *	0.03 * *	0.001 *	0.00 *	0.04 * *
	(25.75–25.85)	(36.72–36.73)	(25.64–25.84)	(36.68–36.70)	(2.54–2.63)
Scad	0.04 * *	0.07	0.003 *	0.00 *	0.17
	(25.58)		(25.74–25.84)	(36.68–36.69)	

* $P \leq 0.01$.
* * $0.01 < P \leq 0.05$.

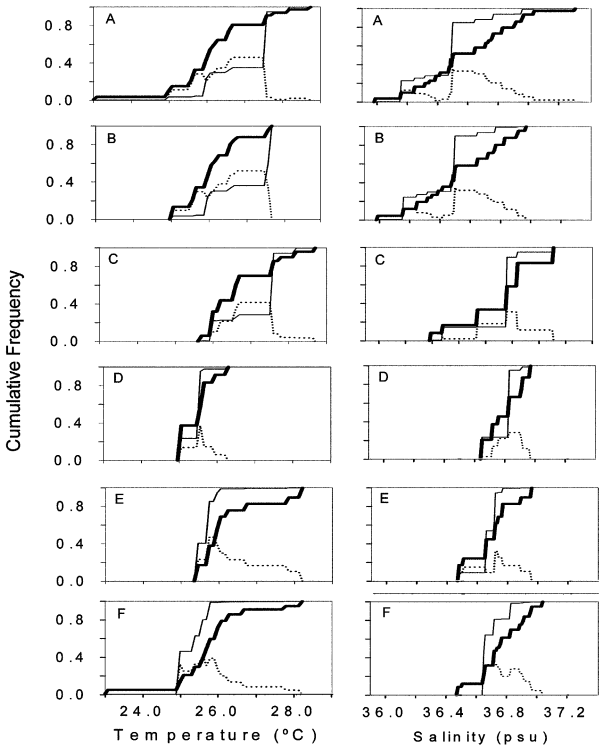

Fig. 3. CFD of the habitat variables, temperature (left) and salinity (right) during the July/August 1997 survey; $f(t)$: thick line; $g(t)$ where t is an index: thin line; absolute difference between $g(t)$ and $f(t)$: dotted line. (A) Atlantic thread herring all area; (B) Atlantic thread herring adult; (C) Atlantic thread herring juvenile; (D) scaled herring; (E) round sardinella; (F) scad.

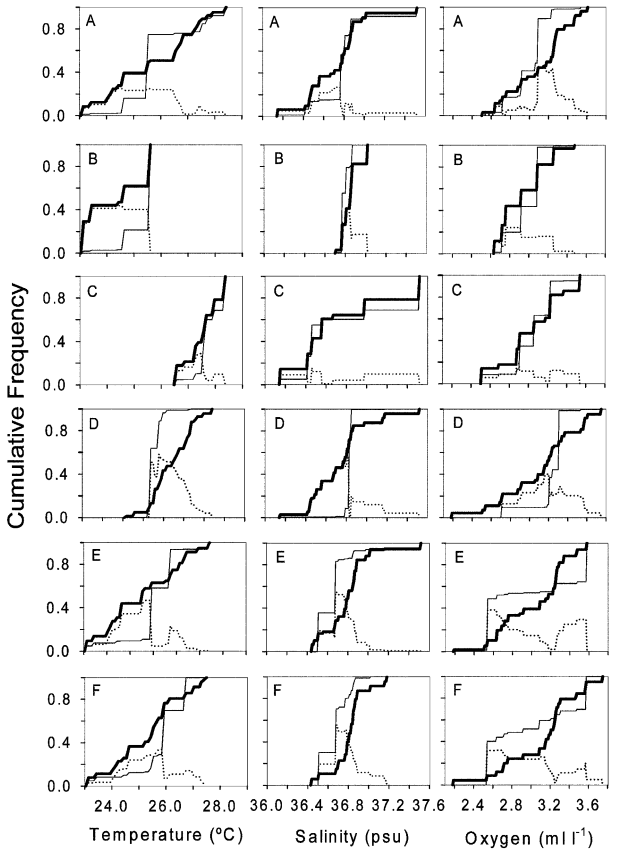

Fig. 4. CFD of the habitat variables, temperature, salinity, and oxygen (from left to right) during the December 1997 survey; $f(t)$: thick line; $g(t)$: thin line; absolute difference between $g(t)$ and $f(t)$: dotted line. (A) Atlantic thread herring all area; (B) Atlantic thread herring adult; (C) Atlantic thread herring juvenile; (D) scaled herring; (E) round sardinella; (F) scad.

Atlantic thread herring in December 1997, the larger one was at the base of La Guajira Peninsula and the smaller one was in the south, between Buritaca River and Camarones (Fig. 1). These two patches seemed to reflect population structure, since individuals from the south were much smaller (averaging 12.1 cm total length) than individuals from the north (27.1 cm average total length). In this sense, we also examined these two populations separately, the northern aggregation (adults) showed significant association with temperature and salinity ($P < 0.01$), while the southern aggregation (juvenile) was only associated with temperature ($P < 0.05$). The adults and juveniles of the Atlantic thread herring showed different association ranges with temperature. The Atlantic thread herring adults were associated with cooler temperatures whereas the juvenile with warmer temperatures. Scaled herring, round sardinella and scad were associated with similar temperatures (Table 1, Fig. 4). Scaled herring showed a strong significant relationship ($P < 0.01$) with all three environmental variables under study. Similarly, sardinella showed significant relationships with temperature, salinity ($P < 0.01$), and oxygen ($P < 0.05$). However, round sardinella preferred conditions of lower salinity and oxygen than the scaled herring. The scad showed a strong significant relationship with temperature and salinity ($P < 0.01$), but not with oxygen (see Fig. 4). Only two of the four species, scaled herring and round sardinella, showed significant relationships with oxygen ($P < 0.05$), the latter tolerating conditions of lower oxygen.

4. Discussion

The main upwelling coastal ecosystems in temperate zones are characterized by strong seasonal or permanent equatorial winds, a vertical current structure, and a persistent wind-induced offshore drift of surface waters (Brink, 1983). These ecosystems present high rates of primary productivity (Roy, 1998; Mackenzie, 2000), and they usually support large populations of pelagic fish (Pauly and Tsukuyama, 1987; Cury and Roy, 1989). In tropical environments, such as the Colombian Caribbean Sea, these conditions are quite different. Generally, two monsoon or trade wind seasons replace the four seasons of temperate zones, differentiated by wind patterns, rainfall, and currents. In addition, the concentration of dissolved nutrients is lower, except in upwelling areas (Johanes, 1978).

Our results suggest that the dynamics of the seasonal upwelling in the northern zone of the Caribbean Colombian Sea is a significant factor in modulating the spatial distribution of the small pelagic species. In the December 1997

survey (i.e. the period of greater influence of seasonal upwelling), the Atlantic thread herring is normally found in this region, although it avoids the centre of the upwelling. This species has a seasonal migratory behaviour towards the open sea during periods of increased wind strength or when upwelling intensifies. These conditions produce an increase in the turbulence of coastal areas, forcing the Atlantic thread herring to move towards clearer waters offshore (Valdes and Sotolongo, 1983). In the northern area, the adults of the Atlantic thread herring prefer lower temperatures and higher salinity, while the juvenile aggregations are found further south. This could be of importance because the growth rate of the individuals is affected by temperature. As shown by Heath (1992), clupeid juveniles with adequate food supply and within a favourable temperature range will increase their growth rate by approximately 10% for every 1 °C. Accordingly, a nursery area with higher temperatures should promote a faster development of the swimming and feeding capacity and thus a drop of the natural mortality. Sardinella was strongly associated with temperature in both surveys (25.64–25.85 °C), which would indicate a preference for relatively cold waters (Johnson and Vaught, 1986; Anon., 1989; Cervigón, 1991). It is also extremely stenohaline and is never found in waters with salinities below 35 (Longhurst and Pauly, 1987). This is in line with our results, since in both surveys, round sardinella was found in areas having salinities of 36.7 for the region off Riohacha. At the same time, environmental preference ranges of scad were similar to those of round Sardinella.

All studied species showed strong associations with lower temperatures. This is typical for areas influenced by the seasonal upwelling, which at this time of year (mid-December–April) is at the maximum due to the presence of stronger trade winds. The main centre of the upwelling is in the area between Gallinas Point and La Vela Cape. The exception being the juvenile aggregation of the Atlantic threads herring which preferred higher temperatures in the December survey. For salinity, all species showed strong association patterns preferring higher salinities at the upwelling influenced area. Once again, the exception being the Atlantic threads herring juveniles that showed no significant relationship with salinity. During the December survey, the region between Camarones and the Tayrona National Park was characterized by an increase in surface temperature in an inshore direction. It is important to note that in this region an aggregation of Atlantic thread herring juveniles was found that had not reached mature size ($L_{50\%}$ = 22.8 cm) (Finucane and Vaught, 1986), but that they were about to reach recruitment length (L_r = 15.9 cm) (www.Fishbase.org). This leads to the hypothesis that the region between Camarones and the Tayrona National Park may be an important retention and nursery area for the Atlantic thread herring. Manjarrés et al. (1998) found that the largest concentrations of zooplankton were found in the area between Gallinas Point and Riohacha. This is in agreement with our results that show that the region influenced by the upwelling off La Guajira Peninsula may be an appropriate habitat for communities of small pelagic due to the increase in productivity and the quantity of available food for these species.

Acknowledgements

During the course of writing of this manuscript J.P., A.R. and R.W. were supported by the School of Graduate Students Scholarship, Universidad de Concepción, to complete an M.Sc. degree in Fisheries; and RQ was funded by the Consorcio para la Investigación del Cambio Global del Pacífico Oriental (IAI). We are thankful to Luis Manjarrés and Jorge Viaña, who organized the surveys from which the data for this work were obtained. The Fishing Program of the INPA-VECEP/UE kindly provided permission for using their data. We would like to thank Ricardo De Pol-Holz and referees for providing helpful comments on the manuscript.

References

Anon, 1989. Prospecciones de los recursos pesqueros de la áreas de plataforma entre Surinam y Colombia. Institute of Marine Research, NORAD/UNDP/FAO Programme, Bergen.

Blanco, J., 1986. Resultados Crucero de Prospección Acústico-Pesquera. Desarrollo de la Pesca Artesanal de la región de Santa Marta. COLCIENCIAS-CIID-FES, Bogotá, pp. 127–150.

Brink, K.H., 1983. The near-surface dynamics of coastal upwelling. Prog. Oceanogr. 12, 223–257.

Bula-Meyer, G., 1990. Oceanografía. Caribe de Colombia. Fondo José Celestino Mutis, Colombia, pp. 51–66.

Cervigón, F., 1991. Los peces Marinos de Venezuela. Fundación científica Los Roques, Vol. 1 Caracas.

Cury, P., Roy, C., 1989. Optimal environmental window and pelagic fish recruitment success in upwelling areas. Can. J. Fish. Aquat. Sci. 46, 670–680.

D'Amours, D., 1993. The distribution of cod (*Gadus morhua*) in relation to temperature and oxygen level in the Gulf of St. Lawrence. Fish. Oceanogr. 2, 24–29.

Finucane, J., Vaught, R., 1986. Species profile of Atlantic thread herring, *Opisthonema oglinum* (Lesueur, 1818). NOAA. Tech. Mem. 182.

Foote, K., 1987. Fish target strengths for use in echo integrator surveys. J. Acoust. Soc. Am. 82, 981–987.

Heath, M.R., 1992. Field investigations of the early life history stages of marine fish. Adv. Mar. Biol. 28, 1–174.

Johanes, R.E., 1978. Reproductive strategies of coastal marine fishes in the tropics. Env. Biol. Fish. 3, 65–84.

Johnson, A., Vaught, R., 1986. Species profile of Spanish sardine *Sardinella aurita*. NOAA. Tech. Mem. 187.

Longhurst, A.R., Pauly, D., 1987. Ecology of Tropical Oceans. Academic Press, San Diego.

Mackenzie, B.R., 2000. Turbulence, larval fish ecology and fisheries recruitment: a review of field studies. Oceanol. Acta 23, 357–375.

MacLennan, D., Simmonds, E.J., 1992. Fisheries Acoustics. Chapman and Hall, London.

Manjarrés, L., Rodríguez, G., Vergara, A., Arteaga, E., Rodríguez, Y., Arévalo, J., Viaña, J., Galvis, R., Amaya, F., García, D., Páramo, J., De León, G., 1998. Crucero de evaluación de peces pelágicos pequeños en el Caribe colombiano UE-INPA/VECEP/PELAG/9711. Informe final. Programa Regional de Pesca UE-INPA/VECEP ALA/92/43, Santa Marta.

Paramo, J., Roa, R., 2003. Acoustic-geostatistical assessment and habitat-abundance relations of small pelagic fish from the Colombian Caribbean. Fish. Res. 60, 309–319.

Paramo, J., Viaña, J., 2003. Evaluación hidroacústica del machuelo (*Opisthonema oglinum*) y la sardina (*Sardinella aurita*), en la zona norte del Caribe colombiano durante julio-agosto y diciembre de 1997. Bol. Inv. Mar. Cost. INVEMAR, Santa Marta, 31.

Pauly, D., Tsukuyama, I., 1987. The Peruvian Anchoveta and its Upwelling Ecosystem: Three Decades of Change. ICLARM, Stud. Rev.

Perry, R.I., Smith, S.J., 1994. Identifying habitat associations of marine fishes using survey data: an application in the Northwest Atlantic. Can. J. Fish. Aquat. Sci. 51, 589–602.

Pujos, M., Pagliardini, J., Steer, R., Vernette, G., Weber, O., 1986. Influencia de la contra-corriente norte colombiana para la circulación de las aguas en la plataforma continental: su acción sobre la dispersión de los efluentes en suspensión del río Magdalena. Bol. Cient. CIOH. Cartagena 6, 3–15.

Roy, C., 1998. An upwelling-induced retention area off Senegal: a mechanism to link upwelling and retention process. S. Afr. J. Mar. Sci. 19, 89–98.

SIMRAD, 1993. Operator manual. SIMRAD EK-500 Scientific Echo Sounder, Bergen.

Valdes, E., Sotolongo, M., 1983. Algunos aspectos de la Biología y Pesquería del machuelo (*Opisthonema oglinum*) de la plataforma suroccidental cubana. Rev. Cub. Pesq. 3, 65–67.

Available online at www.sciencedirect.com
SCIENCE DIRECT®
Aquatic Living Resources 16 (2003) 247–253
Aquatic Living Resources
www.elsevier.com/locate/aquliv

Acoustical-optical assessment of Pacific herring and their predator assemblage in Prince William Sound, Alaska

Gary L. Thomas, Richard E. Thorne *

Prince William Sound Science Center, P.O. Box 705, Cordova, AK 99574, USA

Accepted 1 April 2003

Abstract

The Pacific herring *Clupea pallasi* population in Prince William Sound (PWS), Alaska, is both a valuable commercial resource and an important forage species for marine fish and wildlife. Historically, the herring were managed by a combination of age-structured models and egg deposition estimates. When these methods predicted a large return for spring 1993 that failed to materialize, we began surveying with echointegration–purse seine methods. After a decade of acoustic surveys, we show the new approach yields highly precise biomass estimates, which are consistent with historical measures of the miles of beach spawning. When compared, we show the traditional methods overestimated stock biomass, which resulted in harvest rates approaching 40%. In contrast, the acoustic methods are most likely to underestimate biomass. Since the acoustic estimates can be quickly obtained, we recommend their use to set harvest quotas for the fishery in the spring just prior to harvest. The shift from the traditional preseason to inseason management practices for herring in PWS is consistent with the Precautionary Principle by the fact that protection of the spawning population does not rely on the ability of science to predict how the population is changing. Furthermore, synoptic infrared measurements on our night-time acoustic surveys revealed herring to be the most important winter forage to marine birds and wildlife in PWS, including the endangered Steller sea lion *Eumetopias jubatus*. Given the importance of forage to marine birds and wildlife in the North Pacific during the extended winter conditions (October–March), the implementation of inseason management for herring using echointegration–purse seine techniques may be the most effective method to restore depressed populations of marine birds and mammals in the North Pacific.

Keywords: Acoustic surveys; Pacific herring; Inseason management; Steller sea lions

1. Introduction

The Pacific herring (*Clupea pallasi*) population in Prince William Sound (PWS) has supported an intermittent commercial fishery over the last century due to large fluctuations in biomass (Roundsefell, 1929; Thomas et al., 1991). There has been considerable speculation on how oil spills, disease and climate influence stock biomass fluctuation, but overfishing as a factor in population declines was not well documented (Bailey et al., 1995; Brown et al., 1996; Marty et al., 1998). However, new evidence suggests that overfishing may have played a role in the recent declines of the PWS stock.

The importance of accurate stock assessment procedures for herring management is increased by the fact that Pacific herring in PWS are one of the most important forage fish available to marine wildlife in the winter (Thomas et al., 1991; Thomas and Thorne, 2001). Furthermore, many piscivorous species in the Gulf of Alaska, including the endangered Steller sea lion (*Eumetopias jubatus*), have experienced major declines that are attributed to food limitation (DeMaster and Atkinson, 2002).

Historically, the herring in PWS were managed by a combination of age-structured models, egg deposition estimates and test fishing. In 1993, these traditional, preseason methods predicted a large spring return that failed to materialize. As a consequence, the local fishers union, Cordova District Fishermen United, secured funding for a fall 1993 acoustic survey to ascertain the status of the herring stock.

Although this was the first acoustic survey of the PWS herring biomass, Pacific herring stocks from Alaska to California have been assessed with acoustic techniques for management purposes since the early 1970s (Thorne, 1977a, b; Trumble et al., 1982; Thorne et al., 1983; Thorne and Tho-

* Corresponding author.
E-mail address: thorne@pwssc.gen.ak.us (R.E. Thorne).

doi:10.1016/S0990-7440(03)00044-5

mas, 1990; Thomas and Thorne, 2001). In most cases, these acoustic estimates of biomass were part of a preseason prediction for establishing harvest quotas for the following spring. The requirements for the acoustic surveys were well established: (1) comprehensive coverage of the population, (2) biological information on species and size composition, and (3) correct target strength scaling (Thorne, 1983a). Thomas et al. (2002) document our research into the target strength scaling. This paper focuses on improvements to comprehensive coverage of the population and the collection of biological information.

The initial acoustic survey in PWS confirmed that a population collapse had occurred (DeCino et al., 1995; Thomas et al., 1997). Subsequently, acoustic surveys of the adult herring were conducted during fall in 1994 and 1995, and during early spring since 1995. The objectives of this paper are to: (1) describe the survey techniques that were developed to assess this herring stock, (2) compare the acoustic estimates with traditional herring assessment techniques, and (3) discuss the value of acoustic monitoring of herring to research, management, the economy and the ecosystem.

2. Methods

Effective survey design begins with a consideration of the objectives, which in turn leads to requirements for precision (Thorne, 1983a). Our initial objective was to assess the abundance of Pacific herring in PWS as input to fishery management decisions. For precision, we looked at historic data on the stock fluctuation and concluded that we wanted to be able to detect an annual change in the population level of about ±20% with 95% probability.

The next step was a consideration of the sampling tools available for assessment. We had at our disposal various net sampling techniques, scientific (down-looking) acoustics, commercial sonars, and aerial surveys. The paramount consideration was the sampling power relative to the requirements for precision. Based on previous measurements, we estimated that we needed about 5% coverage to achieve 20% precision (Scheaffer et al., 1986). Since our scientific acoustic system sampled the depth ranges occupied by herring at a rate equivalent to 6 m^2 s^{-1}, 5% coverage would require 2.4 ship-years of effort to representatively sample the 9000 km^2 of PWS. As that level was not feasible, it was clear that we needed either sampling tools with even higher power, a more effective survey design, or both.

We knew from previous investigations that the bulk of the adult Pacific herring population in PWS characteristically exhibits four seasonal distributions: (1) a post-spawning, feeding migration to the ocean that usually starts in May, (2) a post-feeding migration to protected regions of PWS for over-wintering in October, (3) an over-wintering aggregation behavior in protected shoreline regions from November through March, and (4) a migration to spawning beaches in April.

Acoustic techniques are impractical on feeding and post-feeding migrations of herring because: (1) the population is moving along physical and biological gradients that vary annually, (2) the vertical distribution of the feeding fish can vary by the diversity of available prey organisms, (3) the herring are mixed into a complex assemblage of plankton and nekton making separation of targets difficult, and (4) the population is undergoing rapid change in growth and survival so its biological parameters are quite unstable. Vilhjálmsson and Carscadden (2002) came to the same conclusion for Icelandic capelin (*Mallotus villosus*) after 20 years of acoustically surveying. In addition, the spawning migrations to the beaches represent their own complexity because the fish are moving rapidly and occupying shallow rocky and kelp infested habitats that are not conducive to sampling. By elimination, we are left with the fall-winter period. In contrast to spring-summer periods, the herring population at this time is the most contagious and temporally, geographically and biologically stable. Initial survey data suggested that the bulk of the over-wintering herring occupy less than 1% of the surface area of PWS. The scientific acoustic system could cover that area in less than 8 days. However, those areas need to be located.

We ultimately developed a four-stage sampling approach (Cochran, 1977): (1) aerial and sonar reconnaissance, (2) verification and mapping, (3) repeated echointegrations and (4) subsampling school groups for biological information. The goal of the first step, aerial and sonar reconnaissance was to locate areas suspected of holding school-groups. Both aerial survey and sonar techniques have extremely high sampling power. This stage was assisted by historical information and local fishers' knowledge of the site fidelity of over-wintering herring. From the fishers we learned that predator assemblages (primarily Steller sea lions, humpback whales, glaucus and glaucus-winged gulls, common murres and pelagic cormorants) aggregated in herring over-winter areas, which facilitated locating school groups by aerial surveys. From fisheries and subsistence hunters operating in the Sound during the winter, we developed a network of sentinel observers to alert us about predator or subsurface fish aggregations that were observed on their acoustics. In general, we discovered that herring began to aggregate in the Sound in the late October, and as winter approached the distribution shifted to more protected areas that were usually close to major spring spawning locations.

The second stage of the survey was conducted at night with a dark-vessel to minimize boat avoidance and take advantage of a more favorable vertical distribution of the herring (Thomas et al., 1997). Its goal was to verify the presence of herring in suspect areas and develop a map of the area occupied by the school-groups using a searchlight sonar, echosounder and GPS plotter. Again, the high sampling power of the sonar allowed us to rapidly delineate the boundaries of herring concentrations.

The third stage of the survey was echointegration. Once the boundaries of the herring distribution were established,

an echointegration survey using scientific echosounders (Thorne, 1983a, b, MacLennan and Simmonds, 1992) was conducted to estimate the fish density. Echointegration estimates of density were made with one to three frequencies (38, 70 and 120 kHz) following a zigzag survey track. We separated the zigs from the zags to create two series of parallel transects. The searchlight sonar remained in continuous operation during the echointegration measurement phase of the survey (1) to verify absence of school avoidance to the vessel, (2) to monitor the school group to end of the transect, and (3) to avoid collision with submerged rocks and the shoreline.

All echointegration systems were fully calibrated using procedures documented in Foote et al. (1987). Two replicate estimates of biomass per unit surface area were obtained from the two sets of parallel transects in each survey, in addition to estimates from multiple frequencies. The zig-zag survey was then repeated multiple times to develop a sufficient number of independent estimates to achieve the desired precision. A weighted mean estimate was calculated for each parallel-transect survey, with weighting by transect duration. The mean biomass per unit surface area was extrapolated over the area covered by the survey, which was determined from the GPS data. The repeated survey estimates were used to determine the precision of the biomass estimates (Scheaffer et al., 1986).

The fourth and final stage of the herring surveys was to sample the previously echointegrated, herring school-groups for biological information using a commercial purse seine (McClatchy et al., 2000). This step was implemented by providing a second vessel with the coordinates of a herring school for sampling. The purse seines used ranged in depth from 18 to 31 m (10–17 fathoms) and had range of 1–2 cm stretched mesh in the bunt. We used a random sample of only one to three seine catches to collect the biological information due to the large size of the commercial seine used. The species and size composition of the net catches were used to estimate target strengths for converting backscatter to biomass. The density of the herring school-groups was too high even at night to collect reliable in situ target strengths.

Initial estimates of Pacific herring biomass from these surveys were based on a target strength to length relationship for Pacific herring of $TS = 26.5 \log L - 76.4$, where L is length in cm. This equation had evolved from many different sources including in situ measurements of individual herring, comparisons with catches and comparisons with independent measures of abundance (Thorne, 1977a; Trumble et al., 1982). Subsequently, we conducted ex situ experiments to better understand the target strength characteristics (Thomas et al., 2002). These experiments indicated that the target strength assumption was reasonable, and corrections for the historical survey results were not necessary. However, subsequent surveys have incorporated the changes associated with depth that are recommended by Thomas et al. (2002).

Visual observations of predators (sea lions, other marine mammals and birds) were integrated into the acoustic surveys beginning in 2000 (Thomas and Thorne, 2001). Visual observations during hours of darkness used a Texas Instruments Model M100 "NightSight" (27 × 18° field of view) or a Raytheon Model 200 "NightSight" (12 × 6° field of view). Steller sea lions and whales were enumerated along the acoustic transects, while major bird concentrations and activities were logged.

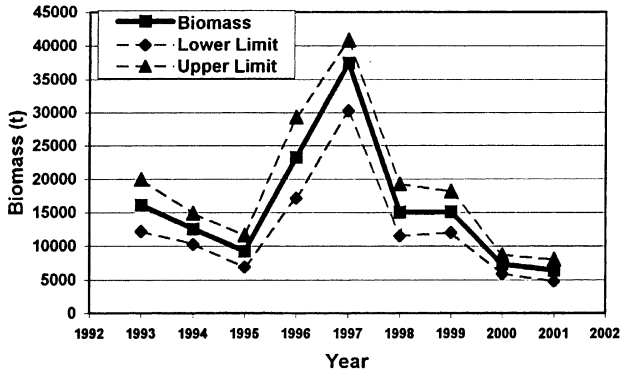

Fig. 1. Results of acoustic biomass herring estimates in PWS (dashed lines are 95% confidence limits).

3. Results

3.1. Annual biomass assessments

The initial two acoustic surveys estimated an abundance of 16 082 metric tons (t) in the fall of 1993 and 12 555 t in fall 1994 (Fig. 1). With a moratorium on fishing, the population rebuilt to 23 203 and 37 498 t in the spring of 1995 and 1996, respectively. However, after reopening the commercial fishery, the acoustic surveys in the springs of 1998 and 1999 showed a decline to about 17 000 t. After test fishing in the spring of 1999, management cancelled the fishery. The spring survey of 2000 and 2001 showed the population to have fallen to a new, all-time lows of 7281 and 6384 t, respectively.

3.2. Comparison with historical techniques

Historical information on the abundance of Pacific herring in PWS consists of commercial catch records, aerial estimates of the length (mile-days) of spawn (milt) patches along beaches and herring spawn (egg) deposition surveys (Biggs et al., 1992; Donaldson et al., 1992; Funk, 1994). The commercial catch records date back to 1969, whereas the mile-days of spawn date to the early 1970s. Egg deposition surveys were conducted in 1981–1982, 1988–1992, and 1994–1997. In addition, the Alaska Department of Fish and Game (management) has used various sources of information to make forecasts of run biomass using an age-structured assessment model since 1980 (Baker et al., 1991; Sharp et al., 1996; Quinn et al., 2001).

The Alaska Department of Fish and Game continues to measure mile-days of spawn, as it has since 1974. As this was

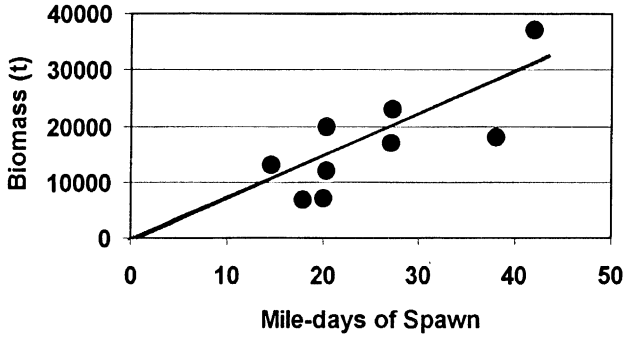

Fig. 2. The relationship between acoustic biomass estimates and the miles-of-spawn indice ($Y = 697X$, $r^2 = 0.75$) for herring in PWS, 1993–2002.

the most complete data record, we compared the estimates of the mile-days of spawn and acoustic estimates of biomass between 1993 and 2002 and found a positive correlation with a coefficient of 0.75 (Fig. 2).

The mile-days of spawn index was used as a relative abundance indicator. However, since it correlated well with the acoustic estimates, we used the correlation to convert mile-days of spawn to an absolute estimate of biomass, and hind-cast herring abundance back to 1973. The hind-cast indicates that the population showed a general increase to a peak in 1988 of about 100 000 t, followed by a rapid decline after the *Exxon Valdez* oil spill in 1989 (Fig. 3).

The egg deposition estimates were in general agreement with this hind-cast except for 1990–1992. During this time, the hind-cast estimates indicated a population in decline, while the egg deposition estimates indicated a major increase in population abundance. Similarly, the age-structured analysis produced estimates that increased from 108 671 t in 1988 to 120 658 t in 1992, at a time when the mile-days of spawn were decreasing (Sharp et al., 1996).

It is apparent that the harvest quotas were driven by the estimates from the egg deposition surveys and age-structured analysis. During the 1990–1992 interval when the hind-cast estimates indicate that the biomass was decreasing, the harvests were increasing. In fact, in 1991 and 1992, the exploitation rates were 0.35 and 0.39, respectively, based on the hind-cast estimates. Between 1990 and 1992, 40 000 t were

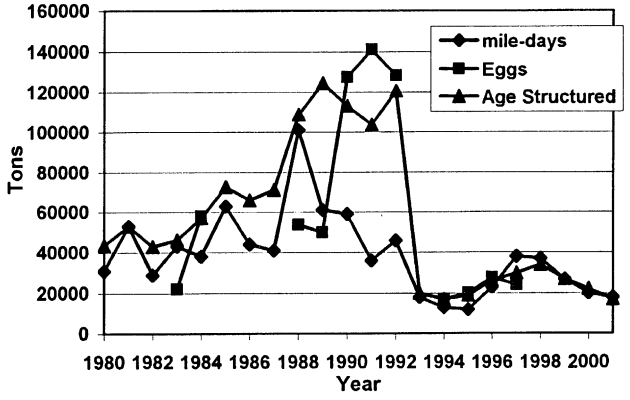

Fig. 3. Comparison of estimates from the age-structured model, egg deposition and mile-days of milt converted to absolute values.

removed from a population that the hind-cast estimated at 61 000 t in 1989.

With the collapse of herring, management placed a moratorium on fishing from 1994 to 1996. The population experienced favorable recruitment in 1994 and 1996 to reach a biomass of between 30 000 and 40 000 t (Kirsch and Thomas, 1997). Since this biomass exceeding the management threshold for spawning biomass (22 000 t) commercial fishing was resumed in spring 1997. The harvest quota was placed at 5000 t. Unfortunately, the next spring after this fishery the acoustic survey estimated that the population dropped to 15 029 ± 4150 t, which was below the management threshold. However, the age-structure model did not reflect this decline (Fig. 3). Consequently, management opened another fishery for spring 1998 with a quota of 5000 t. Subsequently, the acoustic estimates of the population declined to only 7281 t by 2000 (Thorne, 2000). The mile-days of spawn reflected the increase between 1995 and 1997 as well as a decrease between 1997 and 1998, and subsequent decreases between 1998 and 2001. By 1999, it was obvious to all estimators that the population had fallen below threshold, and a fishing moratorium was again imposed that remains in effect to this date. However, post-mortem indicates that the exploitation rate on the declining population in 1998 was about 33%.

3.3. Predator aggregations

Our initial objective was to develop an effective assessment tool for herring management. In pursuit of that goal, we observed that herring were the target of many predators. Our observations of the coincidence of herring and Steller sea lions led to our discovery of night-time foraging by Steller sea lions on herring (Thomas and Thorne, 2001). Over a 3-year period, we found strong correlations ($r^2 = 0.88$–0.98) between our acoustic estimates of biomass and synoptic counts of Steller sea lions at various locations of overwintering herring (Thorne and Thomas, 2002). Subsequent comparisons between our annual estimates of herring in PWS and the long-term census data on Steller sea lion abundance in PWS taken at The Needle, which is the major haul-out within PWS (Kruse et al., 2000; Sease et al., 2001) also show a very strong correlation. The herring population declined by 88% between 1989 and 2000, while the Steller sea lion count declined 86% (Fig. 4). Further, the Steller count in 1973 was 25% of the peak count in 1990, while the herring miles of spawn the first year it was measured, 1974 was 22% of its peak value measured in 1988. Steller sea lion counts also declined after 1989 at sites adjacent to PWS. The average decline between 1989 and 2000 for the three major adjacent sites, Wooded Island, Seal Rocks and Point Elhrington, was 72%. This substantial decline contrasts with the overall trend in the Eastern Gulf of Alaska, which was a minor decline.

The combination of acoustics and infrared sensors also showed close associations between herring and marine bird foraging activity at night. The sea bird assemblage was domi-

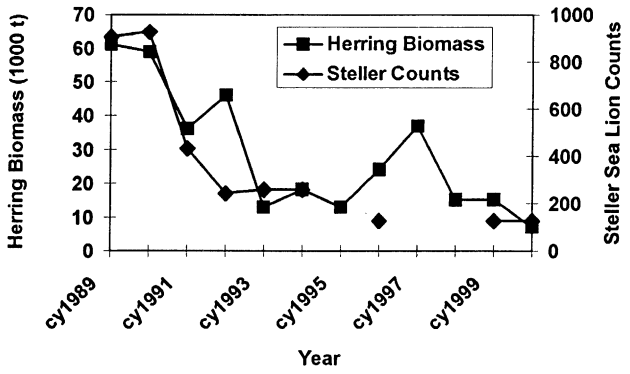

Fig. 4. Comparison of Steller sea lion counts and herring abundance in PWS, 1989–2000. Steller sea lion counts are from NMFS/ADF&G census at The Needle.

nated by two species, glaucous gulls and pelagic cormorants, but murres were also common. While all three species were highly correlated with the herring abundance, the glaucous gulls were also closely associated with the Steller sea lions. The foraging behavior of the Steller sea lions in most cases consisted of stunning the herring, then feeding on the stunned fish at the surface. That behavior apparently facilitated feeding by the gulls.

4. Discussion

The estimates of the PWS herring population from the acoustic techniques correlated well with the mile-days of spawn index. That result alone is not a strong verification. All techniques are subject to sources of variability and bias. However, when the relationship is used to hind-cast the population trends, the result reveals a very logical and rational basis for the historical population changes. It appears that the herring population from 1973 to 1988 was relatively stable and slightly increasing. However, the hind-cast estimates clearly show a sharp decline subsequent to the *Exxon Valdez* oil spill in 1989 that included impacts of recruitment failure and disease. Unfortunately, that decline was not detected because the egg deposition and age-structured models were suggesting a substantial increase from 1989 to 1993 (Sharp et al., 1996) when our evidence indicates the population was actually declining. As a result, harvest rates approached 40% during 1991 and 1992. These relatively high harvest rates on a declining population clearly accelerated the decline. The subsequent collapse argues against the accuracy of the estimates from the egg deposition surveys and age-structured analysis. An increasing mortality following the oil spill could be at least a partial explanation for failure of the age-structured analysis, since an assumption of constant natural mortality is implicit in the approach. The failure of the egg deposition method may reflect the problem of large extrapolations.

We used the regression model that forced the relationship between the acoustic biomass estimates and the mile-days of spawn index through the origin because of the theoretical relationship between the two parameters. The slope of the relationship would be about 10% higher using the general regression equation. However, the same conclusion would be reached with both regression models.

In contrast to the overestimation problem that appears to have resulted from both the egg deposition and age-structured methods during the 1989–1992 period, the acoustic surveys of herring only overestimate if non-herring targets are counted, incorrect TS is used to convert backscatter to biomass, or calibration is erroneous. We have isolated surveys to times when the herring are in single species aggregations of adults. We verify species and age composition. We have verified the TS function for use with herring. Our calibration procedures are meticulous and consistent. Consequently, we do not see overestimation as a problem. Underestimation by truncating fish schools or missing concentrations can still occur and not be detected, but considerable evidence from various survey experiments suggests such errors are minor (Thomas et al., 1997). In addition, minor underestimation is acceptable since it adheres to the Precautionary Principle (O'Riordan, 1992; Dovers and Handmer, 1995). An additional consideration is that the variance of our acoustic estimates is based on variability among complete surveys, rather than a measure of internal variability as is the case with egg deposition surveys. It is interesting that the best fit occurs between the acoustics and the miles of spawn. Both are based on techniques with very high sampling power.

The strong correlation between our estimates of herring biomass and the NMFS/ADF&G census counts of Steller sea lions provides additional support for the accuracy of the herring biomass estimates. We have established that Steller sea lions extensively and almost exclusively target herring during the extended Alaskan winter period (Thomas and Thorne, 2001; Thorne and Thomas, 2002). Consequently, it is not surprising to see similar trends in abundance. Conversely, the correlation with herring demonstrates that it is important to accurately assess major forage stocks in order to understand population fluctuations of important, and often endangered, predators.

While the acoustic estimates correlated well with the mile-days of spawn, it is important to note that the mile-days of spawn measurement occurs too late to impact the fishery for that year. In contrast, the spring acoustic surveys can be conducted immediately prior to a fishery opening. If acoustic surveys had been in place as the primary management tool, the overfishing that took place in 1991, 1992 and 1998 most likely would not have occurred. The economic and ecological consequences of incorrect management are substantial. The fishery remains closed to this date, and many piscivorous species suffered substantial declines.

5. Conclusion

This study points out two major advantages of acoustic techniques (1) direct assessments can be made immediately prior to a harvest, (2) the most likely direction of error is

toward underestimation. In contrast, both the egg deposition surveys and the age-structured analysis are indirect and both depend on assumptions of constant natural mortality over the subsequent year. It is clear in this case that erroneous deterministic and indirect measures of herring biomass were harmful to herring stocks and the fisheries and wildlife that depended upon them.

While error toward underestimation is preferable to overestimation, the error can be minimized by a well-considered survey design. Our experience shows that a thorough understanding of the distributional characteristics of the target population is a critical factor for accurate assessment.

An important additional benefit of accurate and consistent long-term monitoring of a major forage species such as herring is an improved understanding of the auxiliary populations that depend upon the abundance of that forage. Such information is critical to improved understanding of ecosystem health and function.

Acknowledgements

Many people and institutions have contributed to this effort over the years. We are especially appreciative of the support of the Oil Spill Recovery Institute's (OSRI) Advisory Board and Scientific and Technical Committee, Captains Dave Butler of the FV *Kyle David*, Jack Babbic of the FV *Miss Kaylee*, Dave Bradshaw of the RV *Montague* and Steve Moffitt of the Alaska Department of Fish and Game in Cordova. Funding for preparation of this manuscript was provided by OSRI.

References

Bailey, K.M., Piatt, J.F., Royer, T.C., Macklin, S.A., Reed, R.K., Shima, M., Francis, R.C., Hollowed, A.B., Somerton, D.A., Brodeur, R.D., Ingraham, W.J., Anderson, P.J., Wooster, W.S., 1995. ENSO events in the Northern Gulf of Alaska, and effects on selected marine fisheries. CalCOFI. Rep. 36, 78–96.

Baker, T.T., Wilcock, J.A., McCracken, B.W., 1991. Stock assessment and management of Pacific Herring in Prince William Sound, Alaska, 1990. Alaska Department of Fish and Game. Technical Fish. Rep. 64, 22–91.

Biggs, E.D., Haley, B.E., Gilman, J.M., 1992. Historic database for Pacific herring of Prince William Sound, 1973–1991. Alaska Department of Fish and Game, Anchorage, AK Regional Information Rep. 2C91-11.

Brown, E.D., Norcross, B.L., Short, J.W., 1996. An introduction to studies on the effects of the *Exxon Valdez* oil spill on early life history stages of Pacific herring, (*Clupea pallasi*), in Prince William Sound, Alaska. Can. J. Fish. Aquat. Sci. 53, 2337–2342.

Cochran, W.G., 1977. Sampling Techniques. Wiley, New York.

DeCino, R., Wilcock, J.A., Patrick, E.V., Thorne, R.E., Thomas, G.L., 1995. Acoustic estimate of herring biomass in the Green Island area of Prince William Sound, Alaska, 1993. Alaska Department of Fish and Game Regional Information Rep. No. 2A95-27.

DeMaster, D., Atkinson, S., 2002. Steller sea lion decline: is it food? II University of Alaska Sea Grant Program AK-SG-02-02.

Donaldson, W., Morstad, S., Simpson, E., Biggs, E., 1992. Prince William Sound management area 1991 annual finfish management Report. ADF&G, Comm. Fish. Div., Anchorage, AK Regional Information Rep. No. 2A92-09.

Dovers, S.R., Handmer, J.W., 1995. Ignorance, the precautionary principle and sustainability. Ambio 24, 92–97.

Foote, K.G., Knudsen, H.P., Vestnes, G., MacLennan, D.N., Simmonds, E.J., 1987. Calibration of acoustic instruments for fish density estimation: a practical guide. Int. Coun. Explor. Sea, Coop. Res. Rep. 144, 1–57.

Funk, F.C., 1994. Forecast of the Pacific herring biomass in Prince William Sound, Alaska, 1993. Regional Information Report No. 5J93-06. Alaska Department of Fish and Game, Juneau, Alaska.

Kirsch, J., Thomas, G.L., 1997. Acoustic biomass estimate of adult herring in Prince William Sound, Alaska, in spring 1997. Contract Report to Alaska Department of Fish and Game. Prince William Sound Science Center, Cordova, AK .

Kruse, G.H., Funk, F.C., Geiger, H.J., Mabry, K.R., Savikko, H.M., Siddeek, S.M., 2000. Overview of state-managed marine fisheries in the Central and Western Gulf of Alaska, Aleutian Islands and Southeastern Bering Sea, with reference to Steller sea lions. Alaska Department of Fish and Game, Div. Comm. Fish., Juneau, AK Regional Information Rep. 5J00-10.

Marty, G.D., Freiberg, E.F., Meyers, T.R., Wilcock, J.A., Farver, T.B., Hinton, D.E., 1998. Viral hemorrhagic septicemia virus, *Ichthyophonus hoferi*, and other causes of morbidity in Pacific herring (*Clupea pallasi*) in Prince William Sound, Alaska, USA. Dis. Aquat. Org. 32, 15–40.

MacLennan, D.N., Simmonds, E.J., 1992. Fisheries Acoustics. Chapman and Hall, London.

McClatchy, S., Thorne, R.E., Grimes, P., Manchet, S., 2000. Ground-truth and target identification for fisheries acoustics. Fish. Res. 47, 173–191.

O'Riordan, R., 1992. The Precautionary Principle in Environmental Management. CSERGE GEC working paper, 92-103. Center for Social and Economic research on the Global Environment, University of East Anglia, Norwich, England.

Quinn II, T.J., Marty, G.D., Wilcock, J., Willette, M., 2001. Disease and population assessment of Pacific herring in Prince William Sound, Alaska. In: Funk, F., Blackburn, J., Hay, D., Paul, A., Stephanson, R., Toresen, R., Witherell, D. (Eds.), Herring Expectations for a New Millennium, pp. 363–379 Alaska Sea Grant, A.J., College Program, AK-SG-01-04.

Roundsefell, G.A., 1929. Contribution to the biology of the Pacific herring, *Clupea pallasi*, and the condition of the fishery in Alaska. US Department of Commerce, Bureau of Fisheries, Fish Doc. 1080.

Scheaffer, R.L., Mendenhall, W., Ott, L., 1986. Elementary Survey Sampling. third ed. Duxbury Press, Boston.

Sease, J.L., Taylor, W.P., Loughlin, T.R., Pitcher, K.W., 2001. Aerial and land-based surveys of Steller sea lions (*Eumetopias jubatus*) in Alaska, June and July 1999 and 2000. National Marine Fisheries Service. Alaska Fisheries Center, Seattle, WA, pp. 52 NOAA Technical Memorandum NMFS-AFSC-122.

Sharp, D., Morstand, S., Wilcock, J.A., 1996. Prince William Sound management area herring report to the Alaska Board of Fisheries Alaska Department of Fish and Game, Anchorage, Alaska. Regional Information Rep. 2A96-40.

Thomas, G.L., Backus, E.H., Christensen, H.H., Weigand, J., 1991. Prince William Sound/Copper River/North Gulf of Alaska Ecosystem. J. Dobbins Associates Inc., Washington, DC.

Thomas, G.L., Patrick, E.V., Kirsch, J., Allen, J.R., 1997. Development of a multi-species model for managing the fisheries resources of Prince William Sound. In: Hancock, D.A., Smith, D.C., Grant, A., Beumer, J.P. (Eds.), Developing and Sustaining World Fisheries Resources–the State of Science and Management. CSIRO Publishing, Collingwood, Australia, pp. 606–613 2nd World Fisheries Congress.

Thomas, G.L., Thorne, R.E., 2001. Night-time Predation by Steller Sea Lions. Nature 411, 1013.

Thomas, G.L., Kirsch, J., Thorne, R.E., 2002. Ex situ target strength measurements of Pacific herring and Pacific sand lance. North Am. J. Fish. Manage. 22, 1136–1145.

Thorne, R.E., 1977. Acoustic assessment of hake and herring stocks in Puget Sound, Washington, and southeastern Alaska. In: Margets, A.R. (Ed.), Hydroacoustics in Fisheries Research. Rapp. P.V. Réun. Cons. Int. Explor. Mer, 170, pp. 265–278.

Thorne, R.E., 1977. A new digital hydroacoustic data processor and some observations on herring in Alaska. J. Fish. Res. Board Can. 34, 2288–2294.

Thorne, R.E., 1983. Hydroacoustics. In: Nielson, L., Johnson, D. (Eds.), Fisheries Techniques. American Fisheries Society, Bethesda, MD (chapter 12).

Thorne, R.E., 1983. Assessment of population abundance by echo integration. Proc. Symp. Assess. Micronekton. Biol. Ocean. J. 2, 253–262.

Thorne, R.E., 2000. Biological Monitoring of Herring and Pollock in Prince William Sound. Annual Progress Report to Oil Spill Recovery Institute. Prince William Sound Science Center, Cordova, AK.

Thorne, R.E., Trumble, R., Lemberg, N., Blankenbeckler, D., 1983. Hydroacoustic assessment and management of herring fisheries in Washington and southeastern Alaska. FAO Fish. Agric. Org. United Nations Fish. Rep. 300, 269–277.

Thorne, R.E., Thomas, G.L., 1990. Acoustic observation of gas bubble release by Pacific herring. Can. J. Fish. Aquat. Sci. 47, 1920–1928.

Thorne, R.E., Thomas, G.L., 2002. Evaluation of Changes in the Foraging Behavior of Steller Sea Lions in Response to Precipitous Declines of the Herring Population in Prince William Sound, Final Report to National Marine Fisheries Service, SSLRI Project #31. Prince William Sound Science Center.

Trumble, R., Thorne, R.E., Lemberg, N., 1982. The Strait of Georgia herring fishery: a case of timely management aided by hydroacoustic surveys. Fish. Bull. 80, 381–388.

Vilhjálmsson, H., Carscadden, J.E., 2002. Assessment surveys for capelin in the Iceland-East Greenland-Jan Mayen area, 1978–2001. ICES Mar. Sci. Symp. 216, 1096–1104.

Available online at www.sciencedirect.com
SCIENCE DIRECT®
Aquatic Living Resources 16 (2003) 255–263
Aquatic Living Resources
www.elsevier.com/locate/aquliv

Causes and effects of underwater noise on fish abundance estimation

Ron B. Mitson [a,*], Hans P. Knudsen [b]

[a] *Acoustec, Lowestoft, UK*
[b] *Institute of Marine Research, Bergen, Norway*

Accepted 23 January 2003

Abstract

The power of modern research vessels using diesel engines means significant levels of noise may be radiated underwater. At low frequencies a surveying vessel must not cause fish avoidance behaviour when it is using trawl or acoustic assessment methods. All the main mechanisms that form the essential propulsion system are described and discussed in terms of underwater radiated noise. Diesel engines, generators and propulsion motors contribute significantly to the low frequency spectrum and an illustration is given of underwater noise when an unsuitable propulsion system is used. Avoidance behaviour by a herring school is shown due to a noisy vessel, by contrast there is an example of no reaction of herring to a noise-reduced vessel. Propellers are major sources of both low and high frequency noise. The latter should not reduce echo sounder detection range, nor contaminate echo integrator recordings. Underwater noise levels from four vessels with different machinery and propulsion characteristics are seen in relation to ambient noise levels at 18 kHz. Fish detection is examined in relation to sea background noise and vessel self-noise. Calculated detection ranges for fish target strength classes from –30 to –60 dB at 38 kHz are shown for six vessels travelling at 11 knots, based on self-noise measurements. Echo sounder noise levels from several vessels at 120 and 200 kHz are tabulated. Beyond 100 kHz the effect of vessel-radiated noise is usually insignificant; levels up to that frequency are proposed in the International Council for the Exploration of the Sea (ICES) Cooperative Research Report No. 209 of 1995.

Keywords: Vessel noise; Vessel avoidance; Fish detection

1. Introduction

Fisheries management requires unbiased estimates of the stocks. Currently, the estimates are made mostly by trawl and acoustic surveys whose accuracy depends on sampling an undisturbed natural distribution of the populations. A survey vessel should ideally not affect the behaviour of fish in its vicinity and should be capable of using its scientific echo sounder and sonar systems to their maximum capabilities. A low underwater radiated noise signature is the key to success in these matters and this was recognised by the International Council for the Exploration of the Sea (ICES) with the publication of Cooperative Research Report No. 209 (CRR 209, Mitson, 1995). This document was the first in which a limiting noise level recommendation was made on the basis of available scientific evidence. In 1999 a guidance note on machinery characteristics, http://www.ices.dk/pubs/crr/guide209.htm, was issued to advise that a noise reduced vessel should always be in this state when running at, or under, a speed of 11 knots. It is unacceptable for a vessel to have a special ‘survey’ mode.

A few noise-reduced fisheries research vessels were built more than 30 years ago but these fail to meet current noise recommendations by a significant margin. Although their machinery configuration was similar to more recent vessels, improvements in all aspects of the important technologies mean that it is now feasible to achieve low levels of underwater radiated noise as recommended by CRR 209. Prior to this report, FRV “Corystes” came into service in 1988, having been built to a stringent underwater noise specification set by the owners. A good result was reported by Kay et al. (1991) after modifications during the latter part of construction. This gave confidence when FRV “Scotia” was designed and built to a similar engineering specification where meeting the CRR 209 recommendations formed part of the building contract. Important lessons learned from FRV’s “Corystes” and “Thalassa” led to a satisfactory outcome when noise measurements were made in 1998.

* Corresponding author.
E-mail address: acoustec@acoustec.co.uk (R.B. Mitson).

doi:10.1016/S0990-7440(03)00021-4

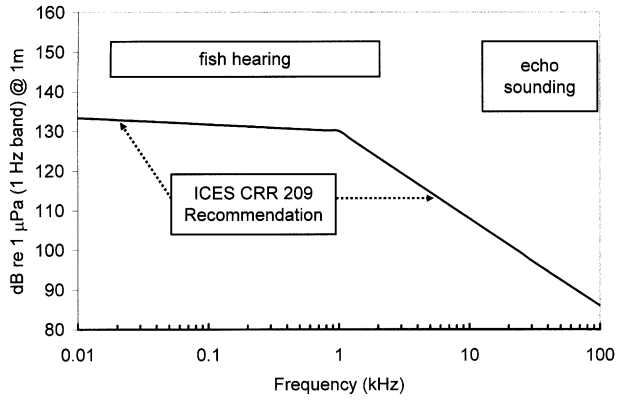

Fig. 1. This shows the maximum underwater radiated noise levels recommended by the ICES CRR 209 (1995) "Underwater Noise of Research Vessels: Review and Recommendations" at vessel speeds up to and including 11 knots. This report is referred to throughout the text as CRR 209.

2. Method

We examine matters relating to the implementation of noise reduction measures necessary to achieve the levels recommended in CRR 209, shown in Fig. 1. Precautions must be taken on many aspects of vessel design to meet these levels, which should not be exceeded at any vessel speed up to and including 11 knots over the frequency spectrum of 10 Hz to 100 kHz. To put the matter of underwater radiated noise and its potential to cause fish avoidance behaviour into perspective fish hearing is briefly mentioned.

The main machinery for running and propulsion of the vessel is examined in general terms with some details of successful and unsuccessful arrangements being identified. When a vessel has been constructed to meet the CRR 209 levels, proof of compliance has to be obtained and recommended measurement procedures are described.

Details from two separate experiments to determine the effects of a noisy vessel on herring concentrations are described and one experiment, also on herring, using a noise-reduced vessel. We consider the other important factor, the effect of high frequency underwater radiated noise on the detection capabilities of scientific echo sounders. Measurements from several vessels at 18, 120 and 200 kHz are compared. At 38 kHz the detection depths of six vessels are shown for a range of fish target strengths.

This paper aims to provide details of ambient sea noise and the origins and/or levels of vessel radiated and self-noise that can reduce the accuracy and effectiveness of acoustic and trawl surveys.

3. Results

3.1. Fish hearing in relation to vessel noise

It is appropriate to start by referring to fish hearing because of the importance of a survey vessel being able to sample by acoustics or trawl a natural fish distribution undisturbed by radiated noise. At frequencies below about 2 kHz, the CRR 209 graph represents a level above which fish are likely to show avoidance behaviour. Although most commercial fish have a hearing capability extending from a few hertz (Sand and Karlsen, 1986) to possibly tens of kilohertz (Astrup and Møhl, 1993; Dunning et al., 1992) the lower and upper extremes have limited sensitivity. The lowest hearing threshold is 75 dB re 1 µPa at 150 Hz with a 6 dB bandwidth of about 220 Hz for cod (Chapman and Hawkins, 1973). Herring have the same sensitivity but a much greater bandwidth to about 1.5 kHz (Enger, 1967; Blaxter et al., 1981). Both cod and herring are important commercial species so the potential effect of vessel noise is based on their sensitivity and hearing bandwidth. For some other species the possible distances for avoidance behaviour are shown by Mitson (2000).

3.2. Machinery configuration

Much of the necessary machinery to drive and operate a ship produces vibration, within the frequency range of 10 Hz to 1.5 kHz, with the consequence of radiation in the form of pressure waves from the hull. For economic and practical purposes, a distance limit has to be set beyond which no fish avoidance behaviour should occur and in CRR 209 this is set at 20 m from the vessel. To aim for a limit closer to the vessel would increase costs significantly and make the task of noise reduction more difficult.

Currently, the only proven method to produce a low noise vessel suitable for fisheries research is by use of diesel-electric propulsion. This arrangement has several advantages, including relative ease of isolating the main generators from the hull because no mechanical connection is needed to the electric propulsion motor. A successful arrangement has proved to be a 'generating set' (genset) comprising a diesel engine, coupled to an alternator, both of which are mounted on a rigid frame sometimes called a raft. Two stages of isolation by special mounts are arranged for the engine, typically allowing a reduction of vibration of more than 40 dB to be achieved between the engine base and its seating in the hull. To stiffen the raft the alternator is often bolted directly down with a flexible coupling driving it from the engine. Vibration from the alternator caused by magnetic forces has to be taken into account. A particular problem, which must be avoided is due to a form of alternator construction where straight 'slots' are used to accommodate the windings. This causes the generation of a "slot-passing" frequency, f_{Hz} = (number of slots × the engine rpm/60), with a subsequent high vibration level transmitted to the hull via the mountings which can occur in the range of fish hearing. Instead, it is necessary to use herringbone or skewed slot construction techniques to minimise this effect.

The size and number of gensets is chosen according to the power requirements of the vessel and varies between two and four sets for existing vessel designs. Construction of the hull seating for the gensets must aim to achieve maximum stiffness for the purpose of further reducing the transmission of vibration and the subsequent radiation of noise into the water.

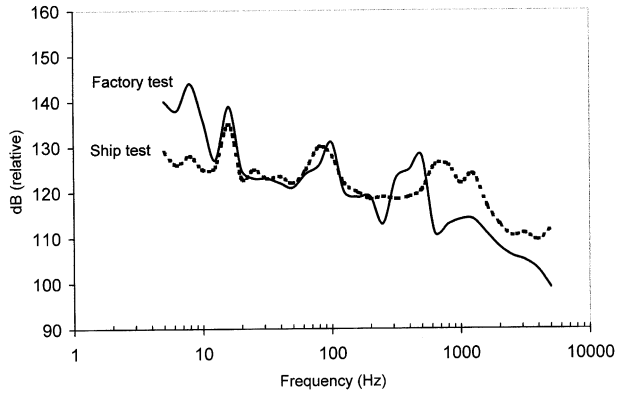

Fig. 2. Showing the measured vibration characteristics of a combined diesel engine and generator set (genset) on 85% load before and after its installation in a vessel.

An impression can be gained of the importance of this process in Fig. 2, showing the change of levels that occurred between factory testing and subsequent installation in the vessel. In this figure note the significant reduction in vibration below 10 Hz but an increase above 600 Hz. For herring, the increase between about 600 Hz and 1.5 kHz shown in this figure could be important. Such an example illustrates the attention to detail that has to accompany the design and construction of all noise reduced vessels and the installed machinery.

The convenience of alternating current (AC) as an electrical power supply is that the voltage supplied from the genset alternators can easily be transformed to different voltages to supply all the vessels requirements. But a propulsion system, known as AC/AC, is now proven to be unsatisfactory because it uses an AC motor where vibration, hence noise levels, are inherently high and this arrangement should not be used. An example of the underwater noise from such a system is seen in Fig. 3 when the vessel was moving at 10 knots. Such high levels of the noise peaks are unsatisfactory. The situation is made worse because a characteristic of this type of propulsion means that the frequency of these peaks varies as the vessel speed changes, moving them across the frequency range of fish hearing.

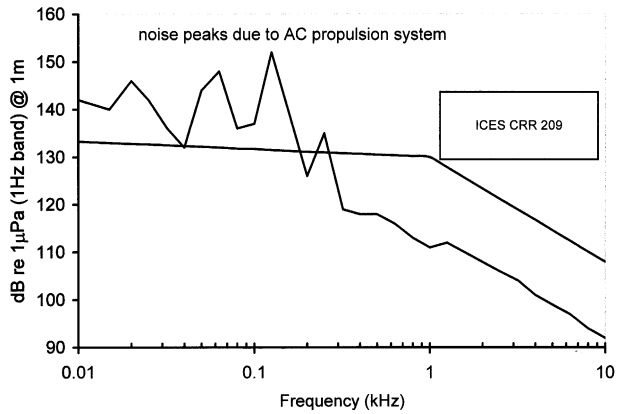

Fig. 3. Underwater radiated noise from FRV “Thalassa” at 10 knots. The peaks are associated with vibration of the propulsion motor due to the AC electrical drive used. Due to the excellent propeller design a very low level of propeller cavitation is evident above 300 Hz.

For a low noise vessel, AC must be converted to direct current (DC), to provide a smooth drive with speed control to the propulsion motor. This system is known as AC/DC and is specified for all vessels currently building to meet the CRR 209 recommendation.

The DC propulsion motor is coupled directly to the propeller and handles the full power needed to drive the vessel so it is ‘hard-mounted’ to the hull and must, therefore, have a very low level of vibration. For this reason its construction must use a herringbone or skewed slot design technique as stated above for the alternators. From 0, to perhaps 150 or 180 rpm, the motor drives the propeller, which produces a broad frequency spectrum of noise but for the present, we consider only the low frequency aspects. As the number of propeller blades increases, the pressure per blade is less and the risk of the phenomenon of cavitation is reduced. However, the overall efficiency is also reduced and a satisfactory compromise has been accepted for most vessels with the use of five blades. FRV “Thalassa” is an exception with six blades and she has an excellent performance at high frequencies but any low frequency benefit is lost due to the AC propulsion.

3.3. Vessel noise signatures

In addition to broad band propeller noise there is a phenomenon known as ‘singing’ where a discrete tone is produced by the propeller, usually due to physical excitation of the trailing edges of the blades. Despite this well-known effect, manufacturers often fail to provide an adequate anti-singing trailing edge on their propellers with the result that very high tone levels can occur in the frequency range of fish hearing.

Often the most prominent features in the low frequency signature of a noise reduced vessel are the propeller blade rate and twice this rate. Blade rate is the frequency f at which the blades pass the closest section of the hull, where f_{Hz} = (number of blades × propeller shaft rpm)/60. The level of these ‘tones’ can vary slightly according to the trim of the vessel. Another feature might be the propeller shaft rate. Bandwidths as narrow as 0.375 Hz are used to obtain measurements for identification of the major individual contributions to the signature. Two peaks might be due to a five-bladed propeller where the blade rate at 130 rpm is at 10.8 and 21.6 Hz at twice the rate. From the diesel engine, the cylinder firing rate ×2 and the crankshaft rate ×1 can usually be identified, with their harmonics blending into many other noises at higher frequencies. The running speed of the engine is f_{Hz} = (rpm/60), typical engine speeds for noise reduced vessels are 750 or 1000 rpm. It is expected that the quality of machinery selected for vessels, plus associated isolation measures, will mean that transmission of line frequencies (tones) will be minimised.

The overall signature of a vessel comprises noise from many machinery sources. Pumps in particular are often sig-

nificant producers of noise from vibration and at higher frequencies from turbulent flow. Sharp angles and high flow rates in pipework can also cause cavitation and even small items of machinery might produce quite high levels. As noise and vibration levels of the main machinery items is reduced, the importance of smaller objects increases. For example, the ringing of a telephone hard-mounted on an engine room bulkhead, has been detected underwater at a distance of about 1 km.

3.4. Determining the vessel noise signature

Investigation of a noise signature involves two operations. A 'static' ranging with the vessel held securely between moorings. This provides an opportunity to identify the frequency spectrum and levels from particular pieces of machinery. A typical exercise of this sort involved 187 operations, with different items being switched on and off and results recorded from each of them. The main dynamic noise ranging operation involves a series of runs at specified speeds through a noise range. This comprises hydrophones about 100 m on either side of the vessel track for port and starboard (beam) measurements, preferably placed 30 m or more metres deep. The slant ranges between the centre point of the vessel and the hydrophones are corrected to 1 m. There are usually one or more hydrophones under the line of the vessel's passage for keel aspect noise measurements. Noise ranges are normally operated for naval purposes and fisheries research vessels are recommended to use these amenities. This is because of the experienced staff with a high standard of facilities and procedures available, which are based on appendices A, B and C of NATO STANAG 1136. The NATO procedures do not require an allowance for Lloyd's mirror effect. In some limited circumstances the use of a portable noise range described by Enoch and McGowan (1997) might be suitable for noise ranging FRV's.

For any vessel, there are angular differences in radiated noise emanating from sections of the hull. Historically, the normal series of measurements made during noise ranging have been taken separately but simultaneously from the port and starboard sides. These often show differences in levels as a result of the layout of machinery within the hull. The third octave band measurements are reduced to a 1 Hz band then averaged to give a simplified picture of the noise signature. Simultaneously, narrow band measurements are made to determine if significant levels of line frequencies (tones) are present. Keel aspect noise levels can be important for a fisheries vessel because the directivity of the hull at low frequencies is greatest in that aspect. On one vessel, this was measured as 6 dB greater than the beam measurements at frequencies below 100 Hz. It is relatively recently that keel aspect noise levels have been specified but it is clear that knowledge of these levels is a necessary requirement. When a vessel runs over the top of a school, fish are suddenly subjected to a higher noise level, which may cause a sharp diving reaction as seen by Olsen et al. (1983).

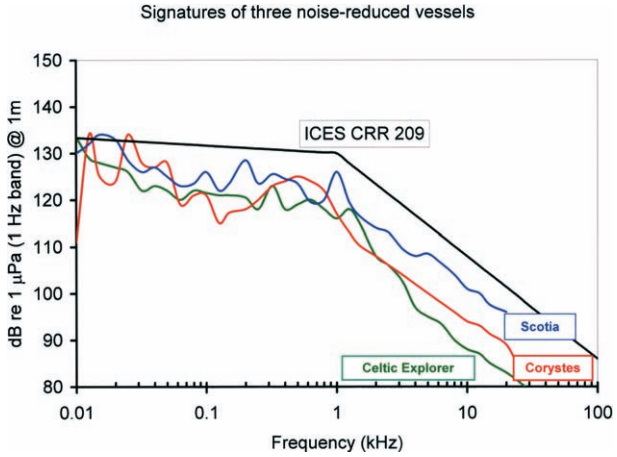

Fig. 4. Underwater radiated noise signatures of three noise-reduced vessels, FRV's "Corystes" "Scotia", "Celtic Explorer" shown for vessel speeds of 11 knots in relation to the CRR 209 levels.

Signatures of three noise-reduced vessels, whose measurements were carried out to the NATO standard, are compared in Fig. 4 to the CRR 209 recommended levels. These vessels were running at 11 knots and have similar configurations of machinery although the manufacturers are not the same for all items. FRV "Corystes" was built 7 years before CRR 209 was published. For her, the blade rate and twice the rate are seen to cross the line slightly but thereafter a significant margin exists. A more diffuse low frequency deviation is seen in the signature of FRV "Scotia" which is partly due to the blade rate and a flow induced resonance. The latest vessel is FRV "Celtic Explorer" whose blade rate level barely touches the line and at frequencies above 3 kHz the levels are very low, giving the potential for a good fish detection capability.

3.5. Observed effects of vessel low-frequency noise

There are many reports of fish avoidance caused by research vessels, e.g. Buerkle (1977), Olsen (1979), Diner and Massé (1987), Goncharov et al. (1989), Misund (1993), Soria et al. (1996), Arrhenius et al. (2000) and Vabø et al. (2002). The latter authors studied vessel avoidance behaviour of wintering spring-spawning herring during an acoustic abundance estimation survey being carried out by FRV "Johan Hjort". Observations of echo energy from schools were made from a downward-looking echo sounder transducer submerged at 12 m when the survey vessel approached and passed the surface marker at close range. There is a difficulty in associating avoidance behaviour with the speed of this vessel because of the highly variable levels of noise that occur, primarily due to changes of propeller pitch. No details are given of the pitch settings used during the experiments but, for example, there are also two available propeller shaft speeds of 100 and 125 rpm, each of which can produce a vessel speed of 8 knots by different pitch settings. At this speed it can be seen from Fig. 5 that noise levels of either 164 or 144 dB occur. These translate into possible fish reaction ranges of 790 and 79 m, respectively.

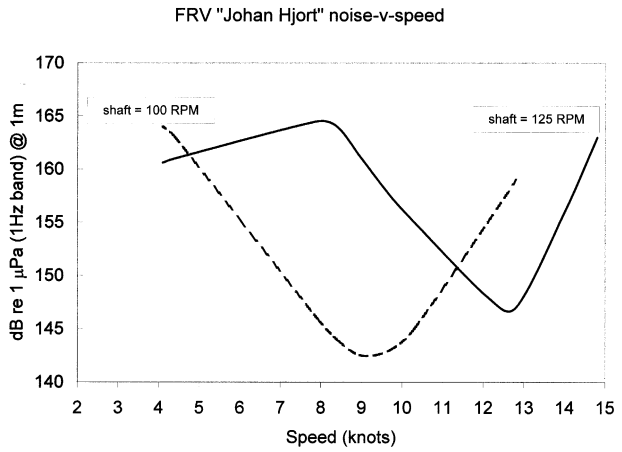

Fig. 5. Variation of underwater radiated noise with speed of FRV "Johan Hjort" resulting from changes of propeller pitch and the optional propeller shaft rpm of 100 or 125. These noise levels occur at a frequency of about 100 Hz.

FRV "Johan Hjort" was also used in 2002 for a large scale systematic investigation of how vessel avoidance by herring may affect abundance estimation. Data from one of about 50 passes made during the experiment are shown in Fig. 6A, B, illustrating the reaction of a herring layer to the approach of the vessel and the effect on the received echo energy. A full data analysis is in preparation for publication by Ona et al. The recordings were made from a stationary EK 60, 38 kHz echo sounder, mounted in a floating buoy system, described by Godø and Totland (1999) and Godø et al. (1999), when the research vessel passed close by. It seems clear from the recordings that the high power pulse transmission from the echo sounder had no effect on the fish aggregation. During the experiment, the 38 kHz echo sounder of FRV "Johan Hjort" was turned off so as not to disturb the buoy recordings, 18 kHz was used instead.

In Fig. 6A, the effects on the echo recording from the layer of herring are caused by FRV "Johan Hjort" running at a nominal 10 knots from a distance 1.2 km up to and passing alongside the buoy to within 8-10 m at 0 min, then receding. Fig. 6B helps to quantify the results of the avoidance behaviour by showing how the mean depth of the echo energy changed as the vessel approached and passed the buoy. The radiated level of noise from the vessel appears to start affecting the fish aggregation at about 1.75 min prior to the closest approach when a downward trend begins in the depth of the echo.

This corresponds to a distance of 540 m. FRV "Johan Hjort" was using a propeller shaft speed of 125 rpm, giving a radiated noise level sufficient to cause fish avoidance behaviour at 560 m distance when travelling at 9 knots but it reduces to 355 m at 10 knots. Fig. 5 shows that large changes in noise level occur for a small change in speed. Fig. 6A, B indicate a relatively quick recovery after the vessel's closest point of approach. The nature of the curve that follows suggests abnormal fish activity continues for sometime as the vessel travels away from the buoy.

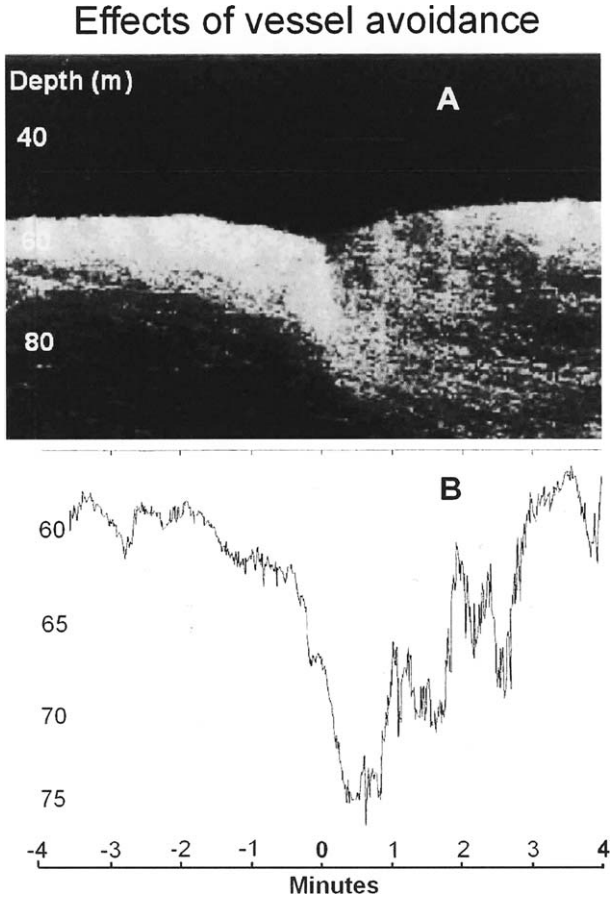

Fig. 6. (A) The time depth record was taken from a buoy mounted echo sounder and shows a herring school exhibiting vessel avoidance behaviour during a passage of the FRV "Johan Hjort" from about 1200 m to within 8–10 m of the recording buoy. (B) This shows the change in mean depth of the recorded echo energy due to the passage of FRV "Johan Hjort".

Variability in the response of fish to nearby vessels has been reported and more observations are needed to investigate this matter. It might be due to the physiological state of the fish at different seasons of the year, or local environmental factors such as salinity, temperature or water transparency. Thermal gradients in the sea can cause radiated noise to be directed either upwards or downwards depending on the gradient. These may reduce or even prevent noise reaching the fish, the so-called 'afternoon effect' due to heating in the upper layers of water.

3.6. Low-noise research vessel survey

Fish avoidance behaviour experiments, using research vessels, can be expensive but it is hoped that effort will be directed towards such work as the number of noise-reduced vessels increases. Evidence is available from an example reported by Fernandes et al. (2000) to show that a vessel noise-reduced to the CRR 209 recommendation does not induce avoidance behaviour by fish. A herring survey in the North Sea was conducted during July 1999 by FRV "Scotia" during part of which an autonomous underwater vehicle (AUV) known as Autosub was used for comparative mea-

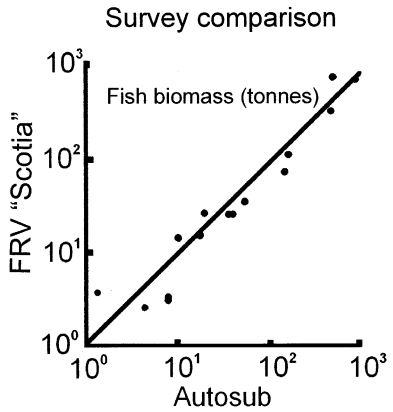

Fig. 7. Results from a herring survey made by FRV "Scotia" and the AUV Autosub, showing significant correlation ($r = 0.935$, $P < 0.001$) of the strata averaged biomass estimates from these vessels; after Fernandes et al. (2000). This indicates that the noise-reduced FRV "Scotia" did not cause any vessel avoidance behaviour to be exhibited.

surements on a large aggregation. This vehicle has an extremely low level of radiated noise, Griffiths et al. (2001), typically between 20 and 40 dB less than FRV "Scotia", by reason of being a small, battery powered device, with minimum moving parts. Autosub has a limited speed of about 4 knots, which had to be matched by FRV "Scotia" for this experiment. It was reasonable to assume that the results would be valid for the normal survey speed because the noise signature of FRV "Scotia" is almost identical at 4 and 11 knots up to 1 kHz. Autosub was deployed 200–800 m ahead of the FRV on eight transects in water 60–180 m deep using the same scientific echo sounder as the FRV. It passed very close indeed to the herring school but caused no more than a localised compression, typical of a close approach by a predator in visual range. If the FRV radiated noise was at a level to cause a reaction from these fish, it was expected that it would detect a smaller quantity than Autosub. The correlation between the two vessels is seen in Fig. 7, which indicates that no avoidance behaviour took place.

3.7. Noise at echo sounder frequencies

If a vessel is sufficiently quiet that it does not disturb fish in its vicinity it also needs the capability to detect them, determine their target strength (size) distributions and assess the population distribution and density (MacLennan and Simmonds, 1992). Very sensitive scientific echo sounders operating at frequencies above 10 kHz are used for these purposes (Mitson, 1983) and there are two main sources of noise that can restrict their capabilities, the ambient noise due to natural forces and vessel self-noise.

3.8. Underwater ambient noise

Ambient noise in the sea, due to sea-state, shows great variability as a result of the many sources from which it arises, so any levels quoted are averages from a number of situations (Ross, 1987). Wind blowing on the surface is a significant cause (Urick, 1983) but as frequency increases, typically above 100 kHz, thermal (molecular agitation) noise begins to increase and become more important (Mellen, 1952). In this paper, we will use metres per second, m s^{-1}, for the wind speed. For unusual local circumstances, such as heavy rain, noise can rise by about 20 dB for a wind speed of 1.5 m s^{-1} when rainfall increases from 1 to 7 mm h^{-1} (Scrimger et al., 1989). Below 1 kHz, ambient noise is not likely to affect fisheries acoustic surveys, although fish behaviour may be modified if the level is high enough to mask their hearing.

3.9. Fish detection

The ultimate theoretical limit, to detection of fish echoes, is the level of ambient noise in the sea. Echo sounders, operating at the lower frequencies, are most vulnerable to this noise because above 1 kHz it decreases by about 20 dB per decade. The lowest frequency normally used for fish detection and assessment purposes is 18 kHz, and at this frequency, a typical echo sounder might expect to receive a signal of 76 dB re 1 μPa from a single fish of –40 dB target strength (TS) at 600 m depth. Ambient noise is about 22 dB re 1 μPa for a wind speed of 1.5 m s^{-1}, and at 20 m s^{-1} this has increased to 48 dB. When corrected for echo sounder bandwidth these levels become 49 and 76 dB re 1 μPa, respectively, so for the higher wind speed this fish would not be detected. There is little to be done about high ambient noise levels other than reduce the echo sounder receiver bandwidth which is usually linked to the transmitted pulse duration, so has other implications.

If weather conditions are good, fish detection is mainly limited by the self-noise of the vessel. This refers essentially to noise generated on, or by the vessel, which is received by the echo sounders and sonars, a major source being the propeller. It is noise due to the presence of the vessel and not to the surrounding medium. Mechanisms which cause self-noise are also capable of radiating noise into the sea but it is important to keep a clear distinction between self and radiated noise. Echo sounders and sonars are normallysituated within the near-field of these sources and the noise they receive is different from that in the radiated far-field. At 18 kHz, the wind-induced noise is likely to be dominant but frequencies above 70–100 kHz are more prone to limitation by thermal noise. Fig. 8 compares the self-noise levels at 18 kHz of four research vessels running at speeds from 3 to 12 knots. Ambient noise levels related to wind speeds from 3 to 20 m s^{-1} are included.

This figure shows that for FRV's "G.O. Sars" and "Johan Hjort" self-noise exceeds sea-state noise for wind speeds below 5 m s^{-1}, whilst for FRV "Bjarni Saemundsson" self-noise rises sharply with vessel speed from a low level below ambient noise due to a wind of 3 m s^{-1} almost reaching the level from a 20 m s^{-1} wind at 11 knots. For FRV "Thalassa" the ambient noise at 3 m s^{-1} wind speed is only slightly greater than vessel self-noise over much of her speed range. This is due to an exceptionally low noise propeller.

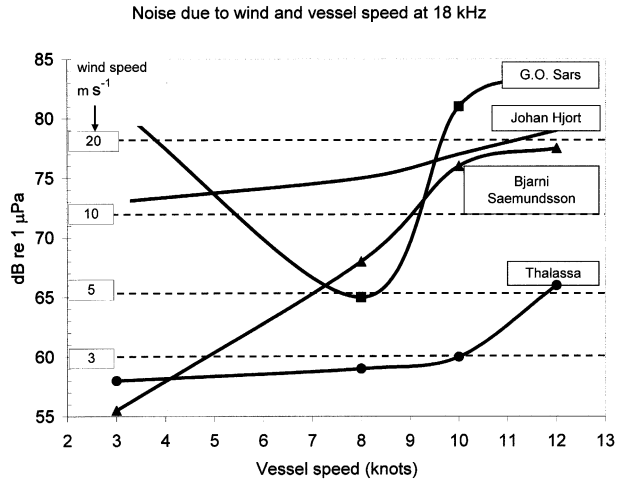

Fig. 8. A comparison of the self noise measured on four vessels at a frequency of 18 kHz when travelling at speeds between 3 and 12 knots. Ambient noise levels in the sea due to wind speed are also shown.

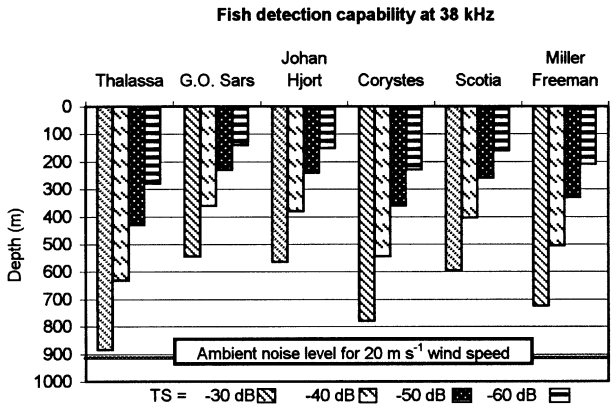

Fig. 9. The fish detection depth capability of six vessels at 38 kHz is shown for four classes of fish target strength. Calculated from self noise and radiated noise measurements.

At echo sounder frequencies, the propeller is the most significant source of self-noise, although orifices in the hull, projections, and rough surfaces, can also play a part. This noise becomes severe when one or more of the common types of propeller cavitation, tip, blade, sheet, hub is fully established. The use of controllable pitch (CP) propellers in vessels means that alteration of the blade pitch angle, sometimes combined with changes of propeller shaft speed, results in a highly variable generation of noise as seen in Fig. 5. Another example of this is FRV "G.O. Sars" in Fig. 8. This type of propeller is discredited for vessels used in fisheries research. For present day purposes, attention is given to the design of fixed pitch propellers where high frequency noise is more directly related to shaft speed as seen for FRV "Thalassa" in Fig. 8. Such designs must adequately meet the criteria of low noise, whilst being capable of achieving sufficient pulling power for trawls and the desired maximum free-running speed. The approximate rate of reduction in propeller noise is 20 dB per decade. In ICES CRR 209, the aim above 1 kHz was to achieve a maximum limit of 130–22 log f_{kHz} at vessel speeds up to, and including, 11 knots. In choosing a maximum of 11 knots for the low noise condition, the ICES Study Group took into account the fact that few of the vessels existing at that time were capable of exceeding such a speed without risking corruption of the echo integration process due to self-noise. Difficulties in realising a propeller design to meet the three conflicting criteria above were also recognised. Progress is being made in this respect with FRV "Thalassa" being one example and a recent design for FRV "Celtic Explorer" has achieved very low levels of noise, particularly at high frequencies.

Detecting individual fish is a demanding task, depending on the actual target strength and range from the transducer. Taking these factors into consideration, as range increases so the received signal grows weaker until it is ultimately at the same level as the noise and cannot be detected. At lower frequencies, although absorption losses are less, wind induced noise is higher, so this carries the risk of reducing the detection range of the echo sounder. Noise levels for three wind speeds at 18 kHz are shown in Fig. 8 but results are not available from vessels built to the ICES CRR 209 recommended levels at this frequency.

When the wind speed is high it also induces motion of the vessel, causing turbulence and air bubbles beneath the hull. This has a deleterious effect on the performance of transducers mounted there through attenuation and signal blocking. In the past this has meant restricting the speed of the vessel. Now, the problem has been reduced in some vessels by the use of a 'drop keel' or 'centreboard' projecting to about 3 m below the hull with transducers fitted at the bottom surface, an idea introduced by Ona and Traynor (1990). As a result of this innovation there is greatly improved performance in bad weather and the limiting factor to surveying may no longer be noise from turbulence, or from signal blocking, but safety to engage in tasks such as trawling or other overboard activities.

Fig. 9 shows the fish detection predictions for six vessels at 38 kHz, related to their noise levels when operating at 11 knots. The signal to noise ratio used was 10 dB and the fish target strengths are from –30 to –60 dB. A bandwidth of 976 Hz was assumed. The same source level was used for each vessel calculation. For reference purposes the detection limit due to ambient noise is shown for the wind blowing at 20 m s^{-1}. It is interesting to note the difference in detection range of the vessels, which is directly related to the performance of their propellers. Those for FRV's "Corystes", "Thalassa" and "Miller Freeman" were optimised for low noise and consequently these vessels have the better fish detection capabilities. FRV "Thalassa" has an excellent six-bladed propeller but those on FRV's "Corystes", "Scotia" and "Miller Freeman" are five-bladed. The latter has a new design of highly skewed propeller provided at a recent refit. FRV "Scotia" noise measurements were taken with the drop-keel down at 3 m. When it was at 0 m, with the transducer face flush to the hull, the 38 kHz noise level was 2 dB greater. This vessel does not have an optimised propeller so her detection capability is slightly less than that should be. Both

Table 1
Self noise levels (dB re 1 μPa) relative to vessel speed measured at 120 and (200) kHz

Vessel	Speed (knots)					
	2	4	6	8	10	11
B. Saemundsson	75.5	75.5	75.5	75.5	75.5	75.5
G.O. Sars	67 (78)	67 (78)	67 (78)	67 (78)	67 (78)	67 (78)
Johan Hjort	74 (95)	74 (95)	74 (95)	74 (92)	74 (92)	74 (94)
Scotia			62 (62.5)	62 (63.8)	63.5 (64.8)	64 (64.8)
Thalassa	66.5	66.5	66.5	66.5	67	67
Miller Freeman	63.6	63.6	64.2	63.7	63.7	64.1

the FRV's "G.O. Sars" and "Johan Hjort" have controllable pitch, four-blade propellers.

Higher frequencies of 120 and 200 kHz are used in some surveys and it can be seen from the measured self-noise levels in Table 1 that vessel speed has little effect, except perhaps in the case of FRV's "Scotia" and "Thalassa", where there is a slight increasing trend at 120 kHz. FRV "Miller Freeman" uses a CP propeller for speed control and a small variability is seen but the flat response from the other vessels could be due to detection of thermal noise level in the sea. At 120 kHz, this is about 26 dB re 1 μPa, resulting in 61 dB for a bandwidth of 3096 Hz. In some instances internal receiver noise or electrical interference can be significant at these frequencies. At 200 kHz, the thermal level is about 30 dB, so in a bandwidth of 1953 Hz the receiver level would be 63 dB. At this frequency, there is little indication of vessel speed affecting results, apart from FRV "Johan Hjort" where some variation is seen but her levels are much higher than the other vessels, probably due to receiver noise.

4. Discussion

The effects of vessel radiated noise on fish and on their detection by echo sounder have been well recognised and documented in many papers and reports. Here we have attempted to expand details in some of the important areas to explain causes and possible effects of such noise on surveys of fish abundance. Firstly, vessel mechanisms that produce low frequency noise within the hearing frequencies of fish. We then draw attention to aspects of high-frequency underwater noise, including vessel self-noise and ambient levels in the sea with comparison of their effects where appropriate. The most significant effect on fish abundance estimation is likely to be that of low-frequency noise causing vessel avoidance behaviour by fish which can bias acoustic and trawl survey results. Problems may be compounded when results are needed from the combination of acoustic data with bottom trawl data, as is the case for pelagic and semi-demersal species. Fish may be driven out of the path of the vessel where they will be missed by the echo sounder, or, into or out of the path of a trawl. Some reports show that fish may be driven into the path of a net which otherwise would not have been caught (Saetersdal, 1969; Ona and Godø, 1990; Dorchenkov, 1986) thereby distorting the natural distribution estimates.

At echo sounding frequencies the noise levels for several vessels have been taken as the basis for calculating detection depths of several target strength classes in Fig. 9. Considerable differences are seen between the vessels, thereby emphasising the need for low noise propellers to obtain maximum performance from the echo sounders. In the case of older fixed pitch propellers, where noise is a problem, a palliative is reduction of speed. For vessels with CP propellers this remedy is not effective because of the extreme variability of radiated noise with change of blade pitch, hence speed.

Ambient noise levels in the sea are unlikely to have a major effect on acoustic or trawl surveys unless conditions are exceptional, or when working in deep water with fish recorded as single targets (Reynisson, 1996). At frequencies greater than 100 kHz the performance restrictions may be due to limitations of the echo sounder receivers rather than thermal noise in the sea, or possibly to electrical interference on the vessels. Turbulence and bubble sweep down under the hull will remain a problem where vessels are not fitted with a drop keel, or do not use a towed transducer.

Is there an alternative to the type of noise reduced vessel outlined in this paper? For a full capability in fisheries and oceanography research the answer appears to be no. However, AUV's have a potential for very low noise levels shown by measurements on Autosub and the experiment to survey a herring aggregation in conjunction with FRV "Scotia" was reported above. Such a vehicle might be usefully employed where circumstances are favourable, e.g. using it when controlled from a noisy vessel. This use would require careful planning in regard to the distance at which the AUV could 'safely' be deployed (relative to the noise of the parent vessel). When used from a noise-reduced vessel an extended survey area could prove an advantage but obtaining a representative trawl sample from the recorded fish would be a drawback.

Fisheries research vessels will continue to be designed and built. Due to the long time interval between the building of a vessel and its subsequent replacement, to say nothing of the cost, it is vital that lessons learned in the building and construction process of each vessel are carefully assessed and appropriate action taken to benefit from them. It is suggested that the ICES community should take steps to publish details of their vessels design and performance achieved because of the need to not only set suitable standards but to minimise the cost of these projects.

The major engineering design problems appear to have been solved by:

- careful attention to detail in the selection of high quality, low vibration diesel engines and alternators for the main generating sets. These items must be adequately isolated and the composite assemblies installed on stiff seatings in the hull. Associated pipe work has to be isolated to reduce transmission of vibration.
- Use of a DC propulsion motor with a low level of vibration when running from an electrical drive with a minimum of 24-pulses (the so-called AC/DC system). This motor must be firmly seated in the hull. Four new vessels including FRV's "Celtic Explorer", "CEFAS Endeavour", the replacement "G.O. Sars" and the "Oscar Dyson" use AC/DC propulsion. Investigations show there are no significant differences between the installed costs of AC/DC and AC/AC propulsion systems. Since high power electronic control systems are used for propulsion there is a need to ensure that electromagnetic compatibility (EMC) is carefully specified to reduce the effects of electrical interference on the scientific echo sounders and other instruments.
- Having specially designed, noise-reduced, multi-bladed, fixed-pitch propellers with anti-singing features.

The new fisheries research vessels for Ireland, the UK, Norway and the USA, built to conform to the ICES CRR 209 (Mitson, 1995) recommendation will be coming into service during the next year and it is hoped that information on their design and performance will be made available to add to current knowledge on the subject of underwater radiated noise and its effect on fish abundance estimation.

Acknowledgements

The authors wish to thank several colleagues at the Institute of Marine Research in Bergen, the Alaska Fisheries Science Centre in Seattle, at IFREMER in France and the Marine Institute of Ireland in Galway. Also, the referees for their helpful comments and detailed criticism.

References

Arrhenius, F., Bethke, E., Cardinale, M., Hakansson, N., 2000. Intercalibration of nautical area scattering coefficients between research vessels. Arch. Fish. Mar. Res. 48, 31–42.

Astrup, J., Møhl, B., 1993. Detection of intense ultrasound by the cod (*Gadus morhua* L). J. Exp. Biol. 182, 71–80.

Blaxter, J.H.S., Gray, J.A.B., Denton, E.J., 1981. Sound and startle responses in herring shoals. J. Mar. Biol. Assoc. UK 61, 851–869.

Buerkle, U., 1977. Detection of trawling noise by Atlantic cod (*Gadus morhua* L). Mar. Behav. Physiol. 4, 233–242.

Chapman, C.J., Hawkins, A.D., 1973. A field study of hearing in the cod (*Gadus morhua* L). J. Comp. Physiol. 85, 147–167.

Diner, N., Massé, J., 1987. Fish school behaviour during echo surveys observed by an acoustic device. Proceedings of International Symposium on Fisheries Acoustics 21–24 June. Seattle, WA, USA, pp. 14.

Dorchenkov, A.E., 1986. Estimation of fish numbers and biomass in the bottom zone through acoustic technique. Rybnoe Khozyaistov (in Russian) 5.

Dunning, D.J., Quentin, E., Ross, D., Geoghegan, P., Reichle, J.J., Menzies, J.K., Watson, J.K., 1992. Alewives avoid high-frequency sound. N. Am. J. Fish. Manage. 12, 407–416.

Enger, P.S., 1967. Hearing in Herring. Comp. Biochem. Physiol. 22, 527–538.

Enoch, P.J., McGowan, S., November 1997. Accurate Measurement of Ownship Acoustic Signature. Sea Technol., 15–20.

Fernandes, P.G., Brierley, A.S., Simmonds, E.J., Millard, N.W., McPhail, S.D., Stevenson, P., Squires, M., 2000. Fish do not avoid survey vessels. Nature 604, 35–36.

Godø, O.R., Totland, A., March 1999. Bergen Acoustic Buoy (BAB)–A Tool for Remote Monitoring of Marine Resources. Joint IASA/EASA meeting, Berlin Paper 2 p. A010. p. 4.

Godø, O.R., Somerton, D., Totland, A., 1999. Fish behaviour during sampling as observed from free floating buoys-Application for bottom trawl survey assessment. ICES CM 1999/J:10.

Goncharov, S.M., Borisenko, E.S., Pyanov, A.T., 1989. Jack mackerel school defence reaction to a surveying vessel. Prog. Fish. Acoust. UK Inst. Acoustics 11, 74–78.

Griffiths, G., Enoch, P., Millard, N.W., 2001. On the radiated noise of the Autosub autonomous underwater vehicle. ICES J. Mar. Sci. 58, 1195–1200.

Kay, B.J., Jones, D.K., Mitson, R.B., 1991. FRV Corystes: A purpose-built Fisheries Research Vessel. The Royal Institution of Naval Architects, London, pp. 12 (Spring meetings 1991).

MacLennan, D.N., Simmonds, E.J., 1992. Fisheries Acoustics. Chapman and Hall, London.

Mellen, R.H., 1952. Thermal noise limit in the detection of underwater acoustic signals. J. Acoust. Soc. Am. 24, 478.

Misund, O.A., 1993. Avoidance behaviour of herring (*Clupea harengus*) and mackerel (*Scomber scombrus*) in purse seine capture situations. Fish. Res. 16, 179–194.

Mitson, R.B., 1983. Fisheries Sonar. Fishing News Books. Blackwell Science, Oxford, UK.

Mitson, R.B. (Ed.), 1995. Underwater Noise of Research Vessels: Review and Recommendations. ICES Coop. Res. Rep. No. 209, 61.

Mitson, R.B., 2000. Fish avoidance: the vessel noise factor. ICES ASC: Incorporation of External Factors in Marine Resources Surveys (K) CM 2000/K:16.

Olsen, K., 1979. Observed avoidance behaviour in herring in relation to passage of an echo survey vessel. ICES CM B: 19 (mimeo).

Olsen, K., Angell, J., Pettersen, F., Løvik, A., 1983. Observed fish reactions to a surveying vessel with special reference to herring, cod, capelin and polar fish. In: Nakken, O., Venema, S.C. (Eds.), Symposium on Fisheries Acoustics, Bergen, Norway. FAO Fish. Rep. 300, 139–149.

Ona, E., Godø, O.R., 1990. Fish reaction to trawling noise: the significance for trawl sampling. Rapp. P-v Réun. Cons. Int. Explor. Mer. 189, 159–166.

Ona, E., Traynor, J.J., 1990. Hull mounted protruding transducer for improved echo integration in bad weather. ICES CM B: 3, 1–10.

Reynisson, P., 1996. Evaluation of threshold-induced bias in the integration of single fish echoes. ICES J. Mar. Sci. 53, 345–350.

Ross, D., 1987. Mechanics of Underwater Noise. Pergamon Press (reprinted Peninsula Publishing (1976 Chap. 4, 8, 10).

Saetersdal, G., 1969. Review of information on the behaviour of gadoid fish. FAO Fish. Rep. 62, 210–215.

Sand, O., Karlsen, H.E., 1986. Detection of infrasound by the Atlantic cod. J. Exp. Biol. 125, 197–204.

Scrimger, J.A., Evans, D.J., Yee, W., 1989. Underwater noise due to rain—Open ocean measurements. J. Acoust. Soc. Am. 85, 726–731.

Soria, M., Fréon, P., Gerlotto, F., 1996. Analysis of vessel influence on spatial behaviour of fish schools using a multi-beam sonar and consequences for biomass estimates by echo sounder. ICES J. Mar. Sci. 53, 453–458.

Urick, R.J., 1983. Principles of Underwater Sound. McGraw-Hill Book Company.

Vabø, R., Olsen, K., Huse, I., 2002. The effect of vessel avoidance of wintering Norwegian spring spawning herring. Fish. Res. 58, 59–77.

Available online at www.sciencedirect.com
SCIENCE DIRECT®
Aquatic Living Resources 16 (2003) 265–270
Aquatic Living Resources
www.elsevier.com/locate/aquliv

Avoidance behaviour in cod (*Gadus morhua*) to a bottom-trawling vessel

Nils Olav Handegard [a,b,*], Kathrine Michalsen [a], Dag Tjøstheim [b]

[a] *Institute of Marine Research, P.O. Box 1870 Nordnes, 5817 Bergen, Norway*
[b] *Department of Mathematics, University of Bergen, P.O. Box 7800, 5020 Bergen, Norway*

Accepted 18 December 2002

Abstract

The reaction of fish induced by a trawling vessel was measured using the Bergen Acoustic Buoy. It is a free-floating buoy with a split beam echo sounder system. Individual fish trajectories were obtained by target tracking methods, and average swimming velocities as a function of depth and time before and after passage of the vessel was calculated. A measure for the change in behaviour was applied, showing a significant response during and after propeller passage. The change in horizontal displacement speed is significant at all depths, while the change in vertical displacement velocity is significant at all but one layer of depth. The horizontal reaction seems to occur a bit later than the diving reaction. After the main response, a slightly higher mean horizontal displacement speed was observed for the deepest layers. This indicates a change in the fish state after being exposed to the vessel/gear.

Keywords: Cod avoidance; Target tracking; Abundance estimates; Acoustic buoy; Bottom trawl

1. Introduction

When assessing the abundance of cod and haddock in the Barents Sea, the bottom trawl survey and the acoustic measurements produce two independent estimates. In order to combine these estimates, and arrive at an absolute abundance estimate of the stock, the fishing efficiency of the trawl and the reaction of the fish relative to the vessel and gear must be known (Ona and Godø, 1990; Aglen et al., 1999). This paper presents a quantitative methodology for measuring individual response of fish to a trawling vessel, as opposed to changes in density. The method is also capable of quantifying the change in behaviour as the vessel passes.

Fish avoidance of a vessel has been reported both in acoustic surveys (Olsen, 1971; Olsen et al., 1983; Olsen, 1990), and in trawl surveys (Ona, 1988; Ona and Godø, 1990; Nunnallee, 1991). It has been reported that cod react as early as 200 m in front of the vessel propeller (Ona, 1988), and that this reaction occurs between the surface and 200 m depth. Buerkle (1977) reported that Atlantic Cod is able to detect a trawling vessel at a range of at least 2.5 km.

In swept area indices, the effective fishing height of the trawl is taken to be constant between hauls. But as shown by Aglen et al. (1999), this is not always the case. In response to vessel and gear, fish in the pelagic zone may swim towards the bottom. The bottom trawl will thus catch fish that were originally higher in the water column than the height of the trawl opening. Vertical herding might be dependent on the size of the fish and their vertical distribution patterns. Effective fishing heights of 30 m for large fish and 4 m for small fish were used for estimating the amount of fish unavailable to the bottom trawl in Aglen et al. (1999).

This paper shows that by using a free-floating buoy with a split beam echo sounder system, the actual response of single individuals can be measured, not only responses measured as changes in water column S_A values. The method used here also makes it possible to measure the mean displacement of individual fish in both the horizontal and vertical direction, and to compare the two. To our knowledge, this has not been done before, and it is an important step towards estimating the effective fishing volume of the bottom trawl.

2. Materials and method

The experiment was conducted with "R/V G.O. Sars" off the coast of Finnmark (72°N 25°E) from 12 to

* Corresponding author.
E-mail address: nilsolav@imr.no (N.O. Handegard).

doi:10.1016/S0990-7440(03)00020-2

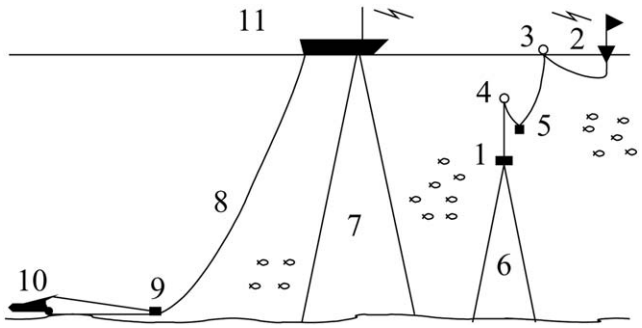

Fig. 1. Overview of the experimental set-up. Note that the figure is schematic and that the scale is not real. Numbers (1) to (6) designate the acoustic buoy. (1) is the transducer with the compass, (2) is the buoy with PC, GPS, Simrad EK60 echo sounder and communication systems. (3 and 4) are the floats and (5) is the weight for stabilising the transducer movement. (6) is the acoustic beam of the EK60 buoy echo sounder. (7) is the beam of the on board mounted echo sounder (operated only at 18 kHz), (8) is the trawl warps, (9) is the trawl doors, (10) is the trawl and (11) is the "R/V G.O. Sars".

21 March 2001. The data were collected using the Bergen Acoustic Buoy (Godø et al., 1999). The buoy is free floating and contains a Simrad EK60 split beam echo sounder, a computer, various communication instruments, GPS and a battery package. Communication to the vessel is maintained through a spread spectrum radio connection with a data transfer rate of 115.2 KB s. This allows for continuous update of echogram, compass data, buoy GPS position and remote control. The transducer is mounted in a stainless steel rig, which is equipped with a compass for continuous recording of transducer direction. The rig is balanced with floaters and weights to stabilise it during operation, and to reduce the effect of surface waves, cf. Fig. 1. The depth of the transducer can be regulated by the placement of the floaters and counterweights on the cables. The transducer depth varied between 37 and 47 m with a median of 44 m.

The change in fish behaviour was measured by passing the buoy 16 times during bottom trawling (Campelen, 1800). The buoy was passed as close as possible. The distance measured by the GPS between the centreline of the vessel and the buoy GPS varied from 48 to 53 m with a median of 53 m. The buoy drift was monitored by the buoy GPS system and the trawl position was monitored by the Simrad ITI system. This information was used to ensure that the trawl passed within the beam of the buoy. The horizontal distance from the trawl to the buoy, measured by the ITI system and the buoy GPS, varied from 42 to 257 m with a median of 45 m. Two times the buoy was passed with a pelagic trawl. These hauls were used only to identify the species distribution higher up in the water column. Table 1 gives an overview of the catches from the trawl hauls.

2.1. Target tracking

The EK60's single target detection algorithm was used to obtain single targets of fish within the echo beam. As shown by Brede et al. (1990), it is possible to connect the detected single targets to tracks. A target-tracking algorithm similar to the Wintracker algorithm (Ona and Hansen, 1991; Ona, 1994) was used, i.e. a track gate box around the last detection in the track is used to search for the next candidate for the track. The size of this box is given in Table 2. In addition, if the track contains more than five pings, a regression is ap-

Table 1
Bottom trawl catches in weight (kg) by species. Tows conducted during daytime are denoted by D, and tows conducted during night time by N

Date	Time	Day/Night	Catch weight (kg)				
			Cod	Haddock	Saithe	Redfish	Total
14-March-2002	02:50	N	376	14	3	4	398
	07:57[a]	D	350	22	78	24	475
	14:04	D	468	35	212	12	727
	16:43	N	535	40	10	5	590
	19:06[b]	N	0	0	0	0	0
	20:50	N	119	8	0	6	132
	22:10	N	58	0	2	3	63
15-March-2002	00:30	N	103	12	14	8	137
	02:24	N	116	22	21	2	162
	19:45	N	150	32	17	4	204
	21:20	N	101	21	20	5	147
16-March-2002	19:03[b]	N	0	0	0	0	0
	21:10[b]	N	0	0	0	0	0
	23:36[a]	N	1050	22	3	2	1077
17-March-2002	10:37[b]	D	0	0	0	0	0
	18:07	N	247	26	5	4	282
	21:53	N	328	15	59	7	408
	22:12	N	229	23	23	18	293
Total			4494	316	567	112	5489
Proportion			82%	6%	10%	2%	100%

[a] Pelagic stations (no buoy measurements).
[b] Stations where the trawl net was open.

Table 2
Parameters used in the target detection algorithm and the target-tracking algorithm

Description	Value
EK60 settings	
Min. echo length	0.8
Max. echo length	1.8
Max. phase dev.	8.0
Max. gain comp.	6.0
Target tracking parameters	
Max. ping skip	5 # ping
Max. depth difference	0.5 (m)
Max. *XY* difference	15 (m)
Min. regression limit	5 # ping
Max. regression limit	10 # ping

plied up to the last 10 pings of the track. This is used to predict the position of the next detection. Then the prediction will be the centre of the track gate instead of the last ping in the track. Five successive missing pings are allowed in the tracking process. When an assignment conflict occurs, the track is terminated. Only tracks of six pings and more are used in the analysis.

The warps produce signals that could easily be mistaken as fish echoes. To avoid any interference with the analysis of fish behaviour, registrations that could be interpreted as warps were manually removed in every passing.

After initial tracking, a constant velocity track,

$$\hat{\mathbf{x}}(t_k) = \mathbf{a} + \mathbf{v}(t_k - t_1)$$

is fitted. Here $\hat{\mathbf{x}}(t_k)$ is the estimated three-dimensional position in the echo beam at time t_k and $\mathbf{v}$ and $\mathbf{a}$ are parameters to be estimated. The fitting is by least squares, i.e. by minimising

$$SS = \sum_k \| \tilde{\mathbf{x}}(t_k) - \hat{\mathbf{x}}(t_k) \|^2$$

where $\tilde{\mathbf{x}}(t_k)$ is the initial track from the tracking process and $\|\cdot\|$ is the Euclidean norm with $\| \mathbf{x} \|^2 = \sum_{i=1}^{3} x_i^2$ for $x = [x_1, x_2, x_3]$. An example is given in Fig. 2.

The estimated velocity, $\hat{\mathbf{v}}$, is called the displacement velocity. This may be different from the swimming velocity if the fish swims in a curved line, or if the current varies in the water column. The mean depth, the mean time and the estimated constant velocity for each track were combined into a dataset containing all tracks from all passings.

2.2. Behavioural indicators

The estimated displacement velocities are binned into groups referred to as running mean (RM) windows, cf. Fig. 3. We let *j* be the index for the depth bin and *i* for the time bin. The binning is based on the mean depth and mean time for each track. Inside each RM window the mean horizontal displacement speed, $H_{i,j}$, and the mean vertical displacement velocity, $V_{i,j}$, are calculated with standard error. The vertical components of each $\hat{\mathbf{v}}$ for each track inside the RM window

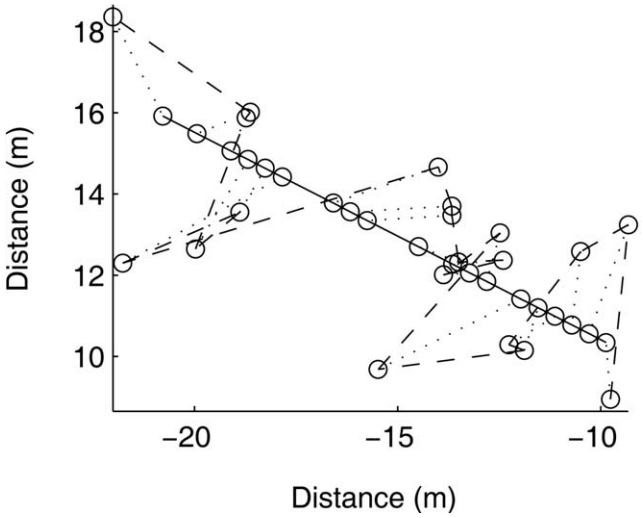

Fig. 2. The dashed line is the measured track, $\tilde{\mathbf{x}}(t_k)$, and the straight line is the mean displacement vector, $\hat{\mathbf{x}}(t_k)$. The distance between each data point, the dotted line, is minimised in a least square sense. The figure shows the projection on the *xy*-plane.

are used to calculate $V_{i,j}$, and the absolute values of the horizontal components are used to calculate $H_{i,j}$. Positive vertical axis in the coordinate system is pointing from the bottom to the surface, and diving is, therefore, negative. Note that $H_{i,j}$ is not a velocity since it has no direction.

2.3. Statistical analysis

Since the RM windows have identical time steps, $H_{i,j}$ and $V_{i,j}$ at each depth *j* comprise a time series, $\{y_i\}$. The response in terms of $H_{i,j}$ and $V_{i,j}$ seems to start during vessel passing, rise to a maximum and then fall off again, cf. Fig. 4. A second order polynomial in time could model such an effect, but could not detect any non-symmetric effects, i.e. a steeper incline or decline. Therefore, a third order polynomial was chosen. The polynomial is fitted to parts of the time series, from t_0 to t_1, where t_0 is the initial time point of the polynomial fitting and t_1 is the end point, cf. Fig. 4. Outside this interval, the fitted curve, $\hat{y}$, cf. Eq. (1), is set to $\bar{y}_0$, where $\bar{y}_0$ is the mean of the time series where the fish is assumed to be

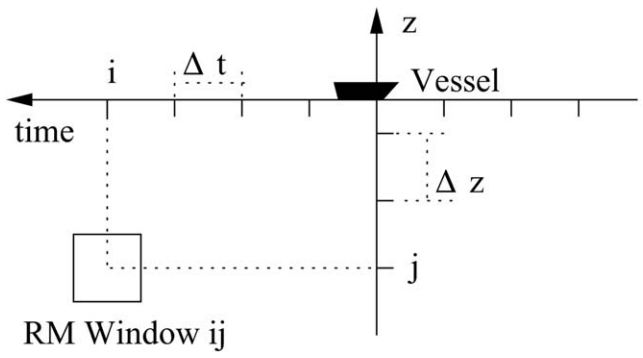

Fig. 3. The behavioural indicators are calculated within each RM window. The size of the RM window is set to Δz = 50 m and Δt = 60 s. At 3 knots, 60 s corresponds to 90 m. Note that negative time is before vessel passing.

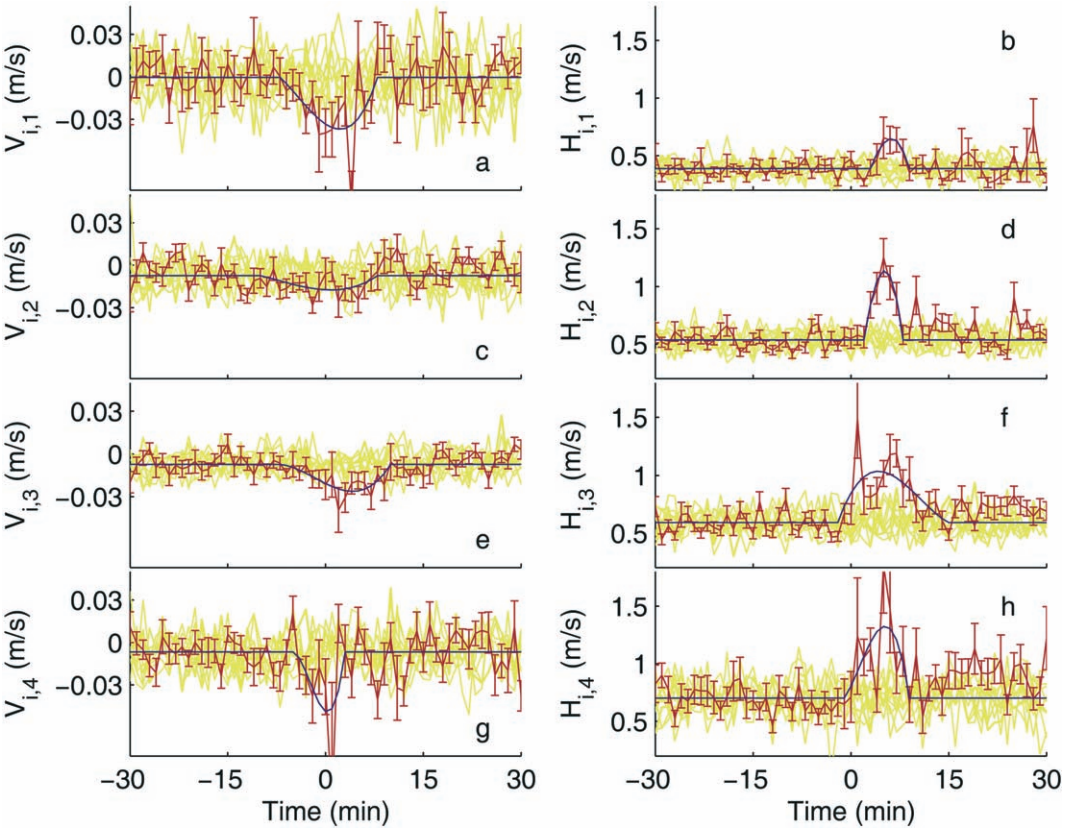

Fig. 4. Yellow curves show 10 realisations of the simulated series under $\{y_i^*\}$, red curves show the time series $\{y_i\}$ plotted with standard error and blue curves show the fitted line, $\{y_i\}$, for each time series. The first panel column shows the mean vertical displacement velocity, $H_{i,j}$, and the second panel column show horizontal displacement speed, $V_{i,j}$. Panels (a) and (b) show depths from –75 to –125 m, panels (c) and (d) from –125 to –175 m, panels (e) and (f) from –175 to –225 m and panels (g) and (h) depths from –225 to –275 m. Negative time is before vessel passing, and positive time is after vessel passing (transducer).

undisturbed, i.e. from the start of the series until 5 min before vessel passing, so that

$$\hat{y}(t) = \begin{cases} \sum_{m=0}^{3} a_m t^m \; t \in [t_0\, t_1] \\ \bar{y}_0 \;\; t \notin [t_0\, t_1] \end{cases} \quad (1)$$

In addition, the polynomial is forced to have only one maximum, and $\hat{y}$ is forced to be continuous, thus leaving three or four parameters to be estimated. All combinations of t_0 and t_1, such that $t_0 < t_1$, are tried, and the combination with the lowest square error is chosen. As an indicator for reaction, the maximum or the minimum value for the fitted curve,

$$y_{\text{ext}} = \begin{cases} \min(\hat{y}), & \text{for the time series based on } V_{i,j} \\ \max(\hat{y}), & \text{for the time series based on } H_{i,j} \end{cases}$$

is used. Since we would like to test for a diving reaction, the minimum value is used for series based on $V_{i,j}$.

Under the null hypothesis, H_0, of no response, we expect that $y_{\text{ext}} = \bar{y}_0$. We assume no dependence of autocorrelation type in the time series under H_0. The standard error of each behavioural indicator in each RM window gives an estimate of the precision of the behavioural indicator. This information is used to simulate the time series under H_0. Independent bootstrap type samples, $\{y_i^*\}$, are drawn according to y_i^*: $N(\bar{y}_0, \; s_p)$, where p is drawn from 1, ..., n. Here n is the length of the undisturbed time series and s_p is the standard error for the pth value of the time series. Standard errors for autocorrelation estimates under H_0 are obtained from the simulated time series. This is compared to autocorrelation estimates for the observed time series. No indication of dependence is found in the undisturbed part of the time series. This supports our assumption of independence in the time series under H_0.

The time series are simulated 5000 times, and a distribution for y_{ext} under H_0 is obtained for both behavioural indicators for all bins of depth. One-sided confidence intervals, cf. Table 3, are obtained by taking the empirical percentiles from this distribution, with the level of α=0.05. If y_{ext} for the original non-simulated data is located outside this confidence interval, it means that a significant velocity change has taken place.

After being exposed to the vessel and gear, the fish may be in another state, i.e. higher alertness. This is investigated by testing the difference in the mean for the behavioural indicators, between the undisturbed situation and the situation after the main response. To simplify, we have used an ordinary t-test even though this is not quite correct in view of the variable standard error from one RM window to another.

Table 3
The results from the analysis where H/V is the behavioural indicator, depth is the depth range for the RM window, t_0 is the start time of the polynomial, t_{ext} is the time where the polynomial has its maximal value, t_1 is the time for the end point of the polynomial, SS is the sum of squares for the fitted line and y_{ext} is the max/min point of the polynomial. Conf. is the confidence interval for y_{ext} under H_0

H/V	Depth (m)	t_0 (s)	t_{ext}	t_1	SS	y_{ext}	Conf. α = 0.05	Significant
$V_{i,1}$	[–75 to –125]	–7.0	2.2	8.0	0.0137	–0.0370	[–0.035, 1)	Y
$V_{i,2}$	[–125 to –175]	–10.0	0.8	8.0	0.0046	–0.0174	[–0.029, 1)	N
$V_{i,3}$	[–175 to –225]	–7.0	4.2	10.0	0.0025	–0.0263	[–0.025, 1)	Y
$V_{i,4}$	[–225 to –275]	–3.0	0.3	2.0	0.0162	–0.0671	[–0.034, 1)	Y
$H_{i,1}$	[–75 to –125]	3.0	6.2	9.0	0.4007	0.648	(–1, 0.5530]	Y
$H_{i,2}$	[–125 to –175]	2.0	5.2	8.0	0.6600	1.139	(–1, 0.7251]	Y
$H_{i,3}$	[–175 to –225]	–2.0	4.2	15.0	1.1551	1.035	(–1, 0.8269]	Y
$H_{i,4}$	[–225 to –275]	–1.0	5.3	9.0	2.5361	1.326	(–1, 1.0159]	Y

3. Results

The trawl catches consisted of cod (*Gadus morhua*), haddock (*Melanogrammus aeglefinus*), saithe (*Pollachius virens*) and redfish (*Sebastes*). Cod dominated the catches at all times, cf. Table 1. Throughout the sampling period, the catches varied considerably in weight, especially for cod, but no significant trend over the experimental period was found. The number of trawl stations during daytime was too few to make any conclusion about diel differences.

By trawling at 3 knots the trawl will, at these depths, arrive 8–10 min after the vessel passing. The vessel passing, $t = 0$, is when the vessel mounted transducer passes the buoy.

The time series, $\{y_i\}$, the fitted curves, $\{\hat{y}_i\}$ and a sample of simulated series under $\{y_i^*\}$, are given in Fig. 4. The fish reacts to the gear/vessel both by diving and by horizontal movements. The diving, particularly in the upper channels of depths, seems to start earlier than the horizontal reaction and the horizontal reaction seems to be closer to the warps, cf. Table 3 columns 2–5 and Fig. 4. By comparing columns 7 and 8 of Table 3, it is seen that the change in $H_{i,j}$ for each j is significant in all layers of depth, and the change in $V_{i,j}$ for each j is significant in all but one channel of depth. Moreover, the change in $H_{i,j}$ seems to be more pronounced than in $V_{i,j}$. The number of registrations is lower in the upper depth channels.

The change in $H_{i,j}$ for each j between the undisturbed situation and the situation after the "main response" is significant for some of the depths, cf. Table 4. This is also evident by inspecting Fig. 4 f,h. There seems to be no such effect for the diving velocity.

4. Discussion

The target-tracking algorithm connects the single targets from the EK60's single target detection algorithm. However, there may be cases where it fails. If fish dive tilted downwards, or swim fast, some echoes may be lost, and the target will not be tracked as one single individual. However, the maximum vertical movement (0.5 m s^{-1} at a ping rate at 1 s) and the maximum horizontal movement (15 m s^{-1} at ping rate at 1 s) is set well above the detected vertical and horizontal movement (i.e. 0.06 and 1.32 m s^{-1}). Missing pings are also allowed in the algorithm, cf. Table 2. If the fish density is too high, the fish will not be resolved into single targets by the EK60's single target detection algorithm. If the behaviour is different at these densities, this behaviour will not be detected. If the target-tracking algorithm fails to connect two parts of a track, the data will not be independent, i.e. one individual will count as two. The buoy transducer is not fixed, and cyclic movement in the transducer may lead to errors in the tracking process. By fitting a constant velocity line to the tracks, and by avoiding short tracks, this problem will be reduced. If one would like to analyse more detailed fish behaviour, this problem needs to be addressed. Improvements of the tracking algorithm may include a filter to estimate the transducer tilt and roll and methods to take into account the measurement error (work in progress).

The observed change in $H_{i,j}$ seems to occur closer to the warps than the change in $V_{i,j}$, at least in the upper layers of depth, cf. Fig. 4. It seems to be a stronger diving response to the vessel/propeller, and a stronger horizontal movement towards the warps. The warps are believed to produce a low frequency sound with a maximum intensity at ≈7 Hz (unpub-

Table 4
Comparing the horizontal displacement speeds from the undisturbed situation with the swimming speeds after the main response. Significantly higher speeds were found at depths from –175 to –275 using a *t*-test. Estimation of the sample variance is based on both groups (pooled). No significant difference was found for the vertical velocity

Depth (m)	Method	Var.	DF	*t*-value	Pr > |*t*|	Significant
[75–125]	Pooled	Equal	40	–0.80	0.4278	N
[125–175]	Pooled	Equal	40	–1.73	0.0914	N
[175–225]	Pooled	Equal	40	–3.99	0.0003	Y
[225–275]	Pooled	Equal	40	–5.62	<0.0001	Y

lished data), and the fish may react to low frequency sound (Sand and Karlsen, 1986).

The higher $H_{i,j}$ after the main response indicates that the fish are more alert after being stimulated by the vessel and gear. In future experiments, the time series should be extended to assess when the null situation is restored. Even though measures have been taken to reduce the effect of transducer tilt and roll, transducer movement due to turbulence from the vessel could also explain this effect. It is, therefore, important to improve the method to filter out the transducer tilt/roll effect.

Fish may respond to several stimuli from the vessel/gear (Wardle, 1993). These stimuli could for instance be the noise at different frequencies measured at different depths, visually detectable stimuli, etc. If the fish reacts to the visual stimuli from the warps, the distance to the warp, corrected for light levels, could be correlated with the change in behaviour. The reaction could also be correlated to the different noise levels at different frequencies. This may tell whether the fish reacts to the visual stimuli or noise stimuli, and from which source these stimuli originate.

When more data is obtained, the binning of the displacement velocities for each track could be extended to three spatial dimensions instead of time and depth only, resulting in a three dimensional field for the displacement velocity. The positioning of the track in relation to the vessel could be measured with GPS data from the buoy and the vessel. This velocity field could be used in a model to predict the distribution of fish at any given time, starting from a fixed position in time and space. This could give us some indication of the fishing height of the bottom trawl, and also of the horizontal displacement, from the time the vessel passes to the trawl doors appear. Knowledge of this is important to combine the bottom-trawl- and the acoustic-index into one value, and ultimately to undertake absolute abundance estimation of cod and haddock in the Barents Sea.

Acknowledgements

Parts of the data analysis were conducted at the International Institute for Applied Systems Analysis (IIASA), Austria, at the Adaptive Dynamics Network (ADN) group, under supervision of Dr. Ulf Dieckmann. We are grateful to the crew on R/V “G.O. Sars” for skilful handling of the buoy system and to Dr. Vidar Hjellvik for giving us his target-tracking algorithm. Finally we are grateful to an anonymous referee for several valuable comments.

References

Aglen, A., Engås, A., Huse, I., Michalsen, K., Stensholt, B., 1999. How vertical distribution may effect survey results. ICES J. Mar. Sci. 56, 345–360.

Brede, R., Kristensen, F.H., Solli, H., Ona, E., 1990. Target tracking with a split-beam echo sounder. Rapp. P.-v. Réun. Cons. Int. Explor. Mer 189, 254–263.

Buerkle, U., 1977. Detection of trawling noise by Atlantic cod (*Gadus morhua* L. Mar. Behav. Physiol. 4, 233–242.

Godø, O.R., Somerton, D., Totland, A., 1999. Fish behaviour during sampling as observed from free floating buoys–application for bottom trawl survey assessment. ICES CM 1999/J:10.

Nunnallee, E., 1991. An investigation of the avoidance reactions of Pacific whiting to demersal and midwater trawl gear. ICES CM 1991, B:5.

Olsen, K., 1971. Modern Fishing Gear of the World, chapter Influence of Vessel Noise on the Behaviour of Herring. Fishing News (Books) Ltd, London, pp. 191–193.

Olsen, K., 1990. Fish behaviour and acoustic sampling. Rapp. P.-v. Réun. Cons. Int. Explor. Mer 189, 147–158.

Olsen, K., Angell, J., Pettersen, F., Løvik, A., 1983. Observed fish reactions to a surveying vessel with special reference to herring, cod, capelin and polar cod. FAO Fish. Rep. 300, 131–138.

Ona, E., 1988. Trawling noise and fish avoidance, related to near-surface trawl sampling. In: Sundby, S. (Ed.), Proceedings from Workshop on Year Class Variations as Determined from Pre-recruit Investigations, vol. 1. Bergen, Norway, 20–30 September 1988.

Ona, E., 1994. Recent developments of acoustic instrumentation in connection with fish capture and abundance estimation. p. 200–216. In: Fernø, A., Olsen, S. (Eds.), Marine Fish Behaviour in Capture and Abundance Estimation. Fishing News Books, Blackwell Science, Ltd.

Ona, E., Godø, O.R., 1990. Fish reaction to trawling noise: the significance for trawl sampling. P.-v. Réun. Const. Int. Explor. Mer 159–166.

Ona, E., Hansen, D., 1991. Software for target tracking with split-beam echo sounders. User Manual. Institute of Marine Research, Bergen, Norway, October 1991.

Sand, O., Karlsen, H., 1986. Detection of infrasound by the Atlantic cod. J. Exp. Biol. 125, 197–204.

Wardle, C., 1993. Fish behviour and fishing gear. In: Pitcher, T.J. (Ed.), Behaviour of Teleost Fishes, chapter 18. Fish and Fisheries Series 7. Chapman & Hall.

Available online at www.sciencedirect.com
SCIENCE DIRECT®
Aquatic Living Resources 16 (2003) 271–275
Aquatic Living Resources
www.elsevier.com/locate/aquliv

Sounds produced by herring (*Clupea harengus*) bubble release

Magnus Wahlberg *,[1], Håkan Westerberg

Institute of Coastal Research, National Board of Fisheries, Sweden

Accepted 19 December 2002

Abstract

In the herring (*Clupea harengus*), the swim bladder is connected to both the alimentary canal and the anal opening. The anterior duct is used for filling the swim bladder with air. Gas release from the anal opening is often observed when the fish is scared or during ascent and descent. Here, the sounds produced by such a gas release are studied. The fish was kept in a low-pressure chamber. As the ambient pressure was reduced, the gas in the swim bladder expanded and was emitted through the anal opening. Herring sounds were also recorded in a fish trap and in the field. The characteristic sound made by herring during gas release is denoted as the pulsed chirp. This pulsed chirp is 32–133 ms long ($N = 11$) and consists of a series of 7–50 ($N = 11$) transient pulses with a continuous reduction of the frequency emphasis (centroid frequency of first pulse 4.1 kHz and of last pulse 3.0 kHz, $N = 11$). The source level of the chirp is 73 ± 8 dB re 1 μPa rms (root mean square) at 1 m ($N = 19$). The pulsed chirp is not known to be produced by any other marine animal and may be a good fingerprint for identifying schools of clupeid fish by natural predators, fishery scientists and fishermen. A model for the generation of the pulsed chirp is presented and tested on existing data.

Keywords: Bioacoustics; Sound production; Gas release; Herring

1. Introduction

The herring (*Clupea harengus*) is quantitatively the most important fish species of northern Europe. During decades of intense research, we have learned about its migratory, diurnal and foraging behavior, and about its role in the marine food web (Klinkhardt, 1996). In spite of this, little is known about herring sound production and communication. In this study, we focus on acoustic signals produced by herring.

Compared to most other fish species, herring has excellent hearing abilities (Enger, 1967). In clupeid fish, the swim bladder connects to the inner ear, which facilitates the perception of sound. This hydro-acoustic detection system is in close contact to the lateral line canal system on the head of the fish (Blaxter et al., 1981) and works well for the perception of both acoustic pressure as well as hydrodynamic displacement signals.

Another feature of the herring anatomy is the connection between swim bladder both to the stomach and to the anal opening (Fig. 1; Bennett, 1879–1880). Herring does not seem to produce gas in the swim bladder as many other fish species do (Fahlén, 1967; Blaxter and Batty, 1984). Air is inhaled at the surface, swallowed and transported into the swim bladder through a small canal, *ductus pneumaticus* (Klinkhardt, 1996; Fig. 1).

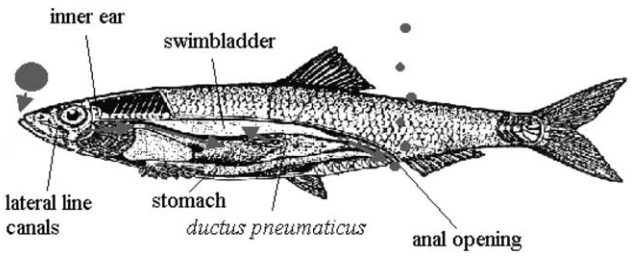

Fig. 1. The airways of herring (*Clupea harengus*). Redrawn from Klinkhardt (1996). The assumed path of air (see text) is indicated with gray circles and arrows.

It is well known among fishermen that herring schools can release air, producing clouds of bubbles that may be observed at the surface (Muus and Dahlstrøm, 1974; Thorne and Thomas, 1990; Nøttestad, 1998). Bubbles are usually released through the anal opening, connected to the swim bladder (Fig. 1). Sometimes, bubbles are released through the mouth (personal observation). Such bubbles may originate from air

* Corresponding author.
E-mail address: magnus.wahlberg@biology.au.dk (M. Wahlberg).

[1] Present address: Center for Sound Communication, Department of Zoophysiology, University of Aarhus, C. F. Møllers Allé Building 131, 8000 Aarhus C, Denmark.

doi:10.1016/S0990-7440(03)00017-2

that has not yet been transferred to the swim bladder. Gas may be released both during ascent and decent and as a response to distress (Nøttestad, 1998). It has been suggested that the air release may work as an optic and acoustic screen that confuses predators (Nøttestad, 1998).

Herring is known to produce sounds (Murray, 1831; Marshall, 1962; Hering, 1964; Fish and Mowbray, 1970; Freytag, 1971; Schwarz and Greer, 1984). Previous studies performed to investigate sound production have, to our knowledge, not reported the source level of such sounds, nor have they suggested how the sounds are produced. Both these pieces of information are important to evaluate the possible function of the sound.

In this study, we report on the sound production during herring gas release. We estimate source level of herring sounds and investigate a potential sound-production mechanism.

2. Materials and methods

Herring sound production was studied with controlled experiments and field observations. The recording system consisted of a BK 8101 (sensitivity –184 dB re 1 V/μPa) and an Atlantic Research LC32 hydrophone (–202 dB re 1 V/μPa) connected via a custom-built amplifier to a Sony TCD-D7 DAT recorder (recording band width 0.1–22 kHz). Data were digitally transferred to the computer via a *U2A* digital interface (*Egosys Inc.*) and subsequently analyzed using *Matlab* (*MathWorks, Inc.*) and *Cool Edit 2000* (*Syntrillium Inc.*) software. Visual observations were made using underwater video cameras.

2.1. Low-pressure chamber (LPC)

Herring were caught live in nets on the Swedish west coast. The fish were carefully removed from the nets and transported to shore in 20 l buckets. The fish were submerged into a transparent water-filled plexi glass cylinder connected to a vacuum pump and a manometer. A hydrophone was mounted on an aluminum rig together with the fish container. The distance from the anal opening of the fish to the hydrophone was 8 cm. The hydrophone was located on the right-hand side of the fish, 90° from the sagittal plane. A custom-built housing with an underwater video camera (*Bischke*) monitored the rear end of the fish from the opposite side of the hydrophone. The rig was lowered into the harbor to a depth of 2 m (the sea floor being at more than 5 m depth). As the pressure in the fish container was decreased (down to a minimum of 0.1 bar), the air inside the swim bladder of the fish expanded and the fish was forced to release air through the anal opening. This experiment permitted sound recordings of live herring in an almost free acoustic field. Additional measurements with the pressure chamber were made in Hårsfjärden and Söderhamn on the Swedish Baltic Sea coast. A total of 20 fish were tested with the LPC. The fork length of the fish was 19.8 ± 1.6 cm (mean ± 1 S.D., $N = 17$; the length of three fish was not measured). The acoustic impedance of plexi glass is close to that of water, so that sound attenuation through the walls of the cylinder could be neglected.

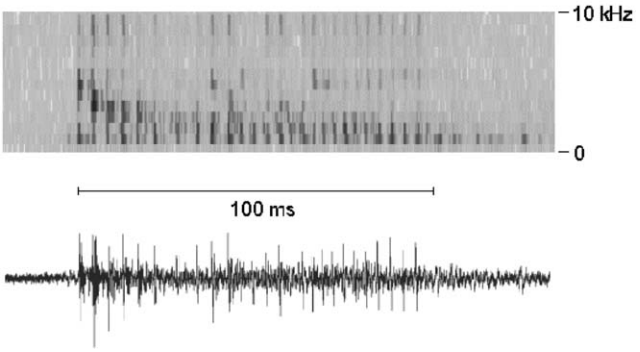

Fig. 2. The pulsed chirp of a herring, recorded in the Swedish archipelago of the Bothnean Bay during the spawning season in June. Top: Spectrogram (filter bandwidth 1.5 kHz). Bottom: Oscillogram, synchronized with the spectrogram.

2.2. Recordings at herring trap net

The only Swedish herring trap is situated close to the town of Söderhamn in the Gulf of Bothnia. This trap resembles Danish herring pond nets (von Brandt, 1964): a leader net directs the fish into a series of funnel-formed net gates that end in a 5 × 3 × 3 m bag. At the time of recording, about 4 tons of live herring were circling inside the trap. A hydrophone was lowered into the bag of the trap, together with an underwater video camera. An extra hydrophone was kept about 15 m outside the net enclosure as a control. Recordings were made in flat calm weather for two days and nights in June 1997. About 10 h of recordings were made.

2.3. Field recordings in a spawning bay

Half a kilometer from the fish trap in Söderhamn (see above), there is a 10 × 30 m bay with a maximum water depth of 2–3 m. This bay is known to be a spawning site of herring. During the spawning season in early June 1997, we deployed two hydrophones from a small rowing boat late at night in flat calm weather. The hydrophone depths were 1 and 2 m, the hydrophones were located vertically one above the other. Two hours of recordings were made.

3. Results

During the recordings with the LPC, in the fish trap and in the spawning bay, sounds were recorded from the herring. The most prominent signal consisted of a series of pulses, where each pulse had a lower frequency emphasis than the previous one (Fig. 2). This sound, we call the pulsed chirp.

In the LPC experiments, 19 out of 20 herrings produced sounds that could be analyzed. The source level of the chirps ranged from 55 to 90 dB re 1 μPa rms (root mean square) at

1 m (73 ± 8 dB, mean ± 1 S.D.; N = 19). The rms intensity was calculated over the length of the signal within the –3 dB points of the signal envelope function. Sounds were first heard at an ambient pressure of 0.2 ± 0.1 bar (N = 19), corresponding to a five-fold increase of the swim bladder air volume.

Each pulsed chirp lasted 0.9–16.2 s (4.2 ± 4.8 s; N = 10) in the LPC experiments, and 32–133 ms (83 ± 28 ms; N = 11) in the field recordings from the spawning bay. Each chirp contained 7–50 (17 ± 13; N = 11) pulses in the field recordings. In the LPC experiments, there were up to hundreds of pulses within a single chirp.

Eleven chirps from the spawning bay were chosen for more detailed measurements of signal properties. The centroid frequency (the frequency splitting the spectra into two halves of equal energy; Au, 1993) ranged from 3.0 to 5.1 kHz (4.1 ± 0.8 kHz; N = 11) for the first pulse of a chirp, and from 2.2 to 4.6 kHz (3.0 ± 0.9 kHz, N = 11) for the last pulse. The mean-square bandwidth (the S.D. of the spectrum; Au, 1993) was 1.2–3.9 kHz (2.4 ± 0.7 kHz; N = 11) for the first pulse, and 1.6–4.9 kHz (2.9 ± 1.0 kHz; N = 11) for the last pulse of the chirp. The interval between pulses ranged from 1.2 to 12.8 ms (5.7 ± 3.1 ms; N = 9) at the start, and from 0.8 to 7.1 ms (4.5 ± 1.9 ms; N = 9) at the end of the chirp.

During the LPC experiments, chirps were only heard when air was emitted from the anal opening of the fish. From visual observations of the video recordings, it was estimated that each bubble detaching from the herring had a radius of about 0.5–1.5 mm. In the herring trap recordings, no bubbles were released from the fish observed with the video camera. The hydrophone inside the trap recorded large amounts of pulsed chirps, whereas these sounds were barely detectable on the hydrophone outside the trap. This made us confident that the sounds were produced inside the trap. During the field recordings, the visibility was not sufficient to observe whether the fish released bubbles or not, but herring was regularly observed to gulp air at the surface.

4. Discussion

4.1. The biological significance of the pulsed chirp

The pulsed chirp (Fig. 2) has previously been observed in recordings of herring (Schwarz and Greer, 1984). To our knowledge, there have been no reports of any other marine animal producing this kind of sound. Eels (*Anguilla anguilla*; J. P, Lagardère, personal communication) and some other fish species (e.g. weakfish, *Cynoscion regalis*; Sprague, 2000; see Fish and Mowbray, 1970 for other examples) are known to produce transient sounds of similar frequency content as the herring pulses, but these sounds do not seem to have the frequency decay between consecutive pulses characteristic for the pulsed chirp. However, some other members of the Clupeid family, such as *Sprattus sprattus* and *Sardina* also have a canal from the swim bladder to the anal opening. Even though recordings of these species are unknown to us, one may predict that they produce sounds similar to herring. The pulsed chirp may serve as a fingerprint to detect and identify Clupeid fish schools by using passive acoustics. The time-band width product (Au, 1993) of the signal is large, in the order of 100–1000, so that they are feasible for automatic detection as well as localization techniques using cross-correlation and matched filtering. As the ratio of the acoustic wavelength and the source size is much larger than one (around 400), we expect the sound to radiate almost omnidirectionally around the fish. This also facilitates automated detection.

It is not clear as to why herring release bubbles. If the swim bladder produced gas at depth, this gas would expand as the fish ascends. Instead of absorbing the gas (as most teleosts do), it would be convenient for the herring to release the superfluous gas through the anal opening. However, experiments have shown that the herring swim bladder may not produce any gas (Fahlén 1967, Blaxter and Batty, 1984). If gas only enters the swim bladder through inhalation at the surface, there is no physical reason why gas has to be released during ascent. Also, herring gas release has been observed both by ascending and descending schools (Nøttestad, 1998). In our study, pulsed chirps were heard from fish caught in a trap and in a shallow spawning bay, where ascent and descent was restricted to a few meters. These observations indicate that gas release, rather than being a physical response, is a behavioral response (such as stress or predator avoidance; see Nøttestad, 1998). It has been suggested that the bubble release could be a way for the herring to distract predators, such as killer whales (Nøttestad, 1998; see also Similä and Ugarte, 1993).

It may be inferred from the audiogram of the herring (Enger, 1967) that they can hear the bubble release from other fish at a distance up to around a meter. This is larger than the typical distance between individual fish in a herring school (Radakov, 1973; Domenici et al., 2000). Therefore, the individual herring can probably hear the bubble release from their nearest neighbors within a school. Whether or not these sounds have any meaning for the fish has to await further acoustic and behavioral observations. It is also possible that predators, such as killer whales *(Orcinus orca)* and harbor porpoises *(Phocoena phocoena)* can detect herring from listening to the sounds of schools releasing bubbles. Herring reacts on the echolocation sounds made by killer whales (Wilson and Dill, 2002). Thus, the pulsed chirp may be a cue for the predator to find the school without disclosing its presence with sonar.

4.2. A model for pulsed chirp generation

A possible mechanism for the sound production of the pulsed chirp is air bubble oscillations, which are known to produce sound efficiently under water (Longuet-Higgins, 1989). When small quantities of air are pressed through the anal opening of the fish, pulses could be produced as the external bubble oscillates while attached to the anal opening by surface tension. For every portion of air added, the at-

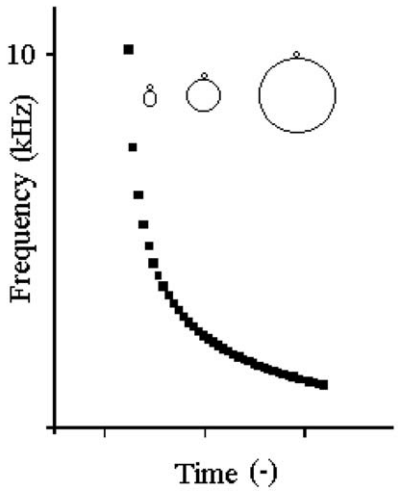

Fig. 3. Visualization of the proposed model of herring chirp generation (for details see text): the air bubble is attached to the anal opening and is filled by air parcels of constant volume from the anal duct. Each air parcel causes the bubble to resonate and thereby produces a pulse. For the consecutive pulse, the bubble has grown, and the frequency emphasis is lower. The expected spectrogram of a pulsed chirp from this model is shown. The time scale is arbitrary.

tached bubble is given an impulse to oscillate and generate sound at its resonance frequency, which is determined by its size and the ambient pressure (Plessett and Prosperetti, 1977). When the attached bubble grows large enough, it will detach and ascend towards the surface.

We propose that the mechanism behind the generation of each chirp is the formation and release of a single bubble from the anal opening. This explains the decay of the centroid frequency throughout the pulses within a chirp, as the resonance frequency of the attached bubble decreases when it gets larger (Plessett and Prosperetti, 1977). In Fig. 3, the spectrogram of a pulsed chirp is depicted, modeled according to the sound production mechanism proposed here. The simulated chirp is similar to the temporal and the frequency structure of a pulsed chirp when a series of air portions of equal volume is added to the bubble. More detailed simultaneous hydrophone and video studies of the sound generation process would clarify whether this sound production model is realistic.

This model may also explain why the frequency content of the pulses varies as a function of the ambient pressure (Fig. 4). The black lines in Fig. 4 show the resonance frequency of air bubbles of radii 0.5 and 1.5 mm as a function of the ambient pressure. The bubble resonance frequencies circumscribe the measured centroid frequency of the last pulse within a chirp, both for the LPC and the spawning bay recordings. This may indicate that the released bubble size is between 0.5 and 1.5 mm radius, which is also what was estimated from visual inspection of the video uptakes from the experiments with the LPC. Fig. 4 predicts that the frequency content of the chirps would increase with depth. Further recordings of herring at different known depths are necessary to test this prediction. The conjecture is corroborated qualitatively by observations from submarines recording herring schools at depths down to 50 m.

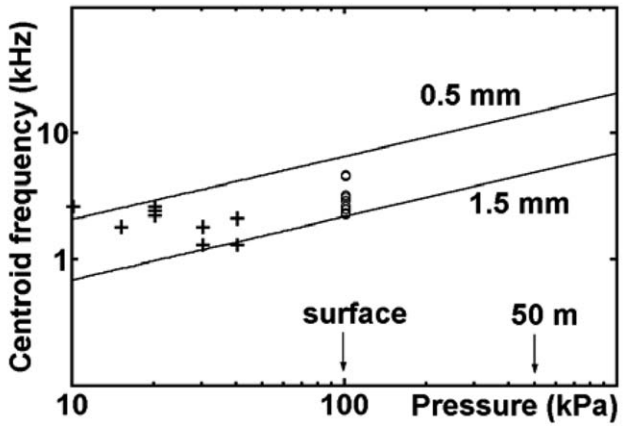

Fig. 4. The centroid frequency of the last pulse of herring chirps and the ambient pressure. '+' data are from LPC experiments, and 'o' data are from field recordings of spawning herring. The lines correspond to the resonance frequency of air bubbles of radius 0.5 and 1.5 mm. The arrows indicate the ambient pressure at the sea surface and at a depth of 50 m. For details and definitions, see text.

During LPC experiments, sound was only heard while air was released from the anal opening. During the fish trap recordings, no bubble release was observed in synchrony with the recorded pulsed chirps. One reason for this could be that the visibility of the water was limited to a few meters and that the gas release was sporadic in time and space; therefore, fish outside visual detection range may have released the air and produced the sound. Another explanation is that herring may produce sound without releasing air. A possible sound production mechanism in such cases is the internal transportation of air within the alimentary–swim bladder canals.

Acknowledgements

The Swedish Navy provided funding, logistics and support. Fernando Ugarte kindly loaned us underwater video uptakes of herring schools.

References

Au, W.W.L., 1993. The Sonar of Dolphins. Springer-Verlag, New York.
Bennett, F.W., 1879–1880. On a communication between the air-bladder and the cloaca in the herring. J. Anat. Phys. 14, 405–406.
Blaxter, J.H.S., Batty, R.S., 1984. The herring swim bladder: loss and gain of gas. J. Mar. Biol. Assoc. UK 64, 441–459.
Blaxter, J., Denton, E.J., Gray, J.A.B., 1981. Acousticolateralis system in clupeid fishes. In: Tavolga, W.N., Fay, R.R. (Eds.), Hearing and Sound Communication in Fishes. Springer-Verlag, New York, pp. 39–56.
Domenici, P., Batty, R.S., Similä, T., 2000. Spacing of wild schooling herring while encircled by killer whales. J. Fish Biol. 57, 831–836.
Enger, P., 1967. Hearing in herring. Comp. Biochem. Physiol. 22, 527–538.
Fahlén, G., 1967. Hydrostatic function of the gas bladder of *Clupea harengus*. L. Acta Univ. Lund II, 3–49.
Fish, M., Mowbray, W., 1970. Sounds of Western North Atlantic Fishes. The Johns Hopkins Press, Baltimore 207 p.

Freytag, G., 1971. Practical applications and limitations in the method of fish finding by passive listening. In: Kristjonsson, H. (Ed.), Modern Fishing Gear of the World, vol. 3. Fishing News Ltd., London, pp. 51–55.

Hering, G., 1964. Die Pfeiftöne des Herings. Schiffbautechnik 3, 150–151.

Klinkhardt, M., 1996. Der Hering *Clupea harengus*. Spektrum Akademischer Verlag, Heidelberg.

Longuet-Higgins, M., 1989. Monopole emission of sound by asymemetric bubble oscillations. Part 1. Normal modes. J. Fluid. Mech. 201, 525–541.

Marshall, N., 1962. The biology of sound-producing fish. Symp. Zool. Soc. Lond., 45–60.

Murray, J., 1831. Voice of fishes. Mag. Nat. Hist. 148.

Muus, B., Dahlstrøm, P., 1974. Havfisk og fiskeri. GEC Gads Forlag, Copenhagen, pp. 64–68.

Nøttestad, L., 1998. Extensive gas bubble release in Norwegian spring-spawning herring (*Clupea harengus*) during predator avoidance. ICES J. Mar. Sci. 55, 1133–1140.

Plessett, M., Prosperetti, A., 1977. Bubble dynamics and cavitation. Annu. Rev. Fluid. Mech. 9, 145–185.

Radakov, D.V., 1973. Schooling in the Ecology of Fish. J. Wiley & Sons, Chichester.

Schwarz, A., Greer, G., 1984. Responses of Pacific herring, *Clupea harengus pallasi*, to some underwater sounds. Can. J. Fish. Aquat. Sci. 41, 1183–1192.

Similä, T., Ugarte, F., 1993. Surface and underwater observations of cooperatively feeding killer whales in northern Norway. Can. J. Zool. 71, 1494–1499.

Sprague, M.W., 2000. The single sonic muscle twitch model for the sound-production mechanism in the weakfish, *Cynoscion regalis*. J. Acoust. Soc. Am. 108, 2430–2437.

Thorne, R.E., Thomas, G.L., 1990. Acoustic observations of gas bubble release by Pacific herring (*Clupea harengus pallasi*. Can. J. Fish. Aquat. Sci. 47, 1920–1928.

von Brandt, 1964. Fishing Catching Methods of the World. Fishing News Ltd., London, pp. 191.

Wilson, B., Dill, L.M., 2002. Pacific herring respond to simulated odontocete echolocation sounds. Can. J. Fish. Aquat. Sci. 59, 542–553.

Available online at www.sciencedirect.com
SCIENCE DIRECT®
Aquatic Living Resources 16 (2003) 277–282
Aquatic Living Resources
www.elsevier.com/locate/aquliv

Visualizing fish movement, behavior, and acoustic backscatter

Richard H. Towler [a,*], J. Michael Jech [b], John K. Horne [a]

[a] University of Washington, School of Aquatic and Fishery Sciences, Box 355020, Seattle, WA 98195, USA
[b] NOAA Northeast Fisheries Science Center, Woods Hole, MA 02543, USA

Accepted 27 January 2003

Abstract

Acoustic surveys of aquatic organisms are notorious for large data sets. Density distribution results from these surveys are traditionally graphed as two-dimensional plots. Increasing information content through wider acoustic frequency ranges or multiple angular perspectives has increased the amount and complexity of acoustic data. As humans are visually oriented, our ability to assimilate and understand information is limited until it is displayed. Computer visualization has extended acoustic data presentation beyond two dimensions but an ongoing challenge is to coherently summarize complex data. Our goal is to develop visualizations that portray frequency- and behavior-dependent backscatter of individual fish within aggregations. Incorporating individual fish behavior illustrates group dynamics and provides insight on the resulting acoustic backscatter. Object-oriented applications are used to visualize fish bodies and swimbladders, predicted Kirchhoff-ray mode (KRM) backscatter amplitudes, and fish swimming trajectories in three spatial dimensions over time. Through the visualization of empirical and simulated data, our goal is to understand how fish anatomy and behavior influence acoustic backscatter and to incorporate this information in acoustic data analyses.

Keywords: Acoustics; Backscatter; Kirchhoff-ray mode; Target strength; Visualization

1. Introduction

Fisheries acoustic surveys collect large data sets. A common challenge when presenting any large data set is to parsimoniously represent data characteristics (e.g. amplitudes, ranges, variances), while maximizing the amount of information portrayed. Acoustic data contain quantitative information on density and size distributions of backscattering organisms. An important analytic task is to partition the backscattered energy into categories representing size classes, species, or species groups. Classification of acoustic backscatter utilizes echo amplitude or echo envelope metrics when targets can be resolved, or patterns of backscatter from aggregations when targets are not resolvable. Fluctuations in backscatter amplitudes from an individual impede consistent and accurate classification of single targets. Variability in the amount of sound reflected by an aquatic organism is caused by the transmission of sound through water and by a suite of biological factors including anatomy, physiology, and behavior.

Simultaneously measuring the influence of all biological factors on backscatter amplitudes is not yet possible. As an alternative, numeric and analytic models estimate backscatter as a function of biological or physical factors of interest. Backscatter models augment experimental measures by predicting echo amplitudes from individuals under known conditions. To illustrate by example, Kirchhoff-ray mode (KRM) backscatter models (Clay and Horne, 1994) have been used to characterize frequency- and behavior-dependent backscatter of individual and aggregations of fish (Horne and Jech, 1999; Jech and Horne, 2001). Visualization of results include backscatter response surfaces over a designated range of aspect angles, lengths, and carrier frequencies (Fig. 6, Horne and Jech 1999; Fig. 5, Horne et al., 2000) and in interactive representations of fish bodies, swimbladders, and the corresponding acoustic backscatter ambits (Jech and Horne, 2001, Fish3d www.acoustics.washington.edu).

One approach used to examine how biological factors influence echo amplitudes integrates modeling of organism behavior with acoustic measurements of fish distributions in computer visualizations. These visualizations should present large data sets in a coherent and comprehensive manner; reveal several levels of detail within data sets; avoid distor-

* Corresponding author.
E-mail address: rtowler@u.washington.edu (R.H. Towler).

doi:10.1016/S0990-7440(03)00011-1

tion of measurements; prompt the viewer to think about mechanisms that cause observed patterns; and encourage comparisons among data sets (Tufte, 1983). This paper was motivated by an interest in visualizing three-dimensional swimming behavior and the resulting effects on acoustic backscatter. Simulations of adult walleye pollock (*Theragra chalcogramma*) and capelin (*Mallotus villosus*) dynamics are integrated with backscatter models to visualize the influence of fish anatomy, orientation, and kinematics on acoustic measurements. We believe that visualization enhances the understanding of backscatter variability and can be used to improve conversions of acoustic data to biological meaningful numbers such as fish length, density, and abundance.

2. Materials and methods

Our goal is to integrate echosounder properties with fish anatomy, backscatter model predictions, and fish trajectories to visualize factors that influence patterns in backscatter data. Three autonomous visualizations are integrated into a single computer application. First, digitized walleye pollock and capelin anatomy are visualized with the corresponding frequency-dependent acoustic backscatter. Second, the movements of fish within schools are visualized from the perspective of a transducer or a member of the school. Third, these two components are integrated to visualize the effect of fish orientation and movement on echo amplitude. Interaction among the three components is facilitated using object-oriented programming.

Object-oriented programming is a ubiquitous feature of computer applications from games to scientific simulations. An object-oriented approach improves efficiency and flexibility of computer programming by coupling data and a set of actions within an object class. An object class defines the data that are stored in an object and the actions that can be performed on the object. Objects are derived from classes. Each object is an instance of a class with its' own unique set of data that can be queried, manipulated, and visualized. The three classes used in this application correspond to the echosounder, fish anatomy and associated backscatter, and fish behavior. The echosounder class includes transducer properties; the echofish class includes acoustical, anatomical, and behavioral characteristics of individual fish; the trajectory class defines fish movements in a shoaling and schooling simulator (Fig. 1).

The echosounder class contains all properties of the echosounder and transducers used in the application: location, orientation, beam width, and frequency. The echosounder tabulates backscatter by determining which targets are in the beam, calculating the incident angle relative to the target's local axes, and then querying each target for a backscatter value. Backscatter amplitudes incorporate target orientations (i.e. tilt and roll) within the beam but are not corrected for transducer beam patterns. Echo amplitudes are equivalent to on axis targets at a variety of tilt and roll angles.

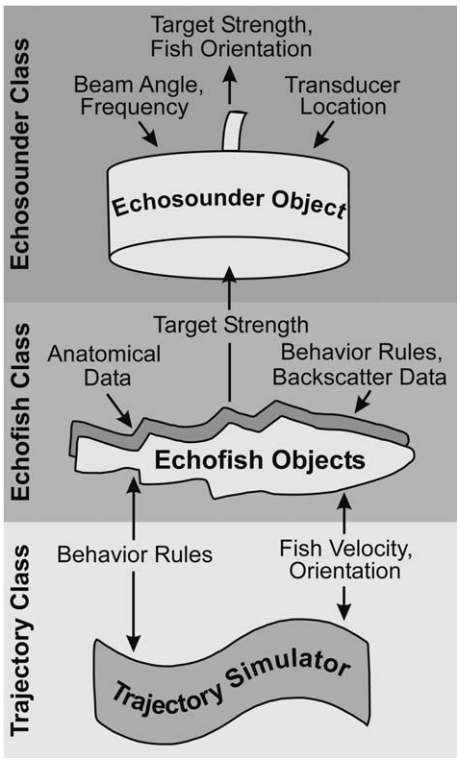

Fig. 1. Schematic diagram showing the relationship between the visualization classes, objects, and data.

The echofish class combines individual fish anatomical and acoustic data with behavioral and physical properties. The echofish class defines the location in space, velocity, and the orientation as physical properties of echofish objects. The anatomical data stored in an echofish object are used to create a three-dimensional model of the fish used in the display. Acoustic backscatter data, either modeled or empirical, can be queried at specified tilt and roll orientations of an echofish object. Because the echofish was designed to interact with any number of behavior simulators, specific behavioral parameters are not defined in this class. The echofish class can read and write behavioral parameters so that behavior simulators can define and modify parameters at any time. This permits simulators with varying parameter requirements to interact with echofish through a common interface and permits each echofish to be parameterized independently if needed.

Fish behavior is simulated by the trajectory class. Fish velocities are calculated using a three-dimensional shoaling and schooling model. The formation and maintenance of fish aggregations is based on opposing forces of attraction and repulsion among individuals (Parr, 1927; Breder, 1954; Horne, 1995). Magnitudes of attraction and repulsion forces are a function of the distance between individuals, canceling at the mean distance between individuals. Parameter values of the behavioral model are based on experimental or empirical observations adapted to approximate walleye pollock and capelin kinematics. In our simulations, all fish are acoustically resolved at any frequency. One walleye pollock is

chosen as the "lead" fish among the 20 echofish objects in the simulation. This pollock follows a specified trajectory through the acoustic beam six times at a depth of approximately 100 m. The force of attraction between the lead and follow fish is 10 times greater than that among follow fish. Trajectories of the 19 "follow" fish generally followed the lead fish and included a random force to add individual behavior. Locations and orientations of the "follow" fish were recorded at 0.1 s intervals for approximately 5 min. Attraction and repulsion forces among group members are calculated at each time interval and a random force is added as an additional behavioral component. All forces are summed and new location, orientation, and velocity values are updated for each fish.

Acoustic backscatter data for walleye pollock and capelin are generated using a KRM model (Clay and Horne, 1994). Anatomical data used in model calculations are generated by digitizing dorsal and lateral radiographs of walleye pollock and capelin bodies and swimbladders. Three-dimensional grids used to display fish bodies and swimbladders are generated from anatomical measurements (Jech and Horne, 2002). Grid points between the dorsal and lateral planes are elliptically interpolated at 2° intervals. In the KRM model, the fish body is represented by a set of contiguous fluid-filled cylinders that surround a set of contiguous gas-filled cylinders representing the swimbladder. Backscatter from each cylinder in the body and the swimbladder is computed and then added coherently to estimate total backscatter as a function of fish length, orientation (i.e. tilt and roll), and acoustic wavelength. Values for the speed of sound through water, fish body, and swimbladder are set at 1470, 1575 and 345 m s^{-1}. Densities of the fish and surrounding medium are set at 1070 kg m^{-3} for the fish body, 1.24 kg m^{-3} for the fish swimbladder, and 1030 kg m^{-3} for seawater. Full details of the model can be found in Clay and Horne (1994), Jech et al. (1995), or the appendix in Horne and Jech (1999). KRM models are used to predict backscatter within 30° of normal incidence. For the visualizations, we calculated backscatter at 38 and 120 kHz at a resolution of 2° in both tilt and roll planes. These backscatter values are assumed to incorporate all echosounder gains.

The simulation data enabled real-time comparisons of target strength variability within or among individual walleye pollock and capelin. Each fish in the aggregation traveled in the same general direction, while being influenced by surrounding fish and its own behavior. Location, orientation, and backscatter data are recorded for each fish at 38 and 120 kHz as they passed through the beam. Simulation transducers with beam widths of 10° are placed at the surface in the center of the domain.

3. Results

A three-dimensional surface (i.e. backscatter ambit, cf. Jech and Horne, 2002) visualizes the effects of fish anatomy and orientation on echoamplitude (Fig. 2). The amplitude of each point in the backscatter matrix is represented in the ambit by color (purple = low, red = high) and by the distance from the surface to intersection of the *x*, *y*, and *z* axes. The dominant feature of all ambits is the high amplitude band of backscatter near the vertical axis. Maximum backscatter occurs at an angle corresponding to the angle of the swimbladder relative to the sagittal axis of the fish body. Among gadoids, the swimbladder is generally tilted 5–10° toward the posterior. The backscatter ambits indicate that the walleye pollock swimbladder (Fig. 2a,b) deviates more from horizontal (9°) than the swimbladder (2°) of the capelin (Fig. 2c,d). For this walleye pollock, peak dorsal backscatter amplitude occurs when the fish swims head down at an angle of 81°. Typical of all teleosts, backscatter amplitudes decrease as incident angles approach the head or tail of the fish in dorsal/ventral and lateral planes. Echo amplitudes are more sensitive to tilt and roll at higher fish length (L) to acoustic wavelength (λ) ratios. As L/λ increases, the directionality of the backscatter increases and the number of "ridges" and "folds" in backscattering ambits increases. As an example, compare the 'roughness' of the ambits at 120 kHz (Fig. 2b,d) to that at 38 kHz (Fig. 2a,c).

A view of a fish aggregation from a 120 kHz transducer's perspective (Fig. 3a) shows the orientation and target strength of individual fish as they pass through the beam at approximately 100 m depth. Fish in the walleye pollock aggregation are shallower than the capelin on the right side of the panel. The backscatter amplitude of each fish is color-coded using the same 256 color scheme used in the backscatter ambit displays (Fig. 2). Target strengths range from near minimum to near maximum for fish of the same species within the school. We can also view the same school by using the perspective of a fish within the aggregation (Fig. 3b). Tilt and roll angles differ among individuals, but the coordinated motion of the aggregation is evident. When the application is running, orientations and corresponding backscatter amplitudes of any fish can be queried in the display.

To illustrate the effect of behavior on frequency-dependent target strengths, orientations and apparent lengths of a walleye pollock and a capelin are plotted as they pass through the transducer beams. Target strengths of the walleye pollock are consistently greater than that of the capelin at both frequencies (Fig. 4a). In the time segment shown, target strengths of walleye pollock at 120 kHz fluctuate by as much as 15 dB between successive measurements. Similar fluctuations, although not as large, occur at 38 kHz. Fluctuations in target strength for both species correspond to large changes in tilt angles (Fig. 4b). Negative changes in tilt angles represent head down tilts relative to horizontal. Positive changes in roll angle correspond to roll angles on the right half of the fish relative to dorsal incidence. Large changes in target strength do not always correspond to large changes in roll angle. Higher roll values can also correspond to higher off-axis angles relative to the transducer.

The apparent length of the walleye pollock and capelin are tracked at each time step. We used published target strength-

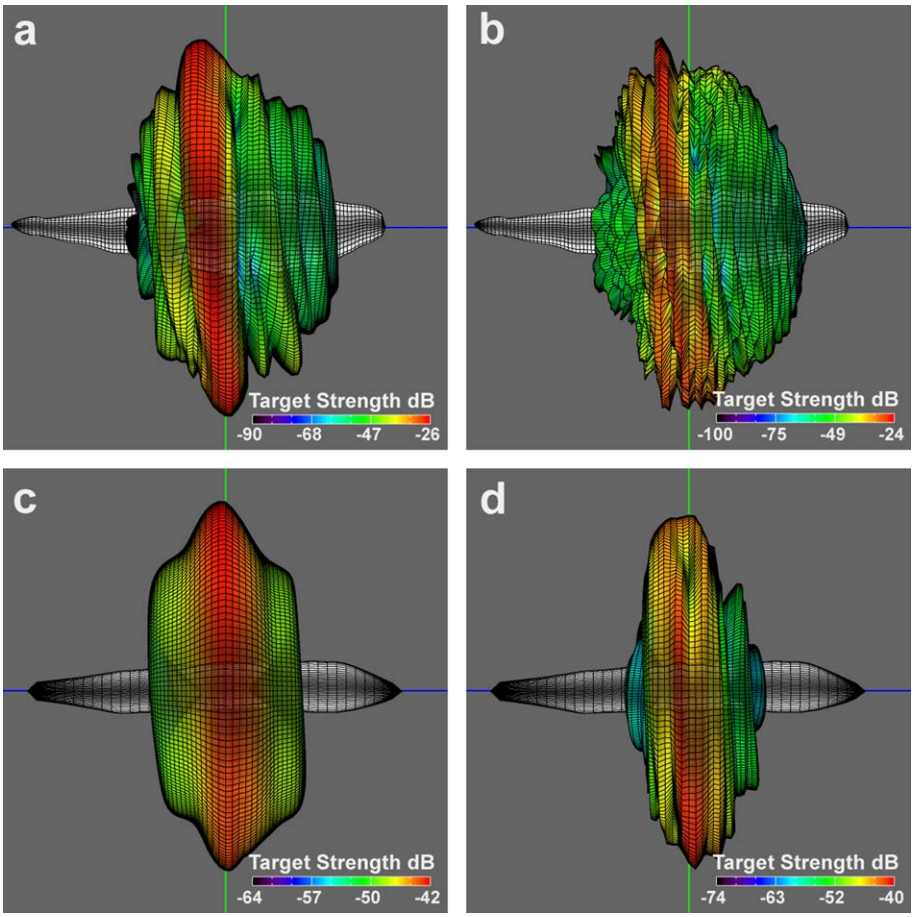

Fig. 2. Acoustic backscatter ambits of a 425 mm walleye pollock (*Theragra chalcogramma*) at (a) 38 kHz and (b) 120 kHz and a 134 mm capelin (*Mallotus villosus*) at (c) 38 kHz and (d) 120 kHz. Backscatter amplitude is represented as distance from the center of the axes and color-coded using red for high amplitude and blue for low amplitude. Target strengths are resolved at 2° in the tilt plane and 2° in the roll plane. Maximum amplitude occurs when the swimbladder is orthogonal to the incident wave front. Note that the color scale minimum and maximum values differ among panels.

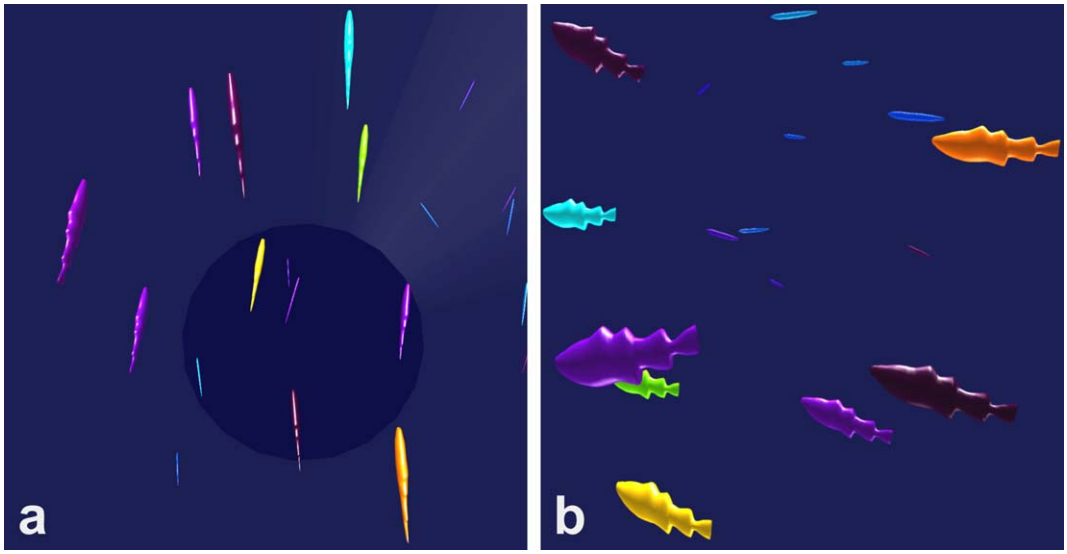

Fig. 3. Snapshots of the Walleye pollock (*Theragra chalcogramma*) and capelin (*Mallotus villosus*) visualization from (a) a 120 kHz transducer's and (b) a fish's perspective of the aggregation. The dark circle in the echosounder perspective delineates the 10° beamwidth of the transducer. Each fish is color-coded depending on the KRM backscatter model prediction of target strength (dB). Color codes range from dark purple (low) to red (high) depending on tilt and roll.

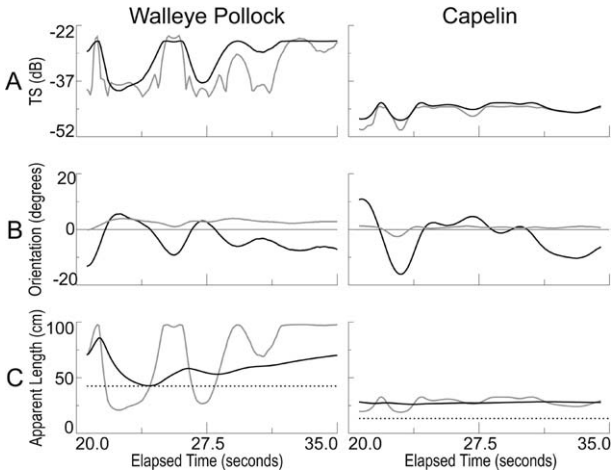

Fig. 4. Tracking of a Walleye pollock (*Theragra chalcogramma*) and capelin (*Mallotus villosus*) (a) predicted target strengths (dB) at 38 kHz (black) and 120 kHz (gray), and (b) orientation: tilt (degrees, positive head up, black), roll (degrees, positive right side, gray) relative to the sagittal and vertical axes of the fish. (c) Apparent length (cm, gray) of each fish is tracked over time using TS = 20 log(L_{cm})-66 (Traynor and Williamson, 1983) for pollock and TS = 20 log(L_{cm})-73.1 (Rose, 1998) for capelin. Dashed lines are the true length of each fish. Black lines are the running mean of each fish's apparent length.

length regression equations for pollock (Traynor and Williamson, 1983) and capelin (Rose, 1998) to translate KRM-predicted target strength to fish lengths (Fig. 4c). Variability in the apparent length of walleye pollock is much greater than that observed in capelin. This is expected, as the range of target strengths predicted for the walleye pollock is larger than that for the capelin. The actual length of each fish is plotted as a dashed line for reference. Apparent length as a running average is plotted for each fish. As the number of echoes increased, accuracy of the length estimation does not always increase.

4. Discussion

Scientific visualization continues to expand its role in fishery research and management. This expansion is due in part to concomitant increases in data volume and in access to computer-based visualization tools. Fisheries acoustic research and management applications are no exception. Visualization facilitates the display and initial analysis of spatially or temporally indexed data and is used to convey technical information to scientists, managers, and other decision makers. Following the lead of other scientific visualization efforts (e.g. Kemp and Meaden, 2002), our goal is to facilitate the discovery and extraction of spatial and temporal patterns from complex data. Our design objectives for this project were:

- to provide dynamic visualizations (Andrienko et al., 2001) that incorporate data exploration;
- to view pattern in data and to view process in simulation;
- to incorporate change or evolution of variables (DiBiase et al., 1992);
- to manage data independent of visualization;
- to interactively manipulate visualization attributes.

Our simulations use a known population of animals with specified behaviors. Simulating fish trajectories provides the advantage of knowing the position and orientation of each individual at every time step. KRM backscatter models are used to predict target strengths for any individual within the acoustic beam based on the orientation (pitch, yaw, roll) at each time step (i.e. echosounder received pulse). This analytic visualization integrates three-dimensional movement with numeric backscatter modeling over time, fulfills the need to integrate data from several sources (Kemp and Meaden, 2002; Stanley et al., 2002), and enables the analysis of derived data sets (Musick and Critchlow, 1999; Lucas, 2000). Two unique features of this application distinguish it from other analytic methods: visual comparison of individual target strengths over time instead of areal or volumetric backscatter summaries and the potential to generate and visualize data for target discrimination among fish sizes or species.

The object-oriented design of the simulation provides a flexible environment to create additional objects or applications. Object classes created for this visualization can be assigned additional attributes and be used in ways not originally conceived during initial development. The use of object classes also eases collaboration and group participation in application development. Objects contain both routines and data that represent an identifiable item with a well-defined role in the application (Smith and Tockey, 1988). Objects appeal to human cognition, are more resilient to change than non-object-oriented programs and allow for faster application development (Booch, 1994).

In our simulation, individual behavior influenced group dynamics and backscatter amplitudes of any fish within an aggregation. The field study by MacLennan et al. (1990) is one of the first investigations to quantify individual and group behaviors while measuring fish target strengths. Tilt-dependent target strengths have been reported for caged (e.g. Edwards and Armstrong, 1983) and tethered (e.g. Nakken and Olsen, 1977; Foote and Nakken, 1978) fish. Fluctuations in target strengths influence accuracy of acoustic size to organism size conversions. Simulating fish trajectories provides the advantage of knowing the position and orientation of each individual within our virtual school. Foote (1980a, b) advocates including fish orientation distributions when establishing relationships between acoustic size and fish length. Combining the ability to track the influence of individual or group behavior on target strength and simultaneously tabulating echo amplitude frequency distributions provides an additional tool when analyzing the causes of backscatter variability. A logical next step would use Boolean operators to combine backscatter amplitudes into target discriminatory metrics.

The visual dominance of human perception poses interesting challenges when analyzing multidimensional data. Graphing one or two variables is easily done in black and

white. Graphing multiple variables in multiple dimensions requires creative thinking. The use of color expands our capability to present echo amplitude predictions from both individual and aggregations of fish. Our challenge was to design a visualization that coherently portrayed relationships among frequency, backscatter amplitude, fish species, orientation, and behavior. The use of multiple images with different characteristics (i.e. fish size and orientation) allows and encourages comparison among images in real time (Tufte, 1990). We hope that the results of this work will directly increase the understanding of fish ensemble structure and dynamics, improve accuracy of acoustic target recognition, and enhance the collection and visualization of acoustic data.

Acknowledgements

This study was funded by the US Office of Naval Research (N00014-00-1-0180). We thank an anonymous reviewer for comments that clarified this paper.

References

Andrienko, N., Andrienko, G., Gatalsky, P., 2001. Exploring changes in census time series with interactive dynamic maps and graphics. Computational Stat. 49, 141–152.

Booch, G., 1994. Object-oriented Analysis and Design with Applications. Benjamin/Cummings Publishing Co., CA, pp. 589.

Breder Jr, C.M., 1954. Equations descriptive of fish schools and other aggregations. Ecology 35, 361–370.

Clay, C.S., Horne, J.K., 1994. Acoustic models of fish: the Atlantic cod (*Gadus morhua*). J. Acoust. Soc. Am. 96, 1661–1668.

DiBiase, D., MacEachren, A.M., Krygier, J.B., Reeves, C., 1992. Animation and the role of map design in scientific visualization. Cartography GIS 19, 201–214.

Edwards, J.I., Armstrong, F., 1983. Measurement of the target strength of live herring and mackerel. FAO Fish. Rep. 300, 69–77.

Foote, K.G., 1980a. Effect of fish behavior on echo energy: the need for measurements of orientation distributions. J. Cons. Int. Explor. Mer 39, 193–201.

Foote, K.G., 1980b. Averaging of fish target strength functions. J. Acoust. Soc.Am. 67, 504–515.

Foote, K.G., Nakken, O., 1978. Dorsal-aspect target strength functions of six fishes at two ultrasonic frequencies. Fisken of Havet Ser. B 1978, 1–96.

Horne, J.K., 1995. Spatial variance of mobile aquatic organisms: capelin and cod in coastal Newfoundland waters. Ph. D. Thesis, Memorial University of Newfoundland. pp. 185.

Horne, J.K., Jech, J.M., 1999. Multi-frequency estimates of fish abundance: constraints of rather high frequencies. ICES J. Mar. Sci. 56, 184–199.

Horne, J.K., Walline, P.D., Jech, J.M., 2000. Comparing acoustic model predictions to in situ backscatter measurements of fish with dual-chambered swimbladders. J. Fish Biol. 57, 1105–1121.

Jech, J.M., Horne, J.K., 2001. Effects of in situ target spatial distributions on acoustic density estimates. ICES J. Mar. Sci. 58, 123–136.

Jech, J.M., Horne, J.K., 2002. Three-dimensional visualization of fish morphometry and acoustic backscatter. Acoust. Res. Lett. Online 3, 35–40.

Jech, J.M., Schael, D.M., Clay, C.S., 1995. Application of three sound scattering models to threadfin shad (*Dorosoma petenense*). J. Acoust. Soc. Am. 98, 2262–2269.

Kemp, Z., Meaden, G., 2002. Visualization for fisheries management from a spatiotemporal perspective. ICES J. Mar. Sci. 59, 190–202.

Lucas, A., 2000. Representation of variability in marine environmental data. In: Wright, D., Bartlett, D. (Eds.), Marine and Coastal Geographical Information Systems. Taylor and Francis, London, pp. 53–70.

MacLennan, D.N., Magurran, A.E., Pitcher, T.J., Hollingworth, C.E., 1990. Behavioral determinants of fish target strength. Rapp. P.-v. Réun. Cons. Int. Explor. Mer. 189, 245–253.

Musick, R., Critchlow, T., 1999. Practical lessons in supporting large-scale computational science. SIGMOD Record 28, 49–57.

Nakken, O., Olsen, K., 1977. Target-strength measurements of fish. Rapp. P.-v. Réun. Cons. Int. Explor. Mer. 170, 52–69.

Parr, A.E., 1927. A contribution to the theoretical analysis of the schooling behavior of fishes. Occasional Papers of the Bingham Oceanography College 1, 1–32.

Rose, G.A., 1998. Acoustic target strengths of capelin in Newfoundland waters. ICES J. Mar. Sci. 55, 918–923.

Smith, M.K., Tockey, S.R., 1988. An integrated approach to software requirements definition using objects. Proceedings of Ada Expo 1988. Galaxy Productions, Frederick, MD, pp. 21.

Stanley, R.D., Kieser, R., Hajirakar, M., 2002. Three-dimensional visualization of a widow rockfish (*Sebastes entomelas*) shoal over interpolated bathymetry. ICES J. Mar. Sci. 59, 151–155.

Traynor, J.J., Williamson, N.J., 1983. Target strength measurements of walleye pollock (*Theragra chalcogramma*) and a simulation study of the dual beam method. In: Nakken, O., Venema, S.C. (Eds.), Symposium on fisheries acoustics. Selected papers of the ICES/FAO Symposium on Fisheries Acoustics. Bergen Norway, 21–24 June, 1982. FAO Fisheries Report 300. pp. 112–124.

Tufte, E.R., 1983. The Visual Display of Quantitative Information. Graphics Press. Cheshire, CT, pp. 197.

Tufte, E.R., 1990. Envisioning Information. Graphics Press. Cheshire, CT, pp. 126.

Available online at www.sciencedirect.com
SCIENCE DIRECT®
Aquatic Living Resources 16 (2003) 283–292
Aquatic Living Resources
www.elsevier.com/locate/aquliv

Diel spatial distribution and feeding activity of herring (*Clupea harengus*) and sprat (*Sprattus sprattus*) in the Baltic Sea

Massimiliano Cardinale *, Michele Casini, Fredrik Arrhenius, Nils Håkansson

Institute of Marine Research, National Board of Fisheries, P.O. Box 4, 45321 Lysekil, Sweden

Accepted 18 December 2002

Abstract

We analysed Baltic Sea pelagic fish (herring and sprat) spatial and temporal distribution, size distribution at different depths and time of the day and diel feeding pattern. In 1995 the study area was investigated by acoustic survey for 3 d, 3, 4 and 11 October, to investigate spatial and temporal distribution of pelagic fish. The area was divided in four different transects forming a survey quadrate of 15 nautical miles of side. The survey quadrate was ensonified each day four times in the 24 h. In 1997 the acoustic survey was conducted in the same area and in the same week of the year to analyse the diel feeding cycle of herring and sprat and their size distribution by depth and time of the day using pelagic trawls. Fish abundance, from 1995 survey, was statistically different among days and survey quadrates. However, from our data it is not clear whether the variation stems from random dispersion or directed movements occurring at the temporal small-scale. Pelagic fish were dispersed during the night at the surface and aggregated during the day at the bottom. They aggregated at dawn and dispersed at dusk at the surface. For herring this distribution pattern coincided with peaks of stomach fullness analysed in the 1997 survey, while sprat seemed to continue feeding during the whole day time. Larger herring were deeper in the water column than smaller individuals. Diel vertical migrations (DVM) of pelagic fish likely mirrored zooplankton diel vertical movements and it was reasonably in response to optimal predation conditions in the sea and possibly intertwined with predation avoidance and bioenergetic optimisation.

Keywords: Baltic Sea; Pelagic fish; Diel vertical migrations; Diel aggregation patterns; Feeding activity

1. Introduction

Schooling behaviour is dependent on different environmental and physiological factors among which feeding and anti-predation risk represent crucial cues (Ona, 1990; see Pitcher, 1993 for a review). However, although spatial and temporal dynamics of fish school structure have been widely investigated in the past, most of the studies referred to tank or aquaria experiment (see Pitcher, 1993 for a review) while analyses in the field are limited (Hansson, 1993; Fréon et al., 1993, 1996; Torgesen et al., 1997; Orlowski, 1998, 1999, 2000; Stokesbury et al., 2000). In the last 30 years, the increased use of hydroacoustic surveys for stock assessment (MacLennan and Simmonds, 1992) has widened the possibility of spatial and temporal structure investigation of pelagic fish in the open sea. The general view is that pelagic fish are highly dispersed at night and aggregated during the day (Blaxter and Holliday, 1969; Hansson, 1993; Fréon et al., 1996). Azzali et al. (1985) defined a model to describe the distribution of pelagic fish during dawn and dusk, arguing that fish disperse rapidly at dusk and aggregate slowly at dawn. This general result has been challenged by Fréon et al. (1996) who observed an opposite pattern analysing data from acoustic survey in the Mediterranean Sea.

Diel vertical migration (DVM) is behaviour common to both invertebrate and vertebrate aquatic organisms (e.g. Lampert, 1989; Levy, 1990a, b; 1991; Steinhart and Wurtsbaugh, 1999). Three major hypotheses (foraging, bioenergetics and predator avoidance) explain the adaptive significance of DVM in pelagic fish. They predict that either they would mirror prey daily movements (i.e. foraging), select water temperature (i.e. bioenergetics) in order to maximise their growth rate (Levy, 1990a, b; Wurtsbaugh and Neverman, 1988; Neverman and Wurtsbaugh, 1994) or reduce to a minimum the exposure to predators (i.e. predator avoidance) (Levy, 1987, 1990b; Clark and Levy, 1988). However, stud-

* Corresponding author.
E-mail address: massimiliano.cardinale@fiskeriverket.se (M. Cardinale).

doi:10.1016/S0990-7440(03)00007-X

ies on the vertical and horizontal structure of pelagic fish schools over the 24-h relating DVM with feeding behaviour in the marine environment are, to our knowledge, scarce in the literature (e.g. Blaxter, 1985), limited to tank experiment (Sogard and Olla, 1996) and lacking for the Baltic Sea.

Nevertheless, inferences on DVM of pelagic fish related to foraging may be done from lakes where DVM by zooplankton has been extensively studied (Levy, 1990a, b, 1991; De Stasio, 1993; Allison et al., 1996; Steinhart and Wurtsbaugh, 1999). Allison et al. (1996) showed peaks in feeding activity of pelagic fish (cichlids) at dawn and dusk in the Lake Malawi related to the DVM of their prey, i.e. zooplankton. Levy (1990b) and Stockwell and Johnson (1999) evaluated the relative importance of different factors explaining DVM of salmon in lakes arguing that a multifactor hypothesis (foraging, bioenergetics and predator avoidance) provided the most realistic explanation of the adaptive significance of DVM in pelagic fish.

The Baltic Sea pelagic ecosystem is constituted by the top-piscivores cod (*Gadus morhua*) and the major pelagic planktivores, herring (*Clupea harengus*) and sprat (*Sprattus sprattus*). Nektobenthos is represented essentially by *Mysis* sp. while zooplankton is dominated by calanoid copepods, but cladocerans and rotifers can be abundant (Rudstam et al., 1994). Hansson et al. (1990) investigated DVM of zooplankton (occupying the deeper and darker water during the day and the upper water column in the night) in the Baltic Sea arguing that this phenomenon was essentially explainable by anti-predation behaviour.

In this paper we investigated pelagic fish (herring and sprat) (a) horizontal movements at the temporal small-scale (data from 1995 survey), (b) DVM and degree of aggregation (data from 1995 survey) and (c) size distribution at different depth and time of the day and diel feeding pattern (data from 1997 survey).

2. Materials and methods

2.1. Surveys design and collection of data

2.1.1. Survey 1995

In October 1995 an acoustic survey was conducted onboard the Swedish research vessel “Argos” in an area south of the Bornholm depth in the southern part of the Baltic Sea (Fig. 1). The 1995 survey was used to estimate the diel spatial distribution of pelagic fish. Recordings of acoustic data of fish were made by SIMRAD EK400 and EK500 38 kHz split-beam echo-sounders. These data were supplemented with geographical position from Global Positioning System in terms of geographical co-ordinates (latitude and longitude). The echo integrator data were collected from 10 m below the sea surface (transducer at 8 m depth) to 1 m above the seabed. Data were recorded using the Simrad BI500 software package on a SUN Sparc IPC computer and stored on DAT tapes. The echo sounder provides a mean integrated value for each 0.1 nautical mile (nm; 1 nm = 1.852 km).

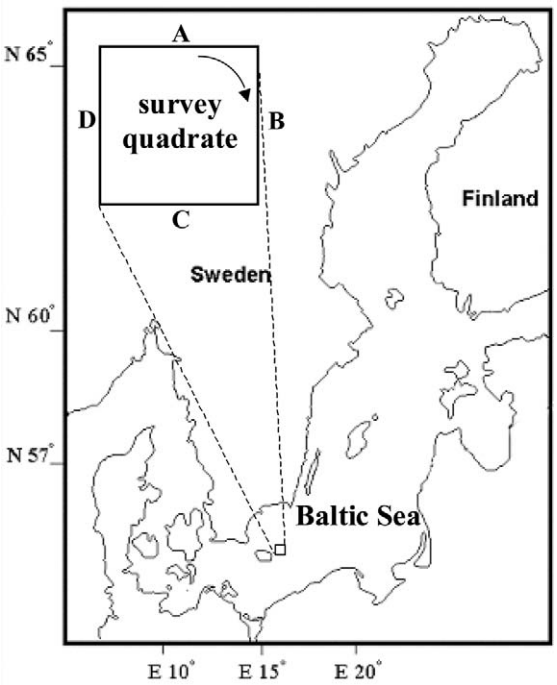

Fig. 1. Study area and sampling design during the 1995 survey. The survey quadrate, constituted by four transects (A–D), was ensonified four times each day (3, 4 and 11 October).

The area investigated was divided in four transects forming a survey quadrate of 15 nm per side (Fig. 1). The survey quadrate was ensonified four times during the 24-h (0–6, 6–12, 12–18, 18–24 h) with a standard vessel speed of 10 knots. The survey was conducted for 3 d on the 3, 4 and 11 October. During the experiment weather conditions were good with a stable high-pressure and variable wind, sunrise was at 05:00 UT (Universal Time) and sunset at 16:30 UT. All the hours mentioned in this study refer to UT. The moon was in its first increasing quarter. The area was chosen because of a high concentration of fish as estimated by the acoustic device. Profiles of water temperature (°C), salinity (psu) and oxygen (ml l^{-1}) content were recorded at 0, 2.5, 5, 10, 15, 20, 30, 40, 50, 60, 70 and 80 m depth using a CTD (Conductivity Temperature Depth) probe.

2.1.2. Survey 1997

In the 1997 an acoustic survey was conducted onboard the Swedish research vessel “Argos” in the same area and in the same period of the year as in the 1995 survey (Fig. 1). The 1997 survey was conducted to estimate the diel feeding cycle of pelagic fish (herring and sprat) and analyse their species and size distribution by depth and time of the day. Individuals of herring and sprat were collected during the 24-h in 3 d using a pelagic trawl net. Fishing was performed with two different pelagic trawls (14–17 m vertical opening; 21 mm stretched mesh size in the cod-end). Size-selectivity of the two trawls used was not statistical different (Bethke et al., 1999). Standard fishing speed was 3–4.5 knots and hauls lasted for approximately 30 min (Bethke et al., 1999). Catches were sorted at species level and a sub-sample of

300 herring and 200 sprat individuals for each haul was measured (total length) to the nearest 0.5 cm for length-frequency distribution analysis. Individual fish were immediately frozen onboard and then processed in the laboratory. A random sample of about 100 herring and 50 sprat for each haul was collected for feeding analysis. In the laboratory, each fish collected was measured (total length) to the nearest 0.5 cm and weighed to the nearest 0.1 g and the stomachs investigated for fullness. A simple approach to calculate feeding cycle in the field is to estimate the proportion of fish with food in the stomach during the 24-h. It simply requires an estimate of the percentage of empty stomachs randomly collected. The effort to collect the data is irrelevant in comparison with other models, particularly when dealing with big sample areas such as the marine environment (Bromley, 1994).

3. Statistical analysis

3.1. Survey 1995. Spatial distribution of fishes during the 24-h

Processed S_a values were used as an index of fish abundance in the sea. In the southern Baltic Sea, herring and sprat constitutes more than 97% of the pelagic fish biomass (Orlowski, 2001). Therefore, the estimated S_a values were assumed to reflect essentially the biomass of herring and sprat and were used as an index of pelagic fish density in the sea. S_a values were transformed (Ln S_a valves + 1) to conform to assumptions of homogeneous variance, normality and linearity (Sokal and Rohlf, 1995). Data were divided into four depth strata (10–20, 21–40, 41–60, 61–80 m) and fish abundance at the different depth strata during the 24-h was compared using Variance Components Analysis and Factorial ANOVA in Statistica computer package (Statistica, 1995). HSD post-hoc tests (Sokal and Rohlf, 1995) were used for mean comparisons. To define changes in degrees of fish aggregation among different hours and depth strata we used the coefficient of variation (CV %) among point estimates of fish abundance as an index (Hilborn and Mangel, 1997). We assumed that when fish are dispersed the variance should be the lowest and when fish are highly aggregate the largest.

3.2. Survey 1997. Diel feeding cycle and species/size distribution of pelagic fish

We estimated the length–frequency distributions of herring and sprat and the proportion of the two species in the catch during the day (05:30–16:30) and night (17:30–04:30) at the surface (10–40 m) and at the bottom (41–80 m). Kolmogorov-Smirnov tests (K-S test) (Sokal and Rohlf, 1995) were used to compare length–frequency distributions. The significance level was set at 5% for all the statistical tests used in the analyses.

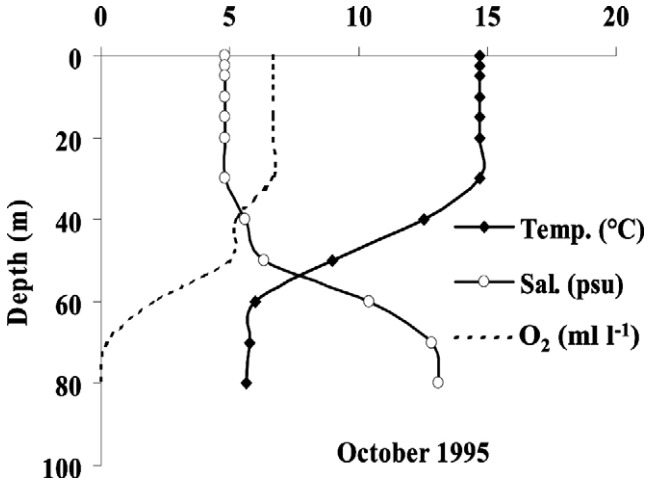

Fig. 2. Depth profiles of temperature, salinity and oxygen content in the study area during the 1995 survey.

4. Results

4.1. Survey 1995. Spatial distribution of fishes during the 24-h

Profiles of water temperature (°C), salinity (psu) and oxygen (ml l^{-1}) content are shown in Fig. 2. A thermocline occurred between 30 and 50 m, salinity was between 5–6 psu down to 40 m and increased to 13 at 80 m depth. Oxygen values were comprised between 6 and 7 ml l^{-1} within 0–40 m decreasing to 0 ml l^{-1} at 70 m depth. Overall, distinct variability was observed in both the horizontal and vertical distribution of fish abundance in space and time. Variables 'day' and 'survey quadrate' and their first interaction term significantly contributed while variable 'transect' did not contribute to explain the total variance of fish abundance during the experiment (Table 1). Fish abundance was significantly different among days (HSD-test), although without a defined pattern (Fig. 3). An increase in fish abundance occurred between the first (October 3) and the second day (October 4) followed by a significant decrease (HSD test; $P < 0.05$) in the third day (October 11) in all the different transects except in D. Here the difference between the second and third day was not significant (HSD test; $P > 0.05$). Fish abundance differed significantly (Table 1) also between different survey quadrates among days and transects but without a well-defined trend during the 24-h (Fig. 3).

The contribution of the variable 'time' to the total variance was not significant for any of the 3 d while 'depth' and 'depth × time' interaction term contributed significantly to the total variance (Table 1). Therefore, we used the 24-h as a single transect testing for diel differences in fish abundance at the different depth strata. Differences in fish abundance occurred among different depth strata during the 24-h (Table 1). Fishes were most abundant between 41 and 80 m (i.e. the deeper part of the thermocline) during the day (HSD test; $P < 0.01$). During the afternoon they migrated to the upper layer (10–40 m) and reached the largest values at the surface

Table 1
Results of Variance Components Analysis and Factorial ANOVA of the 1995 acoustic survey data. d.f. = degrees of freedom; MS = mean square; *P* = probability level, ns (not significant) = $P > 0.05$. {*n*}·{n_x}is the interaction factor between the different variables tested

All days	d.f. effect	MS effect	d.f. error	MS error	*F*	*P*
{1}day	2	54.9	8.0	10.3	5.34	<0.05
{2}survey quadrate	3	17.4	9.2	4.5	3.86	<0.05
{3} transect	3	5.3	8.0	10.0	0.53	ns
{1}·{2}	6	2.9	18.6	1.0	2.81	<0.05
{1}·{3}	6	8.4	18.0	1.0	8.39	<0.01
{2}·{3}	9	2.6	18.0	1.0	2.64	<0.05
{1}·{2}·{3}	18	1.0	6979.0	0.2	6.57	<0.01
October 3						
{1}time	23	25.5	79.6	106.6	0.24	ns
{2}depth	4	407.0	78.8	72.4	5.62	<0.01
{1}·{2}	79	69.0	12038.0	2.1	33.58	<0.01
October 4						
{1}time	23	37.0	80.1	122.9	0.30	ns
{2}depth	5	711.1	78.9	70.7	10.06	<0.01
{1}·{2}	78	86.0	12797.0	2.1	40.72	<0.01
October 11						
{1}time	23.0	12.3	81.7	20.9	0.59	ns
{2}depth	5.0	210.7	78.1	14.4	14.63	<0.01
{1}·{2}	78.0	14.6	11232.0	0.4	38.22	<0.01

(10–20 m) (i.e. above the thermocline), during the night (Fig. 4). Fish abundance in the upper stratum (10–20 m) was larger during the night when compared with deeper strata (HSD test; $P < 0.01$) except in October 3.

The coefficient of variation (CV %, considered as an index of fish aggregation) among point estimates of fish abundance increased sharply at dawn reaching the highest values during the day. The CV % decreased after 14 h reaching the minimum values at night. This trend was common to all 3 d examined (Fig. 5). CV % was always larger in the upper layer (10–40 m) compared to the deeper layer (41–80 m) (ANOVA; $P < 0.05$) while no significant differences were detected within the upper (10–20 vs. 21–40 m) and the deeper (41–60 vs 61–80 m) layers (ANOVA; $P > 0.05$) (Fig. 5).

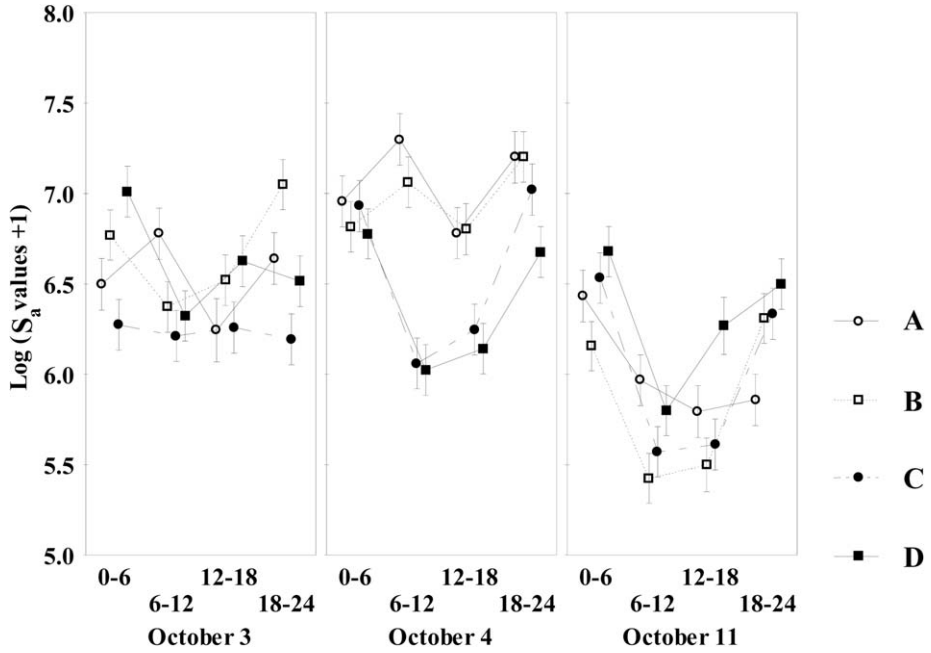

Fig. 3. Log transformed S_a-values estimated for the four transects (A–D) constituting the survey quadrate. The survey quadrate was ensonified four times during the 24 h (0–6, 6–12, 12–18, 18–24 h) for 3 d during the 1995 survey.

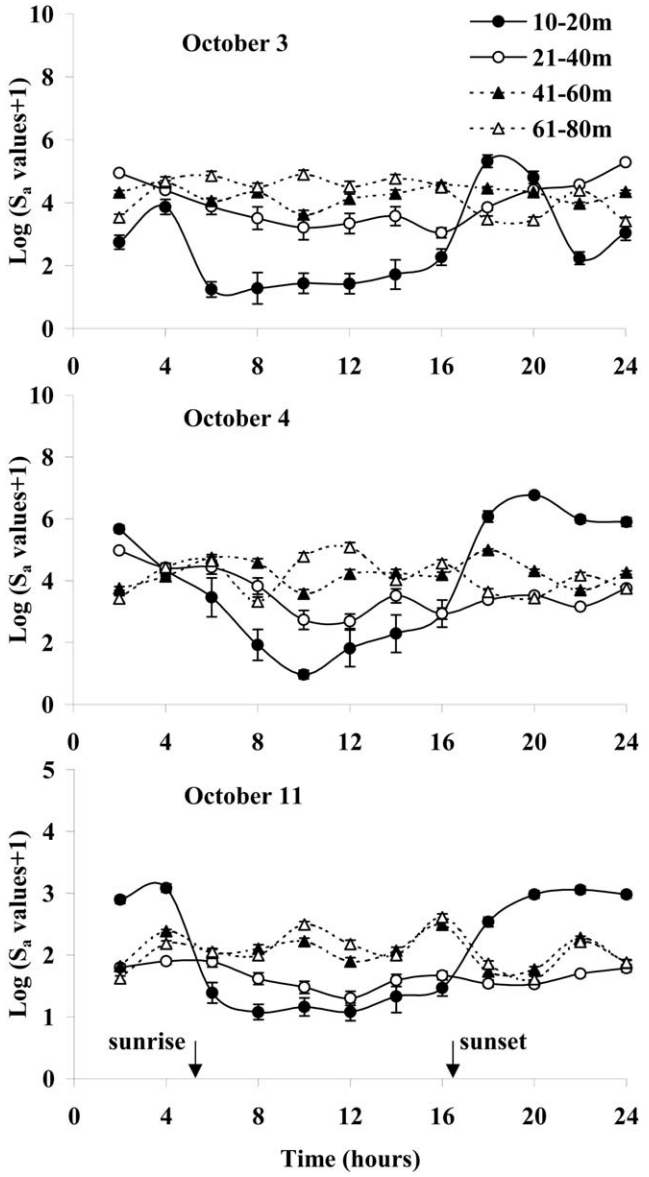

Fig. 4. Log transformed S_a-values (divided in four depth strata) estimated for 3 d over the 24 h during the 1995 survey.

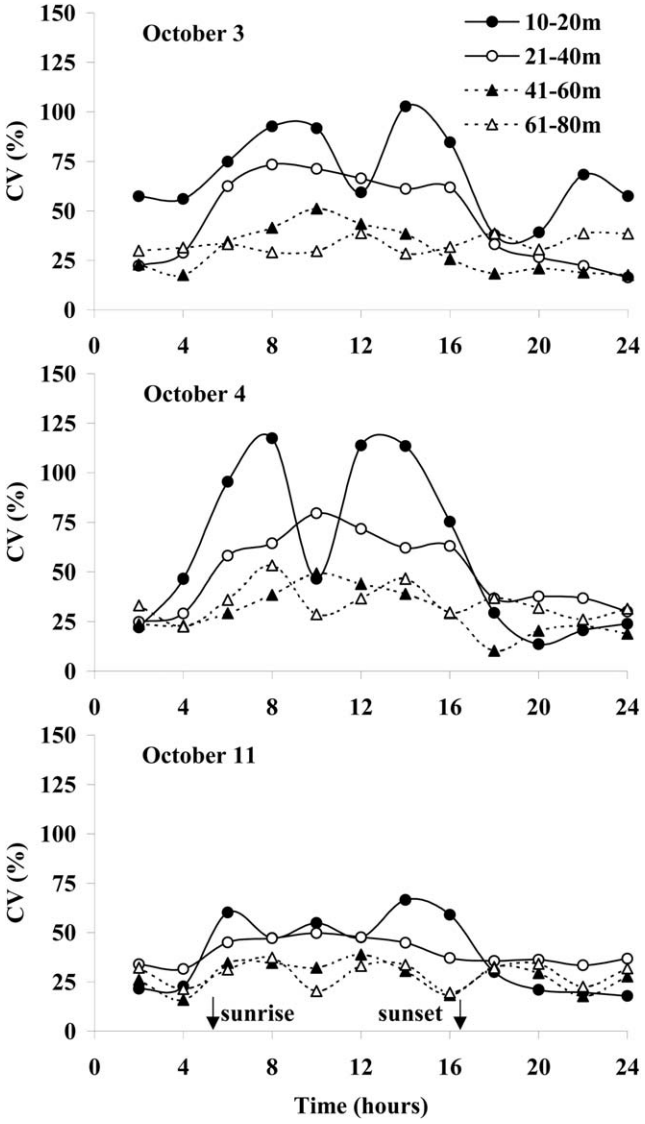

Fig. 5. Coefficient of variation (%) of log transformed S_a-values (divided in four depth strata) estimated over the 24 h for 3 d during the 1995 survey. High and low coefficient of variation (%) indicate fish aggregation and fish dispersion, respectively.

Fig. 6 shows the degree of fish aggregation and dispersion as visualised by the echograms at dawn (a), during the day (b), at dusk (c) and during the night (d).

We also calculated the rates of change (increase or decrease) of CV % during the 4-h preceding (4–7 h) and following (16–19 h) the peaks of maximum aggregation (7 and 16 h, respectively). The rate of change (δ) of the CV % was calculated as:

$$\delta = \frac{cv_{1st} - cv_{4\ th}}{cv_{4\ th}}$$

where *cv*1st is the first hour of the dawn (4 h) and dusk (16 h), and *cv*4th is the last hour of dawn (7 h) and dusk (19 h).

The results of this analysis showed that δ was always larger (ANOVA; $P < 0.05$) at dawn compared to dusk in all days analysed (Fig. 7).

4.2. Survey 1997. Diel feeding cycle and species/size distribution of pelagic fish

The analysis of echograms showed in 1997 the same DVM pattern of pelagic fish as described for the 1995 survey (see section above) (data not shown). This pattern is common to all the other surveys conducted in the study area since 1979 (Nils Håkansson, pers. comm.).

Trawl stations data and percentages of herring and sprat in the catches are presented in Table 2. When comparing length–frequency distributions of herring and sprat during day and night at two different depths, herring length–frequency distributions were statistically different both during day and night. Larger herring individuals were more abundant at the bottom compared to smaller individuals (K-S test; $P < 0.05$) (Fig. 8a). On the other hand, sprat did not show any

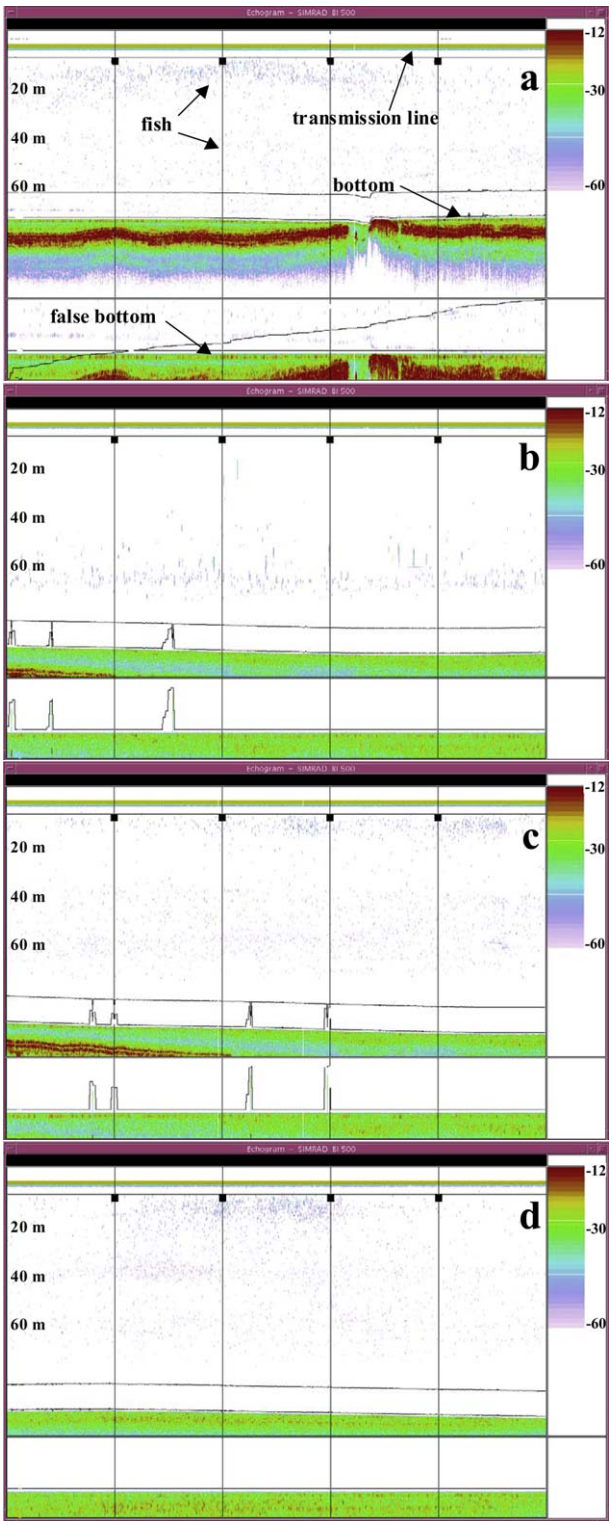

Fig. 6. Echograms of fish vertical distribution recorded during the 1995 survey at different time of the day: (a) dawn, (b) day, (c) dusk and (d) night. The colour scale on the right side of the echograms indicates the strength of the echoes. Red and blue colours indicate strong and weak echoes, respectively. The transmission line corresponds to the depth of the transducer (8 m).

statistical difference in length–frequency distribution at different depth either during the day or night (Fig. 8b).

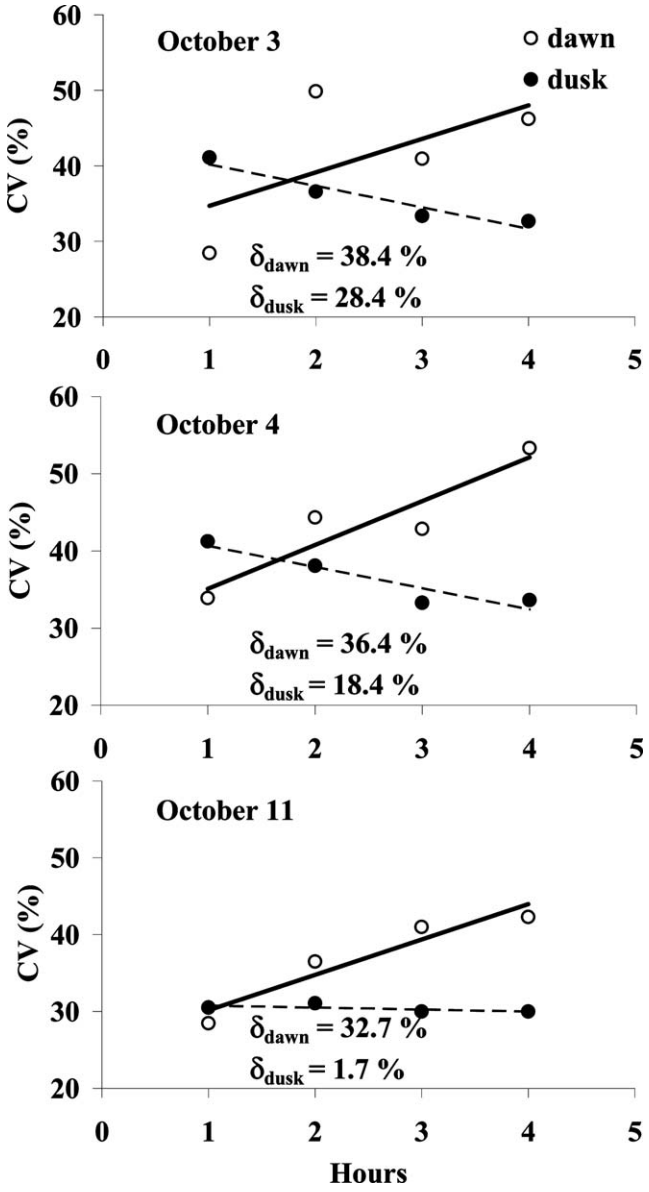

Fig. 7. Changes in the coefficient of variation (%) of log transformed S_a-values estimated during the 4h preceding (4–7) and following (16–19) the peaks of maximum aggregation estimated during the 1995 survey. High and low rate of change (δ) indicate rapid and slow fish aggregation (dispersion), respectively.

There was no statistical difference in the proportion of herring in the pelagic catch at different depth (surface and bottom) during either the day (one-sided test; n_{tot} = 20; P = 0.46; % herring = 26.31 and 28.36 at the surface and bottom, respectively) or night (one-sided test; n_{tot} = 12; P = 0.21; % herring = 29.26 and 54.58 at the surface and bottom, respectively). However, a larger proportion of herring was always present at the bottom both during the day and night.

Fig. 9 shows the proportion of herring and sprat individuals with food in the stomach during the 24-h. There were two peaks for herring, at dawn (~95%) (between 5 and 7 h) and at dusk (~60%) (between 16 and 18 h). The largest proportion of herring with empty stomachs was between 11 and 13 h. The data for sprat showed a peak during the morning (be-

Table 2
Summary of the 1997 trawl stations data. Only herring and sprat were considered in the catch analysis

Haul								Wind		Trawl data			Proportion in the catch	
Date	UT	Latitude			Longitude		Bottom Depth	Direction	Strenght	Mean depth	Duration	Speed	Herring	Sprat
							(m)		($m\ s^{-1}$)	(m)	(min)	(knot)	(Wet weight)	
970930	1526	633	N	56°28'	E	16°45'	58	N	4	42	29	3.9	0.27	0.73
970930	1721	634	N	56°27'	E	16°45'	58	N	9	45	19	4.0	0.07	0.93
970930	1948	635	N	56°22'	E	16°45'	60	NNW	7	35	14	3.9	0.20	0.80
970930	2103	636	N	56°22'	E	16°45'	60	NW	7	33	15	4.1	0.51	0.49
971001	1015	644	N	55°56'	E	17°03'	46	E	4	36	29	4.0	0.12	0.88
971001	1224	645	N	55°55'	E	17°09'	47	Var.	2	37	29	4.0	0.17	0.83
971001	1628	646	N	55°48'	E	16°31'	57	SW	4	37	30	3.8	0.31	0.69
971001	1753	647	N	55°47'	E	16°27'	57	SW	6	48	30	3.8	0.44	0.56
971002	1053	648	N	55°40'	E	14°29'	50	WNW	6	40	30	4.1	0.52	0.48
971002	1224	649	N	55°40'	E	14°29'	50	WNW	16	40	31	4.0	0.47	0.53
971002	1442	650	N	55°35'	E	14°36'	70	NW	15	53	30	3.8	0.76	0.24
971002	1619	651	N	55°35'	E	14°36'	70	NW	16	55	31	3.8	0.79	0.21
971002	2332	652	N	55°57'	E	15°24'	47	N	13	34	30	3.9	0.37	0.63
971003	0104	653	N	55°58'	E	15°24'	47	N	13	35	30	3.9	0.23	0.77
971006	1422	654	N	55°57'	E	15°23'	47	SSW	3	39	31	3.7	0.03	0.97
971006	1620	655	N	55°57'	E	15°22'	47	SSW	3	40	30	4.0	0.04	0.96
971006	2201	657	N	55°33'	E	15°03'	84	SW	4	37	30	3.8	0.17	0.83
971006	2326	658	N	55°33'	E	15°03'	84	SW	2	34	31	3.8	0.15	0.85
971007	0758	659	N	55°23'	E	15°20'	90	SSE	6	64	30	3.8	0.36	0.64
971007	0933	660	N	55°23'	E	15°21'	90	SE	7	71	30	3.7	0.26	0.74
971007	1111	661	N	55°21'	E	15°25'	92	SSE	7	64	30	3.5	0.13	0.87
971007	1233	662	N	55°21'	E	15°25'	92	SSE	7	66	30	3.4	0.24	0.76
971007	1855	664	N	55°28'	E	15°04'	75	SSE	5	57	30	4.5	0.05	0.95
971008	1855	665	N	55°36'	E	14°44'	75	W	7	22	30	3.6	0.10	0.90
971008	1106	666	N	55°36'	E	15°10'	75	WSW	10	60	30	3.7	0.29	0.71
971008	1331	667	N	55°35'	E	15°10'	75	WSW	7	54	30	3.7	0.26	0.74
971008	1854	668	N	55°30'	E	15°03'	76	SW	6	36	30	3.8	0.09	0.91
971009	0554	669	N	55°29'	E	15°02'	85	SW	8	61	30	3.5	0.12	0.88
971009	1801	670	N	55°28'	E	15°05'	75	SW	11	58	30	3.6	0.14	0.86

tween 8 and 10 h) and a minimum during the night. Differently from herring, a large proportion of sprat stomachs contained preys during the day-time. The proportions of sprat full stomachs were point estimates; therefore standard errors were not available.

5. Discussion

Acoustic techniques represent a powerful method to detect and estimate the abundance of fish in the sea (MacLennan and Simmonds, 1992). However, they present a number of important limitations to acknowledge when discussing results from acoustic surveys. One important problem is that when fish occurs in dense concentrations, non-linear effects may bias the accuracy of abundance estimates (MacLennan and Simmonds, 1992; Fréon et al., 1996; Orlowski, 2000). Differences between night and day estimates have been reported (e.g. Aglen, 1983; Unger and Brandt, 1989; Amin and Nugroho, 1990; Schalk et al., 1990) and they were plausibly due to the high degree of patchiness of pelagic fish during the day (Orlowski, 1999, 2000). Usually, in order to exclude or reduce the contribution of horizontal migration to the variation of fish abundance, the surveyed area is limited to a single transect and the experimental time to some days. Hansson (1993) has shown, in a limited study area, that total fish abundances estimated with acoustic survey indicated no large-scale immigration or emigration between the study area and the surroundings. Our data showed that pelagic fish abundance was significantly different for different survey quadrates and days (temporal small-scale) but not for different transects (spatial small-scale). Moreover, no defined trend in pelagic fish abundance was present among days. Therefore, from our data it is not clear whether the variation stems from random dispersion or directed movements occurring at the temporal small-scale. Differences in fish abundance among survey quadrates could be due to bias in the S_a estimates caused probably by the non-linearity effect at different degrees of fish aggregation or by depth dependence of S_a estimates (Ona et al., 2001).

Hence, the lower values of fish abundance occurring during the day-time in some of the days and transects may be partially due to the high degree of fish aggregation as confirmed by the trend of the coefficient of variation among points estimates (a proxy for fish aggregation). On the other hand, when analysing the diel variation of pelagic fish abundance at the different depth strata, the contribution of the

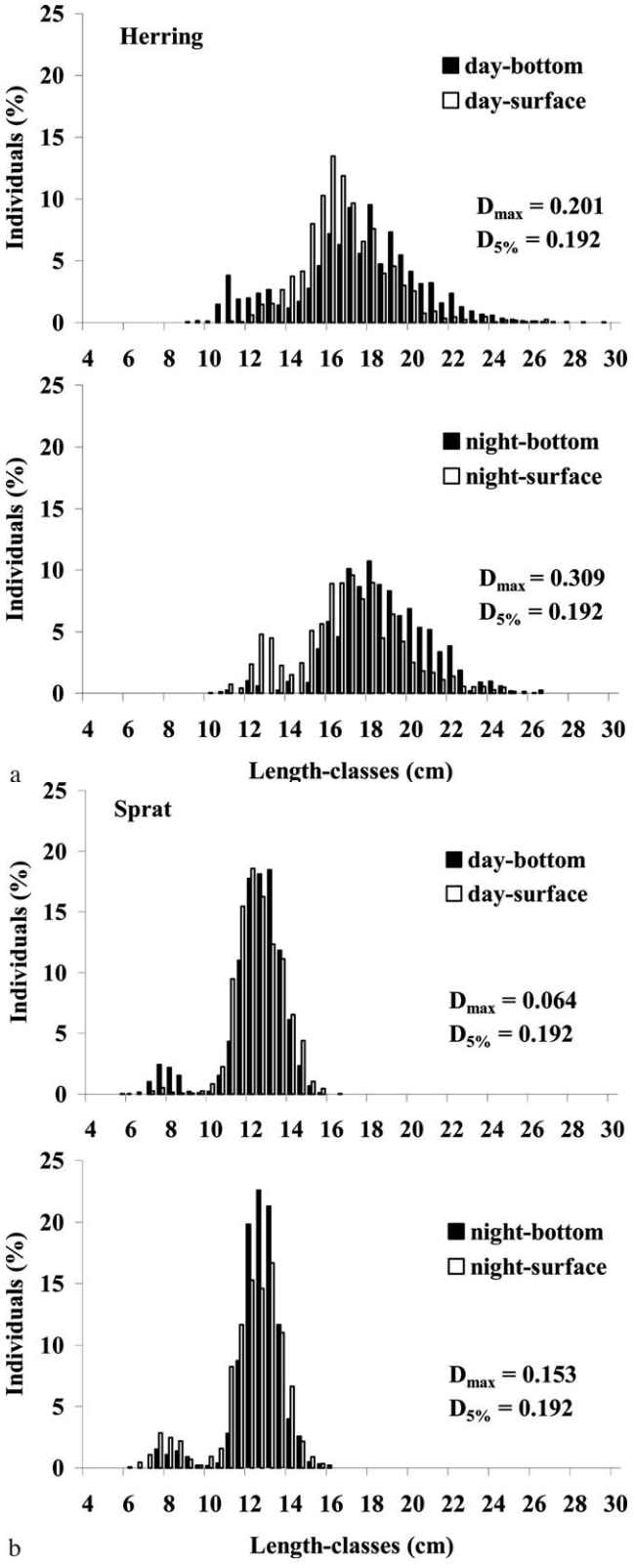

Fig. 8. Length–frequency distribution of herring (a) and sprat (b) during the day and night at the bottom and surface during the 1997 survey.

variable 'time' to the total variance was not significant for any of the 3 d. Therefore, although being aware of technical problems behind S_a values estimates, we assumed that diel

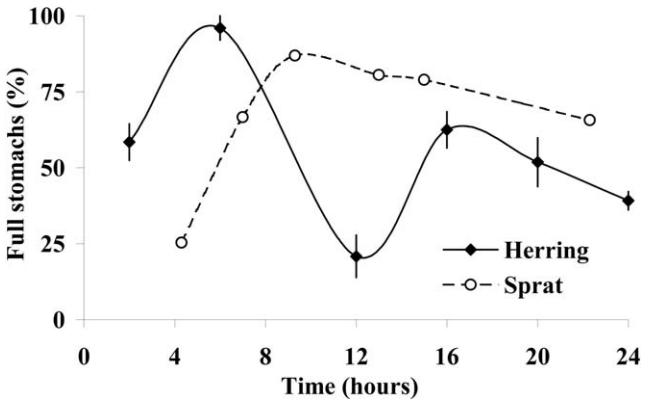

Fig. 9. Daily patterns of full stomachs (%) of herring and sprat sampled during the 1997 survey. Standard errors (bars) were not available for sprat.

trends of fish abundance at different depth were correctly described by S_a estimates. Thus, they reflected essentially the process of vertical migration of fish at the different depth strata during the 24-h and, in a minor extent, horizontal migration or immigration and bias in the acoustic estimates.

Defining school patchiness or aggregation is also a difficult task (Fréon et al., 1996). In this paper, we used the coefficient of variation between point estimates of fish abundance to elucidate diel patterns in pelagic fish patchiness at different depths. The results showed that fish aggregated fast at dawn at the upper layer (10–40 m). After the sunrise they migrated deeper forming denser schools and remained in the deepest layer (41–80 m) during the day. Nevertheless, the degree of fish aggregation was higher for fish stationed at the upper layer (10–40 m), this being possibly explainable as a fish anti-predation behaviour (e.g. Pitcher, 1993). Our results confirmed previous studies describing pelagic fish aggregation during the 24-h (e.g. Blaxter and Holliday, 1969; Fréon et al., 1996). Fréon et al. (1996) suggested that aggregation at dawn is fast due to visual cues and that fish actively swim together forming schools. Conversely, the model of Azzali et al. (1985) predicted that at dusk fish disaggregate fast while at dawn the reforming of the school takes longer. Our data agree with Fréon et al. (1996) showing on the surface a fast (likely to be mainly active) aggregation at dawn and a slower (likely to be mainly passive) dispersion at dusk. To better understand the observed patterns, we have chosen to discuss results from the 1995 acoustic survey with stomachs and length data of herring and sprat collected from the same area and period during the 1997 acoustic survey. We remind that the DVM pattern of pelagic fish, as indicated by the acoustic device, was the same for the two surveys and for all the surveys conducted in the study area since 1979. Stomachs analysis showed that the fast aggregation at dawn on the surface water well correlated to the highest values of stomach fullness in herring individuals. Zooplankton in the Baltic Sea perform large DVM moving to the surface during the night and to the bottom during the day plausibly to avoid zooplanktivorous fish visual predation (Hansson et al., 1990). This implies that zooplankton catchability is reasonably highest, due to fish optimal visual conditions, at the dawn and dusk

when zooplankton is distributed at the surface. This may explain why pelagic fish aggregate for feeding on the surface water at dawn, predating on zooplankton before it starts to migrate to deeper strata. The same pattern occurs at dusk when fish migrates to the surface from the deeper strata. Again, zooplankton is migrating from the bottom towards the surface at that time of the day and is again predated by pelagic fish as showed by herring stomach fullness index. A two-time feeding cycle (dawn-dusk) has been previously showed for young-of-the-year herring in the northern Baltic Sea (Arrhenius and Hansson, 1994a, b) and for cichlids in lake Malawi (Allison et al., 1996). Sprat, however, reached its peak in feeding activity later than herring and continued feeding during the day time. This could be explained by the different feeding preferences of the two species. Sprat feed exclusively upon zooplankton (Starodub et al., 1992) while herring (particularly large individuals) feed also upon nektobethos (Arrhenius and Hansson, 1994a, b). Nektobethos, compared to zooplankton, perform limited DVM and is closer associated to the dark bottom (Hansson et al., 1990). Since both herring and sprat are highly selective visual feeders (Blaxter and Hunter, 1982; Arrhenius, 1998; Viitasalo et al., 2001), the time available for herring for feeding could be less than for sprat and restricted only to dawn and dusk when nektobenthos is in the water column and visible to them. On the other hand, sprat may possibly have more time available for feeding before zooplankton reach, during the day, the darkest layer of the water column. The proposed explanations could reflect in the different diel patterns of stomach fullness observed in this study. During the night, fish were dispersed in the upper water stratum (10–20 m) as well as zooplankton (Hansson et al., 1990) but they were not actively feeding.

According to our data, DVM of pelagic fish in the Baltic Sea is well explained in terms of trade-offs between the three major adaptive hypotheses (Levy, 1990a, b; Wurtsbaugh and Neverman, 1988; Neverman and Wurtsbaugh, 1994). During the day, pelagic fishes appeared at the surface for a short time, likely feeding at dawn and dusk on aggregating zooplankton before it moves down to the bottom, since the availability of plankton organisms in the upper layers is evidently higher and light condition reasonably optimal (Orlowski, 2000). On the contrary, fish spend most of the day-time at deeper areas probably to avoid predation by predatory fish and sea birds. During the night, when predation risk by sea birds is minimised, pelagic fishes were found at the surface water presumably selecting warmer water to maximise their growth rate (Levy, 1990a, b; Wurtsbaugh and Neverman, 1988; Neverman and Wurtsbaugh, 1994; Orlowski, 2000).

Interestingly, our data showed a statistical difference in length–frequency distribution of herring both during the day and night at different depths, with larger herring more abundant at the bottom than smaller individuals. The same trend was not true for sprat. Such differences in size distribution of the two species may again be explained by differences in their feeding habits (see above). As stated above, sprat and smaller herring feed upon zooplankton (Starodub et al., 1992) while larger herring prefer nektobenthos (Arrhenius and Hansson, 1994a, b). Therefore, larger herring individuals were found to be more abundant close to the bottom compared to smaller herring probably because feeding on nektobenthos.

Concluding, results from this study showed that variability of fish distribution and abundance is large at the temporal small-scale although from our data it is not clear whether the variation stems from random dispersion or directed movements occurring at the temporal small scale. DVM of pelagic fish in the Baltic Sea is a well-defined process and it is correlated with their feeding behaviour including differences in diet habits among individuals of different size. Nevertheless, patterns of vertical diel migration of pelagic fish described in this study represent a more general ecological phenomenon. Fish vertical migrations mirrored in zooplankton diel movements in the water column likely in response to optimal predation conditions in the sea and plausibly intertwined with predation avoidance and bioenergetic optimisation.

References

Aglen, A., 1983. Random errors of acoustic fish abundances estimates in relation to the survey grid density applied. Fisheries Acoustic Symposium, Bergen Norway, 21–24 June 1982. In: Nakken, O., Venema, S.C. (Eds.), FAO Fish. Rep., 300, pp. 293–298.

Allison, E.H., Irvine, K., Thompson, A.B., Ngatunga, B.P., 1996. Diets and food consumption rates of pelagic fish in lake Malawy. Fresh water Biol. 35, 489–515.

Amin, E.M., Nugroho, D., 1990. Acoustic surveys of pelagic fish resources in the Banda Sea during August 1984 and February–March 1985. Neth. J. Sea Res. 25, 621–626.

Arrhenius, F., 1998. Food intake and seasonal changes in energy content of young Baltic Sea sprat (*Spratttus sprattus* L. ICES J. Mar. Sci. 55, 319–324.

Arrhenius, F., Hansson, S., 1994. In situ food consumption by young-of-the-year Baltic Sea herring *Clupea harengus*: a test of prediction from a bioenergetics model. Mar. Ecol. Prog. Ser. 110, 145–149.

Arrhenius, F., Hansson, S., 1994b. Erratum Re Arrhenius, F., Hansson, S., 1994a. Mar. Ecol. Prog. Ser. 114, 314. Mar. Ecol. Prog. Ser. 110, 145–149.

Azzali, M., Buracchi, G., Conti, S., Gambetti, S., Luna, M., 1985. Relationship between the forms of pelagic fish distribution and nychtemeral periods. A tentative model of behaviour. Oebalia 11, 471–488.

Bethke, E., Arrhenius, F., Cardinale, M., Håkansson, N., 1999. Comparison of the selectivity of different research trawls in the hydroacoustic surveys. Fish. Res. 44, 15–23.

Blaxter, J.H.S., 1985. The herring: a successful species? Can. J. Fish. Aquat. Sci. 42 (suppl. 1), 21–30.

Blaxter, J.H.S., Holliday, F.G., 1969. The behaviour and physiology of herring and other clupeids. Adv. Mar. Biol. 1, 261–393.

Blaxter, J.H.S., Hunter, J.R., 1982. The biology of clupeoid fishes. Adv. Mar. Biol. 20, 1–225.

Bromley, P., 1994. The role of gastric evacuation experiments in quantifying the feeding rates of predatory fish. Rev. Fish Biol. Fish. 4, 36–66.

Clark, A.N.W., Levy, D.A., 1988. Diel vertical migration by juvenile sockeye salmon and the antipredation window. Am. Nat. 131, 271–290.

De Stasio Jr, B.T., 1993. Diel vertical and horizontal migration by zooplankton: population budget and diurnal deficit. Bull. Mar. Sci. 53, 44–64.

Fréon, P., Gerlotto, F., Soria, M., 1996. Diel variability of school structure with special reference to transition periods. ICES J. Mar. Sci. 53, 459–464.

Fréon, P., Soria, M., Mullon, C., Gerlotto, F., 1993. Diurnal variation in fish density estimates during acoustic surveys in relation to spatial distribution and avoidance reaction. Aquat. Living Resour. 6, 221–234.

Hansson, S., 1993. Variation in hydroacoustic abundance of pelagic fish. Fish. Res. 16, 203–222.

Hansson, S., Larsson, U., Johansson, S., 1990. Selective predation by herring and mysids, and zooplankton community structure in a Baltic Sea coastal area. J. Plankton Res. 12, 1099–1116.

Hilborn, R., Mangel, M., 1997. The ecological detective. Confronting models with data. Princeton University Press, Princeton, New Jersey.

Lampert, W., 1989. The adaptive significance of diel vertical migration of zooplankton. Func. Ecol. 3, 21–27.

Levy, D.A., 1987. Review of the ecological significance of diel vertical migration by juvenile sockeye salmon (*Oncorhynchus nerka*). Sockeye Salmon (*Oncorhynchus nerka*) Population Biology and Future Management. In: Smith, H.D., Margolis, L., Wood, C.C. (Eds.), Can. Spec. Pub. Fish. Aquat. Sci. 96, pp. 44–52.

Levy, D.A., 1990. Reciprocal diel vertical migration behaviour in planktivores and zooplankton in British Columbia lakes. Can. J. Fish. Aquat. Sci. 47, 1755–1764.

Levy, D.A., 1990. Sensory mechanism and selective advantage for diel vertical migration behaviour in juvenile sockeye salmon, *Oncorhynchus nerka*. Can. J. Fish. Aquat. Sci. 47, 1796–1802.

Levy, D.A., 1991. Acoustic analysis of diel vertical migration behaviour of *Mysis relicta* and kokanee (*Oncorhynchus nerka*) within Okanagan Lake, British Columbia. Can. J. Fish. Aquat. Sci. 48, 67–72.

MacLennan, D.N., Simmonds, E.J., 1992. Fisheries acoustic. Fish and Fisheries Series 5. Chapman & Hall, London 336 p.

Neverman, D., Wurtsbaugh, W.A., 1994. The thermoregulatory function of diel vertical migration for a juvenile fish, *Cottus extensus*. Oecologia 98, 247–256.

Ona, E., 1990. Physiological factors causing natural variations in acoustic target strength of fish. J. Mar. Biol. Assoc. UK 70, 107–127.

Ona, E., Svellingen, I., Fosseidengen, J.E., 2001. Target strength of herring during vertical excursions. ICES Fisheries Acoustics, Science and Technology Working Group (FAST), Seattle, April 2001, 1–16.

Orlowski, A., 1998. Acoustic methods applied to fish environmental studies in the Baltic Sea. Fish. Res. 34, 227–237.

Orlowski, A., 1999. Acoustic studies of spatial gradients in the Baltic: implications for fish distributions. ICES J. Mar. Sci. 56, 561–570.

Orlowski, A., 2000. Diel dynamics of acoustic measurements of Baltic fish. ICES J. Mar. Sci. 57, 1196–1203.

Orlowski, A., 2001. Behavioural and physical effect on acoustic measurements of Baltic fish within a diel cycle. ICES J. Mar. Sci. 58, 1174–1183.

Pitcher, T.J., 1993. Behaviour of teleost fishes. Fish and Fisheries Series 7. second ed. Chapman & Hall, London.

Rudstam, L.G., Aneer, G., Hildén, M., 1994. Top-dawn control in the pelagic Baltic ecosystem. Dana 10, 159–173.

Schalk, P.H., Zijlstra, J.J., Witte, J.I.J., 1990. Spatial and seasonal differences in acoustic recordings of the Banda Sea (Indonesia), obtained with a 30 kHz echosounder. Neth. J. Sea Res. 25, 611–620.

Sogard, S.H., Olla, B.L., 1996. Diel patterns of behaviour in juvenile walleye pollock, *Theragra chalcogramma*. Env. Biol. Fish. 47, 379–386.

Sokal, R.R., Rohlf, F.J., 1995. Biometry. third ed. W.H. Freeman and Company, New York.

Starodub, M., Shvetsov, F., Hoziosky, S., 1992. The feeding of sprat in eastern Baltic. ICES C.M. 1992/J:26.

Statistica, 1995. Statistica for Windows. Statsoft, Inc. and its licensors, 1984–1996.

Steinhart, G.B., Wurtsbaugh, W.A., 1999. Under-ice diel vertical migration of *Oncorhynchus nerka* and their zooplankton prey. Can. J. Fish. Aquat. Sci. 56 (Suppl. 1), 152–161.

Stokesbury, K.D.E., Kirsch, J., Brown, E.D., Thomas, G.L., Norcross, B.L., 2000. Spatial distributions of Pacific herring, *Clupea pallasi*, and walleye Pollock, *Theragra chalcogramma*, in Prince William Sound, Alaska. Fish. Bull. 98, 400–409.

Stockwell, J.D., Johnson, B.M., 1999. Field evaluation of a bionergetics-based foraging model for kokanee (*Oncorhynchus nerka*). Can. J. Fish. Aquat. Sci. 56 (Suppl. 1), 140–151.

Unger, P.P., Brandt, S.B., 1989. Seasonal and diel changes in sampling conditions for acoustic surveys of fish abundance in small lakes. Fish. Res. 7, 353–366.

Torgesen, T., Kartvedt, S., Melle, W., Knutsen, T., 1997. Large scale distribution of acoustical scattering layers at the Norwegian continental shelf and the eastern Norwegian Sea. Sarsia 82, 87–96.

Viitasalo, M., Flinkman, J., Viherluoto, M., 2001. Zooplanktivory in the Baltic Sea: a comparison of prey selectivity by *Clupea harengus* and *Mysis mixta*, with reference to prey escape reactions. Mar. Ecol. Prog. Ser. 216, 191–200.

Wurtsbaugh, W.A., Neverman, D., 1988. Post-feeding thermotaxis and daily vertical migration in a larval fish (Lond.). Nature 333, 846–848.

Available online at www.sciencedirect.com
SCIENCE DIRECT®
Aquatic Living Resources 16 (2003) 293–298
Aquatic Living Resources
www.elsevier.com/locate/aquliv

Split-beam target tracking can be used to study the swimming behaviour of deep-living plankton in situ

Thor A. Klevjer *, Stein Kaartvedt

Department of Biology, University of Oslo, P.O. Box 1064, Blindern 0316, Oslo, Norway

Accepted 24 January 2003

Abstract

A scattering layer consisting mainly of krill (*Meganyctiphanes norvegica*) was studied with a submersible transducer, to assess the behaviour of individual organisms in situ by means of split-beam target tracking. Individuals were resolved and tracked, but a rapid increase in average swimming speeds with depth suggested that inaccuracies in the angular estimates affected the estimates. Attempts were made to smooth the tracks during post-processing. Smoothed speeds suggested that most (>78%) invertebrates swam at speeds below 12 cm s^{-1} (mode ~4 cm s^{-1}), with components of speed larger in the horizontal plane than in the vertical.

Keywords: Behaviour; Invertebrate; Swimming; Speed; Target tracking

1. Introduction

Knowledge of natural behaviour is needed in order to get sensible results from models for predator-prey encounter and individual somatic growth (Gerritsen and Strickler, 1977; Torres and Childress, 1983). However, little is known about the swimming behaviour of individual euphausiids in situ (Jaffe et al., 1999), and until recently no non-intrusive method has been available.

Split-beam target tracking (TT) is a relatively new approach for studying individual behaviour (Brede et al., 1990), and the method has so far mainly been aimed at fish (for instance: Huse and Ona, 1996; Torgersen and Kaartvedt, 2001). TT has the capability to measure swimming speed independently of visibility, with a minimum of disturbance (Arrhenius et al., 2000). The main disadvantages are that the true identity of the studied organisms can only be inferred (MacLennan and Simmonds, 1992), and that the accuracy and precision of the measurements are variable (Ehrenberg and Torkelson, 1996; Mulligan and Chen, 2000).

Røstad (2000) used a hull-mounted 120 kHz transducer to track individual krill in shallow water during nighttime. However, for krill in the deep-scattering layer, the ranges involved preclude the use of hull-mounted transducers for studies of individual behaviour due to large sampling volumes, low signal-to-noise ratio (SNR) and low spatial resolution. In this study, we explore the possibility of using a submerged transducer to unveil the behaviour of individual macrozooplankton (mainly krill, *Meganyctiphanes norvegica*), at depth.

2. Materials and methods

The study was conducted in the Oslofjord, Norway, at position (59°48'N, 10°34'E) in the period between 15 and 17 March 2000. This particular station was chosen because the calm conditions of the inner Oslofjord facilitated manoeuvring and deployment of a free-hanging transducer, and also because the pelagic community at this 120 m deep location has been described through several previous studies, establishing krill as a major component of the fauna and acoustic targets at 120 kHz (Onsrud and Kaartvedt, 1998; Bagøien et al., 2000; Kaartvedt et al., 2002).

Backscattering data were collected at 38 and 120 kHz with a Simrad EK500 split-beam echo sounder (software version 5.3) from the RV "Trygve Braarud". The ship used three anchors to avoid drift. From the hull-mounted transducers, a scattering layer starting at ~75 m was observed at 120 (Fig. 1A) but not at 38 kHz.

* Corresponding author.
E-mail address: t.a.klevjer@bio.uio.no (T.A. Klevjer).

doi:10.1016/S0990-7440(03)00013-5

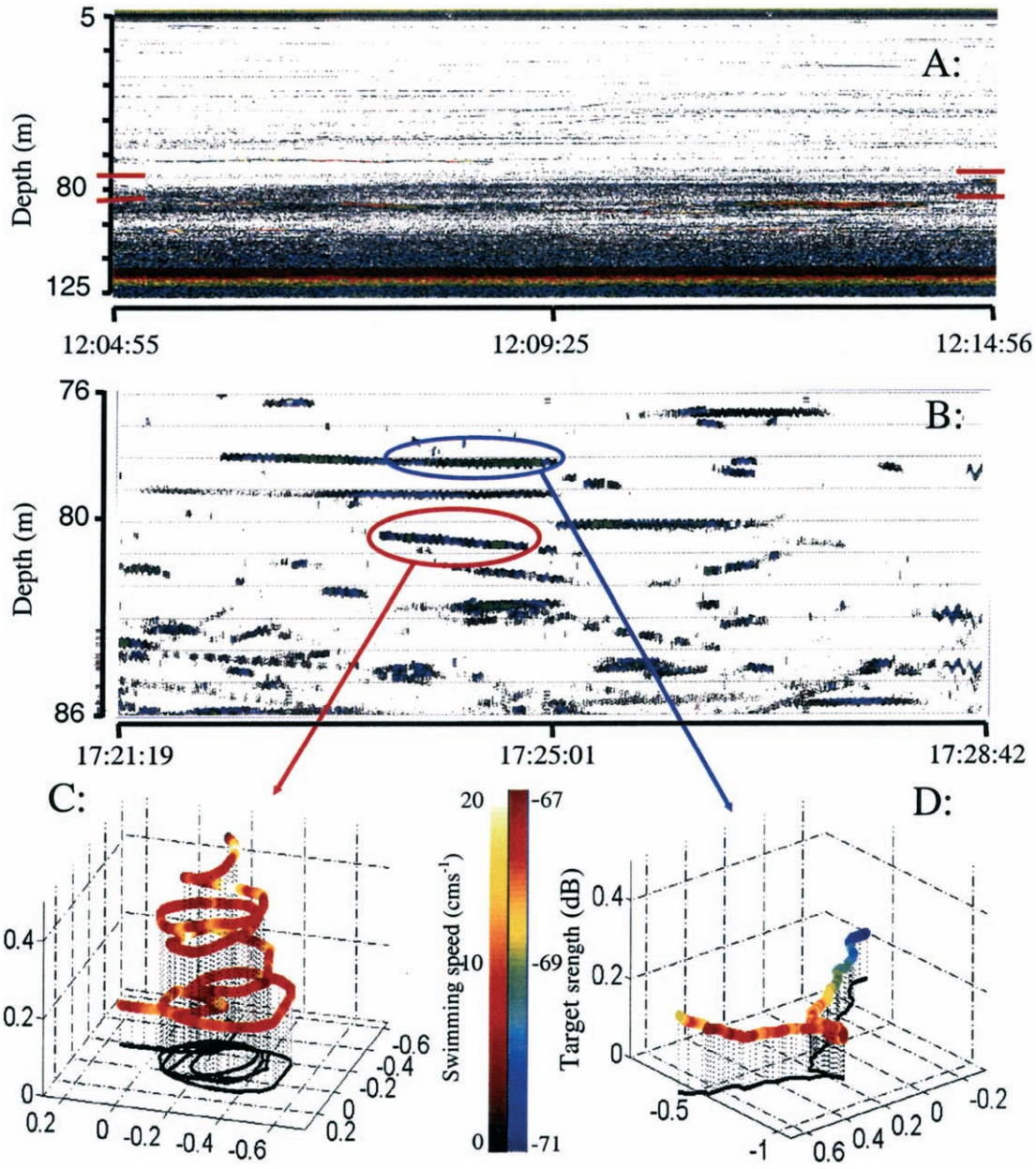

Fig. 1. (A) Echogram from hull-mounted 120 kHz transducer, S_v-threshold = –77 dB, showing the situation shortly after the submersible transducer was raised. The area bounded by horizontal red lines shows the depth-range covered by the printouts from the submersible transducer. (B) Echogram-printout from submersible transducer with 10 m range, showing the depth range of the scattering layer with greater resolution. (B) was printed during daytime on 15th March 2000. (C) Tracking and smoothing performed on targets found within circle in B. The target was tracked for 135 echoes, average smoothed speed was ~8 cm s^{-1}, and average TS –74.1 dB. XYZ-scales in meters. Horizontal plane in figure corresponds to the real horizontal plane. (D) Track recorded simultaneouly with track in (C); totally 125 echoes, average smoothed speed ~3 cm s^{-1}, average TS –68.2 dB.

For this particular study, ground-truthing was performed within and above the observed scattering layer with a pelagic trawl. The trawl had an aperture of about 100 m^2, mesh size near the opening was 20 cm, declining to 1 cm near the cod end, and was towed horizontally at two knots for about 30 min. All the fish and subsamples of krill were frozen from the catch, for later species determination and length measurement (for fish tail-fork length, for krill telson-rostrum length, Sameoto et al., 1993) in the lab.

A downward-looking, submersible 120 kHz transducer was deployed at ~66 m to allow close inspection of the scattering layer and resolution of individual targets (Fig. 1B). Their swimming trajectories were established using specially made software for split-beam TT (Ona and Hansen, 1992),

and data were imported into Matlab for presentation of three-dimensional (3D) swimming tracks and target strengths (TS) (Fig. 1C,D). The submersible transducer was connected to the echo sounder via 100 m of cable. Due to logistic problems, the transducer was not calibrated prior to the deployment.

The transducer had a vertical resolution of 3 cm, while the angular resolution was 0.13°. Pulse duration was set at 0.3 ms, while the average ping rate was ~2.3 s^{-1}.

Echo data interpreted by the EK500 as originating from a single source and with TS (uncalibrated value) higher than –83 dB, were collected from this transducer in the period from 14 h 52 on the 15th to 09 h 23 on the 16th (local time), most of the tracks were therefore recorded during nighttime. The settings used required a minimum of 10 returned echoes to define a track, allowing for one missing echo (except for the illustrations presented in Fig. 1C,D) and a (arbitrary) maximal vertical excursion of 10 cm between echoes.

Registrations of single individuals were easily identified from printouts with high vertical resolution, showing the depth range 10–20 m from the transducer (Fig. 1B). This allowed a manual check of whether wave-movement corrupted the estimated swimming speeds. Also tracks recorded deeper than this were accepted. Swimming speeds were calculated by dividing the sum of movements in a track by the track duration.

Comparisons between day and night relative invertebrate numbers were made from counts of individual traces on echogram-printouts, the traces were identified as invertebrates on the basis of trace-colour on the 40LogR paper-prints. These numbers were then converted to numerical densities.

Since a free-hanging transducer was used, the swimming speeds estimated through the TT-procedure were subjectively examined for the effect of wave-motion generated by passing ships. Tracks recorded in periods with the passing ships were discarded. Since three anchors moored the vessel, the drift was assumed to be minimal. The potential influence of currents at depth was not accounted for.

Bias against fast swimmers may be introduced by requiring a minimum of 10 echoes to define a track (Torgersen and Kaartvedt, 2001). Errors are also introduced through the systems finite resolution (Brede et al., 1990), and by erroneous angle measurement (Mulligan and Chen, 2000), both factors expected to increase ping-to-ping swimming speeds. Since the resolution is inversely proportional to depth, and the angular error increase with decreasing SNR (Ehrenberg and Torkelson, 1996), it was expected that the average of estimated swimming speeds would increase with depth.

Interpolation of position by using adjacent echoes may increase the precision of the measurements (Fleischman and Burwen, 2000). We tried to remove the effect of the finite resolution and erroneous angle measurements by assuming that small, rapid fluctuations in positions were caused entirely by these error sources. This was done by further post-processing the tracks with a simple three-step routine, effectively forming a filter against short, rapid movements. The first step was aimed at reducing the effect of the discrete resolution, and gave echo (n), the same position as echo (n – 1) if echo (n – 1) had the same position as either of echoes n + 1 to n + 3. The second step was aimed at reducing the effect of erroneous measurements, and interpolated the position of echo (n) if the position was not between positions (n – 1) and (n + 1). The last step fitted a 3 (5 point for vertical data) point running mean to the data, further smoothing the effect of the resolution. In all steps, the first and last measurements of a track were kept unchanged, and the corrections were performed separately on both of the angular measurements (and steps 1 and 3 on the depth-data).

Swimming speeds were then recalculated on the basis of these estimated positions.

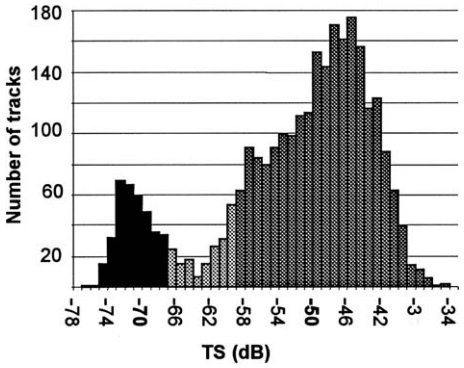

Fig. 2. TS-distribution of tracked organisms; black interpreted as invertebrate, dark grey as fish, light grey not included in any group.

3. Results

The system had the capability to resolve individual plankton scatterers at their daytime depth, enabling the study of behaviour of individuals (Fig. 1C,D). A largely bi-modal TS-distribution of tracked individuals (Fig. 2) suggested that fish could be separated from invertebrates on the basis of average TS. Conservatively, tracks with average TS less than –68 dB were ascribed to invertebrates, and tracks above –60 dB to fish. A total of 2253 tracks passed the criteria, of which 359 were interpreted as originating from invertebrates. Fish tracks were mostly obtained at night. Only four invertebrate tracks were observed beyond 20 m from the transducer. Invertebrate tracks lasted from 3.7 to 82.1 s, with an average track duration of 10.4 s.

The invertebrates of the daytime trawl-catches from the depth of the scattering layer were dominated by the krill *M. norvegica*, with some ctenophores present in the catch (Table 1). The trawl-catches also contained fish (Table 1), but no fish larvae were found. Average daytime densities of invertebrates in the depth interval of 76–86 m were 0.30 individuals m^{-3} (S.D. = 0.15, N = 62), while nighttime densities were 0.09 individuals m^{-3} (S.D. = 0.05, N = 80). Roughly 70% of the invertebrates therefore performed diel migration.

Table 1
Total trawl catch. Maximum depth is the average depth of the bottom rope of the trawl. Trawling distance refers to the horizontal distance the trawl covered at the designated depth. Small gobies were not discerned among the krill in haul 2, but they may have been present. The presence of gelatinous plankters was noted in both hauls, but these organisms were destroyed beyond recognition or enumeration. Krill volumes were measured with 0.25 l jars

Species	Number caught	Mean length	Range
Haul 1		Maximum depth	
Trawl distance ~0.675 nmi		~77 m	
Sprat (*Sprattus sprattus*)	10	9.8 cm	7.3–11.2 cm
Crystal goby (*Crystallogobius linearis*)	>50	3.0 cm	3.4–3.7 cm
Krill (*Meganycthiphanes norvegica*)	0.25 l	[b]	[b]
Haul 2		Maximum depth	
Trawl distance ~0.8 nmi		~89 m	
Sprat (*Sprattus sprattus*)	5	9.0 cm	5.5–11.0 cm
Crystal goby (*Crystallogobius linearis*)	[a]	[b]	[b]
Mueller's pearlside (*Maurolicus muelleri*)	6	5.3 cm	2.6–6.2 cm
Whiting (*Merlangitus merlangus*)	2	[b]	33–39.5 cm
Krill (*Meganycthiphanes norvegica*)	9.75 l	3.1 cm	2–4 cm

[a] Probably present, but could not be separated from the krill.
[b] Not measured or not applicable.

The average uncorrected horizontal component of the swimming speed in average increased rapidly with range (Fig. 3A), though variations between tracks were large. The filtered (corrected) estimates also increased with depth, albeit at a much lower rate. The effect of the smoothing procedure on two simultaneous tracks is illustrated in Fig. 3B,C.

The distributions of corrected swimming speeds showed a mode around 4 cm s^{-1} (Fig. 4) for the invertebrate tracks and a mode around 12 cm s^{-1} for the fish, both distributions being positively skewed with means 9 and 21 cm s^{-1}. Most invertebrates only had small vertical velocities, and the vertical components of swimming speed were below 1.6 cm s^{-1} in more than 90% of the tracks, with an average vertical component of 0.9 cm s^{-1}(Fig. 4). The fish showed more vertical mobility, the average vertical component was 2.9 cm s^{-1}, there behaviours were confirmed by visual inspections of the echogram-printouts.

4. Discussion

The results showed the possibility of describing the in situ behaviour of individual macrozooplankton with existing technology. Based on the trawling and the results from previous investigations at the sampling site (Onsrud and Kaartvedt, 1998; Kaartvedt et al., 2002), the tracks ascribed to invertebrates were probably dominated by krill. However, some of the tracks showed very low swimming speeds coupled with systematic changes in TS. Though also these observations may have been of krill, they could alternatively be explained by ctenophores or jellyfish slowly changing their orientation while swimming through the beam (cf. Fig. 1D). The gelatinous invertebrates were not sampled quantitatively with the gear used, and their relative importance is therefore uncertain. Since nighttime trawling was not performed, the identity of the non-migrating proportion remains uncertain.

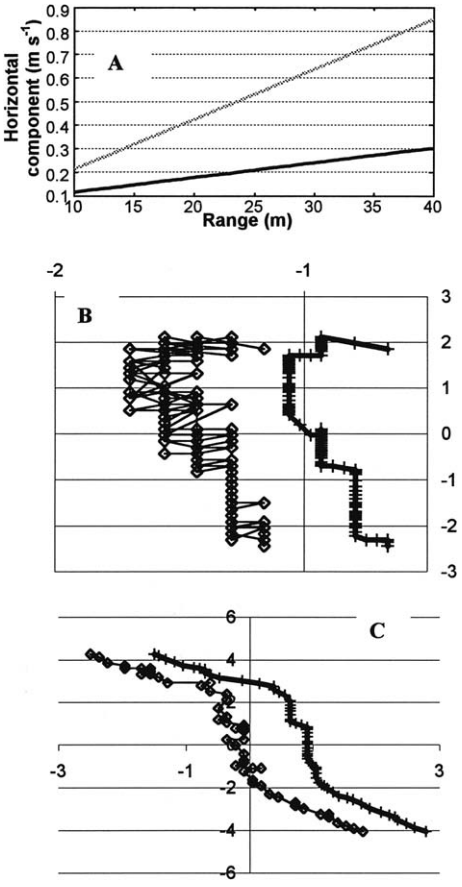

Fig. 3. (A) Regression of horizontal speed component vs. average range to track, all data (except periods of wave-action). Grey line: Unsmoothed estimates: $y = 0.0212x - 0.002$, $R^2 = 0.0588$. Black line: Smoothed estimates: $y = 0.0062x + 0.0526$, $R^2 = 0.0611$. $N = 2253$. (B) and (C) depict the effect of the smoothing on two simultaneous tracks, track (B) is an invertebrate and C is a fish. Only the horizontal projections are shown, with scales in degrees, smoothed tracks (marked by +) offset from the original positions (marked by diamonds). (B) Range 16 m, average TS –71.0 dB, track consists of 177 echoes recorded during 82.07 s, average speed without smoothing 8.4 cm s^{-1}, with smoothing 2.5 cm s^{-1}. (C) Range 19 m, average TS –45.1 dB, track consists of 63 echoes recorded during the first 28.73 s of track in (B), average speed without smoothing 13.7 cm s^{-1}, with smoothing 11.0 cm s^{-1}.

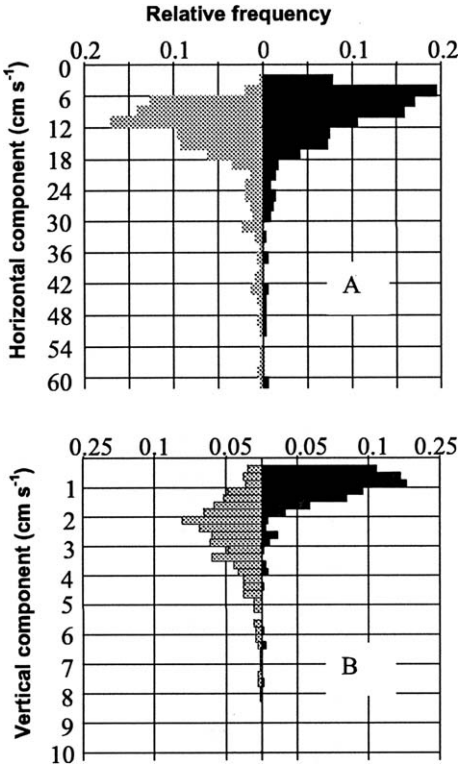

Fig. 4. (A) Distributions of horizontal component of swimming speed for the invertebrate group, left (grey) uncorrected average speeds, right (black) smoothed estimates. (B) The same distributions for the vertical component.

The uncalibrated peak TS-values obtained for invertebrates seemed relatively high compared to values measured for Antarctic krill (Foote et al., 1990), but were in accordance with previous calibrated measurements of *M. norvegica* at the same location (Røstad, 2000). Regardless of the absolute accuracy of the measurements, the bi-modal distribution of TS suggested that there was little possibility of misinterpreting fish as invertebrate.

4.1. Validity of single-echoes and tracks

Due to physical limitations of the single-echo detection-filters in the EK500, an unknown proportion of the accepted echoes stems from noise and multiple scattering (Soule et al., 1997). Since the probability of accepting such false registrations in consecutive pings is low, TT is commonly employed to sort out the echoes created by valid single sources (Ehrenberg and Torkelson, 1996). The relatively strict settings used for the TT procedure and the relatively low densities observed made us believe that false registrations of echoes were not a major problem within our tracks.

There was a restricted range of observation for the weak targets, effectively 10–18 m, probably related to the strict settings used in the single-echo detection-filters (Soule et al., 1997) and decreasing SNR. During day, this restricted range was also influenced by higher numerical densities, but even at night, when the numbers of organisms were lower, few invertebrate tracks were recorded beyond 20 m.

Ping-to-ping velocities estimated directly from the positions given by the echo sounder are biased high, and as long as there is measurement error this will always be the case (Mulligan and Chen, 2000). A lower estimate can be gained by calculating the speed between the first and the last positions in the track (Arrhenius et al., 2000), but since many of the tracks sampled in situ are bound to have some curvature, this method tends to underestimate the real speeds. Mulligan and Chen (2000) suggested that a better estimate could be obtained by fitting a smoothed trajectory to the data, and suggested that further post-processing of the positional data was needed when describing the swimming behaviour of organisms using acoustic data.

The smoothing procedure used made the estimated swimming speeds less dependent on range (Fig. 3A). A certain increase in average estimated speeds with depth was expected, due to the increasing proportion of fish tracks with range, as well as bias against fast swimming fish closer to the transducer, due to the narrowing beam. However, it may have introduced artefacts in the tracks by filtering out small scale and rapid within-track behaviour, as there is a possibility that some of the perceived errors in the positions are in fact caused by actual behaviour, though we believe that this generally was not the case (Fig. 3B,C).

The measured swimming speeds ascribed to krill seem to be reasonable. Assuming a length corresponding to the mode of the observed length distribution (3.5 cm), the mean and modal swimming speed were ~2 and ~1.1 body-lengths (BL) s^{-1}, respectively. All observed swimming speeds for invertebrates were within the bounds of the swimming capabilities of krill (up to 11 BL s^{-1}; Kils, 1982). Jaffe et al. (1999) recorded a swimming speed of 0.5–1 BL s^{-1} for the krill *E. pacifica* in Saanich Inlet.

Acknowledgements

We thank the crew aboard RV “Trygve Braarud” and Anders Røstad for help during the sampling, and Rita Amundsen and Sidsel Øverås for help with the analysis. Constructive criticism from a reviewer improved the manuscript.

References

Arrhenius, F., Benneheij, B.J.A.M., Rudstam, L.G., Boisclair, D., 2000. Can stationary bottom split-beam hydroacoustics be used to measure fish swimming speed in situ? Fish. Res. 45, 31–41.

Bagøien, E., Kaartvedt, S., Øverås, S., 2000. Seasonal vertical migration of *Calanus* spp. in Oslofjorden. Sarsia 85, 299–311.

Brede, R., Kristensen, F.H., Solli, H., Ona, E., 1990. Target tracking with a split-beam echo sounder. Rapp. P.-v. Reun. Cons. Int. Explor. Mer. 189, 254–263.

Ehrenberg, J.E., Torkelson, T.C., 1996. Application of dual-beam and split-beam target tracking in fisheries acoustics. ICES J. Mar. Sci. 53, 329–334.

Fleischman, S.J., Burwen, D.L., 2000. Correcting for position-related bias in estimates of the acoustic backscattering cross-section. Aquat. Living Resour. 13, 283–290.

Foote, K.G., Everson, I., Watkins, J.L., Bone, D.G., 1990. Target strengths of Antarctic krill (*Euphausia superba*) at 38 and 120 kHz. J. Acoust. Soc. Am. 87, 16–24.

Gerritsen, J., Strickler, J.R., 1977. Encounter probabilities and community structure in zooplankton: a mathematical model. J. Fish. Res. Board Can. 34, 73–82.

Huse, I., Ona, E., 1996. Tilt angle distribution and swimming speed of overwintering Norwegian spring spawning herring. ICES J. Mar. Sci. 53, 863–873.

Jaffe, J.S., Ohman, M.D., De Robertis, A., 1999. Sonar estimates of daytime activity levels of *Euphausia pacifica* in Saanich Inlet. Can. J. Fish. Aquat. Sci. 56, 2000–2010.

Kaartvedt, S., Larsen, T., Hjelmseth, K., Onsrud, M.S.R., 2002. Is the omnivorous krill *Meganyctiphanes norvegica* primarily a selectively feeding carnivore? Mar. Ecol. Prog. Ser. 228, 193–204.

Kils, U., 1982. The swimming behavior, swimming performance and energy balance of Antarctic krill, *Euphausia superba*. BIOMASS Sci. Ser. 3, 1–122.

MacLennan, D.N., Simmonds, E.J., 1992. Fisheries Acoustics. Chapman and Hall, London.

Mulligan, T.J., Chen, D.G., 2000. Comment on 'Can stationary bottom split-beam hydroacoustics be used to measure fish swimming speed in situ? Fish. Res. 49, 93–96.

Ona, E., Hansen, D., 1992. Software for target tracking of individual fish with split-beam echo sounders. USER MANUAL. Institute of Marine Research, Bergen.

Onsrud, M.S.R., Kaartvedt, S., 1998. Diel vertical migration of the krill *Meganyctiphanes norvegica* in relation to physical environment, food and predators. Mar. Ecol. Prog. Ser. 171, 209–219.

Røstad, A., 2000. Et akustisk studie av fordeling og atferd til fisk og krill i indre Oslofjord. M.Sc. Thesis, University of Oslo.

Sameoto, D., Cochrane, N., Herman, A., 1993. Convergence of acoustic, optical, and net-catch estimates of euphausiid abundance: use of artificial light to reduce net avoidance. Can. J. Fish. Aquat. Sci. 50, 334–346.

Soule, M., Barange, M., Solli, H., Hampton, I., 1997. Performance of a new phase algorithm for discriminating between single and overlapping echoes in a split-beam echosounder. ICES J. Mar. Sci. 54, 934–938.

Torgersen, T., Kaartvedt, S., 2001. In situ swimming behaviour of individual mesopelagic fish studied by split-beam echo target tracking. ICES J. Mar. Sci. 58, 346–354.

Torres, J.J., Childress, J.J., 1983. Relationship of oxygen consumption to swimming speed in *Euphausia pacifica*. Effects of temperature and pressure. Mar. Biol. 1 (74), 79–86.

Available online at www.sciencedirect.com
SCIENCE DIRECT®
Aquatic Living Resources 16 (2003) 299–306
Aquatic Living Resources
www.elsevier.com/locate/aquliv

Spawning of herring: day or night, today or tomorrow?

Georg Skaret [a,b], Leif Nøttestad [b,*], Anders Fernö [a,b], Arne Johannessen [a], Bjørn Erik Axelsen [b]

[a] *Department of Fisheries and Marine Biology, Bergen High-Technology Centre, University of Bergen, 5020 Bergen, Norway*
[b] *Institute of Marine Research, P.O. Box 1870 Nordnes, 5817 Bergen, Norway*

Accepted 20 December 2002

Abstract

Diel variations in schooling patterns and spatial dynamics during spawning were studied in Norwegian spring-spawning herring (*Clupea harengus*) off south-western Norway by acoustic surveying, diel cycle experiments and school tracking by sonar, and bottom gillnet sampling. Herring formed horizontally extensive, loosely packed demersal layers shortly after darkness. At night, the fish disappeared in the acoustic dead zone, but lifted off the bottom early in the following mornings. At daytime the herring reorganised into dense pelagic schools. The evening descent to the spawning habitat was considered as part of a precautionary strategy towards visual predators, as the bottom is a high-risk zone for archetypal pelagic fish like herring. Large numbers of gadoids, which are potential herring predators, were present in the area. Herring not ready to spawn dominated the bottom samples in 4 out of 5 days, suggesting that pre-spawning herring followed the descent of ripe herring. The herring spawning layers shifted in a south-easterly direction from day to day in diel spawning waves.

Keywords: Acoustics; Schooling dynamics; Timing of spawning; Herring

1. Introduction

Herring (*Clupea harengus* L.) have a pelagic lifestyle, but spawn demersally (Runnstrøm, 1941; Stacey and Hourston, 1982; Aneer et al., 1983). They spawn over a relatively short period annually (Blaxter and Hunter, 1982), and up to 10–15 times during a lifespan (Blaxter and Hunter, 1982; Slotte, 1999). The population of Norwegian spring-spawning herring spawns along the coast from Lofoten to Lista (Runnstrøm, 1941; Dragesund et al., 1997) during early spring.

Herring is a schooling species (Blaxter and Hunter, 1982; Pitcher, 1983; Fernö et al., 1998), that forms highly synchronised and polarised groups (Breder, 1976; Pitcher, 1983). Predator protection is the primary function of schooling (Pitcher and Parrish, 1993), and there is evidence that herring trade off predation risk for reproduction, which ultimately affects the size, shape, density and vertical distribution of the schools (Misund, 1993; Nøttestad et al., 1996; Axelsen et al., 2000). Before spawning, herring become risk-averse to maximise the likelihood of completing reproduction. Schools immigrating to the spawning location are large, densely packed, and swim fast and deep (Nøttestad et al., 1996), hence increasing the efficiency of synchronised escape manoeuvres and decreasing the risk of detection by predators (Pitcher and Parrish, 1993). After spawning, feeding becomes more important, and herring form smaller, more loosely packed schools near the surface (Stacey and Hourston, 1982; Nøttestad et al., 1996).

For a successful reproduction, eggs and milt must be deposited on a suitable bottom substrate (Runnstrøm, 1941; Rajasilta et al., 1997). The spawning is not fully synchronised and herring remain at the spawning site for 3–5 days (Nøttestad et al., 1996; Axelsen et al., 2000). The maturity states of individuals differ amongst and within schools at the same site (Nøttestad et al., 1996; Axelsen et al., 2000), leading to a highly dynamic, and poorly understood schooling behaviour (Nøttestad et al., 1996). Generally, schools of Norwegian spring-spawning herring on the spawning grounds are observed as horizontally elongated demersal layers within a few meters off bottom (Runnstrøm, 1941; Johannessen et al., 1995). However, pelagic schools with high packing densities above demersal layers were observed by Nøttestad et al. (1996), and Axelsen et al. (2000) observed a single spawning school split into a pelagic and a demersal component staying in continuous contact. Herring staying

* Corresponding author.
E-mail address: leif.nottestad@imr.no (L. Nøttestad).

doi:10.1016/S0990-7440(03)00006-8

pelagically presumably reduce predation risk, as staying near the bottom is associated with high risk due to the reduced number of potential escape directions (Axelsen et al., 2000). Large gadoids feed on herring and herring eggs during the spawning season (Toresen, 1991; Høines et al., 1995; Høines and Bergstad, 1999). Gadoids are visual predators and the predation risk for spawning herring should, therefore, be higher in daylight than in darkness.

Herring is one of the worlds most studied species (Blaxter and Hunter, 1982). Despite this, only a few studies have investigated schooling behaviour right before and during spawning (Nøttestad et al., 1996; Mackinson, 1999; Axelsen et al., 2000), and these studies did not explore possible diel variations. Our main goal was, therefore, to investigate diel variation in school patterns and spatial dynamics during spawning in relation to the maturation state of the fish and external factors like predation.

2. Materials and methods

2.1. Study area

The study was carried out off Karmøy (59°15'N, 5°05'E), on the west coast of Norway, from 29 March to 3 April 2000. During the study period, the time of sunrise changed from 05:12 to 05:00 h and the time of sunset from 18:13 to 18:22 h. Two research vessels; the "Håkon Mosby" and the "Hans Brattstrøm" were utilised in the study. A known spawning location extending about 2 nmi^2 with high densities of herring was selected in order to map the schooling dynamics during the spawning process. The bottom depth ranged from 30 to 40 m. The weather was generally cloudy with light north-westerly winds not exceeding 10 m s^{-1} during the study period, although the wind speed increased towards the end of the study.

2.2. Experimental design

Two exploratory mini-surveys were conducted in order to map the distribution of the fish in the area. Based on the fish distributions, two survey grids were fixed for the school dynamic study, one designed to cover the horizontal extent of the spawning layer (zigzag) and one to estimate the fish density in the adjacent spawning area (parallel) (Fig. 1a). The two surveys were repeated three and four times, respectively. In order to map the vertical movements of fish over time, two 24 h diel cycle experiments were conducted on 2 and 3 April. During these experiment the ship was positioned immediately above the demersal spawning layers, continuously recording the vertical distribution and fish density using the echosounder. The Dynamic Positioning System (DPS) of "Håkon Mosby" was utilised in order to keep the vessel at a fixed location (within an area of 25 m^2) during the experiments. Unfortunately, relatively rough weather conditions caused some formation of air bubbles in the surface layer, effectively reducing the usable materials from the diel cycle experiments to 14 and 8 h for diel cycle 1 and 2, respectively.

2.3. Acoustic recordings

Both research vessels were equipped with Simrad EK 500 echo sounders running 38 kHz transducers, while "Hans Brattstrøm" operated an additional Simrad EQ 55 (49 kHz) echo sounder used for mapping of the spawning layer on the bottom. Acoustic recordings were scrutinized according to catch composition and signal characteristics. The acoustic diel cycle data from the EK 500 were post-processed using Bergen Echo Integrator system (BEI) (Knudsen, 1990), averaging the nautical area scattering coefficient s_A (m^2 nmi^{-2}) (MacLennan et al., 2002) over 10 min intervals. Sonardata Echoview v.2.10 © software was used to analyse the school dynamic parameters, including depth (m) and vertical extent (m), volume density S_V (dB re 1 m^2) and s_A (m^2 nmi^{-2}). A total of 246 herring aggregations (schools, layers) were analysed. The range resolution was about 10 cm (500 bins on 50 m operational range). The fish densities of the spawning layers recorded using the EK 500 unit were estimated according to (Foote et al., 1997):

$$\mathrm{TS} = 20 \log_{10}(L) - 71.9$$

where L is the mean total fish length in cm obtained from the gill net samples. The total biomass of the spawners was estimated using the horizontal area of the demersal layer. The packing densities of the schools ρ_V were calculated according to:

$$\rho_v = \frac{s_A}{1852^2 \langle \sigma_{sp} \rangle \Delta z}$$

where s_A is the nautical area scattering coefficient of the school, $\langle \sigma_{sp} \rangle$ is the mean spherical scattering cross section (m^2) (MacLennan et al., 2002), and Δz is the depth over which the acoustic data were integrated, i.e. the vertical extension of the school EV_{school} (m).

The diel cycle observations were divided in eight 3-h time periods starting at 24 UTC (local time = UTC + 2 h). The vertical school extension EV_{school} (m), the distance from the school midpoint to the bottom BD_{school} (m) and the linear mean volume backscattering (mm^2), corresponding to $V \cdot s_V$ in the terminology adopted by MacLennan et al. (2002), were averaged for all time periods.

A Kaijo Denkij KCH 1827 multi-beam scanning sonar on the "Hans Brattstrøm" was used to check for pelagic schools migrating in and out of the spawning area (Nøttestad et al., 1996). The horizontal area, and swimming speed and direction of recorded schools were estimated (Axelsen et al., 2000). Subsequent to the tracking, the schools were recorded using the EK 500 unit in order to estimate the vertical extension, depth and acoustic density of the schools.

2.4. School categories

The herring aggregations were categorised according to their position in the water column: *Pelagic schools*: >90% of the herring located above the bottom layer (>10 m off the bottom); *Demersal layers*: >90% located within the bottom

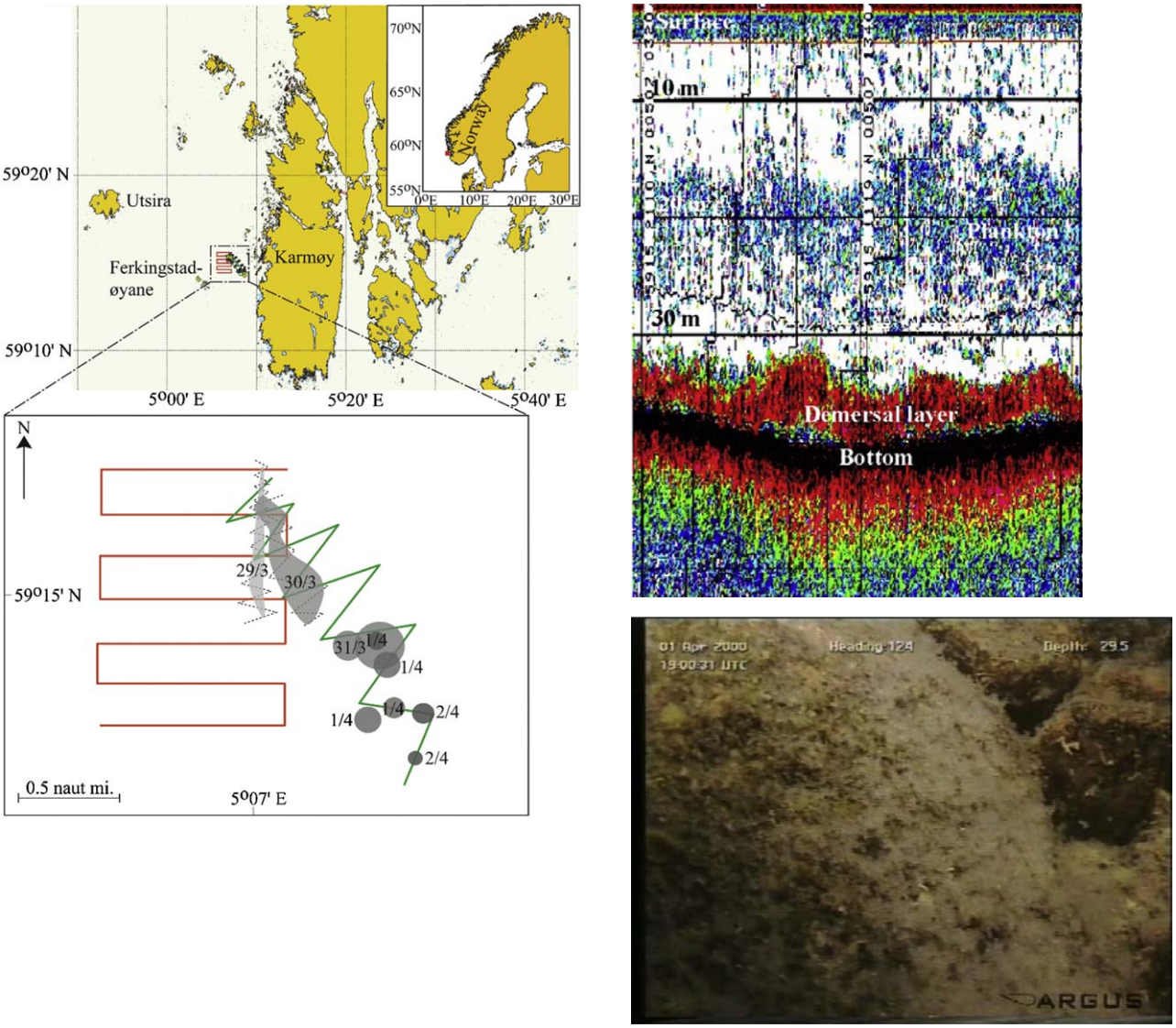

Fig. 1. (a) Distribution of demersal layers based on acoustic recordings with different shadings for each day. The red, parallel track indicates the spawning area survey (repeated four times), the green zig-zag track the distribution survey for demersal layers repeated three times, and the black adaptive localisation and mapping surveys. (b) S_V echogram at 38 kHz of a demersal layer of herring. (c) Eggs deposited on a boulder at the studied spawning site.

layer; and *Transition schools*: 10–90% located within the bottom layer and 10–90% above the bottom layer.

2.5. Biological sampling

Herring samples were obtained daily from 30 March to 3 April using 25 m long by 4 m high gillnets (mesh size: 37 mm when @ 5 kg) set on the seabed overnight. This mesh size is selective towards adult herring above 20 cm total length, but is inefficient towards juveniles. The influence of juvenile fish at the spawning grounds of Norwegian spring-spawning herring is, however, negligible (Johannessen et al., 1995). Total fish length, total wet weight and gonad maturity index GI (1–8) (Anonymous, 1962) were determined for all sampled fish. Two predator samples were obtained using 25 m long by 4 m high gill nets (90 mm meshes), and one sample using a Super Campelen demersal shrimp trawl.

3. Results

Fig. 1b shows an S_V echogram at 38 kHz of a demersal layer of spawning herring. The spawning substrate was closely examined using the Remotely Operated Vehicle (ROV) “Aglantha” and consisted mostly of boulders, rocks and gravel, with herring eggs deposited in thick layers on the bottom (Fig. 1c). The seawater temperature and salinity, as recorded during daily CTD-profiling, ranged from 5 to 6 °C and from 33 to 34‰, respectively.

3.1. Horizontal dynamics

The demersal layers of spawning herring moved in a south-easterly direction from day to day, with a total horizontal displacement of about 0.8 nmi during the study period (Fig. 1a), with overlapping distributions between the first 2 days and between the third and fourth day, otherwise not.

Table 1
Multi-beam sonar tracking. Linear fish density corresponds to SV (dB re 1 m^{-1}) in the linear domain (* the last school was not successfully integrated)

Time	Track duration (min)	Swimming speed (m s^{-1})	Direction	Linear fish density (mm^2)	Biomass (tons)	EV_{school} (m)	A_{school} (m^2)	BD_{school} (m)
12:34	27	0.11	W	430 ± 160	16	19.5 ± 3.7	841 ± 40	14.3 ± 3.4
17:27	96	0.15	SE	600 ± 740	15	14.2 ± 3.0	491 ± 95	9.2 ± 3.4
14:12	78	*	W	*	*	20	1708 ± 142	13

The biomass of the two spawning layers observed on 29 and 30 March was estimated to be 30 and 42 tons, respectively. The herring were too patchy distributed the remaining days to obtain reliable estimates. Altogether three schools were identified and tracked using the multi-beam sonar, and two of these successfully integrated using the EK 500 system (Table 1).

3.2. Vertical dynamics

Demersal spawning layers were usually recorded in the evening. The proportion of demersal layers relative to other school categories, was highest between 18:00 and 24:00 h (>80%). Little herring was recorded between 24:00 and 03:00 h, and only in one of the diel cycle experiments. Pelagic schools and transition schools dominated at daytime (>70%) and the demersal layers recorded were small.

Schools were distributed shallower during the day than at night (General Linear Model (GLM ANOVA, $P < 0.001$)) (Fig. 2a) and were closer to the bottom between 21:00 and 24:00 h than in all time intervals between 06:00 and 18:00 h (Tukey's range test (HSD), $\alpha = 0.05$). Also the vertical school extension changed with time (GLM ANOVA, $P < 0.001$) (Fig. 2b): from 18:00 to 24:00 h the vertical school extension was lower than in all daytime intervals from 09:00 to 18:00 h (HSD, $\alpha = 0.05$).

Little herring was recorded at nighttime during the diel cycle experiments, which is reflected in the low acoustic densities for herring ($s_A < 1000\ m^2\ nmi^{-2}$) between 21:00 and 04:00 h (Fig. 3a). The densities increased rapidly around 04:00 in both experiments, as the herring layers lifted off the bottom. Between 21:00 and 04:00 h most of the fish (>80%) were located in the bottom channel, while 40–100% of the herring was pelagic (>10 m over the bottom) between 04:00 and 12:00 h (Fig. 3b).

3.3. Packing densities

The school packing density changed over time (GLM ANOVA, $P = 0.001$) (Fig. 4a), and was higher between 15:00 and 18:00 h than in all other periods (HSD, $\alpha = 0.05$). The packing density also differed between school categories (GLM ANOVA, $P = 0.002$) (Fig. 4b). Transition schools (3.0 $N_{herr}\ m^{-3}$) and pelagic schools (1.9 $N_{herr}\ m^{-3}$) were on average more tightly packed than demersal layers (<0.8 $N_{herr}\ m^{-3}$), but only the difference between transition schools and demersal layers was significant in our test (HSD, $\alpha = 0.05$).

3.4. Fish size and maturity state

A total of 423 individuals were sampled. The total fish lengths ranged from 16 to 38 cm (mean 33.2 ± 1.9 cm [S.D.]), and total wet weights from 27 to 500 g (301.3 ± 54.7 g), varying little between samples. The catches were dominated by 8-years-olds (67.5%). The majority of the herring (92.1%) had empty stomachs, and only one individual was caught with a full stomach. The stomach contents consisted of calanoid copepods and copepodites, or of herring eggs (Skaret et al., 2002). An increase in the prevalence of running and spent individuals and a decrease of pre-spawning individuals

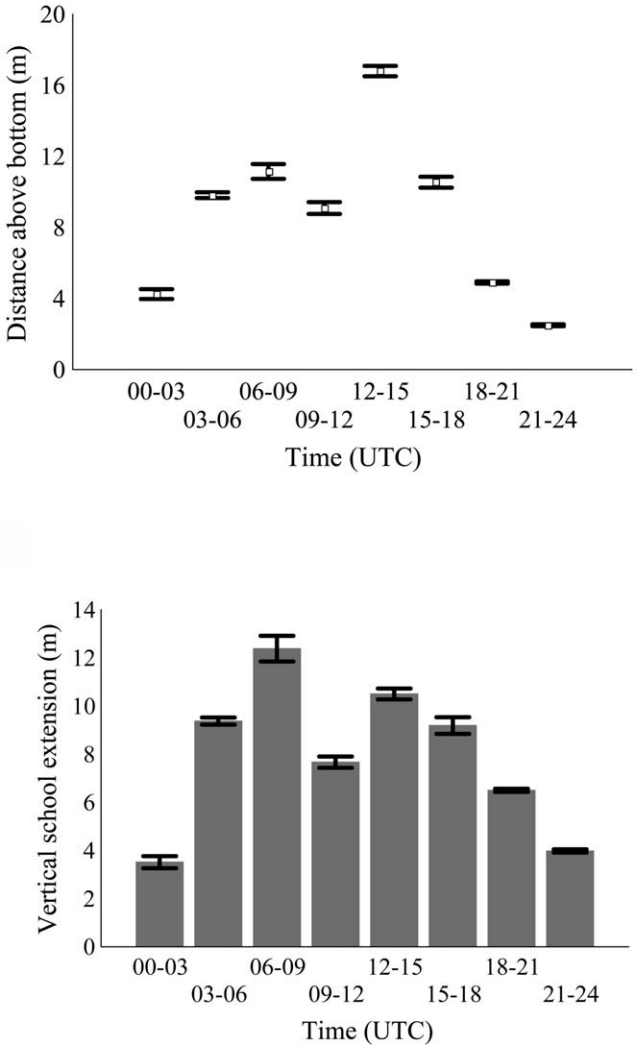

Fig. 2. (a) Mean school distance above bottom (BD_{school}) ±2 standard error (S.E.) (m), measured from the vertical midpoint of the school. (b) Mean vertical school extension (EV_{school}) ±2 S.E. (m).

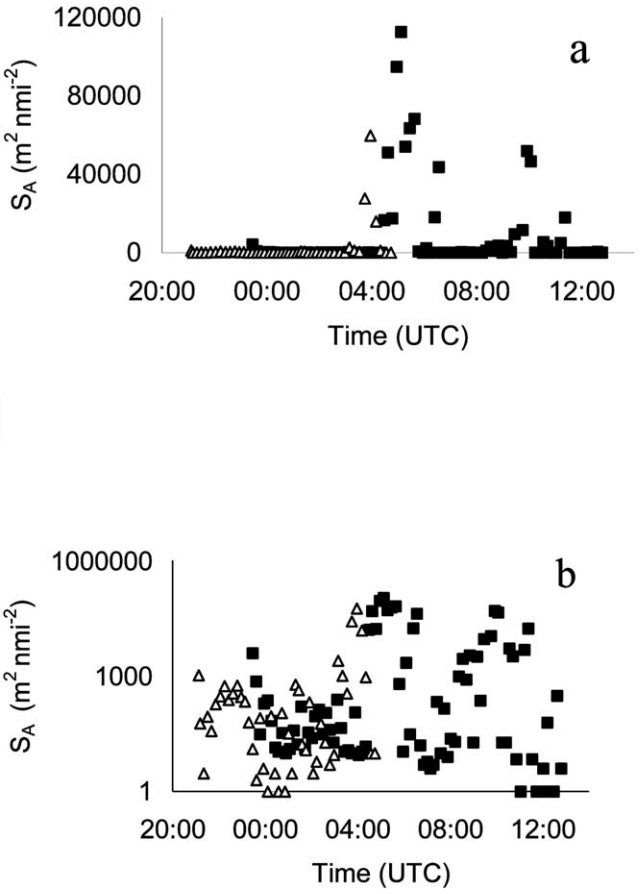

Fig. 3. (a) Mean area backscattering coefficients (s_A, m^2 nmi^{-2}) of herring integrated over 10 min intervals during the diel cycle stations 1 (■) and 2 (Δ) on linear (a) and $\log_{10}$ (b) scales. Sunrise was at ~05.00.

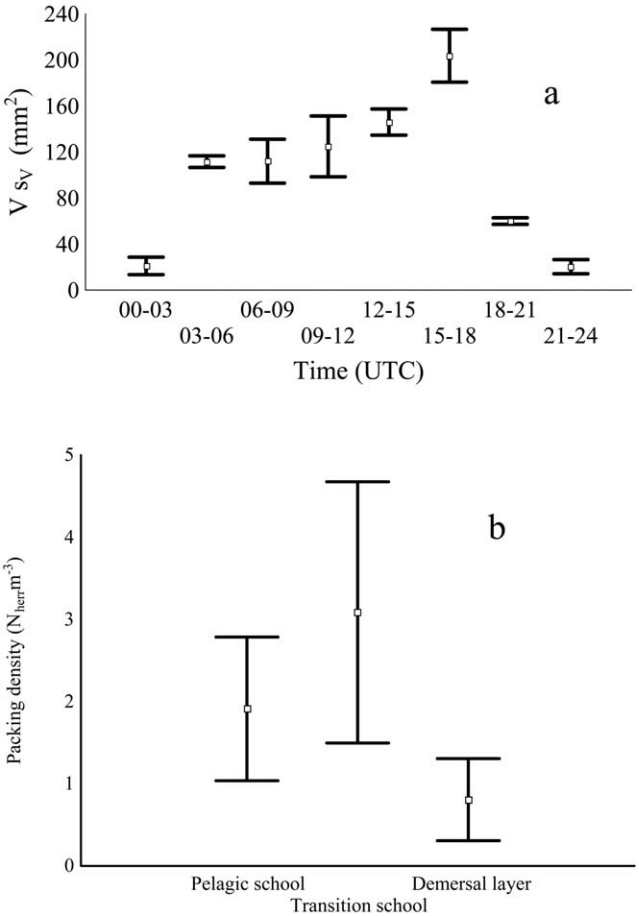

Fig. 4. (a) Linear fish density (mm^2), or S_V (dB re 1 m^{-1}) in the linear domain (MacLennan et al., 2002) of herring ±2 S.E. during the diel cycle. (b) Mean packing density (N_{herr} m^{-3}) of herring ±2 S.E. for the different school categories.

were observed from the first to the final observation day (Fig. 5). The samples from the middle of the period (1 and 2 April) contained more pre-spawning fish than the first two samples (30 and 31 March), but the sample sizes in the former two were small and may not be representative for the population.

3.5. Predators

Potential fish predators caught in gillnet and bottom trawl samples are shown in Table 2. Both of the saithe from the gillnet sample had stomachs that were filled with herring eggs. Only one pollock from the bottom trawl sample had been feeding on herring eggs, but a large proportion (73–78%) of the cod, haddock and saithe had consumed herring eggs. No predators with remnants of herring were caught.

4. Discussion

4.1. Distribution and individual state of the herring

Demersal layers of herring were located at shallow depths (30–40 m) on gravel and stone bottom in bank water with salinities between 33 and 34 and temperatures of 5–6 °C (Runnstrøm, 1941). There were several indications that most of the herring schools remained at the study site throughout the study period. No immigrating schools, characterized by large size, high packing density and fast and deep swimming

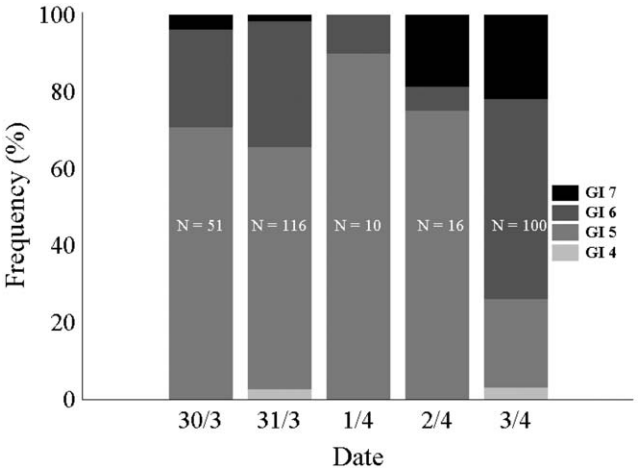

Fig. 5. Distribution of gonad maturity indexes (GI) from day to day in the gillnet samples (*N*: number of herring sampled; GI 4,5: pre-spawning; GI 6: running; GI 7: spent) (Anonymous, 1962).

Table 2
Numbers and size ranges of potential fish predators caught in the trawl and gillnet samples

Predator species	Sample gear	Size-range (cm)	*n*
Pollack *Pollachius pollachius*	Trawl	33–62	98
Cod *Gadus morhua*	Trawl	29–53	42
Haddock *Melanogrammus aeglefinus*	Trawl	17–49	23
Saithe *Pollachius virens*	Trawl	37–59	4
	Gillnet	33–35	2

(Nøttestad et al., 1996) were recorded, and only one school emigrating from the spawning ground was observed. This is consistent with the similar estimated biomasses of the demersal layers during the first two study days, the similar length and age distributions of the samples, and the increase in the proportion of running and spent individuals in the demersal layers from the first (<30%) to the last (>70%) day of the study, suggesting progressive spawning (Axelsen et al., 2000). Herring may have different motivations to remain at the spawning ground. Spent herring may stay at the spawning ground to feed on zooplankton (Nøttestad et al., 1996; Axelsen et al., 2000) and herring eggs (Skaret et al., 2002), or await for other herring to complete spawning and reduce predation risk by leaving the area in larger groups (Pitcher and Parrish, 1993; Axelsen et al., 2000). According to the maturation index, most sampled herring were, however, prespawners, assumingly remaining at the spawning ground to complete spawning.

4.2. Diel schooling pattern

The observed schooling behaviour throughout the 24-h cycle from the acoustic records is schematically illustrated in Fig. 6. After dark (18:00–24:00 h) herring concentrated close to the bottom in horizontally extended demersal layers, with few herring observed outside layers. At nighttime (24:00–03:00 h), only a few small patches of herring were observed close to the bottom. Fish may have avoided the vessel, but no avoidance manoeuvres were observed, and herring have high reaction thresholds during spawning

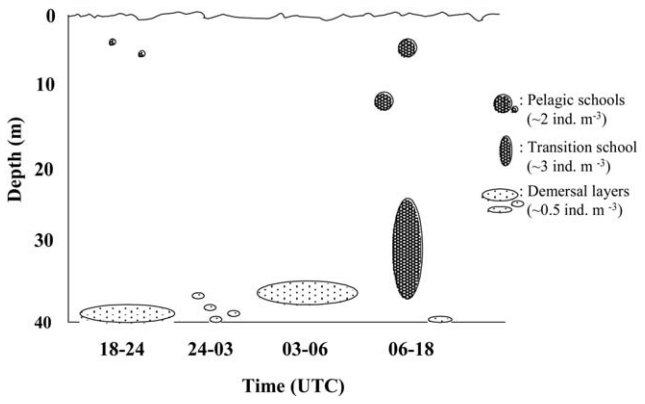

Fig. 6. Generalised schematic illustration of the observed diel pattern in vertical distribution, school shape and packing density of the spawning herring.

(Mohr, 1971; Misund, 1990). Fish schools may disaggregate in darkness (Shaw, 1961; Welsby et al., 1964), but very low light intensities are required for herring to school and spawn (Craig and Priestley, 1960; Kjørsvik et al., 1990; Johannessen et al., 1995). The low recordings at night are thus assumed to be herring staying close to the bottom, where fish echoes and bottom echoes cannot be distinguished (Ona and Mitson, 1996). Spawning herring staying within the acoustic dead zone have been reported before (Johannessen et al., 1995). Our diel cycle observations also showed that nearly all herring recorded at night were located within 10 m from the bottom, and that demersal layers seemed to lift from the bottom around dawn.

During daytime (06:00–18:00 h) pelagic schools, transition schools and small demersal layers were observed indicating a reorganisation of schools. Some transition schools may represent a transition between demersal layers and pelagic schools, whereas others are presumably searching schools. The two “transition” schools being tracked swam deep and had low net swimming speed, characteristic for searching schools (Nøttestad et al., 1996). Slow-swimming transition schools may have visible contact with the bottom to search for suitable spawning substrate, while maintaining group integrity in the pelagic zone for predator avoidance (Axelsen et al., 2000, 2001).

4.3. Timing of spawning

Blaxter and Hunter (1982) suggested that herring depend on light to spawn, but spawning has been reported to take place in darkness (Kjørsvik et al., 1990; Johannessen et al., 1995). Herring may thus adjust spawning time in order to optimise survival and reproduction. As herring adopt low-risk behavioural strategies (Vabø and Nøttestad, 1997; Fernö et al., 1998; Axelsen et al., 2000, 2001), the formation of demersal layers in the evening could be a precautionary behaviour towards predators. The predation pressure at Karmøy is high during the spawning season (Toresen, 1991; Høines et al., 1995, Høines and Bergstad, 1999), and even though none of the sampled gadoids in this study had herring in their stomachs, their size makes them potential predators (Høines et al., 1995). An archetypal pelagic fish like herring is vulnerable when staying on the bottom due to the reduced number of escape directions (Pitcher and Parrish, 1993; Axelsen et al., 2000, 2001). Staying on the bottom should, therefore, be less risky in darkness, since visual predators are less active at low light levels (Løkkeborg and Fernö, 1999).

Earlier studies have shown that the timing of spawning may differ from the one observed here (Johannessen et al., 1995; Nøttestad et al., 1996; Slotte, 1998). This is to be expected taking into account the dynamic trade-off between survival and reproduction changing with prevailing conditions (Magurran, 1993). The present study was conducted at the end of the spawning season (Johannessen et al., 1995; Skaret et al., 2001), with low herring densities compared to the peak of spawning (Johannessen et al., 1995; Slotte and

Dommasnes, 2000). Predation risk decreases with increasing school size due to the dilution effect (Magurran et al., 1985; Milinski, 1993; Axelsen et al., 2001), and the reaction to predators should hence be stronger at the end of the spawning season than at the peak of spawning. Intra-specific competition for a successful deposition of spawn may also influence spawning behaviour (Rajasilta et al., 1997). High competition at the spawning peak may compel herring to spawn during the day even though predation risk is high.

4.4. Spatial dynamics and spawning time of individual herring

The school packing density was high during the day, and mean school packing densities of ~3.0 N_{herr} m^{-3} for transition schools is high compared to packing densities for herring schools at different times and areas along the Norwegian coast (1.3-1.9 N_{herr} m^{-3}) (Misund, 1993). High packing densities of pre-spawning herring at the spawning location have been reported before (Misund, 1993; Nøttestad et al., 1996; Tremorrow and Claytor, 1998; Axelsen et al., 2000), and herring in the pre-spawning phase may reduce the distance to school neighbours as a precautionary behaviour towards predators. Aggregation prior to spawning should also facilitate the exchange of olfactory stimuli. The low packing density (0.8 N_{herr} m^{-3}) of demersal layers could be connected to the low predation risk at night.

Directional spawning has earlier been reported in North Sea herring (Stratoudakis et al., 1998) and the movement direction has been related to current patterns (Lacoste et al., 2001). The occurrence of directional spawning could be connected to the thickness of the egg mats as thick layers may induce high egg mortalities (Runnstrøm, 1941; Taylor, 1971). The shift of spawning site from day to day demonstrates that the search for suitable spawning substrate continues throughout the spawning period.

Interestingly, pre-spawning herring dominated over ripe herring at the bottom in four of five gillnet samples, indicating that herring are present in the demersal layers irrespective of their maturation state, and that they repeat the diel schooling pattern at least once before spawning. It might be argued that pre-spawning fish could have spawned during the night if they had not been caught. However, our biological data indicate that the same herring stayed at the spawning ground for several days and no herring with partly emptied gonads were found, suggesting that spawning took place in one batch.

Why do herring then stay in a high-risk zone if they are not ready to spawn? The determined behaviour of ripe individuals heading for the bottom may influence pre-spawning individuals to follow in connection with the collective behaviour of schools (Fernö et al., 1998; Axelsen et al., 2000; Huse et al., 2002). The ripening process of pre-spawning herring could also be accelerated by staying in close contact with ripening individuals near the bottom in a low-risk period during the night. The release of olfactory stimuli triggers the deposition of milt in males (Ware and Tanasichuk, 1989), which is needed to induce spawning in both sexes (Stacey and Hourston, 1982; Sherwood et al., 1991).

In conclusion, the horizontal shift of spawning site from day to day demonstrates that the search for suitable spawning substrate continues throughout the spawning period. The pronounced vertical migration is presumably a functional response to predation combined with the fact that herring have to spawn at the bottom. The absence of herring outside the demersal layers at night and the domination of pre-spawning individuals on the bottom indicate that herring performed spawning waves moving in a south-easterly direction from day to day.

Acknowledgements

We are grateful to the crew on board RV “Hans Brattstøm” and RV “Håkon Mosby”, and to Anne-Britt Skaar Tysseland for help in editing the figures.

References

Aneer, G., Florell, G., Kautsky, U., Nellbring, S., Sjöstedt, L., 1983. In situ observations of Baltic herring (*Clupea harengus membras*) spawning behaviour in the Askö-Landsort area, northern Baltic proper. Mar. Biol. 74, 105–110.

Anonymous, 1962. Recommendations adopted by the Herring Committee. Rapp. P.-V. Réun. Cons. Int. Explor. Mer. 1, 71–73 (Appendix 1).

Axelsen, B.E., Nøttestad, L., Fernö, A., Johannessen, A., Misund, O.A., 2000. “Await” in the pelagic: a dynamic trade-off between reproduction and survival within a herring school splitting vertically during spawning. Mar. Ecol. Prog. Ser. 205, 259–269.

Axelsen, B.E., Anker-Nilssen, T., Fossum, P., Kvamme, C., Nøttestad, L., 2001. Pretty patterns but a simple strategy: predator-prey interactions between juvenile herring and Atlantic puffins observed with multibeam sonar. Can. J. Zool. 79, 1586–1596.

Blaxter, J.H.S., Hunter, J.R., 1982. The biology of the clupeoid fishes. Adv. Mar. Biol. 20, 1–224.

Breder Jr., C.M., 1976. Fish schools as operational structures. Fish. Bull. US 74, 471–502.

Craig, R.E., Priestley, R., 1960. Photographic studies of fish populations. Nature, London 188, 333–334.

Dragesund, O., Johannessen, A., Ulltang, Ø, 1997. Variation in migration and abundance of Norwegian spring spawning herring (*Clupea harengus* L.). Sarsia 82, 97–106.

Fernö, A., Pitcher, T.J., Melle, V., Nøttestad, L., Mackinson, S., Hollingworth, C., Misund, O.A., 1998. The challenge of the herring: making optimal collective decisions. Sarsia 83, 149–167.

Foote, K.G., Ostrowski, M., Røttingen, I., Slotte, A., 1997. Abundance estimation of Norwegian spring spawning herring wintering in the Vestfjord system December 1996 ICES CM/FF:13.

Høines, Å.S., Bergstad, O.A., 1999. Resource sharing among cod, herring, saithe and pollack on a herring spawning ground. J. Fish Biol. 55, 1233–1257.

Høines, Å.S., Bergstad, O.A., Albert, O.T., 1995. The food web of a coastal spawning ground of the herring (*Clupea harengus*). Proceedings of the Mare Nor Symposium on the Ecology of Fjords and Coastal Waters. In: Skjoldal, H.R., Hopkins, C., Erikstad, K.E., Leinaas, H.P (Eds.), Ecology of Fjords and Coastal Waters. Elsevier Science, Amsterdam, pp. 17–22.

Huse, G., Railsback, S., Fernö, A., 2002. Modelling changes in migration pattern of herring collective behaviour and numerical domination. J. Fish Biol. 60, 571–582.

Johannessen, A., Slotte, A., Bergstad, O.A., Dragesund, O., Røttingen, I., 1995. Reappearance of Norwegian spring spawning herring (*Clupea harengus* L.) at spawning grounds off south-western Norway. Proceedings of the Mare Nor Symposium on the Ecology of Fjords and Coastal Waters. In: Skjoldal, H.R., Hopkins, C., Erikstad, K.E., Leinaas, H.P (Eds.), Ecology of Fjords and Coastal Waters. Elsevier Science, Amsterdam, pp. 347–363.

Kjørsvik, E., Lurås, I.J., Hopkins, C.E.H., Nilssen, E.M., 1990. On the intertidal spawning of Balsfjord herring (*Clupea harengus* L.). ICES CM, H30.

Knudsen, H.P., 1990. The Bergen echo integrator: an introduction. J. Cons. Int. Explor. Mer 47, 167–174.

Lacoste, K.N., Munro, J., Castonguay, M., Saucier, F.J., Gagne, J.A., 2001. The influence of tidal streams on the pre-spawning movements of Atlantic herring, *Clupea harengus* L., in the St Lawrence estuary. ICES J. Mar. Sci. 58, 1286–1298.

Løkkeborg, S., Fernö, A., 1999. Diel activity pattern and food search behaviour in cod, *Gadus morhua*. Environ. Biol. Fish. 54, 345–353.

Mackinson, S., 1999. Variation in structure and distribution of pre-spawning Pacific herring shoals in two regions of British Columbia. J. Fish Biol. 55, 972–989.

MacLennan, D.S., Fernandes, P.G., Dalen, J.D., 2002. A consistent approach to definitions and symbols in fisheries acoustics. ICES J. Mar. Sci. 59, 365–369.

Magurran, A.E., 1993. Individual differences in fish behaviour. second ed. In: Pitcher, T.J (Ed.), The Behaviour of Teleost Fishes. Chapman & Hall, London, pp. 441–477.

Magurran, A.E., Oulton, W.J., Pitcher, T.J., 1985. Vigilant behaviour and shoal size in minnows. Z. Tierpsychol. 67, 167–178.

Milinski, M., 1993. Predation risk and feeding behaviour. second ed. In: Pitcher, T.J (Ed.), The Behaviour of Teleost Fishes. Chapman & Hall, London, pp. 285–305.

Misund, O.A., 1990. Sonar observations of schooling herring: school dimensions, swimming behaviour, and avoidance of vessel and purse seine. Rapp. P.-V. Réun. Cons. Int. Explor. Mer 189, 135–146.

Misund, O.A., 1993. Dynamics of moving masses: variability in packing density, shape, and size among herring, sprat, and saithe schools. ICES J. Mar. Sci. 50, 145–160.

Mohr, H., 1971. Behaviour patterns of different herring stocks in relation to ship and midwater trawl. In: Kristjonsson, H (Ed.), Modern Fishing Gear of the World 3. Fishing News Books, London, pp. 368–371.

Nøttestad, L., Aksland, M., Beltestad, A., Fernö, A., Johannessen, A., Misund, O.A., 1996. Schooling dynamics of Norwegian spring spawning herring (*Clupea harengus*) in a coastal spawning area. Sarsia 80, 277–284.

Ona, E., Mitson, R.B., 1996. Acoustic sampling and signal processing near the seabed: the deadzone revisited. ICES J. Mar. Sci. 53, 677–690.

Pitcher, T.J., 1983. Heuristic definitions of shoaling behaviour. Anim. Behav. 31, 611–613.

Pitcher, T.J., Parrish, J.K., 1993. Functions of shoaling behaviour in teleosts. second ed. In: Pitcher, T.J (Ed.), The Behaviour of Teleost Fishes. Chapman & Hall, London, pp. 364–439.

Rajasilta, M., Paranko, J., Laine, P.T., 1997. Reproductive characteristics of the male herring in the northern Baltic Sea. J. Fish Biol. 51, 978–988.

Runnstrøm, S., 1941. Quantitative investigations on herring spawning and its yearly fluctuations at the west coast of Norway. Fisk Dir. Skr. (Ser. Havunders.) 6, 5–71.

Shaw, E., 1961. Minimal light intensity and the dispersal of schooling fish. Bull. Inst. Oceanogr. 1213, 8.

Sherwood, N.M., Kyle, A.L., Kreiberg, H., Warby, C.M., Magnus, T.H., Carolsfeld, J., Price, W.S., 1991. Partial characterization of a spawning pheromone in the herring *Clupea harengus pallasi*. Can. J. Zool. 69, 91–103.

Slotte, A., 1998. Patterns of aggregation in Norwegian spring spawning herring (*Clupea harengus* L.) during the spawning season. ICES CM, J32.

Slotte, A., 1999. Differential utilisation of energy during wintering and spawning migration in Norwegian spring spawning herring. J. Fish Biol. 54, 338–355.

Slotte, A., Dommasnes, A., 2000. Distribution and abundance of Norwegian spring spawning herring during the spawning season in 2000. Cruise Report Institute of Marine Research (IMR), Bergen, Norway.

Skaret, G., Axelsen, B.E., Nøttestad, L., Fernö, A., Johannessen, A., 2002. Herring as cannibals. J. Fish Biol. 61, 1050–1052.

Skaret, G., Fernö, A., Nøttestad, L., Johannessen, A., Axelsen, B.E., 2001. Impact of herring spawning behaviour on acoustic abundance estimates. ICES CM, Q22.

Stacey, N.E., Hourston, A.S., 1982. Spawning and feeding behaviour of captive Pacific herring (*Clupea harengus palassi*). Can. J. Fish. Aquat. Sci. 39, 489–498.

Stratoudakis, Y., Gallego, A., Morrison, J.A., 1998. Spatial distribution of developmental egg ages within a herring *Clupea harengus* spawning ground. Mar. Ecol. Prog. Ser. 174, 27–32.

Taylor, F.H.C., 1971. Variation in hatching success in Pacific herring (*Clupea harengus pallasi*) eggs with water depth, temperature, salinity, and egg mass thickness. Rapp. P.-V. Réun. Cons. Int. Explor. Mer 160, 34–41.

Toresen, R., 1991. Predation on the eggs of Norwegian spring spawning herring (*Clupea harengus*) on a spawning ground on the west coast of Norway. ICES J. Mar. Sci. 48, 15–21.

Tremorrow, M.V., Claytor, R.R., 1998. Detection of Atlantic herring (*Clupea harengus*) schools in shallow waters using high-frequency sidescan sonars. Can. J. Fish. Aquat. Sci. 55, 1419–1429.

Vabø, R., Nøttestad, L., 1997. An individual based model of fish school reactions: predicting antipredator behaviour as observed in nature. Fish. Oceanogr. 6, 155–171.

Ware, D.M., Tanasichuk, R.W., 1989. Biological basis of maturation and spawning waves in Pacific herring (*Clupea harengus pallasi*). Can. J. Fish. Aquat. Sci. 46, 1776–1784.

Welsby, V.G., Dunn, J., Chapman, C., Sharman, D.P., Priestley, R., 1964. Further uses of electronically scanned sonar in the investigation of behaviour of fish. Nature, London 203, 588–589.

Available online at www.sciencedirect.com
SCIENCE DIRECT®
Aquatic Living Resources 16 (2003) 307–312
Aquatic Living Resources
www.elsevier.com/locate/aquliv

Fish schooling behaviour in the northwest North Sea: interspecific associations measured by acoustic survey

Doug J. Beare [a,*], David G. Reid [a], Eddie McKenzie [b]

[a] *FRS, Marine Laboratory, Victoria Road, Torry, Aberdeen AB11 9DB, Scotland, UK*
[b] *Department of Statistics and Modelling Science, University of Strathclyde, Glasgow G1 1XH, Scotland UK*

Accepted 3 March 2003

Abstract

This study investigates whether pelagic fish schools of different species or groupings (e.g. herring, "surface herring", "gadoids", mackerel, sprat and sandeels) were positively or negatively associated with each other in time and space. To do this, statistical models were fitted to pre-processed acoustic fisheries data to reveal how pelagic school prevalence varied with respect to spatial (latitude and longitude) and temporal (time of day) information. The model outputs, which take the form of probabilities fitted to the presence or absence of schools, were then used to calculate correlation coefficients, which are useful for measuring association between pairs of variables. Results depended upon the specific species pairs under investigation. Herring and "surface herring" were, for example, very generally sympatrically associated with each other in both space and time, while herring and gadoid schools, on the other hand, had allopatric distributions.

Keywords: Fisheries; Herring; Gadoids; Acoustics; Inter-specific associations; Correlation coefficients; Statistical models

1. Introduction

The Marine Laboratory, Aberdeen conducts annual acoustic surveys of the Orkney/Shetland area during July each year (Bailey et al., 1998). The principal objective of the surveys is to estimate the total biomass of herring (*Clupea harengus*) for use as an index in the annual assessment of the stock (Anonymous, 2001), although the data have also been used to answer questions relating to various aspects of herring biology (Bailey et al., 1998; Maravelias and Reid, 1995, 1997; Maravelias et al., 1996; Reid and Maravelias, 2001). However, data relating to the abundance of other schooling species, also collected during the surveys, have not been analysed until now. In this paper, we address the shortfall by demonstrating how statistical models can be used to expose how school prevalence among different pelagic species groups varies with respect to spatial (latitude, longitude) and temporal (time of day) information (Beare et al., 2002). The baseline data output by these statistical models are then incorporated into an assessment of whether the schools of different species groups are positively, or negatively, associated with each other in space and time. The specific hypothesis addressed by this study can be summarised as follows:

"At any specific point in space, and at any time of day, do schools of species group A avoid, or tend to congregate with, schools of species group B?"

2. Materials and methods

2.1. Acoustic data

The investigation used acoustic survey data collected during six surveys carried out by the FRS Marine Laboratory, Aberdeen during July in 1991 and 1993-1997 (Fig. 1). The data were collected by a Simrad EK500 38-kHz echosounder and stored using the B1500 format, which were then transformed into matrices, each number corresponding to an individual calibrated back-scattering strength sample from a single echosounder transmission. Data summarising the school characteristics were then extracted using image-processing software (ImagePro Plus, Media Cybernetics), combining image filtering algorithms with interactive decisions by the operator (Reid and Simmonds, 1993). The detection threshold for schools was set at -60 dB, providing the best effective beam angle for the school volume backscatter (Sv) of the schools retained (Reid et al., 2000). After thresholding, a single morphological filter pass eliminated small objects and clarified larger ones. Remaining objects detected were classified as schools, and then separated into species

* Corresponding author.
E-mail address: d.beare@marlab.ac.uk (D.J. Beare).

doi:10.1016/S0990-7440(03)00041-X

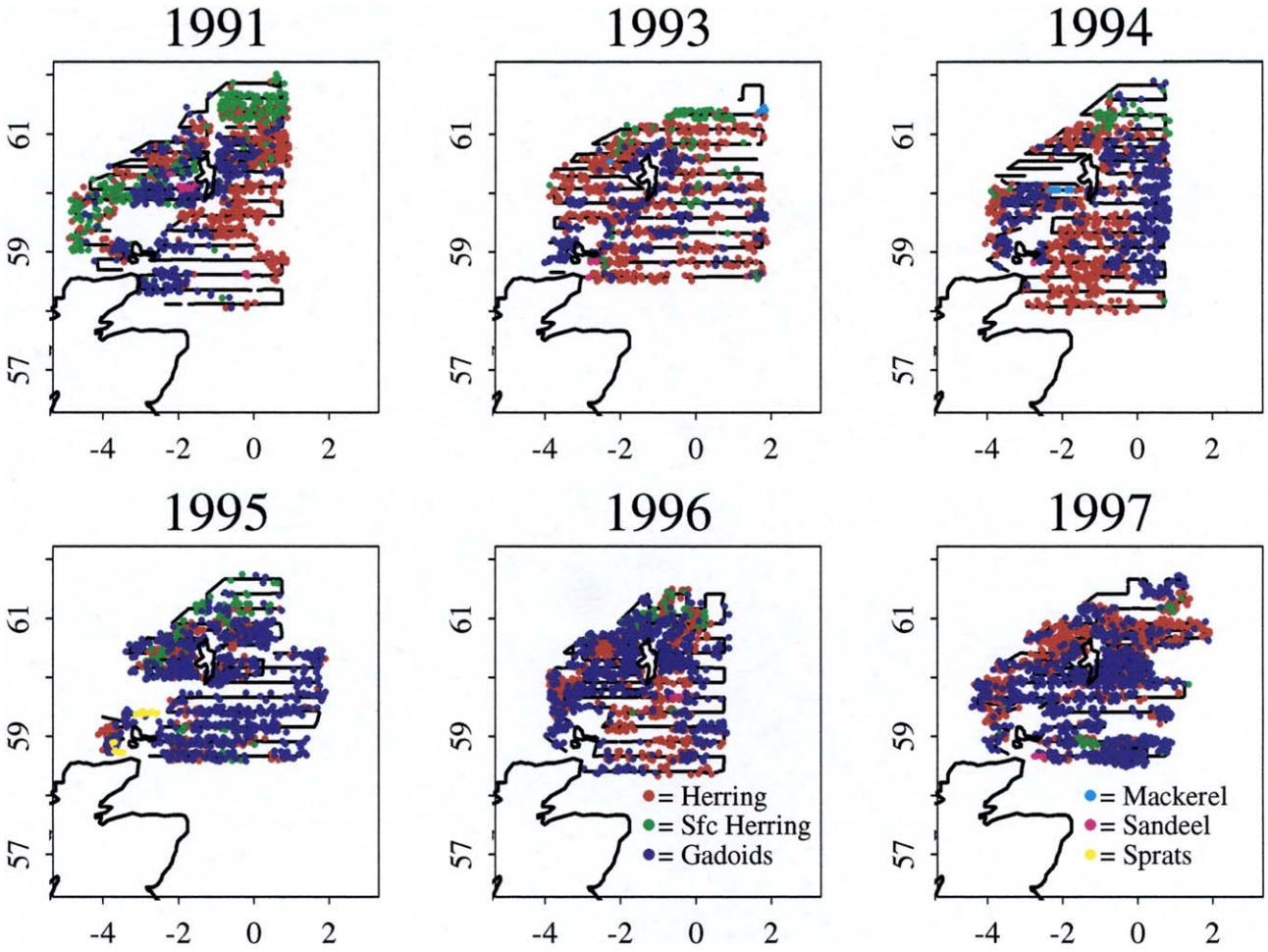

Fig. 1. July acoustic survey data northwest of Scotland. The solid black line represents the survey track; the dots, positive recordings of herring (red), surface herring (green), gadoids (blue), mackerel (turquoise), sandeel (pink), and sprats (yellow) (NB, random noise was added to each observation in both the *x* and *y* dimensions to reflect sample density).

groups. The following taxonomic groups were identified: herring, "surface herring", "gadoids", mackerel, sandeels and sprats. School classification to taxonomic group was carried out according to the standard procedure used for the ICES International Surveys (Simmonds et al., 1992). The allocation of schools to species principally involves the use of ground truth data from pelagic trawling. During the course of an average survey 20-50 trawl stations will be carried out opportunistically on the largest echotraces. During subsequent analyses, the results of these trawl hauls, and the experience of the operator will be used to assign each echotrace to a taxonomic group. The process is subjective to some degree, although it has been shown to be relatively robust and reasonably operator independent (Reid et al., 1998). It was generally possible during these surveys to identify schools of pelagic fish, e.g. herring, mackerel (*Scomber scombrus*), sandeel (*Ammodytes* sp.) and sprats (*Sprattus sprattus*). Most such schools sampled were monospecific, or occasionally mixtures of herring and sprat, or herring and mackerel. Herring schools were generally found, either as small, sharp echotraces near the surface (<20 m), or as relatively high energy marks within 50 m of the seabed. Mackerel schools were identified as large, mid water traces with a weaker backscatter than similar sized herring schools, and they also tended to have a higher backscatter at high frequencies (120 and 200 kHz). Sandeel schools were large and irregular in shape. Sprat schools were similar to the deeper type of herring schools, but could be separated using the trawl data. The "gadoid" category represents a species assemblage made up of Norway pout (*Trisopterus esmarkii*), whiting (*Merlangius merlangus*), haddock (*Melanogrammus aeglefinus*) or saithe (*Pollachius virens*), with smaller numbers of other gadoid species. The fish are usually young (1-2 years), small (maximum 20 cm) and found in discrete schools close to the seabed.

2.2. Statistical analyses

The acoustic data were collected continually along each transect during the surveys (Fig. 1). The transects were then divided into one nautical mile elementary distance sampling units (EDSUs), which minimises the degree of spatial autocorrelation between successive samples (Simmonds et al., 1992). Three species pairs were then selected, based on the

amount of available data (e.g. herring and surface herring; herring and gadoids; gadoids and surface herring). For convenience, the species from each pair were denoted as A and B. We then categorised each EDSU with respect to each schooling pair (A, B) as follows: (the corresponding probability is also shown in each case)

- Category 0: neither species A nor B recorded in the EDSU (P_{00});
- Category 1: only species A recorded in the EDSU (P_{A0});
- Category 2: only species B recorded in the EDSU (P_{B0});
- Category 3: both A and B recorded in the EDSU (P_{AB}).

(Note: mackerel, sandeels and sprats could not be examined in such detail due to data-sparsity, and for these groups we noted only whether or not they were recorded in each EDSU with no attention paid to whether other species were present).

For each pair (A, B), the observed EDSUs are a sample from a multinomial distribution such that the probability of observing n_i occurrences of category i for $i = 0, 1, 2, 3$ in an EDSU is given by

$$P_{00}^{n_0} P_{A0}^{n_1} P_{B0}^{n_2} P_{AB}^{n_3} \quad (1)$$

The four probabilities are modelled as functions of predictive variables known for each EDSU. In this case, these are latitude, longitude and time of day. We write the vector of these values for the kth observed EDSU as z_k. Modelling a multinomial distribution can be achieved in various ways (Cox, 1989) but one simple approach involves rewriting Eq. (1) above in terms of nested conditional events. In this case, we obtain

$$\prod_{i=1}^{3} p_i^{n_i} (1 - p_i)^{n_0 + \ldots + n_{i-1}} \quad (2)$$

where $p_3 = P_{AB}$, $p_2 = P_{B0}/(1 - P_{AB})$ and $p_1 = P_{A0}/(1 - P_{AB} - P_{B0})$. Thus, we have reduced the multinomial probability to three binomial probabilities, which can be modelled separately, i.e. we can estimate each of (p_1, p_2, p_3) as functions of the predictor variables z_k. Here, we use generalised additive models (GAMs) for each binomial (Hastie and Tibshirani, 1990). It is straightforward then to recover the original probabilities (P_{00}, P_{A0}, P_{B0}, P_{AB}) as functions of the predictor variables.

Specific details of model selection protocols are described elsewhere in the literature (Augustin et al., 1998; Borchers et al., 1997a,b). Once a GAM was selected for each survey, spatial grids at approximately a 10th of a degree latitude and 5th of a degree longitude for nine different times of day (04:00, 06:00, 08:00, 10:00, 12:00, 14:00, 16:00, 18:00, 21:00 h) were constructed. Parameters from the fitted models were then used to interpolate over the grids producing spatio-temporally (time of day in this context) resolved surfaces, together with the appropriate standard errors.

2.3. Measuring association

The probability values, output by the statistical models (GAMs) were then used to calculate correlation coefficients between each possible pair of species groups according to the following expression:

$$r = \frac{P_{AB} - (P_A \cdot P_B)}{\sqrt{P_A(1 - P_A)\, P_B(1 - P_B)}} \quad (3)$$

where P_A (or P_B), for example, equals the probability of recording pelagic species group A (or B) within each EDSU whether or not the other species is also recorded, i.e. mathematically, $P_A = P_{A0} + P_{AB}$, and similarly, $P_B = P_{B0} + P_{AB}$. All of the probabilities were estimated, for specific locations and times of day, using the GAMs described above. The correlation coefficient was used here as a measure of the 'association' in time and space between the schools of different species; a high positive value indicating positive association, i.e. a tendency for the two species to be present or absent simultaneously. Negative association or a high negative correlation coefficient is, therefore, a tendency for only one species to be present in an EDSU at a particular time and location.

Note that for binary data, as here, the lower limit of the correlation coefficient r is given, not by -1, but by the greater of $-\sqrt{P_A P_B/(1 - P_A)(1 - P_B)}$ and its reciprocal (Cox, 1989). Thus, since P_A and P_B are functions of location and time we have divided the negative correlations by the magnitude of the appropriate lower limit so that the output may be interpreted in the usual way.

3. Results

3.1. Prevalence of schools in relation to location and time of day

The data for positive recordings of each species group (Fig. 1) indicate that their spatial distributions have varied considerably between the survey years (July 1991, 1993-1997 (Beare et al., 2002)). Herring schools, for example, were more concentrated around Shetland in 1991, but much more sparsely distributed throughout the survey area in 1993 (Fig. 1). Similarly, gadoid schools were recorded predominantly in the shallow areas between Orkney and Shetland, and around their coasts in 1991 and 1995 (Fig. 1), whereas in 1994 gadoids were more commonly observed in the east of the study area (Fig. 1).

GAMs were fitted to estimate the probabilities as smooth functions of latitude, longitude and hour of day. As an example, the most appropriate model for the 1991 herring data had the functional form: Lo(longitude, latitude) + Lo(time of day), where Lo denotes a locally weighted regression smoother, LOWESS (Cleveland and Devlin, 1988). In scientific terms, the selection of this model implies the assumption that the shape, and not just the level, of herring school prevalence from east to west (longitude) depended crucially on the distance north or south (latitude). Similarly, the selection of time of day independently from the locational information (latitude and longitude), indicates that herring school prevalence has the same shape of diel aggregation/dis-

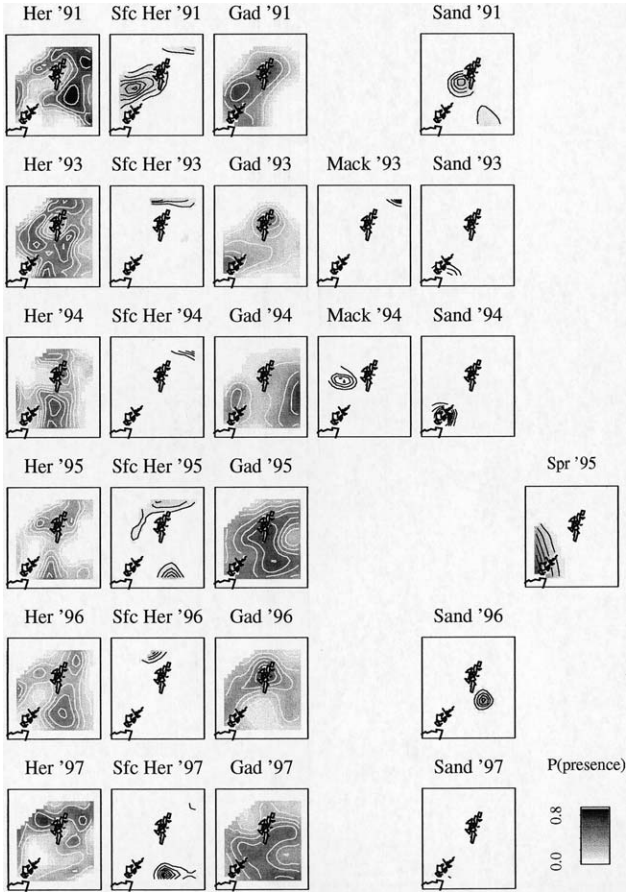

Fig. 2. Prevalence of herring (column 1), surface herring (column 2), gadoids (column 3), mackerel (column 4), sandeel (column 5), and sprats (column 6) estimated for each survey at 10:00 h (July 1991 and 1993-1997) using GAMs.

aggregation behaviour (Pitcher, 1993) across the study region (Fig. 1), and only the overall level (corresponding to abundance) changes according to location. After similar exploration and experimentation, the same, or at least very similar, model formulations were selected to describe the data for the other species groupings and survey combinations.

The spatial patterns output by the selected GAMs for each species grouping and survey year combination are plotted in Fig. 2 . The first column of Fig. 2 represents the probability of recording a herring school given there were no surface herring, during each survey. Herring spatial distributions were fairly similar between years, and high probabilities of occurrence were typical west of Orkney and Shetland, along the continental shelf edge, and also in the Fair Isle Channel area to the southeast of Shetland. Herring were always rare (1991, 1993–1997) over the relatively shallow ridge between Orkney and Shetland (Fig. 2).

In spite of the evidence for a degree of inter-annual stability in spatial distribution, there were also notable differences between the six surveys. In 1991, for example, the chance of recording herring schools was high west of Shetland, but low in the same area between 1994 and 1996 (Fig. 2). Herring schools recorded on, or very near the surface, were comparatively rare, but most likely to be encountered to the north and west of Shetland. The spatial distribution of gadoids was highly variable between surveys, in terms of both shape and level (Fig. 2). In July 1991 and 1993, for example, gadoids were most common over the relatively shallow ridge between Orkney and Shetland, whereas by 1994 they were more abundant east of Shetland (Fig. 2). Mackerel schools were seen west of Shetland during July 1993 and 1994, although they are rarely recorded on acoustic survey, because of a low target strength caused by their lack of a swimbladder (Foote et al., 1987). Sandeel and sprat schools were also comparatively unusual (Fig. 2), but characteristic of the shallower areas around Orkney, Shetland, and mainland Scotland.

Since the effect of time of day on school prevalence was estimated independently from the spatial information (see Table 1), its shape is the same across the entire study area, only the overall level being able to change with location. The chance of recording herring schools was highest during the day between 05:00 and 19:00 h in all 6 years surveyed. Gadoid schools were also most commonly recorded during daylight, although they varied in detail between surveys. Mackerel, sandeel and sprat schools were recorded rarely throughout the surveys, and probabilities were correspondingly low. Mackerel and sprat were more likely to be detected in the afternoon, while sandeel schools were more commonly observed in the morning between 06:00 and 10:00 h.

3.2. Spatial associations for a fixed time of day

In order to examine the association between the different species groups, correlation coefficients, *r*, were calculated using probabilities output by the GAMs described above. Since there was a clear inter-annual, or between survey, effect in the data (see Figs. 1 and 2) correlations were examined separately for each year. Unfortunately mackerel, sandeel and sprat were omitted from this part of the study because of data sparsity caused, either by their failure to be detected by the echosounder, or by their actual relative rarity (e.g. Fig. 2) in the survey area.

Correlation coefficients at 10:00 h, between herring and surface herring for all six surveys are plotted in the first column of Fig. 3, followed by the association between herring and gadoids (column 2, Fig. 3), and finally between surface herring and gadoids (column 3, Fig. 3). Correlations were of mixed sign between herring and surface herring. There were positive associations along the continental shelf north of Shetland, where herring abundance is usually high (Fig. 2), and generally negative associations in the shallow areas where the gadoids are most prevalent. There were large, negative correlations in space between herring and gadoid schools around Orkney and Shetland, although there was some evidence of positive association between herring and gadoids at the periphery of the study region (Fig. 3). The association between surface herring and gadoids was also generally negative in space and varied considerably between surveys (Fig. 3).

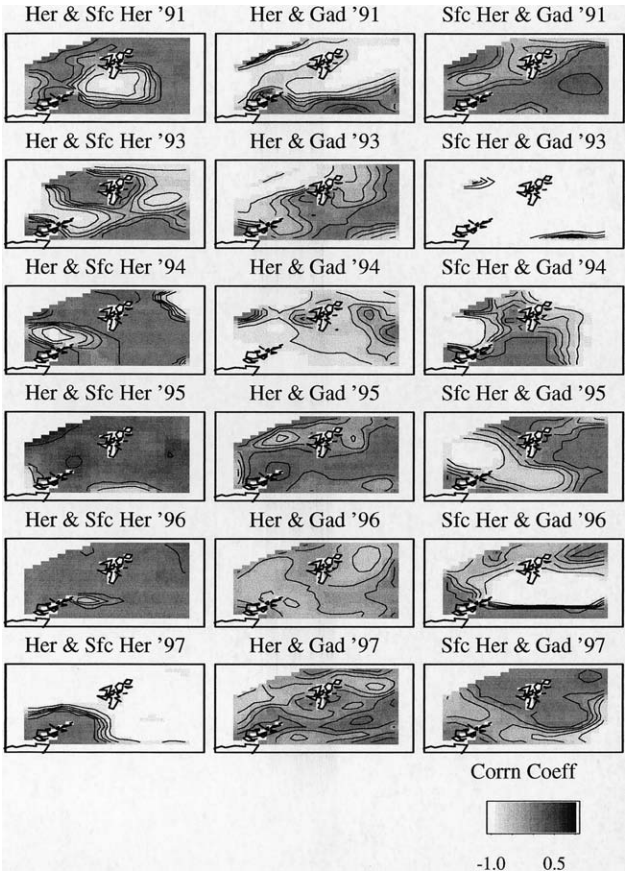

Fig. 3. Spatial variation in association between three species pairs (e.g. herring, surface herring and gadoids) at 10:00 h for each of the six July acoustic surveys. Units are correlation coefficients calculated using Eq. (3).

3.3. Temporal (time of day) associations for a fixed location

Correlation coefficients calculated for the 1991 survey are displayed as a function of time of day, for an arbitrarily selected location west of Shetland, in Fig. 4. The horizontal line (Fig. 4) is a zero correlation, below which association is negative and vice versa. The correlation coefficient estimated between herring and surface herring remained negative throughout the day, suggesting fairly stable negative associations (Fig. 4). Herring and gadoids, however, were much more strongly, negatively associated with each other (e.g. Fig. 4). There was a pronounced time of day effect with the herring and gadoid schools least negatively associated with each other at noon.

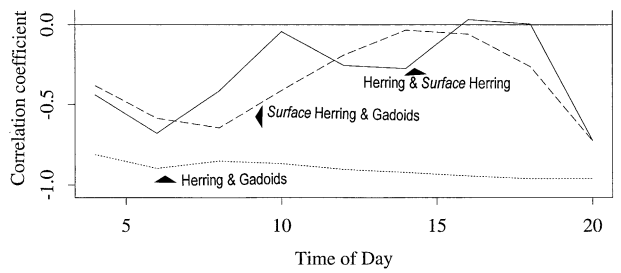

Fig. 4. Daily variation in association between the three species pairs (e.g. herring and surface herring; herring and gadoids; surface herring and gadoids) at an arbitrary location west of Shetland during the 1991 survey. Units are correlation coefficients computed using Eq. (3).

4. Discussion

During the study, we have demonstrated the potential value of acoustic data for exploring the spatial interactions between fish assemblages according to their taxonomic groupings. The use of statistical models has further enabled us to summarise spatial and temporal (time of day) distributions of the various schooling groups. In addition, the probability of positive observations for pairs (e.g. herring and gadoids) of species groups both being recorded, within each EDSU at the same time of day, could be modelled, allowing unusually detailed examination of relative associations between the groups in space/time contexts.

The usual approach to such problems is to calculate Pearson rank correlation coefficient between abundances of, say, species A and species B. But for these data, however, that approach could not be taken because there is only one observation available in each EDSU, i.e. one count of species group A and one of species group B. Binary or presence/absence models were used because most of the data (>80%) are actually zero, i.e. any particular EDSU is most likely to have no schools present at all. Therefore, any costs due to the binary simplification, in terms of lost information at higher levels of school abundance, are compensated for by a statistically robust protocol for dealing with zeros, which ultimately allows reasonable model selection to take place. Moreover, the four probabilities, estimated at each EDSU, also then enable an estimation of 'association' (spatio-temporally resolved correlation coefficients), which would not be possible otherwise because of the data-sparsity alluded to above. A further advantage of our method is that correlation or association is examined at a much higher level of detail than could be achieved using more conventional methodologies. The chance of finding only species A in an EDSU, only species B, both species A and B together, and neither species A or B can be estimated here, and there are thus four different possibilities for correlation between any species pair instead of two.

The schools of most of the species groups studied here were most likely to be recorded by echosounder during the daytime period. This may not be because there are necessarily more fish present, but because of regular diel transitions between densely packed school formations in daylight, and individual, or small groups of, fish in darkness. Schooling is believed to be, primarily, a predator avoidance behaviour (Pitcher, 1993) in that an individual fish is less likely to be eaten in a large aggregation than when alone. Schools are often depicted as breaking up at night as the behaviour is largely in response to visual cues. Interestingly, in this study, sprat schools were most abundant in the evening, which is contrary to typical behaviour evidenced, for example, by herring. It should be noted, however, that sprats are not particularly common in most of the survey area.

The mainly positive associations observed (Fig. 3) between the two categories of herring schools along the continental shelf edge was contrary to expectations. In a previous study, Reid and Maravelias (2001) showed that, over short spatial scales, herring schools related differently to topography and substrate depending on their relative position in the water column. Schools close to the seabed showed good correlation with particular substrates and bottom features, while no such relationship could be seen for the surface schools. The finding of the present work indicates that the two herring school categories are positively associated with each other where herring numbers are high, and for the purposes of stock estimation, could be handled together, using the same biological data (e.g. length frequency and weight-length relationships).

Herring and gadoid schools were more strongly, negatively associated with each other than herring and surface herring (Figs. 3 and 4) suggesting that herring and gadoids occupy different environmental niches. An alternative possibility is that the adult herring may be actively predating on the small gadoids, which make up this assemblage. Again, from a survey analytical perspective, the negative association between the herring and the gadoids is useful, as it suggests that they tend not to be co-located, and so echotraces are less likely to be wrongly allocated. A problem in interpreting this observation is that the "gadoid" category comprises a number of species (predominantly whiting, haddock, Norway pout and saithe, but including others). Additionally, these schools or aggregations would vary in terms of species composition across the survey area. Unfortunately, the survey is not designed to differentiate gadoid species, and this would be difficult to achieve retrospectively, as the trawls were principally conducted to identify pelagic species and differentiate those from the gadoid assemblage.

In conclusion, the present study has shown that the school distribution of a pelagic species such as herring can be shown to have a relationship with the distribution of other fish species, occupying the same general area. In this case, the associations were mostly negative and rather weakly positive (Figs. 3 and 4), suggesting that the schools of pelagic fish occupy space (Fig. 3) and time of day (Fig. 4) in different ways. This information can be added to the corpus of data on other biotic and abiotic correlates with herring distribution presented in previous papers (Bailey et al., 1998; Maravelias and Reid, 1995, 1997; Maravelias et al., 1996). The combined picture from all these studies is one of a complex interaction between the spatial distribution of the herring and many aspects of their environment. In addition, the study has shown that the different types of herring school—surface and deep—are positively associated in space and time of day, and can be analysed as a single population.

Acknowledgements

We would like to thank the European Union for partially funding this work within the CLUSTER project (FAIR CT96.1799) and our colleagues at the Marine Laboratory, Aberdeen who participated in the herring acoustic surveys. We would also like to acknowledge Mr. Richard Aukland for developing the latest version of our image processing system, and for extracting the "school" database used in this study.

References

Anonymous, 2001. Report of the herring assessment working group for the area south of 62N. ICES CM 2001/ACFM:12, ICES, Hamburg.

Augustin, N.H., Borchers, D.L., Clarke, E.D., Buckland, S.T., Walsh, M., 1998. Spatiotemporal modelling for the annual egg production methods of stock assessment using generalized additive models. Can. J. Fish. Aquat. Sci. 55, 2608–2621.

Bailey, M.C., Maravelias, C.D., Simmonds, E.J., 1998. Changes in the spatial distribution of autumn spawning herring (*Clupea harengus* L.) derived from annual acoustic surveys during the period 1984-1996. ICES J. Mar. Sci. 55, 545–555.

Beare, D.J., Reid, D.G., Petitgas, P., 2002. Spatio-temporal patterns in herring (*Clupea harengus* L.) school abundance and size in the NW North Sea: modelling space time dependencies to allow examination of the impact of local school size. ICES J. Mar. Sci. 59, 469–479.

Borchers, D.L., Buckland, S.T., Priede, I.G., Ahmadi, S., 1997. Improving the precision of the daily egg production method using generalized additive models. Can. J. Fish. Aquat. Sci. 54, 2727–2742.

Borchers, D.L., Richardson, A., Motos, L., 1997. Modelling the spatial distribution of fish eggs using generalized additive models. Ozeanografika 1, 103–120.

Cleveland, W.S., Devlin, S.J., 1988. Locally-weighted regression: an approach to regression analysis by local fitting. J. Am. Stat. Assoc. 83, 596–610.

Cox, D.R., 1989. Analysis of Binary Data. Chapman and Hall,, London.

Foote, K.G., Knudsen, H.P., Vestnes, G., MacLennan, D.N., Simmonds, E.J., 1987. Calibration of acoustic instruments for fish density estimation: a practical guide. ICES Coop. Res. Rep., 144.

Hastie, T., Tibshirani, R., 1990. Generalized additive models. Chapman and Hall, London.

Maravelias, C.D., Reid, D.G., 1995. Relationship between herring (*Clupea harengus*, L.) distribution and sea surface salinity and temperature in the northern North Sea. Sci. Mar. 59, 427–438.

Maravelias, C.D., Reid, D.G., 1997. Identifying the effects of oceanographic features and zooplankton on prespawning herring abundances using generalized additive models. Mar. Ecol. Prog. Ser. 147, 1–9.

Maravelias, C.D., Reid, D.G., Simmonds, E.J., Haralabous, J., 1996. Spatial analysis and mapping of acoustic survey data in the presence of high local variability: geostatistical application to the North Sea herring. Can. J. Fish. Aquat. Sci. 53 (7), 1497–1505.

Pitcher, T.J., 1993. Ecology, behaviour and exploitation in fish shoals. Nord. Semin. -Arb. Rapp. 572, 53–56.

Reid, D.G., Maravelias, C.D., 2001. Relationships between herring school distribution and seabed substrate derived from RoxAnn. ICES J. Mar. Sci. 58, 1161–1173.

Reid, D.G., Scalabin, C., Petitgas, P., Messe, J., Aukland, R., Carrerra, P., Georgakarakos, S., 2000. Standard protocols for the analysis of school based data from echosounder surveys. Fish. Res. 47, 125–136.

Reid, D.G., Simmonds, E.J., 1993. Image analysis techniques for the study of fish school structure from acoustic survey data. Can. J. Fish. Aquat. Sci. 50, 886–893.

Reid, D.G., Fernandes, P.G., Bethke, E., Coopers, A., Goetze, E., Makansson, N., Pedersen, J., Staehr, K.J., Simmonds, E.J., Toresen, R., Tortensen, E., 1998. On visual scrutiny of echograms for acoustic stock estimation. ICESCM/J, 3.

Simmonds, E.J., Williamson, N.J., Gerlotto, F., Aglen, A., 1992. Acoustic survey design and analysis procedure: a comprehensive review of current practice. ICES Coop. Res. Rep., 187.

Available online at www.sciencedirect.com
SCIENCE DIRECT®
Aquatic Living Resources 16 (2003) 313–316
Aquatic Living Resources
www.elsevier.com/locate/aquliv

Avoidance behaviour of *Alosa fallax fallax* to pulsed ultrasound and its potential as a technique for monitoring clupeid spawning migration in a shallow river

Jim Gregory *, Peter Clabburn

Environment Agency Wales, Rivers House, St. Mellons Business Park, St. Mellons, Cardiff, Wales CF3 0LT, UK

Accepted 3 March 2003

Abstract

A hydroacoustic monitoring technique to quantify and assess the ecological requirements for migration of the anadromous clupeid, *Alosa fallax fallax* (twaite shad) was developed, and its effectiveness studied, on the River Wye in Wales. The acoustic monitoring technique was a side aspect application, with two transducers fixed permanently to the riverbank and the acoustic beam from each aimed horizontally across the river towards the opposite bank, perpendicular to flow. Two split-beam echo sounders and transducers were deployed, each operating at different frequencies (200 and 420 kHz). Using a combination of these two frequencies it was possible to demonstrate that shad show strong avoidance behaviour to sound transmitted at 200 kHz and would not pass the monitoring site when sound was transmitted at this frequency. They remained unaffected by sound transmitted at 420 kHz and were observed migrating upstream in large, loosely aggregated shoals. From visual observations above and below the water, shoals were estimated to comprise of many hundreds of individuals, covering a size range of between 30 and 45 cm. Only a few individuals could be resolved by the acoustic system operating at 420 kHz, and it was therefore, not possible to obtain a count of fish by "target tracking" single shad. However, by transmitting 200 kHz sound pulses on a 50% duty cycle the seasonal and daily patterns of shad migration were derived from the analysis of data gathered by the acoustic system operating at 420 kHz.

Keywords: Fish behaviour; Split-beam; Shad

1. Introduction

It is clear from research into the sensitivity of fish to sound that some species of clupeiforms are unique amongst fish in being able to detect high frequencies.

Published sensitivities for other teleost fish range from 10 Hz to 1 kHz (Popper, 2000) with the odd exception like the Atlantic cod (*Gadus morhua*) demonstrating sensitivity up to 38 kHz (Astrup and Møhl, 1993). However, most fish detect a much lower range of frequencies, as typified by the anadromous Atlantic Salmon (*Salmo salar*) which has been found to detect frequencies within the 10–380 Hz range (Hawkins and Johnstone, 1978).

Studies conducted on the Alewife, *Alosa pseudoharengus* (Dunning et al., 1992; Ross et al., 1996), Blueback herring, *Alosa aesivalis* (Nestler et al., 2002) and American shad, *Alosa sapidissima* (Popper and Carlson, 1998) showed avoidance responses to sound at frequencies over 120 kHz. The highest frequency to solicit a response was 180 kHz for American shad.

More recent research has indicated that this ability to detect ultrasound may be limited to the alosids. Mann et al. (2001) used auditory brainstem response to show that the alosid gulf menhaden (*Brevoortia patronus*), detected frequencies over 100 kHz but the bay anchovy(*Anchoa mitchilli*), scaled sardine (*Harengula jaguana*) and Spanish sardine (*Sardinella aurita*) did not respond to frequencies over 4 kHz.

This study describes observations on the behaviour of a species of clupeid, the twaite shad (*Alosa fallax fallax*), when subjected to two frequencies of pulsed ultrasound, 200 and 420 kHz, as they migrate up the River Wye along the border between England and Wales. It discusses a potential technique that utilises this behaviour to discriminate and enumerate shoals of shad and assess the ecological requirements for the migration of twaite shad as they pass an acoustic fish

* Corresponding author.
E-mail address: jim.gregory@environment-agency.gov.uk (J. Gregory).

doi:10.1016/S0990-7440(03)00024-X

counter deployed primarily to count salmon passage. The twaite shad is an anadromous species that enters freshwater to spawn between April and June.

This study is different from previous studies in that it describes empirical observations of fish behaviour to sound in a natural river environment rather than at an impoundment or a measured brainstem response. It is a study on a European species of anadromous fish and demonstrates an avoidance reaction to a higher frequency of sound (200 kHz) than previously published for any fish species.

It also illustrates a method of utilising this behaviour to discriminate alosid species from others and assess fish migration using a fixed location acoustic counter.

2. Methods

An acoustic echo sounder (HTI model 243) has been deployed on the lower reaches of the River Wye to monitor salmon migration since 1995. The split-beam transducer is aimed horizontally to the river bed and perpendicular to the river flow across the 30-m width. A second acoustic system and transducer operating at a frequency of 420 kHz was deployed next to the 200 kHz transducer, aimed in the same way.

The 420 kHz system was operated continuously from April to July to cover the migration period for twaite shad into the River Wye. Data from the acoustic systems were collected and analysed during this period. The 200 kHz system was operated for 30 min every hour and deactivated for 30 min. Data were collected and analysed for the 30 min of operation each hour.

Observations on fish behaviour as they approached the acoustic beams were recorded on video cameras deployed from the bank in air and from underwater cameras deployed at various ranges across 26 m of the 30 m river width. Maximum water depth was around 2.5 m. The water clarity in the Wye enabled shoals of shad to be clearly identified from bank side observations as they swam upstream.

Observations on fish behaviour were made:

- During continuous operation of the 200 kHz system.
- Immediately following the disabling of the 200 kHz system.
- During the continuous operation of the 420 kHz system, with the 200 kHz system deactivated for 30 min of every hour.

Acoustic data were collected and analysed for all three periods.

2.1. Technical specifications of the two acoustic systems

The acoustic parameters of the sound pulse generated by the 200 and 420 kHz systems were standardised as much as possible. The major parameter settings used are shown in Table 1.

Table 1
Pulse transmission details for the two frequencies used

Parameter	Setting	
	420 kHz	200 kHz
Frequency (kHz)	420	200
Maximum processing range (m)	26	20
Source level (reference pressure 1 μPa at 1 m)	202 dB	2218 dB
Ping rate (s^{-1})	20	20
FM slide or CW pulse	CW	CW
Transmit pulse width (ms)	0.2	0.2
Transmit power (dB W)	18	24
Nominal transducer beam width (in degrees off axis of the –3 dB points of the beam)	2.8° vertical × 10° horizontal	2.8° vertical × 10° horizontal

3. Results

3.1. Shad behaviour under constant operation of the 200 kHz system

Shoals of shad migrating upstream were seen to abruptly reverse direction when they came within 5 m of the acoustic beam axis as it pointed towards the opposite river bank. Every shoal that approached the beam demonstrated this behaviour and returned downstream. It was not possible to tell how many different shoals approached the acoustic beam or how many approaches each shoal made. However, after several days under this operating regime, a very large "super" shoal of shad containing what looked like many thousands of individuals had formed downstream of the acoustic beam. This shoal circulated about 30 m downstream and made repeated approaches to the acoustic beam without passing through it. The underwater cameras recorded just two fish breaking away from the main shoal and passing through the acoustic beam.

During this operating regime, two changes to the transmit parameters of the acoustic system were made and the results observed. The parameters changed were transmit power and ping rate. Changing the transmitted pulse rate from 20 s^{-1} down to 1 s^{-1} made no observable difference to shoal behaviour. After lowering the transmit power to give a source level of 185 dB, the shad would swim much further upstream, and closer to the acoustic beam, before turning away and swimming downstream as before.

3.2. Shad behaviour on deactivation

On the deactivation of the 200 kHz system, approaching shad shoals passed upstream through the previously ensonified area without any apparent hesitation. If the 200 kHz system was activated when a shoal was within the beam of its transducer, the individual fish demonstrated an immediate "C" body shape startle response and scattered in different directions.

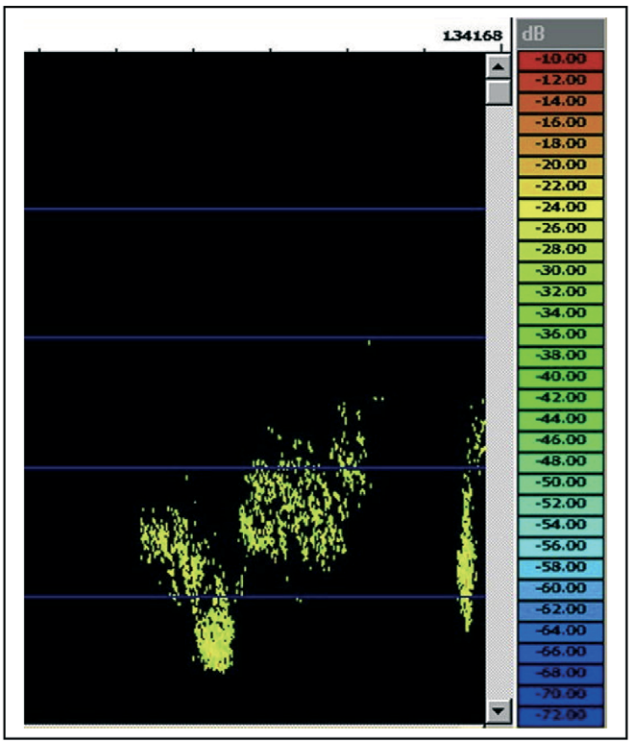

Fig. 1. Echogram display of shad shoals passing through the acoustic beam of the 420 kHz system. The horizontal lines are 5 m range intervals, representing a range of 0–25 from top to bottom. The echogram represents 4 min of data collection.

3.3. Shad behaviour during 60 min duty cycle of the 200 kHz system

During the 30 min each hour the 200 kHz system was deactivated, all shad shoal approaches observed resulted in unhindered passage. Estimations of the number of individual fish in the shoals ranged from 10 to many hundreds. The lengths of individual fish were estimated to range from 30 to 45 cm. All shad shoal approaches made during the 30 min of 200 kHz activation resulted in a failure to pass upstream.

4. Acoustic data results

The large aggregations of echoes on the echogram shown in Fig. 1 came from shoals of shad moving upstream. It was assumed that these are shad shoals because a corresponding echo pattern was not detected during activation of the 200 kHz system. These shoals were also confirmed by the underwater video camera array.

The fish were travelling too close to each other to resolve individual targets and it was not possible to obtain a count of fish by "target tracking" single shad. The fish migrated in large shoals from which only a very few individuals could be resolved by the acoustic system. However, shoals of shad could clearly be identified from the echogram and criteria developed to distinguish individual shoals so that the spatial and temporal migration patterns could be derived for shoal migration. A direction of travel for each shoal could be assigned by examining the average position of echoes in the horizontal plane. The change in average position over time as the shoal passed through the beam was used to determine positive (upstream) movement or negative (downstream) movement.

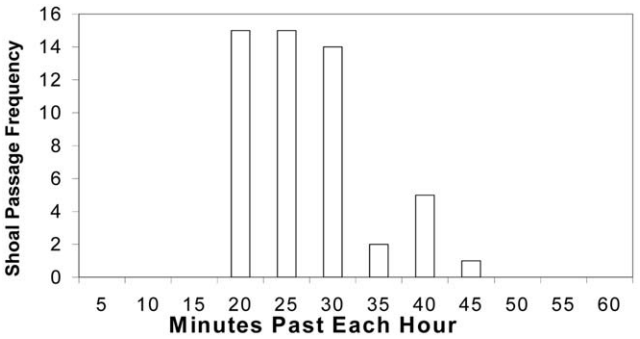

Fig. 2. Distribution of shoal passage within each hour for a 2-week period in May 2000. The 200 kHz system is active from 45 to 15 min.

The avoidance response of shad shoals to 200 kHz is clearly demonstrated in Fig. 2. The data displayed are from a 2-week sub-sample during the early part of the shad migration period. The 200 kHz system was active for half an hour from 45 min past each hour. All shoals passed the site when the 200 kHz system was deactivated, with one exception. This one exception passed upstream when the 200 kHz system was briefly shut down for maintenance.

The upstream spawning migration of twaite shad during 2000 is shown in Fig. 3, together with the subsequent downstream migration of post-spawning shoals. The river flow in cubic metres per second is also displayed.

Fig. 4 shows the diel distribution of upstream and downstream migrating shad shoals for 2000. Movement past the counter was much reduced from 21:00 to 03:00, with a peak in activity around dawn. This is a similar distribution to that found for allis shad (*Alosa alosa*) on the Dordogne in South West France by Travade et al. (1998).

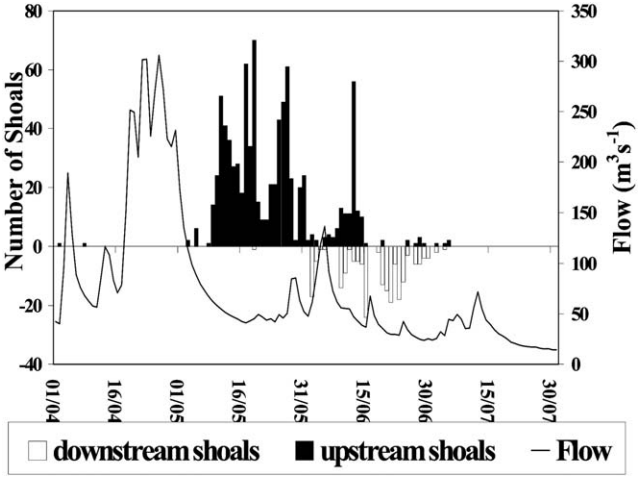

Fig. 3. The number of upstream and downstream migrating shad shoals detected by the 420 kHz acoustic system during 2000, in relation to river flow.

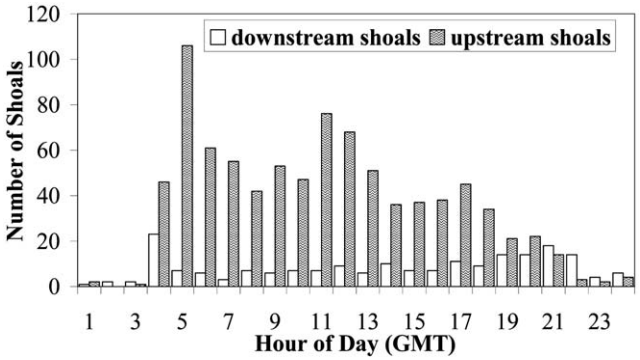

Fig. 4. Diel distribution of shoal migration.

5. Discussion

Twaite shad demonstrate a very strong avoidance reaction to a sound pulse transmitted at 200 kHz and would not pass upstream of a transducer aimed across a 30-m width of river. This behaviour remained unchanged on the variation of the ping rate. A lowering of the transmit power appeared to reduce the fishes sensitivity to the transmitted pulse. Only two fish were observed on the underwater video array to leave a shoal and pass upstream through the beam. It was not possible to tell from the video images whether these "break-away" fish were Twaite shad that may have become acclimatised to the sound or were the less abundant Allis shad, *A. alosa*, which are thought to be present in the Wye. Guillard and Colon (2000) monitored twaite shad with a 70 kHz acoustic system on the River Rhône in France with no reported avoidance reaction.

Twaite shad behaviour on the River Wye appeared unaffected by a sound pulse with similar characteristics transmitted at 420 kHz. Shoals of shad were observed passing through the acoustic beam without hesitation. This allowed them to be detected and enumerated by the acoustic system.

Although it was not possible to obtain a count of fish by "target tracking" single shad, shoals could be counted and spatial and temporal distribution patterns derived. On the Wye there were no other fish species shoaling at this time of year so species apportionment of these shoals was not an issue. However, it would be possible to apportion acoustic shoal or individual counts as either clupeid or not clupeid based on the difference in the number of events counted when the 200 kHz system was activated compared to periods of deactivation. In this way, the dual frequency technique could be used to distinguish and enumerate clupeids sensitive to ultrasound in situations where other shoaling fish species are present.

Although two shoals of shad were first recorded migrating upstream in early April, the main run did not begin until the 10th May when flows had dropped to 50 $m^3\ s^{-1}$. When river flows increased to over 100 $m^3\ s^{-1}$, there was a marked decrease in upstream migration. Although water temperatures were not recorded, they would have been rising during May as the river flow dropped. Boisneau et al. (1985) and Guillard and Colon (2000) have reported positive correlation of shad migration with water temperature for *A. alosa*. Downstream migration was first recorded on 1st June, with the last shoal being detected on 4th July. Upstream migrating shoals continued to be detected into early July.

Very little upstream migration occurred during the hours of darkness (22:00–03:00), although the peak in downstream movement corresponded to decreasing light levels in the evening. Similar patterns of movement have been reported for the American shad, *A. sapidissima*, from observations made by underwater video cameras (Haro and Kynard, 1997).

Echo integration, as used in the marine environment to estimate shoal densities, was not considered applicable to data collected from a shallow river using a horizontally aimed transducer as many of the key assumptions required for the echo integration technique do not appear to hold true under these circumstances. However, enumeration of shoals and assessment of their run timing characteristics is possible.

Acknowledgements

The authors would like to thank the Environment Agency Wales and the Country side Council for Wales for their support of this work.

References

Astrup, J., Møhl, B., 1993. Detection of intense ultrasound by the cod *Gadus morhua*. J. Exp. Biol. 182, 71–80.

Boisneau, P., Mennesson, C., Baglinière, J.L., 1985. Observations sur l'activité de migration de la grande alose, *Alosa alosa* L, en Loire (France). Hydrobiologia 128, 277–284.

Dunning, D.J., Ross, Q.E., Geoghegan, P., Reichle, J.J., Menezes, J.K., Watson, J.K., 1992. Alewives avoid high-frequency sound. North Am. J. Fish. Manage. 12, 407–416.

Guillard, J., Colon, B., 2000. First results on migrating shad *Alosa fallax* and mullet *Mugil cephalus* echocounting in a lock on the Rhône River (France) using a split-beam sounder, and relationships with environmental data and fish caught. Aquat. Living Resour. 13, 327–330.

Haro, A., Kynard, B., 1997. Video evaluation of passage efficiency of American shad and sea lamprey in a modified ice harbour fishway. North Am. J. Fish. Manage. 17, 981–987.

Hawkins, A.D., Johnstone, A.D.F., 1978. The hearing of the Atlantic salmon, *Salmo salar*. J. Fish. Biol. 13, 655–673.

Mann, D.A., Higgs, D.M., Tavolga, W.N., Souza, M.J., Popper, A.N., 2001. Ultrasound detection by clupeiform fishes. J. Acoust. Soc. Am. 109, 3048–3054.

Nestler, J.M., Goodwin, R.A., Cole, T.M., Degan, D., Dennerline, D., 2002. Simulating movement patterns of blueback herring in a stratified Southern impoundment. Trans. Am. Fish. Soc. 131, 55–69.

Popper, A.N., 2000. Hair cell heterogeneity and ultrasonic hearing: recent advances in understanding fish hearing. Phil. Trans. Soc. London Ser. B Biol. Sci. 355, 1277–1280.

Popper, A.N., Carlson, T.J., 1998. Application of sound and other stimuli to control fish behaviour. Trans. Am. Fish. Soc. 127, 673–707.

Ross, Q.E., Dunning, D.J., Menezes, J.K., Kenna, M.J., Tiller, G., 1996. Reducing impingement of alewives with high frequency sound at a power plant intake on Lake Ontario. North Am. J. Fish. Manage. 16, 548–559.

Travade, F., Larinier, M., Boyer-Bernard, S., Dartiguelongue, J., 1998. Performance of four fish pass installations recently built on two rivers in South West France. In: Jengwirth, M., Schmutz, S., Weiss, S (Eds.), Fish Migration and Fish By-pass Channels. Fishing News Books.

Available online at www.sciencedirect.com
SCIENCE DIRECT®
Aquatic Living Resources 16 (2003) 317–324
Aquatic Living Resources
www.elsevier.com/locate/aquliv

Vertical migration and dispersion of sprat (*Sprattus sprattus*) and herring (*Clupea harengus*) schools at dusk in the Baltic Sea

L.A. Fredrik Nilsson [a,*], Uffe Høgsbro Thygesen [b], Bo Lundgren [c], Bo Friis Nielsen [a], J. Rasmus Nielsen [b], Jan E. Beyer [b]

[a] *Informatics and Mathematical Modelling, Technical University of Denmark, Building 321, 2800 Kgs. Lyngby, Denmark*
[b] *Department for Marine Fisheries Research, Danish Institute for Fisheries Research, Charlottenlund Slot, 2920 Charlottenlund, Denmark*
[c] *Department for Marine Fisheries Research, Danish Institute for Fisheries Research, North Sea Centre, 9850 Hirtshals, Denmark*

Accepted 10 January 2003

Abstract

In populations of herring (*Clupea harengus*) or sprat (*Sprattus sprattus*), one typically observes a pattern of schools forming at dawn and dispersing at dusk, usually combined with vertical migration. This behaviour influences interactions with other species; hence a better understanding of the processes could contribute to deeper insight into ecosystem dynamics. This paper reports field measurements of the dispersal at dusk and examines two hypotheses through statistical modelling: that the vertical migration and the dissolution of schools is determined by decrease in light intensity, and that the dissolution of schools can be modelled by diffusion, i.e. active repulsion is not required. The field measurements were obtained during 3 days in March at one location in the Baltic Sea and included continuous hydroacoustical monitoring, trawl samples, and hydrographical CTD data. Echogram patterns were analysed using the school detection module in Echoview® and local light intensities were calculated using a model for surface illuminance. The data and the analysis support that schools migrate upwards during dusk, possibly trying to remain aggregated by keeping the local light intensities above a critical threshold, that schools initiate their dissolution when ambient light intensity drops below this critical threshold, and that fish subsequently swim in an uncorrelated random walk pattern.

Keywords: Random walk; Dispersion of schools; Light; Clupeids; Baltic

1. Introduction

When collecting hydroacoustic data in the Baltic, one commonly sees a fast change in the echogram structure at dawn and dusk. The day situation is often characterized by aggregations of clupeids close to the bottom, whereas there are disperse targets in the whole water column during the night. The pattern is similar to that of herring in the North Sea (Blaxter and Parrish, 1965; Blaxter, 1985), however, in the Baltic, a large proportion of the schools do not migrate vertically—they disperse in the initial phase of the transition close to the bottom. It is possible that most of the predator–prey interactions take place during the twilight period (Major, 1977; Clark and Levy, 1988); the swift changes seen on the echograms may be an indication of this. There are indications that both herring and sprat, and their main predator, cod, are feeding during dusk and dawn (Blaxter and Parrish, 1965; Adlerstein and Welleman, 2000) and consequently these periods could be very important for the population dynamics. This motivates an investigation of the spatial structure and how it changes during dusk and dawn.

The dominant species of fish in the Baltic Proper are sprat (*Sprattus sprattus*), herring (*Clupea harengus*), cod (*Gadus morhua*), and flounder (*Platichtys flesus*). Due to the relative scarcity of species, especially among schooling fishes, the Baltic is a well-suited study area for the transition between schooling and dispersed state in clupeids, since it is relatively easy to know what species one is studying and since the possible number of interactions between different species is few.

While there is some consistency as to where and when schools can be found, it remains much less clear why and how the transitions occur. One specific question is if school-

* Corresponding author.
E-mail address: afn@imm.dtu.dk (L.A.F. Nilsson).

doi:10.1016/S0990-7440(03)00039-1

ing fish actively spread out at dusk, or if schools simply diffuse as their members cease to maintain the structure. This article approaches this question by estimating the time constant of dissolution, assuming passive diffusion, and comparing with observed transition times. Another open question is how directly the dispersal is related to the decrease in light. We examine this issue by estimating the local light intensity at the position of observed schools.

2. Materials and methods

2.1. Data sampling and analysis

Data were collected during a survey with R/V Dana 12–14 March 2002. Two Simrad EY500 split-beam echosounders were continuously recording at 38 and 120 kHz, respectively. The hydroacoustical data were stored electronically. The transducers were hull mounted, and the echosounders were calibrated using standard procedures (Foote et al., 1986). Fish were collected using a TV3-trawl; it was used as a bottom trawl except for night hauls on March 14, when it was used for pelagic hauls. Hydrographical data were collected several times a day with a Seabird SBE911PLUS CTD equipped with a light sensor (Biospherical/Licor) that measures the photosynthetically active radiation (PAR). The collection of fish was performed during both day and night on approximately the same site.

The location at approximately 16° 20' E, 55° 45' N was chosen to be representative of the Bornholm basin with respect to species composition and depth range; the depth at this location was 55–65 m. The fish caught were minced and afterwards discarded into the sea at a dumping site 5 nmi away downstream in order to avoid disturbances to the study site. Steaming speed to and from the dumping site was 12 knots, otherwise the ship was operated at approximately 3 knots in order to make the acoustical data independent of whether the ship was trawling or not. The current direction was registered using an acoustic Doppler current profiler.

The hydroacoustical data were analysed using the Echoview software, version 2.20. The lower threshold for acceptance of volume backscattering values, S_v was set to –60 dB for echo-integration and school-detection procedures. The school detection parameters were set heuristically and the distances were based on GPS positions. The settings for the 38 kHz sounder were (120 kHz settings within parentheses): minimum school length 2 (1.20) m, minimum school height 2 (1.20) m, minimum connected height 1.5 (0.6) m, maximal vertical linking distance 3 (2) m, maximal horizontal linking distance 3 (7) m.

Both the EY500 and the Echoview software have algorithms for detecting the bottom. However, due to bad weather with high swell on March 14, the bottom identification did not perform well. Improved bottom values for pings were identified using a Matlab program searching for the maximum increase of echo level between samples near the expected depth obtained from nearby pings. Furthermore, to compensate for ship movements due to the swell, a C++ program was used to produce new raw data files in which data in relevant telegrams were shifted up or down in order to get bottom points aligned with a smoothed bottom line obtained by a moving average with Gaussian weights. The end result was a smoother bottom (see Fig. 1) and echogram patterns more comparable with the days with calm weather. We did not correct for bubbles under the ship. Regions that evidently were affected by this phenomenon were excluded from the analysis. Data from 0.5 m above bottom to 15 m below surface were included in the echo-integration and school-detection procedures. The upper limit was chosen since observed fish densities were very low above this depth and in order to exclude bubble noise on March 14.

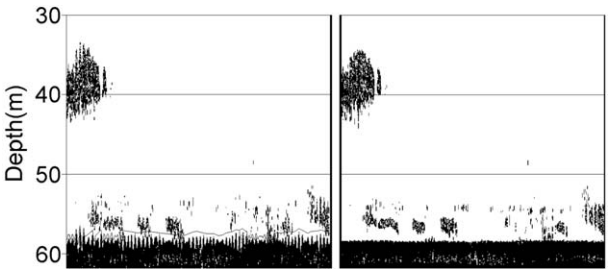

Fig. 1. Detail of echogram from March 14. Bottom is unsmoothed in the left panel, smoothed in the right.

The ship is equipped with a Licor PAR light sensor placed on the top of the ship, but its sensitivity was insufficient for measuring light intensities at dawn and dusk. Instead the light variations for twilight were estimated using a model by Janiczek and De Young (1987), which gives surface illuminance given time, date, geographical position and cloudiness. The cloudiness is given as four factors, corresponding to:

a Average clear sky, less than 70% of the sky covered by (scattered) clouds; the direct rays of the Sun or Moon are unobstructed relative to the location of interest.
b The Sun or Moon is easily visible but direct rays are obstructed by thin clouds.
c The direct rays of the Sun or Moon are obstructed by average clouds.
d Dark stratus clouds cover the entire sky (rare).

In the computer program, these conditions a–d correspond to dividing the calculated illuminance with a factor 1, 2, 3, 10, respectively. The model is quite crude (see Fig. 2). Since the sky was clear for most of the time, we have chosen to use the factor 1 or condition a.

The attenuation of light by water was estimated from the Seabird PAR data using a linear regression of the logarithm of light intensity on depth:

$$\ln I(z) = \ln I(0) - Kz \quad (1)$$

where $I(z)$, $I(0)$ are the light intensities at z and 0 m depth, respectively, and K is the attenuation coefficient. K was found to vary between 0.131 and 0.167 m^{-1}. We chose to proceed with a value of 0.16 m^{-1}, which is higher than the average value for the layer of interest, arguing that the rays of light during dusk come from a more or less horizontal light source.

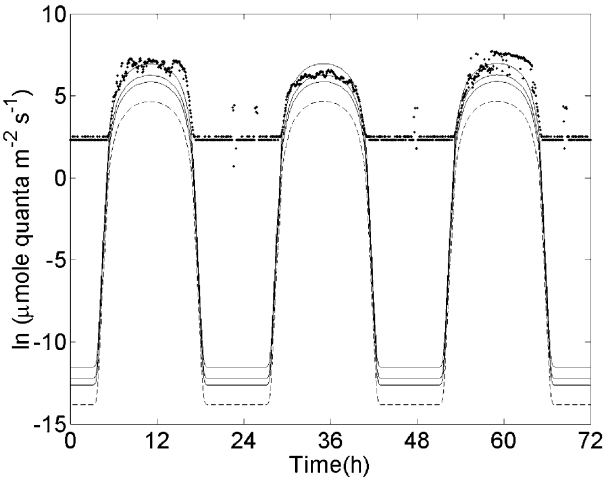

Fig. 2. Plot of logarithmic light intensities ln(µmol quanta s^{-1} m^{-2}). The dots are the measurements from the quantum light meter on R/V Dana. The black lines correspond to the four different cloud situations in the model for illumination (uppermost—clear, lowest—sky covered with stratus clouds). Horizontal scale is hours.

The attenuation is somewhat higher in the layer 0–10 m but we do not take this into account, since the relative effect of this is the same for all days and since only data below 15 m were analysed.

The surface illuminance from the model is given in lux, but the attenuation constant is based on PAR. We choose to use the factor 0.01953 µmol quanta s^{-1} m^{-2} lux^{-1} (Brock, 1981) to convert illuminance to surface PAR irradiance, assuming a standard daylight spectral distribution.

2.2. Migration process in relation to light levels

For every ping, the depth at which the local light intensities would correspond to 0.01, 0.1, 1 lux, respectively, were calculated using the daylight model and the attenuation coefficient. These light levels were chosen a priori since it has been reported that schooling ceased in this interval (Blaxter and Parrish, 1965; Iida and Mukai, 1996). The data were then displayed in the echograms as lines of equal irradiance. The schools followed the lines (see Fig. 3). With the Echoview school-detection module, we obtained the mean depth of a school and the time at which the school was recorded. In the same way as above, time was used to calculate the light intensity at the mean depth of the school. For data well within the transition period (17.25–18 UMT), we tested the model:

$$Y_{ij} = \alpha_i + \beta_i X_{ij} + \varepsilon_{ij} \quad (2)$$

where Y_{ij} is the natural logarithm of the light intensity at the depth of the centre of the jth school at the ith day, α_i, β_i are constants for day i, and X_{ij} is the depth of the jth school on day i, and ϵ_{ij} are independent and identically distributed normal variables with zero mean and variance σ^2. The log-transformation was necessary to meet the standard assumptions for linear regression.

2.3. Modelling the dissolution of schools by diffusion

This section constructs a model of the diffusion of schools and proposes three different time constants describing the duration of the process. With all three approaches, the number of fish in a typical school is Poisson distributed with mean $\bar{N}$ and the sizes of different schools are stochastically independent. At the starting point (dusk), all fish in the school are positioned at a single point in the plane. Then, instantly, all social forces are removed and each fish performs an independent random walk. The difference between the models is in how schools are placed at the starting point, and which criterion is used for the schools to have dissolved.

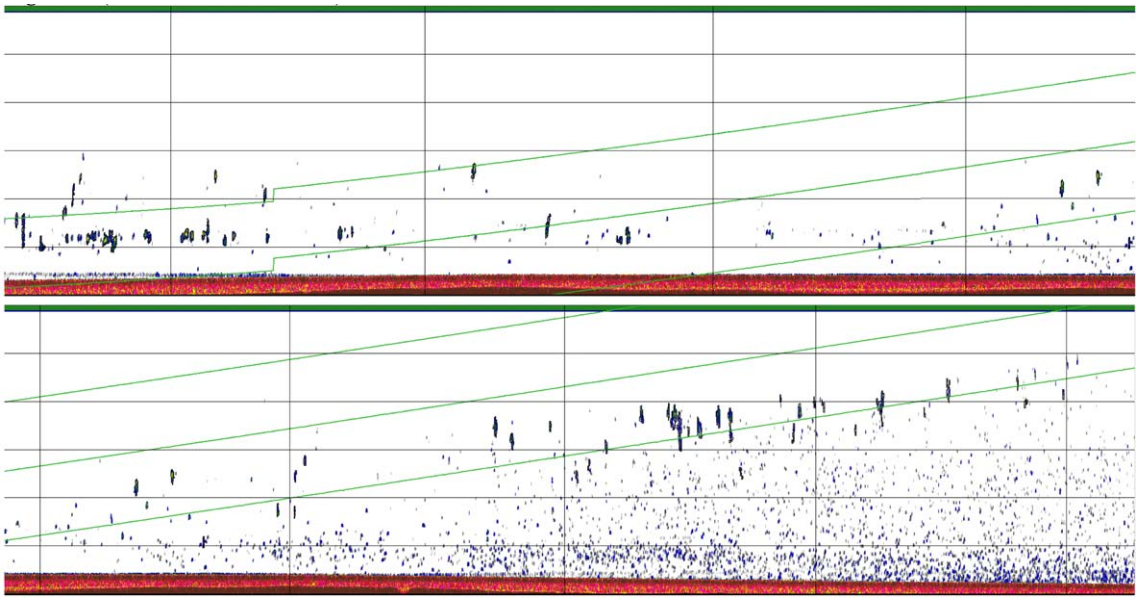

Fig. 3. The vertical migration of schools and dissolution at dusk on March 13. The three green parallel lines that rise from left to right are lines of equal light intensity. The step in the lines (left, top) is due to sunset. Distance between horizontal lines are 10 m and 0.5 nmi between vertical lines.

2.3.1. Dispersion from regularly spaced schools

At time $t = 0$ (dusk), a school is located at each node in a regular two-dimensional grid with grid length L. At times $t > 0$, each individual fish performs a random walk in two dimensions with intensity σ^2. The expected time until an individual fish has displaced itself a distance Δx from its starting point is (e.g. Berg, 1992).

$$\frac{\Delta x^2}{2\,\sigma^2} \tag{3}$$

If we insert $L/2$ for Δx, then we obtain roughly the time until the individual is halfway between two school centres; hence we cannot determine from which school the individual originated. Based on this argument, we would find that the time to dissolution of the schools is

$$\frac{1}{8}\frac{L^2}{\sigma^2} \tag{4}$$

Although this argument is somewhat sketchy, we shall see below that more elaborate modelling leads to similar answers.

2.3.2. Statistical detection of school structure

Using the same model as above, the individual fish constitute a Poisson point process (Stoyan et al., 1995) which is fully specified by its density $\rho(x,y,t)$. This density satisfies the partial differential equation (e.g. Berg, 1992):

$$\frac{\partial \rho(x, y, t)}{\partial t} = \frac{1}{2}\,\sigma^2\,\nabla^2\,\rho(x, y, t) \tag{5}$$

and can be expressed in terms of its Fourier series (Farlow, 1983):

$$\rho(x, y, t) = \sum_{k=-\infty}^{\infty}\sum_{l=-\infty}^{\infty} A_{kl}(t)\,\exp\left(i2\pi\,\frac{kx + ly}{L}\right) \tag{6}$$

Here, the coefficients $A_{kl}(t)$ are determined by the initial conditions, and are equal to:

$$A_{kl}(t) = \frac{\bar{N}}{L^2}\exp\left(-\frac{1}{2}\,\sigma^2\left(\frac{2\pi}{L}\right)^2(k^2 + l^2)\,t\right) \tag{7}$$

The shape of the solution is quickly dominated by the smallest non-zero eigenvalue, $-1/2\sigma^2\,(2\pi\,L)^2$, obtained with wave numbers $k^2 + l^2 = 1$.

At time T, we hypothetically sample two square regions, each of area $L^2/4$. One area, A, is centred around $(x,y) = (0,0)$ so that the initial position of the school is in the dead centre. The other, B, is centred at $(x,y) = (L/2,L/2)$ i.e. the point in space furthest away from the schools.

The number of fish found in region A, N_A, is then Poisson distributed with mean EN_A:

$$EN_A = \int_A \rho(T)\,\mathrm{d}x\,\mathrm{d}y = \sum_{k,l} A_{kl}(T)\,H_A(k, l) \tag{8}$$

where

$$H_A(k, l) = \int_A \exp\left(2\,\pi i\,\frac{kx + ly}{L}\right)\mathrm{d}x\,\mathrm{d}y = f(k)\,f(l) \tag{9}$$

and

$$f(k) = \int_{-L/4}^{L/4} \exp\left(2\,\pi i\,\frac{kx}{L}\right)\mathrm{d}x \tag{10}$$

We have that $f(k)$ is equal to $L/2$ when k is zero, otherwise it is $\frac{L}{2\,\pi i k}\left(\exp\left(\frac{\pi}{2}\,ik\right) - \exp\left(-\frac{\pi}{2}\,ik\right)\right)$. The latter expression is equal to 0 when k is even and non-zero. When k is odd, we have $f(k) = L/(\pi k)$, if $k = ..., -11, -7, -3, 1, 5, 9,...$, and $f(k) = -L/(\pi k)$, if $k = ..., -9, -5, -1, 3, 7, 11,....$ Now, focusing on the long-term behaviour, we consider only the lowest eigenvalue obtained with $k^2 + l^2 = 1$. Then

$$EN_A \approx \frac{L^2}{4}A_{0,0}(T) + \frac{L^2}{2\pi}\,(A_{0,1}(T) + A_{1,0}(T) + A_{0,-1}(T) + A_{-1,0}(T)) = \frac{\bar{N}}{4} + \frac{2\,\bar{N}}{\pi}\exp\left(-\frac{\sigma^2}{2}\left(\frac{2\pi}{L}\right)^2 T\right) \tag{11}$$

Correspondingly,

$$EN_B \approx \frac{L^2}{4}A_{0,0}(T) - \frac{L^2}{2\pi}\,(A_{0,1}(T) + A_{1,0}(T) + A_{0,-1}(T) + A_{-1,0}(T)) = \frac{\bar{N}}{4} - \frac{2\,\bar{N}}{\pi}\exp\left(-\frac{\sigma^2}{2}\left(\frac{2\pi}{L}\right)^2 T\right) \tag{12}$$

The criterion for the schools to have dissolved is that the $N_B > N_A$ with a certain probability $P = 1/2 - \alpha$. Approximating the Poisson distributions with Gaussians, we find

$$N_B - N_A \sim N\left(\frac{4\,\bar{N}}{\pi}\,e^{-\frac{\sigma^2}{2}\left(\frac{2\pi}{L}\right)^2 T}, \frac{\bar{N}}{2}\right) \tag{13}$$

And P is the probability of $N_B - N_A > 0$ which can then be approximated as

$$P = \frac{1}{2} - \alpha = \Phi\left(-\frac{4\,\sqrt{2\,\bar{N}}}{\pi}\,e^{-\frac{\sigma^2}{2}\left(\frac{2\pi}{L}\right)^2 T}\right) \tag{14}$$

where Φ is the standard Gaussian distribution function. Equivalently,

$$T = -\frac{L^2}{2\pi^2\,\sigma^2}\ln\left(\frac{\pi}{4\,\sqrt{2\,\bar{N}}}\,q\left(\frac{1}{2} + \alpha\right)\right) \tag{15}$$

where $q(1/2+\alpha)$ is the $(1/2+\alpha)$-quantile of the standard Gaussian distribution.

According to this expression for T, the natural time scale of the dissolution process is L^2/σ^2. In this time unit, we may plot T as a function of α for different values of N. This is done in Fig. 4. The most striking feature of the plot is the plateau, implying a fairly rapid transition from high levels of aggregation ($\alpha \approx 0.4$) to low levels of aggregation ($\alpha \approx 0.1$). This is comforting since it implies that the estimated transition time is not very sensitive to the exact choice of α, i.e. the critical level of aggregation. With this approach, the dependence on $\ln N$ is also quite natural; more fish in the school makes it easier to detect differences when they exist.

2.3.3. Dispersion from randomly placed schools

This model is a Poisson cluster model, using the terminology of stochastic geometry (Stoyan et al., 1995): schools are placed randomly in the plane according to a Poisson point process in 2D with intensity λ_s. To obtain the same density as in the previous model, we must have $\lambda_s L^2 = 1$. As before, school sizes are independent and identically Poisson distributed with mean $\bar{N}$, all fish within a school are co-located at

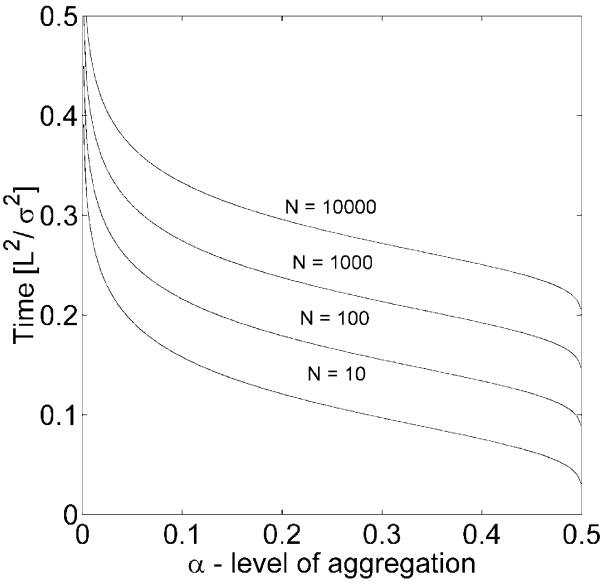

Fig. 4. Time against level of aggregation.

the school centre at time $t = 0$, and for time $t > 0$, each individual performs an independent Brownian motion with intensity σ^2.

At some later time t, the stochastic geometry becomes a Cox process, i.e. a conditional Poisson point process. To be specific, given the school centres, the density of the fish originating from the particular school is a Gauss bell, and the total density is the superposition of all these Gauss bells.

For a Poisson process, we can define the entropy as

$$I = -E \ln \rho(x, y) \tag{16}$$

i.e. minus the logarithmic density at a "typical point".

If only one school is present at position $(x,y) = (0,0)$, then at time t, individual fish will be distributed according to a Poisson process with density

$$\rho(x, y, t) = \frac{\bar{N}}{2\pi\sigma^2 t} e^{-\frac{1}{2}\frac{x^2+y^2}{\sigma^2 t}} \tag{17}$$

leading to an entropy

$$I = 1 + \ln 2\pi + \ln \sigma^2 t - \ln \bar{N} \tag{18}$$

where $\sigma^2 t$ is the variance in the 2D Gauss bell at time t. For low values of t, the schools do not interact and the same expression holds for the Poisson cluster model. As t grows, the entropy will gradually approach its limit in which the density is constant

$$\rho_\infty = \bar{N}\lambda_s \tag{19}$$

which leads to an entropy of $-\ln \bar{N}\lambda_s$. One way of assessing the time duration of the transition is to assume that the initial growth of entropy continues and then report the time where this entropy reaches the steady-state value. We find:

$$1 + \ln 2\pi + \ln \sigma^2 t - \ln \bar{N} = -\ln \lambda_s - \ln \bar{N} \tag{20}$$

or

$$t = \frac{1}{2\pi e \lambda_s \sigma^2} \tag{21}$$

2.4. Estimation of parameters

The inter-school distance was obtained with Echoview's school-detection module. Mean target strength was calculated from the TS relation (Foote, 1987) for clupeids and the length-distribution of caught herring and sprat. This was used to calculate the number of fish per school, assuming that schools could be described as vertical cylinders. The mean school area is (MacLennan and Simmonds, 1992) $\bar{A} = \frac{3\pi}{8}\bar{L}_0^2$, where $\bar{L}_0^2$ is the mean of squared length of schools.

3. Results

For the bottom and pelagic hauls, the catch consisted of more than 70% and 97% of clupeids, respectively (see Table 1). The size distributions were the same for bottom and pelagic hauls for sprat and herring (Fig. 5); the schools on the echograms are most likely sprat and herring.

The model for the relation between depth of school centres and local light conditions was significantly better at describing data than $Y_{ij} = \alpha_i$, i.e. that the logarithm of the light was independent of depth ($P < 0.002$). The model could be reduced to a model with a common slope; all β_i are equal (see Fig. 6). The model could not be reduced more, e.g. to zero slope or a common intercept. The residual plots did not indicate that the model was inappropriate. Since the error variance was high, the part of the variation that could be explained by the model was rather low, 0.22.

The distance between schools was found to be 70–200 m, the number of clupeids per school was 400–900, and the mean area was in the range 120–220 m^2.

Table 1
The weight and percentage of the species caught in the bottom hauls

Species	Common name	Fraction in bottom hauls	Fraction in pelagic hauls
Sprattus sprattus	Sprat	0.636	0.798
Clupea harengus	Herring	0.094	0.177
Platichtys flesus	Flounder	0.011	0
Gadus morhua	Cod	0.257	0.025
	Other species	0.002	≤ 0.001
Total weight (kg)		4387	914

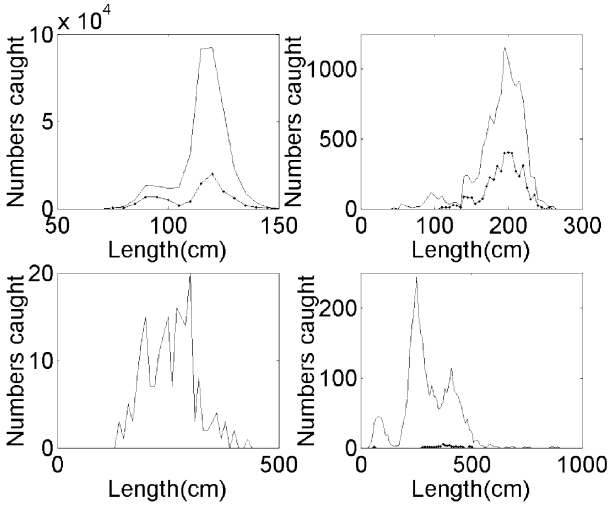

Fig. 5. The total numbers caught '—' in 20 hauls within a certain length-class of the dominant species sprat, herring, flounder and cod (top left, top right, bottom left, bottom right). The line joining dots '•—' shows fish caught with pelagic hauls (three hauls).

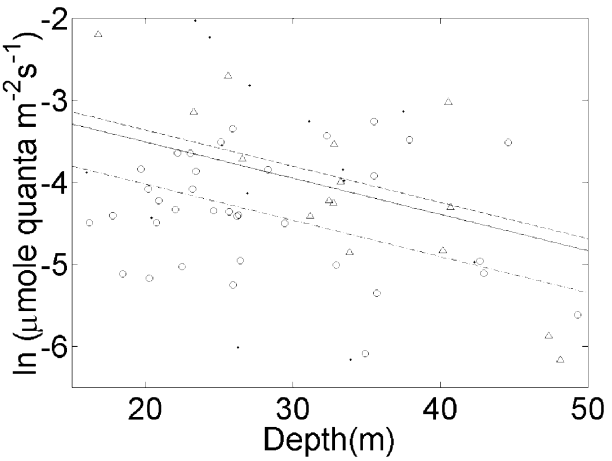

Fig. 6. Relationship between logarithm of light intensity at school centre and depth of school centre for 12–14 March 2002. Data from 12 March '•', 13 March 'o' and 14 March '△'. Fitted model for 12 March '—', 13 March '— —', and 14 March ' — —'.

Comparing the three suggested time constants of the transition, only the second time constant is based on statistical identification of school structures and hence grows with the number of fish in a typical school. Except for this difference, the time constants scale identically. Furthermore, for a school size between 10 and 10 000 fish, the estimated time constants are all of the same order of magnitude, i.e. between 0.05 and 0.3, measured in the time unit L^2/σ^2. In summary, a useful time constant of the dissolution process is about 0.1 L^2/σ^2 and after 0.3 L^2/σ^2, it is fair to say that the process has ceased.

To estimate L^2, we note that the average distance between schools during the daytime is 70–200 m. Since the width of the transect at the bottom is 7–8 m (7° beam width), this implies a school density of maximum one school per 490 m^2 and minimum one school per 1600 m^2.

To obtain a rough estimate of the diffusivity, we assume a swimming speed of one body length per second and a body length of 0.1 m, and a relaxation time (time between turns) of the swimming direction of 10 s. This yields $\sigma^2 = 0.1$ m^2 s^{-1} (Berg, 1992). The fraction $\frac{L^2}{\sigma^2}$ is then in the interval between 4900 and 16,000 s. Multiplying the former with 0.1 and the latter with 0.3, we obtain that the time for schools to dissolve is in the range between 8 and 80 min.

These models all assume that the fish in a school at time $t = 0$ are located at the same point. In reality, the size of a school is measurable compared to the typical distance between schools and thus the time constants should be seen as upper bounds.

4. Discussion

Some authors (Weston and Andrews, 1990; Fréon et al., 1996) have proposed that the dissolution, or expansion of schools may be due to a diffusion process, but not specified the underlying mechanism. In this paper, a simple model for the dissolution of schools is proposed, where the fish in a school disperse as uncorrelated random walkers. The models presented are based on few parameters and should be easy to use to compare with data in different regions. The estimated transition times are comparable to those observed, indicating that active dispersal is not required to explain the observed change in the pattern. Iida and Mukai (1995) obtained similar values for the dispersion of Kokkanee schools, 50 min; whereas Fréon et al. (1996) showed that, in Senegalese waters, the transition took several hours, but the expected values depend on the local conditions.

The results given by Orlowski (2001) suggest that there is a slower transition in the Baltic at dusk for herring and sprat that takes approximately 4 h; however that result is based on S_v per 30 min, not school identification. The slower transition could be explained with planktonic prey emerging from the bottom at dusk and that the fish dispersing close to the bottom are hungry enough to risk feeding and dispersing where the predation risk probably is very high since cod are close to the bottom. If the planktonic prey are rising slowly, then may be the dispersed fish close to the bottom follow their prey toward the surface, which would give rise to a slower transition phenomenon. This leads to an anisotropy that may give different time scales depending on whether the solution is determined in the horizontal or in the vertical plane. In a similar approach to Orlowski (2001), Giannoulaki et al. (1999) obtained a transition for sardines in the northern Aegean Sea that took several hours; it may be that the averaging done using S_v and the modelling of the vertical migration with relatively low order trigonometric polynomials give longer dispersion times.

Schools follow roughly the lines of equal light intensity, but with high variation. The fact that the schools rise faster than the lines of equal irradiance (i.e. $\beta < 0$) is difficult to explain. However, it should be noted that the differences

between the light intensities at the end points of the fitted lines are very small and perhaps the estimated slope β is an artefact of the methodology. In any case, the slope β being significantly different from 0 in the statistical sense should not overshadow the observation that schools appear to remain at similar light levels. It is encouraging that the models catch this feature despite the simplicity in their assumptions and the uncertainty on the parameters. The log-transformation of the light data makes biological sense, since the response of eyes is approximately logarithmic.

The fact that the model could not be reduced to a common intercept may be due to real differences between days or that the cloudiness factor in the model for the light illuminance is the same for the different days, while the light levels seem to differ between days (see Fig. 2).

The high variation in the results is partly due to few measurements. However, diurnal vertical migration is highly variable (e.g. Blaxter and Parrish, 1965; Appenzeller and Legget, 1995); it can vary over season, and is probably dependent on tides, the physiological status of the fish as well as predators (Blaxter and Parrish, 1965).

Appenzeller and Leggett (1995) showed that the modus and the upper 95 percentile of the biomass distribution of rainbow smelt (*Osmerus mordax*) closely follow the lines of constant local light intensities, whereas the lower 95 percentile did so to a lesser extent. The range of the vertical distribution was narrower during day than night. They also noted that the smelt formed dense schools during day, which dispersed during night. Based on our results, it is possible that the widening of the distribution is due to schools dissolving, and that the upper parts that followed light levels more closely were schools rising.

Future work should be aimed at describing the internal and external state of the schooling fish in the Baltic. Is the crepuscular period the time at which the clupeids are eating, being eaten, neither or both? Stomach data of both clupeids and cod with high temporal resolution could help to answer that question. If the dispersion pattern of a school were studied with sonar, this could possibly give the local swimming speeds of the fish, and a better overview of the process. In addition, it would be interesting to follow the individual fish during the dispersal of schools in laboratory tanks, such as was done by Blaxter and Parrish (1965). With modern tracking techniques, it should be able to obtain more information about the behaviour and motion of the individual fishes, and it might be important and informative to incorporate the predatory behaviour of cod in relation to clupeids, since predation is not a static risk but a dynamic process dependent on prey behaviour (Lima, 2002).

5. Conclusion

Schools of herring and sprat tend to follow lines of equal light intensity when they migrate towards the surface at dusk in the Baltic, whereas this is not the case for the dispersing fish. In contrast to other studies showing the phenomenon that migrating fish follow lines of equal light intensity, we have found that a large part of the schooling fish dispersed close to the bottom. This causes a widening of the depth distribution, which may be attributed to differences in hunger or some other internal factor. Three different measures for the time until schools are dispersed are presented, these agree quite well with the time-scales viewed on the echograms. The times depend on few parameters and should be useful in comparisons.

Acknowledgements

We wish to thank the crew of the R/V Dana for excellent work and the DIFRES personnel for processing the fish. The research was supported by the SLIP research school under the Danish Network for Fisheries and Aquaculture Research (www.fishnet.dk) financed by the Danish Ministry for Food, Agriculture and Fisheries and the Danish Agricultural and Veterinary Research Council. The work is part of a larger project ‘Development of improved models of fisheries impact on marine fish stocks and ecosystems’ also funded by the Danish Ministry for Food, Agriculture and Fisheries.

References

Adlerstein, S.A., Welleman, H.C., 2000. Diel variation of stomach contents of North Sea cod (*Gadus morhua*) during a 24-h fishing survey: an analysis using generalized additive models. Can. J. Fish. Aquat. Sci. 57, 2363–2367.

Appenzeller, A.R., Leggett, W.C., 1995. An evaluation of light-mediated vertical migration of fish based on hydroacoustic analysis of the diel vertical movement of rainbow smelt (*Osmerus mordax*). Can. J. Fish. Aquat. Sci. 52, 504–511.

Berg, H.C., 1992. Random Walks in Biology. 2d ed., Princeton Universtity Press, Princeton.

Blaxter, J.H.S., 1985. The herring: a successful species? Can. J. Fish. Aquat. Sci. 42 (Suppl. 1), 21–30.

Blaxter, J.H.S., Parrish, B.B., 1965. The importance of light in shoaling, avoidance of nets and vertical migration by herring. J. Cons. Perm. Int. Explor. Mer 30, 40–57.

Brock, T.D., 1981. Calculating solar radiation for ecological studies. Ecol. Model. 14, 1–19.

Clark, C.W., Levy, D.A., 1988. Diel vertical migrations by juvenile sockeye salmon and the antipredation window. Am. Nat. 131, 271–290.

Farlow, S.J., 1983. Partial Differential Equations for Scientists and Engineers. John Wiley & Sons, New York (Reprinted by Dover, 1992).

Foote, K.G., 1987. Fish target strengths for use in echointegrator surveys. J. Acoust. Soc. Am. 82, 981–987.

Foote, K.G., Aglen, A., Nakken, O., 1986. Measurements of fish target strength with a split-beam echosounder. J. Acoust. Soc. Am. 80, 612–621.

Fréon, P., Gerlotto, F., Soria, M., 1996. Diel variability of school structure with special reference to transition periods. ICES J. Mar. Sci. 53, 459–464.

Giannoulaki, M., Machias, A., Tsimenides, N., 1999. Ambient luminance and vertical migration of the sardine *Sardina pilchardus*. Mar. Ecol. Prog. Ser. 178, 29–38.

Iida, K., Mukai, T., 1995. Behavior of Kokanee *Oncorhynchus nerka* in Lake Kuttara observed by echo sounder. Fish. Sci. 61, 641–646.

Janiczek, P.M.J., De Young, J.A., 1987. Computer programs of Sun and Moon illuminance with contingent tables and diagram. Circ. US Nav. Obs. 171, 1–131.

Lima, S.L., 2002. Putting predators back into behavioural predator–prey interactions. Trends Ecol. Evol. 17, 70–71.

MacLennan, D.N., Simmonds, E.J., 1992. Fisheries Acoustics. Chapman and Hall, London.

Major, P.F., 1977. Predator–prey interactions in schooling fishes during periods of twilight: a study of the Silverside *Pranesus insularum* in Hawaii. Fish. Bull. 75 (2), 415–426.

Orlowski, A., 2001. Behavioural and physical effect on acoustic measurements of Baltic fish with a diel cycle. ICES J. Mar. Sci. 58, 1174–1183.

Stoyan, D., Kendall, W.S., Mecke, J., 1995. Stochastic Geometry and its Applications. 2d ed. Wiley, New York.

Weston, D.E., Andrews, H.W., 1990. Seasonal sonar observation of the diurnal schooling times of fish. J. Acoust. Soc. Am. 87, 673–680.

Available online at www.sciencedirect.com
SCIENCE DIRECT®
Aquatic Living Resources 16 (2003) 325–331
Aquatic Living Resources
www.elsevier.com/locate/aquliv

Acoustic study of fish and invertebrate behavior in a tropical reservoir

Marie Prchalová [a,*,b], Vladislav Draštík [a,b], Jan Kubečka [a], Boonsong Sricharoendham [c], Fritz Schiemer [d], Jacobus Vijverberg [e]

[a] *Hydrobiological Institute AS CR, Na Sádkach 7, 370 05 České Budějovice, Czech Republic*
[b] *Faculty of Biological Sciences, University of South Bohemia, 370 05 České Budějovice, Czech Republic*
[c] *National Inland Fisheries Institute, Bangkok, Thailand*
[d] *Department of Limnology, University of Vienna, Austria*
[e] *NIOO–KNAW Centre for Limnology, The Netherlands*

Accepted 11 March 2003

Abstract

The fish and invertebrate behavior of the Ubol Ratana Reservoir, Thailand, were monitored using up- and downlooking split beam sonar located at a fixed location. In the same area and period, ichthyoplankton nets and multimesh gillnets were used. The bulk of targets, recorded by acoustics and direct capture, consisted both of fish 3–4 cm long and insect larvae 0.2–1 cm long. Diurnal patterns of behavior were very distinct: during the daytime, invertebrates were hidden in the bottom and most fish stayed in compact shoals. Time course of acoustic fish biomass and abundance was very variable due to shoaling. Only the largest fish were recorded as solitary targets. At night, the whole acoustic range was filled with targets and the time course of fish biomass (5–15 kg ha^{-1}) and abundance (20–45 thousand individuals ha^{-1}) were more constant. The biomass increased mostly at surface layers. Fish appeared in the evening in the water column 1 h earlier and stayed there in the morning 1 h longer than invertebrates. Dawn and dusk are good periods for studying fish before invertebrates outnumber them. Apart from fish, according to the target strength, swimming speed and depth distribution, at least four groups of water invertebrates were distinguished acoustically, some with extremely fast vertical movement (7–9 cm s^{-1} vertical speed). Comparison of up- and downlooking observations gave comparable results in midwater layer outside the near-field of the transducer. The uplooking approach can be more suitable for night records; downlooking for the day.

Keywords: Acoustics; Echospecies; Target strength; Acoustic tracking and identification; Behavioral pattern

1. Introduction

Acoustic surveys of tropical lakes and reservoirs are much less numerous than similar surveys of temperate waters (Guillard, 1998; Schiemer et al., 2001; Tumwebaze et al., 2002). The main reason is smaller research intensity in developing countries. Another important reason may be the much more complex animal community, which is less known and may complicate interpretation of echosounder records. This paper represents a part of an attempt to estimate fish community of a large and relatively shallow reservoir in Thailand. The aim of this study was to establish acoustic conditions, potential limitations, fish size distribution and diurnal cycle of animal behavior in the reservoir.

2. Materials and methods

2.1. Study area

The reservoir Ubol Ratana (16° 30'–16° 55' N; 102° 20'–102° 40' E) in Thailand, Khon-Kaen Province, belongs to the belt of tropical monsoon climate. The year of impoundment was 1965. The water surface area is 410 km^2, maximal depth is 19.5 m and average depth is 6.2 m (Pholprasith and Virapat, 1995; Simon et al., 2001). In 2000, ichthyofauna consisted of 67 species from 18 families. Most species are from families Cyprinidae, Cobitidae and Bargidae. Majority of

* Corresponding author. Fax: +420-38-5300248.
E-mail address: marie.prchalova@bf.jcu.cz (M. Prchalová).

doi:10.1016/S0990-7440(03)00047-0

Table 1
Parameters of sonar system

Simrad EY 500—split beam echosounder	
Operating frequency	120 kHz
Transmission power	63 W
Simrad ES 20-7 G—circular beam transducer	
Nominal 3 dB beam angle	7°
Face diameter	11 cm
Transceiver	
Pulse duration	0.1 ms
Frequency bandwidth	12 kHz
Pulse repetition rate	10 Hz
Single echo detector	
Min. and max. returned pulse width	0.6- to 1.8-fold transmitted pulse duration
Max. off axis distance	6 dB
Max. phase deviation	10 phase steps
TS threshold for 40 log *R* TVG	–79 dB
S_V threshold for 20 log *R* TVG	–65 dB

total fish biomass is represented by family Cyprinidae—90%, and then Clupeidae—5–10% (Pholprasith and Sirimongkonthaworn, 1999). Small clupeids are very abundant in the open water. The fixed location acoustic study was done at the sampling station 5 (Simon et al., 2001), which is located in the dam region with depth of 10 m. The distance from the shore was more than 3 km, the Secchi-disc transparency 1 m, dissolved oxygen concentration 7.1 mg l^{-1}, temperature 23.5 °C (no thermal stratification). The station was chosen due to good representativeness for the lacustrine part of the reservoir and good access.

2.2. Field survey

The Ubol Ratana Reservoir was studied during 9–11 February 2000 by the sonar system set as described in Table 1. According to the manufacturer, the safe start of the far-field is located 1 m from the transducer. This was verified by the in situ experiments with the standard target insonified at 10 cm distances from the transducer. From the distance of 90 cm onwards, the echo intensity from the standard target remained constant (40 log *R* time-varied-gain, TVG). The sonar system was calibrated with a tungsten-carbide standard target (32 mm; MacLennan and Simmonds, 1992). The echosounder was driven by a personal computer and all data were immediately stored on the hard disc of the PC. An accumulator 12 V battery powered whole sonar system and the computer.

The first 24 h run of records (12:30 9 February–2:30 10 February) was recorded with the uplooking position of the beam with the transducer mounted on the bottom facing vertically to the surface. Upward-looking vertical position was ensured by the heavy counterbalancing weight mounted to the cable socket of loosely held transducer. The second

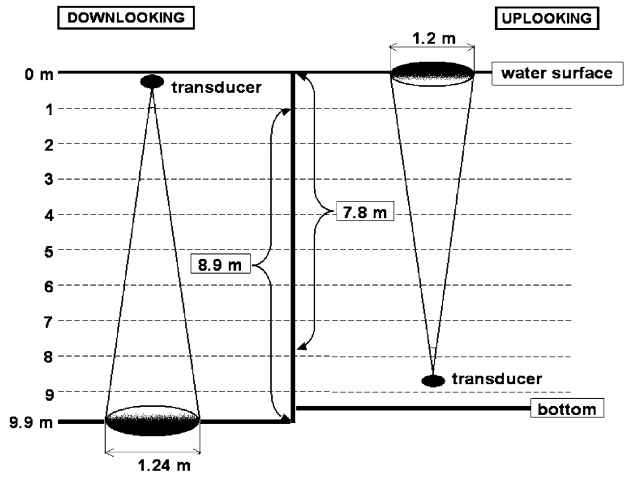

Fig. 1. Designs of up- and downlooking surveys with dividing of water column into depth layers and with diameters of acoustic beams in the furthest distance from the transducer. Uplooking transducer had slightly shorter range due to the holding frame and shallower site.

24 h run (13:15 10 February–12:00 11 February) was recorded with downlooking vertical beaming with the transducer mounted closely to the rectangle float. During calm weather of our survey, this setup ensured vertical orientation of the acoustic beam. Recording sites for two approaches were nearly the same, but due to some microhabitat differences, the uplooking site was slightly shallower than the downlooking site (Fig. 1). Recording range was also shortened due to the height of transducer holding frame (60 cm). The transducer had 130 m long cable and the sonar system was placed on anchored floating platform 100 m away from the transducer. Blind zone by the phase boundaries was about 15 cm thick.

The open water of the reservoir near the acoustic station was sampled by 5 min tows by an ichthyoplankton tow-net and multimesh gillnets. The parameters for the ichthyoplankton net were 1 m in diameter, mesh size 1.5 mm and design was similar as described in Wanzenböck et al. (1997). Gillnets were of bar mesh sizes 5, 6.25, 8, 12.5, 15.5, 19.5, 24, 29, 35, 43 and 55 mm set for whole 24 h period, emptied every 4 h. Total length (mm) of all captured animals was measured.

2.3. Post processing

Sizes of all acoustically detected single targets were identified using Love's equation (Love, 1977) for 120 kHz for simplicity. Majority of fish have swimbladder and many of the invertebrates have gas inclusions. There is no direct information on target strength TS of local animals available. The biomass of fish was calculated with the length–weight relationship for Sri Lankan fish provided by Dr. U. Amarasinghe from the Kelaniya University, Sri Lanka. The marginal length for distinguishing between two main categories of targets—'fish' and 'invertebrates'—was set at average TS value –60.5 dB, which corresponds approximately to 15 mm (Love, 1977). This threshold corresponds to low frequency groups of both targets and captured animals as shown at

Table 2
Four diurnal periods in up looking and downlooking

Period	Uplooking	Downlooking
Daytime	12:30–17:30	13:15–17:45
	7:00–12:30	6:45–11:45
Dusk	17:30–18:45	17:45–19:00
Night	18:45–5:45	19:00–5:45
Dawn	5:45–7:00	5:45–6:45

Fig. 5. 'Large fish' were defined as longer than 270 mm (~–36.5 dB in TS). Simrad EP 500 post-processing software was used for biomass and abundance estimation. The elementary sampling unit for this analysis was recording of one 5 MB*.dg* file (Simrad EY 500 software), which took 16–18 min. The records were processed by scaling total integrated volume backscattering coefficient S_v by average backscattering cross-section ς_{bs} (MacLennan et al., 2002) of a particular layer producing this volume density. This abundance was then proportionally distributed into 3 dB TS frequency groups according to TS frequency distribution. For fish and invertebrate tracking (connecting neighboring hits into one animal record), we used Sonar 5 software (Balk and Lindem, 2002; mostly manual tracking with maximum ping gap of 1 ping and minimum 5 echoes in a track). Attention was paid to tortuosity of the targets, only targets with the smooth trajectory through the beam were accepted.

Uplooking records were divided into seven depth layers from the surface (0–7.8 m). Downlooking records were divided into nine depth layers from 1 to 9.9 m. The data from the first 1 m from the transducer were not used due to the near-field. Each layer was 1 m thick except the shallowest one, which was in uplooking 1.8 m and the deepest one in downlooking 0.9 m thick (Fig. 1). In presentation of results, the layers are given from the true surface of the reservoir for both up- and downlooking. The records were divided into four diurnal periods—daytime, night, dusk and dawn (Table 2).

3. Results

3.1. Comparison of up looking and downlooking approaches

The values of total fish biomass, abundance and average weight attained comparable levels in most time intervals (Table 3). Fish recorded by uplooking had usually larger average weight and non-significantly smaller abundance. The only significant difference was found for night, when the layer 1–2 m contained extremely abundant targets in downlooking. Daytime records showed the largest differences and variability because of very distinct aggregating behavior. Uplooking records contained significantly less dense shoals. Invertebrates dominated size distribution of both records, but the downlooking records had slightly larger proportion of fish with a smaller modal length (Fig. 5).

3.2. Diurnal development of fish and invertebrate communities

During the daytime, most fish followed general tendency for forming shoals or staying near the bottom. Single fish targets rarely appeared. Invertebrates were not visible acoustically and were most likely hidden in the bottom. For most of the time, the daytime echogram was empty. During early dusk (17:28), shoals disintegrated and single fish appeared mostly in deeper layers. Invertebrates started to rise from the bottom 1 h later than fish (18:30). At night, the entire water column was filled with organisms. Most fish moved then gradually to the upper part of the water column (0–5 m) and stayed there throughout the night. Dawn sequence of events was opposite to the dusk: invertebrates were disappearing approximately 1 h earlier than fish (6:15 ~ last recorded invertebrate targets). At about 5:50, single fish started to descend to deeper waters and gradually disappeared from most of echograms (at about 7:00).

The phenomenon of earlier fish rising from the bottom can be also shown on the diurnal development of the share of fish on total abundance of all targets (Fig. 2). Night pattern was characterized by lower share of fish (5–10%) within deeper layers (5–8 m) and higher fish proportion in the upper layers (0–5 m; 15–25%). Invertebrates represent the rest to 100%. During dusk and dawn, the fish showed two peaks in target composition in the open water. They stayed in the open water as single targets longer than invertebrates. During both day and night, invertebrate targets prevailed. During the daytime, the sizing of targets is much less reliable due to aggregation and the proportion of fish fluctuated vigorously. During the night, enormous amounts of invertebrates emerged from the bottom and outnumbered fish, which were present as single targets as well.

Table 3
Difference in total average fish biomass (*B*) and abundance (*A*) between uplooking (Up) and downlooking (Down) from the same depth layers (1–8 m); one way ANOVA, *P*-level of 0.001. Average weight was calculated as *B*/*A*

Period	Biomass (kg ha^{-1})					Abundance (individuals ha^{-1})					Average weight (g)	
	Up		Down		*P*	Up		Down		*P*	Up	Down
	Mean	S.D.	Mean	S.D.		Mean	S.D.	Mean	S.D.		Mean	Mean
Daytime	2.3	6.3	7.8	18.9	0.145	5 800	19 400	34 400	86 400	0.087	0.40	0.23
Dusk	15.4	9.8	10.5	8.6	0.478	20 000	12 200	23 700	20 300	0.765	0.77	0.44
Night	6.4	2.8	6.7	3.3	0.687	26 500	7 600	34 700	9 100	<0.001	0.24	0.19
Dawn	2.5	1.4	6.8	3.6	0.519	16 800	5 100	29 300	16 200	0.189	0.32	0.23
24 h	5.2	5.8	7.3	11.8	0.175	17 100	16 700	33 700	52 500	0.012	0.30	0.22

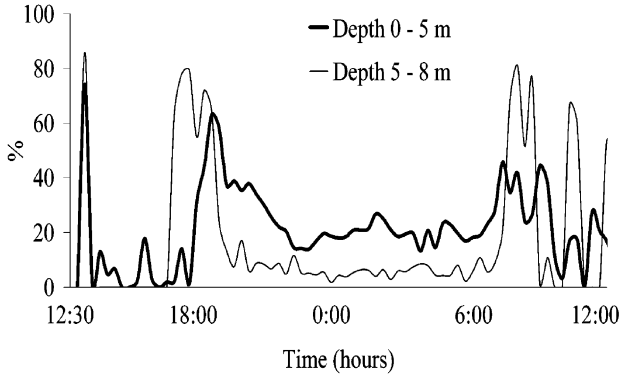

Fig. 2. Relative proportion of fish in total number of all recorded targets in two different parts of the water column; uplooking.

3.3. Biomass, abundance and average weight of fish

These three characteristics were calculated only for fish targets, TS > – 60.5 dB. Biomass, abundance and average weight of fish followed a typical diurnal development. Appearance of fish shoals during the daytime caused extensive variation of fish biomass (Fig. 3, Table 3). During the night, the biomass stabilized on the level of 5–10 kg ha^{-1} and the hectaric abundance ranged between 20 and 45 thousand individuals, both showed less fluctuations and probably are more representative than the variable daytime data. The smallest average weight of fish was recorded at night. Slightly larger fish dominated single target population during the dusk while tiny fish were still in numerous small shoals.

Vertical distribution of fish biomass changed during the diurnal cycle (Fig. 4). During the day, the bottom layer (9–9.9 m) in downlooking contained high values of biomass. This peak consisted of bigger fish (average weight of 1.76 g, ~50 mm, ~–50.5 dB), which did not seem to join the shoals. These fish seem to belong to the genus *Puntioplites* according to gillnets sampling. Another peak in daytime vertical distribution of fish biomass was recorded in upper layers especially by downlooking. Shoaling fish mostly composed this biomass. Night distribution of fish biomass was more even and more similar when recorded by different transducer deployments. The biomass was higher in upper layers; near-bottom peak of biomass was missing.

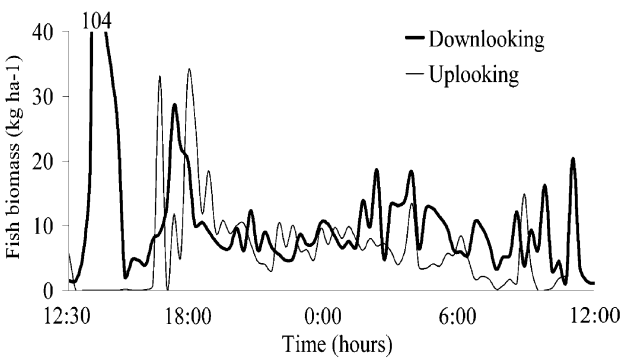

Fig. 3. The development of total fish biomass at all depth layers from up- and downlooking.

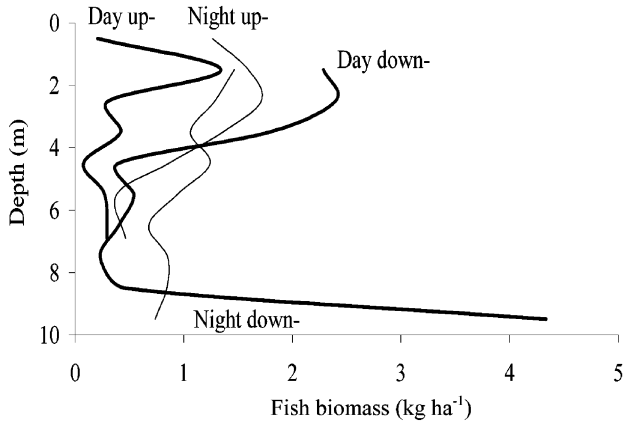

Fig. 4. Comparison of the vertical development of fish biomass during the daytime and the night in up- and downlooking. Thick line—day, thin line—night.

Occurrence of larger fish (≥27 cm, ~275 g, ~–36.5 dB) was extremely sporadic. The longest detected target corresponded to 37 cm. The greatest frequency of larger fish was in the bottom layer in downlooking, but only with a density of 0.5 individual ha^{-1}. Low density of larger fish could be influenced by relatively small sampling volume.

3.4. Categories of acoustic targets

Fig. 5 gives the comparison between reconstructed target size by up-and downlooking acoustics with the direct capture by ichthyoplankton nets (the same depth layers, nighttime). Both approaches showed two peaks of two main groups of organisms: the first peak belongs to invertebrates with modal values from 3.5 to 5.1 mm (~–72.5 to –69.5 dB). The second peak belongs to fish with values from 31 to 44 mm (~–54.5 to –51.5 dB). After recalculating the acoustic length-frequency structure only for fish (>15 mm), the majority of fish individuals (70% in uplooking, 75% in downlooking, the same depth layers, nighttime) was represented by targets 22–44 mm long. According to direct catches, this peak consisted mostly of genus *Clupeichthys*, which was the most abundant fish from ichthyoplankton nets and also from gillnets. This genus covered length range from 22 to 44 mm of total length in catches from ichthyoplankton nets and range 30–58 mm from gillnets, with the most abundant size class 35–37 mm. In both acoustic and direct capture results, the invertebrate peak outnumbered the fish peak. The only exception was the bottom layer in downlooking, where frequencies in peaks were nearly equal. Modal length of small fish observed by the uplooking appeared slightly longer compared to downlooking.According to target strength, swimming and vertical speed, we were able to distinguish at least six categories of acoustic targets (acoustic species, echospecies), which are presented in Table 4 and are shown on echogram (Fig. 6). The pattern of echogram appearance (TS, duration-in-beam and change-in-range) was the initial criterion for discrimination of individual tracks into groups. Acoustic targets were analyzed from dusk and dawn in up- and downlooking. These

Table 4
Definition of categories of acoustic targets analyzed from dusk and dawn in uplooking and downlooking. The total length was calculated according to Love's general equation (1977)

Category of acoustic targets (number of tested targets)	Total length (mm)	Target strength (dB)			Swimming speed (cm s^{-1})			Vertical speed (cm s^{-1})		
	Mean	Mean	S.D.	*	Mean	S.D.	*	Mean	S.D.	*
Fish (160)	42	–52.1	1.96	a	10.5	0.8	k	1.7	0.2	x
Slow targets (80)	3	–72.3	0.45	b	1.6	0.3	l	0.1	0.0	y
Ascending targets (40)	15	–60.5	0.71	c	2.4	0.1	l	1.6	0.2	x
Extreme targets (71)	10	–64.4	0.73	d	7.5	1.4	m	6.9	1.3	z
Standing targets (20)	13	–61.8	2.27	c	2.5	1.0	l	0.2	0.3	y
Subsurface liv. particles	<1.6	<–79	–	–	–	–	–	–	–	–

$swim.speed = \sqrt{Vx^2 + Vy^2 + Vz^2}$. *Vi*, velocity in *x*, *y* and *z* direction, respectively, between first and last echo; *Vz*, vertical speed (all speed calculations done according to Balk and Lindem, 2002).

periods were appropriate for this kind of observation due to presence of single fish and invertebrates, which were spreading to the water column from the bottom. One way ANOVA rejected the hypothesis of homogeneity of parameters (TS, swimming and vertical speed) of echospecies (*P*-level < 0.001). Echospecies labeled with different letters in column* of Table 4 were found significantly different in selected parameters (*P*-level < 0.05; Tukey HSD test).

4. Discussion

4.1. Patterns of open water community

Short survey of a relatively shallow reservoir revealed the potential of vertical acoustic application in a complex system. Up- and downlooking approach usually provided comparable results. Uplooking can be more suitable for night recording, because more fish were in the upper part of the water column where there is the largest sampling volume. On the other hand, downlooking was more effective in recording fish during daytime, when single larger fish tended to stay at the bottom layer. Both approaches have shown very distinct diurnal patterns of behavior like shoaling (Fréon et al., 1996; Helfman, 1993; MacLennan and Simmonds, 1992; Schiemer et al., 2001) during the day and shoal disintegration during the night and invertebrate emergence during the night. Acoustic study and direct sampling (Sricharoendham, personal communication) confirmed previous findings (Schiemer et al., 2001) that the fish community of a tropical reservoir is usually represented by huge numbers of tiny forage fish (average weight less than 1 g). This is very different compared to similar studies of temperate lakes and reservoirs where the weight of fish is 1–2 orders higher (Arrhenius et al., 2000; Čech and Kubečka, 2002).

4.2. Interpretation of echospecies

If we combine results from direct catch (Fig. 5) with categories of acoustic targets (Table 4), we can attempt to interpret some echospecies as reservoir animals. The combination is based on comparison of reconstructed total length

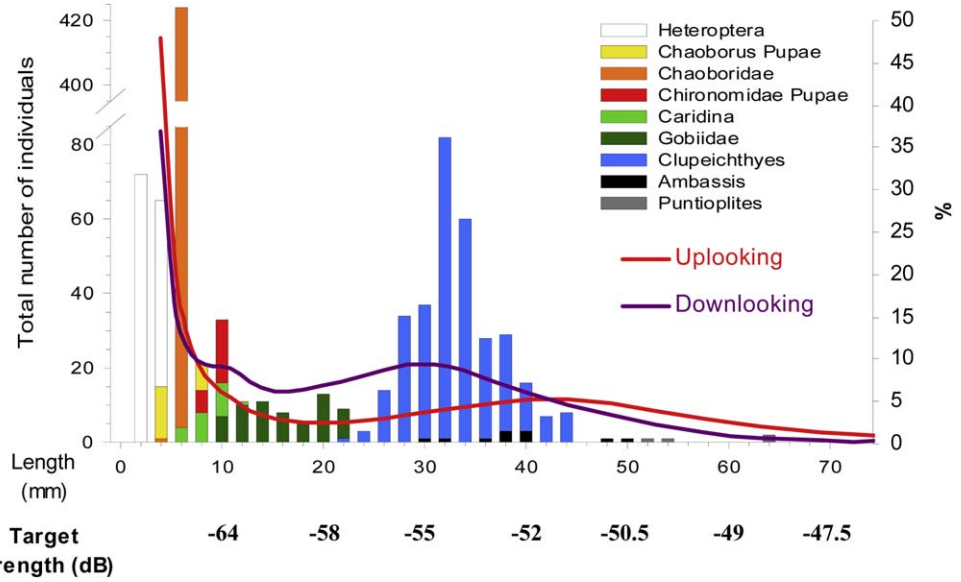

Fig. 5. Illustrative figure of size structure of invertebrates, ichthyoplankton and fish from night direct catch of ichthyoplankton nets (left *x*-axis with total number of individuals) and night acoustic length frequency structure in up- and downlooking (right *y*-axis with %). Values of TS corresponding to the length classes are given below *x*-axis.

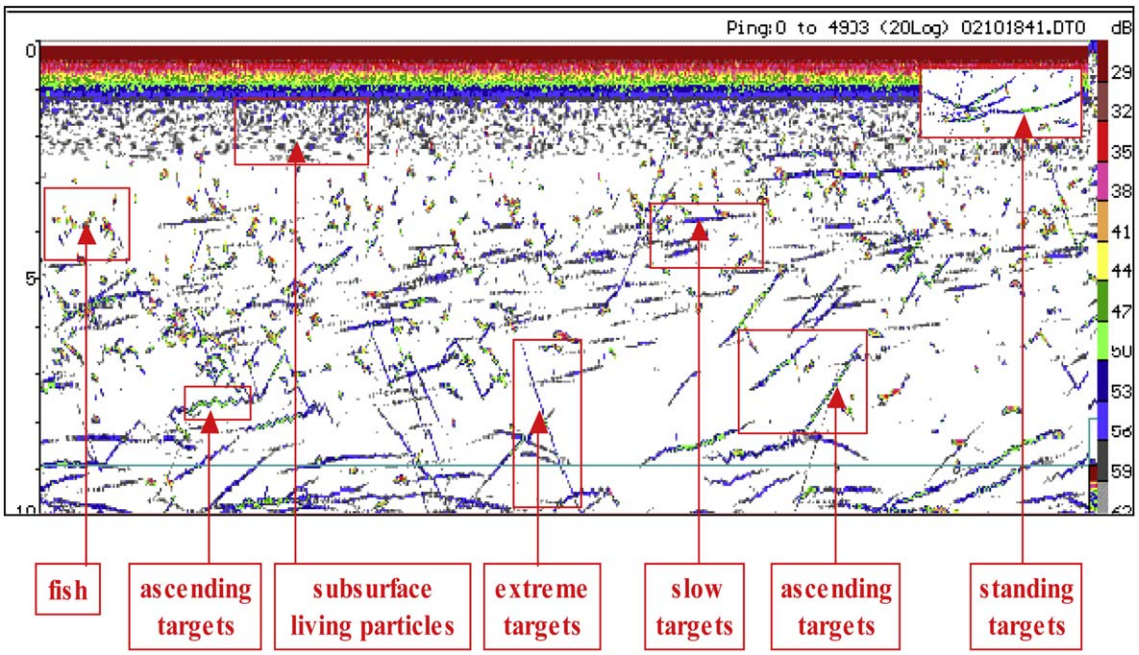

Fig. 6. Echogram image of six categories of echospecies—all categories are shown on this echogram were recorded during the dusk by downlooking transducer except category of standing targets, which was pasted from dawn record by uplooking transducer. Numbers of acoustic targets correspond to numbers in Table 4. *X*-axis corresponds to time (approximately 16 min) and *y*-axis is depth.

and swimming speed of organisms and one has to be aware that much more information about a complex system would be necessary for sound comparison. Also the application of general relationship of Love (1977) to all targets may be a big approximation, but it gives at least some idea about animal physical sizes when direct observations are absent. The latest larval fish studies (Rudstam et al., 2002) show that Love's equations (1977) are suitable for early juveniles (7–40 mm).

The first category is undoubtedly fish. They were swimming actively through whole acoustic beam. With average reconstructed total length of 42 mm, they were likely to belong to the genus *Clupeichthys*, which represented most fish in the catch of ichthyoplankton nets and smallmesh gillnets.

The second category (slow targets, reconstructed length of about 3 mm) is likely to consist of *Chaoborus* larvae and pupae. This echospecies represented the majority of invertebrate targets recorded in the open water and most of the catch of towed ichthyoplankton nets. They were present in all layers without any apparent swimming. This rather planktonic behavior distinguishes them from more nektonic echospecies of categories 3 and 4.

The third category (ascending targets, reconstructed length of about 15 mm) contained relatively fast rising organisms but with slow horizontal moving. They occurred during dusk and mainly in the lower part of the water column. Rarely they were also swimming down. Many of these targets exhibited fine oscillating movement while rising as shown in Fig. 6. With their average length, they match only to fish from family Gobiidae, but this is unlikely due to their patterns of movement. This pattern could correspond with behavior of pupae or maybe shrimps of genus *Caridina*.

The fourth category (extreme targets, reconstructed length of about 10 mm) had very expressive patterns of fast vertical movement, which does not agree with any pattern of movement of other organisms, shown in Fig. 6. The range of vertical speed was from 6 to 9 cm s^{-1}. Their movement was both ascending and descending. They appeared on records relatively scarcely (one individual per 2–4 min of record), but were present during all night and twilight observations. The patterns could represent some water Coleoptera or Heteroptera. Small Heteroptera have similar TS in temperate waters (Kubečka et al., 2000).

The fifth category of standing targets with average reconstructed length of about 13 mm appeared only during dawn in uplooking for a relatively short time (20 min) and only under the surface (up to 2 m). According to reconstructed length, they correspond to Gobiidae or *Caridina* but the swimming pattern does not resemble nekton. These targets created very long subsurface tracks while standing in a beam for a long time. Their temporal occurrence under the surface with nearly no moving in horizontal direction could indicate their affiliation with pupae of Chironomidae (10 mm; Fig. 5).

The last group was subsurface living particles present all night and during the twilight. These targets were too small for single target analysis with respect to the recording threshold. The size was smaller than –79 dB and they can only be observed in lower threshold echograms. They formed relatively compact belt under the surface down to 2 m of depth. They could be formed by the aggregations of zooplankton or algae. Dominant phytoplankton species, filamentous blue–green alga *Cylindrospermopsis raciborski* (Cyanophyta/Cyanobacteria), contained aerotopes, gas-filled vesicles, which allow floatation (Rott et al., 2002).

5. Conclusion

Open water of a tropical reservoir was found to be a comfortable environment for acoustic study of animal behavior. Both approaches of fixed location acoustic study—up- and downlooking—of the Ubol Ratana gave comparable results in all main characteristics of observed community.

Apparent circadian pattern of community behavior was found. Daytime records fluctuated significantly due to occurrence of fish shoals. Shoals varied in size and appeared with no apparent regularity. Single fish were during daytime mostly close to the bottom. Night records showed many hours of relatively stable behavioral pattern with much more equal dispersion of single targets. During dark, we also observed invertebrates, which were rising from the bottom during dusk. At dawn, fish and invertebrates were going down to the bottom and disappeared from the water column as single targets. Both small fish and invertebrates seemed to rely on darkness as a protective period for colonizing open water, this period started 1 h earlier and lasted 1 h longer for the fish. In most depth layers, except the deepest, invertebrates outnumbered the fish.

Due to more stable dispersion of community during night, the time course of biomass, abundance and average weight of fish was relatively regular. Vertical development of fish biomass showed that fish were at daytime on the bottom and surface layers and over night they were mainly in the upper part of the water column. Vertical development of abundance and average weight indicated that larger fish were in the bottom layer.

According to target strength, speed pattern of moving, depth and diurnal distribution, we are able to distinguish six acoustic species. The results show the potential of acoustic tracking for non-intrusive observation of behavior of individual echospecies even in a complex and diverse tropical ecosystem.

Acknowledgements

This study was supported by FISHSTRAT Project funded by European Commission and by Grant Agency of the Czech Academy of Sciences (project no. A 601 72 01 and program K 600 51 14). We thank anonymous referees and the editor for their constructive comments on this manuscript. We are also beholden to Gregory P. Setliff for revision of English.

References

Arrhenius, F., Benneheij, B.J.A.M., Rudstam, L.G., Boislair, D., 2000. Can stationary bottom split-beam hydroacoustics be used to measure fish swimming speed in situ? Fish. Res. 45, 31–41.

Balk, H., Lindem, T., 2002. Sonar4 and Sonar5-Pro Post Processing Systems. Lindem Data acquisition, Norway, pp. 155–189.

Čech, M., Kubečka, J., 2002. Sinusoidal cycling swimming pattern of reservoir fishes. J. Fish Biol. 61, 456–471.

Fréon, P., Gerlotto, F., Soria, M., 1996. Diel variability of school structure with special reference to transition periods. ICES J. Mar. Sci. 53, 459–464.

Guillard, J., 1998. Daily migration cycles of fish populations in a tropical estuary (Sine-Saloum, Senegal) using a horizontal-directed split-beam transducer and multibeam sonar. Fish. Res. 35, 23–31.

Helfman, G.S., 1993. Fish behaviour by day, night and twilight. In: Pitcher, T.J (Ed.), Behaviour of Teleost Fishes. Chapman & Hall, London, pp. 479–512.

Kubečka, J., Frouzová, J., Čech, M., Peterka, J., Ketelaars, H.A.M., Wagenwoort, A.J., Papáček, M., 2000. Hydroacoustic assessment of pelagic stages of freshwater insects. Aquat. Living Resour. 13, 361–366.

Love, R.H., 1977. Target strength of an individual fish at any aspect. J. Acoust. Soc. Am. 62, 1397–1403.

MacLennan, D.N., Fernandes, P.G., Dalen, J., 2002. A consistent approach to definitions and symbols in fisheries acoustics. ICES J. Mar. Sci. 59, 365–369.

MacLennan, D.N., Simmonds, E.J., 1992. Fisheries Acoustics. Chapman & Hall, London, pp. 68–88.

Pholprasith, S., Virapat, C., 1995. The management of fisheries in the Ubolratana Reservoir for a sustainable fishery. In: Petr, T., Morris, M. (Eds.), Regional Symposium on Sustainable Development of Inland Fisheries Under Environmental Constraints, Bangkok, Thailand, FAO Fish. Rep. No. 512, pp. 177–184.

Pholprasith, S., Sirimongkonthaworn, R., 1999. The fish community of the Ubolratana Reservoir, Thailand. In: van Densen, W.L.T., Morris, M.J. (Eds.), Fish and Fisheries of Lakes and Reservoirs in Southeast Asia and Africa. Westbury Publishing, Otley, pp. 103–115.

Rott, E., Peerapornpisal, Y., Ingthamjitr, S., Silva, E.I.L., 2002. Phytoplankton seasonality in reservoirs under monsoon climate in Sri Lanka and Thailand. 4th International Conference on Reservoir Limnology and Water Quality. České Budějovice, Czech Republic, pp. 290–291.

Rudstam, L.G., VanDe Valk, A.J., Scheuerell, M.D., 2002. Comparison of acoustic and Miller high-speed sampler estimates of larval fish abundance in Oneida Lake, New York. Fish. Res. 57, 145–154.

Schiemer, F., Amarasinghe, U., Frouzova, J., Sricharoendham, B., Silva, E.I.L., 2001. Ecosystem structure and dynamics—a management basis for Asian reservoirs and lakes. In: De Silva, S.S. (Ed.), Reservoir and Culture-based Fisheries: Biology and Management. Australian Centre for International Agricultural Research, Canberra, pp. 215–226.

Simon, D., de Jesus, C., Boonchuwong, P., Mohottala, K., 2001. The role of reservoir and lacustrine fisheries in rural development: comparative evidence from Sri Lanka, Thailand and the Philippines. In: De Silva, S.S. (Ed.), Reservoir and Culture-based Fisheries: Biology and Management. Australian Centre for International Agricultural Research, Canberra, pp. 56–65.

Tumwebaze, R., Getabu, A., Bayona, J., MacLennan, D.N., Cowx, I.G., 2002. Fisheries of Lake Victoria: an underwater perspective. In: Cowx, I.G. (Ed.), Management and Ecology of Lake and Reservoir Fisheries. Fishing News Books, Blackwell Science, Oxford, pp. 70–83.

Wanzenböck, J., Matěna, J., Kubečka, J., 1997. Comparison of two methods to quantify pelagic early life stages of fish. Arch. Hydrobiol. Spec. Issues Adv. Limnol. 49, 117–124.

Available online at www.sciencedirect.com
SCIENCE DIRECT®
Aquatic Living Resources 16 (2003) 333–338
Aquatic Living Resources
www.elsevier.com/locate/aquliv

New applications of hydroacoustic methods for monitoring shallow water aquatic ecosystems: the case of mussel culture grounds

Patrice Brehmer [a,*], François Gerlotto [b], Jean Guillard [a,1], Fabien Sanguinède [a], Yvon Guénnegan [c], Dominique Buestel [d]

[a] *Institut de Recherches pour le Développement, CRHMT/UR061 and US004, BP 171, 34203 Sète, France*
[b] *Institut de Recherches pour le Développement, Casilla 53390 Correo Central, Santiago-1, Chile*
[c] *Institut français de recherche pour l'exploitation de la mer, CRHMT/RH, BP 171, 34203 Sète, France*
[d] *Institut français de recherche pour l'exploitation de la mer COP, BP 7004, 98719 Taravao, Tahiti, French Polynesia*

Accepted 7 March 2003

Abstract

The development of acoustics tools and methods for monitoring anthropized ecosystems represents a new field for the application of acoustics. Monitoring such an environment was not possible with single vertical echo sounders, due to the fact that the artificial structures and the natural targets were not distinguishable. Monitoring data were collected along the French Mediterranean coastline, during five short surveys of mussel culture longline areas. Both the *Reson Seabat 6012* multibeam sonar (455 kHz) and the *Simrad SR 240* omnidirectional sonar (23.75 kHz) were used for target detection. The former tools allow accurate allocation of the different types of echoes to artefacts, fish schools and scattered fish. The school characteristics collected included morphological, geographical (GPS, school location), and behavioural (connections with the longlines). An acoustic survey undertaken with the same hardware near the study area allowed the comparison of fish schools and the TS distribution of individual fish in the open sea and in the mussel area. These data permitted us to evaluate the ecological impact of a mussel culture on the ecosystem, in a context of predation behaviour of fish on these longlines. Finally, the acoustic data revealed the configuration of each concession and the level of charge of each line. We discuss the applicability of this technology for in situ real time monitoring for joint management of such ecosystems. The information can allow littoral cooperative management or incorporating it into an ecosystem approach.

Keywords: Multibeam sonar; Monitoring; Fish school; Mussel longline; Artificial reef; Ecosystem

1. Introduction

The conflicts engendered by the multiple uses of coastal ecosystems (fisheries, tourism, aquaculture, etc.) are becoming a major challenge for the environmental friendly development and exploitation of these areas. Since 1988, the development and management of several artificial reefs (Lacroix et al., 2002) and mussel culture fields in open sea along the French Mediterranean coastline have become a major economical activity (Loste and Cazin, 1993). First experimented in 1976 near Sète (the most important fisheries harbour along the French Mediterranean coastline), these developments have induced several changes in the ecosystem. In 1996, new and heavy predation on mussels by Sparids was reported illustrating the need for exploited anthropized ecosystems to be monitored. Currently, acoustic observations are usually the only applicable monitoring method, as the area is too wide and turbid for routine visual observations and fishing gears cannot be deployed because of the great number of the artefacts present in the area. However, in such anthropized ecosystems, a scientific echo sounder alone may not permit the definition of specific targets because of these submerged artefacts (Fig. 1). In the mussel aquaculture ground (MG), the echoes of longline structures cannot be distinguished from the echoes of fish and schools (Fig. 2). This paper wants to demonstrate how the adaptation of acoustic methods with multibeam sonar makes it possible to monitor such a complex environment. Some illustrative preliminary results are presented.

* Corresponding author.
E-mail address: brehmer@ird.fr (P. Brehmer).
[1] Institut National de Recherche Agronomique, CARRTEL, BP 511, 74203, Thonon les Bains, France.

doi:10.1016/S0990-7440(03)00042-1

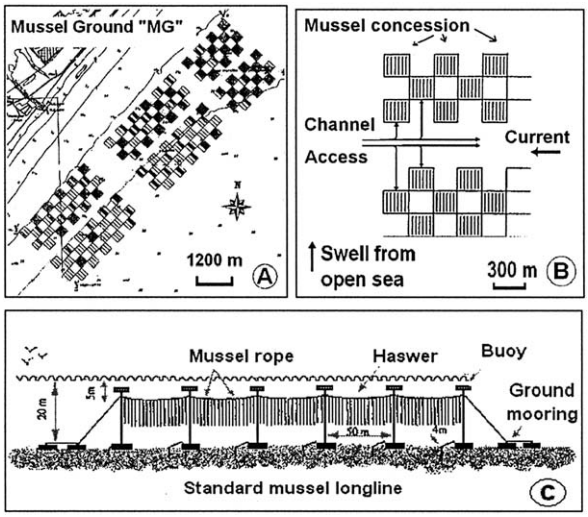

Fig. 1. Structure of the mussel ground, in open sea; channel access; the mussel production area (a) constituted by two longlines each; channel access (b) the mussel longlines are fixed by ground mooring and hung with buoy (c), the mussel ropes are hooked on the hawser, the main horizontal rope (after Lost and Cazin, 1993).

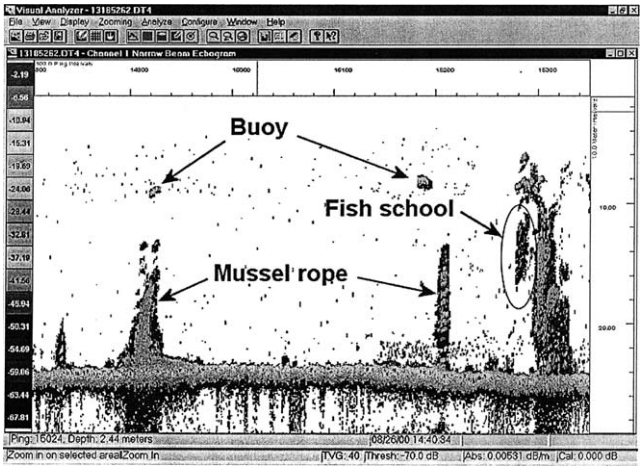

Fig. 2. A vertical echogram obtained with a *Biosonics DT 5000* in the mussel ground (MG). It is impossible to discriminate the fish school (circled) from the mussel longline structure on the vertical echosounder (VES) records without information delivered by the multibeam side scan sonar (MBS).

2. Materials and methods

2.1. Acoustic devices and mussel culture grounds

Data were collected from five surveys during the summer of 2000 and 2001 using small boats adapted to manoeuvre inside the aquaculture field. In 2001, a set of observations were recorded aboard the 30 m R/V "l'Europe" out and near the MG using a portable echo sounder (VES) (either *Simrad* EY500 or *Biosonics* DT 5000, previously calibrated (Foote, 1987)) and a mutibeam side scan sonar *Reson Seabat 6012* (MBS) (Table 1). The latter was set on a vertical plane perpendicular to the vessel route, with the main axis either vertical (i.e. observing from 45° port to 45° starboard below the boat) or lateral (directed 45°, observing from 0° to 90° below the boat). Aboard the R/V "l'Europe", a long-range multibeam omnidirectional sonar (LOS) was employed following the methodology developed by Brehmer and Gerlotto (2000) to test the applicability of such tools in shallow waters. The total MG area, prohibited to navigation, covers 2754 ha (Fig. 1a). Each concession (3 ha each) contained two mussel longlines of 250 m length, usually at 5 m depth from the surface and, between 20 and 30 m deep (Fig. 1c). The longline structure was standard, where the hawser (main rope) was suspended horizontally by buoys and fixed to the bottom by secondary ropes each 50 m, hooked by ground mooring concrete blocks (Fig. 1c). The mussel ropes were hung vertically below the hawser.

2.2. Sampling methods

Morphometric and spatial data were collected on a total of 191 fish schools (140 inside the mussel area and 51 outside) with the MBS. A total of 7457 target strength (TS) values were processed on scattered fish using the VES: 1455 TS values outside the MG (night); 3467 inside (night); 605 inside (night with artificial light); 1527 inside (day).

The MBS and VES data were recorded simultaneously. The MBS video images allow clear discrimination of fish and artefact echoes (Fig. 3). Once the discrimination has been completed, the corresponding vertical echogram can be easily cleaned (Fig. 2). Then the biological target analysis, from VES and digital MBS, is performed and the main school parameters are measured (Gerlotto et al., 1999, 2001). The MBS images from the longline structure allow for three-dimensional reconstruction. Two sets of images were collected, those obtained with the vessel crossing the longline and those with the vessel parallel to the longline (Fig. 3). Three levels of mussel abundance on the mussel ropes were defined according to the MBS imagery: full, medium (in growth), and empty.

The same measurements on schools and scattered fish were performed outside the MG area (5 nautical miles far from the MG on the same isobaths) with the same acoustic devices and boat. No artificial reef and structure were encountered in this area. In the 2000 survey (IRD, Ifremer, SRCM) "lamparo" experiments (lighting 500 W) 2 m above the sea surface (Nédélec and Prado, 1990) were conducted during which TS values were collected.

3. Results

The fish, school and mussel long line can be discriminated separately by acoustic methods. The results displayed here are methodological, and give some information on the kind of information a multibeam sonar can provide in such anthropized ecosystems, by the way of some examples. The three most important points that concern the observation are description of fish schools, the analysis of individuals (and specially fish TS), and the representation of the artificial structures such as the mussel longline present in the area.

Table 1
Main characteristics and settings of the acoustic devices: the multibeam sonar (MBS), the vertical echosounder (VES) and the long-range multibeam omnidirectional sonar (LOS) used during the surveys 2000 and 2001

Type	*Reson Seabat 6012*	*Biosonics DT5000*	*Simrad EY500*	*Simrad SR 240*
Acronym	MBS	VES	VES	LOS
Surveys	07/2000;04–05/2001*	07/2000	07/2001;04–05/2001	10/2001
Periods	Day/night (day)*	Day/night	Day/night	Day
Frequency (kHz)	455	129	70	23.75
Nb. beams	60	1 dual beam	1 split beam	32
Beam shape	1.5° × 22°	11° × 11°	11° × 11°	11.5° × 11.25°
TVG	20 log *R*	40 log *R*	20 and 40 log *R*	30 log *R*
Power	7–8	–	–	Full
Gain	4–5	–	–	9
Ping rate	7/s	Auto	Auto	Auto
Pulse duration (ms)	0.06	0.4	0.3	8
Range (m)	50 (50/100)*	Auto	Auto	800
Beam position	Vertical (45°)*	Vertical	Vertical	Tilt –2° to –5°
Sound celerity (m s^{-1})	1500	1485	1505	–
Recording	Video + digital (video)*	Digital	Digital	Digital
Zoom	1	–	–	–
Scale	Linear	–	–	–
Smoothing	Off	–	–	On
Software	*Sbiviewer 5.01*	*DT analyser*	*Movies+ 3.3a*	*Infobancs 3.0*

* During surveys in 2002

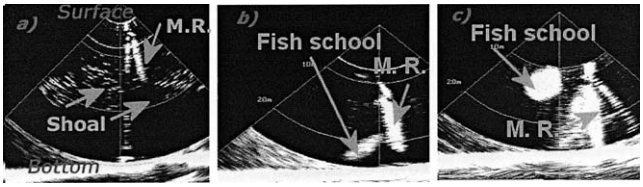

Fig. 3. Multibeam sonar display in lateral view (vertical transducer). Shoal around the mussel rope (a), 30 m-deep from surface (top) to bottom; fish schools near a mussel rope, M.R (b and c).

3.1. Fish schools

No school was detected during night surveys. The 191 schools recorded (Fig. 5) were on average 6.9 m in width, 3.4 m in height and 13.7 m in length (the maximal value was 120 m recorded outside the MG). The average distance from the bottom (altitude) was 5.1 m and their distance from the boat was 26.5 m (the minimum distance recorded was 2 m and occurred outside the MG). When the schools were observed simultaneously with a longline (n = 79; Fig. 3), their average distance to the structure was 15.3 m. Two phenomena that let us suspect that the schools could be attracted by the structure are: (i) no or very few schools were recorded in the access channel during the surveys, and (ii) due to the limited range and the directivity of the sonar beam, it was not always possible to record, on a single frame, the schools and the structure. Therefore, most of the 191 observed schools were actually close to the longline (unlike the limited number of 79 recordings with school and longline may suggest). The vertical distribution of fish schools was predominantly close to the bottom (0–8 m altitude) but inside the MG the fish school was detected in the whole water column (Brehmer, 2001), except during rough weather (above 5 m or below 18 m). Horizontally, the fish schools were distributed over all the MG with a low density in the access channel except that they were more abundant on the open seaside of the MG during rough weather. The fish school characteristics were highly variable inside the MG (standard deviation: length, 6.7 m; height, 2.0 m; width, 3.4 m and altitude 4.3 m) and varied according to the time of the day (Brehmer, 2001). The biggest schools were recorded at midday (from 1 ½ h before to 1 ½ h after the zenith) and close to the bottom. The fish school morphometrics and position inside and outside the MG were significantly different (MANOVA, $P < 0.05$) (Fig. 5); that is, schools were smaller, shallower and farther from the boat (avoidance)

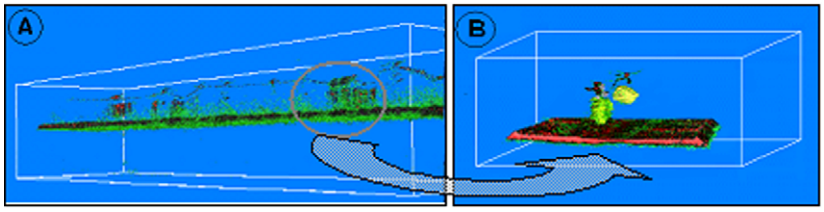

Fig. 4. Three-dimensional view of a mussel long line (a) and an enlargement of a fish school (b: zoom) from multibeam side scan sonar (MBS) processed data. The software allows identifying and measuring separately all the individual structures; b: the fish school (in yellow), the mussel rope (in green), the hawser and buoy (in grey), bottom (in red).

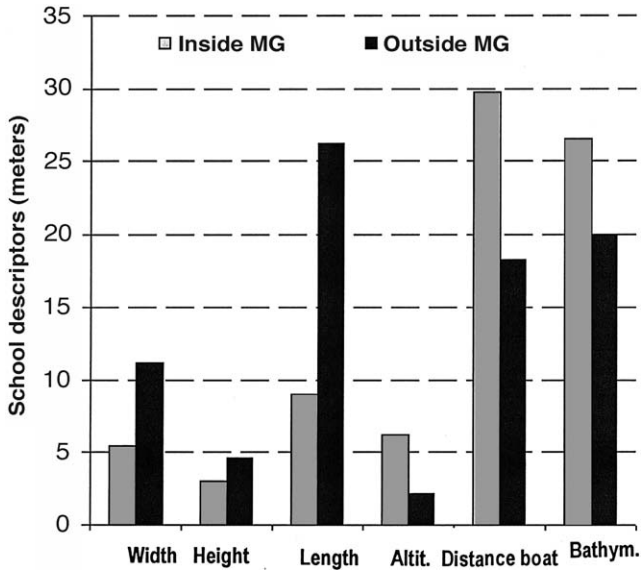

Fig. 5. Comparison of the fish school sonar descriptors, obtained inside and outside the mussel culture ground.

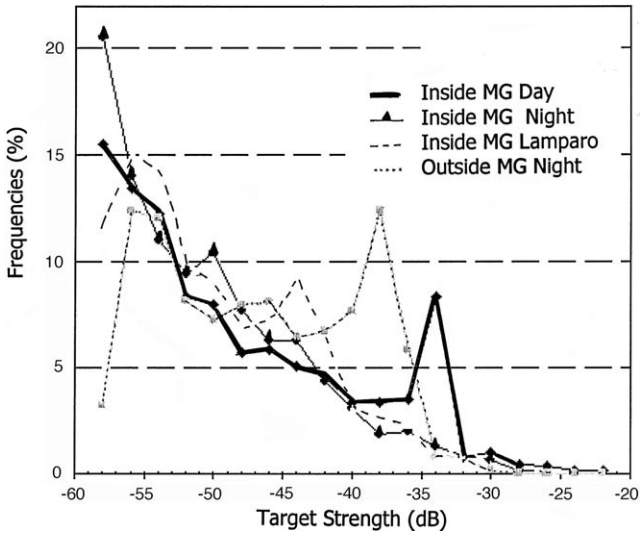

Fig. 6. Comparison of TS (in dB) obtained outside and inside the mussel culture ground (MG), at a same depth (20–30 m): during the day, and during the night, with and without the "*lamparo*" light attraction experiment.

inside the MG. There were no significant correlations between the fish school descriptors (correlation matrix, $P < 0.05$).

Fish school abundance, calculated as number per kilometre of transect, was higher inside the MG (2.3 school km^{-1}) than outside (1.9 school km^{-1}), but the volume (length × width × height) was six times higher outside the MG. Limited visual observations by divers (inside, summer 2000) and by trawl operation (outside, summer 2001) indicated the presence of the same dominant species: *Sardina pilchardus*, *Engraulis encrasicholus*, *Boops boops* and *Trachurus trachurus*.

3.2. Individual fish (Target Strength)

As expected, the overview of the echograms showed the usual pattern of fish in schools during the day and scattered during the night (Freon et al., 1996). Comparison of all the TS values by non-parametric tests (Kruskal–Wallis) showed no differences ($P < 0.05$) amongst the four TS distributions (Fig. 6). Nevertheless, the TS distributions indicate the presence of a higher percentage of small fishes inside the MG than outside (Fig. 6), yet the maximum TS values were collected inside the MG. On average, the TS values were higher outside the MG. During the "lamparo" experiments, there was a shift towards large targets compared with the night TS values inside the MG (Fig. 6). However, on average, there is no real change.

3.3. Mussel longline structure

Our results show that, using MBS, technology it was possible to:

- locate and count (GPS, vertical position) the mussel longlines in each concession;
- evaluate the mussel charge by segment (50 m) into the three categories described above and acoustically document directly the disappearance of mussel ropes due to predation;
- observe the vertical behaviour of mussel rope in the water column (Figs. 3 and 4);
- note the existence of lost or clandestine longlines, and record the bottom relief;
- document and monitor the interaction of fish and fish schools in the MG.

Digital MBS data processing via *Sbiviewer* software (Gerlotto et al., 1999) and MBS video recordings also allow reconstructing the longlines in three dimensions and the characterization of the longlines (Fig. 4). It takes less than 10 min to record a longline exhaustively. Consequently, the total area of 2754 ha with 242 mussel longlines distributed on 171 concessions can be fully recorded in 1 week.

The behavioural ecology of schools relative to the longline was explored (e.g. attraction effect as described above). Fig. 4 shows the three-dimensional reconstruction of a school close to the part of the longline where the mussel charge is the most abundant. This kind of three-dimensional imagery allows an accurate evaluation of the influence of the longline features on school distribution and behaviour. LOS observations were undertaken with a *Simrad SR240* (filter: *Reverberation Control Gain*/strong, *Ping to Ping*/strong, *Auto Gain Control*/off) on the MG (Table 1). The data show that the fixed longline can be discriminated from the mobile biological target. This provides information on the time of residence of fish schools and their horizontal swimming behaviour around the mussel longline structure.

4. Discussion

The objective of this project was to discriminate fish schools from non-biological targets. The objective has been successful. Our results confirmed that the combined use of

VES and MBS digital and analogical video data allows an accurate discrimination of the fish echoes, individuals as well as in schools, from the non-biological target in a complex environment (mussel longline structure). These results have to be supplemented by systematic species recognition using fishing, underwater observation or acoustic identification (multifrequencies, school shape, etc.). However, shoal measurement (Pitcher, 1983) and the definition of mussel charge require specific tests (i.e., standardization by direct in situ observation).

Detection of predators was not achieved.

Simultaneous use of multibeam sonar and classical echo sounder allowed discriminating artefact echoes from schools. For this work, we used a MOVIES+ function (Weill et al., 1993; Berger et al., 2001) to zoom on each "false echo" and delete them before a complete process of VES (echo integration, TS measurement, fish school discrimination). A similar procedure could be used to discriminate trees and fish in non-deforested dams (Cardenas et al., 1988).

The local managers have planed to restructure the area. The MBS can provide useful information on the under water structures and 3D topography for such purposes. Our methodology allows recording all the mussel longlines and detection of clandestine or lost longlines, even those unseen from the surface. An exhaustive mapping of the MG production is made possible. It is possible to locate, count, observe the state of the mussel longlines in the MG, and to deliver data for a global management of the area. All these data are complementary and are of great interest to the local administrative managers and fisheries or aquaculture scientists.

The information provided by our study can help in evaluating the catchability coefficient of fish and schools by different fishing techniques. Fishing with light appears to be efficient on certain targets, and samples inside the channel may not provide any useful information (weak abundance) (Brehmer, 2001).

The TS values indicate the presence of big fish, suspected to be Sparids as described by the professionals (Moran, pers. comm.), inside the MG in night time. Small fish are four times more abundant inside the MG than outside (Fig. 6). This could be due to the refuge effect of the structures (reduced current and area prohibited to navigation), with the presence of higher taxonomic composition (fauna and flora) of the suspended mussel rope unit due to their interaction with the environment (Mazouni et al., 2001; Deslous-Paoli et al., 1998). The mussel aquaculture can play a central role in nitrogen renewal in the water column (Mazouni et al., 1998) and shellfish farming nutrient transformation increases ecosystem productivity even if the filtration pressure keeps phytoplankton biomass at low level (Deslous-Paoli et al., 1998). A concept of "mussel rope forest" is defended in the book of Lacroix et al. (2002), for increasing the potential of artificial reef attraction. Fig. 5 shows the opposite for schools inside and outside the MG. Conversely, the TS data show no significant differences in the distribution inside/outside; the predominant species are the same. Since the species are the same, the school morphological variation must be related to different behavioural motivations inside and outside the MG.

We were unable to draw any conclusion on the effect of such structures as artificial reefs (fish biomass attraction and/or production) but we pointed out the differences in fish behaviour inside and outside the MG. Attraction seems evident, if measured in terms of biodiversity, but the mechanisms have not been quantified or identified. The sampling survey design must be adapted to investigate the potential attraction of such "artificial reefs". The comparison of fish school spatial structure with a spatial point process approach (Petitgas et al., 1996) and biomass assessment could be a good indicator of the "reef effect" on the fish resources coupled with species richness study (Bayley and Peterson, 2001). Productivity needs a multiyear study (fish assessment, evaluation of biomass and diversity on the mussel longline fauna and flora) with at least, bi-annual surveys to take into consideration the species seasonality (water temperature variations). The methodology we developed provides information for a rational management of the coastline, such as inventory of mussel culture, effect of artificial reefs, and fish behaviour. A regularly use of this methodology will insure an evaluation of the evolution of pelagic fish population around the MG according to the MG activities. A comparative approach at annual or seasonal scale (temperature and salinity variation observed seasonal change of the taxonomic richness of biofouling (Souchu et al., 1997; Mazouni et al., 2001)) should provide information for fisheries scientist and local manager. The methodology can be applied on natural or artificial reef as plane sand bottom under Fish Aggregation Devices (Hunter and Mitchel, 1967).

An optimized methodology could be added with information obtained by LOS, to use MBS with ping sector of 180° (Gerlotto et al., 1999; Mayer et al., 2002), Radio-Acoustic Positioning and Telemetry (O'Dor et al., 2000) and Ultrasonic Telemetry (Bolden, 2000) for an exhaustive view of fish behaviour.

5. Conclusion

The integration of observations into three dimensions allows several exploratory options and an overview of the fish behaviour. Fish structure, fish aggregation dynamics, swimming behaviour, time of residence, catchability, spatial occupancy, diel variations, interaction with the mussel rope, etc. and a complete fish school database can be built with the three devices VES, MBS and LOS (Brehmer et al., 2002). Automation of digital sonar data acquisition and analysis software would provide more reliable information on school characteristics.

The aim of our work, to observe fish in a shallow water ecosystem, was successfully achieved. However, an important unexpected result was the demonstration of the capacity of modern acoustic systems to monitor such areas, at several levels. The results of this study clearly demonstrate that the MBS technology can be used for the discrimination between

the non-biological targets like the mussel longline and biological echoes such as shoals and fish schools. In addition, the technology permits the evaluation of lost and/or clandestine gears, evaluation of the global impact of aquaculture structures on the whole ecosystem, as well as changes and shifts in the trophic levels of the area. Although some technical and methodological improvements have to be designed, a wide field of activities is open to underwater acoustics, and the methods may be available to managers to monitor their activities in detail. If the management of human activities and exploitation must be considered in an ecosystem-based approach, being able to describe in detail and in a qualitative as well as quantitative way, the whole system becomes critical. Acoustic methods, such as the one we presented in this paper, seem to be able to provide this kind of information on the different parameters of the ecosystem. It seems clear that an integrated approach of the mussel culture ground, gathering in a synoptic data base: the artificial structure, the aquaculture status of the mussels and the fish behaviour and abundance, will be of great help to evaluate the potential of an area, and the ecological health of an anthropized ecosystem.

Acknowledgements

To the Languedoc Roussillon region which supports this program by the measure 13.4.4, 03-04/01; CPER 2000-2006. To the Mediterranean aquaculture farmers of SRCM-ASA for their participation. We are also grateful to the anonymous reviewers who contributed to improve the text. The research facilities were provided by the new centre of Mediterranean and tropical fisheries research (CRHMT: IRD, Ifremer and University of Montpellier II).

References

Bayley, P.B., Peterson, J.T., 2001. An approach to estimate probability of presence and richness of fish. Trans. Am. Fish. Soc. 130, 620–633.

Berger, L., Durand, C., Marchalot, C., 2001. Movies+ User Manual version 3.3. Ifremer, Brest.

Bolden, S.K., 2000. Using ultrasonic telemetry to determine home range of a coral-reef fish. In: Sibert, J.R., Nielsen, J.F. (Eds.), Electronic Tagging and Tracking in Marine Fisheries. Kluwer Academic Publishers, London, pp. 167–179.

Brehmer, P., Gerlotto, F., 2000. Methodology concept and preliminary analysis on omnidirectional sonar data. In: Zakharia, M.E., Chevret, P., Dubail, P. (Eds.), Proceedings of the Fifth European Conference on Underwater Acoustics. Commission Européenne, Luxembourg, pp. 1527–1532.

Brehmer, P., 2001. Observations acoustiques de bancs de poissons autour de filières à moules en mer ouverte à l'aide d'un sonar multi-faisceaux à haute résolution (455 kHz) : application au lotissement conchylicole de Sète-Marseillan. Doc Sci. IRD-Region LR 13.4.4 Montpellier, France.

Brehmer, P., Gerlotto, F., Rouault, A., 2002. In situ inter-standardization of acoustic data: an integrated database for fish school behaviour studies. Acta Acoust. 88, 730–734.

Cardenas, L., Petit, J.J., Nova, D., 1988. Hydroacoustic surveys of Guri lake (Venezuela) a preliminary assay on the quantification and distribution of fish biomass. Mem. Cien. Nat. La Salle 47, 77–90.

Deslous-Paoli, J.M., Souchu, P., Mazouni, N., Juge, C., Dagault, F., Chardy, P., 1998. Relationship between environment and resources: impact of shellfish farming on a Mediterranean lagoon (Thau, France). Oceanol. Acta 21, 831–843.

Freon, F., Gerlotto, F., Soria, M., 1996. Diurnal variation of school structure with special reference to transition periods. ICES J. Mar. Sci. 53, 459–464.

Foote, K.G., 1987. Calibration of acoustic instruments for fish density estimation: a practical guide. ICES Coop. Res. Rep. No. 144.

Gerlotto, F., Soria, M., Fréon, P., 1999. From two dimensions to three: the use of multibeam sonar for a new approach in fisheries acoustics. Can. J. Fish. Aquat. Sci. 56, 6–12.

Gerlotto, F., Brehmer, P., Buestel, D., Sanguinede, F., 2001. A method for acoustics monitoring of a mussel longline ground using vertical echosounder and multibeam sonar. ICES CM/R:01.

Hunter, J.R., Mitchel, C.T., 1967. Association of fishes with floatam in the offshore waters of central America. Fish. Bull. 66, 13–29.

Lacroix, D., Dao, J.-C., Veron, G., Buestel, D., Mellon, C., Lagardere, J.P., Coves, D., Charbonnel, E., 2002. Les récifs artificiels : aménagement du littoral et repeuplement. In: Lacroix, D. (Ed.), Bilans et perspectives, Ifremer.

Loste, C., Cazin, F., 1993. La conchyliculture en mer ouverte en Languedoc Roussillon, situation en 1992. Région Languedoc Roussillon CEPRALMAR Montpellier.

Mayer, L., Li, Y., Melvin, G., 2002. 3D visualization for pelagic fisheries research and assessment. ICES J. Mar. Sci. 59, 216–225.

Mazouni, N., Gaertner, J.-C., Deslous-Paoli, J.-M., 2001. Composition of biofouling communities on suspended oyster cultures: an in situ study of their interactions with the water column. Mar. Ecol. Prog. Ser. 214, 93–102.

Mazouni, N., Deslous-Paoli, J.-M., Landrein, S., 1998. Impact of oyster culture on nutrients and oxygen fluxes in a coastal lagoon. Oceanol. Acta 21, 845–858.

Nédélec, C., Prado, J., 1990. Definition and classification of fishing gear categories. FAO Fish. Tech. Pap. 222.

O'Dor, R.K., Aitken, J.P., Babcock, R.C., Bolden, S.K., Seino, S., Zeller, D.C., Jackson, G.D., 2000. Using radio-acoustic positioning and telemetry (RAPT) to define and assess marine protected areas (MPAs). In: Sibert, J.R., Nielsen, J.F. (Eds.), Electronic Tagging and Tracking in Marine Fisheries. Kluwer Academic Publishers, London, pp. 147–158.

Petitgas, P., Monimeau, L., Brehmer, P., Gerlotto, F., 1996. Characterising the spatial distribution of fish schools with a point process approach: a first application on sonar recordings. ICES CM96/B:31.

Pitcher, T.J., 1983. Heuristic definitions of shoaling behaviour. Anim. Behav. 31, 611–613.

Souchu, P., Gasc, A., Cahet, G., Vaquer, A., Collos, Y., Deslous-Paoli, J.-M., 1997. Biogeochemical composition of Mediterranean waters outside Thau Lagoon. Estuar. Coast. Shelf. Sci. 44, 275–284.

Weill, A.C., Scalabrin, C., Diner, N., 1993. MOVIES-B: an acoustic detection description software. Application to shoal species classification. Aquat. Living Resour. 6, 255–267.